frontiers | Research Topics

# Innovations in surgical oncology

**Edited by**
Beatrice Aramini and Jeroen Van Vugt

**Published in**
Frontiers in Oncology
Frontiers in Surgery

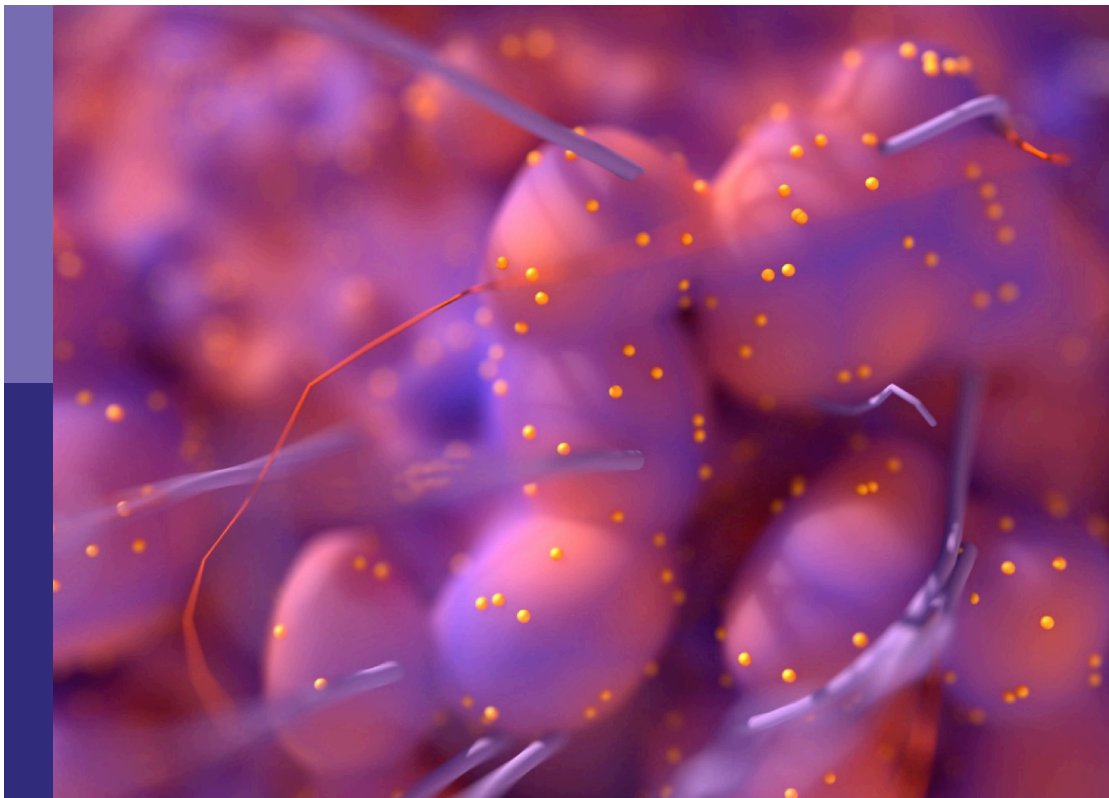

ISSN 1664-8714
ISBN 978-2-8325-3316-1
DOI 10.3389/978-2-8325-3316-1

## About Frontiers

Frontiers is more than just an open access publisher of scholarly articles: it is a pioneering approach to the world of academia, radically improving the way scholarly research is managed. The grand vision of Frontiers is a world where all people have an equal opportunity to seek, share and generate knowledge. Frontiers provides immediate and permanent online open access to all its publications, but this alone is not enough to realize our grand goals.

## Frontiers journal series

The Frontiers journal series is a multi-tier and interdisciplinary set of open-access, online journals, promising a paradigm shift from the current review, selection and dissemination processes in academic publishing. All Frontiers journals are driven by researchers for researchers; therefore, they constitute a service to the scholarly community. At the same time, the *Frontiers journal series* operates on a revolutionary invention, the tiered publishing system, initially addressing specific communities of scholars, and gradually climbing up to broader public understanding, thus serving the interests of the lay society, too.

## Dedication to quality

Each Frontiers article is a landmark of the highest quality, thanks to genuinely collaborative interactions between authors and review editors, who include some of the world's best academicians. Research must be certified by peers before entering a stream of knowledge that may eventually reach the public - and shape society; therefore, Frontiers only applies the most rigorous and unbiased reviews. Frontiers revolutionizes research publishing by freely delivering the most outstanding research, evaluated with no bias from both the academic and social point of view. By applying the most advanced information technologies, Frontiers is catapulting scholarly publishing into a new generation.

## What are Frontiers Research Topics?

Frontiers Research Topics are very popular trademarks of the *Frontiers journals series*: they are collections of at least ten articles, all centered on a particular subject. With their unique mix of varied contributions from Original Research to Review Articles, Frontiers Research Topics unify the most influential researchers, the latest key findings and historical advances in a hot research area.

Find out more on how to host your own Frontiers Research Topic or contribute to one as an author by contacting the Frontiers editorial office: frontiersin.org/about/contact

# Innovations in surgical oncology

**Topic editors**

Beatrice Aramini — University of Bologna, Italy

Jeroen Van Vugt — Erasmus Medical Center, Netherlands

**Citation**

Aramini, B., Van Vugt, J., eds. (2023). *Innovations in surgical oncology*. Lausanne: Frontiers Media SA. doi: 10.3389/978-2-8325-3316-1

# Table of contents

frontiers | Frontiers in Oncology

TYPE Editorial
PUBLISHED 09 August 2023
DOI 10.3389/fonc.2023.1257762



OPEN ACCESS

EDITED AND REVIEWED BY
Francesco Giovinazzo,
Agostino Gemelli University Polyclinic (IRCCS), Italy

*CORRESPONDENCE
Beatrice Aramini
beatrice.aramini@gmail.com
beatrice.aramini2@unibo.it

†These authors share first authorship

RECEIVED 12 July 2023
ACCEPTED 21 July 2023
PUBLISHED 09 August 2023

CITATION
Aramini B, Masciale V and van Vugt JLA (2023) Editorial: Innovations in surgical oncology.
*Front. Oncol.* 13:1257762.
doi: 10.3389/fonc.2023.1257762



# Editorial: Innovations in surgical oncology

Beatrice Aramini[1*†], Valentina Masciale[2†] and Jeroen L. A. van Vugt[3]

[1]Division of Thoracic Surgery, Department of Medical and Surgical Sciences (DIMEC) of the Alma Mater Studiorum, University of Bologna, Giovanni Battista Morgagni—Luigi Pierantoni Hospital, Forlì, Italy, [2]Division of Oncology, Laboratory of Cellular Therapy, Department of Medical and Surgical Sciences for Children & Adults, University-Hospital of Modena and Reggio Emilia, Modena, Italy, [3]Department of Surgery, Erasmus Medical Center (MC) University Medical Center, Rotterdam, Netherlands

KEYWORDS

**innovation, surgical technique, training, surgical simulators, minimally invasive & robotic surgery**

Editorial on the Research Topic
Innovations in surgical oncology

Innovation describes the continuous process of developing and defining new surgical techniques (1, 2). In recent years, the increased introduction of minimally invasive surgical (MIS) approaches has been achieved for solid malignant tumor removal (3–5). The importance of creating new MIS approaches for curing cancer with the benefit of reduced hospital length of stay, less pain, and rapid recovery has motivated innovators to implement robotic surgery (6, 7). This is one of the reasons why innovative engineering solutions have been adopted, that is, to overcome the challenges of these new approaches, decrease costs, and help surgeons achieve the most effective results and clinical outcomes, improving the quality of life of the patients (8, 9). For example, robots and medical simulators have successfully addressed the limitations and revolutionized minimal surgical access (10, 11). The introduction of robots into operating rooms has resulted in improvements in the surgeon's control and visual field (12). Additional benefits have been noted, even for the patient: less tissue damage, shortened hospitalization time to an average of 3–4 days, decreased psychological impact on the patient, reduction of infection risk with the MIS approach, reduction of unwanted surgical complications (e.g., vessel sectioning and nerve damage), and fewer assistants in the operating room (13, 14).

Furthermore, training using surgical simulators offers several benefits and advantages primarily for future surgeons (15). These simulators can be used as a wet laboratory, with a reduced "human cost" considering potential adverse patient outcomes, and surgeons-in-training can learn in a relaxed environment (16). In addition, the progressive development of simulators improves learning approaches, which involve novel methods that are different from the traditional methods. However, while the importance of these new approaches to improving the learning curve of new surgeons' is an attractive and acceptable adjunct to surgical curricula, the simulators cannot replace the experiences of surgical preceptors (17). The recent establishment of simulation programs in all surgical fields is beneficial for future surgical training, improving patient care and providing surgeons with the opportunity to overcome limitations without anxiety, which is generally considered the norm during the

surgical maturation progress (18). The goals of emerging companies have been changed by these enthusiastic approaches, with the new focuses being to provide solutions to overcome the electro-mechanical limitations of the current robotic surgical systems and to build new surgical simulators to address some of the obstacles faced when performing open surgical procedures (19, 20).

Advances in surgery have focused on minimizing the invasiveness of surgical procedures, and a significant paradigm shift has occurred for some procedures in which surgeons no longer directly touch or see the structures on which they operate (21). Advancements in video imaging, endoscopic technology, and instrumentation have made it possible to convert procedures in many surgical specialties from open surgeries to endoscopic procedures (22). Computers and robotics can be used to facilitate complex endoscopic procedures via voice control over the networked operating room, enhancement of dexterity to facilitate microscale operations, and the development of simulator trainers to enhance the learning of new, complex operations (23). Robotic surgery and medical simulators have dramatically altered and improved procedures, and these two methods share several features: both use a mechanized interface that provides visual patient reactions in response to the actions of the health care professional (simulation also includes touch feedback), both use monitors to visualize the progression of the procedure, and both use computer software applications to interface with the health care professional. Both technologies are experiencing rapid adoption, and they are modalities that allow physicians to perform increasingly complex minimally invasive procedures while enhancing patient safety.

It should also be considered that the advent of new molecular diagnostic technologies has improved treatment approaches in multiple branches of medicine, including surgery. The biosocial medicine approach aims to explain how people's lifestyles impact their health (24, 25). This approach could be revolutionary for medical practice, paving the way for the introduction of biology to patient care. In addition to the biology of the patient, their biography—or lived experience—should be considered; in this way, biosocial medicine offers a unique signature for each patient. It all started with the idea that the patient is the focus of their own clinical care—although statistical and demographic information is also necessary to ensure the provision of precise medicine—and that clinicians should focus on the real person whom they are treating. Currently, progress is rapidly being made in biology, as the world could appreciate in the management of the global COVID-19 pandemic through the advent of the new mRNA vaccines, thanks to advances in genomic and molecular sciences. This progress may represent the basis for the establishment of precision medicine in clinical practice using tailored treatment based on the signature of the patient (26, 27).

This Research Topic includes a broad selection and unique mix of papers from pioneering researchers showing innovations in surgical oncology.

## Author contributions

BA: Conceptualization, Writing – original draft, Writing – review & editing. VM: Supervision, Visualization, Writing – review & editing. JvV: Conceptualization, Visualization, Writing – review & editing.

## Conflict of interest

The authors declare that the research was conducted in the absence of any commercial or financial relationships that could be construed as a potential conflict of interest.

## Publisher's note



## References

1. Birchley G, Ives J, Huxtable R, Blazeby J. Conceptualising surgical innovation: an eliminativist proposal. *Health Care Anal* (2020) 28(1):73–97. doi: 10.1007/s10728-019-00380-y

2. Flessa S, Huebner C. Innovations in health care-A conceptual framework. *Int J Environ Res Public Health* (2021) 18(19):10026. doi: 10.3390/ijerph181910026

3. Phelps HM, Lovvorn HN3rd. Minimally invasive surgery in pediatric surgical oncology. *Children (Basel).* (2018) 5(12):158. doi: 10.3390/children5120158

4. van Dalen EC, de Lijster MS, Leijssen LG, Michiels EM, Kremer LC, Caron HN, et al. Minimally invasive surgery versus open surgery for the treatment of solid abdominal and thoracic neoplasms in children. *Cochrane Database Syst Rev* (2015) 1 (1):CD008403. doi: 10.1002/14651858.CD008403.pub3

5. Yutaka Y, Ng CSH. Editorial: Recent advances in minimally invasive thoracic surgery. *Front Surg* (2023) 10:1182768. doi: 10.3389/fsurg.2023.1182768

6. Gonçalves AA, Freire De Castro Silva SL, Pitassi C, Brauer M, Gois S, de Oliveira SB. Innovation in cancer treatment: the impacts of robotic-assisted surgery adoption at the Brazilian National Cancer Institute. *Stud Health Technol Inform* (2020) 272:123–6. doi: 10.3233/SHTI200509

7. Ashrafian H, Clancy O, Grover V, Darzi A. The evolution of robotic surgery: surgical and anaesthetic aspects. *Br J Anaesth* (2017) 119(suppl_1):i72–84. doi: 10.1093/bja/aex383

8. Bajwa J, Munir U, Nori A, Williams B. Artificial intelligence in healthcare: transforming the practice of medicine. *Future Healthc J* (2021) 8(2):e188–94. doi: 10.7861/fhj.2021-0095

9. Johnson KB, Wei WQ, Weeraratne D, Frisse ME, Misulis K, Rhee K, et al. Precision medicine, AI, and the future of personalized health care. *Clin Transl Sci* (2021) 14(1):86–93. doi: 10.1111/cts.12884

10. Sone K, Tanimoto S, Toyohara Y, Taguchi A, Miyamoto Y, Mori M, et al. Evolution of a surgical system using deep learning in minimally invasive surgery (Review). *BioMed Rep* (2023) 19(1):45. doi: 10.3892/br.2023.1628

11. Badash I, Burtt K, Solorzano CA, Carey JN. Innovations in surgery simulation: a review of past, current and future techniques. *Ann Transl Med* (2016) 4(23):453. doi: 10.21037/atm.2016.12.24

12. Shah J, Vyas A, Vyas D. The history of robotics in surgical specialties. *Am J Robot Surg* (2014) 1(1):12–20. doi: 10.1166/ajrs.2014.1006

13. Tran K, Bell C, Stall N, Tomlinson G, McGeer A, Morris A, et al. The effect of hospital isolation precautions on patient outcomes and cost of care: A multi-site, retrospective, propensity score-matched cohort study. *J Gen Intern Med* (2017) 32 (3):262–8. doi: 10.1007/s11606-016-3862-4

14. Dharap SB, Barbaniya P, Navgale S. Incidence and risk factors of postoperative complications in general surgery patients. *Cureus* (2022) 14(11):e30975. doi: 10.7759/cureus.30975

15. Badash I, Gould DJ, Patel KM. Supermicrosurgery: history, applications, training and the future. *Front Surg* (2018) 5:23. doi: 10.3389/fsurg.2018.00023

16. Hu YG, Liu QP, Gao N, Wu CR, Zhang J, Qin L, et al. Efficacy of wet-lab training versus surgical-simulator training on performance of ophthalmology residents during chopping in cataract surgery. *Int J Ophthalmol* (2021) 14(3):366–70. doi: 10.18240/ijo.2021.03.05

17. Agha RA, Fowler AJ. The role and validity of surgical simulation. *Int Surg* (2015) 100(2):350–7. doi: 10.9738/INTSURG-D-14-00004.1

18. Brandão CMA, Pêgo-Fernandes PM. HANDS-ON: training simulation in surgery. *Sao Paulo Med J* (2023) 141(3):e20231413. doi: 10.1590/1516-3180.2022.1413230223

19. Cepolina F, Razzoli RP. An introductory review of robotically assisted surgical systems. *Int J Med Robot.* (2022) 18(4):e2409. doi: 10.1002/rcs.2409

20. Enayati N, De Momi E, Ferrigno G. Haptics in robot-assisted surgery: challenges and benefits. *IEEE Rev BioMed Eng.* (2016) 9:49–65. doi: 10.1109/RBME.2016.2538080

21. Palep JH. Robotic assisted minimally invasive surgery. *J Minim Access Surg* (2009) 5(1):1–7. doi: 10.4103/0972-9941.51313

22. Kumar A, Yadav N, Singh S, Chauhan N. Minimally invasive (endoscopic-computer assisted) surgery: Technique and review. *Ann Maxillofac Surg* (2016) 6 (2):159–64. doi: 10.4103/2231-0746.200348

23. Mack MJ. Minimally invasive and robotic surgery. *JAMA* (2001) 285(5):568–72. doi: 10.1001/jama.285.5.568

24. Blair ED. Molecular diagnostics and personalized medicine: value-assessed opportunities for multiple stakeholders. *Per Med* (2010) 7(2):143–61. doi: 10.2217/pme.10.1

25. Traversi D, Pulliero A, Izzotti A, Franchitti E, Iacoviello L, Gianfagna F, et al. Precision medicine and public health: new challenges for effective and sustainable health. *J Pers Med* (2021) 11(2):135. doi: 10.3390/jpm11020135

26. Li T, Huang T, Guo C, Wang A, Shi X, Mo X, et al. Genomic variation, origin tracing, and vaccine development of SARS-CoV-2: A systematic review. *Innovation (Camb).* (2021) 2(2):100116. doi: 10.1016/j.xinn.2021.100116

27. Chabanovska O, Galow AM, David R, Lemcke H. mRNA - A game changer in regenerative medicine, cell-based therapy and reprogramming strategies. *Adv Drug Delivery Rev* (2021) 179:114002. doi: 10.1016/j.addr.2021.114002

frontiers | Frontiers in Oncology

TYPE Methods
PUBLISHED 22 August 2022
DOI 10.3389/fonc.2022.980050



OPEN ACCESS

EDITED BY
Beatrice Aramini,
University of Bologna, Italy

REVIEWED BY
Carmine Conte,
Agostino Gemelli University Polyclinic (IRCCS), Italy
Gaetano Valenti,
Kore University of Enna, Italy

*CORRESPONDENCE
Lingya Pan
panly@pumch.cn

†These authors have contributed equally to this work and share first authorship

SPECIALTY SECTION
This article was submitted to Surgical Oncology, a section of the journal Frontiers in Oncology

RECEIVED 28 June 2022
ACCEPTED 02 August 2022
PUBLISHED 22 August 2022

CITATION
Shan Y, Jin Y, Li Y, Gu Y, Wang W and Pan L (2022) Rectosigmoid sparing en bloc pelvic resection for fixed ovarian tumors: Surgical technique and perioperative and oncologic outcomes.
*Front. Oncol.* 12:980050.
doi: 10.3389/fonc.2022.980050



# Rectosigmoid sparing en bloc pelvic resection for fixed ovarian tumors: Surgical technique and perioperative and oncologic outcomes

Ying Shan†, Ying Jin†, Yan Li, Yu Gu, Wei Wang and Lingya Pan*

Department of Obstetrics and Gynecology, National Clinical Research Center for Obstetric and Gynecologic Diseases, Peking Union Medical College Hospital, Chinese Academy of Medical Sciences and Peking Union Medical College, Beijing, China

**Purpose:** Patients with advanced ovarian cancer often undergo en bloc rectosigmoid resection with total hysterectomy to completely debulk the pelvis. We describe a unique rectosigmoid sparing en bloc pelvic resection technique for fixed ovarian tumors infiltrating the colon wall.

**Methods:** From July 2020 to June 2021, 20 patients with advanced epithelial ovarian cancer (EOC) underwent rectosigmoid sparing en bloc pelvic resection successfully at our institution. We summarized our surgical technique and the peri-operative and oncological outcomes.

**Results:** Twenty cases with bowel infiltration achieved en bloc pelvic resection with rectosigmoid tumorectomy in a centripetal fashion. Only two patients required mucosal repair. None of the patients experienced any complications associated with en bloc resection. No pelvic recurrence occurred within the median follow-up time of 12 months.

**Conclusion:** Rectosigmoid sparing en bloc pelvic resection may be feasible for select patients with fixed ovarian tumors infiltrating the colon wall.

KEYWORDS

**rectosigmoid sparing, en bloc pelvic resection, ovarian cancer, surgical technique, tumorectomy**

## Introduction

Ovarian cancer is the most lethal of all gynecologic malignancies. Surgery with complete residual tumor removal (R0 resection) is the recommended treatment and has the greatest prognostic impact (1, 2). To obtain complete cytoreduction, patients with advanced ovarian cancer often undergo en bloc rectosigmoid resection with total hysterectomy to completely debulk the pelvis. Hudson published the first report describing this technique, termed "radical oophorectomy", which was specifically designed for the intact removal of a fixed ovarian tumor en bloc along with the attached peritoneum and surrounding structures (3). Since then, it has been adopted by many medical institutions around the world (4–9). The rectosigmoid colon is frequently involved in these cases, and rectosigmoid colon resection is performed in 25%–58% of all patients (5, 10–13). Anastomotic leakage is the most feared complication. Common complications are persistent urinary, defecatory, and sexual dysfunction due to autonomic nervous system damage arising from surgery (13). However, considering that epithelial ovarian cancer (EOC) tumors usually involve part of the wall of the colon and are limited to the serosa in 45% of cases (14), ulceration into the rectum is very rare (15). Moreover, since the goal of debulking surgery is the complete removal of macroscopic neoplasms, not radical resection, it is feasible to perform an en bloc pelvic resection with tumorectomy for tumors that are fixed in the pelvis and infiltrate the rectosigmoid colon, avoiding colectomy. The purpose of this paper is to describe a rectosigmoid sparing en bloc pelvic resection technique for fixed ovarian tumors infiltrating the colon wall. We summarize our surgical technique and the peri-operative and oncological outcomes.

## Materials and methods

From July 2020 to June 2021, among the patients who underwent primary or interval debulking surgery, 20 patients with advanced EOC received rectosigmoid sparing en bloc pelvic resection successfully at the Department of Gynecologic Oncology Peking Union Medical College Hospital. Relative contraindications to the procedure include a Gynecologic Oncology Group performance status score of ≥3 and/or a tumor distribution that precludes an attempt to achieve complete resection, namely, extensive tumor infiltration of the small bowel mesenteric root, unresectable involvement of the porta hepatis, large-volume (≥1 cm) unresectable extra-abdominal metastasis (e.g., pulmonary), or multiple unresectable parenchymal liver metastases.

The surgical procedures are shown in Table 1. Steps such as retroperitoneal exposure, infundibulopelvic ligament ligature, ureterolysis, uterine artery ligature, retrograde hysterectomy, and retrograde rectovaginal septum dissection have been described in many reports on Hudson procedures. These procedures were accomplished using a retroperitoneal approach. The para-rectal and presacral spaces were not intentionally exposed. After rectovaginal septum dissection and tumor-involved mesosigmoid and mesorectal peritoneum shaving, the entire segment of the affected peritoneum and uterus was dissected and removed as a part of the false capsule. Since a tumor that is fixed to the Douglas pouch can infiltrate the rectosigmoid colon, in these cases, the attached tumor held in place by the rectosigmoid colon was left on the colon to serve as the bottom of the false capsule, as shown in Figure 1A. At this time, evaluations were made by experienced surgeons before tumorectomy. If tumorectomy led to laceration of <30%–40% of the colon wall or if the defect in the seromuscular layer was not too extensive, patients received rectosigmoid sparing surgery. Otherwise, en bloc rectosigmoid resection was performed, because if the area of the colonic defect was too extensive, there would be a high risk of colon fistula or stricture after repairment. Tumorectomy was performed in a centripetal fashion with a monopolar device. After complete resection of the tumor held by the rectosigmoid colon (Figure 1B), the whole specimen was removed intact with the false capsule (Figure 1C). The seromuscular layer was repaired with interrupted sutures; sometimes sutures perpendicular to the long axis of the bowel were not required (Figure 1D). The two-layer repair was performed if mucosal defects were observed.

## Results

The median age of the patients was 62 years (range 28–75 years). High-grade serous ovarian cancer (HGSOC) was the predominant histological type and was detected in 16 of 20 (80%) patients. The most common International Federation of Gynecology and Obstetrics (FIGO) stage was IIIC, which was confirmed in 90% of patients. Detailed data on the preoperative characteristics are shown in Table 2. Intraoperative and postoperative outcomes are shown in Table 3. Optimal debulking was achieved in all patients; 19 of 20 achieved R0 (no residual tumor), and only one had a residual tumor less than 2 mm on the mesentery of the small intestine. The median duration of the procedure was 230 min (range 175–340 min). The time interval from surgery to the start of chemotherapy was 9 days (range 7–13 days). The surgical complexity score (introduced by Aletti) (16) of 20 patients was 6–9; instead of rectosigmoidectomy and anastomosis, tumorectomy accounted for 3 points in this system since they shared many of the same steps. The median estimated blood loss (EBL) was 500 cc (range 300–1,200 cc). No tumors were observed to infiltrate the mucosa, and interrupted repair of the seromuscular layer was performed in 18 patients. The mucosal repair was performed, and total parenteral nutrition was provided to two patients (10%) because of a mucosal defect caused by tumorectomy.

TABLE 1 Surgical steps of rectosigmoid sparing en bloc pelvic resection.

1. Pelvic parietal peritoneum dissection, accession to the retroperitoneal space
2. Ligation of the infundibulo-pelvic ligament
3. Isolation of the ureter laterally
4. Retrograde mobilization of the bladder peritoneum with access to the vesico-vaginal space
5. Ligation of uterine vessels at the level of ureter and parametrial resection
6. Colpotomy
7. Recto-vaginal septum dissection
8. Tumor involved mesorectal and mesosigmoid peritoneum shaving
9. Rectosigmoid tumorectomy in a centripetal fashion and bowl defects repairment

The size of the solid tumor fixed in the Douglas pouch was measured by CT. The median length of the long axis was 51 mm (range 36–68 mm), and the median length of the bowel with a serosal defect was 10 cm (range 3–20 cm).

No patient experienced complications associated with en bloc resection, and no stricture or subsequent obstruction occurred after bowel repair. Two patients had pleural effusion because of diaphragmatic peritoneal stripping, and one had deep vein thrombosis (DVT). There was no readmission within 30 days and no surgery-related deaths.

After surgery, all patients were administered six cycles of standard adjuvant chemotherapy (carboplatin area under curve 5 and paclitaxel 175 mg/m$^2$). The time interval from surgery to the start of chemotherapy was 9 days (range 7–13 days). No pelvic recurrence occurred during the median follow-up time of 12 months.

## Discussion

En bloc pelvic resection of ovarian cancer with fixed tumors in the pelvis was first reported by Hudson 60 years ago (3). In principle, this technique consists of the removal of the entire Douglas pouch, serving as a false capsule of the tumor. The cardinal feature of this procedure is the approach to the retroperitoneal space, in which extensive intraperitoneal tumors are not involved, so dissection can be performed in a centripetal fashion, ensuring maximum safety to the surrounding vital structures, particularly if the pelvic organs can no longer be clearly identified.

When bowel infiltration is suspected, en bloc resection of the rectosigmoid colon is the most frequently performed variation of the Hudson procedure (4, 6, 8, 9, 17–21). Indications for rectosigmoid resection (RR) vary across centers. For instance, RR has been indicated for extensive involvement of the cul-de-sac and rectosigmoid colon in some reports (7), while it has been indicated for bowel wall infiltration even in cases with only superficial

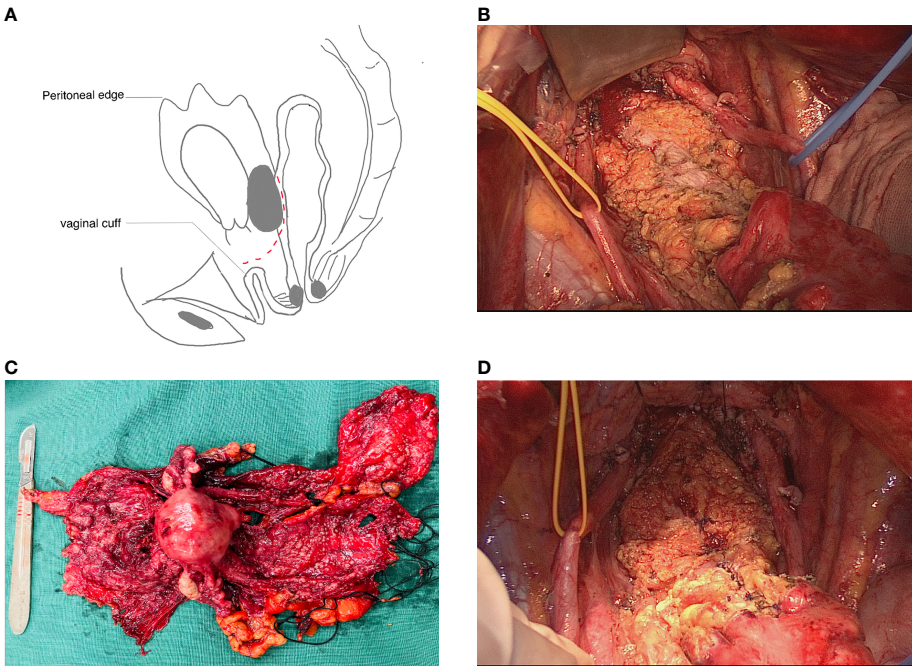


FIGURE 1
Rectosigmoid sparing en bloc pelvic resection for fixed ovarian tumors. **(A)** Tumor attaching the intact specimen was left on the colon as the bottom of the false capsule. Cutting plane is shown as a dashed line. **(B)** Seromuscular defections (black arrow) after complete resection of implants on the rectosigmoid colon. **(C)** The whole specimen was removed intact with a false capsule. **(D)** Seromuscular layer was repaired with interrupted sutures.

TABLE 2 The clinical characteristics of the included patients.

| Variable | Value/no. of patients (N = 20) |
|---|---|
| **Median age (years)** | 62 (range 28–75) |
| **Type of surgery** | |
| PDS | 15 |
| IDS | 5 |
| **Tumor histology** | |
| HGSOC | 16 |
| LGSOC | 2 |
| Musinous | 2 |
| **FIGO stage** | |
| IIIc | 18 |
| IVA | 2 |

PDS, primary debulking surgery; IDS, Interval debulking surgery; HGSOC, high-grade serous ovarian carcinoma; LGSOC, low-grade serous ovarian carcinoma; FIGO, International Federation of Gynecology and Obstetrics.

involvement in other reports (13, 14). Considering the complications that can occur after RR, rectosigmoid mesorectal-sparing resection can maximize the blood supply to colorectal anastomosis and minimize the risk of both anastomotic leakage and pelvic autonomic nervous system dysfunction (22). However, there is still the risk of anastomotic leakage.

If the tumor penetrates the muscularis of the colon but has a limited (≤2 cm) longitudinal extent, a full-thickness "wedge-shaped" segment of the anterior rectal wall can be sharply excised. Plotti (23) reported a similar method for partial rectosigmoid resection, which was performed when the complete removal of the disease led to laceration of <30%–40% of the intestinal wall circumference. The oncologic outcomes of 5-year overall survival and optimal debulking rates were not significantly different from those obtained with total rectosigmoid resection. This more conservative approach to the rectum seems to be a feasible approach for over 40% of patients with advanced ovarian cancer and rectosigmoid colon involvement.

However, it should be noted that unlike colon cancer, it is very rare for ovarian tumors to ulcerate into the rectum. Histopathological findings from the main studies on primary debulking with RR in patients with advanced ovarian cancer (AOC) have revealed superficial infiltration in a very large percentage of cases, with the infiltration being limited to the serosa or subserosa in 28%–71% of cases. Based on this view, some studies have asserted that conservative ablation may be safe and effective, like RR (14). However, the criterion of no gross residual tumor is preferred for optimal cytoreduction instead of R0 resection in these patients.

Unlike radical surgery, debulking surgery aims to achieve complete resection of all visible diseases (24–28), and considering that there is a boundary between the solid tumor and bowel wall, it is feasible to achieve complete resection in a rectosigmoid sparing fashion. Kim et al. (29) published the first report on the impact of tumorectomy without bowel resection for affected rectosigmoid lesions on EOC survival outcomes and operation-related morbidity. Their results revealed that the survival outcomes of patients treated with tumorectomy were not inferior to those of patients treated with RR if optimal debulking could be guaranteed. However, notably, the cohort excluded patients who had rectosigmoid lesions infiltrating up to the muscle, and the tumorectomy procedure used was a kind of serosectomy technique performed in patients with superficial bowel infiltration.

We developed a novel technique that achieved complete resection with tumorectomy in an en bloc manner for tumors fixed in the pelvis, even some with seromuscular infiltration, in which case rectosigmoid resection was required using the traditional Hudson procedure.

Since it may be difficult to distinguish the severity of bowel infiltration, the most important decision regarding whether rectosigmoid sparing or not was not made at the beginning of the surgery; this is the major difference compared with several modified en bloc resection planned anastomosis procedures, in which rectosigmoid bowel division is performed at the start of the surgery.

Sometimes tumors fixed in the pelvis seemed to infiltrate the bowel wall in the Douglas pouch, but only peritoneum and part of mesocolon involvement were found after peritoneum shaving. Hertel et al. (13) reported that bowel infiltration was not found on histopathologic examination in 27% of patients who underwent RR. For these patients who had exclusive involvement of the cul-de-sac but no bowel infiltration, retrograde hysterectomy and excision of the involved peritoneum in an en bloc manner should be performed without bowel resection. Moreover, extensive disease in the peritoneum and tumors fixed in the pelvis may cause the colon to be distorted or folded such that the severity of bowel infiltration cannot be evaluated objectively until retrograde rectovaginal septum dissection and mesosigmoid and mesorectal peritoneum shaving are complete. After this step, only the tumor as the bottom of the false capsule remained on the rectosigmoid colon,

TABLE 3 Intra-operative and post-operative outcomes.

| Patients no. | Surgery duration (min) | Tumor size (mm) | EBL (cc) | SCS | Length of seromuscular defection (cm) | Mucosal layer repairment | Residual disease | TPN (days) | Overall morbidity | Time between surgery and Cht (days) | Follow-up time (months) | Sites of recurrence |
|---|---|---|---|---|---|---|---|---|---|---|---|---|
| 1 | 175 | 57 * 28 | 400 | 6 | 3 | No | R0 | 0 | | 8 | 18 | – |
| 2 | 270 | 43 * 25 | 500 | 7 | 8 | No | R0 | 0 | | 9 | 17 | – |
| 3 | 240 | 43 * 30 | 600 | 7 | 5 | No | R0 | 0 | | 7 | 16 | – |
| 4 | 340 | 63 * 32 | 1200 | 8 | 6 | Yes | R0 | 4 | | 13 | 15 | Inguinal lymph nodes |
| 5 | 280 | 56 * 40 | 900 | 8 | 10 | Yes | R1 | 4 | | 11 | 15 | – |
| 6 | 195 | 42 * 29 | 300 | 7 | 11 | No | R0 | 0 | | 9 | 14 | – |
| 7 | 210 | 39 * 28 | 350 | 8 | 9 | No | R0 | 0 | | 8 | 13 | – |
| 8 | 195 | 49 * 24 | 500 | 6 | 15 | No | R0 | 0 | | 8 | 13 | – |
| 9 | 240 | 43 * 31 | 400 | 7 | 12 | No | R0 | 0 | | 9 | 13 | – |
| 10 | 330 | 39 * 24 | 1100 | 9 | 6 | No | R0 | 0 | Pleural effusion | 7 | 13 | – |
| 11 | 285 | 36 * 32 | 600 | 7 | 8 | No | R0 | 0 | DVT | 9 | 12 | – |
| 12 | 320 | 63 * 53 | 800 | 7 | 12 | No | R0 | 0 | | 10 | 12 | – |
| 13 | 190 | 44 * 30 | 400 | 7 | 13 | No | R0 | 0 | | 9 | 11 | – |
| 14 | 180 | 53 * 39 | 500 | 8 | 8 | No | R0 | 0 | | 10 | 10 | – |
| 15 | 215 | 67 * 38 | 300 | 8 | 17 | No | R0 | 0 | | 8 | 10 | – |
| 16 | 230 | 48 * 45 | 450 | 8 | 3 | No | R0 | 0 | | 9 | 10 | – |
| 17 | 240 | 57 * 47 | 850 | 9 | 7 | No | R0 | 0 | Pleural effusion | 8 | 9 | – |
| 18 | 220 | 68 * 57 | 550 | 7 | 9 | No | R0 | 0 | | 7 | 8 | – |
| 19 | 230 | 59 * 53 | 450 | 7 | 11 | No | R0 | 0 | | 8 | 8 | – |
| 20 | 225 | 67 * 39 | 600 | 6 | 20 | No | R0 | 0 | | 8 | 7 | – |

Tumor size, size of tumor in Douglas pouch measured in CT; SCS, surgical complexity score; EBL, estimated blood loss; TPN, parenteral nutrition; PDS, primary debulking surgery; Cht, chemotherapy.
*Means by multiply.



10.3389/fonc.2022.980050

so the severity of bowel invasion could be visualized clearly. At this time, evaluation and decisions regarding rectosigmoid sparing can be made by experienced surgeons.

Tumorectomy is the most unique part of our procedure, and several points should be considered to accomplish it successfully. First, to achieve complete resection and avoid cutting through the tumor tissue, the cutting plane should be on the healthy part beneath the border of the tumor and the normal colon, as shown in Figure 1A. Sacrificing complete resection for an intact bowel wall is not the goal of the procedure. Second, since there is a high risk of mucosal defect if cutting is performed too rapidly with a high-level electrical device; thus, setting the monopolar device to a moderate setting and keeping the device moving while identifying the cutting plane will minimize the electrical injury and carbonization of normal tissue. Third, to minimize mucosal defects, tumorectomy should be performed in a centripetal fashion (the point of the tumor that infiltrates deepest into the bowel wall was regarded as the "center"). In our case, since the tumor infiltrated irregularly into the seromuscular layer of the bowel, the cutting route had irregular lines, which should be continually adjusted to identify the relatively loose space in the muscular layer beneath the tumor, leaving the part of the bowel with the deepest tumor infiltration to be separated at the end of the resection. Once mucosal perforation occurs, the best cutting plane will be lost, and the bowel still attached to the tumor must be removed in a full-thickness fashion, causing more mucosal defects, which may cause the procedure to be converted to RR. Proper tension perpendicular to the cutting plane will make it easier to find the cutting plane. However, retracting the tumor attached to the bowel too forcefully will make the bowel wall thinner and increase the risk of perforation.

The largest tumor size in our series measured by CT was 68 * 57 mm, but only a 9-cm serosal defect length was measured, and no mucosal defect was observed after tumorectomy. Two patients with mucosal defects had medium-sized tumors. The size of the tumor fixed in the pelvis at first sight or measured by CT is not the most important factor for considering bowel sparing surgery since the tumor size is not directly related to the depth of bowel infiltration. The depth and width of bowel infiltration are the most important factors, but they cannot be evaluated accurately preoperatively only by CT scan. Several studies in the past have also demonstrated a significant discrepancy between the CT and the surgical findings on bowel involvement (16, 30, 31). In the past decades, a few groups have introduced an exploratory laparoscopy (EXL) before laparotomy (32–35). The advantages of EXL are multiple, including a correct diagnosis based on the histology of tissue biopsy, precise evaluation of disease spread, and better selection of the patients for ultra-radical surgery. The combination of CT and EXL displayed a better diagnostic power on the large bowel involvement than the CT scan alone. Also, it can reliably anticipate the absence of bowel involvement (36). So this preoperative workout should be considered as a method to better discriminate which patients might be eligible for rectosigmoid sparing or resection in our further study. What is more, if a large tumor is packed in the pelvis, even without severe bowel infiltration, there will be no space to perform a tumorectomy since this procedure requires space to clearly expose the bottom of the false capsule and adjust the cutting direction by retracting the tumor in different directions. Presacral space dissection may help to expose the tumor bed under clear visualization.

If mucosal defects occur, two-layer repair should be performed, and sutures should be placed perpendicular to the long axis of the bowel for mucosal repair. Seromuscular defects occurred over a much larger area. There are limited reports on the method of seromuscular repair since bowel resection has been performed in most cases when a muscular invasion was noted. The length of the seromuscular defects in our series was between 3 and 20 cm, and the edges of the defects were irregular. Since the defects were long in some cases and perpendicular repair to the long axis would cause the bowel to fold together, we repaired the defects in an oblique manner to avoid lumen stricturing and bowel folding, which may be safe and effective. Soo et al. (37) reported another safe method of seromuscular repair that formed the rectosigmoid colon into a U-shaped loop, but the lengths of the defects in their reports were 18 cm or less. In particular, the same method of tumorectomy and bowel repair has also been used in upper abdominal surgery in selected cases in our center when seromuscular involvement of the colon caused by omental cake occurred.

In summary, the rectosigmoid sparing en bloc pelvic resection technique described herein may be safe and effective for complete resection in select cases of fixed ovarian tumors infiltrating the colon wall. However, in order to observe the site of recurrence after this procedure, a longer follow-up period is needed, and also, further larger prospective studies are needed to better assess the safety, feasibility, and, most importantly, efficacy in terms of oncological outcomes of this conservative surgical approach.

## Data availability statement

The original contributions presented in the study are included in the article/Supplementary Material. Further inquiries can be directed to the corresponding author.

## Ethics statement

The studies involving human participants were reviewed and approved by Ethics Committee of PUMCH. The patients/participants provided their written informed consent to participate in this study. Written informed consent was

obtained from the individual(s) for the publication of any potentially identifiable images or data included in this article.

## Author contributions

Study conceptualization: LP and YJ; Study design: YS and YJ; Data acquisition: YS, YJ, YG, WW, and YL; Quality control of data and algorithms: YJ and YS; Data analysis and interpretation: YS, YL, and YJ; Statistical analysis: YS; Manuscript preparation: YS and YJ; Manuscript editing: all authors; Manuscript review: LP. All authors contributed to the article and approved the submitted version.

## Funding

This project was supported by the Non-profit Central Research Institute Fund of Chinese Academy of Medical Sciences (2021- PT320-003). Furthermore, this project was also supported by CAMS Innovation Fund for Medical Sciences (CIFMS-2017- I2M-1-002).

## Conflict of interest

The authors declare that the research was conducted in the absence of any commercial or financial relationships that could be construed as a potential conflict of interest.

## Publisher's note



## References

1. du Bois A, Reuss A, Pujade–Lauraine E, Harter P, Ray–Coquard I, Pfisterer J. Role of surgical outcome as prognostic factor in advanced epithelial ovarian cancer: A combined exploratory analysis of 3 prospectively randomized phase 3 multicenter trials: By the arbeitsgemeinschaft gynaekologische onkologie studiengruppe ovarialkarzinom (Ago–ovar) and the groupe d'investigateurs nationaux pour Les etudes des cancers de l'ovaire (Gineco). *Cancer* (2009) 115 (6):1234–44. doi: 10.1002/cncr.24149

2. Ghirardi V, Moruzzi MC, Bizzarri N, Vargiu V, D'Indinosante M, Garganese G, et al. Minimal residual disease at primary debulking surgery versus complete tumor resection at interval debulking surgery in advanced epithelial ovarian cancer: A survival analysis. *Gynecol Oncol* (2020) 157(1):209–13. doi: 10.1016/j.ygyno.2020.01.010

3. Hudson CN. A radical operation for fixed ovarian tumours. *J Obstet Gynaecol Br Commonw* (1968) 75(11):1155–60. doi: 10.1111/j.1471–0528.1968.tb02901.x

4. Clayton RD, Obermair A, Hammond IG, Leung YC, McCartney AJ. The Western Australian experience of the use of en bloc resection of ovarian cancer with concomitant rectosigmoid colectomy. *Gynecol Oncol* (2002) 84(1):53–7. doi: 10.1006/gyno.2001.6469

5. Sonnendecker EW, Beale PG. Rectosigmoid resection without colostomy during primary cytoreductive surgery for ovarian carcinoma. *Int Surg* (1989) 74 (1):10–2.

6. Berek JS, Hacker NF, Lagasse LD. Rectosigmoid colectomy and reanastomosis to facilitate resection of primary and recurrent gynecologic cancer. *Obstet Gynecol* (1984) 64(5):715–20.

7. Bristow RE, del Carmen MG, Kaufman HS, Montz FJ. Radical oophorectomy with primary stapled colorectal anastomosis for resection of locally advanced epithelial ovarian cancer. *J Am Coll Surg* (2003) 197(4):565–74. doi: 10.1016/s1072–7515(03)00478–2

8. Eisenkop SM, Nalick RH, Teng NN. Modified posterior exenteration for ovarian cancer. *Obstet Gynecol* (1991) 78(5 Pt 1):879–85.

9. Barnes W, Johnson J, Waggoner S, Barter J, Potkul R, Delgado G. Reverse hysterocolposigmoidectomy (Rhcs) for resection of panpelvic tumors. *Gynecol Oncol* (1991) 42(2):151–5. doi: 10.1016/0090–8258(91)90336–4

10. Jaeger W, Ackermann S, Kessler H, Katalinic A, Lang N. The effect of bowel resection on survival in advanced epithelial ovarian cancer. *Gynecol Oncol* (2001) 83(2):286–91. doi: 10.1006/gyno.2001.6375

11. Mourton SM, Temple LK, Abu–Rustum NR, Gemignani ML, Sonoda Y, Bochner BH, et al. Morbidity of rectosigmoid resection and primary anastomosis in patients undergoing primary cytoreductive surgery for advanced epithelial ovarian cancer. *Gynecol Oncol* (2005) 99(3):608–14. doi: 10.1016/j.ygyno.2005.07.112

12. Benedetti–Panici P, Maneschi F, Scambia G, Cutillo G, Greggi S, Mancuso S. The pelvic retroperitoneal approach in the treatment of advanced ovarian carcinoma. *Obstet Gynecol* (1996) 87(4):532–8. doi: 10.1016/0029–7844(95)00494–7

13. Hertel H, Diebolder H, Herrmann J, Köhler C, Kühne–Heid R, Possover M, et al. Is the decision for colorectal resection justified by histopathologic findings: A prospective study of 100 patients with advanced ovarian cancer. *Gynecol Oncol* (2001) 83(3):481–4. doi: 10.1006/gyno.2001.6338

14. Gallotta V, Fanfani F, Vizzielli G, Panico G, Rossitto C, Gagliardi ML, et al. Douglas Peritonectomy compared to recto–sigmoid resection in optimally cytoreduced advanced ovarian cancer patients: Analysis of morbidity and oncological outcome. *Eur J Surg Oncol* (2011) 37(12):1085–92. doi: 10.1016/j.ejso.2011.09.003

15. Cornes JS, Thompson HR. Secondary carcinomas presenting as ulcerating tumours of the rectum, with report of two ovarian cases. *Br J Surg* (1960) 48:50–3. doi: 10.1002/bjs.18004820707

16. Aletti GD, Eisenhauer EL, Santillan A, Axtell A, Aletti G, Holschneider C, et al. Identification of patient groups at highest risk from traditional approach to ovarian cancer treatment. *Gynecol Oncol* (2011) 120(1):23–8. doi: 10.1016/j.ygyno.2010.09.010

17. Bridges JE, Leung Y, Hammond IG, McCartney AJ. En bloc resection of epithelial ovarian tumors with concomitant rectosigmoid colectomy: The kemh experience. *Int J Gynecological Cancer* (1993) 3(4):199–202. doi: 10.1046/j.1525–1438.1993.03040199.x

18. Obermair A, Hagenauer S, Tamandl D, Clayton RD, Nicklin JL, Perrin LC, et al. Safety and efficacy of low anterior en bloc resection as part of cytoreductive surgery for patients with ovarian cancer. *Gynecol Oncol* (2001) 83(1):115–20. doi: 10.1006/gyno.2001.6353

19. Sainz de la Cuesta R, Goodman A, Halverson SS. En bloc pelvic peritoneal resection of the intraperitoneal pelvic viscera in patients with advanced epithelial ovarian cancer. *Cancer J Sci Am* (1996) 2(3):152–7.

20. Soper JT, Couchman G, Berchuck A, Clarke–Pearson D. The role of partial sigmoid colectomy for debulking epithelial ovarian carcinoma. *Gynecol Oncol* (1991) 41(3):239–44. doi: 10.1016/0090–8258(91)90316–w

21. Sugarbaker PH. Complete parietal and visceral peritonectomy of the pelvis for advanced primary and recurrent ovarian cancer. *Cancer Treat Res* (1996) 81:75–87. doi: 10.1007/978–1–4613–1245–1_8

22. Rosati A, Vargiu V, Santullo F, Lodoli C, Attalla El Halabieh M, Scambia G, et al. Rectosigmoid mesorectal–sparing resection in advanced ovarian cancer surgery. *Ann Surg Oncol* (2021) 28(11):6721–2. doi: 10.1245/s10434–021–09651–2

23. Plotti F, Montera R, Aloisi A, Scaletta G, Capriglione S, Luvero D, et al. Total rectosigmoidectomy versus partial rectal resection in primary debulking surgery for advanced ovarian cancer. *Eur J Surg Oncol* (2016) 42(3):383–90. doi: 10.1016/j.ejso.2015.12.001

24. Chang SJ, Bristow RE, Ryu HS. Impact of complete cytoreduction leaving no gross residual disease associated with radical cytoreductive surgical procedures on survival in advanced ovarian cancer. *Ann Surg Oncol* (2012) 19(13):4059–67. doi: 10.1245/s10434–012–2446–8

25. Vergote I, Tropé CG, Amant F, Kristensen GB, Ehlen T, Johnson N, et al. Neoadjuvant chemotherapy or primary surgery in stage IIIC or IV ovarian cancer. *N Engl J Med* (2010) 363(10):943–53. doi: 10.1056/NEJMoa0908806

26. Kommoss S, Rochon J, Harter P, Heitz F, Grabowski JP, Ewald–Riegler N, et al. Prognostic impact of additional extended surgical procedures in advanced–stage primary ovarian cancer. *Ann Surg Oncol* (2010) 17(1):279–86. doi: 10.1245/s10434–009–0787–8

27. Rafii A, Stoeckle E, Jean–Laurent M, Ferron G, Morice P, Houvenaeghel G, et al. Multi–center evaluation of post–operative morbidity and mortality after optimal cytoreductive surgery for advanced ovarian cancer. *PloS One* (2012) 7(7):e39415. doi: 10.1371/journal.pone.0039415

28. Eisenkop SM, Spirtos NM, Friedman RL, Lin WC, Pisani AL, Perticucci S. Relative influences of tumor volume before surgery and the cytoreductive outcome on survival for patients with advanced ovarian cancer: A prospective study. *Gynecol Oncol* (2003) 90(2):390–6. doi: 10.1016/s0090–8258(03)00278–6

29. Kim M, Suh DH, Park JY, Paik ES, Lee S, Eoh KJ, et al. Survival impact of low anterior resection in patients with epithelial ovarian cancer grossly confined to the pelvic cavity: A Korean multicenter study. *J Gynecologic Oncol* (2018) 29(4):e60. doi: 10.3802/jgo.2018.29.e60

30. MacKintosh ML, Rahim R, Rajashanker B, Swindell R, Kirmani BH, Hunt J, et al. Ct scan does not predict optimal debulking in stage III-IV epithelial ovarian cancer: A multicentre validation study. *J Obstet Gynaecol* (2014) 34(5):424–8. doi: 10.3109/01443615.2014.899330

31. Axtell AE, Lee MH, Bristow RE, Dowdy SC, Cliby WA, Raman S, et al. Multi–institutional reciprocal validation study of computed tomography predictors of suboptimal primary cytoreduction in patients with advanced ovarian cancer. *J Clin Oncol* (2007) 25(4):384–9. doi: 10.1200/jco.2006.07.7800

32. Deffieux X, Castaigne D, Pomel C. Role of laparoscopy to evaluate candidates for complete cytoreduction in advanced stages of epithelial ovarian cancer. *Int J Gynecological Cancer* (2006) 16(Suppl)1:35–40. doi: 10.1111/j.1525–1438.2006.00323.x

33. Fagotti A, Fanfani F, Ludovisi M, Lo Voi R, Bifulco G, Testa AC, et al. Role of laparoscopy to assess the chance of optimal cytoreductive surgery in advanced ovarian cancer: A pilot study. *Gynecol Oncol* (2005) 96(3):729–35. doi: 10.1016/j.ygyno.2004.11.031

34. Fagotti A, Fanfani F, Vizzielli G, Gallotta V, Ercoli A, Paglia A, et al. Should laparoscopy be included in the work–up of advanced ovarian cancer patients attempting interval debulking surgery? *Gynecol Oncol* (2010) 116(1):72–7. doi: 10.1016/j.ygyno.2009.09.015

35. Zivaljević M, Majdevac I, Novaković P, Vujkov T. The role of laparoscopy in gynecologic oncology. *Med Pregl* (2004) 57(34):125–31. doi: 10.2298/mpns0404125z

36. Tozzi R, Traill Z, Campanile RG, Kilic Y, Baysal A, Giannice R, et al. Diagnostic flow–chart to identify bowel involvement in patients with stage IIC-IV ovarian cancer: Can laparoscopy improve the accuracy of ct scan? *Gynecol Oncol* (2019) 155(2):207–12. doi: 10.1016/j.ygyno.2019.08.025

37. Park SJ, Kim HS. Surgical technique of visceral segmental serosectomy for advanced ovarian cancer. *Gland Surg* (2021) 10(3):1276–8. doi: 10.21037/gs–2019–ursoc–03

frontiers | Frontiers in Oncology

TYPE Original Research
PUBLISHED 16 September 2022
DOI 10.3389/fonc.2022.989316



OPEN ACCESS

EDITED BY
Jeroen Van Vugt,
Erasmus Medical Center, Netherlands

REVIEWED BY
Jiang Chen,
Zhejiang University, China
Eliza Wright Beal,
The Ohio State University,
United States

*CORRESPONDENCE
Aiguo Shen
shag@ntu.edu.cn
Wenjing Zhao
wenjingvivian@163.com

†These authors have contributed equally to this work

SPECIALTY SECTION
This article was submitted to Surgical Oncology, a section of the journal Frontiers in Oncology

RECEIVED 08 July 2022
ACCEPTED 01 September 2022
PUBLISHED 16 September 2022

CITATION
Xia Z, Zhao Y, Zhao H, Zhang J, Liu C, Lu W, Wang L, Chen K, Yang J, Zhu J, Zhao W and Shen A (2022) Serum alanine aminotransferase to hemoglobin ratio and radiological features predict the prognosis of postoperative adjuvant TACE in patients with hepatocellular carcinoma.
*Front. Oncol.* 12:989316.
doi: 10.3389/fonc.2022.989316



# Serum alanine aminotransferase to hemoglobin ratio and radiological features predict the prognosis of postoperative adjuvant TACE in patients with hepatocellular carcinoma

Zicong Xia[1†], Yulou Zhao[1†], Hui Zhao[2], Jing Zhang[1], Cheng Liu[1], Wenwu Lu[1], Lele Wang[1], Kang Chen[1], Junkai Yang[1], Jiahong Zhu[1], Wenjing Zhao[1*] and Aiguo Shen[1*]

[1]Cancer Research Center Nantong, Tumor Hospital Affiliated to Nantong University, Medical School of Nantong University, Nantong, China, [2]Department of Interventional Radiology, Afiliated Hospital of Nantong University, Nantong, China

**Objective:** To explore the prognostic value of radiological features and serum indicators in patients treated with postoperative adjuvant transarterial chemoembolization (PA-TACE) and develop a prognostic model to predict the overall survival (OS) of patients with hepatocellular carcinoma (HCC) treated with PA-TACE.

**Method:** We enrolled 112 patients (75 in the training cohort and 37 in the validation cohort) with HCC treated with PA-TACE after surgical resection at the Affiliated Hospital of Nantong University between January 2012 and June 2015. The independent OS predictors were determined using univariate and multivariate regression analyses. Decision curve analyses and time-dependent receiver operating characteristic curve analysis was used to verify the prognostic performance of the different models; the best model was selected to establish a multi-dimensional nomogram for predicting the OS of HCC patients treated with PA-TACE.

**Result:** Multivariate regression analyses indicated that rim-like arterial phase enhancement (IRE), peritumor capsule (PTC), and alanine aminotransferase to hemoglobin ratio (AHR) were independent predictors of OS after PA-TACE. The combination of AHR had the best clinical net benefit and we constructed a prognostic nomogram based on IRE, PTC, and AHR. The calibration curve showed good fit between the predicted nomogram's curve and the observed curve.

**Conclusion:** Our preliminary study confirmed the prognostic value of AHR, PTC, and IRE and established a nomogram that can predict the OS after PA-TACE treatment in patients with HCC.

KEYWORDS

postoperative adjuvant transarterial chemoembolization, Alanine aminotransferase to hemoglobin ratio, prognosis, nomogram, peritumor capsule, rim-like arterial phase enhancement, hepatocellular carcinoma

# Introduction

Hepatocellular carcinoma (HCC) is one of the most common malignant tumors, the fifth most common malignancy, and the third-leading cause of cancer-related death worldwide; moreover, its incidence and mortality rates are increasing (1). Owing to its high recurrence rate, long-term effects of surgical resection are poor (2, 3). Therefore, transarterial chemoembolization (TACE) and other treatments after surgical resection are increasingly accepted by clinicians (4).

Simultaneously killing cells by restricting blood supply and infusion with chemotherapy drugs are the main contributions of TACE to treating HCC (5). The latest Chinese ***Guidelines for Diagnosis and Treatment of Primary Liver Cancer (2022 Edition)*** recommends postoperative adjuvant TACE (PA-TACE) in case of high-risk recurrence factors, such as tumor thrombus formation and multiple tumors, to reduce recurrence and prolong survival. PA-TACE has been shown to improve the overall survival (OS) of patients with HCC and portal vein tumor thrombus after surgical resection or patients diagnosed with B stage tumors according to the Barcelona Clinic Liver Cancer evaluation system (6, 7). However, whether patients can benefit from PA-TACE remains controversial (8), As the responses to TACE in patients with HCC is variable (9), it is necessary to identify the patients who can benefit from PA-TACE and implement individualized treatments.

The prognosis of HCC is closely related to liver function and systemic conditions. Alanine aminotransferase (ALT) and aspartate aminotransferase (AST) are often indicators of liver function in clinical settings. Many studies have reported the relationship of ALT with the recurrence and low survival rate of hepatitis B virus-related HCC (10, 11). Hemoglobin (Hb) can reflect anemia and be used to predict HCC's prognosis (12). The alanine aminotransferase to hemoglobin ratio (AHR) has been reported to predict progression-free survival in patients treated with TACE (13). However, the relationship between AHR and OS after TACE remains unclear.

In addition, the tumor nature is itself an important factor affecting the prognosis of HCC (14). Imaging is an important examination method for identifying tumor nature before surgery. Computed tomography (CT) is the preferred examination method for HCC because of its efficiency and economic advantages (15). CT is often used to predict the prognosis of TACE, but its radiological features are neglected in this case. However, the predictive ability of multiple markers is often more advantageous than using a single marker. Therefore, in the prognostic model constructed in this study, we included two additional radiological features (rim-like arterial phase enhancement [IRE] and peritumor capsule [PTC]).

This study aimed to explore the relationship between the radiological features of HCC, AHR after surgical resection, and prognosis of PA-TACE. We also constructed a prognostic nomogram including IRE, PTC, and AHR to predict the OS of patients undergoing PA-TACE.

# Materials and methods

## Study patients

Between January 2012 and June 2015, we identified a consecutive series of 149 patients with HCC who underwent PA-TACE at the Affiliated Hospital of Nantong University, Nantong, China. The inclusion criteria for this study were: (1) clinical diagnosis of HCC; (2) PA-TACE within 2 months after surgical resection; (3) complete preoperative images and postoperative serum data; (4) no other malignant tumors; and (5) no extrahepatic metastasis. Thirty-seven patients were excluded based on these criteria: (1) receiving other therapies before surgical resection (n = 24); (2) having radiological images from other hospitals (n = 10); and (3) missing follow-up data (n = 3). Ultimately, 112 patients were included in the study. All patients provided written informed consent before surgery. The patients were randomly divided into training (n = 75) and validation (n = 37) cohorts.

## Data collection and follow-up

The following clinical and laboratory data were extracted from the medical records system: name; age; sex; presence of

cirrhosis; alpha-fetoprotein, AST, ALT, Hb, and albumin levels; white cell, lymphocyte, and platelet counts; and AHR, defined as the ratio of ALT to Hb at the first laboratory examination after surgical resection. Cut-off AHR values were determined using receiver operating characteristic (ROC) curve analysis.

IRE was defined as irregular hyper-enhancement at the tumor edge and hypo-enhancement at the center in the arterial phase. PTC was defined as a capsule-like lesion with clear boundary hyper-enhancement around the tumor parenchyma in the arterial phase (Figures 1A–C). Two radiologists with >5 years of work experience judged whether the patient had IRE or PTC, while being blinded to the patients' AHR. OS was defined as the time from PA-TACE to death or the last follow-up.

## Construction of models and the nomogram

We developed two models to compare the training and validation cohorts. The prognostic value of the two models was determined by decision curve analyses (DCA) and time-dependent ROC analyses. The best model was selected to construct the nomogram for the entire cohort. Model 1 included IRE, PTC, and AHR, and Model 2 included only IRE and PTC.

## Statistical analysis

The t-test was used to analyze continuous variables with a normal distribution. The Wilcoxon rank-sum test was used to analyze continuous variables not conforming to a normal distribution. For classified data, we chose the $\chi^2$ test when each level met the requirements of frequency >5 and total sample size >40; otherwise, the Fisher precision probability test was used. We used the "survival" package in R software, version 3.6.3 (R Foundation for Statistical Computing, Vienna, Austria), to perform univariate and multivariate Cox regression analyses and used variables with a *P*-value <0.1 in univariate analysis for multivariate analysis. In addition, we used the "survival" and "stdca.R" packages in R to perform DCA for evaluating the clinical application of different models and the nomogram (16). Time-dependent ROC curves were analyzed using the "timeROC" package in R and visualized by the ggplot2 package (17). The nomogram and calibration curves were analyzed and visualized using the "rms" package in R.

All statistical analyses were performed using SPSS, version 26.0 (IBM Corp., Armonk, NY, USA) and R software version 3.6.3. We considered a *P*-value <0.05 as statistically significant.

# Results

## Patient characteristics

The patient characteristics of the two cohorts are shown in Table 1. The death status ($P = 0.139$) and OS ($P = 0.194$) did not significantly differ between the training and validation cohorts. In addition, the clinical parameters, laboratory data, and radiological characteristics were similar between the training and validation cohorts. These findings indicate no significant difference in baseline data between the two cohorts; the two cohorts were homogeneous and comparable, which served as basis for our subsequent analysis.

## Prognostic factors of OS in the training cohort

First, we determined the optimal AHR cut-off value to be 0.940, with an area under the curve (AUC) of 0.554 (95% confidence interval [CI]: 0.410–0.698), sensitivity of 28.6%, and specificity of 93.6% (Table 2). Univariate analysis showed that PTC (hazard ratio [HR] = 0.314; 95% CI: 0.135–0.732; $P = 0.007$) and AHR >0.94 (HR = 6.376; 95% CI: 2.584–15.735; $P < 0.001$) were risk factors for OS (Table 3). Second, we


FIGURE 1
Enhanced CT for PTC **(A)**, IRE **(B)**, and both PTC and IRE **(C)**, CT, computed tomography; PTC, peritumor capsule; IRE, rim-like arterial phase enhancement.

10.3389/fonc.2022.989316

TABLE 1 Baseline patient data in the two cohorts.

| Characteristic | Training cohort n = 75 | Validation cohort n = 37 | *P* |
|---|---|---|---|
| **Sex, n (%)** | | | 0.259 |
| **Female** | 12 (16%) | 10 (27%) | |
| **Male** | 63 (84%) | 27 (73%) | |
| **AFP, n (%)** | | | 0.211 |
| **<400** | 53 (70.7%) | 21 (56.8%) | |
| **≥400** | 22 (29.3%) | 16 (43.2%) | |
| **IRE, n (%)** | | | 0.081 |
| **Absent** | 47 (62.7%) | 16 (43.2%) | |
| **Present** | 28 (37.3%) | 21 (56.8%) | |
| **PTC, n (%)** | | | 1.000 |
| **Absent** | 42 (56%) | 21 (56.8%) | |
| **Present** | 33 (44%) | 16 (43.2%) | |
| **Child-pugh, n (%)** | | | 1.000 |
| **A** | 3 (4%) | 1 (2.7%) | |
| **B** | 72 (96%) | 36 (97.3%) | |
| **Cirrhosis, n (%)** | | | 0.794 |
| **Absent** | 23 (30.7%) | 13 (35.1%) | |
| **Present** | 52 (69.3%) | 24 (64.9%) | |
| **Status, n (%)** | | | 0.139 |
| **Alive** | 47 (62.7%) | 17 (45.9%) | |
| **Dead** | 28 (37.3%) | 20 (54.1%) | |
| **Age, mean ± SD** | 55.17 ± 9.66 | 54.49 ± 9.39 | 0.722 |
| **AST, mean ± SD** | 41.77 ± 33.25 | 39.32 ± 14.19 | 0.669 |
| **ALT, mean ± SD** | 45.72 ± 39.78 | 41 ± 24.38 | 0.509 |
| **ALB, mean ± SD** | 38.58 ± 4.58 | 37.6 ± 4.05 | 0.269 |
| **WBC, mean ± SD** | 5.09 ± 1.5 | 4.72 ± 1.1 | 0.193 |
| **LY, mean ± SD** | 1.65 ± 0.53 | 1.51 ± 0.46 | 0.160 |
| **PLT, mean ± SD** | 153.31 ± 61.86 | 151.46 ± 57.89 | 0.880 |
| **Hb, mean ± SD** | 142.59 ± 16.37 | 137.32 ± 13.87 | 0.096 |
| **OS day, mean ± SD** | 1666.93 ± 800.56 | 1459.05 ± 773.56 | 0.194 |

AFP, alpha-fetoprotein; IRE, irregular rim-like arterial phase enhancement; PTC, peritumor capsule; AST, aspartate aminotransferase; ALT, alanine aminotransferase; ALB, albumin; WBC, white blood cell; LY, lymphocyte count; PLT, platelet count; Hb, hemoglobin; OS, overall survival; SD, standard deviation.

performed multivariate analysis on parameters with a *P*-value <0.1 in univariate analysis. The result showed that IRE (HR = 2.8; 95% CI: 1.186–6.608; $P = 0.019$), PTC (HR = 0.401; 95% CI: 0.166–0.965; $P = 0.041$), and AHR >0.94 (HR = 6.698; 95% CI: 2.561–17.519; $P < 0.001$) were independent predictors of OS (Table 3). We observed no significant differences in IRE in univariate analysis (hazard ratio [HR] = 2.204; 95% CI: 0.990–4.906; $P = 0.053$). However, after multivariate analysis, IRE became an independent prognostic factor for OS.

## Optimal model for predicting the OS of patients treated with PA-TACE

We established two models: Model 1, consisting of IRE, PTC, and the AHR; and Model 2, consisting of IRE and PTC. This design allowed us to observe differences in radiological characteristics with or without the AHR. Based on the 2-year DCA of the training cohort, Models 1 and 2 had a similar clinical net benefit (Figure 2A), but the clinical net benefit of Model 1 at

TABLE 2 \Cut-off value and AUC of the AHR after surgical resection.

| Parameter | Cut-off value | AUC | Sensitivity (%) | Specificity (%) | 95% CI of AUC |
|---|---|---|---|---|---|
| AHR | 0.940 | 0.554 | 28.6% | 93.6% | 0.410-0.698 |

AUC, area under the curve; CI, confidence interval; AHR, alanine aminotransferase to hemoglobin ratio.

10.3389/fonc.2022.989316

TABLE 3 Univariable and multivariable Cox analyses of OS in the training cohort.

| Characteristics | Total (N) | HR (95% CI) Univariate analysis | *P* | HR (95% CI) Multivariate analysis | *P* |
|---|---|---|---|---|---|
| **Age** | 75 | 1.024 (0.983–1.066) | 0.252 | | |
| **Child-pugh** | 75 | | 0.783 | | |
| **B** | 72 | Reference | | | |
| **A** | 3 | 1.329 (0.176–10.038) | 0.783 | | |
| **Cirrhosis** | 75 | 1.128 (0.501–2.539) | 0.772 | | |
| **AFP** | 75 | | 0.114 | | |
| **<400** | 53 | Reference | | | |
| **≥400** | 22 | 1.917 (0.855–4.300) | 0.114 | | |
| **IRE** | 75 | | 0.053 | | |
| **Absent** | 47 | Reference | | | |
| **Present** | 28 | 2.204 (0.990–4.906) | 0.053 | 2.800 (1.186–6.608) | 0.019 |
| **PTC** | 75 | | 0.007 | | |
| **Absent** | 42 | Reference | | | |
| **Present** | 33 | 0.314 (0.135–0.732) | 0.007 | 0.401 (0.166–0.965) | 0.041 |
| **ALT** | 75 | 1.000 (0.999–1.001) | 0.841 | | |
| **Hb** | 75 | 1.009 (0.988–1.030) | 0.422 | | |
| **AHR** | 75 | | < 0.001 | | |
| **≤ 0.94** | 64 | Reference | | | |
| **> 0.94** | 11 | 6.376 (2.584–15.735) | < 0.001 | 6.698 (2.561–17.519) | < 0.001 |

HR, hazard ratio; OS, overall survival; AFP, alpha-fetoprotein; IRE, irregular rim-like arterial phase enhancement; PTC, peritumor capsule; ALT, alanine aminotransferase; OS, overall survival; SD, standard deviation; AHR, alanine aminotransferase to hemoglobin ratio.

4 and 6 years was better than that of Model 2 in the training cohort (Figures 2A–C). In the validation cohort, we found that the net clinical benefit of Model 1 at 2, 4, and 6 years was better than that of Model 2 (Figures 2D–F).

The time-dependent ROC curves indicated AUC values of Model 1 in the training cohort of 0.840, 0.836, and 0.732 at 2, 4, and 6 years, respectively. In contrast, those in the validation cohort were 0.722, 0.793, and 0.776 at 2, 4, and 6 years, respectively (Figures 3A, C). However, the AUC values of Model 2 in the training cohort were 0.810, 0.737, and 0.664 at 2, 4, and 6 years, respectively, whereas those in the validation cohort were 0.687, 0.751, and 0.721 at 2, 4, and 6 years, respectively; lower than those of Model 1 (Figures 3B, D).

The results above show better predictive performance of Model 1 compared to Model 2. Based on its performance, we selected Model 1 as the final model.

## Establishment and verification of the nomogram

We found superior predictive ability of the combination of three indicators to the individual predictive ability. Further, we used PTC, IRE, and the AHR to establish a nomogram to predict the OS of patients treated with PA-TACE (Figure 4). The calibration curve showed a good fit between the predicted curve of the nomogram and the observed curve at 2, 4, and 6 years (Figures 5A–C). Moreover, DCA showed that the nomogram had an excellent net clinical benefit at 2, 4, and 6 years (Figures 5D–F).

# Discussion

In this study, we constructed two models to predict PA-TACE prognosis. Using DCA and ROC analysis, we found better predictive performance of Model 1 compared to Model 2. This shows better predictive performance of the multi-dimensional model than that of simple radiological features. We used these three indicators to establish a nomogram to predict the OS after PA-TACE. The calibration curve showed a good fit between the predicted and observed curves of the nomogram. Clinically, ALT and Hb are part of routine blood tests on admission or discharge. In addition, an important means for diagnosing HCC is enhanced CT examination. The enhanced CT image allows identifying whether the patient has PTC or IRE, information usually included in the radiologist's report. Intervening doctors can quickly obtain these three indicators and predict the OS of patients using our nomogram for assistive judgment of patient suitability for PA-TACE. The current scoring system for TACE includes patients who only received TACE treatment. The data in this study included patients who received PA-TACE after surgery; a more specific concept. Compared with other scoring systems such as HAP and ART, the data in our prognostic model is easier to obtain, having verified clinical effects (18–20).

10.3389/fonc.2022.989316

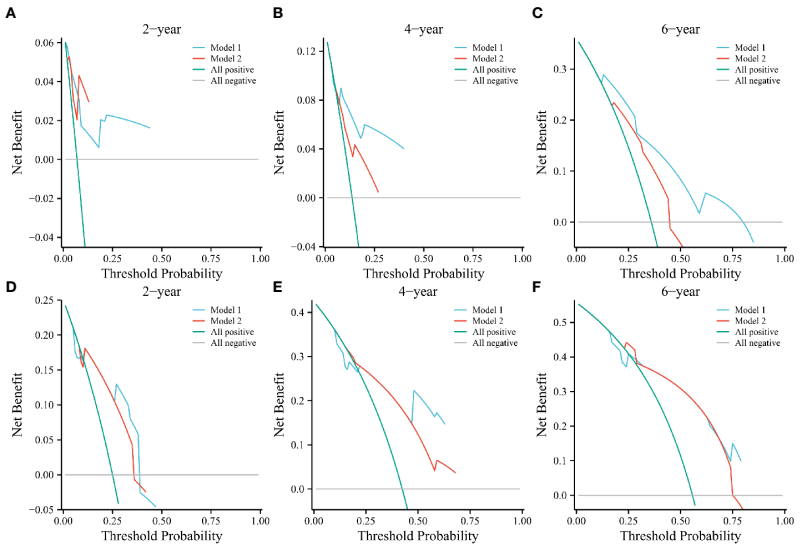


FIGURE 2
Decision curve analyses of Models 1 and 2 at 2, 4, and 6 years in the training **(A–C)** and validation cohorts **(D–F)**. The green and gray line indicates that all patients were dead or alive, respectively. The blue and red line indicates the clinical net benefit of Model 1 and 2 at different threshold probabilities.

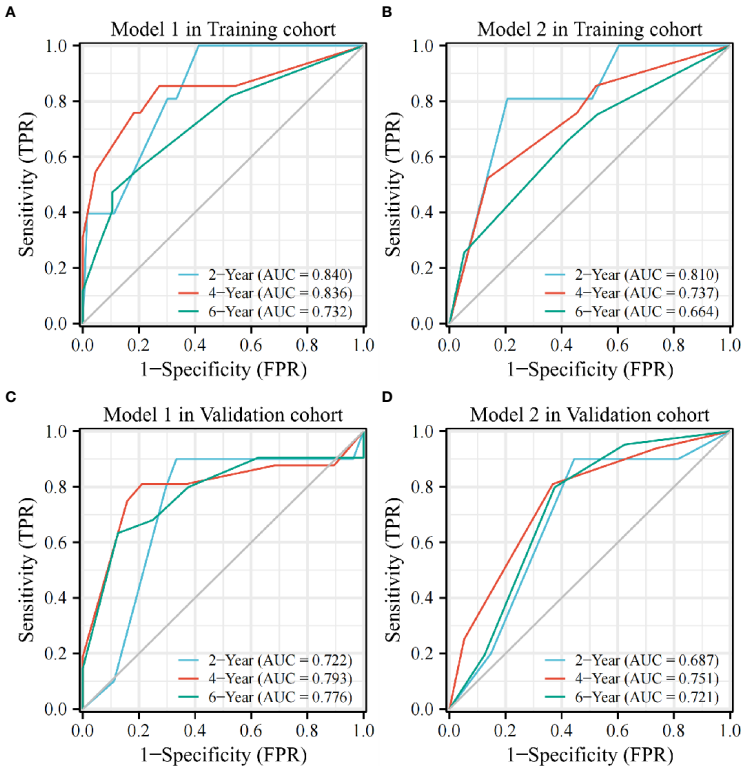


FIGURE 3
The AUC value of Model 1 is higher than that of Model 2 at 2, 4, and 6 years in the training **(A, B)** and validation cohorts **(C, D)**.AUC, area under the curve; TPR, true positive rate; FPR, false positive rate.

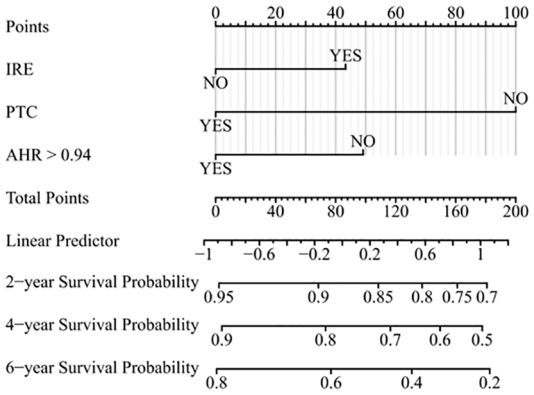


FIGURE 4
Prognostic nomogram for predicting OS of patients treated with PA-TACE. OS, overall survival; PA-TACE, postoperative adjuvant transarterial chemoembolization; IRE, rim-like arterial phase enhancement; PTC, peritumor capsule; AHR, alanine aminotransferase to hemoglobin ratio.

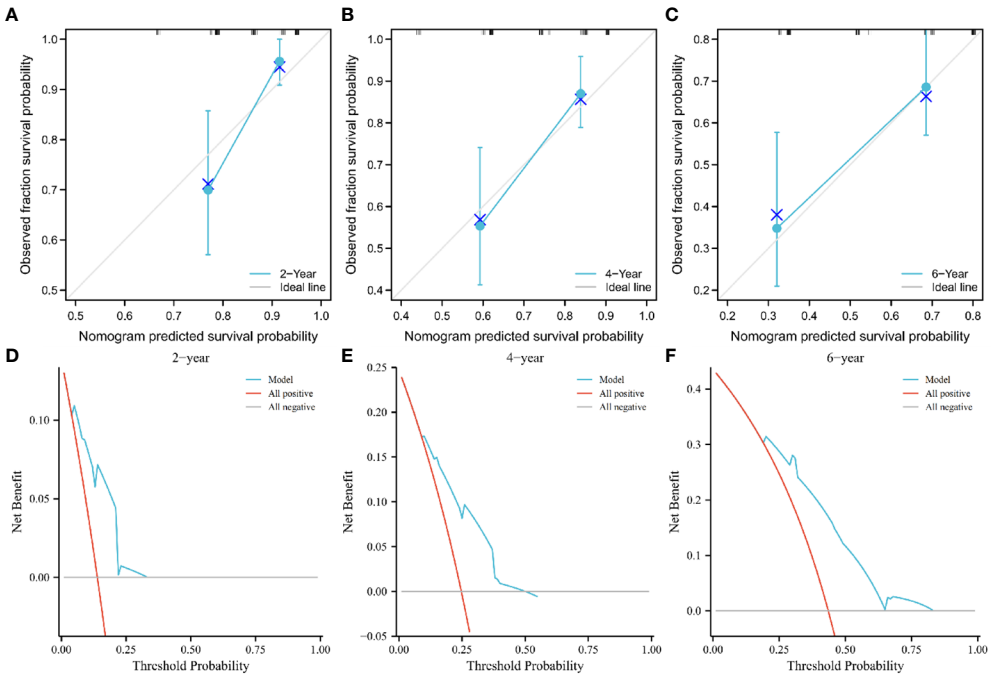


FIGURE 5
Calibration curve showing good fit between the predicted nomogram curve and the observed curve **(A–C)**. DCA of the nomogram at 2, 4, and 6 years. The green and gray line indicates that all patients were dead or alive, respectively. The red line indicates the clinical net benefit of the nomogram at different threshold probabilities **(D–F)**. DCA, decision curve analysis.

Increased ALT indicates damage to liver function and represents the formation of a tumor microenvironment conducive to the development of HCC (21, 22). A decrease in Hb indicates that the oxygen carried by red blood cells is decreased and that the tissue is in a state of hypoxia. A hypoxic microenvironment may increase the expression of angiogenic factors, such as hypoxia-inducible factor 1α and vascular endothelial growth factor, associated with poor prognosis of TACE (23–25). In this study, we found that ALT and Hb cannot be used to predict the OS after PA-TACE, but the AHR was an independent prognostic factor, which may result from the interaction of many factors. Thus, unveiling the underlying mechanism requires further research.

The impact of the presence or absence of PTC on prognosis is controversial (26). Some studies have suggested that PTC prevents HCC invasion. In clinical practice, presence or absence of PTC affects the surgical resection method. The scope of HCC resection with a capsule is often smaller, resulting in less damage to liver function. HCC without a capsule is more likely to spread and cause more significant damage to liver function after surgical resection, which may lead to a worse clinical response of patients to PA-TACE. Surgeons often worry about HCC invasion depth without a capsule and tend to expand the resection area (26–28). In our study, patients with PTC had a better prognosis after PA-TACE than those without. In previous studies, IRE was considered an invasive marker of HCC and associated with early recurrence after radiofrequency ablation (29). Similarly, the present study also found that patients with IRE had a worse prognosis than those without.

This study has few limitations. In the past, PA-TACE was not often used after surgical resection; therefore, few patients were enrolled. Despite the relatively small sample size of our study, our predictive model was verified in the validation cohort. Moreover, our study is a single-center study. In the future, to improve our prognosis model, we will cooperate with other hospitals to improve on the generalizability of our nomogram.

In conclusion, our study used radiological features and serum indicators to establish a nomogram for predicting the OS of patients with HCC treated with PA-TACE. This predictive model can quickly determine whether patients can benefit from PA-TACE after surgical resection of HCC.

## Data availability statement

The raw data supporting the conclusions of this article will be made available by the authors, without undue reservation.

## Ethics statement

Written informed consent was obtained from the individual (s) for the publication of any potentially identifiable images or data included in this article.

## Author contributions

ZX and YZ contributed equally to this research.WZ, AS, and HZ contributed to research concept and design. ZX and YZ contributed to data analysis and interpretation and manuscript writing and editing. WL and LW contributed to acquisition of image. JiaZ, CL, KC, JY, and JiaZ contributed to data acquisition. All authors contributed to the research and agreed to be accountable for the content of the work.

## Funding

This research was supported by grants from the Graduate Innovation Program of Jiangsu Province (No. SJCX21-1466, No.SJCX22-1636, and No.SJCX22-1634), National Natural Science Foundation of China (grant: 82102784), and Natural Science Foundation of Jiangsu Province (BK20221275).

## Acknowledgments

We would like to thank Editage (www.editage.cn) for English language editing.

## Conflict of interest

The authors declare that the research was conducted in the absence of any commercial or financial relationships that could be construed as a potential conflict of interest.

## Publisher's note



## References

1. Calderaro J, Seraphin TP, Luedde T, Simon TG. Artificial intelligence for the prevention and clinical management of hepatocellular carcinoma. *J Hepatol* (2022) 76(6):1348–61. doi: 10.1016/j.jhep.2022.01.014

2. Tabrizian P, Jibara G, Shrager B, Schwartz M, Roayaie S. Recurrence of hepatocellular cancer after resection: patterns, treatments, and prognosis. *Ann Surg* (2015) 261(5):947–55. doi: 10.1097/SLA.0000000000000710

3. Mao S, Yu X, Sun J, Yang Y, Shan Y, Sun J, et al. Development of nomogram models of inflammatory markers based on clinical database to predict prognosis for hepatocellular carcinoma after surgical resection. *BMC Cancer* (2022) 22(1):249. doi: 10.1186/s12885-022-09345-2

4. Wang PX, Sun YF, Zhou KQ, Cheng JW, Hu B, Guo W, et al. Circulating tumor cells are an indicator for the administration of adjuvant transarterial chemoembolization in hepatocellular carcinoma: A single-center, retrospective, propensity-matched study. *Clin Transl Med* (2020) 10(3):e137. doi: 10.1002/ctm2.137

5. Li QJ, He MK, Chen HW, Fang WQ, Zhou YM, Xu L, et al. Hepatic arterial infusion of oxaliplatin, fluorouracil, and leucovorin versus transarterial

chemoembolization for Large hepatocellular carcinoma: A randomized phase III trial. *J Clin Oncol* (2022) 40(2):150–60. doi: 10.1200/JCO.21.00608

6. Hu S, Gan W, Qiao L, Ye C, Wu D , Liao B, et al. A new prognostic algorithm predicting HCC recurrence in patients with Barcelona clinic liver cancer stage b who received PA-TACE. *Front Oncol* (2021) 11:742630. doi: 10.3389/fonc.2021.742630

7. Liu F, Guo X, Dong W, Zhang W, Wei S, Zhang S, et al. Postoperative adjuvant TACE-associated nomogram for predicting the prognosis of resectable hepatocellular carcinoma with portal vein tumor thrombus after liver resection. *Int J Biol Sci* (2020) 16(16):3210–20. doi: 10.7150/ijbs.46896

8. Tong Y, Li Z, Liang Y, Yu H, Liang X, Liu H, et al. Postoperative adjuvant TACE for patients of hepatocellular carcinoma in AJCC stage I: friend or foe? a propensity score analysis. *Oncotarget* (2017) 8(16):26671–8. doi: 10.18632/oncotarget.15793

9. Tang Y, Wu Y, Xue M, Zhu B, Fan W, Li J. A 10-gene signature identified by machine learning for predicting the response to transarterial chemoembolization in patients with hepatocellular carcinoma. *J Oncol* (2022) (2022) 3822773. doi: 10.1155/2022/3822773

10. Cheung YS, Chan HL, Wong J, Lee KF, Poon TC, Wong N, et al. Elevated perioperative transaminase level predicts intrahepatic recurrence in hepatitis b-related hepatocellular carcinoma after curative hepatectomy. *Asian J Surg* (2008) 31 (2):41–9. doi: 10.1016/S1015-9584(08)60056-1

11. Tarao K, Takemiya S, Tamai S, Sugimasa Y, Ohkawa S, Akaike M, et al. Relationship between the recurrence of hepatocellular carcinoma (HCC) and serum alanine aminotransferase levels in hepatectomized patients with hepatitis c virus-associated cirrhosis and HCC. *Cancer* (1997) 79(4):688–94. doi: 10.1002/(SICI)1097-0142(19970215)79:4<688::AID-CNCR5>3.0.CO;2-A

12. Finkelmeier F, Bettinger D, Köberle V, Schultheiß M, Zeuzem S, Kronenberger B, et al. Single measurement of hemoglobin predicts outcome of HCC patients. *Med Oncol* (2014) 31(1):806. doi: 10.1007/s12032-013-0806-2

13. Lin ZH, Li X, Hong YF, Ma XK, Wu DH, Huang M, et al. Alanine aminotransferase to hemoglobin ratio is an indicator for disease progression for hepatocellular carcinoma patients receiving transcatheter arterial chemoembolization. *Tumour Biol* (2016) 37(3):2951–9. doi: 10.1007/s13277-015-4082-y

14. Yoneda N, Matsui O, Kobayashi S, Kitao A, Kozaka K, Inoue D, et al. : Current status of imaging biomarkers predicting the biological nature of hepatocellular carcinoma. *Jpn J Radiol* (2019) 37(3):191–208. doi: 10.1007/s11604-019-00817-3

15. Chen X, Yang Z, Deng J. Use of 64-slice spiral CT examinations for hepatocellular carcinoma (DR LU). *J buon* (2019) 24(4):1435–40.

16. Vickers AJ, Elkin EB. Decision curve analysis: a novel method for evaluating prediction models. *Med Decis Making* (2006) 26(6):565–74. doi: 10.1177/0272989X06295361

17. Ginestet C. ggplot2: Elegant Graphics for Data Analysis. . *Journal of the Royal Statistical Society* (2011) 174(1):245-246. doi: 10.1111/j.1467-985X.2010.00676_9

18. Sieghart W, Hucke F, Pinter M, Graziadei I, Vogel W, Müller C, et al. The ART of decision making: retreatment with transarterial chemoembolization in patients with hepatocellular carcinoma. *Hepatology* (2013) 57(6):2261–73. doi: 10.1002/hep.26256

19. Kadalayil L, Benini R, Pallan L, O'Beirne J, Marelli L, Yu D, et al. A simple prognostic scoring system for patients receiving transarterial embolisation for hepatocellular cancer. *Ann Oncol* (2013) 24(10):2565–70. doi: 10.1093/annonc/mdt247

20. Hucke F, Sieghart W, Pinter M, Graziadei I, Vogel W, Müller C, et al. The ART-strategy: sequential assessment of the ART score predicts outcome of patients with hepatocellular carcinoma re-treated with TACE. *J Hepatol* (2014) 60(1):118–26. doi: 10.1016/j.jhep.2013.08.022

21. Başar O, Yimaz B, Ekiz F, Giniş Z, Altinbaş A, Aktaş B, et al. Non-invasive tests in prediction of liver fibrosis in chronic hepatitis b and comparison with post-antiviral treatment results. *Clin Res Hepatol Gastroenterol* (2013) 37(2):152–8. doi: 10.1016/j.clinre.2012.07.003

22. Suh SW, Lee JM, You T, Choi YR, Yi NJ, Lee KW, et al. Hepatic venous congestion in living donor grafts in liver transplantation: is there an effect on hepatocellular carcinoma recurrence? *Liver Transpl* (2014) 20(7):784–90. doi: 10.1002/lt.23877

23. Lin ZH, Jiang JR, Ma XK, Chen J, Li HP, Li X, et al. Prognostic value of serum HIF-1α change following transarterial chemoembolization in hepatocellular carcinoma. *Clin Exp Med* (2021) 21(1):109–20. doi: 10.1007/s10238-020-00667-8

24. Huang M, Wang L, Chen J, Bai M, Zhou C, Liu S, et al. Regulation of COX-2 expression and epithelial-to-mesenchymal transition by hypoxia-inducible factor-1α is associated with poor prognosis in hepatocellular carcinoma patients post TACE surgery. *Int J Oncol* (2016) 48(5):2144–54. doi: 10.3892/ijo.2016.3421

25. Liu K, Min XL, Peng J, Yang K, Yang L, Zhang XM. The changes of HIF-1α and VEGF expression after TACE in patients with hepatocellular carcinoma. *J Clin Med Res* (2016) 8(4):297–302. doi: 10.14740/jocmr2496w

26. Kim BK, Kim KA, An C, Yoo EJ, Park JY, Kim DY, et al. Prognostic role of magnetic resonance imaging vs. computed tomography for hepatocellular carcinoma undergoing chemoembolization. *Liver Int* (2015) 35(6):1722–30. doi: 10.1111/liv.12751

27. Song L, Li J, Luo Y. The importance of a nonsmooth tumor margin and incomplete tumor capsule in predicting HCC microvascular invasion on preoperative imaging examination: a systematic review and meta-analysis. *Clin Imaging* (2021) 76:77–82. doi: 10.1016/j.clinimag.2020.11.057

28. Zhu YJ, Feng B, Wang BZ, Wang S, Ye F, Ma XH, et al. [Value of gadolinium ethoxybenzyl diethylenetriamine pentaacetic acid enhanced magnetic resonance imaging and diffusion-weighted MR imaging in predicting microvascular invasion in hepatocellular carcinoma and the prognostic significance]. *Zhonghua zhong liu za zhi*. (2021) 43(3):312–7. doi: 10.3760/cma.j.cn112152-20191009-00652

29. Kang TW, Rhim H, Lee J, Song KD, Lee MW, Kim YS, et al. Magnetic resonance imaging with gadoxetic acid for local tumour progression after radiofrequency ablation in patients with hepatocellular carcinoma. *Eur Radiol* (2016) 26(10):3437–46. doi: 10.1007/s00330-015-4190-5

frontiers | Frontiers in Oncology

TYPE Systematic Review
PUBLISHED 18 October 2022
DOI 10.3389/fonc.2022.998159



OPEN ACCESS

EDITED BY
Beatrice Aramini,
University of Bologna, Italy

REVIEWED BY
Maher Hendi,
Sir Run Run Shaw Hospital, China
Lorenzo Cinelli,
San Raffaele Hospital (IRCCS), Italy

*CORRESPONDENCE
Zonglin Li
lizonglin85@163.com

SPECIALTY SECTION
This article was submitted to Surgical Oncology, a section of the journal Frontiers in Oncology

RECEIVED 19 July 2022
ACCEPTED 26 September 2022
PUBLISHED 18 October 2022

CITATION
Dong B, Zhang A, Zhang Y, Ye W, Liao L and Li Z (2022) Efficacy of indocyanine green fluorescence imaging-guided lymphadenectomy in radical gastrectomy for gastric cancer: A systematic review and meta-analysis. *Front. Oncol.* 12:998159. doi: 10.3389/fonc.2022.998159



# Efficacy of indocyanine green fluorescence imaging-guided lymphadenectomy in radical gastrectomy for gastric cancer: A systematic review and meta-analysis

Bo Dong[1], Anyuan Zhang[1], Yuqiang Zhang[1], Wei Ye[1], Lan Liao[1] and Zonglin Li[1,2]*

[1]Department of General Surgery, The People's Hospital of Rongchang District, Chongqing, China, [2]Department of Gastrointestinal Surgery, The Affiliated Hospital of Southwest Medical University, Luzhou, China

**Background:** Indocyanine green (ICG) imaging-guided lymphadenectomy has been introduced in gastric cancer (GC) surgery and its clinical value remains controversial. The aim of this study is to evaluate the efficacy of ICG fluorescence imaging-guided lymphadenectomy in radical gastrectomy for GC.

**Methods:** Studies comparing lymphadenectomy in radical gastrectomy between use and non-use of ICG fluorescence imaging up to July 2022 were systematically searched from PubMed, Web of Science, Embase and Cochrane Library. A pooled analysis was performed for the available data regarding the baseline features, the number of retrieved lymph nodes (LNs), the number of metastatic LNs and surgical outcomes as well as oncological outcomes. RevMan 5.3 software was used to perform the statistical analysis. Quality evaluation and publication bias were also conducted.

**Results:** 17 studies with a total of 2274 patients (1186 in the ICG group and 1088 in the control group) undergoing radical gastrectomy and lymphadenectomy were included. In the pooled analysis, the baseline features were basically comparable. However, the number of retrieved LNs in the ICG group was significantly more than that in the control group (MD = 7.41, 95% CI = 5.44 to 9.37, $P < 0.00001$). No significant difference was found between the ICG and control groups in terms of metastatic LNs (MD = -0.05, 95% CI = -0.25 to 0.16,

*P* = 0.65). In addition, the use of ICG could reduce intraoperative blood loss (MD = -17.96, 95% CI = -27.89 to -8.04, *P* = 0.0004) without increasing operative time (*P* = 0.14) and overall complications (*P* = 0.10). In terms of oncological outcomes, the use of ICG could reduce the overall recurrence rate (OR = 0.50; 95% CI 0.28-0.89; *P* = 0.02) but could not increase the 2-year overall survival rate (OR = 1.25; 95% CI 0.72-2.18; *P* = 0.43).

**Conclusions:** ICG imaging-guided lymphadenectomy is valuable for complete LNs dissection in radical gastrectomy for GC. However, more high-quality randomized controlled trials are needed to confirm this benefit.

KEYWORDS

**gastric cancer, lymphadenectomy, indocyanine green, fluorescence imaging, minimally invasive surgery**

## Introduction

Gastric cancer (GC) is one of the most common cancers worldwide with more than one million new cases and 760,000 deaths in 2020 (1). At present, radical gastrectomy combined with D2 lymphadenectomy is still the most effective treatment for GC (2, 3). The status of lymph nodes (LNs) is a stronger prognostic factor for the survival of GC patients and sufficient lymphadenectomy can improve the prognosis of GC patients (4–6). Howerer, lymphadenectomy for GC is usually performed without the aid of visual instruments and complete lymphadenectomy is sometimes difficult, especially for inexperienced gastrointestinal surgeons, which always results in LNs residue and in turn leads to tumor recurrence as well as the death of these patient. Therefore, the application of intraoperative navigation technology to assist systematic and complete lymphadenectomy is essential for radical gastrectomy.

Indocyanine green (ICG), a lymphatic tracer with minimal adverse effects, can bind intensely with serum proteins *in vivo* and emits fluorescence on exposure to near-infrared rays of wavelength 760-780 nm (7, 8). In recent years, ICG fluorescence imaging for LNs tracing has attracted surgeons' attention and ICG imaging-guided lymphadenectomy has been introduced in GC surgery (9–11). Until now, several studies have reported that ICG imaging-guided lymphadenectomy was applied to GC surgery and showed promising results in increasing the number of retrieved LNs, without increasing operative time and overall complications (12–14). However, whether ICG imaging-guided lymphadenectomy is indeed beneficial for LNs dissection remains unclear. Therefore, further research is needed to validate the efficacy of ICG imaging-guided lymphadenectomy in radical gastrectomy for GC.

The aim of this meta-analysis is to evaluate the efficacy of ICG imaging-guided lymphadenectomy in radical gastrectomy for GC based on the current published studies.

## Methods

This meta-analysis was carried out in line with the Preferred Reporting Items for Systematic Reviews and Meta-Analysis (PRISMA) statement.

### Search strategy

Studies comparing lymphadenectomy in radical gastrectomy between use and non-use of ICG fluorescence imaging up to July 2022 were systematically searched from PubMed, Web of Science, Embase and Cochrane Library. The keywords used for the search were "gastric cancer", "lymphadenectomy" and "ICG". Thus, the following search string was used across the above databases: ["gastric cancer" OR "gastric carcinoma" OR "gastric tumor" OR "stomach cancer" OR "stomach carcinoma" OR "stomach tumor"] AND ["lymphadenectomy" OR "lymph node excision" OR "lymph node dissection"] AND ["indocyanine green" OR "ICG"]. Articles from previously published reviews were also checked for potential articles. The search was conducted independently by two authors (BD and AZ). The search was last performed on July 3, 2022.

### Study selection and data extraction

The included studies met the following criteria: (1) GC patients with laparoscopic or robotic surgery; (2) lymphadenectomy performed in accordance with the guidelines for the treatment of GC; (3) comparative studies

about lymphadenectomy in radical gastrectomy between use and non-use of ICG fluorescence imaging; (4) studies with reported outcome including the number of retrieved LNs in the ICG and control groups; (5) original research published in English. The exclusion criteria were as follows: (1) studies published as reviews, comments, letters, case reports, animal studies and meeting abstracts; (2) studies without the outcome about the number of retrieved LNs; (3) unavailability of effective data for meta-analysis.

Two reviewers (BD and AZ) carried out the screening and extraction process independently. First, studies were screened by titles and abstract. Then, the potential studies were checked for full text. For the eligible articles, the following information from each article was recorded: first author, publication year, country, study interval, study design, study object, sample size, extent of lymphadenectomy, ICG dosage and imaging system. Furthermore, the following clinicopathological parameters were extracted from these studies: sex, age, body mass index (BMI), American Society of Anesthesiologists (ASA) score, tumor size, pathological stage, histologic type, method of gastrectomy, neoadjuvant chemoradiotherapy, the number of retrieved LNs, the number of metastatic LNs, operation time, intraoperative blood loss, overall complications, overall recurrence rate and 2-year overall survival (OS) rate. Results were checked by a third author (ZL).

## Risk of bias assessment

Qualities of the selected studies were assessed according to the Cochrane Handbook. Biases including selection, performance, detection, attrition, reporting and others were evaluated and the outcomes were summarized in the form of a bias graph.

## Statistical analysis

The odds ratio (OR) and mean difference (MD) with their 95% confidence interval (CI) were used as the effect size for dichotomous and continuous variables, respectively. For studies that only reported median and range, data were converted into mean and standard deviation (SD) following the method reported by Hozo SP et al. (15). Heterogeneity among studies was assessed by $\chi^2$ and $I^2$ statistics. fixed-effects models and random-effects models were used in cases of nonsignificant ($I^2 \leq 50\%$) and significant ($I^2 > 50\%$) heterogeneity, respectively. For the assessment of publication bias, a funnel plot was conducted. A $P$ value < 0.05 was considered significant. All of the statistical analyses were performed by RevMan 5.3 software (Cochrane, London, UK).

# Results

## Characteristics of studies

A total of 612 studies were identified, and 17 studies including 15 retrospective studies and 2 randomized controlled trials (RCTs) were ultimately included in this meta-analysis (13, 14, 16–30). The details of the selection procedures are shown to be in line with the PRISMA flowchart (Figure 1). General information from those included studies is summarized in Table 1. The total number of GC patients included was 2274 (1186 in the ICG group and 1088 in the control group). These studies were from five countries (i.e., China, Italy, Korea, Spain and Japan) and were published from 2017 to 2022. The sample size ranged from 20 to 514 patients. Laparoscopic or robotic radical total or distal gastrectomy combined with D1+ or D2 lymphectomy were performed in these studies. Nevertheless, the dosage of ICG and imaging systems considered differed in these studies. According to the Cochrane Handbook, the 17 studies were at slight or moderate risk of bias. The items evaluated for each study are shown in Figure 2.

## Patient- and tumor-related baseline characteristics

For the patient- and tumor-related variables, sex (male and female), age (mean ± SD), BMI (mean ± SD), ASA score (ASA 1/2 and ASA 3/4), tumor size (mean ± SD), pathological stage (stage 1/2 and stage 3/4), histologic type (differentiated and other types), method of gastrectomy (total gastrectomy and distal gastrectomy) and neoadjuvant chemoradiotherapy (with and without) were analyzed. Except for age ($P = 0.0004$) and the method of gastrectomy ($P < 0.00001$), other variables were all comparable between the ICG and control groups ($P > 0.05$) analysed by the fixed-effects models ($I^2 \leq 50\%$) and random-effects models ($I^2 > 50\%$). The baseline parameters between the two groups were basically statistically insignificant, as shown in Figure 3.

## Efficacy of lymphadenectomy

The primary outcome of this study was to assess the efficacy of lymphadenectomy by using ICG fluorescence imaging. Ultimately, 17 studies (2274 patients) (13, 14, 16–30) reporting this outcome were included in our meta-analysis. The pooled analysis revealed that the number of retrieved LNs in the ICG group was significantly more than that in the control group (MD = 7.41, 95% CI = 5.44 to 9.37, $P < 0.00001$) (Figure 4A), but there is no significant difference in terms of metastatic LNs

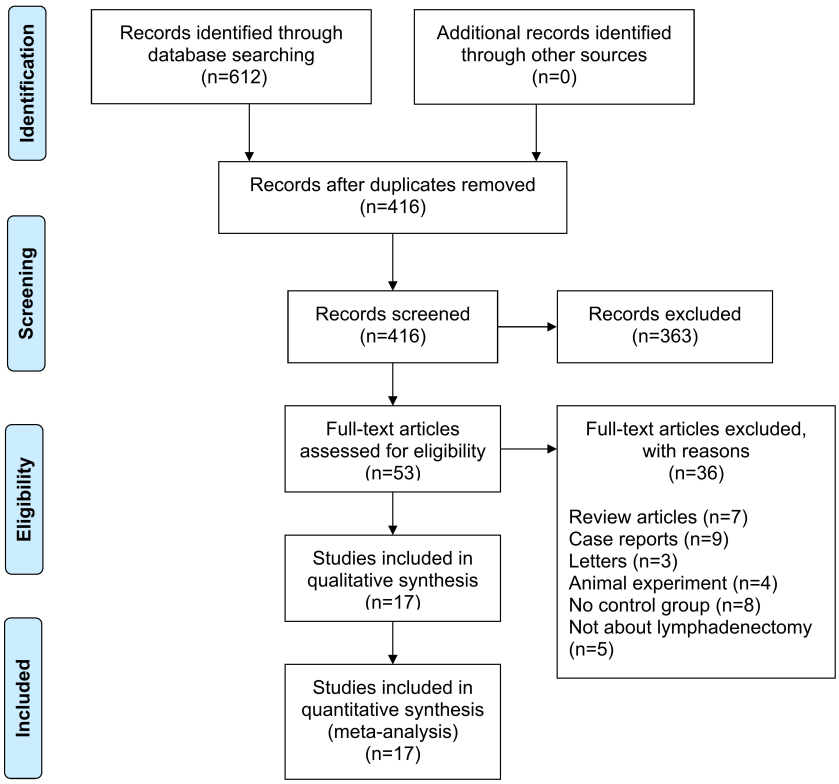


FIGURE 1
PRISMA flowchart of literature search and selection process. *PRISMA* preferred reporting items for systematic review and meta-analysis.

between the ICG and control groups (MD = -0.05, 95% CI = -0.25 to 0.16, $P$ = 0.65) (Figure 4B).

## Surgical outcomes

14 studies (13, 14, 17–21, 23–29) reported the operation time and the pooled analysis showed no difference between the ICG and control groups (MD = −9.38, 95% CI = −21.70 to 2.93, $P$ = 0.14) (Figure 5A). However, 11 studies (13, 16–21, 23, 26–28) reported the intraoperative blood loss and showed that the use of ICG could reduce intraoperative blood loss (MD = -17.96, 95% CI = -27.89 to -8.04, $P$ = 0.0004) (Figure 5B). 12 studies (13, 14, 16–21, 23, 26–28) reported the overall complications and there was a trend that the use of ICG was related to less overall complications with no statistic difference (OR = 0.78, 95% CI = 0.57 to 1.05, $P$ = 0.10) (Figure 5C).

## Oncological outcomes

In terms of oncological outcomes, four studies (19, 21, 22, 28) reported the overall recurrence rate and the pooled analysis showed that the use of ICG could reduce the overall recurrence rate (OR = 0.50; 95% CI 0.28-0.89; $P$ = 0.02) (Figure 6A). However, in terms of postoperative overall survival, two studies (19, 28) reported the 2-year overall survival rate but there was no difference between the ICG and control groups (OR = 1.25; 95% CI 0.72-2.18; $P$ = 0.43) (Figure 6B).

## Publication bias

The funnel plot was used to assess potential publication bias in the meta-analysis of the correlation between the use of ICG fluorescence imaging and the number of retrieved LNs. As shown in Figure 7, the funnel plot was symmetrical, which showed a low risk of publication bias in this study.

# Discussion

GC is one of the most common malignant tumors of digestive tract and radical surgery is the mainstay of treatment, which involves performing gastric resection with negative margins and adequate systemic LNs dissection. The status of

TABLE 1 Characteristics of studies.

| Reference | Country | Study interval | Study object | Study design | Sample size (ICG: Control) | Method of gastrectomy | Extent of lymphadenectomy | ICG dosage | ICG injection method | ICG injection time | ICG imaging system | Outcomes |
|---|---|---|---|---|---|---|---|---|---|---|---|---|
| Chen QY (13) | China | 2018-2019 | pT1-4aN0-3M0 | S;RCT | 129: 129 | laparoscopic TG and DG | D2 | 2.5 mg | endoscopic submucosal injection | 1 day before surgery | Stryker | 1, 2, 3, 4, 5 |
| Cianchi F (14) | Italy | 2014-2018 | pT1-3N0-3M0 | S;R | 37: 37 | laparoscopic TG and DG | D2 | 2.5 mg | endoscopic submucosal injection | 1 day before surgery | Firefly | 1, 2, 3, 5 |
| Huang ZN (16) | China | 2010-2020 | cT1-4N0-3M0 | M;R;PSM | 94: 94 | laparoscopic TG and DG | D2 | 4.5 mg | subserosal injection | intraoperative | Stryker | 1, 4, 5 |
| Kwon IG (17) | Korea | 2012-2014 | pT1-2N0-1M0 | S;R;PSM | 40: 40 | robotic TG and DG | D1+ or D2 | 3 mg | endoscopic submucosal injection | 1 day before surgery | NA | 1, 3, 4, 5 |
| Lan YT (18) | China | 2011-2016 | pT1-4N0-3M0 | S;R | 14: 65 | robotic TG and DG | D1+ or D2 | 6 mg | subserosal injection | intraoperative | NA | 1, 3, 4, 5 |
| Lee S (19) | Korea | 2013-2018 | pT1-4aN0-3M0 | S;R | 74: 94 | laparoscopic or robotic TG | D2 + No. 10 | 1.5-3.0 mg | endoscopic submucosal injection | 1 day before surgery | Firefly and Pinpoint | 1, 3, 4, 5, 6, 7 |
| Liu M (20) | China | 2017-2019 | pT1-4N0-3M0 | S;R | 61: 75 | laparoscopic DG | D2 | 1.25 mg | endoscopic submucosal injection | 20 to 30 hours before surgery | Stryker | 1, 2, 3, 4, 5 |
| Lu X (21) | China | 2015-2019 | pT1-4N0-3M0 | S;R;PSM | 28: 28 | laparoscopic TG, DG and PG | D2 | 2.5 mg | endoscopic submucosal injection | intraoperative | Pinpoint | 1, 3, 4, 5, 6 |
| Maruri I (22) | Spain | 2018-2019 | cT1-4N0-3M0 | S;R | 17: 17 | laparoscopic TG and DG | D1+ or D2 | 3 mg | endoscopic submucosal injection | 18 to 24 hours before surgery | NA | 1, 2, 6 |
| Park SH (23) | Korea | 2017-2018 | pT1-4N0-3M0 | S;R;PSM | 20: 60 | laparoscopic DG | D1+ or D2 | 0.5 mg | endoscopic submucosal injection | intraoperative | Pinpoint | 1, 3, 4, 5 |
| Puccetti F (24) | Italy | 2015-2021 | pT1-3N0-3M0 | S;R | 38: 64 | laparoscopic TG | D2 | 0.25 mg | endoscopic submucosal injection | 12 to 24 hours before surgery | NA | 1, 2, 3 |
| Romanzi A (25) | Italy | 2018-2019 | pT1-4bN0-3M0 | S;R | 10: 10 | robotic DG | D2 | 3 mg | endoscopic submucosal injection | 18 hours before surgery | Firefly | 1, 3 |
| Tian Y (26) | China | 2019-2020 | NA | S;R | 27: 32 | robotic DG | D2 | 5 mg | endoscopic submucosal injection | 1 day before surgery | NA | 1, 3, 4, 5 |
| Ushimaru Y (27) | Japan | 2015-2017 | pT1-4N0-3M0 | S;R;PSM | 84: 84 | laparoscopic TG and DG | D1+ or D2 | 0.1 mg | endoscopic submucosal injection | 1 day before surgery | STORZ | 1, 3, 4, 5 |
| Wei M (28) | China | 2018-2019 | pT1-4aN0-3M0 | S;R | 107: 88 | laparoscopic TG and DG | D2 | 2.5 mg | endoscopic submucosal injection | 12 to 24 hours before surgery | Stryker | 1, 2, 3, 4, 5, 6, 7 |
| Yoon BW (29) | Korea | 2010-2020 | pT1-4aN0-3M0 | S;R;PSM | 21: 42 | laparoscopic DG | D2 | 0.4 mg | endoscopic submucosal injection | 1 day before surgery | NA | 1, 2, 3 |
| Zhong Q (30) | China | 2018-2020 | pT1-4aN0-3M0 | M;RCT | 385: 129 | laparoscopic TG and DG | D2 | 4.5 mg | subserosal injection | intraoperative | Stryker | 1, 2 |

ICG, indocyanine green; S single centre; M, multicentre; R, retrospective study; PSM, propensity score matching; RCT, randomized controlled trial; NA, not available, 1= number of retrieved lymph nodes, 2= number of metastatic lymph nodes, 3=operative time, 4=intraoperative blood loss, 5=overall complications, 6=overall recurrence rate, 7 = 2-year overall survival.



10.3389/fonc.2022.998159

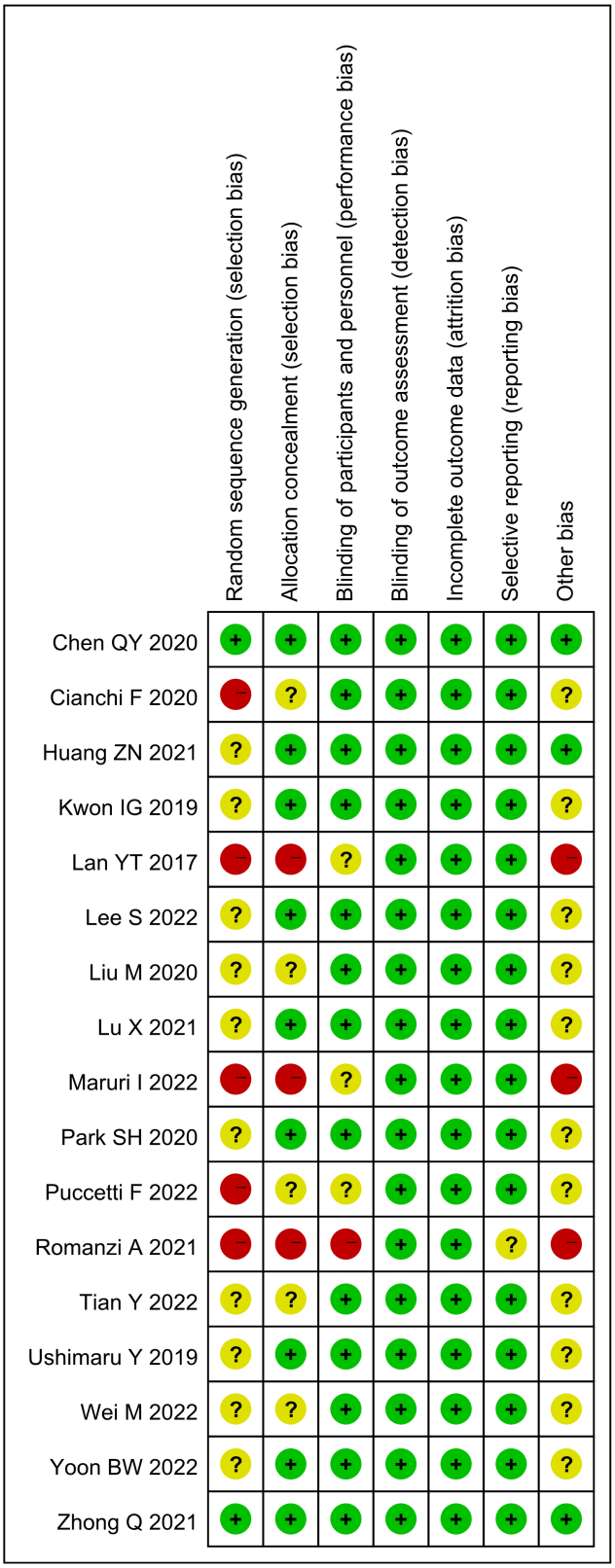


FIGURE 2
Risk of bias summary for the included studies.

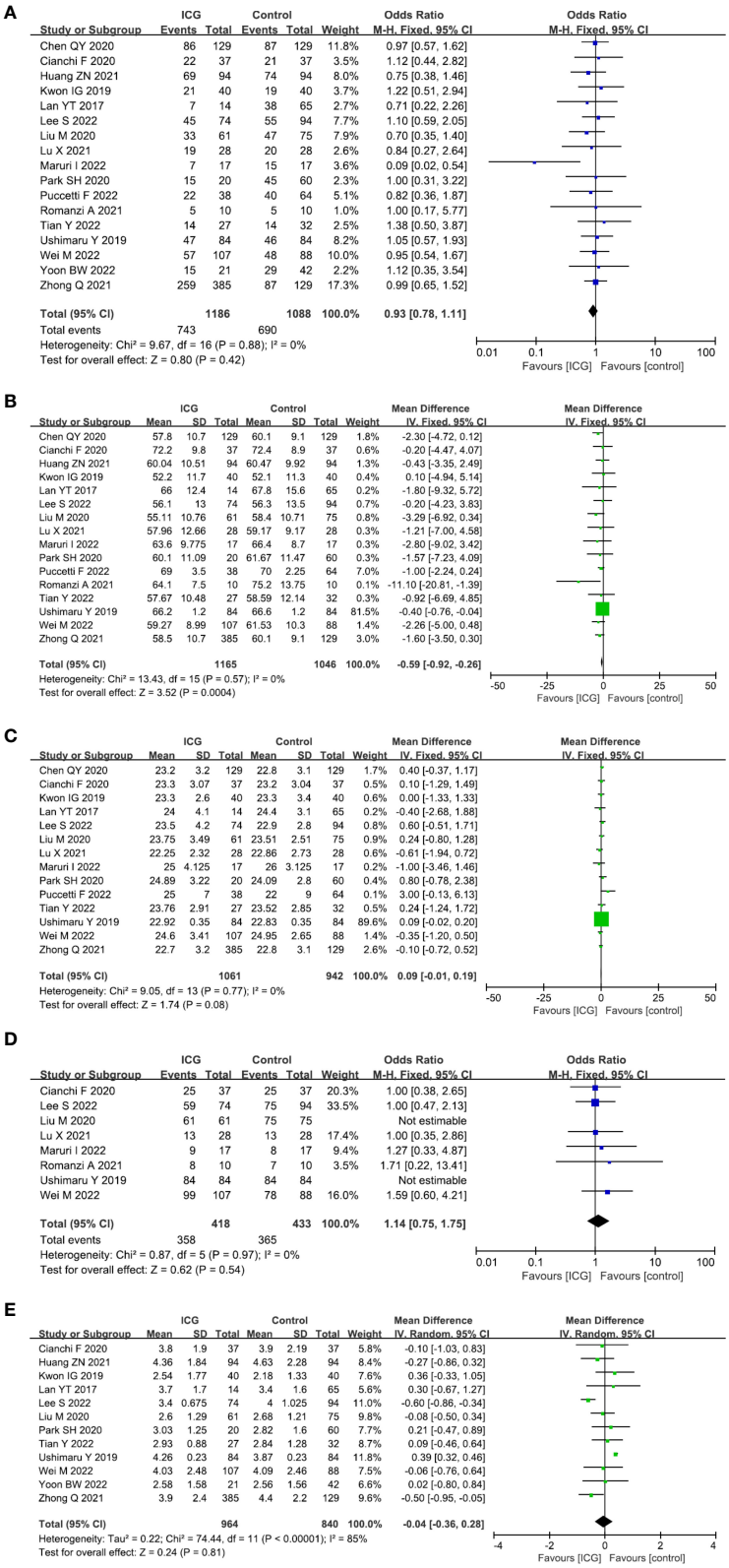


FIGURE 3 (Continued)

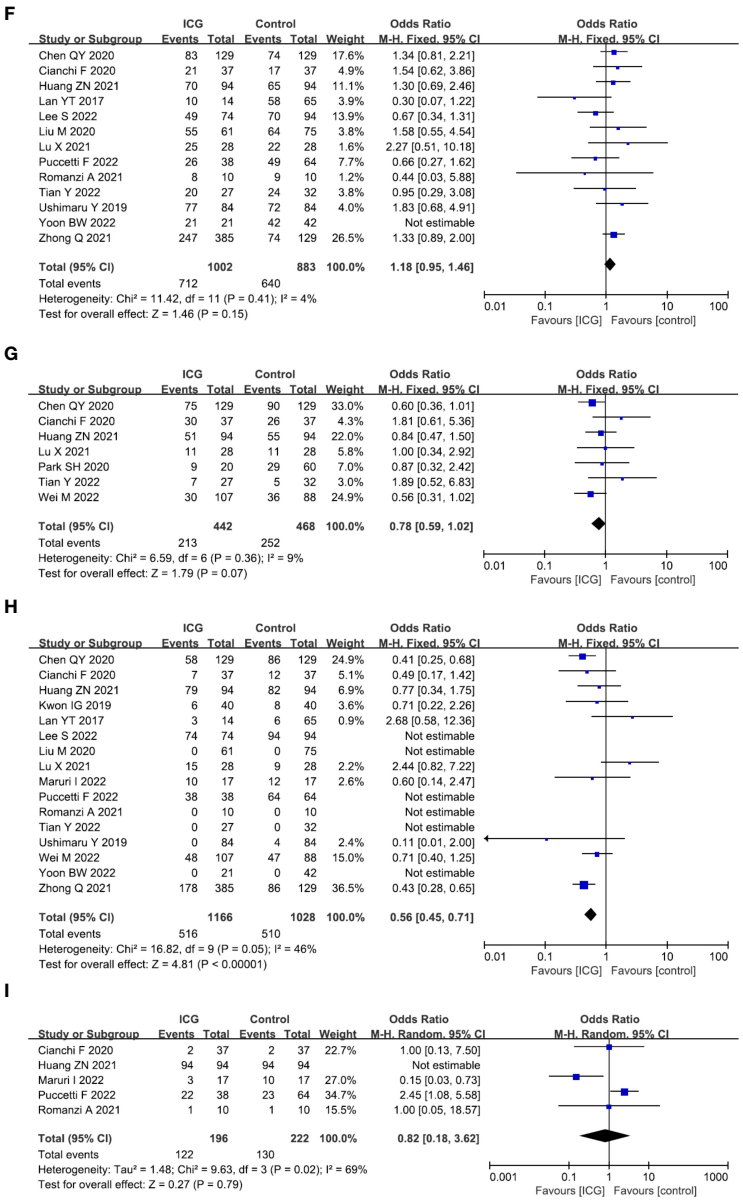


FIGURE 3
Forest plots showing the assessment of baseline features including **(A)** sex, **(B)** age, **(C)** body mass index, **(D)** American Society of Anaesthesiologists score, **(E)** tumor size, **(F)** pathological stage, **(G)** histologic type, **(H)** method of gastrectomy, **(I)** neoadjuvant chemoradiotherapy. *ICG*, indocyanine green.

LNs is a stronger prognostic factor for the survival of GC patients and radical lymphadenectomy can significantly improve the long-term survival (31, 32). In addition, whether or not the resected LNs have metastasis, complete perigastric lymphadenectomy is important for the accurate staging of tumors and the decision of subsequent treatment (33–35). So the retrieval of more LNs in radical gastrectomy has become the special requirement for gastrointestinal surgeons.

Currently, minimally invasive surgery, including laparoscopic and robotic methods, has been widely used in the treatment of GC, especially for early GC (36, 37). However, the oncological efficacy of minimally invasive techniques for the treatment of advanced GC is still controversial because of the concern about not being able to perform an accurate D2 lymphadenectomy and the oncological safety (38, 39). At present, lymphadenectomy in radical gastrectomy is often performed depending on the surgeon's experience and without the aid of visual instruments. However, due to the complex lymphatic drainage and abundant LNs around the stomach, it is often difficult for surgeons, especially for those younger and

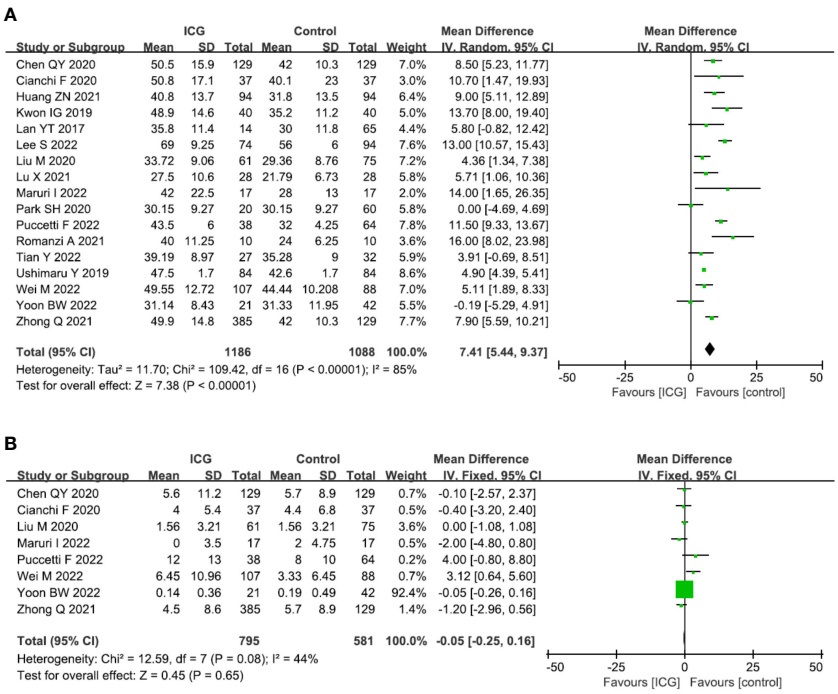


FIGURE 4
Forest plots showing the assessment of lymphadenectomy including **(A)** the number of retrieved lymph nodes, **(B)** the number of metastatic lymph nodes. ***ICG,*** indocyanine green.

inexperienced surgeons, to perform an accurate and effective D2 lymphadenectomy without increasing surgical complications.

In recent years, ICG fluorescence imaging for LNs tracing has attracted surgeons' attention and ICG imaging-guided lymphadenectomy has been introduced in GC surgery. Chen QY et al. (13) performed a RCT and indicated that ICG can noticeably improve the number of retrieved LNs without increased complications in GC patients undergoing D2 lymphadenectomy and they recommend ICG fluorescence imaging should be performed for routine lymphatic mapping during laparoscopic gastrectomy, especially total gastrectomy. Kwon et al. (17) also reported that ICG-guided lymphadenectomy is effective in retrieving more LNs than conventional surgery and had a similar incidence of postoperative complications to conventional surgery. Lee S et al. (19) point out ICG fluorescence imaging-guided lymphadenectomy is an effective tool for complete LNs dissection at the splenic hilum and it may help select patients who do not need splenic hilar LNs dissection during a total gastrectomy. However, Lan et al. (18) reported that the number of retrieved LNs in the ICG group was not improved compared with the non-ICG group. According to the pooled analysis in our study, the number of retrieved LNs in the ICG group was significantly more than that in the control group ($P < 0.00001$) and the use of ICG could reduce intraoperative blood loss ($P = 0.0004$) without increasing operative time ($P = 0.14$) and overall complications ($P = 0.10$). Theoretically, total gastrectomy could obtain more LNs than distal gastrectomy. In our combined analysis, the proportion of total gastrectomy in the ICG group is lower than that in the control group (44.3% vs. 49.6%), but more LNs were obtained, which further indicated that ICG fluorescence imaging-guided lymphadenectomy could increased the number of retrieved LNs. Also, Yoon BW et al. (29) reported that the use of ICG could secure the oncologically safe of proximal resection margin in totally laparoscopic distal gastrectomy, with the advantage of reducing the operation time and has the benefit of locating the tumor. These results suggest that the ICG fluorescence imaging-guided lymphadenectomy is valuable in terms of LNs dissection and short-term outcomes. Nevertheless, the present meta-analysis demonstrated that there was no significant difference in metastatic LNs between the ICG and control groups. The reasons for this outcome may be explained as follows: (1) The metastatic LNs can be removed completely by standard D2 lymphectomy without the use of ICG imaging-guided lymphadenectomy, and (2) Some researchers removed all the fluorescent LNs, even these LNs were outside the extent of D2 lymphectomy (13).

Reducing postoperative tumor recurrence and prolonging patients' survival time are the ultimate goals of standardized and systematic lymphectomy (40–42). Lees et al. (19) reported that

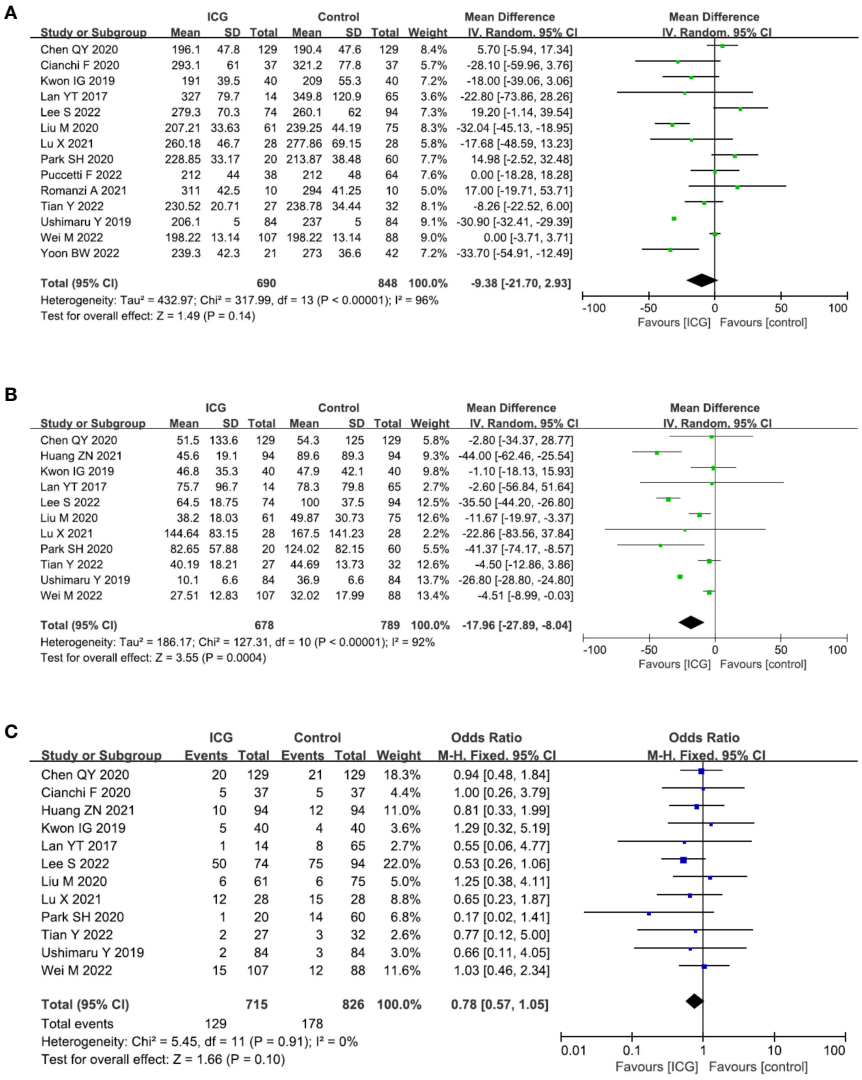


FIGURE 5
Forest plots showing the assessment of surgical outcomes including **(A)** operative time, **(B)** intraoperative blood loss, **(C)** overall complication. *ICG*, indocyanine green.

ICG fluorescence imaging-guided lymphadenectomy could reduce the tumor recurrence rate after surgery, with the recurrence rate 8.1% and 17.0% in the ICG and control groups, respectively. And another two studies also got the similar results (21, 22). However, Wei M et al. (28) pointed out that the tumor recurrence rates were similar between the two groups after surgery, with the recurrence rate 13.1% and 15.9% in the ICG and control groups, respectively. According to the pooled analysis, ICG fluorescence imaging-guided lymphadenectomy could reduce the overall recurrence rate ($P = 0.02$). However, the 2-year OS rates were comparable between the ICG and control groups ($P = 0.43$). Nevertheless, this result does not indicate that ICG fluorescence imaging-guided lymphadenectomy cannot improve the prognosis of GC patients, because there were only two studies reported survival results, and the follow-up period was shorter, without 5-year survival rate. So more studies with longer follow-up are necessary and expected.

Our study has some limitations. Firstly, there were only two RCTs in the included studies, which may increase the risk of selective bias. Therefore, more high-quality RCTs are expected to provide more credible evidence on this issue. Secondly, due to the limitations of data acquisition and language understanding, only English studies were included in this meta-analysis, which may also increase the risk of selective bias. Thirdly, the uses of ICG, including the dosage, injection method, injection time and

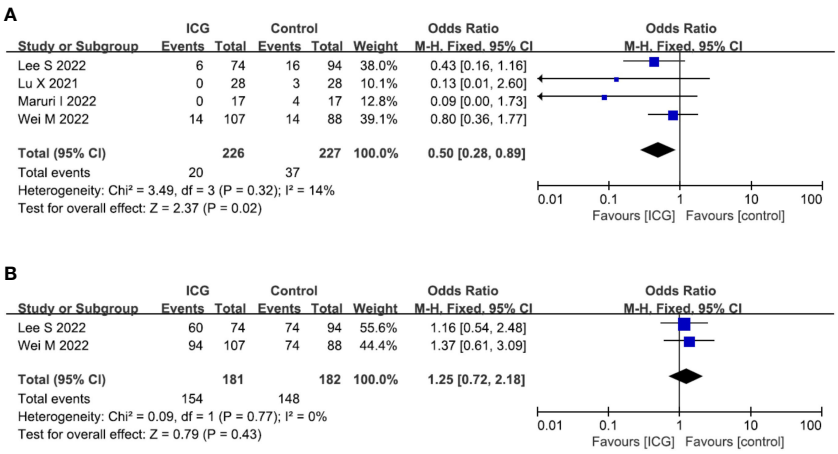


FIGURE 6
Forest plots showing the assessment of oncological outcomes including **(A)** overall recurrence rate, **(B)** 2-year OS rate. *ICG*, indocyanine green; *OS*, overall survival.

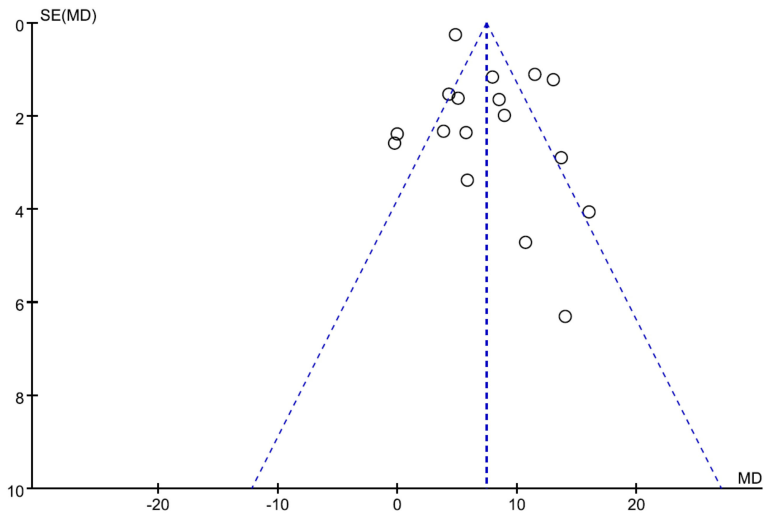


FIGURE 7
Funnel plots of publication bias for the number of retrieved lymph nodes.

ICG imaging system, were all different in these studies, which probably led to heterogeneity in the outcomes.

## Conclusions

Despite the limitations of the included studies, this meta-analysis indicates that ICG fluorescence imaging-guided lymphadenectomy could increase the number of retrieved LNs, reduce intraoperative blood loss and the overall recurrence rate without increasing operative time and overall complications. It is very valuable for complete LNs dissection in radical gastrectomy for GC. Nevertheless, more high-quality prospective studies and RCTs are necessary to confirm this conclusion.

## Data availability statement

The original contributions presented in the study are included in the article/supplementary material. Further inquiries can be directed to the corresponding author.

## Author contributions

ZL made substantial contributions to conception and design for this work. BD, AZ, and ZL collected all the data. BD and ZL were the major contributors in writing the manuscript. YZ, WY, and LL performed critical revision for important intellectual content. All authors read and approved the final manuscript.

## Funding

This work was supported by Scientific Research Project of Southwest Medical University (No.2020ZRQNB026).

## Conflict of interest

The authors declare that the research was conducted in the absence of any commercial or financial relationships that could be construed as a potential conflict of interest.

## Publisher's note



## References

1. Sung H, Ferlay J, Siegel RL, Laversanne M, Soerjomataram I, Jemal A, et al. Global cancer statistics 2020: GLOBOCAN estimates of incidence and mortality worldwide for 36 cancers in 185 countries. *CA Cancer J Clin* (2021) 71:209–49. doi: 10.3322/caac.21660

2. Japanese Gastric Cancer Association. Japanese Gastric cancer treatment guidelines 2018 (5th edition). *Gastric Cancer* (2021) 24:1–21. doi: 10.1007/s10120-020-01042-y

3. Li Z, Song M, Zhou Y, Jiang H, Xu L, Hu Z, et al. Efficacy of omentum-preserving gastrectomy for patients with gastric cancer: A systematic review and meta-analysis. *Front Oncol* (2021) 11:710814. doi: 10.3389/fonc.2021.710814

4. Li ZL, Zhao LY, Zhang WH, Liu K, Pang HY, Chen XL, et al. Clinical significance of lower perigastric lymph nodes dissection in siewert type II/III adenocarcinoma of esophagogastric junction: A retrospective propensity score matched study. *Langenbecks Arch Surg* (2022) 407:985–98. doi: 10.1007/s00423-021-02380-w

5. Ko CS, Jheong JH, Jeong SA, Kim BS, Yook JH, Yoo MW, et al. Comparison of standard d2 and limited lymph node dissection in elderly patients with advanced gastric cancer. *Ann Surg Oncol* (2022) 29:5076–82. doi: 10.1245/s10434-022-11480-w

6. Li Z, Jiang H, Chen J, Jiang Y, Liu Y, Xu L. Comparison of efficacy between transabdominal and transthoracic surgical approaches for siewert type II adenocarcinoma of the esophagogastric junction: A systematic review and meta-analysis. *Front Oncol* (2022) 12:813242. doi: 10.3389/fonc.2022.813242

7. Reinhart MB, Huntington CR, Blair LJ, Heniford BT, Augenstein VA. Indocyanine green: Historical context, current applications, and future considerations. *Surg Innov* (2016) 23:166–75. doi: 10.1177/1553350615604053

8. Li Z, Zhou Y, Tian G, Liu Y, Jiang Y, Li X, et al. Meta-analysis on the efficacy of indocyanine green fluorescence angiography for reduction of anastomotic leakage after rectal cancer surgery. *Am Surg* (2021) 87:1910–9. doi: 10.1177/0003134820982848

9. Park JH, Berlth F, Wang C, Wang S, Choi JH, Park SH, et al. Mapping of the perigastric lymphatic network using indocyanine green fluorescence imaging and tissue marking dye in clinically advanced gastric cancer. *Eur J Surg Oncol* (2022) 48:411–7. doi: 10.1016/j.ejso.2021.08.029

10. Osterkamp J, Strandby RB, Nerup N, Svendsen M, Svendsen LB, Achiam MP. Time to maximum indocyanine green fluorescence of gastric sentinel lymph nodes and feasibility of combined indocyanine green/sodium fluorescein gastric lymphography. *Langenbecks Arch Surg* (2021) 406:2717–24. doi: 10.1007/s00423-021-02265-y

11. Jung MK, Cho M, Roh CK, Seo WJ, Choi S, Son T, et al. Assessment of diagnostic value of fluorescent lymphography-guided lymphadenectomy for gastric cancer. *Gastric Cancer.* (2021) 24:515–25. doi: 10.1007/s10120-020-01121-0

12. Ekman M, Girnyi S, Marano L, Roviello F, Chand M, Diana M, et al. Near-infrared fluorescence image-guided surgery in esophageal and gastric cancer operations. *Surg Innov* (2022) 29(4):540–9. doi: 10.1177/15533506211073417

13. Chen QY, Xie JW, Zhong Q, Wang JB, Lin JX, Lu J, et al. Safety and efficacy of indocyanine green tracer-guided lymph node dissection during laparoscopic radical gastrectomy in patients with gastric cancer: A randomized clinical trial. *JAMA Surg* (2020) 155:300–11. doi: 10.1001/jamasurg.2019.6033

14. Cianchi F, Indennitate G, Paoli B, Ortolani M, Lami G, Manetti N, et al. The clinical value of fluorescent lymphography with indocyanine green during robotic surgery for gastric cancer: A matched cohort study. *J Gastrointest Surg* (2020) 24:2197–203. doi: 10.1007/s11605-019-04382-y

15. Hozo SP, Djulbegovic B, Hozo I. Estimating the mean and variance from the median, range, and the size of a sample. *BMC Med Res Methodol* (2005) 5:13. doi: 10.1186/1471-2288-5-13

16. Huang ZN, Su-Yan, Qiu WW, Liu CH, Chen QY, Zheng CH, et al. Assessment of indocyanine green tracer-guided lymphadenectomy in laparoscopic gastrectomy after neoadjuvant chemotherapy for locally advanced gastric cancer: Results from a multicenter analysis based on propensity matching. *Gastric Cancer.* (2021) 24:1355–64. doi: 10.1007/s10120-021-01211-7

17. Kwon IG, Son T, Kim HI, Hyung WJ. Fluorescent lymphography-guided lymphadenectomy during robotic radical gastrectomy for gastric cancer. *JAMA Surg* (2019) 154:150–8. doi: 10.1001/jamasurg.2018.4267

18. Lan YT, Huang KH, Chen PH, Liu CA, Lo SS, Wu CW, et al. A pilot study of lymph node mapping with indocyanine green in robotic gastrectomy for gastric cancer. *SAGE Open Med* (2017) 5:2104799444. doi: 10.1177/2050312117727444

19. Lee S, Song JH, Choi S, Cho M, Kim YM, Kim HI, et al. Fluorescent lymphography during minimally invasive total gastrectomy for gastric cancer: An effective technique for splenic hilar lymph node dissection. *Surg Endosc.* (2022) 36:2914–24. doi: 10.1007/s00464-021-08584-x

20. Liu M, Xing J, Xu K, Yuan P, Cui M, Zhang C, et al. Application of near-infrared fluorescence imaging with indocyanine green in totally laparoscopic distal gastrectomy. *J Gastric Cancer.* (2020) 20:290–9. doi: 10.5230/jgc.2020.20.e25

21. Lu X, Liu S, Xia X, Sun F, Liu Z, Wang J, et al. The short-term and long-term outcomes of indocyanine green tracer-guided laparoscopic radical gastrectomy in patients with gastric cancer. *World J Surg Oncol* (2021) 19:271. doi: 10.1186/s12957-021-02385-1

22. Maruri I, Pardellas MH, Cano-Valderrama O, Jove P, Lopez-Otero M, Otero I, et al. Retrospective cohort study of laparoscopic ICG-guided lymphadenectomy in gastric cancer from a Western country center. *Surg Endosc.* (2022). doi: 10.1007/s00464-022-09258-y

23. Park SH, Berlth F, Choi JH, Park JH, Suh YS, Kong SH, et al. Near-infrared fluorescence-guided surgery using indocyanine green facilitates secure infrapyloric lymph node dissection during laparoscopic distal gastrectomy. *Surg Today* (2020) 50:1187–96. doi: 10.1007/s00595-020-01993-w

24. Puccetti F, Cinelli L, Genova L, Battaglia S, Barbieri LA, Treppiedi E, et al. Applicative limitations of indocyanine green fluorescence assistance to laparoscopic lymph node dissection in total gastrectomy for cancer. *Ann Surg Oncol* (2022) 29(9):5875–82. doi: 10.1245/s10434-022-11940-3

25. Romanzi A, Mancini R, Ioni L, Picconi T, Pernazza G. ICG-NIR-guided lymph node dissection during robotic subtotal gastrectomy for gastric cancer. a single-centre experience. *Int J Med Robot.* (2021) 17:e2213. doi: 10.1002/rcs.2213

26. Tian Y, Lin Y, Guo H, Hu Y, Li Y, Fan L, et al. Safety and efficacy of carbon nanoparticle suspension injection and indocyanine green tracer-guided lymph node dissection during robotic distal gastrectomy in patients with gastric cancer. *Surg Endosc.* (2022) 36:3209–16. doi: 10.1007/s00464-021-08630-8

27. Ushimaru Y, Omori T, Fujiwara Y, Yanagimoto Y, Sugimura K, Yamamoto K, et al. The feasibility and safety of preoperative fluorescence marking with indocyanine green (ICG) in laparoscopic gastrectomy for gastric cancer. *J Gastrointest Surg* (2019) 23:468–76. doi: 10.1007/s11605-018-3900-0

28. Wei M, Liang Y, Wang L, Li Z, Chen Y, Yan Z, et al. Clinical application of indocyanine green fluorescence technology in laparoscopic radical gastrectomy. *Front Oncol* (2022) 12:847341. doi: 10.3389/fonc.2022.847341

29. Yoon BW, Lee WY. The oncologic safety and accuracy of indocyanine green fluorescent dye marking in securing the proximal resection margin during totally laparoscopic distal gastrectomy for gastric cancer: A retrospective comparative study. *World J Surg Oncol* (2022) 20:26. doi: 10.1186/s12957-022-02494-5

30. Zhong Q, Chen QY, Huang XB, Lin GT, Liu ZY, Chen JY, et al. Clinical implications of indocyanine green fluorescence imaging-guided laparoscopic lymphadenectomy for patients with gastric cancer: A cohort study from two randomized, controlled trials using individual patient data. *Int J Surg* (2021) 94:106120. doi: 10.1016/j.ijsu.2021.106120

31. Dai W, Zhai ET, Chen J, Chen Z, Zhao R, Chen C, et al. Extensive dissection at no. 12 station during d2 lymphadenectomy improves survival for advanced lower-third gastric cancer: A retrospective study from a single center in southern china. *Front Oncol* (2021) 11:760963. doi: 10.3389/fonc.2021.760963

32. Liang Y, Cui J, Cai Y, Liu L, Zhou J, Li Q, et al. "D2 plus" lymphadenectomy is associated with improved survival in distal gastric cancer with clinical serosa invasion: A propensity score analysis. *Sci Rep* (2019) 9:19186. doi: 10.1038/s41598-019-55535-7

33. Zhang YX, Yang K. Significance of nodal dissection and nodal positivity in gastric cancer. *Transl Gastroenterol Hepatol* (2020) 5:17. doi: 10.21037/tgh.2019.09.13

34. Zhang N, Bai H, Deng J, Wang W, Sun Z, Wang Z, et al. Impact of examined lymph node count on staging and long-term survival of patients with node-negative stage III gastric cancer: A retrospective study using a Chinese multi-institutional registry with surveillance, epidemiology, and end results (SEER) data validation. *Ann Transl Med* (2020) 8:1075. doi: 10.21037/atm-20-1358a

35. Komatsu S, Ichikawa D, Nishimura M, Kosuga T, Okamoto K, Konishi H, et al. Evaluation of prognostic value and stage migration effect using positive lymph node ratio in gastric cancer. *Eur J Surg Oncol* (2017) 43:203–9. doi: 10.1016/j.ejso.2016.08.002

36. Omori T, Yamamoto K, Hara H, Shinno N, Yamamoto M, Fujita K, et al. Comparison of robotic gastrectomy and laparoscopic gastrectomy for gastric cancer: A propensity score-matched analysis. *Surg Endosc.* (2022) 36:6223–34. doi: 10.1007/s00464-022-09125-w

37. Lou S, Yin X, Wang Y, Zhang Y, Xue Y. Laparoscopic versus open gastrectomy for gastric cancer: A systematic review and meta-analysis of randomized controlled trials. *Int J Surg* (2022) 102:106678. doi: 10.1016/j.ijsu.2022.106678

38. Rosa F, Alfieri S. Laparoscopic gastrectomy for locally advanced gastric cancer. *JAMA Surg* (2022) 157:545–6. doi: 10.1001/jamasurg.2021.7582

39. Otsuka R, Hayashi H, Uesato M, Hayano K, Murakami K, Kano M, et al. Comparison of estimated treatment effects between randomized controlled trials, case-matched, and cohort studies on laparoscopic versus open distal gastrectomy for advanced gastric cancer: A systematic review and meta-analysis. *Langenbecks Arch Surg* (2022) 407:1381–97. doi: 10.1007/s00423-022-02454-3

40. Kano K, Yamada T, Yamamoto K, Komori K, Watanabe H, Hara K, et al. Association between lymph node ratio and survival in patients with pathological stage II/III gastric cancer. *Ann Surg Oncol* (2020) 27:4235–47. doi: 10.1245/s10434-020-08616-1

41. Wang JW, Chen CY. Prognostic value of total retrieved lymph nodes on the survival of patients with advanced gastric cancer. *J Chin Med Assoc* (2020) 83:691–2. doi: 10.1097/JCMA.0000000000000368

42. Mao M, Zhang A, He Y, Zhang L, Liu W, Song Y, et al. Development and validation of a novel nomogram to predict overall survival in gastric cancer with lymph node metastasis. *Int J Biol Sci* (2020) 16:1230–7. doi: 10.7150/ijbs.39161

frontiers | Frontiers in Oncology

TYPE Original Research
PUBLISHED 25 October 2022
DOI 10.3389/fonc.2022.1003951



OPEN ACCESS

EDITED BY
Beatrice Aramini,
University of Bologna, Italy

REVIEWED BY
Valerio Gallotta,
Agostino Gemelli University Polyclinic (IRCCS), Italy
Carmine Conte,
Agostino Gemelli University Polyclinic (IRCCS), Italy

*CORRESPONDENCE
Hui-ting Sun
94sunhuiting@163.com
Ji-ming Chen
cjming@126.com
Ru-xia Shi
czeyfk@163.com

†These authors share first authorship

SPECIALTY SECTION
This article was submitted to Surgical Oncology, a section of the journal Frontiers in Oncology

RECEIVED 26 July 2022
ACCEPTED 06 October 2022
PUBLISHED 25 October 2022

CITATION
Wei W-w, Zheng H, Shao P, Chen X, Min Y-f, Tang B, Sun H-t, Chen J-m and Shi R-x (2022) Can laparoscopic nerve-sparing ultra-radical hysterectomy play a role in locally advanced cervical cancer? A single-center retrospective study. *Front. Oncol.* 12:1003951. doi: 10.3389/fonc.2022.1003951



# Can laparoscopic nerve-sparing ultra-radical hysterectomy play a role in locally advanced cervical cancer? A single-center retrospective study

Wei-wei Wei[1†], Hong Zheng[1†], Panqiu Shao[1], Xia Chen[2], Yi-fei Min[1], Bin Tang[1], Hui-ting Sun[2*], Ji-ming Chen[1*] and Ru-xia Shi[1*]

[1]Department of Gynecology, The Affiliated Changzhou No. 2 People's Hospital of Nanjing Medical University, Changzhou, China, [2]Department of Reproductive Center, The Affiliated Changzhou No. 2 People's Hospital of Nanjing Medical University, Changzhou, China

**Background and objectives:** The objective of this study is to investigate the outcomes of concurrent platinum-based chemoradiation therapy (CCRT), laparoscopic nerve-sparing ultra-radical hysterectomy (LNSURH), and open radical hysterectomy (ORH) on patients with locally advanced cervical carcinoma (LACC).

**Methods:** A single-center retrospective study was conducted on LACC patients who received CCRT, ORH, or LNSURH from January 2011 to December 2019. Data on age, tumor size, overall survival (OS), disease-free survival (DFS), and early and late morbidities were collected. After 24 months of treatment, patients were asked a series of questions about their urinary, bowel, and sexual activities. Early morbidities were defined as those occurring during or within a month of treatment, whereas late morbidities and complications were defined as those occurring a month after treatment. The postoperative complications were classified with reference to the Clavien–Dindo classification (CD) system.

**Results:** The Kaplan–Meier curves revealed no significant differences in OS and DFS among the three groups ($P$ = 0.106 for DFS and $P$ = 0.190 for OS). The rates of early complications in the CCRT group were comparable with those in the operated groups ($P$ = 0.46). However, late complications were significantly lower in the ORH and LNSURH groups relative to those in the CCRT group. The scores of urinary and bowel functions were restored to the pretreatment state, although the sexual function scores were not satisfactory.

**Conclusions:** The treatments of CCRT, ORH, and LNSURH can be considered options for patients with LACC, as their OS and DFS showed no significant difference. In addition, LNSURH exhibited a lower incidence of late complications and high sexual function scores.

KEYWORDS

locally advanced cervical carcinoma, nerve-sparing radical hysterectomy, laparoscopic surgery, concurrent chemoradiotherapy, disease-free survival

# Introduction

Cervical cancer is the fourth most common malignancy in women across the world (1). Radical hysterectomy (RH) represents the classical treatment for early-stage cervical cancer. Locally advanced cervical carcinoma (LACC) is larger with cervical carcinoma > 4 cm and stage IB2 or IIA2 (2). The exploration of the treatment for LACC has never stopped. According to the National Comprehensive Cancer Network (NCCN) guidelines, both RH and CCRT can be applied as the treatment approach for LACC. However, the NCCN guidelines published in 2014 clearly stated that, for the treatment of stage IB2 (> 4 cm) and IIA2 (> 4 cm) LACC, concurrent chemoradiotherapy should be preferred over surgery. However, due to the differences in the radiotherapy levels and resources, as well as based on the patient's willingness to undertake surgical treatment, surgical treatment remains an indispensable part of the treatment regimen for LACC.

CCRT is the first-line treatment option for LACC (3). However, LACC patients routinely treated with CCRT have demonstrated a poor prognosis, with about one-third of the patients relapsing within 18 months of CCRT (4), with a 5-year survival rate of 50–60% (5). In developing countries such as China, patients often present with different stages of LACC (6). In stages IB3 and IIA2, the possible causes of relapse have been reported to be larger tumors and residual tumor tissues after CCRT. Blidaru et al. (7) reported that, in 2019, 30–40% of patients with surgery for LACC who were following CCRT had residual tumor tissues on pathology examination of their hysterectomized specimen. Despite LACC being larger and with a high possibility of positive lymph nodes, positive parametria, or positive surgical margins that augment the risk of recurrence and the rate of adjuvant radiation after surgery, RH is a treatment option for locally advanced tumors.

The *New England Journal of Medicine* reported that, in 2018, minimally invasive RH was associated with a poor prognosis relative to that with open RH among women with early-stage cervical cancer (8). However, this conclusion has been questioned by several scholars, and the surgical method has been improved; as a result, minimally invasive RH has been deemed a safe approach in terms of the oncological outcomes (9, 10). In 2015, we reported the surgical procedure of LNSRH, with a disease-free survival rate of 90.6% in the LNSRH (11). Based on the results of this past study, we continued to conduct laparoscopic nerve-sparing ultra-radical hysterectomy (LNSURH), open radical hysterectomy (ORH), and CCRT, after providing the patients the relevant information.

To investigate whether patients with LACC can benefit from LNSURH, we evaluated the outcome of LNSURH, RH (RH), and CCRT in patients with LACC. The disease-free survival (DFS), OS, and complications were recorded and analyzed to determine the prognosis and quality of life of these patients.

# Materials and methods

## Study design and patient selection

LACC patients in stages IB3 and IIA2 (74) who had received ORH (29), LNSURH (20), or CCRT (25) from the Affiliated Changzhou No. 2 People's Hospital of Nanjing Medical University between January 2011 and December 2019 were enrolled in this study. All surgical cases were treated by the same surgical team (Prof. Ru-Xia Shi et al.). This study was approved by the hospital's ethics committee (approval number: [2019] YLJSA011).

The subject inclusion criteria were as follows: (1) patients at stages IB3 or IIA2, as defined by the International Federation of Gynecology and Obstetrics (FIGO) staging system (2018) before treatment and with pathologically confirmed cervical squamous cell carcinoma, adenocarcinoma, or adenosquamous; and (2) patients who had RH, LNSURH with pelvic and para-aortic lymphadenectomy, or CCRT.

The subject exclusion criteria were as follows: (1) combination with other malignant tumors, (2) incomplete medical records, and (3) abnormal vital organ functions.

## Surgical procedure

The surgical procedure for LNSURH with pelvic and para-aortic lymphadenectomy was performed under general anesthesia in the dorsolithotomy position. The operation platform was performed by a five-port laparoscopy. The para-aortic lymph node dissection was performed routinely up to the inferior mesenteric artery emergence. If the intraoperative frozen section examination indicated a positive common iliac lymph node, it was performed up to the renal vein level.

A laparoscopic pelvic lymphadenectomy was performed following para-aortic lymphadenectomy. The critical steps of nerve preservation were the development of the anatomical space, identification, selective transection of the uterine nerve branches (UNBs) of the inferior hypogastric plexus (IHP), and sparing of the vesical nerve branches (VNBs). As cervical carcinoma patients at stage IB3 or IIA2 with larger tumor and parametrial infiltration were not deemed suitable for the nerve-sparing procedure, contralateral or partial nerve-sparing RH was performed to preserve some part of the IHP and the pelvic splanchnic nerves (12).

LNSURH has a wider parametrial excision and safeguards the pelvic splanchnic nerve from long-term postoperative complications (e.g., urinary dysfunction, sexual dysfunction, and bowel motility disorders). The key point of LNSURH is depicted in Figure 1. The procedure is summarized as follows:

Step 1: Resection of the uterine artery at the starting position of the internal iliac artery following the development of the pararectal space and paravesical space (Figure 1A).

Step 2: Continue downward to separate the pararectal and paravesical spaces, followed by exposure and isolation of the deep uterine vein. We then exposed the deep uterine vein to reveal the pelvic splanchnic nerve beneath it. Next, we closed the uterine bilateral arteries and veins and then excised the parametrial tissues so as to reduce blood loss (Figure 1B).

Step 3: We pushed the hypogastric plexus bundle laterally and resected the root of the distal uterosacral ligaments (Figure 1C).

Step 4: Vesicouterine ligament (VUL) is located between the bladder and the cervix and is a lamellar structure (Figure 1D). The vesicovaginal ligament (VVL) is located between the bladder and the vagina at the level of the vaginal fornix, which is a posterior portion of the VUL. The VVL is exposed after the excision of the VUL (Figure 1E). Vesical vein is then transected at the edge of the bladder, disconnecting the bladder from the cervix and the upper vagina. The excision of the VUL and the VVL was performed close to the bladder with a wider parametrial excision.

Step 5: We next conducted cross-shaped IHP and isolated the uterine branch from the plexus. The uterine branch division was performed to create a T-shaped nerve plane of the IHP. The T-shaped nerve plane was pushed down before the radical excision of the paracolpium to avoid nerve damage.

Step 6: The uterus was removed through the vagina, and the length of the vagina was 3 cm (Figure 1F).

Step 7: The ultra-radical hysterectomy specimen was obtained (Figures 1G, H).

## Data collection

The data relating to the age of the patients, the tumor size, early complications, and late complications were collected. All patients diagnosed with cervical cancer routinely underwent medical imaging to evaluate the abdomen and the pelvis, respectively, before treatment. LACC was diagnosed by two deputy chiefs or experts supervising the gynecological oncologists. These patients with LACC then underwent RH and LNSURH with pelvic and para-aortic lymphadenectomy or CCRT.

The patients in the RH and LNSURH groups were given adjuvant radiotherapy in case of a risk of tumor recurrence postoperatively. The risk factors included (1) 1 of the high-risk factors such as lymph node metastases, positive resection margins, and parametrial invasion, or (2) >1 of the other risk factors that include deep stromal invasion and lymphovascular space invasion (LVSI) (13–16).

The early complications included myelosuppression, hypohepatia, radiation enteritis, radiocystitis, pelvic lymphatic cyst, angiolymphitis, ureteral vaginal fistula, and radiothermitis. Late complications included obstructive nephropathy, lymphatic reflux disorder, and colorectal fistula. The ureteral vaginal fistula was treated with ureteral stenting. All early complications improved after the treatment.

The Clavien–Dindo (CD) classification system was applied to analyze the post-operative complications (17). It was defined as lower than or equal to grade II (not requiring surgical, endoscopic, or radiological intervention) and higher than or equal to grade III (requiring surgical, endoscopic, or radiological intervention or life-threatening complication or death of a patient).

After discharge from the hospital, the patients were followed up *via* a telephonic and outpatient care interview conducted every 3 months. The follow-up data included the duration of the follow-up; the general health status; complications; time of cancer recurrence; urinary, bowel, and sexual functions; and mortality.

During the follow-up, at least 24 months after the operation or CCRT, the patients were asked to answer a series of questions about their urinary, bowel, and sexual functions. The self-assessed questionnaires consisted of five questions on sexual satisfaction, dyspareunia, defecation condition, urinary incontinence, and urination requiring abdominal assistance, according to the article published by Zhuoyu Sun in 2020 (18).

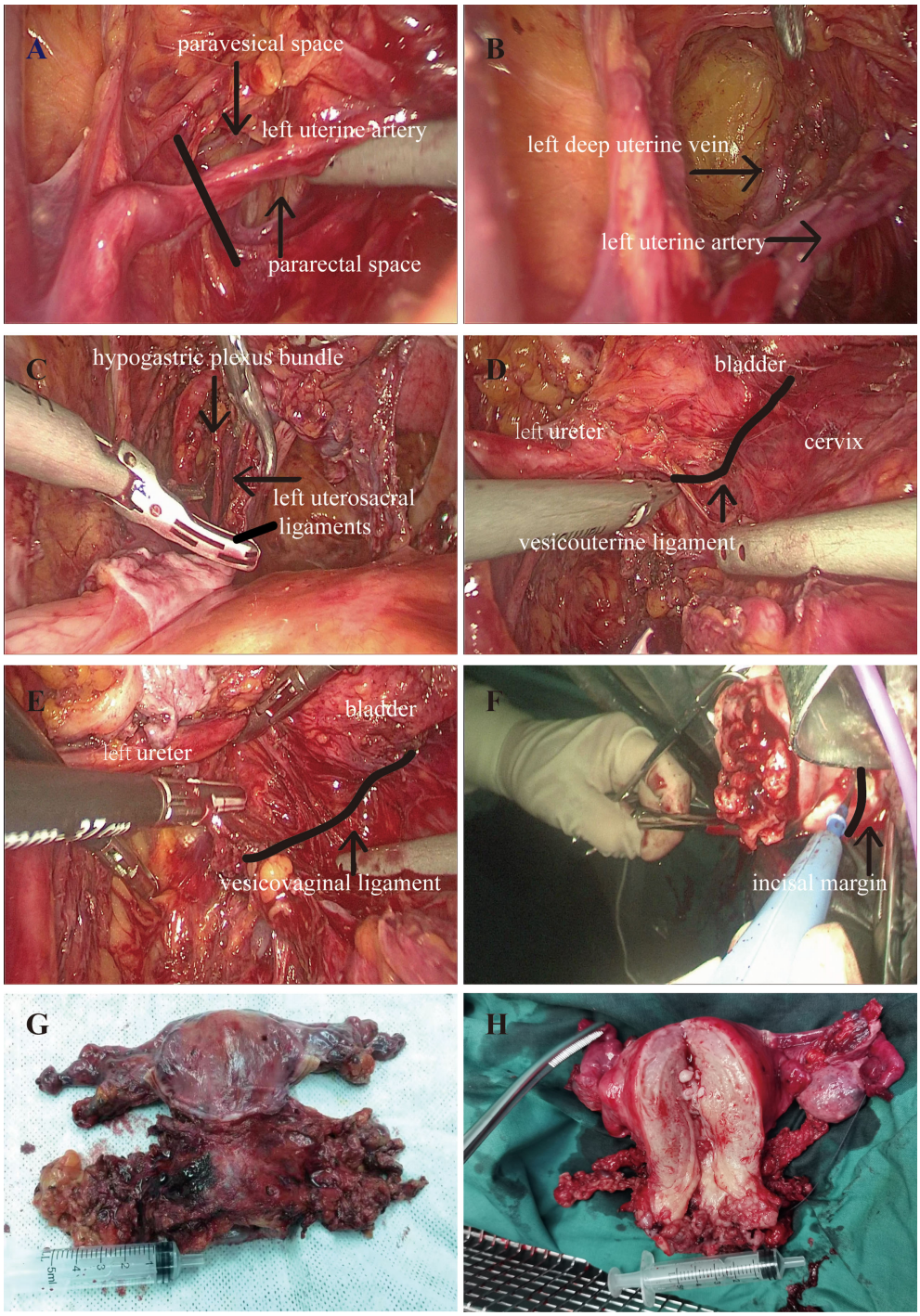


FIGURE 1
Perioperative picture. **(A)** Resection of the uterine artery. **(B)** Isolation of the deep uterine vein. **(C)** Resection of the uterosacral ligaments. **(D)** Resection of the vesicouterine ligament. **(E)** Resection of the vesicovaginal ligament. **(F)** The removal of the uterus. **(G, H)** Ultra-radical hysterectomy specimen.

The scores for each question ranged from 0 to 3, with higher scores indicating a better quality of life.

DFS was considered as the period from surgery or CCRT to cancer recurrence, as identified by biopsy or evaluation by medical imaging. In case of no cancer recurrence, the last follow-up examination or death was considered as the DFS. Overall survival (OS) was regarded as the period from the time of treatment including surgery and CCRT until death from cervical cancer.

## Statistical analysis

We analyzed the factors associated with OS and DFS by multivariate logistic regression analyses. Comparison of continuous data was performed by one-way analysis of variance (ANOVA), and continuous data were expressed as the mean ± *SD*. Comparison of the categorical data was performed by the chi-square test, and categorical data were expressed as percentages. DFS and OS were detected by Kaplan–Meier analysis. We calculated *P* values by log-rank test. $P < 0.05$ was considered to indicate statistical significance. All data were analyzed by SPSS 20.0 (SPSS, IBM, New York, NY).

# Results

## Participant characteristic comparisons

In our study, we assessed 74 patients, with 25, 29, and 20 patients assigned to the CCRT, RH, and LNSRH groups, respectively. Statistical analysis revealed that there were no statistically significant differences in the BMI and tumor size. However, when compared with the CCRT group, the LNSURH and RH groups were significantly younger (Table 1).

## Comparisons of survival after the therapy survival among the three groups

A total of 74 patients showed a median postoperative follow-up time of 39.6 months (0–115 months). The DFS rates were 84.0, 75.9, and 90.0%, whereas the OS rates were 96.0, 93.1, and 100% in the CCRT, ORH, and LNSURH groups in 3 years, respectively. The median DFS times were 49, 53, and 35 months, and the median OS times were 48, 50, and 28 months in the CCRT, ORH, and LNSURH groups, respectively.

The Kaplan–Meier analysis showed that there was no significant difference in the OS and DFS among the CCRT, ORH, and LNSURH groups ($P = 0.106$ for DFS and 0.190 for OS, Figures 2A, B, respectively).

## Early and late complications

The rate of early complications was not statistically significantly different among the CCRT, ORH, and LNSURH groups ($P = 0.46$). When compared with the CCRT group, the rate of late complications in the ORH and LNSURH groups was markedly lower (Table 2).

## Post-treatment functional evaluation

During follow-up, at least 24 months after the procedure, the patients were asked to answer a series of questions about their urination, defecation, and sexual functions. A total of eight patients from the 25 patients in the CCRT group, six of the 29 patients in the ORH group, and nine of the 20 patients in the LNSURH group answered the questionnaires.

The scores of sexual functions were 0.25 ± 0.66, 0.83 ± 1.21, and 1.56 ± 2.31 in the CCRT, ORH, and LNSURH groups, respectively. The scores of urinary and bowel functions were

TABLE 1 Characteristics of the study participants.

| Characteristics | CCRT group (*N* = 25) | ORH group (*N* = 29) | LNSURH group (*N* = 20) | *P* |
|---|---|---|---|---|
| Age, years (mean ±*SD*) | 55.2 ±11.7 | 51.7 ±8.2 | 47.1 ±10.5 | 0.03 |
| BMI | 22.69 (3.28) | 23.69 (3.08) | 23.14 (2.66) | 0.48 |
| Tumor size, cm (mean ±*SD*) | 5.00 (0.94) | 4.53 (0.57) | 4.80 (0.71) | 0.1 |
| FIGO stage, *N* (%) | | | | 0.04 |
| IB3 | 15 (60.00) | 18 (62.07) | 11 (55.00) | |
| IIA2 | 10 (40.00) | 11 (37.93) | 9 (45.00) | |
| Pathology, *N* (%) | | | | 0.141 |
| Squamous cell carcinoma | 21 (84.00) | 27 (93.10) | 15 (75.00) | |
| Adeno/adenosquamous carcinoma | 4 (16.00) | 2 (6.89) | 5 (25.00) | |

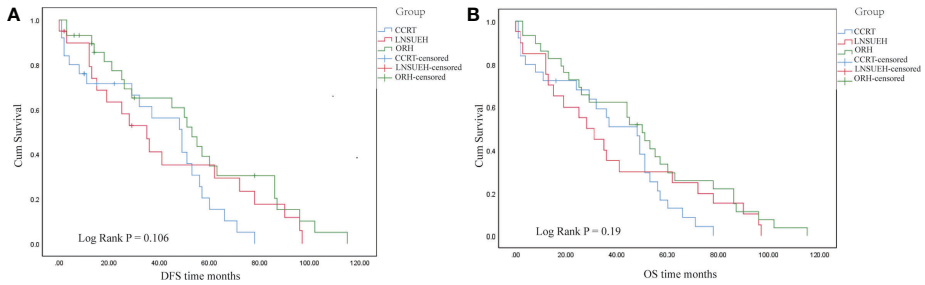


FIGURE 2
Kaplan–Meier survival analyses. **(A)** Comparisons of the disease-free survival (DFS) periods among the three study groups. **(B)** Comparisons of the overall survival (OS) periods among the three groups.

restored to the pretreatment state in all three groups, albeit the sexual function was not satisfactory (Table 3).

## Discussion

Cervical cancer is one of the most common gynecological malignancies across the world. Based on the latest statistics, more than 311,000 women worldwide died of cervical cancer in 2018 alone (19, 20). Most of these patients were diagnosed in the late stage of the disease, making timely estimation of the clinical grade the most important prognostic factor of this tumor. The treatment of LACC has always been a hot issue worthy of research and discussion. Clinically, the main treatment approach for LACC includes radiotherapy and chemotherapy, although the treatment outcome is generally poor. This type of tumor is not easy to control locally, which makes it difficult to operate and easy to relapse and metastasize even after the operation, and the 5-year survival rate is low (21, 22). The latest guideline from the NCCN recommends CCRT, including external radiotherapy and brachytherapy, which is the standard treatment approach for LACC patients (23, 24). Cochrane meta-analysis completed by GOG and the Radiation Therapy Oncology Group (RTOG) demonstrated that, for women with LACC, the 5-year survival rate of CCRT was increased by 6% when compared with that by radiotherapy alone (hazard ratio

TABLE 2 Rate of complications in the CCRT, ORH, and LNSURH groups.

| Complications | CCRT group ($N$ = 25) | ORH group ($N$ = 29) | LNSURH group ($N$ = 20) | $P$ |
|---|---|---|---|---|
| Early complications $N$ (%) | 17 (68) | 18 (62.1) | 10 (50) | 0.463 |
| Myelosuppression | 12 | 10 | 6 | |
| Hypohepatia | 4 | 4 | 3 | |
| Radiation enteritis | 6 | 4 | 2 | |
| Radiocystitis | 3 | 1 | 5 | |
| Pelvic lymphatic cyst | 0 | 2 | 1 | |
| Angiolymphitis | 0 | 1 | 1 | |
| Ureteral vaginal fistula | 0 | 1 | 1 | |
| Radiothermitis | 1 | 0 | 0 | |
| Late complications | 5 (20) | 0 | 1 (5) | 0.015 |
| Obstructive nephropathy | 2 | 0 | 1 | |
| Lymphatic reflux disorder | 1 | 0 | 0 | |
| Colorectal fistula | 2 | 0 | 0 | 0.352 |
| CD | | | | |
| Grade ≤ II | 19 | 17 | 10 | |
| Grade≥ III | 3 | 1 | 1 | |

The early complications included myelosuppression, hypohepatia, radiation enteritis, radiocystitis, pelvic lymphatic cyst, angiolymphitis, ureteral vaginal fistula, and radiothermitis. The same patient often exhibited several early complications simultaneously; hence, the times of early complications were counted by the patients experiencing early complications.
CD, Clavien–Dindo classification.

TABLE 3 The scores for each question in the CCRT, ORH, and LNSURH groups.

| Scores (mean ±*SD*) | CCRT group (*N* = 25) | ORH group (*N* = 29) | LNSURH group (*N* = 20) |
|---|---|---|---|
| Sexual function | 0.25 ± 0.66 | 0.83 ± 1.21 | 1.56 ± 2.31 |
| Rectum function | 2.63 ± 0.99 | 3.00 ± 0.00 | 2.89 ± 0.31 |
| Bladder function | 5.88 ± 0.33 | 5.67 ± 0.75 | 5.56 ± 0.68 |
| Aggregate score | 8.50 ± 1.00 | 9.50 ± 1.61 | 10.00 ± 2.75 |

[HR] = 0.81, $P < 0.001$) (25, 26). Li et al. (27) reported that the 5-year overall response rate of CCRT for the treatment of LACC patients was 67%. A retrospective study compared the curative effects of paclitaxel/ifosfamide/platinum (TIP) and paclitaxel/platinum (TP) on patients with metastatic, recurrent, or persistent cervical cancer. They found that TIP exhibited a higher remission rate than TP without increasing the risks of severe complications (28). Kalaghchi et al. (29) reported that LACC patients exhibited good tolerance to cisplatin and paclitaxel combined chemotherapy and radiotherapy, albeit the tumor response and PFS did not show any improvement. When compared with CCRT combined with platinum monotherapy, CCRT combined with platinum monotherapy could improve the OS and PFS of patients with LACC, albeit it also increased the adverse reactions caused by several chemotherapeutic drugs. A systematic review with meta-analysis that evaluated the efficacy of CCRT and neoadjuvant chemotherapy followed by radical surgery (NACT+S) revealed that, when compared with the CCRT group, the incidence of diarrhea, rectal, and bladder complications in the NACT+S group was lower, although NACT+S exhibited no survival advantage for patients with IB2-IIB cervical cancer (30). Until now, there exists no consensus on whether NACT can significantly improve the prognosis of cervical cancer (31). Therefore, in clinical practice, it is extremely important to select the appropriate chemotherapy scheme in accordance with the patient's actual tolerance. Therefore, the choice of LACC treatment remains a huge problem in the currently available treatment modalities (32).

However, owing to the difference in the advancement of medical and healthcare facilities across the world, there is a deviation in clinical staging before surgery, an imbalance in the radiotherapy resources, limitations of regional-related medical conditions, and the subjective choice made by patients, considering that a considerable number of patients continue to opt for surgical resection as an initial treatment (33–35). In recent years, with the development of the minimally invasive concept, surgical instruments, and relevant technology, laparoscopic RH for cervical cancer has been proved to be safe and effective, thereby gradually replacing the traditional open surgery approach (36, 37). However, the radical effect of this operation and the suitability of its application scope remain controversial. Recent research reports have raised serious concerns about the oncological safety of endoscopic surgery for cervical cancer and highlight the remarkable and alarming increase in the recurrence rate (38, 39). With the rising trend of minimally invasive surgery and the development of laparoscopic technology, along with the advantage of a clear vision offered by the latest laparoscopy techniques, it has become more conducive to preserving the pelvic autonomic nerve structure and further improving the quality of surgery. Since 2008, our research group has been exploring the precise anatomy of radical operation of cervical cancer and the improved operation method for laparoscopic nerve-sparing RH (LNSRH), thereby mastering solid surgical skills and accumulating significant case data. Our previous research preliminarily confirmed that LNSRH can preserve the urinary, colorectal, and sexual functions and arrest lymph node metastasis, rather than the type of hysterectomy, which is independently related to the DFS and OS (40). Several research reports across the world have supported and validated the advantages of nerve-sparing minimally invasive RH (NS-MRH) operation in improving bladder functions and the safety of reducing the pelvic floor dysfunction rate (41, 42). In 2016, a multicenter prospective cohort study on 76 patients with IB2 and IIA2 cervical cancer whose local tumors were >6 cm in size completed laparoscopic nerve-sparing RH (LNRH) and laparoscopic RH (LRH) after neoadjuvant chemotherapy. Their results asserted that LNRH is safe and feasible in the treatment of LACC, although the study followed up the patients for only 1 year and did not conduct any prognosis evaluation (43). A retrospective study evaluated the survival outcome of minimally invasive radical surgery (MI-RS) versus open radical surgery (O-RS) in LACC patients managed by surgery after CT/RT through propensity score analyses. MI-RS and O-RS were found to be associated with similar rates of recurrence, and there was no difference in the early or late complications (44). Moreover, the feasibility of secondary radical resection positively impacts the survival of recurrent

LACC patients submitted to multimodality primary treatments, thus prompting practitioners treating patients with recurrence from cervical cancer to consider a second surgery in the armamentarium of potential therapies (45).

All surgery candidates in this study preferred adjuvant radiotherapy and chemotherapy according to the high-risk factors suggested by their postoperative pathological outcomes. After a median of 39.6 months' long-term follow-up, our results showed that, when compared with conventional chemoradiotherapy, LNSURH plus chemoradiotherapy had no significant difference in the OS and DFS in LACC patients, suggesting that LNSURH preserved the pelvic nerve but did not increase the postoperative recurrence rate. It is therefore recommended that the postoperative survival rate of patients is related to the scope of surgery and the implementation of the principle of no tumor, albeit it has no obvious correlation with the surgical method. After the pelvic nerve is preserved, the bladder function of the patient recovers quickly. Moreover, this way, patients with risk factors who need postoperative adjuvant radiotherapy can receive treatment at the earliest. In this study, the early complications of CCRT, ORH, and LNSURH patients included myelosuppression, hypohepatia, and radiation enteritis, albeit the corresponding incidences were not statistically significantly different among the groups. The long-term follow-up of late complications demonstrated that the rectal and bladder functions recovered to the preoperative state and that the quality of life was improved, although the recovery of sexual functions was not satisfactory; in fact, it was lower than those reported previously (36), which may be attributed to the Chinese women's sexual psychological worries. The results of the present study implied that active adjuvant therapy can help improve the prognosis of patients with LACC. Moreover, laparoscopic para-aortic and pelvic lymphadenectomy provides accurate information about the lymph node status and allows the development of individualized treatment plans for LACC patients, thereby avoiding false-negative (FN) and false-positive (FP) imaging results (46).

To analyze the reasons for good OS and DFS after LNSRH operation, the following factors should be considered: (1) based on nerve preservation, the operation scope is sufficient; and (2) strict implementation of the principle of being tumor-free: (A) removal of the uterus through the vagina; (B) flushing with plenty of water after the operation; (C) lymph node removal on time by bagging; and (D) ensuring that pneumoperitoneum is stable and instrument replacement is minimized.

Comparatively speaking, this retrospective small-sample study involved a selective deviation. Patients who selected LNSRH were younger than those in the CCRT and ORH groups, and they are more enthusiastic about undertaking laparoscopic surgery with nerve preservation. In addition, the quality of life was self-reported by the patients themselves, which implies the possibility of deviation in self-reporting. Therefore, for validation of the present findings, larger randomized trials and longer follow-ups are warranted.

## Conclusions

In summary, the present research supports that the prognosis of LACC patients should be determined by the scope of surgery and tumor-free outcome and not by the difference in the surgical approaches. No significant difference was noted in the OS and DFS among the three study groups, albeit there were more long-term complications of CCRT, such as vaginal fistula, ureteral obstruction (related to the uncleared primary lesion), and obstructive nephropathy. The response to the questionnaires revealed that the sexual life score of the LNSRH group was higher than that of the other two groups.

## Data availability statement

The original contributions presented in the study are included in the article/supplementary material. Further inquiries can be directed to the corresponding authors.

## Ethics statement

This study was approved by the ethics committee of Nanjing Medical University Affiliated Changzhou Second People's Hospital (approval number: [2019] YLJSA011). The patients/participants provided their written informed consent to participate in this study. Written informed consent was obtained from the individual(s) for the publication of any potentially identifiable images or data included in this article.

## Author contributions

JC and RS designed the study and approved the manuscript. HZ and BT collected the clinical data. WW and HS prepared and wrote the original draft, with the reviewing of YM and XC. PS

provided statistical methods. All authors contributed to the article and approved the submitted version.

## Funding

This work was supported by grants from the Changzhou Science and Technology Program (QN201931) and the Changzhou Sci and Tech Program (grant no. CJ20220077 and CJ20210110).

## Acknowledgments

The authors would like to thank those female patients who participated in the study and shared their experiences with us.

## Conflict of interest

The authors declare that the research was conducted in the absence of any commercial or financial relationships that could be construed as a potential conflict of interest.

## Publisher's note



## References

1. Arbyn M, Weiderpass E, Bruni L, de Sanjosé S, Saraiya M, Ferlay J, et al. Estimates of incidence and mortality of cervical cancer in 2018: a worldwide analysis. *Lancet Glob Health* (2020) 8(2):e191–203. doi: 10.1016/S2214-109X(19)30482-6

2. Gallotta V, Chiantera V, Conte C, Vizzielli G, Fagotti A, Nero C, et al. Robotic radical hysterectomy after concomitant chemoradiation in locally advanced cervical cancer: A prospective phase II study. *J Minim Invasive Gynecol.* (2017) 24(1):133–9. doi: 10.1016/j.jmig.2016.09.005

3. Bhatla N, Aoki D, Sharma DN, Sankaranarayanan R. Cancer of the cervix uteri. *Int J Gynaecol Obstet* (2018) 143 Suppl 2:22–36. doi: 10.1002/ijgo.12611

4. Spensley S, Hunter RD, Livsey JE, Swindell R, Davidson SE. Clinical outcome for chemoradiotherapy in carcinoma of the cervix. *Clin Oncol (R Coll Radiol)* (2009) 21(1):49–55. doi: 10.1016/j.clon.2008.10.014

5. Lai JC, Chou YJ, Huang N, Tsai JJ, Huang SM, Yang YC, et al. Survival analysis of stage IIA1 and IIA2 cervical cancer patients. *Taiwan J Obstet Gynecol* (2013) 52(1):33–8. doi: 10.1016/j.tjog.2013.01.006

6. Goss PE, Strasser-Weippl K, Lee-Bychkovsky BL, Fan L, Li J, Chavarri-Guerra Y, et al. Challenges to effective cancer control in China, India, and Russia. *Lancet Oncol* (2014) 15(5):489–538. doi: 10.1016/S1470-2045(14)70029-4

7. Blidaru A, Bordea C, Burcoş T, Duduş L, Eniu D, Ioanid N, et al. Mind the gap between scientific literature recommendations and effective implementation. is there still a role for surgery in the treatment of locally advanced cervical carcinoma? *Chirurgia (Bucur)* (2019) 114(1):18–28. doi: 10.21614/chirurgia.114.1.18

8. Ramirez PT, Frumovitz M, Pareja R, Lopez A, Vieira M, Ribeiro R, et al. Minimally invasive versus abdominal radical hysterectomy for cervical cancer. *N Engl J Med* (2018) 379(20):1895–904. doi: 10.1056/NEJMoa1806395

9. Kanno K, Andou M, Yanai S, Toeda M, Nimura R, Ichikawa F, et al. Long-term oncological outcomes of minimally invasive radical hysterectomy for early-stage cervical cancer: A retrospective, single-institutional study in the wake of the LACC trial. *J Obstet Gynaecol Res* (2019) 45(12):2425–34. doi: 10.1111/jog.14116

10. Kanao H, Matsuo K, Aoki Y, Tanigawa T, Nomura H, Okamoto S, et al. Feasibility and outcome of total laparoscopic radical hysterectomy with no-look no-touch technique for FIGO IB1 cervical cancer. *J Gynecol Oncol* (2019) 30(3):e71. doi: 10.3802/jgo.2019.30.e71

11. Shi R, Wei W, Jiang P. Laparoscopic nerve-sparing radical hysterectomy for cervical carcinoma: Emphasis on nerve content in removed cardinal ligaments. *Int J Gynecol Cancer* (2016) 26(1):192–8. doi: 10.1097/IGC.0000000000000577

12. Sakuragi N, Murakami G, Konno Y, Kaneuchi M, Watari H. Nerve-sparing radical hysterectomy in the precision surgery for cervical cancer. *J Gynecol Oncol* (2020) 31(3):e49. doi: 10.3802/jgo.2020.31.e49

13. Cho HC, Kim H, Cho HY, Kim K, No JH, Kim YB. Prognostic significance of perineural invasion in cervical cancer. *Int J Gynecol Pathol* (2013) 32(2):228–33. doi: 10.1097/PGP.0b013e318257df5f

14. Je HU, Han S, Kim YS, Nam JH, Kim HJ, Kim JW, et al. A nomogram predicting the risks of distant metastasis following postoperative radiotherapy for uterine cervical carcinoma: a Korean radiation oncology group study (KROG 12-08). *Radiother Oncol* (2014) 111(3):437–41. doi: 10.1016/j.radonc.2014.03.025

15. Monk BJ, Wang J, Im S, Stock RJ, Peters WA 3rd, Liu PY, et al. Rethinking the use of radiation and chemotherapy after radical hysterectomy: a clinical-pathologic analysis of a gynecologic oncology Group/Southwest oncology Group/Radiation therapy oncology group trial. *Gynecol Oncol* (2005) 96(3):721–8. doi: 10.1016/j.ygyno.2004.11.007

16. Rotman M, Sedlis A, Piedmonte MR, Bundy B, Lentz SS, Muderspach LI, et al. A phase III randomized trial of postoperative pelvic irradiation in stage IB cervical carcinoma with poor prognostic features: follow-up of a gynecologic oncology group study. *Int J Radiat Oncol Biol Phys* (2006) 65(1):169–76. doi: 10.1016/j.ijrobp.2005.10.019

17. Dindo D, Demartines N, Clavien PA. Classification of surgical complications: a new proposal with evaluation in a cohort of 6336 patients and results of a survey. *Ann Surg* (2004) 240(2):205–13. doi: 10.1097/01.sla.0000133083.54934.ae

18. Sun Z, Huang B, Liu C, Yang Y, Rao Y, Du Y, et al. Comparison of neoadjuvant treatments followed by radical surgery or chemoradiation on quality of life in patients with stage IB2-IIA cervical cancer. *Gynecol Oncol* (2020) 157 (2):536–41. doi: 10.1016/j.ygyno.2020.01.039

19. Cohen PA, Jhingran A, Oaknin A, Denny L. Cervical cancer. *Lancet* (2019) 393(10167):169–82. doi: 10.1016/S0140-6736(18)32470-X

20. Gallardo-Alvarado L, Cantú-de León D, Ramirez-Morales R, Santiago-Concha G, Barquet-Muñoz S, Salcedo-Hernandez R, et al. Tumor histology is an independent prognostic factor in locally advanced cervical carcinoma: A retrospective study. *BMC Cancer* (2022) 22(1):401. doi: 10.1186/s12885-022-09506-3

21. Buskwofie A, David-West G, Clare CA. A review of cervical cancer: Incidence and disparities. *J Natl Med Assoc* (2020) 112(2):229–32. doi: 10.1016/j.jnma.2020.03.002

22. Gaffney DK, Hashibe M, Kepka D, Maurer KA, Werner TL. Too many women are dying from cervix cancer: Problems and solutions. *Gynecol Oncol* (2018) 151(3):547–54. doi: 10.1016/j.ygyno.2018.10.004

23. Datta NR, Stutz E, Gomez S, Bodis S. Efficacy and safety evaluation of the various therapeutic options in locally advanced cervix cancer: A systematic review and network meta-analysis of randomized clinical trials. *Int J Radiat Oncol Biol Phys* (2019) 103(2):411–37. doi: 10.1016/j.ijrobp.2018.09.037

24. Sanna E, Chiappe G, Lavra F, Oppi S, Macciò A. Diagnostic framework of pelvic massive necrosis with peritonitis following chemoradiation for locally advanced cervical cancer: When is the surgery not demandable? a case report and literature review. *Diagnostics (Basel)* (2022) 12(2):440. doi: 10.3390/diagnostics12020440

25. Peters WA 3rd, Liu PY, Barrett RJ 2nd, Stock RJ, Monk BJ, Berek JS, et al. Concurrent chemotherapy and pelvic radiation therapy compared with pelvic radiation therapy alone as adjuvant therapy after radical surgery in high-risk early-

stage cancer of the cervix. *J Clin Oncol* (2000) 18(8):1606–13. doi: 10.1200/JCO.2000.18.8.1606

26. Chemoradiotherapy for Cervical Cancer Meta-analysis Collaboration (CCCMAC). Reducing uncertainties about the effects of chemoradiotherapy for cervical cancer: individual patient data meta-analysis. *Cochrane Database Syst Rev* (2010) 2010(1):Cd008285. doi: 10.1002/14651858

27. Li Z, Yang S, Liu L, Han S. A comparison of concurrent chemoradiotherapy and radiotherapy in Chinese patients with locally advanced cervical carcinoma: a multi-center study. *Radiat Oncol* (2014) 9:212. doi: 10.1186/1748-717X-9-212

28. Choi HJ, Paik ES, Choi CH, Kim TJ, Lee YY, Lee JW, et al. Response to combination chemotherapy with Paclitaxel/Ifosfamide/Platinum versus Paclitaxel/Platinum for patients with metastatic, recurrent, or persistent carcinoma of the uterine cervix: A retrospective analysis. *Int J Gynecol Cancer* (2018) 28(7):1333–41. doi: 10.1097/IGC.0000000000001316

29. Kalaghchi B, Abdi R, Amouzegar-Hashemi F, Esmati E, Alikhasi A. Concurrent chemoradiation with weekly paclitaxel and cisplatin for locally advanced cervical cancer. *Asian Pac J Cancer Prev* (2016) 17(S3):287–91. doi: 10.7314/APJCP.2016.17.S3.287

30. Zou W, Han Y, Zhang Y, Hu C, Feng Y, Zhang H, et al. Neoadjuvant chemotherapy plus surgery versus concurrent chemoradiotherapy in stage IB2-IIB cervical cancer: A systematic review and meta-analysis. *PloS One* (2019) 14(11): e0225264. doi: 10.1371/journal.pone.0225264

31. Tierney JF, Vale C, Symonds P. Concomitant and neoadjuvant chemotherapy for cervical cancer. *Clin Oncol (R Coll Radiol)* (2008) 20(6):401–16. doi: 10.1016/j.clon.2008.04.003

32. Deng T, Gu S, Wu J, Yu Y. Comparison of platinum monotherapy with concurrent chemoradiation therapy versus platinum-based dual drug therapy with concurrent chemoradiation therapy for locally advanced cervical cancer: a systematic review and meta-analysis. *Infect Agent Cancer* (2022) 17(1):18. doi: 10.1186/s13027-022-00433-3

33. Bouvard V, Wentzensen N, Mackie A, Berkhof J, Brotherton J, Giorgi-Rossi P, et al. The IARC perspective on cervical cancer screening. *N Engl J Med* (2021) 385(20):1908–18. doi: 10.1056/NEJMsr2030640

34. Li S, Hu T, Lv W, Zhou H, Li X, Yang R, et al. Changes in prevalence and clinical characteristics of cervical cancer in the people's republic of China: a study of 10,012 cases from a nationwide working group. *Oncologist* (2013) 18(10):1101–7. doi: 10.1634/theoncologist.2013-0123

35. Ceccaroni M, Roviglione G, Malzoni M, Cosentino F , Spagnolo E, Clarizia R, et al. Total laparoscopic vs. conventional open abdominal nerve-sparing radical hysterectomy: clinical, surgical, oncological and functional outcomes in 301 patients with cervical cancer. *J Gynecol Oncol* (2021) 32(1):e10. doi: 10.3802/jgo.2021.32.e10

36. Kohut AY, Kuhn T, Conrad LB, Chua KJ, Abuelafiya M, Gordon AN, et al. Thirty-day postoperative adverse events in minimally invasive versus open abdominal radical hysterectomy for early-stage cervical cancer. *J Minim Invasive Gynecol* (2022) 29(7):840–7. doi: 10.1016/j.jmig.2022.03.014

37. Nitecki R, Ramirez PT, Frumovitz M, Krause KJ, Tergas AI, Wright JD, et al. Survival after minimally invasive vs open radical hysterectomy for early-stage cervical cancer: A systematic review and meta-analysis. *JAMA Oncol* (2020) 6 (7):1019–27. doi: 10.1001/jamaoncol.2020.1694

38. Melamed A, Margul DJ, Chen L, Keating NL, Del Carmen MG, Yang J, et al. Survival after minimally invasive radical hysterectomy for early-stage cervical cancer. *N Engl J Med* (2018) 379(20):1905–14. doi: 10.1056/NEJMoa1804923

39. Wei WW, Wang H, Zheng H, Chen J, Shi RX. Survival impacts of perineural invasion on patients under different radical hysterectomies due to early cervical cancer. *Front Oncol* (2022) 12:889862. doi: 10.3389/fonc.2022.889862

40. Cibula D, Abu-Rustum NR, Benedetti-Panici P, Köhler C, Raspagliesi F, Querleu D, et al. New classification system of radical hysterectomy: emphasis on a three-dimensional anatomic template for parametrial resection. *Gynecol Oncol* (2011) 122(2):264–8. doi: 10.1016/j.ygyno.2011.04.029

41. Bogani G, Rossetti DO, Ditto A, Signorelli M, Martinelli F, Mosca L, et al. Nerve-sparing approach improves outcomes of patients undergoing minimally invasive radical hysterectomy: A systematic review and meta-analysis. *J Minim Invasive Gynecol* (2018) 25(3):402–10. doi: 10.1016/j.jmig.2017.11.014

42. Yang Y, Qin T, Zhang W, Wu Q, Yang A, Xu F. Laparoscopic nerve-sparing radical hysterectomy for bulky cervical cancer (≥6 cm) after neoadjuvant chemotherapy: A multicenter prospective cohort study. *Int J Surg* (2016) 34:35–40. doi: 10.1016/j.ijsu.2016.08.001

43. Ferrandina G, Gallotta V, Federico A, Fanfani F, Ercoli A, Chiantera V, et al. Minimally invasive approaches in locally advanced cervical cancer patients undergoing radical surgery after chemoradiotherapy: A propensity score analysis. *Ann Surg Oncol* (2021) 28(7):3616–26. doi: 10.1245/s10434-020-09302-y

44. Legge F, Chiantera V, Macchia G, Fagotti A, Fanfani F, Ercoli A, et al. Clinical outcome of recurrent locally advanced cervical cancer (LACC) submitted to primary multimodality therapies. *Gynecol Oncol* (2015) 138(1):83–8. doi: 10.1016/j.ygyno.2015.04.035

45. Mezquita G, Muruzabal JC, Perez B, Aguirre S, Villafranca E, Jurado M. Para-aortic plus pelvic lymphadenectomy in locally advanced cervical cancer: A single institutional experience. *Eur J Obstet Gynecol Reprod Biol* (2019) 236:79–83. doi: 10.1016/j.ejogrb.2019.02.033

46. Toure M, Bambara AT, Kouassi KKY, Seka EN, Dia JM, Yao I, et al. Level of concordance of pre-, intra-, and postoperative staging in cervical cancers (TREYA study). *J Oncol* (2017) 2017:8201462. doi: 10.1155/2017/8201462

frontiers | Frontiers in Surgery

TYPE Original Research
PUBLISHED 01 November 2022
DOI 10.3389/fsurg.2022.1013794



OPEN ACCESS

EDITED BY
Jeroen Van Vugt,
Erasmus Medical Center, Netherlands

REVIEWED BY
Armando Rojas,
Catholic University of the Maule, Chile
Filippo Carannante,
Campus Bio-Medico University, Italy

*CORRESPONDENCE
Wenliang Chen
rbchen2015@sina.com

SPECIALTY SECTION
This article was submitted to Surgical Oncology, a section of the journal Frontiers in Surgery

RECEIVED 07 August 2022
ACCEPTED 14 October 2022
PUBLISHED 01 November 2022

CITATION
Bai Z, Bai Y, Fang C and Chen W (2022) Oxidative stress-related patterns determination for establishment of prognostic models, and characteristics of tumor microenvironment infiltration.
Front. Surg. 9:1013794.
doi: 10.3389/fsurg.2022.1013794



# Oxidative stress-related patterns determination for establishment of prognostic models, and characteristics of tumor microenvironment infiltration

Zihao Bai[1], Yihua Bai[1], Changzhong Fang[1] and Wenliang Chen[2]*

[1]Graduate Department, Shanxi Medical University, Taiyuan, China, [2]Department of General Surgery, The 2nd Affiliated Hospital of Shanxi Medical University, Taiyuan, China

Oxidative stress-mediated excessive accumulation of ROS in the body destroys cell homeostasis and participates in various diseases. However, the relationship between oxidative stress-related genes (ORGs) and tumor microenvironment (TME) in gastric cancer remains poorly understood. For improving the treatment strategy of GC, it is necessary to explore the relationship among them. We describe the changes of ORGs in 732 gastric cancer samples from two data sets. The two different molecular subtypes revealed that the changes of ORGs were associated with clinical features, prognosis, and TME. Subsequently, the OE_score was related to RFS, as confirmed by the correlation between OE_score and TME, TMB, MSI, immunotherapy, stem cell analysis, chemotherapeutic drugs, etc. OE_score can be used as an independent predictive marker for the treatment and prognosis of gastric cancer. Further, a Norman diagram was established to improve clinical practicability. Our research showed a potential role of ORGs in clinical features, prognosis, and tumor microenvironment of gastric cancer. Our research findings broaden the understanding of gastric cancer ORGs as a potential target for individualized treatment of gastric cancer and a new direction to evaluate the prognosis.

KEYWORDS

gastric cancer, oxidative stress, tumor microenvironment, microsatellite instability, prognosis

## Introduction

Gastric cancer is the fourth leading cancer with the highest mortality rate globally (1) and a considerable burden on society. In 2020 alone, approx. 760,000 people died of stomach cancer. Surgical treatment, systemic radiotherapy, chemotherapy, immunotherapy, and other therapies have been found beneficial to the treatment of gastric cancer. Still, due to the gastric cancer heterogeneity, the diagnosis is often made at the middle and advanced stage; thus, the therapeutic effect is not particularly effective. Nevertheless, identifying molecular subtypes of gastric cancer based on gene and transcriptome provides a basis for individualized treatment. In addition, the discovery of biomarkers guides immunotherapy and specific drugs treatment of gastric

cancer (2). Oxidative stress can be caused by various reasons, such as ultraviolet radiation, smoking, drinking, intake of non-steroidal anti-inflammatory drugs, etc. Induction of oxidative stress causes ROS accumulation in the body, destroys cell homeostasis, leads to tissue damage, accelerates aging, and then participates in the occurrence of many diseases (3). Oxidative stress is known to play an important role in the occurrence of gastric cancer (4). However, the relationship of oxidative stress with the prognosis of gastric cancer remains largely unclear.

Identifying PD-1/PD-L1 and HER-2 as biomarkers in large cohort studies has helped immensely design the corresponding treatment strategies for clinical application (5). However, such studies are often based on a single biomarker without entirely satisfactory and convincing outcomes (6). Furthermore, previous studies on oxidative stress and gastric cancer have mainly focused on the effect of a single gene or single pathway (7). Thus, there is a growing need to construct a new prognostic marker based on molecular subtypes for the individualized treatment and prognosis of patients with gastric cancer.

In the present study, we aim to establish a scoring model (OE_score), through which patients with GC can be divided into high and low-risk groups for guiding treatment and assessment of prognosis. First, we clustered 732 GC patients based on the genes related to the prognosis of oxidative stress. This clustering revealed the subtypes related to prognosis and immune infiltration of GC. Then, according to the differentially expressed genes (DEGs) identified by these two oxidative stress subtypes, the patients were further divided into two gene subtypes. The model related to oxidative stress was established by the Lasso-Cox method, and thus OE-value was determined. This score was related to many characteristics, such as tumor mutation load, immunotherapy, microsatellite instability, etc. Our findings revealed a potential relationship between oxidative stress, prognosis, immune microenvironment, and immunotherapy response in GC patients. We have identified the potential relationship between oxidative stress and gastric cancer in the current study. In addition, a significant correlation exists between the overall effect of multiple ORGs on GC and the infiltration characteristics of TME. Meanwhile, the OE_score will help guide the individualized treatment of gastric cancer patients besides providing important insights for predicting the response of gastric cancer patients to immunotherapy.

# Methodology

## Acquisition and pre-processing of gastric cancer data resources

The gastric cancer transcriptome data (FPKM value) was downloaded, and corresponding clinical data were obtained from the TCGA official website (https://portal.gdc.cancer.gov/). As the TPM data is considered the same as the transcript from the microarrays (8), after transforming the transcriptomic data into TPM values, the data was merged with the chip data and clinical information of 357 gastric cancer tissues from the "GSE84433" dataset from the Gene Expression Omnibus (GEO) database (https://www.ncbi.nlm.nih.gov/geo/). The background adjustment and quantile normalization of the data were performed as the final data set. The batch effect caused by the non-biotechnology deviation was corrected using the "ComBat" algorithm of the "SVA" package. Patients without complete clinical information were excluded from the data.

## Survival analysis of oxidative stress genes

A total of 608 genes related to oxidative stress were obtained from the Amigo database (http://amigo.geneontology.org/amigo). In addition, 48 genes related to prognosis were screened by the univariate Cox regression and Kaplan-Meier analysis with the "survival" package and "survminer" package. The Log-rank test determined the difference in survival analysis. The adjusted *P*-value by the "LIMMA" package was <.001, indicating the statistical significance of gene for prognosis.

## Consensus clustering and gene set variation analysis (GSVA)

The number and stability of the obtained clusters were determined by the consensus using the clustering algorithm of the "ConsensuClusterPlus" package. Each subgroup after clustering had a certain sample size, and the samples within the group had a certain correlation. In contrast, the correlation between groups decreased after clustering. We used the "GSVA" R package to display and analyze the results of GSVA in a heatmap. The "C2.cp.kegg.v7.4.symbols" data obtained from MSigDB database was used for GSVA. In addition, single-sample gene set enrichment analysis (ssGSEA) was used to determine the level of immune cell infiltration in GC TME and the differences between the subtypes. The grouping effect was determined by principal component analysis (PCA) using the "ggplot2" R package.

## Clinical value of molecular subtypes in GC

The chi-square analysis of age, sex, T, and N stage was performed to obtain clinical information between the two subtypes. In addition, the Kaplan-Meier curve generated by the "survival" and "survminer" R package was used to evaluate the differences in RFS between different subtypes.

## DEG identification and functional annotation

By using the empirical Bayesian method of the "LIMMA" package, we obtained the DEGs. The adjusted *P*-value <0.05 and the fold-change of 1.5 were the screening criteria. We used the "clusterprofiler" R package to analyze the functional enrichment of these DEGs by GO and KEGG to explore the DEGs potential function.

## Construction of the oxidative stress-related prognostic OE_score

By calculating the model score of each patient, the grouping of each sample was obtained, and the corresponding treatment strategy was adopted. First, univariate COX regression was used to screen the DEGs related to the prognosis; then, based on DEGs, the molecular subtypes of GC patients were obtained using the same clustering and acquisition criteria as ORG subtypes. At last, through the "caret" R package, the GC patients were randomly into training ($n = 364$) and test groups ($n = 364$). We used the former to construct oxidative stress-related OE_score. Next, we used DEGs related to prognosis for constructing OE_score and used the "glmnet" R package to reduce the risk of overfitting. Finally, LASSO and multivariate Cox analysis selected the candidate genes to establish OE_score related to prognosis.

The OE_score was calculated as follows:

$$\text{OE\_score} = \Sigma(\text{Expi} * \text{coefi})$$

In the formula, Expi and Coefi represent the expression level of each gene and the corresponding risk coefficient, respectively.

Based on this risk score, the patients were divided into high and low-risk groups according to the median score, and the prognosis was analyzed. According to the median risk score obtained from the training set, the total and the test set were divided into two subgroups, and the Kaplan-Meier survival analysis was carried out. The Log-rank test determined the difference in survival analysis. OE_score was evaluated by generating the receiver operating characteristic (ROC) curve, survival status, and risk scores distribution.

## Independence analysis and applicability of OE_score

Univariate and multivariate COX regression analysis was used to study the independence of OE_score. In addition, a stratified analysis was conducted according to the clinical characteristics of GC patients to determine the predictability of OE_score in different clinical groups.

## Determination of characteristic value of immunotherapy in OE_score-related subtypes

To obtain the difference of immune infiltration of subtypes, the CIBERSORT algorithm was used to quantify the score and infiltration of tumor-infiltrating immune cells in GC TME. The relationship between these 22 immune cells and the genes involved in constructing OE_score were explored. The ESTIMATE algorithm was used to calculate each patient's immune, stromal, and total scores. Further, the risk score was correlated with these scores. In addition, the relationship between these two risk groups and microsatellite instability (MSI), cancer stem cell (CSC), and tumor mutation load (TMB) was assessed. Finally, a boxplot was constructed to show the difference between the two groups of patients to determine the immunotherapeutic value of OE_score.

## Somatic mutation and analysis of chemotherapeutic drugs

The "maftools" R packet was used to process the mutation annotation format (MAF) obtained from the TCGA database to determine the similarities and differences of somatic mutations in GC patients between risk score subgroups. To treat patients in the scoring subgroup more effectively, we used a boxplot to visually present the semi-inhibitory concentration (IC50) value of chemotherapeutic drugs. These drugs concentration used to treat GC were calculated through the "pRRophetic" package, where a lower IC50 value depicts a more favorable chemotherapy regimen.

## Building a predictive nomogram

Based on the results of independent prognostic analysis, a predictive nomogram was built using clinical features and risk scores through the "rms" package. In the predictive line chart, the participating score variables of each sample match a score, and the total score obtained by each score can directly predict the 1-, 3-, and 5-year survival rate of the current sample (9). The calibration map of the predicted line chart was used to compare the gap between the predicted 1-, 3-, and 5-year ideal value and the real value to intuitively evaluate the prediction effect of the forecast line chart.

## Statistical analyses

All statistical analyses were carried out using the R version 4.0.3. The statistical significance was set as $P < 0.05$.

# Results

## Prognostic genes of ORGs in STAD

The analysis process of this study is shown in Figure S1. To explore the role of ORGs in GC, we integrated the TCGA STAD dataset with the expressive data. In contrast, the survival information from the GEO dataset was used to create a new dataset containing 732 samples for further analysis. The details of 732 patients with GC are shown in Supplementary Table S1. Using univariate Cox regression and Kaplan-Meier analysis, 48 ORGs were associated with the prognosis of GC patients. The expression of these genes is shown in Supplementary Table S2, and $P < 0.001$ was selected as the screening threshold.

## Expression of ORGs in STAD

We first used the TCGA STAD dataset to study the differences in the expression of 48 prognosis-related ORGs between STAD and normal gastric tissues. In STAD, a total of 28 ORGs expressions were found to be up-regulated or down-regulated. More specifically, in the STAD group, the expression of RCAN1, IL1A, ALDH3B1, EZH2, EPAS1, PXDN, UCP3, PDGFRB, COL1A1, DHFR, GPX1, AIFM1, JAK2, HYAL2, EDNRA, GCH1, and NOS3 increased, while the expression of NR4A3, CD36, MSRB3, SOD3, CRYAB, SNCA, APOD, BNIP3, SCARA3, GPX3, and PRKAA2 were decreased (Figure 1A, $P < 0.05$). We also constructed a prognostic network map to directly identify the regulatory relationship between these ORGs (Figure 1B, $P < 0.0000001$).

## Genetic changes and ORGs expression in STAD

The incidence of copy number variation (SNV) and somatic mutation of 48 ORGs in STAD was summarized. As shown in Figure 1C, 132 (30.48%) of the 433 samples showed gene mutations. Among them, PXDN mutation frequency was the highest. In addition, we did not find any SNCA or DHFR mutations in any of the GC samples. T > A was the most common SNV type. Figure 1D shows the CNV changes on the chromosomes of the 48 ORGs. The frequency of CNV changes revealed that the 48 ORGs had general CNV changes. The amplification of CNV was mainly seen in APOD, while the loss of copy number mainly occurred in EZH2 and NOS3 (Figure 1E). Combined with the expression of mRNA of genes with obvious changes in CNV, the expression of APOD and MSRB3 was amplified by CNV decreased in GC, while the expression of ORGs amplified by CNV such as EZH2, NOS3, and DHFR was found to be increased in GC. The finding suggests that the change of CNV might be involved in the regulation of mRNA expression in ORGs. However, some genes amplified by CNV, such as HSPA1A, PRKD1, and other genes, did not differ in mRNA expression between the tumor and the normal group. This observation suggests that the change of CNV may be only one of the many factors that regulate the expression of mRNA of ORGs. While there are more factors such as RNA methylation, miRNA, lncRNA, and others that affect the expression of mRNA (10, 11). Our analysis showed significant differences in ORGs between the STAD and normal samples regarding genetic landscape or expression level. This data suggest that the overall effect of oxidative stress-related genes can affect the occurrence and development of GC. In addition, it might change the prognosis of patients by affecting somatic mutation and CNV.

## Identification of GC classification pattern mediated by 48 ORGs

Based on the expression levels of 48 ORGs related to prognosis, two ORGs were identified related to GC subtypes, including 292 cases in ORGs cluster group A and 440 cases in ORGs cluster group B (Figure 2A). The Kaplan-Meier curve revealed that the survival advantage of group B was significantly higher than group A (log-rank test, $P < 0.001$, Figure 2B). The PCA analysis revealed that these two subtypes could be distinguished significantly based on the expression of ORGs (Figure 2C). Heatmap arrangement showed that most of the genes were highly expressed in group A. Specifically, TPM1, PKD2, PRNP, PDGFRB, and GPX7 were significantly expressed in almost all the samples in group A, while SMPD3 and EZH2 were highly expressed in group B (Figure 2D). According to the GSVA, group B was significantly enriched in alanine, aspartate and glutamate metabolism, aminoacyl-tRNA biosynthesis, pyrimidine metabolism, DNA replication, base excision repair, and other pathways. In contrast, the group was significantly enriched in focal adhesion, ECM receptor interaction, dilated cardiomyopathy, hypertrophic cardiomyopathy (HCM), TGF beta signaling pathway, and calcium signaling pathway (Figure 2E). The enrichment of several extracellular matrix-related pathways suggests that oxidative stress may be related to the prognosis of patients by changing the content and composition of the matrix.

## Differences in TME infiltration characteristics between the two subtypes

The difference analysis of immune cells revealed that the expression of Type 17 T helper cell, Neutrophil, CD56dim

10.3389/fsurg.2022.1013794

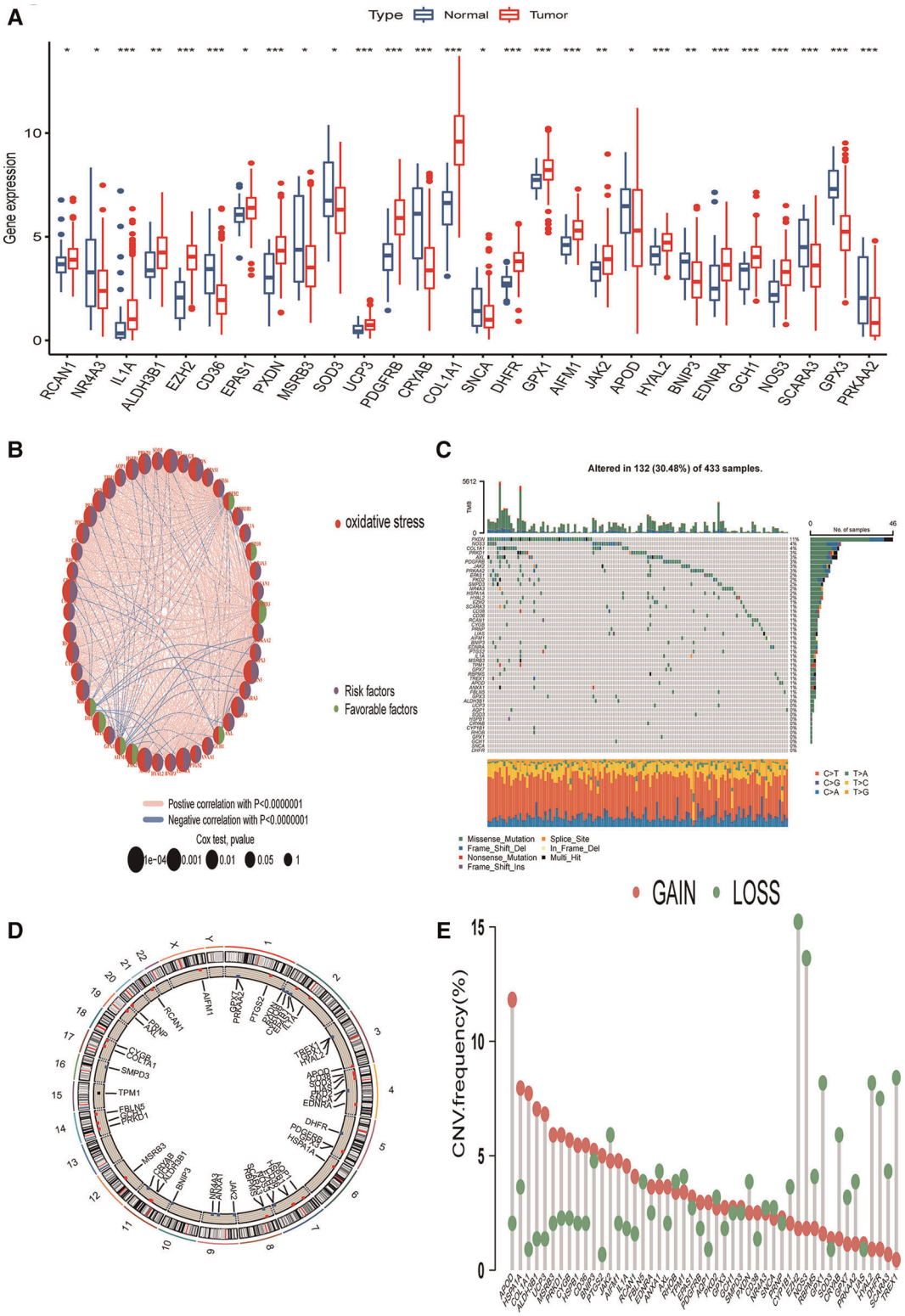


FIGURE 1
Genetic changes and ORGs gene expression in STAD. (**A**) Differentially expressed genes of ORGs in STAD issues and Normal tissues. (**B**) Interaction relationship of 48 ORGs in STAD. (**C**) Mutation type and mutation frequency of ORGs in STAD. (**D**) The location of ORGs in chromosomes. (**E**) The change of CNV of ORGs in the STAD cohort. ORGs, oxidative stress-related genes; STAD, stomach adenocarcinoma; CNV, copy number variant.

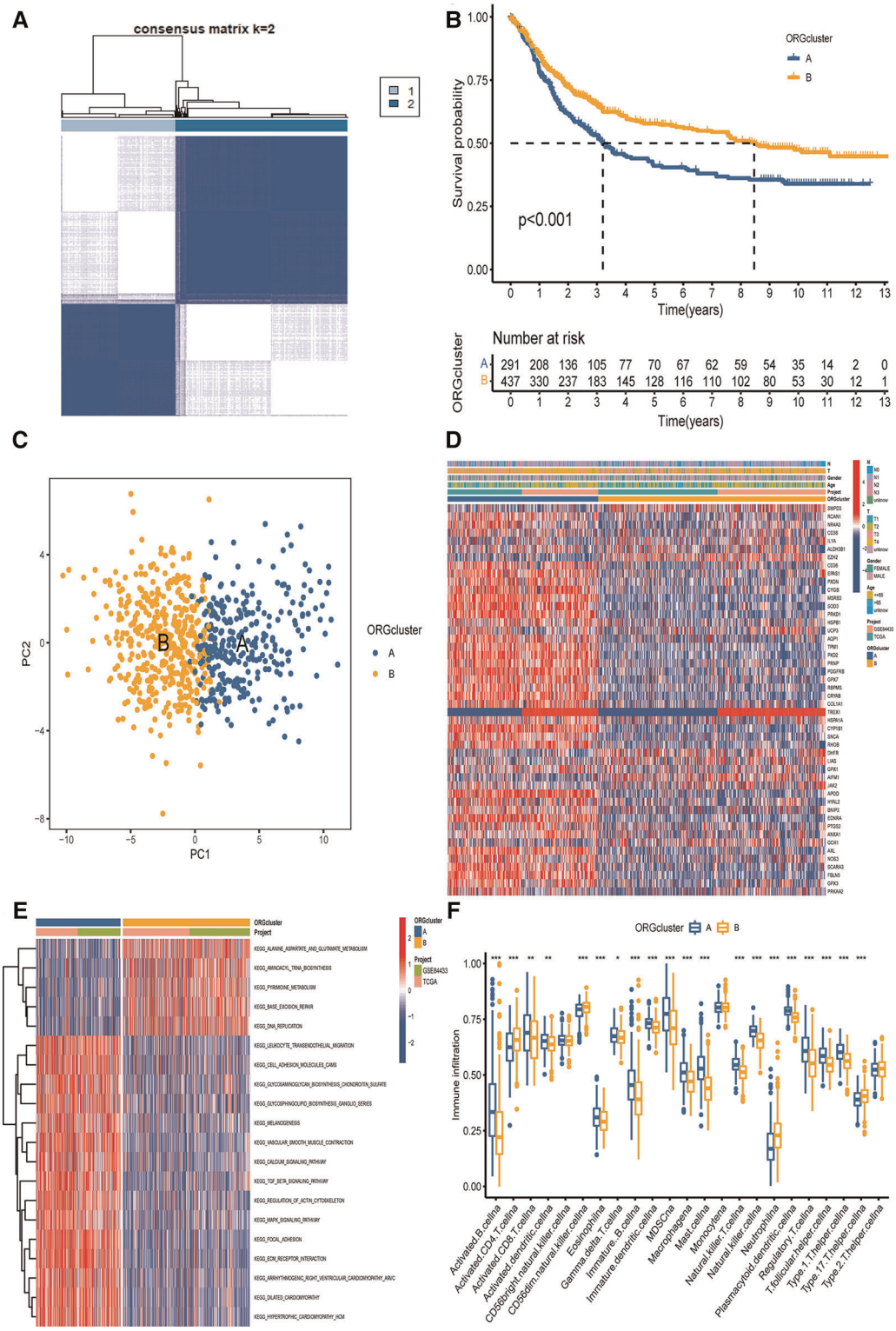


FIGURE 2
The determination of ORGcluster and the study of subtype function. (**A**) The patients with QC were divided into 292 cases in ORGcluster A and 440 cases in ORGcluster B by clustering algorithm. (**B**) PCA analysis of ORGcluster subtypes. (**C**) Differences in survival of ORGcluster subtypes. (**D**) Differences in clinical characteristics and gene expression of ORGcluster subtypes. (**E**) Study on the function of ORGs by GSVA. (**F**) Study on the difference of immune infiltrating cells of ORGcluster subtypes ORGcluster, the cluster of oxidative stress-related genes; GC, gastric cancer; PCA, principal components analysis; GSVA, gene set variation analysis.

natural killer cell, activated CD4 T cell was significantly higher in group B (Figure 2F). Furthermore, a significant difference was observed in the characteristics of TME cell infiltration between the two groups. T cells were associated with the infiltration of myeloid cells, making group B close to the immune-inflamed phenotype, while group A was more similar to the immune–excluded phenotype (12). In addition, these 48 ORGs can well distinguish the two subtypes.

## Acquisition of DEGs and determination of two gene clustering subtypes

To better develop the clinical significance of two types of gastric cancer and develop an appropriate model for gastric cancer patients scoring, we explored the differential genes between the two subtypes and a specific genetic feature. We quantified the gene signature to apply it to the individualized treatment for GC patients. First, to identify the function of each oxidative stress mode, by analyzing the difference between the two subtypes, we obtained 1,358 DEGs related to oxidative stress subtypes. Then, we analyzed these genes using GO and KEGG databases. Our analysis revealed that related genes were significantly enriched in extracellular matrix-related biological processes, while in KEGG analysis, more genes were enriched in focal adhesion pathways (Figures 3A,B). Further, we screened out 593 genes that could be regarded as independent prognostic markers by univariate COX regression (adjusted $P$-value <0.05).

We used these 593 differential genes related to prognosis to construct the gene typing of patients with GC. The unsupervised clustering method identified two GC gene subtypes, including 236 cases in group A and 496 cases in group B (Figure 3C). The survival advantage of group B was significantly higher than group A (Figure 3D). The heatmap arrangement showed that almost all the genes involved in the grouping construction were highly expressed in group A (Figure 3E). Comparing the differential genes between the two groups showed that 43 of the genes involved in ORGs grouping were differentially expressed in gene grouping (Figure 3F).

## Construction of ORGs model

OE_score was established according to the oxidative stress-related DEGs. The data set was randomly divided into a training and a test set with 364 cases. We used the Lasso-Cox regression model to establish a characteristic score related to oxidative stress involving seven genes, named "OE_score".

OE_score = (0.1378* expression of SLCO2A1) + (0.1025* expression of SHISA2) + (0.1034* expression of SERPINE1) + (−0.1752* expression of SMPD3) + (0.0727* expression of GPC3) + (0.0913* expression of CRABP2) + (−0.0856* expression of C1QTNF5).

Further, we determined the value of OE_score by predicting the prognosis of patients. We divided the training patients into the high- and low-risk groups based on the median OE_score (0.949). The low-risk group had an obvious survival advantage (Figure 4B; $P < 0.001$). The low-risk group with the test and the total set had a better prognosis(Figures 4C,D; $P < 0.001$). The consistent distribution of risk scores with survival status indicated the general value of OE_score(Figures 4E–G). The test, training, and total set of these seven genes were expressed, as shown in Figures 4E–G. Meanwhile, the risk scores of ORGs typing and genotyping in group A were higher than group B (Figures 4H,I); this suggests that the subtypes with poor prognosis showed higher risk scores. There may be a correlation between OE_score and immune infiltration expression combined with prognostic analysis and immune infiltration. Therefore, next, we specifically analyzed the immune expression patterns and characteristics of OE_score. Further, our data revealed that OE_score was a good indicator for predicting 1 -, 3- and 5-year survival rates in patients with gastric cancer (Figures 5A–C). In addition, by incorporating the OE_score into the stratified analysis of clinical features, the score had good predictive ability in high and low age groups, different gender groups, and early and late T stage groups (Figures 5D–I). Thus, the OE_score could be used as a promising index to evaluate the prognosis of patients with gastric cancer. Figure 4A illustrates the survival state and distribution of the sample in two ORGcluster, two gene clusters, and high and low-risk groups.

## Building a predictive nomogram

Combined with clinicopathological features and OE_score, a predictive nomogram is essential for clinical intuitive survival probability. The predictive nomogram was established by using independent factors affecting the prognosis of patients with gastric cancer, such as age, T stage, N stage, OE_score, and non-independent factors such as gender (Figures 5J,K, 6A). With the calibration chart, compared with the ideal model, the 3- and 5-year survival rates can be better predicted and applied in the clinic by combining the predictive nomogram of OE_score (Figure 6B). Furthermore, the good prediction of the survival of patients by predictive nomogram showed the rationality of constructing the OE_score, which is helpful to evaluate the prognosis of patients with GC.

## Relationship between ORG-related OE_score and immunotherapy in STAD

Oxidative stress plays a unique and important role in creating and maintaining the tumor immune microenvironment. Therefore, we decided to study the guiding value of OE_score

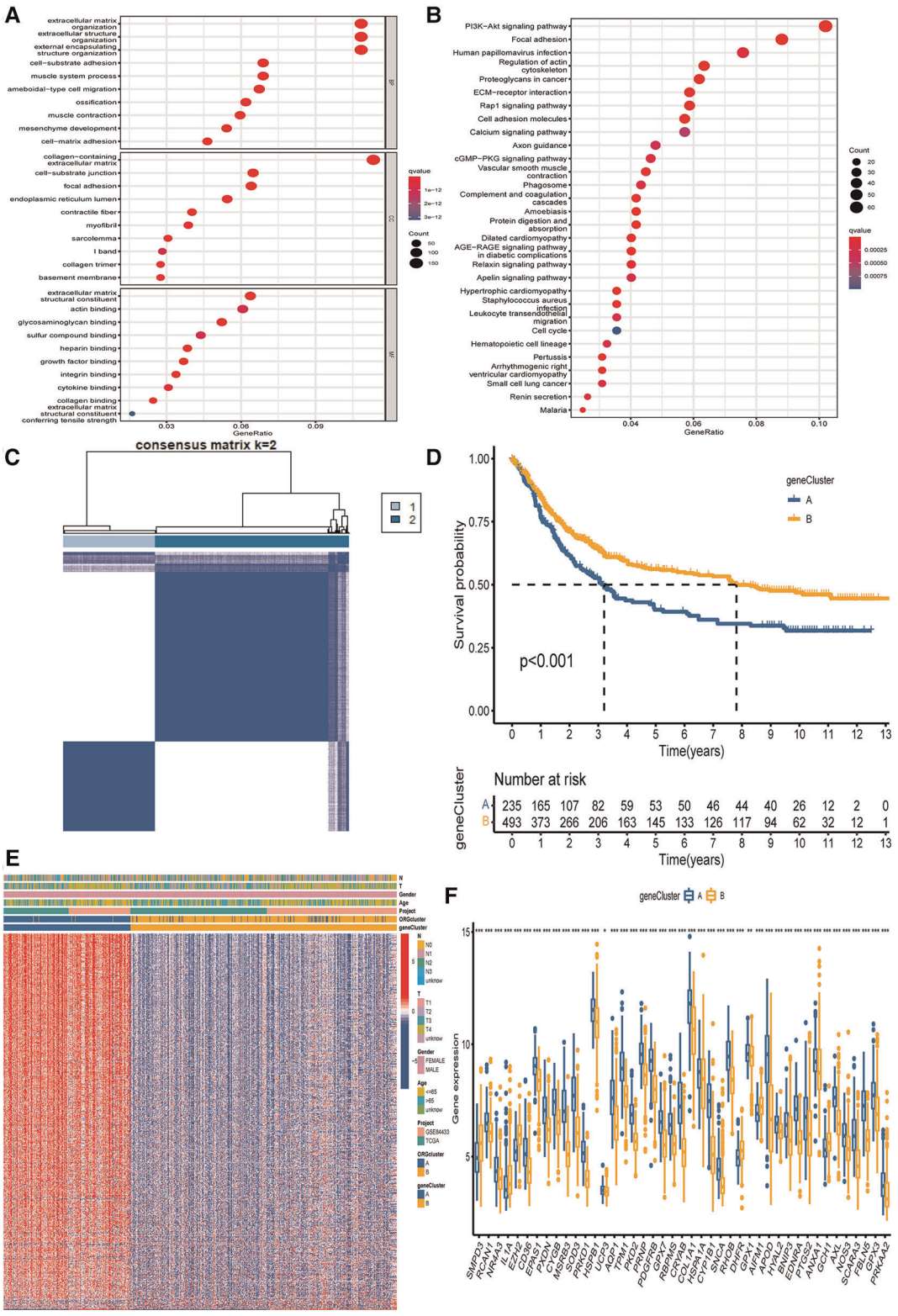


FIGURE 3
The determination of genecluster and the study of subtype function. (**A**,**B**) GO and KEGG on the enrichment of DEGs in difference pathways. (**C**) The clustering results of genecluster were divided into subtype A ($n$ = 236) and subtype B ($n$ = 496). (**D**) Survival analysis results of gene subtypes. (**E**) The difference in the expression of genes involved in the construction of the model between the two subtypes. (**F**) 43 genes involved in ORGcluster also showed differential expression in genecluster. GO, Gene Ontology; KEGG, Kyoto Encyclopedia of Genes and Genomes; DEGs, differentially expressed genes; ORGs, oxidative stress-related genes.

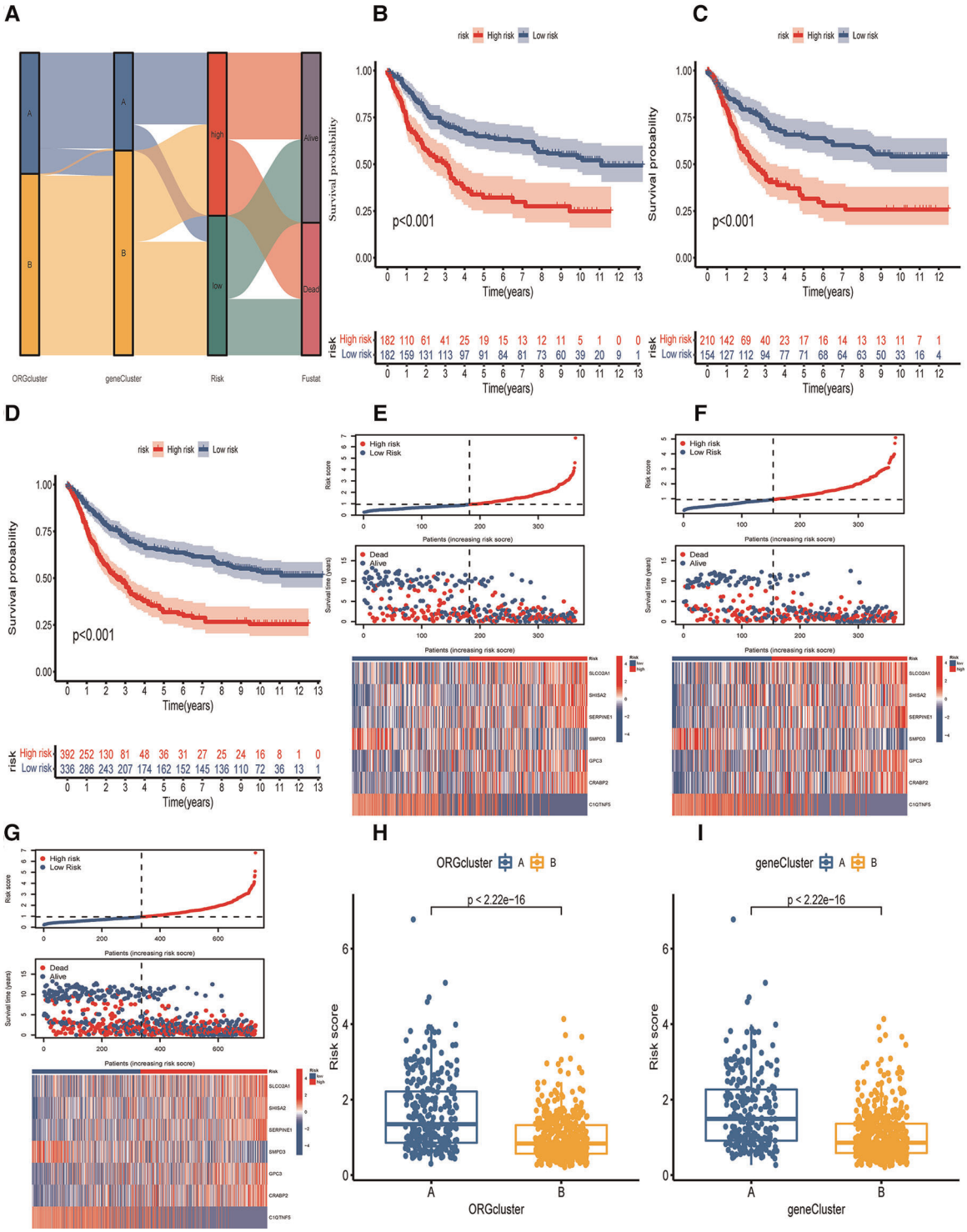


FIGURE 4
Survival analysis or OE_score in training set, test set and total data set. (**A**) Alluvial diagram of the distribution of the survival state of the samples of ORGcluster, genecluster and OE_score subgroups. (**B**) Survival differences between the two subgroups of the training group. (**C**) survival differences between the two subgroups of the test group. (**D**) Survival differences between the two subgroups of the total data set. (**E**) The risk score distribution and survival status in the training group, and the gene expression involved in the construction of OE_score. (**F**) The risk score distribution and survival status in the test, and the gene expression involved in the construction of OE_score. (**G**) The risk score distribution and survival status of the total data set, and participate in the construction of gene express of OE_score. (**H**,**I**) The difference of OE_score between ORGcluster and genecluster subgroups.

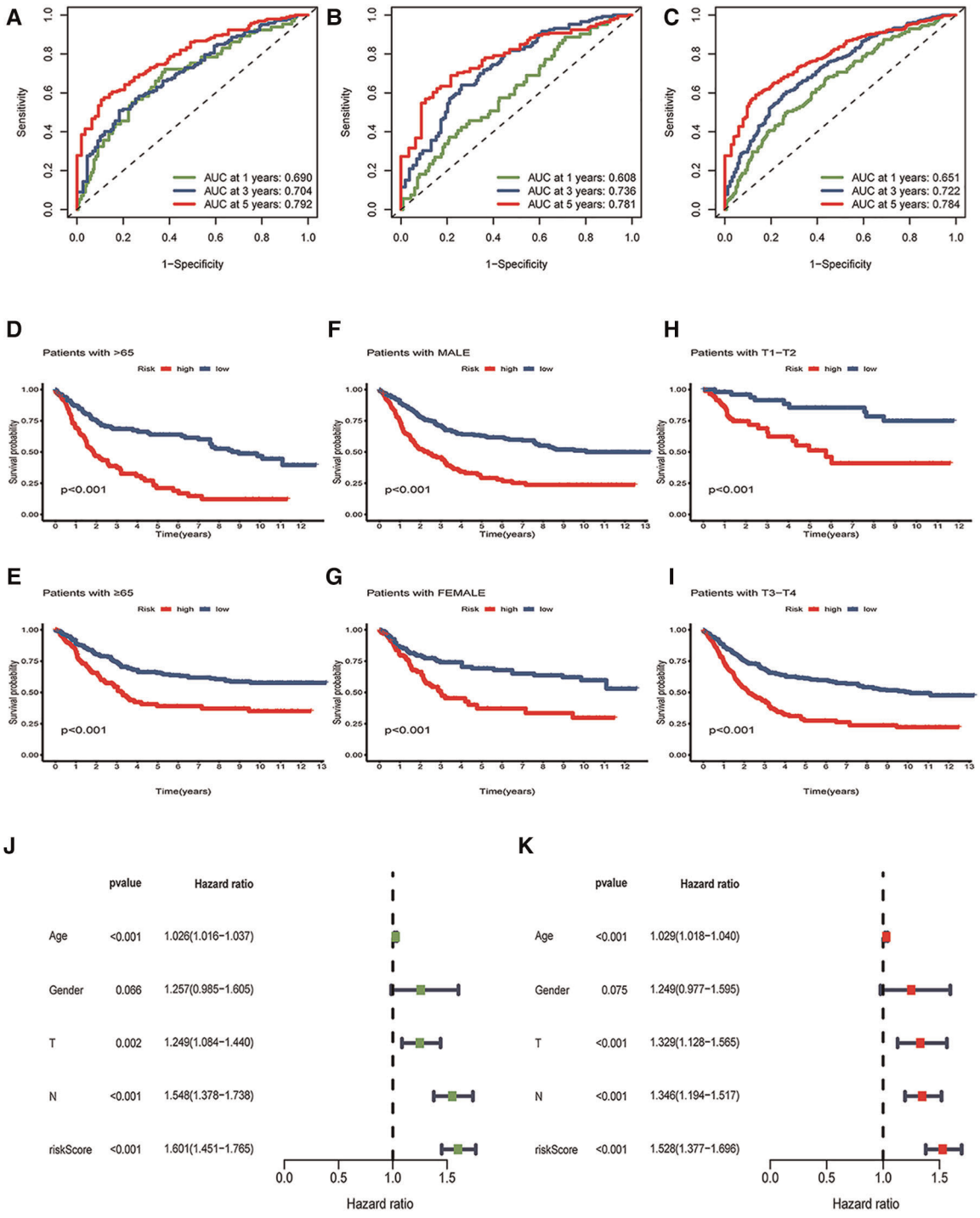


FIGURE 5
Independence analysis and hierarchical analysis of OE_score. (A) Using ROC curve to predict the sensitivity and specificity of 1-, 3-and 5-year survival rates based on OE_score in the training set. (B) Using the ROC curve, the sensitivity and specificity of predicting 1-, 3-and 5-year survival rates based on OE_score in the test set. (C) Using the ROC curve, the sensitivity and specificity of OE_score in predicting 1-, 3-and 5-year survival rates in the total data set. (D–I) Survival analysis of OE_score in high and low age groups, different gender groups and early and late T stage groups. ROC, receiver operating characteristic. (J) Univariate Cox regression analysis was used to determine that OE_score could be used as an independent factor affecting the prognosis of patients with gastric canser. (K) Multivariate Cox regression analysis was used to determine that OE_score could be used as an independent factor affecting the prognosis of patients with gastric cancer.

10.3389/fsurg.2022.1013794

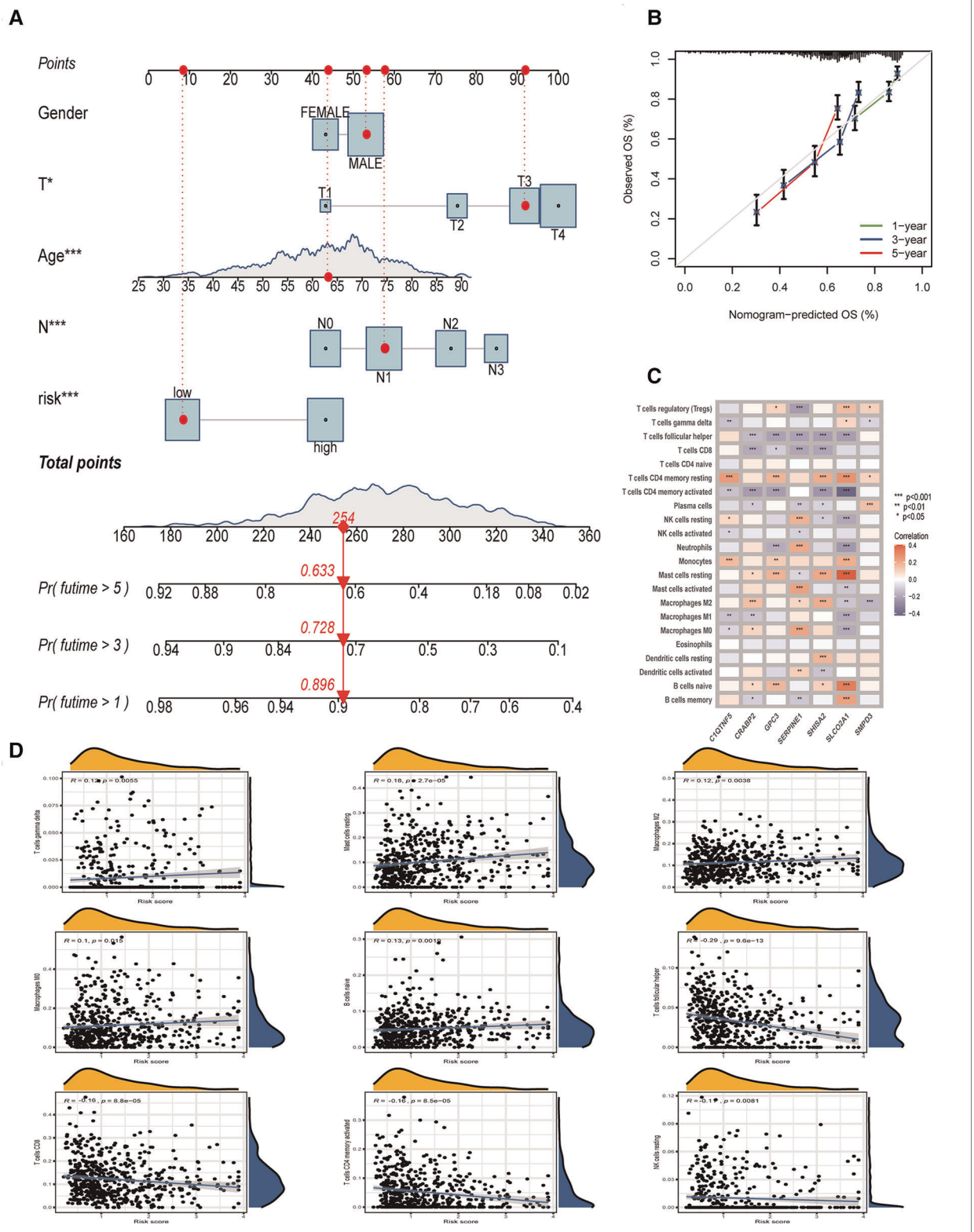


FIGURE 6
The establishment of nomogram, and the relationship between OE_score and tumor immune microenvironment. (A) Nomogram based on OE_score and other clinical factors to predict 1-, 3-and 5-year survival rates in patients with gastric cancer. (B) The calibration plot of the nomogram. (C) The relationship between the genes involved in the construction of OE_score and the expression of immune infiltrating cells. (D) The correlation between OE_score and immune infiltrating cells.

for clinical treatment, especially immunotherapy. By analyzing the expression of genes involved in OE_score and immune infiltrating cells, we found that SERPINE1, SHISA2, and SLCO2A1 were strongly correlated with the expression of most immune infiltrating cells (**Figure 6C**). These genes might have caused the difference in immune characteristics of OE_score groups. In exploring and analyzing the relationship between OE_score and immune cells, a positive correlation was observed between OE_score and the abundance of T cells gamma delta ($R = 0.12$, $P = 0.0055$), Mast cells resting ($R = 0.18$, $P = 2.7 \times 10^{-5}$), Macrophages M2 ($R = 0.12$, $P = 0.0038$), Macrophages M0 ($R = 0.1$, $P = 0.015$) and B cells naive ($R = 0.13$, $P = 0.0019$). However, OE_score and the abundance of T cells follicular helper ($R = -0.29$,$P = 9.6 \times 10^{-13}$), T cells CD8 ($R = -0.16$, $P = 8.8 \times 10^{-5}$), T cells CD4 memory activated ($R = -0.16$, $P = 8.5 \times 10^{-5}$) and NK cells resting ($R = -0.11$, $P = 0.0081$) had the contrary result (**Figure 6D**). Tumors that attract more T cell infiltration are called "hot tumors" and are more sensitive to immunotherapy with better immunotherapeutic effects (13). The negative correlation between OE_score and multiple T cell infiltration suggests that the low-risk group might be close to our definition of "hot tumors" and was more suitable for immunotherapy to treat and delay the disease progression. Meanwhile, these data show a significant correlation between ORGs and tumor immune infiltration. The ESTIMATE algorithm (14) showed that the matrix score increased gradually with the increase of OE_score, while the tumor purity showed a contrasting effect. Still, no significant difference was found in the immune scores between the two groups (**Figure 7A**). The importance of stromal cells was reflected in all aspects of tumors, such as tumor growth, disease progression, and drug resistance (15–17). This suggests that our two subtypes had the GC heterogeneity through the difference of TME cells, thus affecting the outcome of treatment and prognosis.

Several studies have reported that TMB is a new biomarker for assessing the sensitivity of immune checkpoint inhibitors (18). In the present study, we found differences in TMB among different OE_score. The lower group had higher TMB, which indicated that the response to immunotherapy was better (**Figure 7B**). There was a negative correlation between OE_score and TMB ($P = 3.7 \times 10^{-14}$, **Figure 7C**). According to the waterfall chart, up to 94.92% of the 59 samples in the low-risk group had TMB, in which TTN and ARID1A had mutations in 50% of the samples, where missense mutations and multi-hit were the most common types of mutations. Among the 303 samples in the high-risk group, 86.8% had TMB, TTN, and TP53, with the highest probability of mutation (43%). The vast majority of mutation types were missense mutations. TP53 is an important gene involved in oxidative stress (19). The TP53 mutation rate (31%) in the low-risk group was lower than the high-risk group with a poor prognosis (**Figures 7D,E**). MSI is also considered a predictive biomarker of cancer immunotherapy (20). Patients with gastric cancer characterized by MSI-H tend to be more sensitive to immunotherapy, more suitable for related treatments, and exhibit a better prognosis (21). The patients in the low-risk group were characterized by MSI-H, while the patients in the high-risk group tended to show MSS (**Figures 7F,G**). One of the characteristics of MSI-H gastric tumors is the high level of $CD8^+$ T cell infiltration (22). This observation was consistent with our analysis, which might explain the effectiveness of immunosuppressive therapy at checkpoints in patients with MSI-H gastric cancer. Furthermore, we investigated the potential correlation of OE_score and CSC in gastric cancer. **Figure 7H** shows that OE_score was significantly negatively correlated with CSC index ($R = -0.57$, $P < 2.2 \times 10^{-16}$), suggesting that patients with low-risk scores had more obvious stem cell characteristics and low cell differentiation characteristics. Next, to explore the difference in the efficacy of chemotherapy drugs in the two groups of patients, the chemotherapy drugs currently used for the treatment of gastric cancer were used to explore the drug sensitivity related to OE_score. Interestingly, patients with high OE_score had lower IC50 values for Temsirolimus, Pazopanib, Elesclomol, and Dasatinib, while chemotherapeutic drugs Paclitaxel, Etoposide, Vinorelbine, and Mitomycin C had significantly lower IC50 values in patients with low OE_score (**Figures 7I–P**). Taken together, these results suggest that ORGs are associated with drug sensitivity. The analysis of OE_score based on ORGs, immune infiltration, and immunotherapy confirms that OE_score has a certain application value for assessing the effect of GC patients on immunotherapy. Moreover, it has potential significance for selecting treatment methods and assessing the prognosis results of GC patients.

## Discussion

Oxidative stress plays an important role in inflammation and tumor regulation (23); however, the TME and gastric cancer prognostic analysis remains unclear. The overall effect of multiple ORGs on GC and the characteristics of TME infiltration has not been elucidated. This study showed a correlation between the genetic landscape and the transcriptional level of ORGs in GC patients. Based on these 48 ORGs related to prognosis, we obtained two subtypes of ORGs with different clinical characteristics. The clinical features of type A were more obvious, with a worse prognosis. We obtained two gene subtypes based on the DEGs of two ORGs clusters. Our results showed that the ORGs might be an independent predictor of clinical outcome and immunotherapy response in GC. Based on this observation, an accurate and effective prognosis OE_score was constructed, proving its predictive ability. The oxidative stress patterns

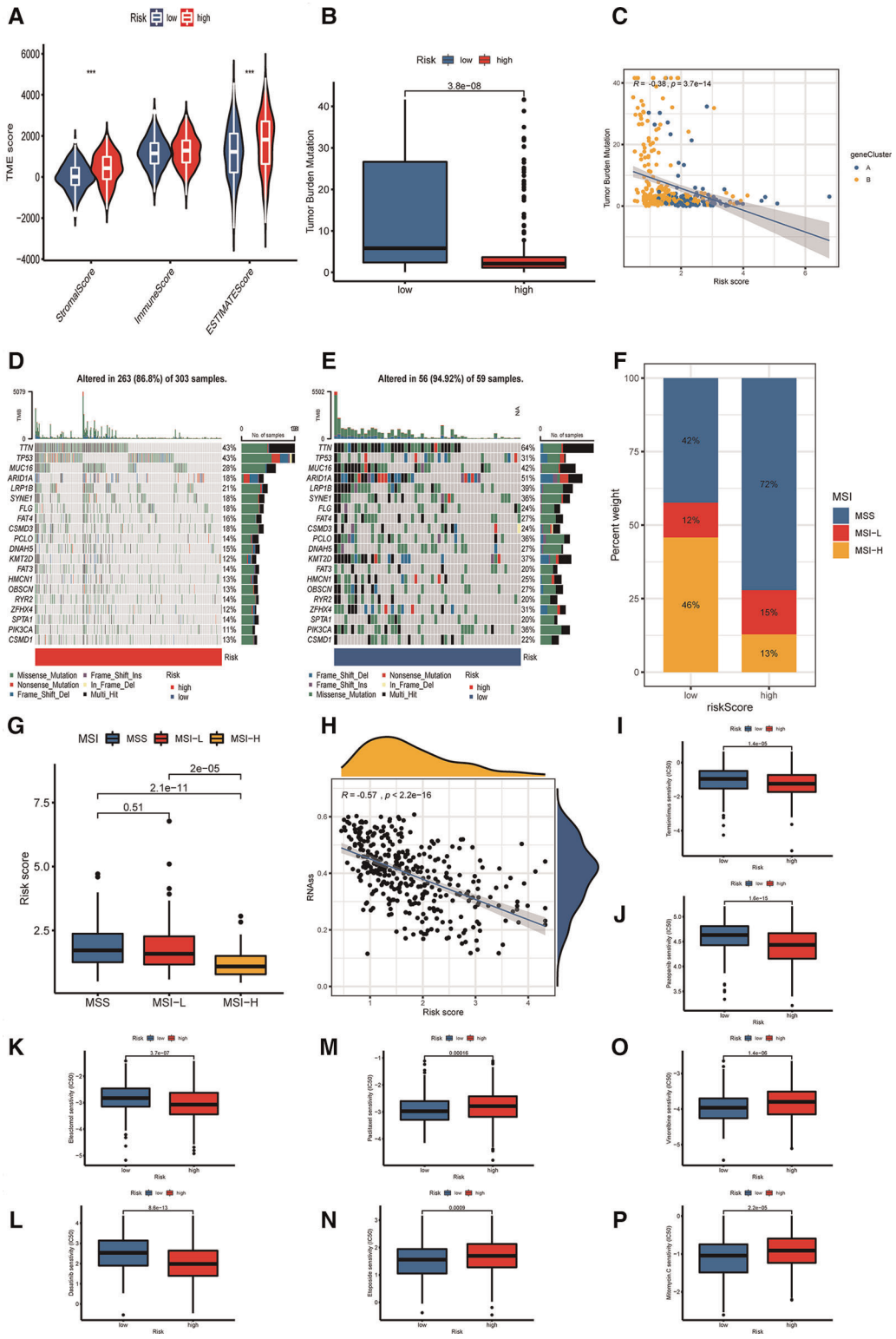


FIGURE 7
The relationship between OE_score and immunotherapy. (**A**) The correlation between the two OE_score-related subtypes and the TME score. (**B**,**C**) The correlation between OE_score and TMB. (**D**,**E**) OE_score high-risk and low-risk groups about the waterfall plot of TMB. (**F**,**G**) The correlation between OE_score and MSI. (**H**) the correlation between OE_score and CSC. (**I**–**P**) Sensitivity of patients with high and low risk of OE_score to various chemotherapautic drugs. TME, tumor microenvironment; TMB, tumor mutation burden; MSI, microsatelllite instability; CSC, cancer stem cell.

related to the occurrence and development of many diseases can be classified into high and low OE_score groups with different characteristics. Notably, there were significant differences in clinical characteristics, prognosis, mutation, TME, immune checkpoint, MSI, CSC index, and drug sensitivity between low-risk and high-risk patients with OE_score. Finally, we combined OE_score with tumor clinical characteristics to establish a quantitative nomogram, making OE_score widely used with a much easier approach. Through this score, we could directly predict the prognosis of patients, understand the occurrence and mechanism for the development of gastric cancer, and provide direct evidence for the treatment.

Although immunotherapy wide used to treat cancer patients has improved the survival rate in advanced stages (III/ IV stage patients). Still, a large number of patients show low responses to immunotherapy. These tumors generally lack lymphocyte infiltration in their microenvironment are often called "cold tumors" (24). Identifying these types of tumors and adopting corresponding treatment strategies might help decide the individualized treatment of tumors in these patients. A significant negative correlation was observed between OE_score and T cells follicular helper, T cells CD8, T cells CD4 memory activated, and NK cells resting. Of note, more $CD8^+$ T cells were expressed in the low-risk group. In a previous phase II trial of pembrolizumab, the $CD8^+$ T cells were associated with the resistance to PD-1 in MSI-H gastric cancer (25). With the increase of $CD8^+$ T cells, patients showed a better therapeutic effect. This observation was consistent with a better prognosis in the low-risk group of OE_score with high-MSI-H and high $CD8^+$ T cell infiltration. In routine clinical practice, there is a lack of peripheral markers analysis to reflect the efficacy of immunotherapy. The OE_score based on the variety of tumor immune infiltrating cells can determine which patients benefit more from immunotherapy. At the same time, a correlation was observed between peripheral immune cells and MSI, PD-1-related therapy.

The $\gamma\delta$T cells, a T cell subtype involved in the innate immune system, usually are double negative for CD4 and CD8 (26). This cell accounts for less than 5% of peripheral blood T cells and is associated with various inflammation and tumors (27, 28). In the study by Donnele Daley et al. (29), human pancreatic ductal adenocarcinoma (PDA) infiltrating $\gamma\delta$T cells were the main regulatory cells for $\alpha\beta$T cell activation. When $\gamma\delta$T cells are absent, many TH1 cells and $CD8^+$ T cells enter into TME and play an immune role. However, little is known about the interaction of $\gamma\delta$T cells with gastric tumors. However, a positive correlation was found between OE_score and $\gamma\delta$T cells. The differences in prognosis of high-risk and low-risk groups suggest that a large number of $\gamma\delta$T cells might be the reason for poor prognosis in high-risk groups. Moreover, $\gamma\delta$T cells can be used as a therapeutic direction for the outcome of the immunotherapy group. The $\gamma\delta$T cells have been used for the preparation of CAR-T and found therapeutically superior from the CAR-T prepared by $\alpha\beta$T cells (30).

Macrophages are one of the most important inflammatory cells in the tumor microenvironment. The Macrophages usually are of unpolarized M0 type and polarized classically activated macrophage (M1) and alternatively activated macrophage (M2) types. The infiltration of a large number of macrophages is often associated with the poor prognosis of gastric cancer (31). Therefore, we used macrophages as one of the prognostic markers. In ORGs classification, subtype A with a poor prognosis showed high expression of Macrophages. While a positive correlation was observed between OE_score and Macrophages M0, Macrophages M2. In-concurrence with previous findings, the high-risk group with poor prognosis expressed more Macrophages M0, Macrophages M2. Generally, M2 macrophages are polarized and participate in tissue repair and antiparasitic response (32). However, M2 macrophages exhibit an immunosuppressive effect in the tumor microenvironment, participate in matrix remodeling, and promote tumor growth and metastasis. Chen et al. (33) have found that CHI3L1 secreted by macrophage M2 can promote the metastasis of gastric and breast cancer cells both *in vitro* and *in vivo*. In addition, the expression of TGF-$\beta$ affected the invasion of TAM and then the invasiveness of gastric cancer. PD-1 is also involved in the process of affecting the phagocytosis of macrophages and changing the tumor progression (34, 35). These studies have demonstrated the potential of monitoring Macrophages and their products as a diagnostic marker for gastric cancer. Of note, the use of depleted TAM or the conversion of TAM M2 to TAM M1 has been tried in anticancer therapy (36). This may also be an attempt to treat patients with higher OE_score.

Previous studies have shown that the mesenchymal stromal cells may participate in the polarization of M2 while promoting the metastasis and EMT of gastric cancer (37). Additionally, M2 macrophages are closely related to the extracellular matrix (ECM) and gastric cancer. The GO analysis of ORGs typing showed that the ORG-related subtypes were enriched in the ECM-related pathways. In KEGG, the focal adhesion pathway also had an obvious enrichment. In GSVA, the focal adhesion and ECM receptor interaction were also significant in expression pathways. The ECM is a complex collection of proteins, proteoglycans, and other molecules, while different tissues often have different structures and components. This difference gives functional and biological characteristics to the corresponding tissue. ECM is not simply involved in cell support and fixation; in gastric cancer, the role of the extracellular matrix has been proved to be involved in the process of disease initiation to metastasis. Importantly, the collagen gene in the focal adhesion pathway is a potential biomarker to distinguish gastric cancer from precancerous lesions (38). Oxidative stress induces ECM regulation and the interaction between oxidative stress. Thus, oxidative stress can

be used as a potential target for treatment (39, 40). However, the effect of oxidative stress on ECM of gastric cancer is not clear. The interaction between extracellular matrix components and oxidative stress still has great potential as a biomarker and drug target for the prognosis of gastric cancer.

The risk score calculated by our scoring system was significantly related to the prognosis of GC patients and can be well distinguished in various characteristics. Based on the differences of TME, TMB, MSI, immunotherapy, stem cell analysis, and chemotherapeutic drugs, we can better distinguish the subtypes of gastric cancer patients. Moreover, this distinction can provide a new reference for individualized analysis and treatment of gastric cancer patients based on these gene expressions. In this study, seven genes (SLCO2A1, SHISA2, SERPINE1, SMPD3, GPC3, CRABP2, C1QTNF5) were used for the construction of OE_score, among which SLCO2A1, SERPINE1, CRABP2, and GPC3 were reported to be associated with gastric cancer (41–44), and play an important role in the occurrence and development of gastric cancer. The increased expression of SERPINE1 can promote tumor progression and angiogenesis by activating the VEGFR-2 signal pathway in gastric cancer (42). GPC3 has also been reported for the prognostic diagnosis of gastric cancer (45). These seven genes involved in constructing OE_score *in vivo* or *in vitro* can be explored further to study their potential regulatory relationship between upstream and downstream genes. The outcome might be useful for a new direction in treating and diagnosing gastric cancer.

Through *in vivo* or *in vitro* experiments, the relationship between genes involved in the construction of OE_score and gastric cancer will be assessed in the next step. Studying the relationship between these genes and the immune microenvironment will also provide important insight. Through single-cell sequencing, specific effects of oxidative stress on individual cells are also the focus of our future research.

This study had several limitations. Firstly, our data were obtained from the public database, and all the samples were retrospective in nature. There was a lack of verification of *in vivo* and *in vitro* experiments and large-scale randomized controlled trials to confirm our findings. Meanwhile, the effects of adjuvant radiotherapy and chemotherapy, neoadjuvant radiotherapy and chemotherapy, and surgical methods could not be fully considered in different cohorts. These limitations might have affected our judgment for assessing the relationship between oxidative stress and the prognosis of GC patients. It is worth mentioning that a variety of key enzymes leading to oxidative stress are involved in the production of reactive oxygen free radicals and active nitrogen free radicals. Meanwhile, antioxidant enzymes such as superoxide dismutase, catalase, and glutathione peroxidase are involved in the defense mechanism against oxidative stress. The variation in the coding genes of these enzymes (single nucleotide polymorphism, SNPs) affects the individual susceptibility to diseases, creates deviation in the gene expression database, and reduces the credibility of the results. In this paper, the biological process of oxidative stress is not analyzed from the point of view of SNPs, diet, physical activity, and several comorbidities. Moreover, these factors can easily affect the expression of oxidative stress genes, which might overshadow the individual differences, leading to biasness and data analysis limitations.

## Conclusions

In the current study, the predictive model based on oxidative stress-related genes along with the characteristics of immune infiltration was explored. In addition, the gene expression, clinicopathological and prognostic characteristics of ORGs cluster, gene cluster, and OE_score established by ORGs were studied.

The comprehensive analysis of ORGs unraveled their extensive relationship with the immune microenvironment, clinical features, and prognosis. The correlation between OE_score with seven genes based on ORGs and prognosis of gastric cancer patients with TMB, MSI, CSC, ECM, chemotherapeutic drugs were studied. The patients with low-risk scores had survival advantages in many aspects. These findings emphasize the potential role of ORGs in targeted therapy and immunotherapy based on patient's individual gene expression characteristics. Furthermore, the combined effect of multiple ORGs on the immune characteristics of gastric cancer is of immense value. The relationship between oxidative stress and gastric cancer is of great significance, providing a reference and basis for guiding the individualized treatment of gastric cancer. Moreover, it might enrich the existing ways of assessing the prognosis and choice of treatment of patients with gastric cancer.

## Data availability statement

The original contributions presented in the study are included in the article/**Supplementary Material**, further inquiries can be directed to the corresponding author/s.

## Author contributions

BZH and CWL forwarded this research's conception. BZH, BYH, FCZ, and CWL collected, processed the data, and completed the research writing. BZH and CWL proofread and revised the research paper. All authors contributed to this study and agreed to the publication of this article in the

present form. All authors contributed to the article and approved the submitted version.

## Acknowledgments

The Natural Science Foundation of Shanxi Province, China (Grant No. 201801D121320).

## Conflict of interest

The authors declare that the research was conducted in the absence of any commercial or financial relationships that could be construed as a potential conflict of interest.

## Publisher's note



## Supplementary material

The Supplementary Material for this article can be found online at: https://www.frontiersin.org/articles/10.3389/fsurg.2022.1013794/full#supplementary-material.

## References

1. Sung H, Ferlay J, Siegel RL, Laversanne M, Soerjomataram I, Jemal A, et al. Global cancer statistics 2020: GLOBOCAN estimates of incidence and mortality worldwide for 36 cancers in 185 countries. *CA Cancer J Clin*. (2021) 71:209–49. doi: 10.3322/caac.21660

2. Joshi SS, Badgwell BD. Current treatment and recent progress in gastric cancer. *CA Cancer J Clin*. (2021) 71:264–79. doi: 10.3322/caac.21657

3. Forman HJ, Zhang H. Targeting oxidative stress in disease: promise and limitations of antioxidant therapy. *Nat Rev Drug Discov*. (2021) 20:689–709. doi: 10.1038/s41573-021-00233-1

4. Han L, Shu X, Wang J. Helicobacter pylori-mediated oxidative stress and gastric diseases: a review. *Front Microbiol*. (2022) 13:811258. doi: 10.3389/fmicb.2022.811258

5. Janjigian YY, Shitara K, Moehler M, Garrido M, Salman P, Shen L, et al. First-line nivolumab plus chemotherapy versus chemotherapy alone for advanced gastric, gastro-oesophageal junction, and oesophageal adenocarcinoma (CheckMate 649): a randomised, open-label, phase 3 trial. *Lancet*. (2021) 398:27–40. doi: 10.1016/S0140-6736(21)00797-2

6. Smyth EC, Gambardella V, Cervantes A, Fleitas T. Checkpoint inhibitors for gastroesophageal cancers: dissecting heterogeneity to better understand their role in first-line and adjuvant therapy. *Ann Oncol*. (2021) 32:590–9. doi: 10.1016/j.annonc.2021.02.004

7. Wang Q, Xu C, Fan Q, Yuan H, Zhang X, Chen B, et al. Positive feedback between ROS and cis-axis of PIASx$\alpha$/p38$\alpha$-SUMOylation/MK2 facilitates gastric cancer metastasis. *Cell Death Dis*. (2021) 12:986. doi: 10.1038/s41419-021-04302-6

8. Conesa A, Madrigal P, Tarazona S, Gomez-Cabrero D, Cervera A, McPherson A, et al. A survey of best practices for RNA-seq data analysis. *Genome Biol*. (2016) 17:1–19. doi: 10.1186/s13059-016-0881-8

9. Richter AN, Khoshgoftaar TM. A review of statistical and machine learning methods for modeling cancer risk using structured clinical data. *Artif Intell Med*. (2018) 90:1–14. doi: 10.1016/j.artmed.2018.06.002

10. Goodall GJ, Wickramasinghe VO. RNA In cancer. *Nat Rev Cancer*. (2021) 21:22–36. doi: 10.1038/s41568-020-00306-0

11. Li M, Zha X, Wang S. The role of N6-methyladenosine mRNA in the tumor microenvironment. *Biochim Biophys Acta Rev Cancer*. (2021) 1875:188522. doi: 10.1016/j.bbcan.2021.188522

12. Chen DS, Mellman I. Elements of cancer immunity and the cancer-immune set point. *Nature*. (2017) 541:321–30. doi: 10.1038/nature21349

13. Liu YT, Sun ZJ. Turning cold tumors into hot tumors by improving T-cell infiltration. *Theranostics*. (2021) 11:5365–86. doi: 10.7150/thno.58390

14. Yoshihara K, Shahmoradgoli M, Martínez E, Vegesna R, Kim H, Torres-Garcia W, et al. Inferring tumour purity and stromal and immune cell admixture from expression data. *Nat Commun*. (2013) 4:1–11. doi: 10.1038/ncomms3612

15. Zhang LN, Zhang DD, Yang L, Gu YX, Zuo QP, Wang HY, et al. Roles of cell fusion between mesenchymal stromal/stem cells and malignant cells in tumor growth and metastasis. *Febs j*. (2021) 288:1447–56. doi: 10.1111/febs.15483

16. Hanus M, Parada-Venegas D, Landskron G, Wielandt AM, Hurtado C, Alvarez K, et al. Immune system, microbiota, and microbial metabolites: the unresolved triad in colorectal cancer microenvironment. *Front Immunol*. (2021) 12:612826. doi: 10.3389/fimmu.2021.612826

17. Seebacher NA, Krchniakova M, Stacy AE, Skoda J, Jansson PJ. Tumour microenvironment stress promotes the development of drug resistance. *Antioxidants (Basel)*. (2021) 10(11):1801. doi: 10.3390/antiox10111801

18. Choucair K, Morand S, Stanbery L, Edelman G, Dworkin L, Nemunaitis J. TMB: a promising immune-response biomarker, and potential spearhead in advancing targeted therapy trials. *Cancer Gene Ther*. (2020) 27:841–53. doi: 10.1038/s41417-020-0174-y

19. Hayes JD, Dinkova-Kostova AT, Tew KD. Oxidative stress in cancer. *Cancer Cell*. (2020) 38:167–97. doi: 10.1016/j.ccell.2020.06.001

20. Park R, Da Silva LL, Saeed A. Immunotherapy predictive molecular markers in advanced gastroesophageal cancer: mSI and beyond. *Cancers (Basel)*. (2021) 13(7):1715. doi: 10.3390/cancers13071715

21. van Velzen MJM, Derks S, van Grieken NCT, Haj Mohammad N, van Laarhoven HWM. MSI as a predictive factor for treatment outcome of gastroesophageal adenocarcinoma. *Cancer Treat Rev*. (2020) 86:102024. doi: 10.1016/j.ctrv.2020.102024

22. Chida K, Kawazoe A, Kawazu M, Suzuki T, Nakamura Y, Nakatsura T, et al. A low tumor mutational burden and PTEN mutations are predictors of a negative response to PD-1 blockade in MSI-H/dMMR gastrointestinal tumors. *Clin Cancer Res*. (2021) 27:3714–24. doi: 10.1158/1078-0432.CCR-21-0401

23. Fishbein A, Hammock BD, Serhan CN, Panigrahy D. Carcinogenesis: failure of resolution of inflammation? *Pharmacol Ther*. (2021) 218:107670. doi: 10.1016/j.pharmthera.2020.107670

24. Rosenbaum SR, Wilski NA, Aplin AE. Fueling the fire: inflammatory forms of cell death and implications for cancer immunotherapy. *Cancer Discov*. (2021) 11:266–81. doi: 10.1158/2159-8290.CD-20-0805

25. Kwon M, An M, Klempner SJ, Lee H, Kim KM, Sa JK, et al. Determinants of response and intrinsic resistance to PD-1 blockade in microsatellite instability-high gastric cancer. *Cancer Discov*. (2021) 11:2168–85. doi: 10.1158/2159-8290.CD-21-0219

26. Lauritsen JP, Haks MC, Lefebvre JM, Kappes DJ, Wiest DL. Recent insights into the signals that control alphabeta/gammadelta-lineage fate. *Immunol Rev*. (2006) 209:176–90. doi: 10.1111/j.0105-2896.2006.00349.x

27. Barros MS, de Araújo ND, Magalhães-Gama F, Pereira Ribeiro TL, Alves Hanna FS, Tarragô AM, et al. $\gamma\delta$ T cells for leukemia immunotherapy: new and expanding trends. *Front Immunol*. (2021) 12:729085. doi: 10.3389/fimmu.2021.729085

28. Li Y, Li G, Zhang J, Wu X, Chen X. The dual roles of human γδ T cells: anti-tumor or tumor-promoting. *Front Immunol*. (2020) 11:619954. doi: 10.3389/fimmu.2020.619954

29. Daley D, Zambirinis CP, Seifert L, Akkad N, Mohan N, Werba G, et al. γδ T cells support pancreatic oncogenesis by restraining αβ T cell activation. *Cell*. (2016) 166:1485–99.e1415.

30. Sebestyen Z, Prinz I, Déchanet-Merville J, Silva-Santos B, Kuball J. Translating gammadelta (γδ) T cells and their receptors into cancer cell therapies. *Nat Rev Drug Discov*. (2020) 19:169–84. doi: 10.1038/s41573-019-0038-z

31. Su CY, Fu XL, Duan W, Yu PW, Zhao YL. High density of CD68+ tumor-associated macrophages predicts a poor prognosis in gastric cancer mediated by IL-6 expression. *Oncol Lett*. (2018) 15:6217–24. doi: 10.3892/ol.2018.8119

32. Hu Q, Lyon CJ, Fletcher JK, Tang W, Wan M, Hu TY. Extracellular vesicle activities regulating macrophage- and tissue-mediated injury and repair responses. *Acta Pharm Sin B*. (2021) 11:1493–512. doi: 10.1016/j.apsb.2020.12.014

33. Chen Y, Zhang S, Wang Q, Zhang X. Tumor-recruited M2 macrophages promote gastric and breast cancer metastasis via M2 macrophage-secreted CHI3L1 protein. *J Hematol Oncol*. (2017) 10:36. doi: 10.1186/s13045-017-0408-0

34. Yan Y, Zhang J, Li JH, Liu X, Wang JZ, Qu HY, et al. High tumor-associated macrophages infiltration is associated with poor prognosis and may contribute to the phenomenon of epithelial-mesenchymal transition in gastric cancer. *Onco Targets Ther*. (2016) 9:3975–83. doi: 10.2147/OTT.S103112

35. Gordon SR, Maute RL, Dulken BW, Hutter G, George BM, McCracken MN, et al. PD-1 expression by tumour-associated macrophages inhibits phagocytosis and tumour immunity. *Nature*. (2017) 545:495–9. doi: 10.1038/nature22396

36. Li J, Cai H, Sun H, Qu J, Zhao B, Hu X, et al. Extracts of Cordyceps sinensis inhibit breast cancer growth through promoting M1 macrophage polarization via NF-κB pathway activation. *J Ethnopharmacol*. (2020) 260:112969. doi: 10.1016/j.jep.2020.112969

37. Li W, Zhang X, Wu F, Zhou Y, Bao Z, Li H, et al. Gastric cancer-derived mesenchymal stromal cells trigger M2 macrophage polarization that promotes metastasis and EMT in gastric cancer. *Cell Death Dis*. (2019) 10:918. doi: 10.1038/s41419-019-2131-y

38. Zhao Y, Zhou T, Li A, Yao H, He F, Wang L, et al. A potential role of collagens expression in distinguishing between premalignant and malignant lesions in stomach. *Anat Rec (Hoboken)*. (2009) 292:692–700. doi: 10.1002/ar.20874

39. Ramos-Tovar E, Muriel P. Molecular mechanisms that link oxidative stress, inflammation, and fibrosis in the liver. *Antioxidants (Basel)*. (2020) 9(12):1279. doi: 10.3390/antiox9121279

40. Martins SG, Zilhão R, Thorsteinsdóttir S, Carlos AR. Linking oxidative stress and DNA damage to changes in the expression of extracellular matrix components. *Front Genet*. (2021) 12:673002. doi: 10.3389/fgene.2021.673002

41. Lopes C, Pereira C, Farinha M, Medeiros R, Dinis-Ribeiro M. Prostaglandin E(2) pathway is dysregulated in gastric adenocarcinoma in a Caucasian population. *Int J Mol Sci*. (2020) 21(20):7680. doi: 10.3390/ijms21207680

42. Teng F, Zhang JX, Chen Y, Shen XD, Su C, Guo YJ, et al. LncRNA NKX2-1-AS1 promotes tumor progression and angiogenesis via upregulation of SERPINE1 expression and activation of the VEGFR-2 signaling pathway in gastric cancer. *Mol Oncol*. (2021) 15:1234–55. doi: 10.1002/1878-0261.12911

43. Yamashita S, Nomoto T, Ohta T, Ohki M, Sugimura T, Ushijima T. Differential expression of genes related to levels of mucosal cell proliferation among multiple rat strains by using oligonucleotide microarrays. *Mamm Genome*. (2003) 14:845–52. doi: 10.1007/s00335-003-2299-3

44. Wichert A, Stege A, Midorikawa Y, Holm PS, Lage H. Glypican-3 is involved in cellular protection against mitoxantrone in gastric carcinoma cells. *Oncogene*. (2004) 23:945–55. doi: 10.1038/sj.onc.1207237

45. Wang B, Xie Y, Zheng L, Zheng X, Gao J, Liu X, et al. Both the serum AFP test and AFP/GPC3/SALL4 immunohistochemistry are beneficial for predicting the prognosis of gastric adenocarcinoma. *BMC Gastroenterol*. (2021) 21:408. doi: 10.1186/s12876-021-01986-0

frontiers | Frontiers in Surgery

TYPE Original Research
PUBLISHED 01 November 2022
DOI 10.3389/fsurg.2022.997819



OPEN ACCESS

EDITED BY
Beatrice Aramini,
University of Bologna, Italy

REVIEWED BY
Zeyu Wu,
Guangdong Provincial People's Hospital, China
Guibin Zheng,
Yantai Yuhuangding Hospital, China

*CORRESPONDENCE
Guoyang Wu
wuguoyangmail@aliyun.com

†These authors have contributed equally to this work and share first authorship

SPECIALTY SECTION
This article was submitted to Surgical Oncology, a section of the journal Frontiers in Surgery

RECEIVED 19 July 2022
ACCEPTED 26 September 2022
PUBLISHED 01 November 2022

CITATION
Kuang P, Wang Y, Wu G, Luo Y, Fu J, Yan W, Lin S, Hong X, Lin F, Lin E and Fu Y (2022) Endoscopic lateral neck dissection *via* the breast and transoral approaches for papillary thyroid carcinoma: A preliminary report. Front. Surg. 9:997819. doi: 10.3389/fsurg.2022.997819



# Endoscopic lateral neck dissection *via* the breast and transoral approaches for papillary thyroid carcinoma: A preliminary report

Penghao Kuang[1†], Yuanyuan Wang[2†], Guoyang Wu[1*], Yezhe Luo[1], Jinbo Fu[1], Wei Yan[1], Suqiong Lin[1], Xiaoquan Hong[1], Fusheng Lin[1], Ende Lin[1] and Yilong Fu[1]

[1]Department of General Surgery, Zhongshan Hospital, Xiamen University, Xiamen, China, [2]Department of Thyroid Surgery, Zhengzhou University First Affiliated Hospital, Zhengzhou, China

**Purpose:** Complete lymph node dissection is essential for the management of papillary thyroid carcinoma (PTC) with lymph node metastasis (LNM). This work aimed to describe the feasibility of endoscopic lateral neck dissection *via* the breast and transoral approach (ELNDBTOA) in PTC patients and the necessity of the addition of the transoral approach.

**Methods:** We included 13 patients with PTC and suspected lateral LNM who underwent ELNDBTOA at the Zhongshan Hospital, Xiamen University. Total thyroidectomy, ipsilateral central lymph node dissection, and selective neck dissection (levels IIA, IIB, III, and IV) were performed endoscopically *via* the breast approach. Residual lymph nodes were further dissected *via* the transoral approach.

**Results:** The mean operation time was 362.1 ± 73.5 min. In the lateral neck compartments, the mean number of retrieved lymph nodes was 36.6 ± 23.8, and the mean number of positive lymph nodes was 6.8 ± 4.7. In further dissection via the transoral approach, lymph nodes in the lateral neck compartment were obtained in nine patients (9/13, 69.2%), and three patients (3/13, 23.1%) had confirmed lateral neck metastases. Transient hypocalcemia occurred in two patients (2/13, 15.4%), and three patients (3/13, 23.1%) developed transient skin numbness in the mandibular area. No other major complications were observed. There was no evidence of local recurrence or distant metastasis during the follow-up period (range, 24–87 months). All patients were satisfied with the good cosmetic outcome.

**Conclusion:** ELNDBTOA is an option with proven feasibility for select PTC patients with LNM, and the addition of the transoral approach is necessary to ensure complete dissection.

KEYWORDS

thyroid, papillary thyroid carcinoma, endoscopic lateral neck dissection, lymph node metastasis, thyroid cancer

Abbreviations

PTC, papillary thyroid carcinoma; LNM, lymph node metastasis; ELNDBTOA, endoscopic lateral neck dissection *via* the breast and transoral approach; SCM, sternocleidomastoid muscle.

# Introduction

Papillary thyroid carcinoma (PTC), the most common malignant thyroid tumor (1), is characterized by a high rate of lymph node metastasis (LNM), mostly in the central lymph nodes and sometimes in the lateral lymph nodes. LNM has a significant impact on PTC prognosis (2). Therefore, ensuring complete and legitimate dissection of the lymph nodes is crucial for the surgical management of PTC with LNM. Improvements in endoscopic thyroidectomy have allowed surgeons more options for lateral neck dissection. Tan et al (3). applied the transoral endoscopic technique during lateral neck dissection for selected patients. Other studies have described the chest-breast (4), chest (5), and breast approaches (6), and others have verified the safety of robot-assisted (7), needle-assisted (8), and video-assisted endoscopic lateral neck dissections (9). However, endoscopic lateral neck dissection *via* the breast and transoral approach (ELNDBTOA) has not been reported. In the breast approach, obstruction by the sternum and clavicles may cause a blind area in the surgical visual field, leading to incomplete dissection. We believe that the addition of the transoral approach can overcome this limitation. Herein, we report our experience using ELNDBTOA in the management of 13 PTC patients analyze the feasibility and of this approach and the necessity of the addition of the transoral approach.

# Materials and methods

## Ethical approval

This study was approved by the Medical Ethics Committee of Zhongshan Hospital, Xiamen University, Xiamen, Fujian, China. Written informed consent was obtained from all individual patients included in this study.

## Patients

Thirteen patients underwent ELNDBTOA by the same surgeon in our department between February 2015 and May 2020. PTC was diagnosed using ultrasonography-guided fine needle aspiration in all patients. Ultrasonography and/or computed tomography findings led to the suspicion of lateral LNM, which was confirmed using fine needle aspiration, *BRAF* mutation analysis, or washout thyroglobulin test.

The inclusion criteria for ELNDBTOA were as follows: (1) PTC with LNM; (2) the maximum diameter of primary tumor less than 4 cm; (3) metastatic lymph nodes not blended with each other or fixed in the neck; (4) no invasion of the neighboring structures, such as the esophagus, trachea, or recurrent laryngeal nerve; (5) no distant metastasis; (6) need for a cosmetic outcome; and (7) provision of informed consent for ELNDBTOA. The following exclusion criteria were used: (1) neck surgical or irradiation history, (2) level I or level V LNM, (3) hyperthyroidism or Hashimoto's thyroiditis, and (4) intolerance to general anesthesia.

Patient demographics, outcomes, and complications were collected retrospectively.

## Surgical procedures

### Total thyroidectomy and central lymph node dissection *via* the breast approach

The preoperative preparations and major procedures of total thyroidectomy and central lymph node dissection *via* the breast approach have been described in detail previously (10). The distribution of trocars is shown in **Figure 1**.

### Lateral neck dissection *via* the breast approach and transoral approach

ELNDBTOA was performed using the following seven steps (**Figure 2**), with intraoperative neuromonitoring:

1) Working space: When total thyroidectomy and central lymph node dissection *via* the breast approach completed, we expanded the working space of the affected side to reach the hyoid level and the lateral margin of the sternocleidomastoid muscle (SCM).
2) Determination of the superior and lateral boundaries: The submandibular gland and posterior belly of the digastric muscle were exposed. The space between the sternal and clavicular heads of the SCM was split to expose the lateral cervical compartment, reaching the posterior margin of the SCM as the lateral boundary. Care was taken to

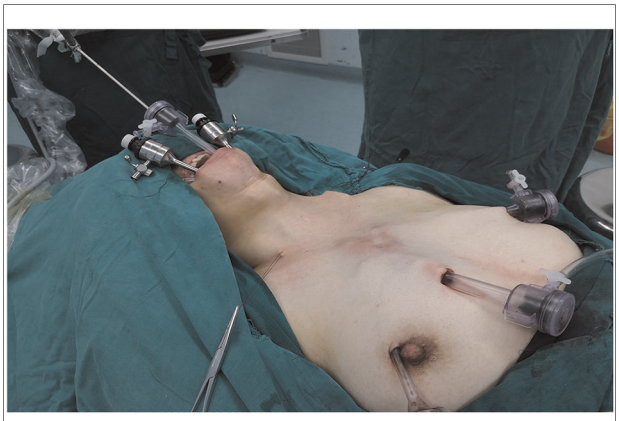

FIGURE 1
The distribution of trocars.

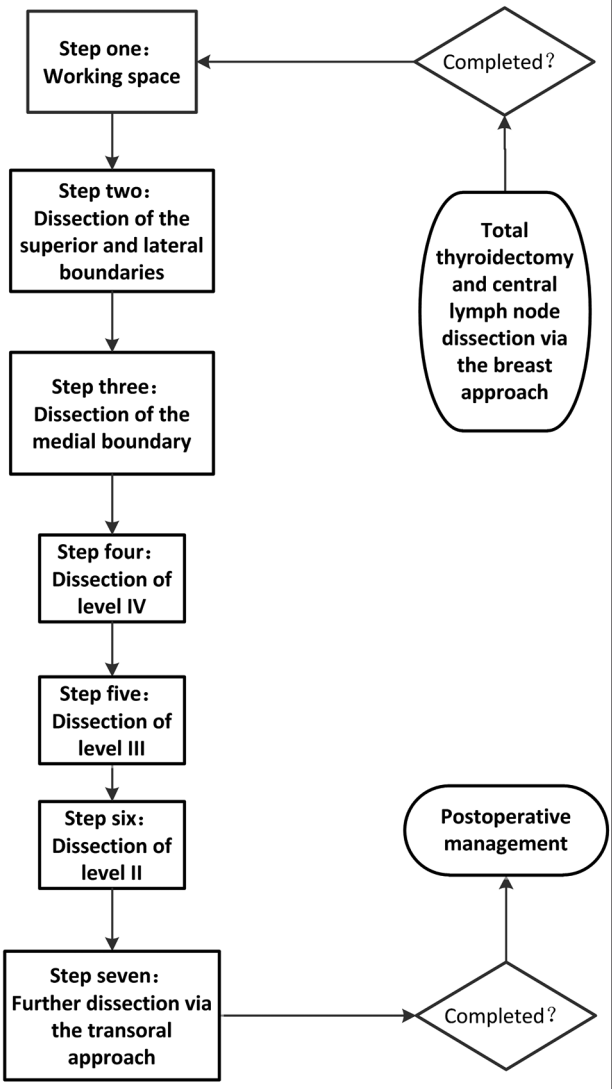


FIGURE 2
Seven steps of ELNDBTOA.

identify and expose the accessory nerve without injuring it. Then, the tissue on the surface of the accessory nerve was dissected, and the superior boundary of level II was determined by cutting off the tissue of the lower edge of the digastric muscle.

3) Dissection of the medial boundary: The omohyoid muscle was exposed and preserved. The tissue of the carotid triangle region, the lymph nodes between the SCM and sternohyoid muscle, and the tissue on the surface of the internal jugular vein were dissected from top to bottom along the lateral margin of the strap muscles. Care was taken to separate the jugular vein angle, and the thoracic duct (left side) or the lymphatic trunk (right side) was clamped with a 5-mm hemolock to prevent chyle leakage.

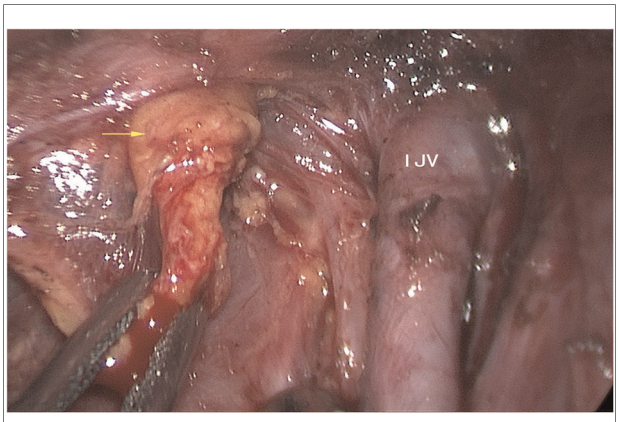


FIGURE 3
The left side residual lymph nodes (yellow arrow). IJV: internal jugular vein.

4) Dissection of level IV: The inferior boundary of the lateral cervical compartment was separated from the jugular vein angle to the posterior margin of the SCM. The level IV tissue was lifted upward; then, level IV was dissected carefully without damaging the transverse cervical artery.
5) Dissection of level III: The lymph nodes of level III were dissected along the internal jugular vein from bottom to top in front of the prevertebral fascia. The lateral margin of level III was removed at the posterior margin of the SCM.
6) Dissection of level II: The lymph nodes of level II were dissected upward until the superior boundary, which had been separated in step 2, was reached. The accessory nerve was properly protected during this process.
7) Further neck dissection *via* the transoral approach and placement of the drainage tube: When these procedures were completed, three 5-mm incisions were made in the oral vestibule (Figure 1). A 5-mm, 30-degree laparoscope was used for observing the operative region. The residual lymph nodes located in levels VI and IV and between the SCM and sternohyoid muscle were dissected and removed carefully through the transoral approach (Figure 3). A total of 1,000 ml of warm saline was used for flushing the surgical region to check for active bleeding, and all incisions were sutured using absorbable sutures. Two drainage tubes were placed: one in the central cervical compartment and the other in the lateral cervical compartment.

## Postoperative management and follow-up

All patients started a semi-liquid diet after a postoperative 6-hour fast. Parathyroid hormone and serum calcium levels (Figure 4) were routinely checked on postoperative day 2. Complications were monitored for quick identification and prompt management. When the intraoperative recurrent laryngeal nerve signal decreased by more than 50%,

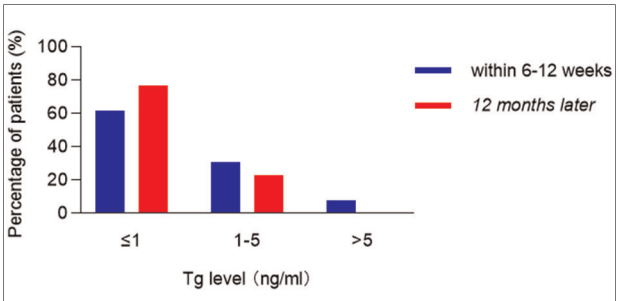


FIGURE 4
The percentage of patients with different postoperative thyroglobulin levels.

intraoperative loss of signal was considered, and the fiberoptic nasopharyngoscope was performed on the first day postoperatively to determine whether there was vocal cord paralysis. If postoperative vocal cord paralysis occurs, according to the duration, temporary recurrent laryngeal nerve injury was diagnosed if it recovers within 6 months, and permanent recurrent laryngeal nerve injury was diagnosed when it lasts more than 6 months. Mild symptoms of hypoparathyroidism may manifest as numbness in the lips, face, and limbs, and twitching of the limbs, while severe symptoms may manifest as spasms of the larynx and diaphragm, causing difficulty in breathing. If the patient was diagnosed with hypoparathyroidism after surgery, symptomatic treatment should be given. If the patient recovers within 6 months, it is temporary hypoparathyroidism. Permanent hypoparathyroidism may be considered if there is no recovery after more than 6 months. The drainage tubes were removed when the volume was less than 15 ml/day. All the patients received thyroid-stimulating hormone suppression therapy, and they were encouraged to undergo radioactive iodine therapy in the oncology department 1–3 months later.

The first follow-up was completed 1 month after operation, and patients were followed up every 6 months thereafter. During the follow-up period, check for tumor recurrence and metastasis (imaging, thyroglobulin, thyroid function, etc.) and observe whether there are appearance deformities, sensory and movement abnormalities in the chest, neck and oral cavity.

## Results

ELNDBTOA was performed successfully with a successful cosmetic outcome in 13 patients (12 women and 1 man; age range, 22–53 years). The average tumor size was 2.1 cm ± 1.1 cm. The mean operation time was 362.1 ± 73.5 min. The mean intraoperative blood loss was 21.5 ± 13.4 ml. In the lateral neck compartments, the mean number of retrieved lymph nodes was 36.6 ± 23.8, and the mean number of positive lymph nodes was 6.8 ± 4.7. In further dissection via the transoral approach, lymph nodes in the lateral neck compartment were obtained in nine patients (9/13, 69.2%), and three patients (3/13, 23.1%) had confirmed LNM. The average length of hospital stay was 5.0 ± 1.2 days. All patients had normal parathyroid hormone and serum calcium levels on postoperative day 2. The clinical characteristics of the patients are shown in **Table 1**.

None of the patients developed major complications (e.g., postoperative bleeding, infection, chyle leakage, and vocal cord paralysis). However, two patients (2/13, 15.4%) had transient hypocalcemia, which was reversed within 2 months, and three patients (3/13, 23.1%) developed transient skin numbness in the mandibular area and recovered within 2 weeks. The median follow-up period was 59 months (range, 24–87 months). There was no evidence of local recurrence or distant metastases. Postoperative thyroglobulin level with levothyroxine suppression was low (<1 ng/ml) in most patients (76.9%) after 12 months. The incisions in the oral cavity and breast healed well in all the patients, and they were satisfied with the good cosmetic outcome.

## Discussion

Because LNM is related to tumor recurrence in PTC patients, lateral neck dissection is the preferred and most efficient curative option for PTC with LNM according to the current guidelines (11). However, a long cervical incision is required for open lateral neck dissection, which is a limitation with regard to cosmetic outcome and medical privacy. Therefore, endoscopic techniques for lateral neck dissection have been explored. Miccoli et al. introduced a video-assisted technique in 2008 (12). Zhang et al (9). later reported that there was no significant difference in the number of lymph nodes obtained between video-assisted and open lateral neck dissection (41.1 ± 12.9 vs. 43.8 ± 13.1, $p = 0.3194$). Yan et al (6). described lateral neck dissection *via* the breast approach, and the mean number of retrieved lymph nodes in the lateral neck compartment was 21.8 (range, 5–42). In the pilot report of the transoral approach, the mean number of retrieved lymph nodes in levels III and IV was 10.9 ± 2.8 (3). However, the breast approach may result in incomplete lymph node dissection. In this study, we aimed to analyze the feasibility and necessity of ELNDBTOA.

### Feasibility and necessity of this technique

The safety and efficacy of radical excision should be the principal areas of focus when considering surgical approaches rather than the cosmetic outcome. In this study, we described endoscopic lateral neck dissection (levels IIA, IIB, III, and IV)

TABLE 1 The clinical characteristics of the patients ($n = 13$).

| Case | Age (years) | Sex | Tumour size (mm) | Operation time (min) | TNM stage | Positive/retrieved number of lymph node (breast approach) | | Positive/retrieved number of lymph node (transoral approach) | |
|---|---|---|---|---|---|---|---|---|---|
| | | | | | | CNC | LNC | CNC | LNC |
| 1 | 40 | F | 33 | 377 | $T2N1_bM0$ | 5/11 | 2/19 | 0/0 | 0/0 |
| 2 | 31 | F | 24 | 331 | $T2N1_bM0$ | 0/0 | 5/31 | 0/0 | 0/0 |
| 3 | 22 | F | 39 | 477 | $T2N1_bM0$ (L)<br>$T1_aN1_aM0$ (R) | 6/8 (L)<br>1/4 (R) | 7/14 (L)<br>0/8 (R) | 0/0 (L)<br>0/1 (R) | 2/2 (L)<br>0/3 (R) |
| 4 | 46 | F | 10 | 268 | $T1_bN1_bM0$ | 1/4 | 2/20 | 0/1 | 0/2 |
| 5 | 34 | F | 26 | 327 | $T2N1_bM0$ | 1/1 | 8/14 | 0/0 | 0/0 |
| 6 | 33 | F | 8 | 423 | $T3N1_bM0$ | 2/3 | 4/40 | 0/0 | 0/3 |
| 7 | 53 | F | 29 | 272 | $T1_aN1_bM0$ | 1/2 | 6/23 | 0/0 | 0/0 |
| 8 | 30 | F | 22 | 497 | $T3N1_bM0$ (L)<br>$T1_aN1_bM0$ (R) | 1/1 (L)<br>2/9 (R) | 15/51 (L)<br>3/49 (R) | 0/0 (L)<br>0/0 (R) | 0/0 (L)<br>1/4 (R) |
| 9 | 25 | F | 8 | 318 | $T3N1_bM0$ | 3/6 | 5/33 | 0/2 | 0/1 |
| 10 | 37 | M | 6 | 335 | $T3N1_bM0$ | 3/6 | 5/21 | 0/1 | 0/4 |
| 11 | 34 | F | 31 | 360 | $T1_bN1_bM0$ | 9/12 | 10/26 | 0/0 | 1/4 |
| 12 | 52 | F | 22 | 423 | $T3N1_bM0$ | 4/9 | 2/33 | 0/0 | 0/9 |
| 13 | 25 | F | 18 | 299 | $T1_bN1_bM0$ | 6/16 | 10/61 | 0/0 | 0/1 |

CNC, central neck compartment; LNC, lateral neck compartment; L, left side; R, right side.

*via* the breast combined with the transoral approach in detail. All 13 patients underwent ELNDBTOA successfully without conversion to open surgery. In the lateral neck compartment, the mean number of retrieved lymph nodes was $36.6 \pm 23.8$, and three patients (3/13, 23.1%) had confirmed LNM. With regard to complications related to the additional transoral ports, three patients had transient skin numbness in the mandibular area, which resolved within 2 weeks. No other patients developed complications from the procedure. There was no tumor recurrence or metastasis during the follow-up period (range, 24–87 months). Hence, ELNDBTOA is considered a safe and effective technique that is worthy of promotion in well-selected patients.

The key to lateral neck dissection is complete resection, since incomplete resection can have serious consequences requiring further treatment. Some patients may need a second surgery or even multiple operations due to nonstandard and incomplete initial surgery. In this report, three patients (23.1%) had confirmed LNM diagnosed during further dissection using the transoral approach, highlighting the necessity of the addition of the transoral approach. This transoral approach is necessary because the surgical visual perspective of the breast approach is blocked by the sternal manubrium and clavicles, which may lead to blinding the area of the visual field, resulting in incomplete dissection in the central neck compartment, level IV, or lymph nodes between the SCM and sternohyoid muscle. In contrast, the transoral approach provides sufficient exposure to the surgical visual field in these areas. Hence, combining the transoral approach with the breast approach for lateral neck dissection is required.

## Surgical extent and patient selection

The optimal surgical extent of lateral neck dissection is still controversial, mainly in the dissection of level IIB and level V lymph nodes. Some authors who are opposed to routine dissection in level IIB and level V argue that the accessory nerve and C4 (the fourth branch of the cervical plexus) could be protected to a certain extent.

The boundaries for lateral neck dissection (level II, level III, and level IV) in this study were as follows: the inferior margin of the posterior belly of the digastric muscle as the superior boundary (Figure 5), the level of the clavicle as the inferior boundary (Figure 6), the medial margin of the common carotid artery as the medial boundary, and the posterior margin of the SCM as the lateral boundary. The reasons for the routine dissection of level IIB: level IIA and level IIB encompass a single piece of tissue, although they are anatomically bounded by the accessory nerve; protecting the accessory nerve would be difficult if a second operation is needed later. Patients with preoperative suspected metastases in level I or V should not undergo ELNDBTOA.

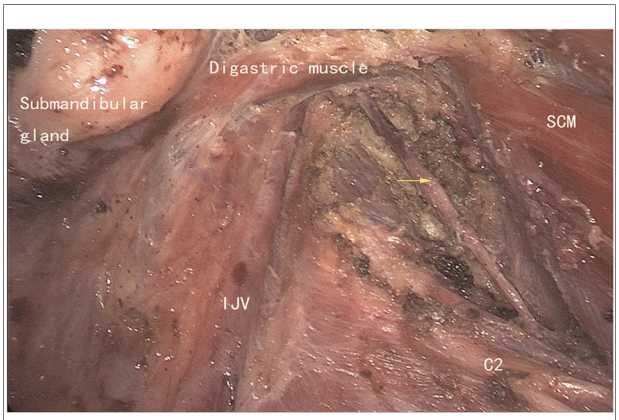


FIGURE 5
The superior boundary (left side). SCM, sternocleidomastoid muscle; IJV, internal jugular vein; C2, the second branch of the cervical plexus; yellow arrow: the accessory nerve.

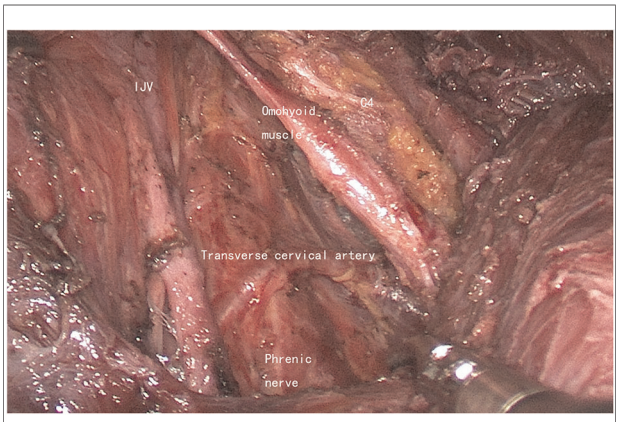


FIGURE 6
The inferior boundary (left side). IJV, internal jugular vein; C4, the fourth branch of the cervical plexus.

Based on our experience, we propose that ELNDBTOA should be performed in patients with a cosmetic requirement who are diagnosed with PTC and suspected LNM in the low position of level IV that may be blocked by the clavicle and sternum.

## The prevention of complications

There are several complications related to lateral neck dissection; therefore, we explored means to prevent these complications in patients undergoing ELNDBTOA.

Chyle leakage has been reported as a common complication of lateral neck dissection (occurring in 5.1% of total thyroidectomies with ipsilateral lateral neck dissection and 6.2% of total thyroidectomies with bilateral lateral neck dissection) (13) probably due to intraoperative injury to the thoracic duct or lymphatic trunk. None of our patients developed chyle leakage. To avoid chyle leakage, we recommend that no energy instruments be used, but a 5-mm hemolock should be used in the dangerous area between the transverse cervical vessels and the venous angle if a cord structure is seen. Chyle leakage should be carefully assessed at the end of surgery. If the thoracic duct or lymphatic trunk is injured, 6-0 Prolene can be used for suturing.

Severe intraoperative bleeding is a thyroid endoscopic surgical emergency, which may not only lead to conversion to open surgery but also cause $CO_2$ embolism. All surgeries were performed endoscopically in this study, and no $CO_2$ embolism occurred. Based on our previous experience with endoscopic thyroid surgery (14), we recommend that surgeons enhance their anatomical knowledge (e.g., of the external carotid vein, all branches of the internal jugular vein, common carotid artery, superior thyroid artery, and SCM perforator parts) and operate with great care. If severe intraoperative bleeding occurs, $CO_2$ embolization should be suspected, identified, and treated promptly.

The accessory nerve is the boundary between level IIA and level IIB. Injury of this nerve leads to paralysis and atrophy of the trapezius, which will significantly affect the patient's postoperative quality of life. None of our patients had accessory nerve injury, and we suggest that the surgeon should make full use of the high resolution of endoscopy to reveal the anatomical structure, expose the accessory nerve, and avoid injury.

## Limitations

The mean operation time was 362.1 ± 73.5 min. This means that the patients were under general anesthesia for a long period. Therefore, surgeons should strengthen their proficiency to shorten the operation time. Moreover, the patient must undergo a rigorous anesthesia tolerance assessment before surgery. Because of the small sample size, a further study including a larger sample size and comparison with the breast approach is needed.

# Conclusion

In conclusion, ELNDBTOA is an option with proven feasibility for select PTC patients with LNM, and the addition of the transoral approach is necessary to ensure complete dissection.

## Data availability statement

The original contributions presented in the study are included in the article, further inquiries can be directed to the corresponding author.

## Ethics statement

The studies involving human participants were reviewed and approved by The Medical Ethics Committee of Zhongshan Hospital, Xiamen University, Xiamen, Fujian, China. The patients provided their written informed consent to participate in this study.

## Author contributions

Conception and design: GW. Development of methodology: PK, YW, YL. Analysis and interpretation of data: JF, WY, SL. Writing of the manuscript: PK, XH, EL, YF. Review of the manuscript: FL, EL, YF. Study supervision: GW. All authors contributed to the article and approved the submitted version.

## Funding

This research was funded by Guidance Project of Xiamen Science and Technology Plan (grant number: 3502Z20224ZD1046).

## Conflict of interest

The authors declare that the research was conducted in the absence of any commercial or financial relationships that could be construed as a potential conflict of interest.

## Publisher's note



## References

1. Cabanillas M, McFadden DG, Durante C. Thyroid cancer. *Lancet*. (2016) 388:2783–95. doi: 10.1016/S0140-6736(16)30172-6

2. Zaydfudim V, Feurer ID, Griffin MR, Phay JE. The impact of lymph node involvement on survival in patients with papillary and follicular thyroid carcinoma. *Surgery*. (2008) 144:1070–7. doi: 10.1016/j.surg.2008.08.034

3. Tan Y, Guo B, Deng X, Ding Z, Wu B, Niu Y, et al. Transoral endoscopic selective lateral neck dissection for papillary thyroid carcinoma: a pilot study. *Surg Endosc*. (2020) 34(12):5274–82. doi: 10.1007/s00464-019-07314-8

4. Guo Y, Qu R, Huo J, Wang C, Hu X, Chen C, et al. Technique for endoscopic thyroidectomy with selective lateral neck dissection via a chest-breast approach. *Surg Endosc*. (2019) 33:1334–41. doi: 10.1007/s00464-018-06608-7

5. Lin P, Liang F, Cai Q, Han P, Chen R, Xiao Z, et al. Comparative study of gasless endoscopic selective lateral neck dissection via the anterior chest approach versus conventional open surgery for papillary thyroid carcinoma. *Surg Endosc*. (2021) 35(2):693–701. doi: 10.1007/s00464-020-07434-6

6. Yan H, Wang Y, Wang P, Xie Q, Zhao Q. "Scarless" (in the neck) endoscopic thyroidectomy (SET) with ipsilateral levels II, III, and IV dissection via breast approach for papillary thyroid carcinoma: a preliminary report. *Surg Endosc*. (2015) 29:2158–63. doi: 10.1007/s00464-014-3911-1

7. Paek SH, Lee HA, Kwon H, Kang K, Park S. Comparison of robot-assisted modified radical neck dissection using a bilateral axillary breast approach with a conventional open procedure after propensity score matching. *Surg Endosc*. (2019) 34:622–7. doi: 10.1007/s00464-019-06808-9

8. Wang B, Weng YJ, Wang SS, Zhao W, Yan S, Zhang L, et al. Feasibility and safety of needle-assisted endoscopic thyroidectomy with lateral neck dissection for papillary thyroid carcinoma: a preliminary experience. *Head Neck*. (2019) 41 (7):2367–75. doi: 10.1002/hed.25705

9. Zhang D, Gao L, Xie L, He G, Chen J, Fang L, et al. Comparison between video-assisted and open lateral neck dissection for papillary thyroid carcinoma with lateral neck lymph node metastasis: a prospective randomized study. *J Laparoendosc Adv Surg Tech A*. (2017) 27:1151–7. doi: 10.1089/lap.2016.0650

10. Wu G, Fu J, Lin F, Luo Y, Lin E, Yan W. Endoscopic central lymph node dissection via breast combined with oral approach for papillary thyroid carcinoma: a preliminary study. *World J Surg*. (2017) 41:2280–2. doi: 10.1007/s00268-017-4015-6

11. Haugen B, Alexander E, Bible K, Doherty G, Mandel S, Nikiforov Y, et al. American thyroid association management guidelines for adult patients with thyroid nodules and differentiated thyroid cancer: the American thyroid association guidelines task force on thyroid nodules and differentiated thyroid cancer. *Thyroid*. (2015) 2016(26):1–133. doi: 10.1089/thy.2015.0020

12. Miccoli P, Materazzi G, Berti P. Minimally invasive video-assisted lateral lymphadenectomy: a proposal. *Surg Endosc*. (2008) 22:1131–4. doi: 10.1007/s00464-007-9564-6

13. Lee Y, Nam K, Chung W, Chang H, Park C. Postoperative complications of thyroid cancer in a single center experience. *J Korean Med Sci*. (2010) 25:541–5. doi: 10.3346/jkms.2010.25.4.541

14. Fu J, Luo Y, Chen Q, Lin F, Hong X, Kuang P, et al. Transoral endoscopic thyroidectomy: review of 81 cases in a single institute. *J Laparoendosc Adv Surg Tech A*. (2018) 28:286–91. doi: 10.1089/lap.2017.0435

frontiers | Frontiers in Surgery

TYPE Original Research
PUBLISHED 04 November 2022
DOI 10.3389/fsurg.2022.1004687



OPEN ACCESS

EDITED BY
Jeroen Van Vugt,
Erasmus Medical Center, Netherlands

REVIEWED BY
Nguyen Minh Duc,
Pham Ngoc Thach University of Medicine, Vietnam
Mijntje Vastbinder,
IJsselland Ziekenhuis, Netherlands

*CORRESPONDENCE
Jianfeng Zeng
zjf202206@163.com

SPECIALTY SECTION
This article was submitted to Surgical Oncology, a section of the journal Frontiers in Surgery

RECEIVED 27 July 2022
ACCEPTED 17 October 2022
PUBLISHED 04 November 2022

CITATION
Yang G, Liu P, Zheng L and Zeng J (2022) Novel peripheral blood parameters as predictors of neoadjuvant chemotherapy response in breast cancer.
Front. Surg. 9:1004687.
doi: 10.3389/fsurg.2022.1004687



# Novel peripheral blood parameters as predictors of neoadjuvant chemotherapy response in breast cancer

Gaohua Yang, Pengju Liu, Longtian Zheng and Jianfeng Zeng*

Department of General Surgery, The Second Affiliated Hospital of Fujian Medical University, Fujian Province, Quanzhou, China

The neutrophil-to-lymphocyte ratio (NLR), platelet-to-lymphocyte ratio (PLR), systemic immune severity index (SII), and prognostic nutritional index (PNI) are associated with the prognosis of gastric, lung, and breast cancers. However, the predictive value of pathological complete response (pCR) rates in patients with breast cancer treated with neoadjuvant chemotherapy (NAC) remains unclear. This retrospective study explored the correlation between each index and the efficacy of neoadjuvant chemotherapy in patients with breast cancer and assessed the relationship between changes before and after neoadjuvant chemotherapy. We enrolled 95 patients with locally advanced breast cancer who received neoadjuvant therapy for breast cancer at the Second Affiliated Hospital of Fujian Medical University from April 2020 to April 2022. Based on postoperative pathology, patients were divided into pCR and non-pCR groups. Between-group differences and efficacy prediction ability of NLR, PLR, SII, and PNI were analyzed. Patient characteristics and changes in NLR, PLR, SII, and PNI before and after neoadjuvant chemotherapy (NAC) were compared between groups. Patients were divided into two groups according to the optimal diagnostic thresholds of the SII before treatment. Between-group differences in terms of neoadjuvant therapy efficacy and patient characteristics were evaluated. The pCR exhibited significantly lower ER ($\chi^2 = 10.227$, $P = 0.001$), PR ($\chi^2 = 3.568$, $P = 0.049$), pretreatment NLR ($\chi^2 = 24.930$, $P < 0.001$), pretreatment PLR ($\chi^2 = 22.208$, $P < 0.001$), pretreatment SII ($\chi^2 = 26.329$, $P < 0.001$), and post-treatment PNI ($P = 0.032$), but higher HER-2 ($\chi^2 = 7.282$, $P = 0.007$) and ΔNLR ($P = 0.015$) than the non-pCR group. ROC curve analysis revealed that the areas under the curve (AUC) of pretreatment SII, NLR, and PLR for predicting pCR of NAC for breast cancer were 0.827, 0.827, and 0.810, respectively, indicating a higher predictive value for response to NAC in patients with breast cancer. According to the Youden index, the optimal cut-off value of SII pretreatment was 403.20. Significant differences in age ($\chi^2 = 6.539$, $P = 0.01$), ER ($\chi^2 = 4.783$, $P = 0.029$), and HER-2 ($\chi^2 = 4.712$, $P = 0.030$) were observed between high and low-SII groups. In conclusion, pretreatment NLR, PLR, and SII can be used as predictors of pCR in patients with breast cancer receiving neoadjuvant chemotherapy. The predictive value of pretreatment SII is higher, and patients with low SII are more likely to achieve pCR.

KEYWORDS

breast cancer, neoadjuvant chemotherapy, neutrophil-to-lymphocyte ratio, platelet-to-lymphocyte ratio, systemic immune severity index

# Introduction

Breast cancer is a malignant tumor with the highest morbidity and mortality among women worldwide. The prevalence of breast cancer is increasing and has become a critical public health issue. Progress in precision medicine has resulted in developments in treatment methods for breast cancer (1). At present, treatment of breast cancer predominantly involves surgery supplemented by systemic therapy and other individualized comprehensive treatment plans (2). However, for locally advanced tumors, such as tumor diameter > 5 cm, axillary lymph node metastasis, or poor molecular type (such as HER-2-positive or triple-negative); or for patients with a ratio of tumor size to breast volume that makes it difficult to preserve breasts, preoperative neoadjuvant drug therapy is often favored to achieve tumor down-staging and reduce recurrence rate in order to prolong patient survival (3). Previous studies have demonstrated that OS and RFS of patients receiving neoadjuvant chemotherapy (NAC) are closely related to the efficacy of neoadjuvant therapy. As patients who achieve pathological complete remission (pCR) with NAC typically have longer survival time, early prediction of efficacy in breast cancer is critical for individualized treatment (4).

The current preoperative NAC regimen for breast cancer is based on factors such as molecular classification and predominantly comprises a 6-cycle TEC or 8-cycle EC-T regimen, that is, taxane combined with anthracycline, For patients with HER-2-positive breast cancer, targeted drugs are often added, such as trastuzumab and pertuzumab. Each cycle consists of 21 days, and evaluations are performed once every three cycles. Surgery is performed after completing the entire NAC course, and the specific efficacy of neoadjuvant therapy is evaluated according to postoperative paraffin pathology. However, there is a paucity of relevant prediction methods in clinical practice for patients who are insensitive to neoadjuvant therapy and delayed treatment. Therefore, there is an urgent need to explore convenient and effective indicators to assist in the clinical evaluation of the efficacy of neoadjuvant therapy in patients with breast cancer. Given the ease of performing blood tests, assessment of peripheral blood-related indicators may hold considerable clinical value for predicting the efficacy of neoadjuvant therapy in patients with breast cancer.

Persistent subclinical inflammation is associated with various diseases, particularly senile diseases (5). Recent studies have reported that chronic inflammation is closely associated with the occurrence and development of cancer (6). Tumor recurrence and metastasis are associated with the biological behavior of tumors and inflammatory responses. In cancer, normal vascular endothelial cells regulate microenvironmental homeostasis that can limit tumor growth, invasion, and metastasis. In contrast, dysfunctional endothelial cells exposed to an inflammatory tumor microenvironment support cancer progression and metastasis (7). For example, the persistent presence of *Helicobacter pylori*-associated gastritis is inseparable from MALT lymphoma.

Neutrophils, platelets, lymphocytes, and albumin are key mediators of chronic inflammation. Based on studies examining different solid tumors, the poor prognosis of gastric, lung, and breast cancers is associated with increased neutrophil/lymphocyte ratio (NLR), platelet/lymphocyte ratio (PLR), systemic immune inflammatory index (SII), and prognostic nutritional index (PNI) (8). However, there is a paucity of studies on the relationship between these inflammatory indicators and the efficacy of neoadjuvant therapy in patients with breast cancer.

Therefore, this study aimed to analyze the relationship of NLR, PLR, SII, and PNI with the efficacy of NAC in patients with breast cancer. To this end, we explored the risk factors affecting the efficacy of NAC in patients with breast cancer and analyzed the relationship between NLR, PLR, SII, and PNI changes pre-NAC and post-NAC to derive pretreatment predictive indicators for individualized breast cancer treatment.

# Materials and methods

## Patients

A total of 95 patients with breast cancer who received preoperative neoadjuvant therapy at the Second Affiliated Hospital of Fujian Medical University between April 2020 and April 2022 were selected as research participants. We extracted detailed treatment information and clinical data from the medical records of all patients. The inclusion criteria were as follows: (1) pathologically diagnosed breast cancer based on ultrasound-guided needle biopsy; (2) completed a course of neoadjuvant therapy; and (3) no other distant organ metastasis. Exclusion criteria were as follows: (1) bilateral, multifocal, inflammatory breast cancer; (2) history of breast surgery or other cancers; (3) had not completed the full course of treatment; and (4) patients with immune-related

diseases, chronic wasting diseases, and blood system diseases that affected blood testing.

## Clinical characteristics

Clinical data of the enrolled patients were collected, including age, NAC regimen, TNM stage, pathological type, histological grade, molecular typing, platelet count, neutrophil count, lymphocyte count, albumin count and efficacy evaluation. Evaluation of efficacy was predominantly based on whether the patient achieved pCR after NAC, i.e., no histological evidence of malignant tumor in the primary breast tumor and metastatic regional lymph nodes or carcinoma restricted to the *in situ* component based on the 2022 China Clinical Tumor Society (CSCO) guidelines for the diagnosis and treatment of breast cancer, which set the positive threshold of ER and PR immunohistochemical detection as 1% and immunohistochemical results of Her-2 (+++) as Her-2 positive. If Her-2 (++), FISH detection was included, and Her-2 status was determined based on FISH results. All patients were TNM-staged according to the American Joint Committee on Cancer guidelines.

## Methods

Based on the results of routine blood and biochemical tests pre- and post-NAC, platelet, neutrophil, lymphocyte, and albumin counts as well as NLR, PLR, SII, and PNI were calculated. NLR and PLR refer to the ratio of neutrophils to lymphocytes and platelets to lymphocytes, respectively. SII was calculated as follows: platelet count × neutrophil count/ lymphocyte count, which reflects inflammation and immune system status. PNI was calculated as follows: albumin (g/L) + 5 × lymphocyte count (109/L). Patients were divided into PCR and non-PCR groups based on postoperative pathology. The efficacy prediction ability of NLR, PLR, SII, and PNI values before treatment and differences in clinicopathological characteristics between the two groups were analyzed. Dynamic changes in NLR, PLR, SII, and PNI were measured. The receiver operating characteristic (ROC) curve was used to determine the optimal cutoff value of SII, that is, the maximum point of the sum of sensitivity and specificity (Youden index), and divided into two groups (high and low) to compare the difference in efficacy of NAC and clinical outcomes between the two groups and between different pathological features.

## Statistical analysis

The database was established using Excel. Data were analyzed and graphed using SPSS 26.0 and GraphPad Prism 9.0 software. Quantitative data conforming to a normal distribution were expressed as $x \pm s$, and two independent samples *t*-test was used for comparison between groups, the U test was used for the non-normal quantitative data, and qualitative data were expressed as the number of cases and percentages, and the comparison between groups was performed by chi-square test. The receiver operating characteristic (ROC) curve was drawn to analyze the predictive value of SII before treatment for pCR. The SII value corresponding to the maximum sum of sensitivity and specificity was the best cut-off value. $P < 0.05$ considered the difference to be statistically significant.

# Results

## Relationship between pCR grouping and clinical characteristics

A total of 95 patients with breast cancer were included in the study. Of patients, 26 achieved pCR after neoadjuvant therapy (pCR rate, 27.4%). Significant differences were observed in ER, PR, and HER-2 expression between the pCR and non-pCR groups (all $P < 0.05$). Patients with ER (−), PR (−), HER-2 (+++) exhibited higher pCR rates. No significant differences between the pCR and non-pCR groups were noted in age, tumor size, lymph node metastasis, and Ki-67 ($P > 0.05$).The data are summarized in (**Table 1**).

## Relationship of NLR, PLR, SII, and PNI with pCR

The 95 enrolled patients were divided into pCR and non-pCR groups. Dichotomous variables passed the $\chi^2$ test, and continuous variables passed the *t*-test. Pretreatment NLR, pretreatment PLR, and pretreatment SII were lower in the pCR group than in the non-pCR group. ($P < 0.001$). Post-treatment PNI and ΔNLR were lower in the non-pCR group ($P < 0.05$). In contrast, pretreatment PNI, post-treatment NLR, post-treatment PLR, SII, ΔPLR, ΔSII, and ΔPNI post-treatment were significantly different to those in the non-pCR group. No significant correlations were noted with the efficacy of NAC (all $P > 0.05$). None of the patients with a high pretreatment NLR achieved pCR. Patients with pretreatment PLR < 118.78 had a 4.5-fold higher rate of pCR compared to those with pretreatment PLR > 118.78. pCR rate was almost five times higher in patients with pretreatment SII < 403.20

TABLE 1 Associations of clinicopathological characteristics with pCR in breast cancer patients.

| Variables | Number | PCR | *n*-PCR | $\chi^2$ | *P*-value |
|---|---|---|---|---|---|
| **Age** | | | | 1.422 | 0.233 |
| ≤50岁 | 49 | 16 | 33 | | |
| >50岁 | 46 | 10 | 36 | | |
| **TNM** | | | | 0.816 | 0.366 |
| ≤II | 44 | 14 | 30 | | |
| >II | 51 | 12 | 39 | | |
| **T** | | | | 0.460 | 0.498 |
| ≤5 cm | 60 | 15 | 45 | | |
| >5 cm | 35 | 11 | 24 | | |
| **N** | | | | 0.531 | 0.466 |
| ≤N1 | 64 | 19 | 45 | | |
| >N1 | 31 | 7 | 24 | | |
| **ki-67** | | | | 2.915 | 0.088 |
| ≤30% | 35 | 6 | 29 | | |
| >30% | 60 | 20 | 40 | | |
| **ER** | | | | 10.227 | 0.001 |
| Negative | 31 | 15 | 16 | | |
| Positive | 64 | 11 | 53 | | |
| **PR** | | | | 3.568 | 0.049 |
| Negative | 40 | 15 | 25 | | |
| Positive | 55 | 11 | 44 | | |
| **HER-2** | | | | 7.282 | 0.007 |
| Low | 47 | 7 | 40 | | |
| High | 48 | 19 | 29 | | |
| **NLR** | | | | 24.930 | 0.000 |
| >2.46 | 39 | 0 | 39 | | |
| <2.46 | 56 | 26 | 30 | | |
| **PLR** | | | | 22.208 | 0.000 |
| >118.78 | 67 | 9 | 58 | | |
| <118.78 | 28 | 17 | 11 | | |
| **SII** | | | | 26.329 | 0.000 |
| >403.20 | 74 | 11 | 63 | | |
| <403.20 | 21 | 15 | 6 | | |

TABLE 2 The relationship between NLR, PLR, SII, PNI and pCR before treatment, after treatment and dynamic changes.

| Variables | PCR | `X ± S | *T*-value | *P*-value |
|---|---|---|---|---|
| **Pre-NLR** | Yes | 1.59±0.53 | −6.278 | <0.001 |
| | No | 2.81±1.36 | | |
| **Pre-PLR** | Yes | 113.46±29.53 | −5.747 | <0.001 |
| | No | 168.01±62.45 | | |
| **Pre-SII** | Yes | 409.34±170.62 | −5.546 | <0.001 |
| | No | 791.64±500.67 | | |
| **Pre-PNI** | Yes | 55.74±4.28 | 0.678 | 0.500 |
| | No | 55.02±4.73 | | |
| **Post-NLR** | Yes | 2.06±1.08 | −1.136 | 0.259 |
| | No | 2.42±1.49 | | |
| **Post-PLR** | Yes | 172.50±95.87 | −1.633 | 0.106 |
| | No | 208.87±97.14 | | |
| **Post-SII** | Yes | 482.81±381.08 | −1.616 | 0.110 |
| | No | 646.90±461.60 | | |
| **Post-PNI** | Yes | 52.01±3.80 | 2.173 | 0.032 |
| | No | 49.95±4.24 | | |
| **ΔNLR** | Yes | 0.47±1.31 | 2.478 | 0.015 |
| | No | −0.39±1.58 | | |
| **ΔPLR** | Yes | 59.04±87.56 | 0.852 | 0.396 |
| | No | 40.85±94.62 | | |
| **ΔSII** | Yes | 73.47±437.56 | 1.724 | 0.088 |
| | No | −144.74±585.86 | | |
| **ΔPNI** | Yes | −3.73±4.74 | 1.688 | 0.095 |
| | No | −5.08±2.84 | | |

than in those with pretreatment SII > 403.20. The data are summarized in (Table 2).

## Predictive value of preoperative NLR, PLR, SII, and PNI for pCR in breast cancer

The area under the curve (AUC) of the ROC curve of NLR, PLR, SII, and PNI was used to assess the ability of preoperative NLR, PLR, SII, and PNI to predict pCR in patients with breast cancer. The AUC, best cut-off value, sensitivity, and specificity of NLR were 0.827 (95% CI: 0.744–0.910, $P < 0.001$), 2.46, 100%, and 56.5%, respectively. The AUC, best cut-off value, sensitivity, and specificity of PLR were 0.810 (95% CI: 0.718–0.901), $P < 0.001$), 118.78, 65.4%, and 84.1%, respectively. The AUC, best cut-off value, sensitivity, and specificity of SII were 0.827 (95% CI: 0.737–0.916, $P < 0.001$), 403.20, 57.7%, and 91.3%, respectively. The AUC of PNI was 0.444 (95% CI: 0.309–0.579, $P > 0.05$), indicating that NLR, PLR, and SII had good predictive values. Of these indices, SII had the largest AUC, and pretreatment PNI did not have significant predictive value. This suggested that pretreatment SII had higher predictive value for the efficacy of NAC in patients with breast cancer.The data are summarized in (Figure 1).

## Relationship between pretreatment SII grouping and clinical characteristics

Based on the optimal cut-off value of the ROC curve, patients were divided into groups with pretreatment SII <403.20 or >403.20. Significant between-group differences were observed in age, ER, and HER-2 status. Patients in the low SII group were predominantly aged ≤50 years, ER (−), and HER-2 (+++), while those in the high SII group were

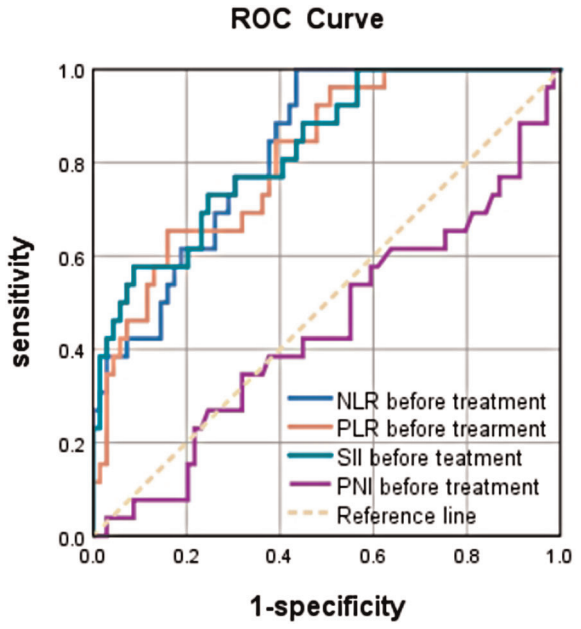


FIGURE 1
Predictive ability of the SII,NLR, PLR and PNI presented by ROC curves.

TABLE 3 Relationships between SII and clinicopathological characteristics.

| Variables | Number | SII<403.20 | SII>403.20 | $X^2$值 | $p$值 |
|---|---|---|---|---|---|
| **Age** | | | | 6.539 | 0.01 |
| ≤50岁 | 49 | 16 | 33 | | |
| >50岁 | 46 | 5 | 41 | | |
| **TNM** | | | | 0.130 | 0.719 |
| ≤II | 44 | 9 | 35 | | |
| >II | 51 | 12 | 39 | | |
| **T** | | | | 0.143 | 0.706 |
| ≤5 cm | 60 | 14 | 46 | | |
| >5 cm | 35 | 7 | 28 | | |
| **N** | | | | 0.366 | 0.545 |
| ≤N1 | 64 | 13 | 51 | | |
| >N1 | 31 | 8 | 23 | | |
| **ki-67** | | | | 0.143 | 0,706 |
| ≤30% | 35 | 7 | 28 | | |
| >30% | 60 | 14 | 46 | | |
| **ER** | | | | 4.783 | 0.029 |
| Negative | 31 | 11 | 20 | | |
| Positive | 64 | 10 | 54 | | |
| **PR** | | | | 2.501 | 0.114 |
| Negative | 40 | 12 | 28 | | |
| Positive | 55 | 9 | 46 | | |
| **HER-2** | | | | 4.712 | 0.030 |
| Low | 47 | 6 | 41 | | |
| High | 48 | 15 | 33 | | |

aged >50 years, with low expression of ER (+) and HER-2. Other indicators, such as tumor size, TNM stage, lymph node metastasis, and PR, were not significantly correlated with the high and low SII groups.The data are summarized in (Table 3).

## Discussion

Breast cancer has emerged as the most common cancer among women worldwide, and its mortality rate ranks first among cancer-related deaths in women, with a gradual upward trend (9). The specific mechanisms underlying the occurrence and development of breast cancer remain unclear. In recent years, the correlation between chronic inflammation and breast cancer has received widespread attention from the medical community (10). Numerous studies have demonstrated a relationship between chronic inflammation and poor prognosis in patients with breast cancer. The occurrence of breast cancer causes cancer cells to accumulate chemotactic inflammatory cells, while chronic inflammation-associated neutrophils regulate the tumor microenvironment (TME) through cytokines and cathepsins to promote cancer cell migration, invasion, and metastasis. A possible underlying mechanism is chronic inflammation-induced production of inflammatory mediators such as interleukin-6 (IL-6) (11). These effects promote angiogenesis in target organs, DNA damage, and gene mutation, which leads to cancer growth and metastasis. Further, nuclear transcription factor-κB (NF-κB), a key factor in inflammation and tumor cells, induces TNF-α and IL-6 chemotactic leukocytes to infiltrate the inflammation site (12). This may contribute to genetic mutations, thereby promoting tumorigenesis. In addition, activation of the STAT-3 and NF-κB signaling pathways stimulates the expression of vascular endothelial growth factor (VEGF) and chemokines (CXC), induces epithelial-to-mesenchymal transition, and ultimately promotes tumor cell proliferation and growth (13). Therefore, we designed this study to investigate the relationship between breast cancer and chronic inflammation.

Neutrophils in the TME can be divided into two types: N1 and N2. N1 neutrophils exert anti-tumor properties and directly kill cancer cells through cytotoxicity, antibody-dependent cytotoxicity, and antigen presentation (14). N2-type neutrophils exert tumor-promoting properties by promoting cancer cell proliferation, pathological angiogenesis, and immune regulation. Queen et al. reported that neutrophils promote the expression of VEGF by releasing oncostatin M and binding to receptors on the cell membrane in breast cancer, thereby activating tyrosine kinase signaling pathways

and transcriptional activators, ultimately promoting tumor invasion (15).

Platelets play a key role in the process of vascular injury repair (16). Platelets store and release vascular regulatory factors, such as VEGF, to increase vascular permeability, promote blood coagulation, and induce vascular endothelial cell migration, thereby promoting tumor angiogenesis (17). Indeed, platelets play an essential role in tumor invasion and metastasis. A retrospective analysis of 180 patients with breast cancer and 100 patients with normal breasts by Liu et al. revealed that the pCR rate of supraclavicular lymph nodes after NAC was 51.8%. In this regard, platelets have predictive value for the prognosis of patients with breast cancer and metastasis. Patients with high platelet counts have poorer prognosis compared to patients with low platelet counts, suggesting that platelet counts may be clinically useful for differentiating high-risk patients (18).

Peripheral blood lymphocytes reflect immune levels and overall nutritional status of the body. CD8 + T lymphocytes promote the anti-tumor ability of endogenous lymphocytes through type I immune responses and release perforin through the perforin-granzyme pathway (19). Natural killer cells can induce dendritic cells to aggregate within the TME by releasing chemokines and killing cancer cells or activating T lymphocytes to initiate specific immune responses through interferon (20). A retrospective analysis of the relationship between tumor-infiltrating lymphocytes and breast cancer by Tianen et al. revealed that regional infiltrating lymphocytes in the tumor could be used as a predictor of the efficacy of neoadjuvant therapy for breast cancer, and neoadjuvant therapy promoted immune infiltration of TILs in the tumor region of patients with breast cancer (21).

Previous studies have confirmed that NLR, PLR, and SII are associated with the prognosis of many malignant tumors, including colon, prostate, and breast cancers, and are closely related to the depth of tumor invasion and lymph node metastasis (22). Gulzade et al. demonstrated that a high NLR could be used as an independent predictor in the differential diagnosis of breast cancer from benign breast disease and could predict sentinel lymph node metastasis (23). Coh et al. analyzed pretreatment NLR in more than 2,000 patients with breast cancer and concluded that 5-year survival in the high NLR group was lower. Further, women with breast cancer in the high NLR group were younger, had larger tumor size, and had a higher risk of lymphatic and distant metastases (24). A retrospective study by Liu et al. reported that increased SII was associated with poorer OS in triple-negative breast cancer ($HR = 2.91$, $P < 0.001$) (25). Chen et al. used an SII of $<602 \times 10^9$/L as the optimal cut-off value and divided patients into high and low SII groups. DFS and OS of patients with breast cancer were higher in the low SII group than in the high SII group, and SII was not significantly associated with the side effects of NAC (26). Multivariate analysis in a propensity score-matched study on the prognostic value of preoperative SII in breast cancer initiated by Hua et al. revealed that SII independently predicted OS ($P = 0.017$) and DMFS ($P = 0.007$) (27). The prognosis of patients is closely associated with histological type, T stage, N stage, PR, HER2, and Ki67 of the tumor. Patients with breast cancer with a high initial SII value should thus receive early supplemental immunotherapy and anti-inflammatory treatment.Our study confirmed that pretreatment NLR, PLR, and SII could be used as predictors of the efficacy of locally advanced neoadjuvant therapy. Further, we observed that pCR was closely associated with ER, PR, and HER-2 but was not significantly related to tumor size or lymph node metastasis. A possible reason is potential bias due to the small sample size of this study. No significant differences were noted in post-treatment NLR, PLR, SII, ΔNLR, ΔPLR, and ΔSII between the two groups, possibly because the measured blood parameters were not sensitive enough to reflect the inflammatory state of the body due to the effects of bone marrow suppression after chemotherapy.

Serum albumin is a key indicator of the nutritional status of the body (28). In the pathological state of cancer, albumin consumption increases, and low albumin weakens immune defense mechanisms, resulting in a vicious circle associated with cancer. Oba et al. observed that DFS was significantly lower in the high ΔPNI group than in the low ΔPNI group (optimal cut-off value: 5.26, $P = 0.015$) when evaluating the prognostic impact of PNI changes in patients with breast cancer receiving NAC. These results suggest that maintaining nutritional status during NAC may lead to better treatment outcomes for patients with breast cancer (29). In our study, there is no significant difference was observed in pretreatment PNI between pCR and non-pCR groups. However, post-treatment PNI was greater in the pCR group than in the non-pCR group ($P = 0.032$). With regard to ΔPNI, the pCR group ($\mathbf{X} = -3.73$) exhibited a smaller decrease compared to the non-pCR group ($\mathbf{X} = -5.08$), although this difference was not statistically significant ($P = 0.095$). A potential explanation is that maintaining good nutritional and immune status during NAC may correlate with the curative effects.

As this was a retrospective single-center study, certain study limitations should be noted. First, the sample size was small, especially in the pCR group, which may have resulted in selection bias. Second, further multicenter studies are required for validation. Furthermore, there is a lack of continuous assessment of neoadjuvant treatment efficacy and lack of comparison with existing imaging methods for assessing neoadjuvant efficacy.

Further research on the relationship between chronic inflammation, inflammation-related parameters, and breast

cancer is warranted to facilitate individualized treatment of breast cancer and prediction of efficacy.

## Conclusions

Pretreatment NLR, PLR, and SII can be used as predictors of pCR in patients with breast cancer undergoing NAC. Pretreatment SII has a higher predictive value, and patients with low SII are more likely to achieve pCR.

## Data availability statement

The raw data supporting the conclusions of this article will be made available by the authors, without undue reservation.

## Ethics statement

The studies involving human participants were reviewed and approved by The Second Affiliated Hospital of Fujian Medical University. The patients/participants provided their written informed consent to participate in this study.

## Author contributions

GY and JZ drafted the manuscript; JZ performed the surgery; PL and LZ collected the clinical data; GY and PL conducted the literature review; and JZ revised the manuscript critically for intellectual content; all authors have read and approved the final manuscript. All authors contributed to the article and approved the submitted version.

## Conflict of interest

The authors declare that the research was conducted in the absence of any commercial or financial relationships that could be construed as a potential conflict of interest.

## Publisher's note

All claims expressed in this article are solely those of the authors and do not necessarily represent those of their affiliated organizations, or those of the publisher, the editors and the reviewers. Any product that may be evaluated in this article, or claim that may be made by its manufacturer, is not guaranteed or endorsed by the publisher.

## References

1. Von Minckwitz G, Untch M, Blohmer JU, Costa SD, Eidtmann H, Fasching PA, et al. Definition and impact of pathologic complete response on prognosis after neoadjuvant chemotherapy in various intrinsic breast cancer subtypes. *J Clin Oncol*. (2012) 30:1796–804. doi: 10.1200/JCO.2011.38.8595

2. Harbeck N, Gnant M. Breast cancer. *Lancet*. (2017) 389(10074):1134–50. doi: 10.1016/S0140-6736(16)31891-8

3. Colomer R, Saura C, Sanchez-Rovira P, Pascual T, Rubio IT, Burgues O, et al. Neoadjuvant management of early breast cancer: a clinical and investigational position statement. *Oncologist*. (2019) 24(5):603–11. doi: 10.1634/theoncologist.2018-0228

4. Cortazar P, Zhang L, Untch M, Mehta K, Costantino JP, Wolmark N, et al. Pathological complete response and long-term clinical benefit in breast cancer: the CTNeoBC pooled analysis. *Lancet*. (2014) 384(9938):164–72. doi: 10.1016/S0140-6736(13)62422-8

5. Chen NN, Dai D. Progress in the role of chronic inflammation in malignant tumors. *Medical Innovation of China*. (2020) 17(14):169–72. doi: 10.3969/j.issn.1674-4985.2020.14.043

6. Galdiero MR, Marone G, Mantovani A. Cancer inflammation and cytokines. *Cold Spring Harb Perspect Biol*. (2018) 10(8):a028662. doi: 10.1101/cshpers-pect.a028662

7. Fridman WH, Zitvogel L, Sautes-Fridman C, Kroemer G. The immune contexture in cancer prognosis and treatment. *Nat Rev Clin Oncol*. (2017) 14(12):717–34. doi: 10.1038/nrclinonc.2017.101

8. Dan J, Tan J, Huang J, Zhang X, Guo Y, Huang Y, et al. The dynamic change of neutrophil to lymphocyte ratio is predictive of pathological complete response after neoadjuvant chemotherapy in breast cancer patients. *Breast Cancer*. (2020) 27(5):982–8. doi: 10.1007/s12282-020-01096-x

9. Azamjah N, Yasaman SZ, Zayeri F. Global trend of breast cancer mortality rate: a 25-year study. *Asian Pac J Cancer Prev*. (2019) 20(7):2015–20. doi: 10.31557/APJCP.2019.20.7.2015

10. Danforth DN. The role of chronic inflammation in the development of breast cancer. *Cancers (Basel)*. (2021) 13:3918. doi: 10.3390/cancers13153918

11. Yu H, Kortylewski M, Pardoll D. Crosstalk between cancer and immune cells: role of STAT3 in the tumour microenvironment. *Nat Rev Immunol*. (2007) 7:41–51. doi: 10.1038/nri1995

12. Zhou Y, Xia L, Liu Q, Wang H, Lin J, Oyang L, et al. Induction of pro-inflammatory response via activated macrophage mediated NF-$\kappa$B and STAT3 pathways in gastric cancer cells. *J Cell Physiol Biochem*. (2018) 47(4):1399–410. doi: 10.1159/000490829

13. Grivennikov SI, Karin M. Dangerous liaisons: sTAT3 and NF-kappaB collaboration and crosstalk in cancer. *Cytokine Growth Factor Rev*. (2010) 21:11–9. doi: 10.1016/j.cytogfr.2009.11.005

14. Kim J, Bae J-S. Tumor-associated macrophages and neutrophils in tumor microenvironment. *Mediators Inflamm*. (2016) 2016:1466–861. doi: 10.1155/2016/6058147

15. Queen MM, Ryan RE, Holzer RG, Keller-Peck CR, Jorcyk CL. Breast cancer cells stimulate neutrophils to produce oncostatin M: potential implications for tumor progression. *J Cancer Res*. (2005) 65(19):8896–904. doi: 10.1158/0008-5472.CAN-05-1734

16. Ahmad A, Wang ZW, Kong DJ, Ali R, Ali S, Banerjee S, et al. Platelet-derived growth factor-D contributes to aggressiveness of breast cancer cells by up-regulating notch and NF-$\kappa$B signaling pathways. *Breast Cancer Res Treat*. (2011) 126:15–25. doi: 10.1007/s10549-010-0883-2

17. Guo Y, Cui W, Pei Y, Xu D. Platelets promote invasion and induce epithelial to mesenchymal transition in ovarian cancer cells by TGF-$\beta$ signaling pathway. *Gynecol Oncol*. (2019) 153(3):639–50. doi: 10.1016/j.ygyno.2019.02.026

18. Liu SQ, Fang J, Jiao DH, Liu ZZ. Elevated platelet count predicts poor prognosis in breast cancer patients with supraclavicular lymph node meta-stasis. *Cancer Manag Res*. (2020) 12:6069–75. doi: 10.2147/CMAR.S257727

19. Liu S, Lachapelle J, Leung S, Gao D, Foulkes WD, Nielsen TO. CD8 + lymphocyte Infiltration is an independent favorable prognostic indicator in basal-like breast cancer. *J Breast Cancer Research: BCR*. (2012) 14(2):R48–R48. doi: 10.1186/bcr3148

20. Böttcher JP, Bonavita E, Chakravarty P, Blees H, Cabeza-Cabrerizo M, Sammicheli S, et al. NK Cells stimulate recruitment of cDC1 into the tumor microenvironment promoting cancer immune control. *Cell*. (2018) 172 (5):1022–37. doi: 10.1016/j.cell.2018.01.004

21. Jin TE, Huang J, Zh X, Guo WL, Ye ZQ, Huang JQ, et al. Tumor infiltrating lymphocytes as a predictive factor for pCR to neoadjuvant treatment in breast cancer. *J Evid Based Med*. (2020) 20(3):175–80. doi: 10.12019/j.issn.1671-5144.2020.03.010

22. Ji YF, Wang HY. Prognostic value of the systemic immune inflammation index in patients with breast cancer: a meta-analysis. *World J Surg Oncol*. (2020) 18:197. doi: 10.1186/s12957-020-01974-w

23. Ozyalvacli G, Yesil C, Kargi E, Kizildag B, Kilitci A, Yilmaz F. Diagnostic and prognostic importance of the neutrophil lymphocyte ratio in breast cancer. *Asian Pac J Cancer Prev*. (2014) 15(23):10363–6. doi: 10.7314/APJCP.2014.15.23.10363

24. Koh CH, Bhoo-Pathy N, Ng KL, Jabir RS, Tan GH, See MH, et al. Utility of pre-treatment neutrophil–lymphocyte ratio and platelet–lymphocyte ratio as prognostic factors in breast cancer. *Br J Cancer*. (2015) 113(1):150–8. doi: 10.1038/bjc.2015.183

25. Liu JX, Shi ZZ, Bai YS, Liu L, Cheng KL. Prognostic significance ofsystemic immune-inflammation index in triple-negative breast cancer. *Cancer Manag Res*. (2019) 11:4471–80. doi: 10.2147/CMAR.S197623

26. Li C, Kong XY, Wang ZZ, Wang XY, Fang L, Wang J. Pretreatment systemic immune-inflammation index is a useful prognostic indicator in patients with breast cancer undergoing neoadjuvant chemotherapy. *J Cell Mol Med*. (2020) 00:1–29. doi: 10.1111/jcmm.14934

27. Hua X, Long ZQ, Zhang YL, Wen W, Guo L, Xia W, et al. Prognostic value of preoperative systemic immune-inflammation index in breast cancer: a propensity score matching study. *Cancer Manag Res*. (2019) 11:4471–80. doi: 10.3389/fonc.2020.00580

28. Li C, Bai P, Kong XY, Huang SL, Wang ZZ, Wang XY, et al. Prognostic nutritional Index (PNI) in patients with breast cancer treated with neoadjuvant chemotherapy as a useful prognostic indicator. *Front Cell Dev Biol*. (2021) 9:656741. doi: 10.3389/fcell.2021.656741

29. Oba T, Maeno K, Takekoshi D, Ono M, Ito T, Kanai T, et al. Neoadjuvant chemotherapy induced decrease of prognostic nutrition index predicts poor prognosis in patients with breast cancer. *BMC Cancer*. (2020) 20:160. doi: 10.1186/s12885-020-6647-4

frontiers | Frontiers in Surgery

TYPE Original Research
PUBLISHED 07 November 2022
DOI 10.3389/fsurg.2022.1039828



OPEN ACCESS

EDITED BY
Jeroen Van Vugt,
Erasmus Medical Center, Netherlands

REVIEWED BY
Stefania Brozzetti,
Sapienza University of Rome, Italy
Ahmed Farag El-Kased,
University of Menoufia, Egypt

*CORRESPONDENCE
Wenjun Liao
liaowenjun120@163.com
Linquan Wu
wulqnc@163.com

†These authors have contributed equally to this work

SPECIALTY SECTION
This article was submitted to Surgical Oncology, a section of the journal Frontiers in Surgery

RECEIVED 08 September 2022
ACCEPTED 17 October 2022
PUBLISHED 07 November 2022

CITATION
Yang J, Li E, Wang C, Luo S, Fu Z, Peng J, Liao W and Wu L (2022) Robotic versus open extended cholecystectomy for T1a–T3 gallbladder cancer: A matched comparison.
Front. Surg. 9:1039828.
doi: 10.3389/fsurg.2022.1039828



# Robotic versus open extended cholecystectomy for T1a–T3 gallbladder cancer: A matched comparison

Jun Yang†, Enliang Li†, Cong Wang†, Shuaiwu Luo, Zixuan Fu, Jiandong Peng, Wenjun Liao* and Linquan Wu*

Department of General Surgery, The Second Affiliated Hospital of Nanchang University, Nanchang, China

**Background:** The feasibility and safety of robotic extended cholecystectomy (REC) are still uncertain. This study was performed to compare the short- and long-term outcomes of REC with those of open extended cholecystectomy (OEC) for T1a–T3 gallbladder cancer.
**Methods:** From January 2015 to April 2022, 28 patients underwent REC in our center. To minimize any confounding factors, a 1:2 propensity score-matching analysis was conducted based on the patients' demographics, liver function indicators, T stage, and symptoms. The data regarding demographics, perioperative outcomes, and long-term oncologic outcomes were reviewed.
**Results:** The visual analogue scale score was significantly lower in the REC than OEC group immediately postoperatively ($3.68 \pm 2.09$ vs. $4.73 \pm 1.85$, $P = 0.008$), on postoperative day 1 ($2.96 \pm 1.75$ vs. $3.69 \pm 1.41$, $P = 0.023$), and on postoperative day 2 ($2.36 \pm 1.55$ vs. $2.92 \pm 1.21$, $P = 0.031$). In addition, the REC group exhibited a shorter time to first ambulation ($P = 0.043$), a shorter time to drainage tube removal ($P = 0.038$), and a shorter postoperative stay ($P = 0.037$), but hospital costs were significantly higher in the REC group ($P < 0.001$). However, no statistically significant difference was found in the operation time ($P = 0.134$), intraoperative blood loss ($P = 0.467$), or incidence of postoperative morbidity ($P = 0.227$) or mortality ($P = 0.289$) between the REC and OEC groups. In regard to long-term outcomes, the 3-year disease-free survival rate was comparable between the OEC and REC groups (43.1% vs. 57.2%, $P = 0.684$), as was the 3-year overall survival rate (62.8% vs. 75.0%, $P = 0.619$).
**Conclusion:** REC can be an effective and safe alternative to OEC for selected patients with T1a–T3 gallbladder cancer with respect to short- and long-term outcomes.

KEYWORDS

gallbladder cancer (GBC), extended cholecystectomy, robotic surgery, propensity score matching, surgical outcomes

Abbreviations
REC, robotic extended cholecystectomy; OEC, open extended cholecystectomy; GBC, gallbladder cancer; PSM, propensity scores matching; OS, overall survival; DFS, disease-free survival; AJCC, American Joint Committee on Cancer; CT, computed tomography; MRCP, magnetic resonance cholangiopancreatography; BMI, body mass index; TB, total bilirubin; ASA, American score of anesthesiologists; ALT, alanine aminotransferase; AST, aspartate aminotransferase; CEA, carcinoembryonic antigen; CA 19-9, carbohydrate antigen; SDs, standard deviations; SMD, standardized mean difference; VAS, visual analog scale.

# Introduction

Gallbladder cancer (GBC) refers to malignant tumors that occur in the gallbladder, including the base, body, neck, and cystic duct. In China, GBC accounts for 0.4%–3.8% of all biliary tract diseases and ranks sixth among all gastrointestinal cancers (1, 2). Moreover, the overall mean survival rate for patients with GBC is 6 months, and the 5-year overall survival rate is 5% (3). Radical resection is the only curative treatment for GBC (4). Therefore, the choice of surgical technique is particularly important, and whether to perform extended resection depends on the patient's preoperative imaging data and intraoperative frozen section results.

Extended cholecystectomy can greatly improve the postoperative survival time and quality of life of patients with GBC, but traditional open extended cholecystectomy (OEC) is associated with many postoperative complications (e.g., bleeding, bile leakage, and poor wound healing) that can lead to slow recovery and a prolonged hospital stay (5–7). However, since the inception of robot-assisted liver resection in 2003, robotic extended cholecystectomy (REC) has gained widespread acceptance (8). The development of robotic surgical systems has promoted treatment of GBC in the past decade, and the number of patients with GBC receiving REC has rapidly increased (9–11).

This study involved patients with stage T1a–T3 GBC according to the 8th edition of the TNM Classification of Malignant Tumors of the American Joint Committee on Cancer (AJCC) who were treated by extended hepatectomy with gallbladder resection (12). We retrospectively analyzed the clinical data of 28 patients with GBC treated with REC. To reduce the confounding bias, a 1:2 propensity score-matching (PSM) analysis was conducted in the REC and OEC groups. The perioperative data and follow-up results were analyzed to provide clinical evidence for more rapid recovery after robotic surgery than after open surgery for the treatment of GBC.

# Patients and methods

## Study design

From January 2015 to April 2022, 28 consecutive patients who underwent REC for the treatment of GBC at the Second Affiliated Hospital of Nanchang University and met the inclusion criteria were analyzed. During the same period, 117 patients who underwent OEC for GBC were also included (**Figure 1**). All patients had undergone preoperative computed tomography (CT) or magnetic resonance cholangiopancreatography as well as a multidisciplinary consultation including surgery, medical oncology, hepatology, and imaging experts. Clinicopathological data were complete. Non advanced malignancy was identified by pre-operative multi-slice spiral enhanced CT and enhanced magnetic resonance imaging combined with cholangiopancreatography. Enhanced CT examination could show the extent of gallbladder wall invasion, whether adjacent organs were involved, and lymph node metastasis (13). Magnetic resonance cholangiopancreatography could clearly show the anatomical relationship of the pancreatic duct and determine whether there was biliary obstruction. Contrast-enhanced magnetic resonance imaging could identify tumor size, liver invasion, vascular invasion, abdominal lymph node metastasis and distant metastasis (14). Before the operation, all patients were also expected to achieve complete resection without combined resection of adjacent organs other than the liver (patients with distant metastasis were excluded). All patients were well enough to tolerate the operation under general anesthesia and had no history of abdominal surgery. The cases of robotic extended cholecystectomy converted to open surgery, suffered major vascular injuries and needed vascular reconstruction were eliminated. Therefore, 28 patients included in this study were not converted to open surgery, suffered major vascular injuries and needed vascular reconstruction. Because of the high cost associated with REC, REC was performed only in patients who voluntarily agreed to undergo robotic surgery after being fully informed of the differences between the conventional open and robotic approaches. The hospital costs of our medical center were composed of the following 9 aspects: cost for comprehensive medical services, diagnostic cost, treatment cost, rehabilitation cost, cost for traditional Chinese medicine, drug cost, cost for blood and blood products, cost for consumables and other cost. We used propensity scores to match patients in a 1:2 ratio according to age, sex, body mass index, albumin concentration, total bilirubin concentration, American Society of Anesthesiologists classification, alanine aminotransferase concentration, aspartate aminotransferase concentration, T stage, and symptoms. The study was conducted in accordance with the Helsinki Declaration of 1,964 and all subsequent amendments, and it was approved by the Ethics Committee of the Second Affiliated Hospital of Nanchang University in China. All patients provided written informed consent.

## Surgical procedures

To effectively demonstrate the surgical procedures of REC, the following text describes a representative case involving a 68-year-old man with stage T1b GBC according to the AJCC 8th edition staging criteria who underwent wedge resection around the gallbladder fossa.

### Preoperative preparation and trocar locations

The patient was placed in the lithotomy position under general anesthesia. The assistant surgeon stood between the

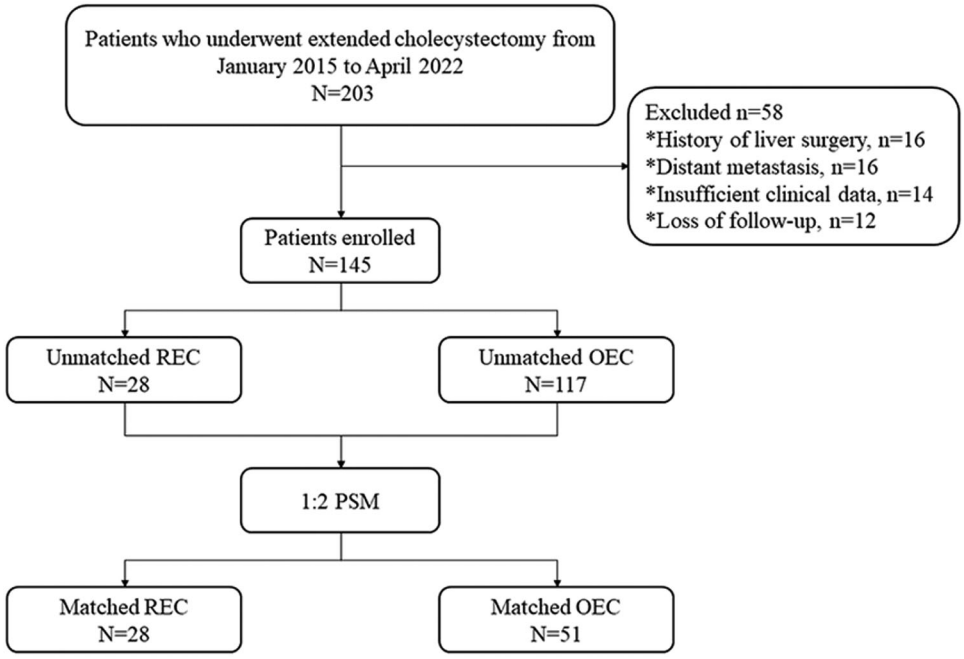


FIGURE 1
Flow chart of study design. REC, robotic extended cholecystectomy; OEC, open extended cholecystectomy; PSM, propensity score matching.

patient's legs with the robot cart located over the patient's head. First, a 12-mm trocar was inserted immediately inferior to the umbilicus using the open technique. Carbon dioxide gas was infused into the intraperitoneal cavity until the pressure reached 14 mmHg. The intra-abdominal space was explored *via* video scope before the other trocars were inserted. The positions of the trocars are shown in Figure 2. These positionings were not absolute but varied instead according to the patient's body size and anatomy. We ensured the space of at least one fist between trocars to minimize interference among instruments. The patient was then placed in the reverse Trendelenburg position and slightly left side down. Robotic arms were docked to each trocar.

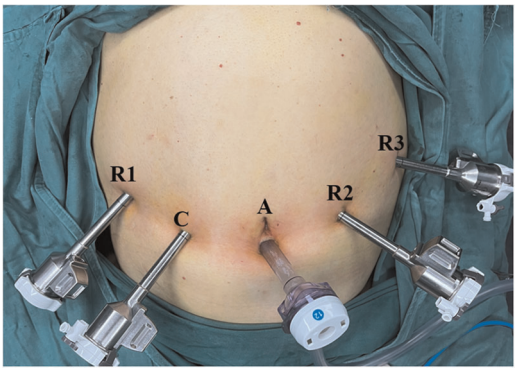


FIGURE 2
Photograph showing positions of the trocars: A, assistant port (12 mm); C, camera port (8 mm); R1, operation port 1 (8 mm); R2, operation port 2 (8 mm); R3, operation port 3 (8 mm).

## Dissection of Calot's triangle and lymph nodes

The left and right perihepatic ligaments and all loose connective tissues in the exposed area of the liver were removed so that the liver was completely free. Dissection then commenced from the right side of porta to the hilum to expose the right lateral wall of the bile duct and portal vein. Calot's triangle was dissected and the cystic duct ligated flush to the common bile duct (Figure 3A). Next, the supraduodenal region of the porta hepatis and hepatoduodenal ligament was dissected to expose the common hepatic artery. The superior border of the pancreas was exposed, and the common hepatic artery was identified. The adipose and connective tissues of the porta hepatis were sharply separated, the lymph nodes of station 12 (12a, 12b, and 12p) were dissected respectively, the adipose and connective tissues of the celiac trunk were sharply separated, and the lymph nodes of stations 8 and 9 were dissected (Figure 3B).

## Liver resection

The transection plane was demarcated with electrocauterization on the liver surface, 2–3 cm from the gallbladder bed (Figure 3C). Controlled low central venous pressure technology and pre-indwelling hepatic portal block tape were routinely used during the operation to reduce the

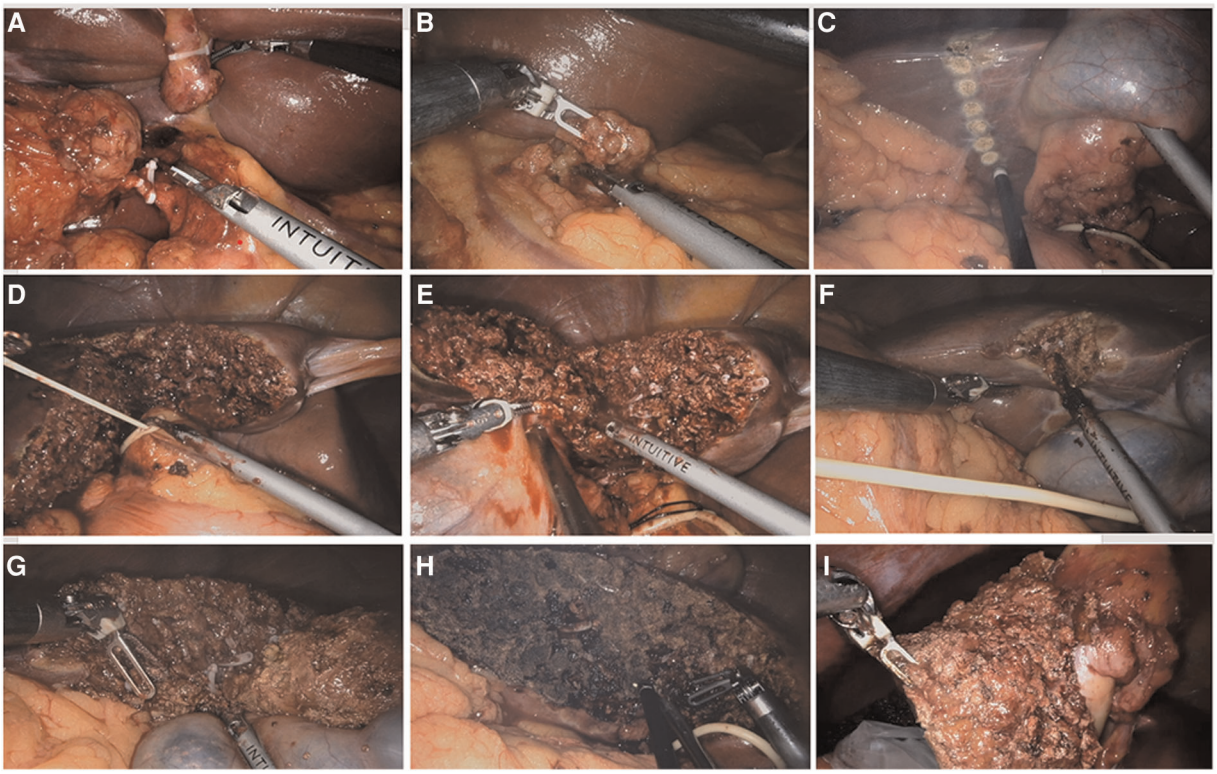


FIGURE 3
Surgical procedures of robotic extended cholecystectomy (A) ligation of cystic artery and cystic duct. (B) Regional lymph node dissection. (C) Hepatectomy line 2–3 cm around the gallbladder bed. (D) Blockage of hepatic portal. (E) Incision of liver tissue on left side of gallbladder along hepatectomy line. (F) Incision of liver tissue on right side of gallbladder along hepatectomy line. (G) Complete resection of liver tumor. (H) Electrocoagulation of liver wound for hemostasis. (I) Removal of specimen.

risk of hepatic vein bleeding (Figure 3D). The parenchymal dissection was carried out with a harmonic scalpel, beginning from the left side (Figure 3E). Visualized vessels and bile ducts were ligated by the clip applier, electrocauterization, or suturing. After the left-side liver dissection was nearly completed, dissection was performed on the right side of the transection line (Figure 3F). Finally, the inferior portion of the liver was dissected upward to complete the liver resection (Figure 3G). The specimen was placed in a specimen bag and set aside in the intra-abdominal space for removal at the end of surgery (Figures 3H,I). Liver wounds with active bleeding or bile leakage were treated with electrocoagulation rods or 4–0 Prolene sutures. After confirming the absence of active bleeding and bile leakage in the liver wound, a drain was placed around the resection plane and tagged on the retroperitoneum. The umbilical incision was extended by an additional 2–3 cm, and a wound protector was applied to prevent port site recurrence.

## Surgical procedures of open extended cholecystectomy

For traditional surgical procedures of open extended cholecystectomy, an inverse L-shaped right subcostal incision was performed. First, Calot's triangle was dissected and the cystic duct ligated flush to the common bile duct. Next, the supraduodenal region of the porta hepatis and hepatoduodenal ligament was dissected to expose the common hepatic artery. The superior border of the pancreas was exposed, and the common hepatic artery was identified. the lymph nodes of stations 8, 9 and 12 (12a, 12b, and 12p) were dissected respectively. Finally, resecting liver tissue 2–3 cm around the gallbladder bed until completing resection of liver tumor.

## Perioperative care and follow-up

All patients in both groups underwent routine preoperative care, such as standard perioperative education, no eating or drinking for 8 h before surgery, and no preoperative bowel preparation or premedication. Postoperative complications were documented and graded according to the Clavien–Dindo classification. The follow-up protocol included a clinical examination, abdominal contrast-enhanced CT, and measurement of serum tumor markers (including carcinoembryonic antigen and carbohydrate antigen) every 3 months.

## Statistical analysis

Continuous data are expressed as mean ± standard deviation, and categorical variables are expressed as *n* (%). The Mann–Whitney *U* test was used to compare continuous variables, and Pearson's chi-square test was used to compare discrete variables. All analyses were performed using SPSS 26.0 software (IBM Corp., Armonk, NY, USA), and the "R-3.5.3-win" R package was used to perform the PSM analysis. The matching was performed in a 1:2 ratio, and a caliper width of 0.2 standard deviations was specified. Kaplan–Meier estimates for overall survival (OS) and disease-free survival (DFS) were compared between the OEC group and the REC group using the log-rank test. A *P* value of <0.05 was considered statistically significant.

# Results

## Clinical characteristics of 145 eligible patients before PSM

Of the 145 eligible patients diagnosed with GBC, 28 (19.3%) underwent REC and 117 (80.7%) underwent OEC. The clinical characteristics of the two groups are shown in Table 1. There were significant differences in the total bilirubin, alanine aminotransferase, and aspartate aminotransferase concentrations ($P = 0.044$, $P = 0.019$, and $P = 0.017$, respectively) before PSM as a result of a conspicuous bias with the pre-described propensity scores (REC group vs. OEC group: 0.254 vs. 0.179, $P < 0.001$) (Figures 4, 5).

## Clinical characteristics of 79 matched patients after PSM

The 28 patients who underwent REC were matched with 51 of the 117 patients who underwent OEC. The propensity scores suggested no bias in the matched groups (REC group vs. OEC group: 0.254 vs. 0.251, $P = 0.647$). Figure 4C shows a dot plot of the covariate balance in terms of the standardized mean difference (SMD) for all the individual covariates; the covariate balance improved in the matched data. A line plot of the SMD and the SMD of all confounders is shown in Figure 4B; the standard deviation of the PS decreased after matching. The clinical characteristics of the matched patients were compared, and no significant differences were shown between the groups, considering all 10 variables (Table 1).

TABLE 1 Patient characteristics according to operation type by unmatched and matched data.

| Variables | Unmatched data | | | Matched data | | |
|---|---|---|---|---|---|---|
| | Control ($n = 117$) | Treated ($n = 28$) | *P*-value | Control ($n = 51$) | Treated ($n = 28$) | *P*-value |
| Age (years) | 55.27 ± 14.10 | 58.50 ± 12.15 | 0.257 | 57.08 ± 13.82 | 58.50 ± 12.15 | 0.610[a] |
| Gender (male/female) | 59/58 | 16/12 | 0.523 | 29/22 | 16/12 | 0.981[a] |
| BMI (kg/m$^2$) | 25.08 ± 3.81 | 24.75 ± 3.48 | 0.279 | 24.21 ± 3.77 | 24.75 ± 3.48 | 0.364[a] |
| Albumin (g/L) | 36.61 ± 4.37 | 38.04 ± 4.48 | 0.968 | 38.06 ± 3.40 | 38.04 ± 4.48 | 0.205[a] |
| TB (μmol/L) | 29.79 ± 30.75 | 23.22 ± 9.76 | **0.044*** | 22.21 ± 14.7 | 23.22 ± 9.76 | 0.261[a] |
| ALT (U/L) | 65.54 ± 66.84 | 42.79 ± 27.18 | **0.019*** | 43.39 ± 27.39 | 42.79 ± 27.18 | 0.415[a] |
| AST (U/L) | 74.57 ± 92.96 | 52.31 ± 38.84 | **0.017*** | 45.17 ± 30.12 | 52.31 ± 38.84 | 0.854[a] |
| ASA | | | | | | |
| ≤2 | 95 | 25 | 0.309 | 47 | 25 | 0.668[a] |
| >2 | 22 | 3 | | 4 | 3 | |
| T stage | | | | | | |
| T1a | 2 | 0 | 0.935 | 0 | 0 | 0.950[a] |
| T1b | 9 | 2 | | 5 | 2 | |
| T2a | 28 | 6 | | 11 | 6 | |
| T2b | 62 | 15 | | 28 | 15 | |
| T3 | 16 | 5 | | 7 | 5 | |
| Symptoms | 51/117 | 13/28 | 0.786 | 27/24 | 13/28 | 0.957[a] |
| PS | 0.179 ± 0.275 | 0.254 ± 0.087 | **<0.001*** | 0.247 ± 0.092 | 0.254 ± 0.087 | 0.674[a] |

Data are expressed as *n* (%) or mean ± standard deviation; BMI, body mass index, TB, total bilirubin; ALT, alanine aminotransferase; AST, aspartate aminotransferase; ASA, American score of anesthesiologists; PS, propensity score. * and bold values indicate statistically significant *P*-value ($P < 0.05$).
[a]Pearson Chi-square tests.

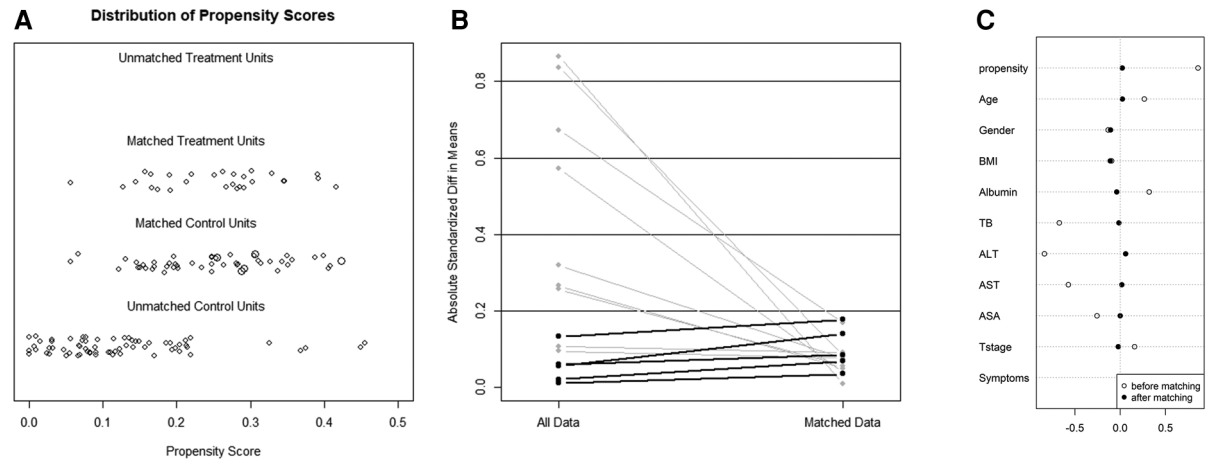


FIGURE 4
The model values of the SMD before and after propensity score-matching analysis. (**A**) The unmatched robotic extended cholecystectomy (treated) and open extended cholecystectomy (control) data were removed, and the matched treatment and control data were preserved. (**B**) The SMD of the propensity score and 10 confounders before and after propensity score matching is depicted in a line plot. (**C**) The SMDs of the propensity score and 10 confounders (age, sex, BMI, albumin, TB, ALT, AST, ASA, T stage, and symptoms) are depicted as hollow dots, and the SMDs of the matched data are depicted as solid dots. SMD, standardized mean difference; BMI, body mass index; TB, total bilirubin; ALT, alanine aminotransferase; AST, aspartate aminotransferase; ASA, American Society of Anesthesiologists classification.

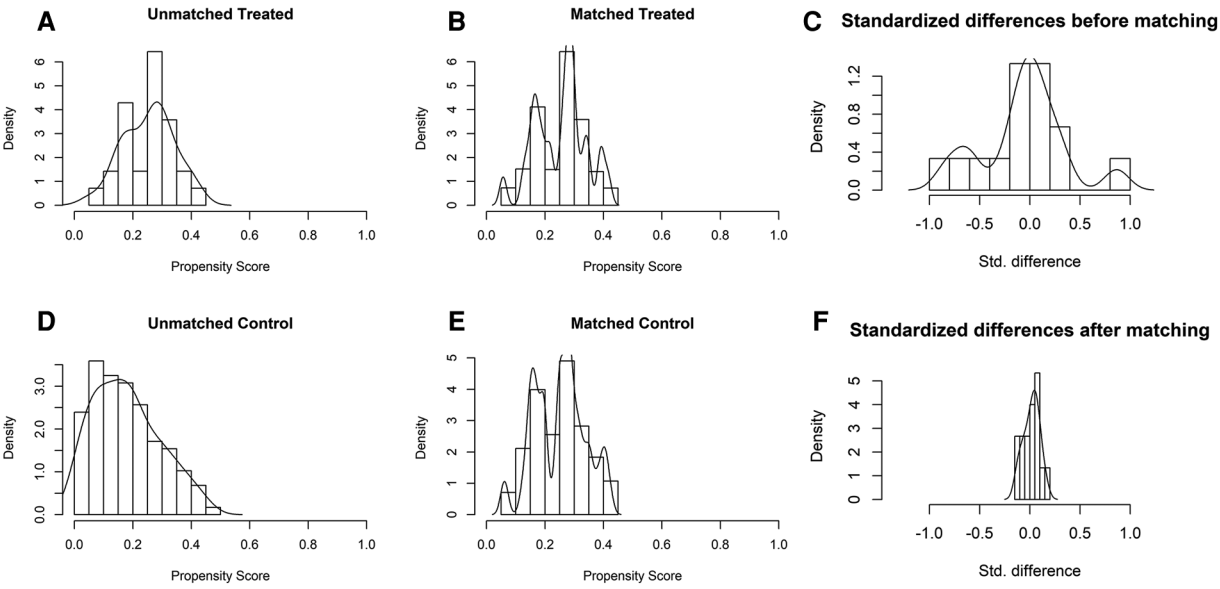


FIGURE 5
Distribution of propensity scores of robotic extended cholecystectomy (treated) and open extended cholecystectomy (control) (**A**,**D**) before and (**B**,**E**) after matching with overlaid kernel density estimate. Histograms with overlaid kernel density estimates of standardized differences (**C**) before and (**F**) after matching.

## Operative outcomes of 79 matched patients after PSM

Patients who underwent REC had a longer operation time (212.39 ± 73.19 vs. 186.75 ± 66.60 min, $P = 0.134$) and lower amount of bleeding (99.11 ± 115.32 vs. 156.08 ± 242.64 ml, $P = 0.467$) than patients in the OEC group. According to the T stage, lymph node metastasis, and distant metastasis of patients with GBC, as well as re-evaluation of the stage and resectability during the operation, 25 patients underwent wedge resection around the gallbladder fossa (REC group, $n = 8$; OEC group, $n = 17$), 42 underwent bisegmentectomy of

segments IVb and V (REC group, $n = 15$; OEC group, $n = 27$), 11 underwent right hemihepatectomy (REC group, $n = 5$; OEC group, $n = 6$), and 1 underwent Right hepatic trisegmentectomy (REC group, $n = 0$; OEC group, $n = 1$) with no significant difference between the two groups ($P = 0.762$). Additionally, the mean number of lymph nodes retrieved was 4.89 ± 2.78 in the REC group and 4.59 ± 2.22 in the OEC group, with no significant difference between the two groups ($P = 0.828$). There were 5 patients with liver cirrhosis diagnosed by pathological examination after operation, and the evaluation of liver function was child A (REC group, $n = 2$; OEC group, $n = 3$, $P = 0.826$). Furthermore, the mean visual analogue scale score after the operation was significantly lower in the REC group immediate postoperatively (3.68 ± 2.09 vs. 4.73 ± 1.85, $P = 0.008$), on postoperative day 1 (2.96 ± 1.75 vs. 3.69 ± 1.41, $P = 0.023$), and on postoperative day 2 (2.36 ± 1.55 vs. 2.92 ± 1.21, $P = 0.031$). However, the time to first ambulation, time to drainage tube removal, and postoperative stay were significantly lower in the REC than OEC group (49.57 ± 16.51 vs. 57.47 ± 16.17 h, $P = 0.043$; 7.86 ± 5.28 vs. 11.08 ± 7.65 days, $P = 0.038$; and 10.11 ± 5.74 vs. 13.65 ± 8.48 days, $P = 0.037$, respectively). But hospital costs were significantly higher in the REC than OEC group (86,174 ± 12,148 vs. 70,400 ± 31,612 yuan, $P < 0.001$). In addition, the incidence of postoperative morbidity and mortality (Clavien–Dindo I–II and III–IV complications) was not statistically significant between the groups (Table 2).

44 patients in OEC group were T1b–T2b, of which 13 patients were diagnosed as GBC by frozen section examination after cholecystectomy, and then underwent wedge resection of liver. The remaining 31 patients underwent extended cholecystectomy directly. 23 patients in the REC group were T1b–T2b, of which 5 were diagnosed as GBC by frozen section examination after cholecystectomy, and then underwent robotic wedge resection of liver. The remaining 18 patients underwent robotic extended cholecystectomy directly.

46 patients in OEC group were T2–T3. Among them, 39 patients were treated with Gimeracil and Oteracil Potassium capsule combined with Gemcitabine chemotherapy after operation, 4 patients refused chemotherapy, and 3 patients could not tolerate chemotherapy. 26 patients in REC group were T2–T3, of which 21 patients were treated with Gimeracil and Oteracil Potassium capsule combined with Gemcitabine chemotherapy after operation, 4 patients refused chemotherapy, and 1 patient could not tolerate chemotherapy.

TABLE 2 Operative outcomes according to operation type after propensity scoring match.

| Variables | Control ($n = 51$) | Treated ($n = 28$) | *P*-value |
|---|---|---|---|
| Operation time, min | 186.75 ± 66.60 | 212.39 ± 73.19 | 0.134[b] |
| Intraoperative blood loss, ml | 156.08 ± 242.64 | 99.11 ± 115.32 | 0.467[b] |
| Hepatic resection site | | | |
| Wedge resection around the gallbladder fossa | 17 | 8 | 0.762[a] |
| Bisegmentectomy of segments IVb and V | 27 | 15 | |
| Right hemihepatectomy | 6 | 5 | |
| Right hepatic trisegmentectomy | 1 | 0 | |
| Number of lymph nodes retrieved | 4.59 ± 2.22 | 4.89 ± 2.78 | 0.828[b] |
| VAS score | | | |
| Immediate postoperative | 4.73 ± 1.85 | 3.68 ± 2.09 | **0.008**[b*] |
| POD1 | 3.69 ± 1.41 | 2.96 ± 1.75 | **0.023**[b*] |
| POD2 | 2.92 ± 1.21 | 2.36 ± 1.55 | **0.031**[b*] |
| First ambulation time, h | 57.47 ± 16.17 | 49.57 ± 16.51 | **0.043**[b*] |
| Drainage tube removal time, days | 11.08 ± 7.65 | 7.86 ± 5.28 | **0.038**[b*] |
| Postoperative morbidity (%) | 11 (21.6%) | 3 (10.7%) | 0.227[a] |
| Clavien–Dindo I–II (%) | 6 (11.8%) | 2 (7.1%) | 0.515[a] |
| Clavien–Dindo III–IV (%) | 5 (9.8%) | 1 (3.6%) | 0.317[a] |
| Postoperative mortality (%) | 2 (3.9%) | 0 | 0.289[a] |
| POS, days | 13.65 ± 8.48 | 10.11 ± 5.74 | **0.037**[b*] |
| Hospital cost, yuan | 70,400 ± 31,612 | 86,174 ± 12,148 | **<0.001**[b*] |

VAS, visual analog scale; POD, postoperative day; POS, postoperative hospital stay; Data are expressed as *n* (%) or mean ± standard deviation; * and bold values indicate statistically significant *P*-value ($P < 0.05$).
[a]Pearson Chi-square tests.
[b]Mann–Whitney *U* test (Wilcoxon rank sum W test).

## Long-term survival outcomes of 79 matched patients after PSM

The mean follow-up duration was 20.1 ± 12.6 months in the OEC group and 16.0 ± 10.7 months in the REC group, with no significant difference between the groups ($P = 0.228$). The median OS in the OEC and REC groups was 30.0 months [95% confidence interval (CI), 16.9–43.1 months] and 35.0 months (95% CI, 13.0–57.0 months), respectively (Figure 6A). The 3-year OS rates were not significantly different between the OEC and REC groups (62.8% vs. 75.0%, respectively; $P = 0.619$). The median DFS in the OEC and REC groups was 22.0 months (95% CI, 12.8–31.2 months) and 20.0 months (95% CI, 14.0–26.0 months), respectively (Figure 6B). The 3-year DFS rates were not significantly different between the OEC and REC groups (43.1% vs. 57.2%, respectively; $P = 0.684$).

# Discussion

Because GBC is accompanied by gallstones or inflammation and lacks specific clinical manifestations, its preoperative and intraoperative diagnosis is difficult. Therefore, the use of adequate and effective imaging methods is very important. Ultrasound is the preferred method for diagnosing gallbladder

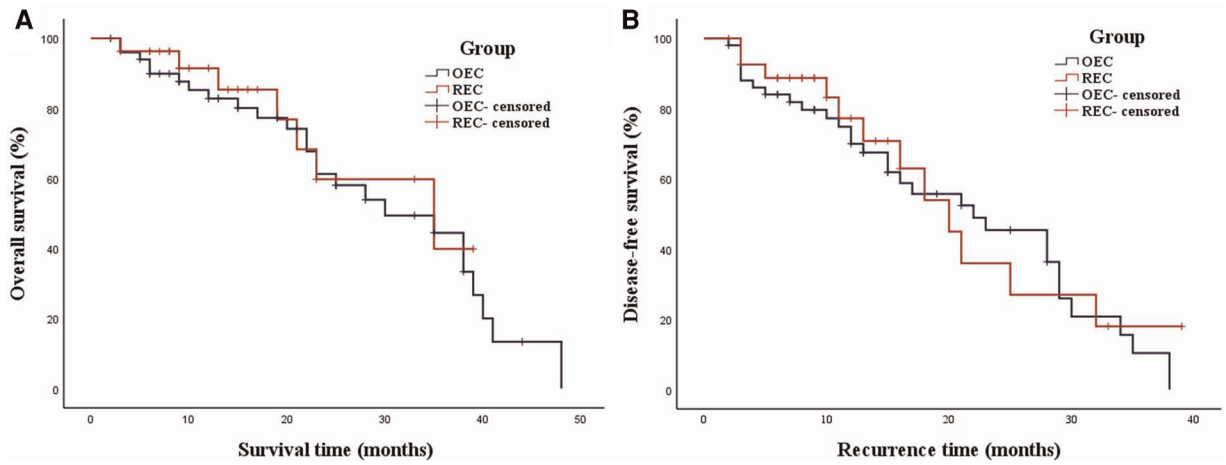


FIGURE 6
Weighted Kaplan–Meier plot for OS and DFS in the OEC and REC groups. (A) The median OS in the OEC and REC groups was 30.0 and 35.0 months, respectively ($P = 0.619$). (B) The median DFS in the OEC and REC groups was 22.0 and 20.0 months, respectively ($P = 0.684$).

disease because of its simplicity and high sensitivity (15). The resolution of CT for GBC lesions, surrounding tissue and organ invasion, and distant metastasis is significantly higher than that of ultrasound; in particular, enhanced CT thin-section scanning technology has a higher recognition rate for small lesions of early GBC (16, 17). Compared with CT, magnetic resonance imaging combined with magnetic resonance cholangiopancreatography can more sensitively display GBC and its involvement with adjacent organs, more clearly show signs of biliary obstruction caused by involvement of the intrahepatic and extrahepatic bile ducts, and help to accurately assess the extent of local tumor invasion (18, 19). Intraoperative frozen pathological examination is also an important diagnostic method for GBC (20). However, because of the limited scope of intraoperative frozen pathological examination, the entire gallbladder wall cannot be included, and it is difficult to distinguish mucosal dysplasia from focal GBC. The sensitivity of intraoperative frozen pathological detection of cancer cells ranges from 64.0% to 84.2%, and the sensitivity increases with the depth of tumor invasion (21, 22). In this study, for patients with T1b–T2b gallbladder cancer, intraoperative frozen sections were mainly used for diagnosis to determine whether extended cholecystectomy was required. For patients with T3 gallbladder cancer, intraoperative frozen sections were used to judge the tumor margin to achieve R0 resection.

Extended cholecystectomy broadly includes liver resection, pancreaticoduodenectomy, portal vein resection, extended regional lymph node dissection, hepatopancreatoduodenectomy, and even right upper abdominal resection (23–26). The scope of liver resection is mainly determined according to the location of the tumor and the extent of infiltration, and it may include gallbladder and liver wedge resection, liver segment resection, hemihepatectomy, or liver trilobectomy (27, 28). For T1a GBC, cholecystectomy is usually sufficient; in the present study, however, two patients with T1a GBC in the OEC group had severe gallbladder abscesses and required liver wedge resection. Nevertheless, the optimal surgical method for T1b GBC remains controversial. Lee et al. found no statistically significant difference in the prognosis between extended cholecystectomy and simple cholecystectomy (27). Therefore, they proposed that radical treatment by simple cholecystectomy can meet the needs of patients with stage T1b GBC. However, there are differing opinions on this issue (29, 30). Because of the particularity of the anatomy of the gallbladder area (31), the gallbladder tissue lacks protection, and tumor cells can metastasize through the blood supply and lymphatic system. The range of GBC micrometastasis can even invade the liver tissue 16 mm from the gallbladder bed. Considering the previous literature and actual clinical experience, our institution prefers the use of liver wedge resection to treat T1b GBC because it meets the principle of a tumor-free technique for surgical treatment. In addition, numerous studies have shown that extended cholecystectomy combined with lymph node dissection can achieve R0 resection for patients with T2 and T3 GBC (32, 33).

In recent years, da Vinci robotic surgeries have been widely used in many fields, because these procedures provide magnified three-dimensional high-definition views as well as motion and tremor filtering. Additionally, the enlarged anatomical structures can reduce unnecessary damage during the operation, especially GBC surgery (34). At the same time, the clear visualization of anatomical structures facilitates safe and effective anastomosis of blood vessels and bile ducts and dissection of lymph nodes. As shown in **Table 3** (9–11, 35–39), previous studies have revealed that REC has numerous advantages including a lower blood loss volume, lower

TABLE 3 Previous reports about the robotic extended cholecystectomy in gallbladder cancer.

| Author. Year | *N* | Operation time (min) | Blood loss (ml) | Postoperative stay (days) | Morbidity | Mortality | ≥T2 stage | Retrieved LNs |
|---|---|---|---|---|---|---|---|---|
| Shen et al. 2012 | 5 | 200 (120–300) | 210 (50–400) | 7 (7–8) | 0 | 0 | 5 (100%) | 9 (3–11) |
| Khan et al. 2018 | 11 | 219 (99–790) | 50 (10–200) | 4 (2–9) | 4 (36.4%) | 0 | 11 (100%) | 5 (0–9) |
| Sucandy et al. 2021 | 15 | 222 (151–323) | 200 (87–357) | 3 (1–8) | 2 (13.3%) | 0 | - | - |
| Ahmad et al. 2020 | 10 | 173 (95–240) | 88 (30–200) | 4 (2–6) | 1 (10.0%) | 0 | 10 (100%) | 2 (0–5) |
| Araujo et al. 2020 | 3 | 392 (376–408) | 186 (60–312) | 3 (3) | 0 | 0 | 0 | 4 (3–6) |
| Goel et al. 2019 | 27 | 295 (200–710) | 200 (20–700) | 4 (2–12) | 1 (3.7%) | 0 | 22 (81.5%) | 10 (2–21) |
| Zeng et al. 2018 | 3 | 243 (165–530) | 175 (50–700) | 4 (2–8) | 0 | 0 | 3 (100%) | 6 (1–11) |
| Byun et al. 2020 | 13 | 188 (153–223) | 271 (0–569) | 7 (5–8) | 2 (15.4%) | 0 | 13 (100%) | 7 (4–10) |
| Our study | 28 | 212 (139–285) | 99 (0–214) | 10 (4–16) | 2 (7.1%) | 0 | 26 (92.9%) | 5 (2–8) |

complication rates, and a shorter postoperative stay. In addition, among patients with GBC, robotic surgery is not inferior to open surgery in terms of the number of lymph nodes resected. In this study, we found no statistically significant difference in the operation time, blood loss, or number of lymph nodes resected between the REC and OEC groups. However, the patients who underwent REC had a shorter postoperative hospital stay ($P = 0.037$) and less pain ($P < 0.05$).

The oncologic outcome after REC in patients with GBC is an important issue. Most previous studies focused on short-term results. For example, Goel et al. (38) reported that the postoperative complication rate was higher after open radical cholecystectomy than after robotic radical cholecystectomy (1 vs. 15 patients, respectively; $P = 0.035$), with only one patient developing major morbidity following robotic radical cholecystectomy. Few studies have compared the long-term outcomes of OEC and REC for patients with GBC, and the present study is the first to compare the OS and DFS of OEC and REC. However, two studies addressed the long-term outcomes after robotic liver resection in patients with hepatocellular carcinoma. Chen et al. (40) reported that robotic liver resection showed a 3-year DFS rate comparable to that of open liver resection in patients with hepatocellular carcinoma (72.2% vs. 58.0%, respectively; $P = 0.062$). Eric et al. (41) compared laparoscopic liver resection and robotic liver resection for hepatocellular carcinoma and found similar 5-year OS (65% vs. 48%, $P = 0.28$) and DFS (42% vs. 38%, $P = 0.65$) between the two groups. In the present study, the median OS in the OEC and REC groups was 30 and 35 months, respectively, and the median DFS was 22 and 20 months, respectively. All patients with GBC in the REC group achieved R0 resection and showed long-term outcomes comparable to those in the OEC group.

In summary, the short- and long-term results in this study indicate that the use of a robotic surgical system for the treatment of GBC is safe, effective, and feasible compared with OEC. There was no difference in the OS or DFS between the two groups. REC was accompanied by less pain, a shorter postoperative hospitalization time, and more rapid postoperative recovery than OEC. Thus, REC is a suitable minimally invasive procedure for the treatment of GBC. Notably, this study had a limited sample size and did not address all types of extended cholecystectomy. This was also a retrospective study with a short follow-up period. The results of this study therefore need to be further confirmed by large-scale multicenter prospective randomized controlled trials and longer-term follow-up.

## Data availability statement

The raw data supporting the conclusions of this article will be made available by the authors, without undue reservation.

## Ethics statement

The studies involving human participants were reviewed and approved by the Ethics Committee of the Second Affiliated Hospital of Nanchang University. The patients/participants provided their written informed consent to participate in this study. Written informed consent was obtained from the individual(s) for the publication of any potentially identifiable images or data included in this article.

## Author contributions

Research design and project supervision: WL, LW. Data collection, statistical analysis and writing: JY, EL. Data

analysis and interpretation: CW, SL. Literature review and manuscript proofreading: ZF, JP. All authors contributed to the article and approved the submitted version.

## Funding

This research was funded by the National Natural Science Foundation of China (NO. 82060447 and NO. 81860431) and Youth Science Foundation of Jiangxi Province (NO. 20192ACBL21036). The funders had no role in the study design, data collection and analysis.

## Acknowledgments

We thank Angela Morben, DVM, ELS, from Liwen Bianji (Edanz) (www.liwenbianji.cn), for editing the English text of a draft of this manuscript.

## Conflict of interest

The authors declare that the research was conducted in the absence of any commercial or financial relationships that could be construed as a potential conflict of interest.

## Publisher's note

All claims expressed in this article are solely those of the authors and do not necessarily represent those of their affiliated organizations, or those of the publisher, the editors and the reviewers. Any product that may be evaluated in this article, or claim that may be made by its manufacturer, is not guaranteed or endorsed by the publisher.

## Author disclaimer

The views and opinions expressed in this article are those of the authors and do not necessarily reflect the official policy or position of the respective funding organizations.

## References

1. Lazcano-Ponce EC, Miquel JF, Muñoz N, Herrero R, Ferrecio C, Wistuba II, et al. Epidemiology and molecular pathology of gallbladder cancer. *CA: Cancer J Clin*. (2001) 51(6):349–64. doi: 10.3322/canjclin.51.6.349

2. Stinton LM, Shaffer EA. Epidemiology of gallbladder disease: cholelithiasis and cancer. *Gut Liver*. (2012) 6(2):172–87. doi: 10.5009/gnl.2012.6.2.172

3. Hundal R, Shaffer EA. Gallbladder cancer: epidemiology and outcome. *Clin Epidemiol*. (2014) 6:99–109. doi: 10.2147/CLEP.S37357

4. Shih SP, Schulick RD, Cameron JL, Lillemoe KD, Pitt HA, Choti MA, et al. Gallbladder cancer: the role of laparoscopy and radical resection. *Ann Surg*. (2007) 245(6):893–901. doi: 10.1097/SLA.0b013e31806beec2

5. Feng JW, Yang XH, Liu CW, Wu BQ, Sun DL, Chen XM, et al. Comparison of laparoscopic and open approach in treating gallbladder cancer. *J Surg Res*. (2019) 234:269–76. doi: 10.1016/j.jss.2018.09.025

6. Agarwal AK, Javed A, Kalayarasan R, Sakhuja P. Minimally invasive versus the conventional open surgical approach of a radical cholecystectomy for gallbladder cancer: a retrospective comparative study. *HPB*. (2015) 17 (6):536–41. doi: 10.1111/hpb.12406

7. Dou C, Zhang Y, Liu J, Wei F, Chu H, Han J, et al. Laparoscopy versus laparotomy approach of a radical resection for gallbladder cancer: a retrospective comparative study. *Surg Endosc*. (2020) 34(7):2926–38. doi: 10.1007/s00464-019-07075-4

8. Giulianotti PC, Coratti A, Angelini M, Sbrana F, Cecconi S, Balestracci T, et al. Robotics in general surgery: personal experience in a large community hospital. *Arch Surg*. (2003) 138(7):777–84. doi: 10.1001/archsurg.138.7.777

9. Byun Y, Choi YJ, Kang JS, Han Y, Kim H, Kwon W, et al. Early outcomes of robotic extended cholecystectomy for the treatment of gallbladder cancer. *J Hepatobiliary Pancreat Sci*. (2020) 27(6):324–30. doi: 10.1002/jhbp.717

10. Shen BY, Zhan Q, Deng XX, Bo H, Liu Q, Peng CH, et al. Radical resection of gallbladder cancer: could it be robotic? *Surg Endosc*. (2012) 26(11):3245–50. doi: 10.1007/s00464-012-2330-4

11. Araujo R, de Sanctis MA, Coelho T, Felippe F, Burgardt D, Wohnrath DR. Robotic surgery as an alternative approach for reoperation of incidental gallbladder cancer. *J Gastrointest Cancer*. (2020) 51(1):332–4. doi: 10.1007/s12029-019-00264-3

12. Chun YS, Pawlik TM, Vauthey JN. 8th edition of the AJCC cancer staging manual: pancreas and hepatobiliary cancers. *Ann Surg Oncol*. (2018) 25(4):845–7. doi: 10.1245/s10434-017-6025-x

13. Kumaran V, Gulati S, Paul B, Pande K, Sahni P, Chattopadhyay K. The role of dual-phase helical CT in assessing resectability of carcinoma of the gallbladder. *Eur Radiol*. (2002) 12(8):1993–9. doi: 10.1007/s00330-002-1440-0

14. Kim SJ, Lee JM, Lee JY, Choi JY, Kim SH, Han JK, et al. Accuracy of preoperative T-staging of gallbladder carcinoma using MDCT. *Am J Roentgenol*. (2008) 190(1):74–80. doi: 10.2214/AJR.07.2348

15. Zhang HP, Bai M, Gu JY, He YQ, Qiao XH, Du LF. Value of contrast-enhanced ultrasound in the differential diagnosis of gallbladder lesion. *World J Gastroenterol*. (2018) 24(6):744–51. doi: 10.3748/wjg.v24.i6.744

16. Rodríguez-Fernández A, Gómez-Río M, Medina-Benítez A, Moral JV, Ramos-Font C, Ramia-Angel JM, et al. Application of modern imaging methods in diagnosis of gallbladder cancer. *J Surg Oncol*. (2006) 93(8):650–64. doi: 10.1002/jso.20533

17. Patkar S, Chaturvedi A, Goel M, Rangarajan V, Sharma A, Engineer R. Role of positron emission tomography-contrast enhanced computed tomography in locally advanced gallbladder cancer. *J Hepatobiliary Pancreat Sci*. (2020) 27 (4):164–70. doi: 10.1002/jhbp.712

18. Lopes Vendrami C, Magnetta MJ, Mittal PK, Moreno CC, & Miller FH. Gallbladder carcinoma and its differential diagnosis at MRI: what radiologists should know. *Radiographics*. (2021) 41(1):78–95. doi: 10.1148/rg.2021200087

19. Bae JS, Kim SH, Yoo J, Kim H, Han JK. Differential and prognostic MRI features of gallbladder neuroendocrine tumors and adenocarcinomas. *Eur Radiol*. (2020) 30(5):2890–901. doi: 10.1007/s00330-019-06588-9

20. You Z, Ma WJ, Deng YL, Xiong XZ, Shrestha A, Li FY, et al. Histological examination of frozen sections for patients with acute cholecystitis during cholecystectomy. *Hepatobiliary Pancreat Dis Int*. (2015) 14(3):300–4. doi: 10.1016/s1499-3872(15)60375-7

21. Azuma T, Yoshikawa T, Araida T, Takasaki K. Intraoperative evaluation of the depth of invasion of gallbladder cancer. *Am J Surg*. (1999) 178(5):381–4. doi: 10.1016/s0002-9610(99)00210-x

22. Yamaguchi K, Chijiiwa K, Saiki S, Shimizu S, Tsuneyoshi M, Tanaka M. Reliability of frozen section diagnosis of gallbladder tumor for detecting

carcinoma and depth of its invasion. *J Surg Oncol.* (1997) 65(2):132–6. doi: 10.1002/(sici)1096-9098(199706)65:2<132::aid-jso11>3.0.co;2-7

23. Kondo S, Nimura Y, Hayakawa N, Kamiya J, Nagino M, Uesaka K. Extensive surgery for carcinoma of the gallbladder. *Br J Surg.* (2002) 89(2):179–84. doi: 10.1046/j.0007-1323.2001.02001.x

24. Tsukada K, Hatakeyama K, Kurosaki I, Uchida K, Shirai Y, Muto T, et al. Outcome of radical surgery for carcinoma of the gallbladder according to the TNM stage. *Surgery.* (1996) 120(5):816–21. doi: 10.1016/s0039-6060(96)80089-4

25. Miyazaki M, Itoh H, Ambiru S, Shimizu H, Togawa A, Gohchi E, et al. Radical surgery for advanced gallbladder carcinoma. *Br J Surg.* (1996) 83 (4):478–81. doi: 10.1002/bjs.1800830413

26. Nakamura S, Nishiyama R, Yokoi Y, Serizawa A, Nishiwaki Y, Konno H, et al. Hepatopancreatoduodenectomy for advanced gallbladder carcinoma. *Arch Surg.* (1994) 129(6):625–9. doi: 10.1001/archsurg.1994.01420300069010

27. Lee SE, Jang JY, Lim CS, Kang MJ, Kim SW. Systematic review on the surgical treatment for T1 gallbladder cancer. *World J Gastroenterol.* (2011) 17 (2):174–80. doi: 10.3748/wjg.v17.i2.174

28. Goetze TO. Gallbladder carcinoma: prognostic factors and therapeutic options. *World J Gastroenterol.* (2015) 21(43):12211–7. doi: 10.3748/wjg.v21.i43.12211

29. Vo E, Curley SA, Chai CY, Massarweh NN, Tran Cao HS. National failure of surgical staging for T1b gallbladder cancer. *Ann Surg Oncol.* (2019) 26(2):604–10. doi: 10.1245/s10434-018-7064-7

30. Hickman L, Contreras C. Gallbladder cancer: diagnosis, surgical management, and adjuvant therapies. *Surg Clin North Am.* (2019) 99(2):337–55. doi: 10.1016/j.suc.2018.12.008

31. Sasaki E, Nagino M, Ebata T, Oda K, Arai T, Nishio H, et al. Immunohistochemically demonstrated lymph node micrometastasis and prognosis in patients with gallbladder carcinoma. *Ann Surg.* (2006) 244 (1):99–105. doi: 10.1097/01.sla.0000217675.22495.6f

32. Shindoh J, de Aretxabala X, Aloia TA, Roa JC, Roa I, Zimmitti G, et al. Tumor location is a strong predictor of tumor progression and survival in T2 gallbladder cancer: an international multicenter study. *Ann Surg.* (2015) 261 (4):733–9. doi: 10.1097/SLA.0000000000000728

33. Araida T, Higuchi R, Hamano M, Kodera Y, Takeshita N, Ota T, et al. Hepatic resection in 485 R0 pT2 and pT3 cases of advanced carcinoma of the gallbladder: results of a Japanese society of biliary surgery survey–a multicenter study. *J Hepatobiliary Pancreat Surg.* (2009) 16(2):204–15. doi: 10.1007/s00534-009-0044-3

34. Choi SH, Han DH, Lee JH, Choi Y, Lee JH, Choi GH. Safety and feasibility of robotic major hepatectomy for novice surgeons in robotic liver surgery: a prospective multicenter pilot study. *Surg Oncol.* (2020) 35:39–46. doi: 10.1016/j.suronc.2020.07.003

35. Khan S, Beard RE, Kingham PT, Fong Y, Boerner T, Martinie JB, et al. Long-term oncologic outcomes following robotic liver resections for primary hepatobiliary malignancies: a multicenter study. *Ann Surg Oncol.* (2018) 25 (9):2652–60. doi: 10.1245/s10434-018-6629-9

36. Sucandy I, Jabbar F, Syblis C, Crespo K, Ross S, Rosemurgy A. Robotic central hepatectomy for the treatment of gallbladder carcinoma. Outcomes of minimally invasive approach. *Am Surg.* (2022) 88(3):348–51. doi: 10.1177/00031348211047457

37. Ahmad A. Use of indocyanine green (ICG) augmented near-infrared fluorescence imaging in robotic radical resection of gallbladder adenocarcinomas. *Surg Endosc.* (2020) 34(6):2490–4. doi: 10.1007/s00464-019-07053-w

38. Goel M, Khobragade K, Patkar S, Kanetkar A, Kurunkar S. Robotic surgery for gallbladder cancer: operative technique and early outcomes. *J Surg Oncol.* (2019) 119(7):958–63. doi: 10.1002/jso.25422

39. Zeng G, Teo NZ, Goh B. Short-term outcomes of minimally invasive surgery for patients presenting with suspected gallbladder cancer: report of 8 cases. *J Minim Access Surg.* (2018) 15(2):109–14. doi: 10.4103/jmas.JMAS_229_17

40. Chen PD, Wu CY, Hu RH, Chou WH, Lai HS, Liang JT, et al. Robotic versus open hepatectomy for hepatocellular carcinoma: a matched comparison. *Ann Surg Oncol.* (2017) 24(4):1021–8. doi: 10.1245/s10434-016-5638-9

41. Lai EC, Tang CN. Long-term survival analysis of robotic versus conventional laparoscopic hepatectomy for hepatocellular carcinoma: a comparative study. *Surg Laparosc Endosc Percutan Tech.* (2016) 26(2):162–6. doi: 10.1097/SLE.0000000000000254

frontiers | Frontiers in Surgery

TYPE Clinical Trial
PUBLISHED 10 November 2022
DOI 10.3389/fsurg.2022.984857



OPEN ACCESS

EDITED BY
Jeroen Van Vugt,
Erasmus Medical Center, Netherlands

REVIEWED BY
Cuizhi Geng,
Fourth Hospital of Hebei Medical University, China
Savo Bou Zein Eddine,
Harvard Medical School, United States
Takeaki Ishizawa,
Osaka Metropolitan University, Japan

*CORRESPONDENCE
Yu D. Han
hanyudi_301@foxmail.com
Yan Han
hanyanzyy@163.com

SPECIALTY SECTION
This article was submitted to Surgical Oncology, a section of the journal Frontiers in Surgery

RECEIVED 02 July 2022
ACCEPTED 21 October 2022
PUBLISHED 10 November 2022

CITATION
Cui L, Wang GF, Li X, Song YQ, Pu WW, Zhang DK, Jiang WQ, Kou YQ, Tan ZQ, Tao R, Han Y and Han YD (2022) Modified low-dose second window indocyanine green technique improves near-infrared fluorescence image-guided dermatofibrosarcoma protuberans resection: A randomized control trial. Front. Surg. 9:984857. doi: 10.3389/fsurg.2022.984857



# Modified low-dose second window indocyanine green technique improves near-infrared fluorescence image-guided dermatofibrosarcoma protuberans resection: A randomized control trial

Lei Cui[1,2], Gao F. Wang[3], Xin Li[4], Yu Q. Song[4], Wen W. Pu[1], De K. Zhang[5], Wei Q. Jiang[2], Ya Q. Kou[2], Zhao Q. Tan[2], Ran Tao[2], Yan Han[2]* and Yu D. Han[2]*

[1]Department of Plastic and Reconstructive Surgery, Plastic Surgery Hospital (Institute), CAMS, PUMC, Beijing, China, [2]Department of Plastic and Reconstructive Surgery, 1st Medical Center of Chinese PLA General Hospital, Beijing, China, [3]Pathology Department, 1st Medical Center of Chinese PLA General Hospital, Beijing, China, [4]Transformation Laboratory, 1st Medical Center of Chinese PLA General Hospital, Beijing, China, [5]Radiology Department, 1st Medical Center of Chinese PLA General Hospital, Beijing, China

**Objective:** Conventional second window indocyanine green (SWIG) technique has been widely attempted in near-infrared fluorescence (NIRF) imaging for intraoperative navigation of tumor radical resection. Nevertheless, the overuse of indocyanine green (ICG) led to an increased risk of drug lethal allergy and high medical cost. This prospective study was to explore clinical application of modified low-dose SWIG technique in guiding dermatofibrosarcoma protuberans (DFSPs) radical resection.

**Method:** Patients with DFSPs were randomly assigned to control and experimental group. The ICG was injected intravenously 24 h before surgery, at a dose of 3.5 mg/kg in the control group and 25 mg/patient in the experiment group, respectively. Intraoperative NIRF imaging included serial views of gross tumor, tumor bed and cross-sectional specimen.

**Results:** Although NIRF imaging of gross tumor and tumor bed in the experimental group demonstrated similar sensitivity and negative predictive value, the specificity and positive predictive value were obviously higher compared to control group. The tumor-to-background ratios of cross-sectional specimens in the experimental group was significantly higher than in the control group ($P = 0.000$). Data in both groups displayed that there was a positive correlation of tumor size in cross-sections between integrated

Abbreviation

DFSP, dermatofibrosarcoma protuberans; MRI, magnetic resonance imaging; CT, computerized tomography; CLI, cerenkov luminescence imaging; NIRF, near-infrared fluorescence; ICG, indocyanine green; SWIG, second window ICG; EPR, enhanced permeability retention; TBR, tumor background ratio; FFPE, formalin fixed paraffin; IHC, immunohistochemical; AJCC, American joint committee on cancer; PPV, positive predictive value; NPV, negative predictive value; BMI, body mass index; MSTS, musculoskeletal tumor society; AJCC, American joint committee on cancer; TMCC, Toronto margin context classification.

histopathologic photomicrographs and NIRF imaging of specimen views ($P = 0.000$). NIRF imaging of cross-sectional specimens had a significant decrease in time cost, and an increase in the ability of examining more surgical margins ($P = 0.000$).

**Conclusion:** This is the first study to demonstrate that a low-dose SWIG technique could improve the accuracy of near-infrared fluorescence image-guided dermatofibrosarcoma protuberans resection.

**Clinical Trial Registration:** ChiCTR2100050174; date of registration: August 18, 2021 followed by "retrospectively registered"

KEYWORDS

intraoperative near-infrared fluorescence imaging, second window indocyanine green technique, dermatofibrosarcoma protuberans, tumor radical resection, tumor-to-background ratios

## Introduction

Dermatofibrosarcoma protuberans (DFSP) originating from the dermis or subcutis is a relatively rare yet stubborn tumor, characterized by infiltrative growth, high risk of local recurrence and extremely uncommon distant metastasis. To improve local control, it is preferably recommended that tumor *en bloc* resection should be performed to acquire adequate surgical margins of at least 2 cm according to conventional histopathology (1–3). Theoretically, three-dimensional micrographic surgery is more preponderant in terms of acquiring negative margins (4, 5). Given labor factor and examining time, however, it is impracticable to perform this procedure in clinical settings, especially in the case of huge tumors with a diameter greater than 2 cm.

With the development of intraoperative navigation, a variety of technologies, such as BrainLab intraoperative 3-dimensional magnetic resonance imaging (MRI) (6, 7), Raman spectroscopy (8), intraoperative computerized tomography (CT) (9), and Cerenkov luminescence imaging (CLI) (10), have been investigated to guide complete tumor removal, as well as locate small or metastatic lesions. In the past decades, the intraoperative MRI or CT surgical units are applied more and more widely in the resection of deep lesions, whereas these approaches were seldom used in the surgery of cutaneous malignant tumor because of sophisticated installation and operating procedure. Nowadays, most of Raman spectroscopy and CLI are at the preclinical stage. Moreover, CLI involves some controversial issues of radiation protection and occupation exposure, which limits the popularity of its clinical practice. In contrast, near-infrared fluorescence (NIRF) imaging using indocyanine green (ICG), a fluorescent contrast dye approved by Food and Administration (FDA), has been greatly broadened from ophthalmology (11), liver surgery (12–14), sentinel lymph nodes biopsy (15), and flap transfer (16) to intraoperative navigation in all sorts of tumor resections. In 2009, Kokudo et al. (17) happened to discover that hepatocellular carcinoma fluoresced strongly when these patients received a routine liver function test by intravenous injection of ICG prior to the surgery, which resulted in a clinical trial to investigate this novel fluorescent imaging techniques. They intravenously injected ICG at a dose of 0.5 mg/kg at least 24 h before surgery. Their study demonstrated that intraoperative real-time ICG-fluorescent imaging enables the highly sensitive identification of hepatocellular carcinoma and metastatic lesions in livers, improving the accuracy of liver resection and surgical staging. ICG is not tumor specific, non-cancerous tissue surrounding the tumor displays fluorescent signal as well. Hence, second window ICG (SWIG) technique based on the enhanced permeability retention (EPR) effect was put forward to improve tumor background ratios (TBRs) by altering the time and dose of ICG injection (18, 19). Nowadays, SWIG approach of high-dose (2.5 mg/kg-5 mg/kg) ICG intravenous infused 24 h prior to surgery has been widely attempted in intraoperative NIRF imaging for identifying tumor margins or discriminating occult cancerous lesions (19–26).

Nevertheless, the dose of ICG was overused on patients and violated package insert in previous clinical trials of SWIG approach, which led to an increased risk of drug lethal allergy and extremely high medical cost. In contrast to excessive dose of ICG, we designated 25 mg ICG for each patient as low-dose approach. Our current research was to explore clinical application of modified low-dose SWIG technique in guiding DFSP radical resection.

## Methods

Patients with DFSPs in heads, extremities or trunk were recruited between October 2019 and May 2022. The main exclusion included seafood/iodine allergy, hyperthyroidism, pregnancy, myasthenia gravis, or acute severe hypertension. The study, registered under chictr.org.cn (ChiCTR2100050174), was approved by the Medical Ethics Committee of the Chinese PLA General Hospital and rigidly

obeyed the principles of the Declaration of Helsinki. All informed consent was obtained before ICG administration.

## NIRF image procedure

The patients enrolled in current research were randomly divided into control and experimental groups with a 1:1 allocation ratio based on block randomization by IBM SPSS software version 20.0 (IBM Corp., Armonk, NY) (Figure 1). The programs of ICG (2.5 mg/ml) ($C_{43}H_{47}N_2O_6S_2$·Na; Danton Pharmaceutical Company) intravenous infusion were as follows: In the control group, the plan of ICG injection was 3.5 mg/kg 24 h before surgery, which referred to the dosage applied in previous research (2.5 mg/kg-5mg/kg). In the experimental group, the designed ICG injection was 25 mg/patient 24 h before surgery. The standard administration protocol included allergy test, antiallergic precondition and intravenous infusion of ICG. 8 mg ICG was injected *via* median cubital vein. After 20 min, if the test result was negative, the antiallergic preconditions consisting of 10 mg dexamethasone sodium phosphate and 20 mg diphenhydramine were administrated. Finally, the surplus ICG was infused intravenously. The adverse effects of ICG were recorded.

Fluorescent camera system (ARGOS NIR-300PT, Jinan Xianweizhineng Technology Co., Ltd) was applied to scan the tumor, with an 785-nm laser excitation source and 830 to 900-nm emission filter. The computer screen with a 3,820 × 2,160 pixel video resolution could offer white light view and pseudocolor view. The probe was positioned 20 cm above the operative area. Initially, the preoperative fluorescence imaging was referred to as "**gross tumor view**". Patients underwent radical tumor resections at a safe margin distance of 2 cm from tumor fluorescent signals. After tumor removal, NIRF imaging was captured by visualizing surgical cavity again to

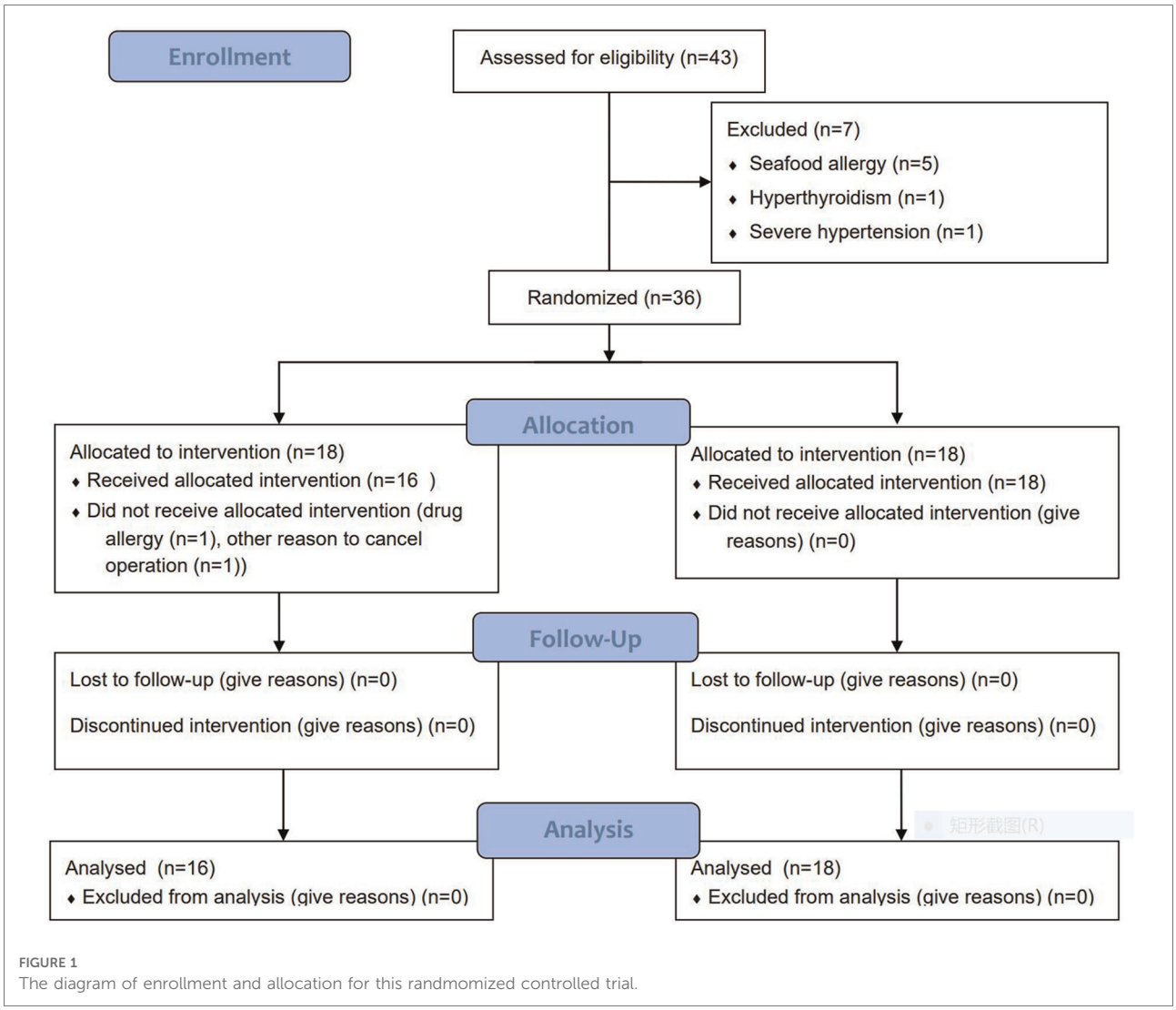


FIGURE 1
The diagram of enrollment and allocation for this randmomized controlled trial.

detect residual cancerous tissues, which was named as "**tumor bed view**". The suspicious lesions discerned by high fluorescent signals were further removed and diagnosed by histopathologic examinations. If there was no fluorescent signal in tumor beds, surgeons were designated to collect tissue as negative tumor base for final histopathologic examination. Sequentially, based on pathologic protocols, representative areas with close margins and the greatest horizontal and perpendicular dimensions of the gross specimens were cut transversely into cross-sections with the thickness of 10 mm in the vertical direction to the skin. Each cross-section was inspected using NIRF probe. The final ICG fluorescence imaging was defined as "**specimen view**", which offered the information of TBRs and tumor size in cross-sectional specimens. The fluorescent imaging of "specimen view" could not affect the range of tumor resection in accordance to panel's recommendation. However, all cross-sections were evaluated by the final pathologic diagnoses. During this phase, the scanning time and number of surgical margins assessed by multiple cross-sections were also compared with conventional rapid frozen pathology. **Figure 2** shows a workflow of the present study.

## Histopathologic diagnosis

After completing "specimen view", the dissected specimen was retrieved to an intact one by suturing. In addition to routine specimen collection, each cross-section was subsequently cut into multiple small portions, the purpose of which was to measure tumor size by assembling into a complete photomicrograph by Adobe Photoshop (PS CC2020, Adobe Systems Incorporated, San Jose, California, USA). Pathological assessment included histologic type, tumor grade and size, and resection margin status. The surgical margins was reported based on the American Joint Committee on Cancer (AJCC) classification/R systems (27), which defines margins as negative (R0), microscopically positive (R1) and macroscopic tumor contamination (R2). Pathologic diagnoses were performed by two experts majoring in soft tissue sarcoma.

## Image analysis

ImageJ (https://imagej.nih.gov/ij/; National Institutes of Health, Bethesda, MD, USA) was used to analyze the TBRs and tumor size in fresh resected cross-sections from NIRF images of specimen views. Region of interest (ROI) size was defined as 100 $mm^2$, given that the diameter of tumor in our study was more than 20 mm and the distance between tumor margin and surgical margin was more than 20 mm. The TBRs were obtained by manually drawing ROI areas of tumor and normal tissue to measure mean grey values on black-and-white images of cross-sectional specimens.

## Statistical analysis

PASS software was used to calculate sample size. Fisher's exact test, Mann-Whitney *U* test or independent *t*-test were used to compare baseline characteristics between two groups. Two-by-two contingency tables were used to calculate the sensitivity, specificity, positive predictive value (PPV) and negative predictive value (NPV) with 95% confidence intervals. TBRs of cross-sectional specimens between two groups were compared by Mann-Whitney *U* test. Spearman correlation analyses were performed to compare the maximum tumor dimension in cross-sections between integrated H&E slides and NIRF imaging of specimen views among respective group. An independent *t*-test was used to analyze the examining time between rapid frozen pathology and NIRF imaging of specimen view. Mann-Whitney *U* test was used to compare number of surgical margins between rapid frozen pathology and NIRF imaging of specimen view. All statistical analyses were performed using IBM SPSS software version 23.0 (IBM Corp., Armonk, NY).

## Results

### Patient characteristics

The needed sample size in this prospective two-arm randomized study was estimated by an alfa-value of 5%, a power of 85% and a difference in TBR of 1 between the two groups. The estimated sample size was 12 patients in each group. Hence, a total of 36 patients were enrolled in our study. 1 patient in the control group developed a skin rash during ICG administration. One operation was cancelled duo to nonmedical reason in the control group. At last, there were 16 patients in the control group and 18 patients in the experimental group (**Figure 1**). There were no significant differences between two groups as regards age ($P = 0.351$), gender ($P = 1.000$), histologic grade ($P = 1.000$), tumor location ($P = 0.943$), tumor size ($P = 0.76$) and body mass index (BMI) ($P = 0.91$). Comparison of patient demographics between two groups are summarized in **Table 1**.

### Analysis of NIRF imaging

16 DFSPs in 16 patients (100%) in the control group displayed significant NIRF imaging on gross tumor views. Four positive fluorescent signals in 4 of 16 patients were detected on tumor bed views, whereas these 4 lesions were

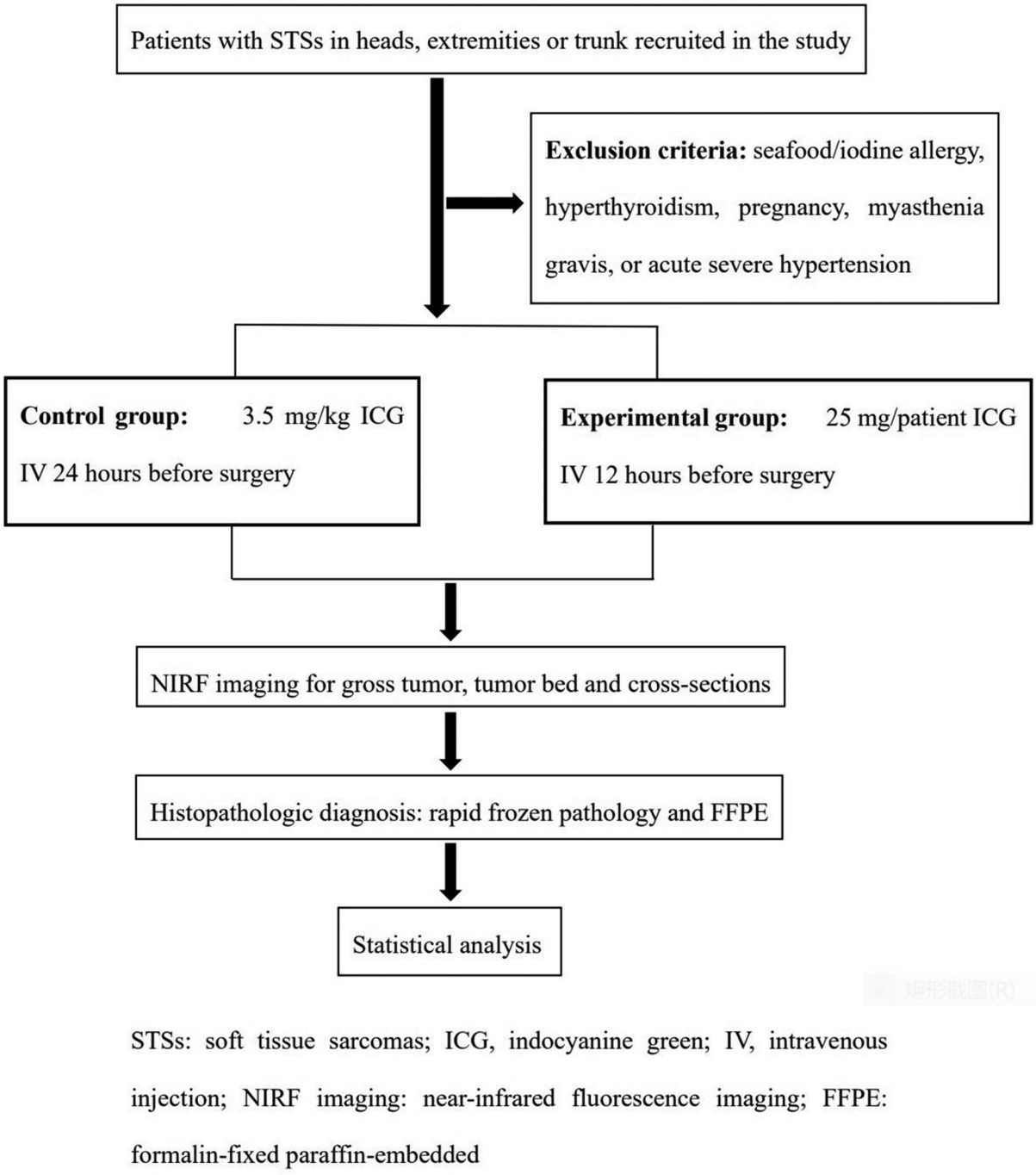


FIGURE 2
The workflow of study.

confirmed as normal tissue or fibrous tissue based on histopathologic diagnoses. Based on the final pathology, the sensitivity, specificity, PPV, and NPV of NIRF imaging were 100%, 75.0%, 80.0%, 100%, respectively (Table 2). All tumors (100%) in the experimental group demonstrated positive NIRF imaging on gross tumor views. Three positive fluorescent signals from tumor bed views were observed in 3 of 18 patients. According to the final histopathology, two of these three suspicious positive tissue were diagnosed as clusters of spindle-shaped CD34-positive neoplastic cells. The other one was normal tissue. In the experimental group, the sensitivity, specificity, PPV, and NPV of NIRF

TABLE 1 Comparison of patient demographics between 2 groups.

| Variable | Control group ($n = 16$) | Experimental group ($n = 18$) | $P$ Value |
|---|---|---|---|
| Age, years, median (interquartile range) | 46.50 (41.00, 53.50) | 41.25 (39.50, 54.30) | 0.351 |
| Gender, female: male ratio | 7:9 | 8:10 | 1.000 |
| Histologic grade (G), low: high ratio | 8:8 | 8:10 | 1.000 |
| Tumor location, $n$ | | | 0.943 |
| Anterior trunk | 3 | 3 | |
| Posterior trunk | 6 | 7 | |
| Lower extremity | 2 | 4 | |
| Upper extremity | 4 | 4 | |
| Head | 1 | 0 | |
| Tumor size, largest diameter, mean ± SD, in centimeter | 5.78 ± 1.53 | 5.83 ± 1.46 | 0.76 |
| Body mass index (BMI), mean ± SD | 24.14 ± 2.80 | 24.25 ± 2.81 | 0.91 |

imaging were 100%, 93.8%, 95.2%, and 100%, respectively (Table 2).

To identify the optimal SWIG technique, we compared the fluorescent intensity of cross-sections in "specimen views" between these two groups. The difference in TBRs of cross-sectional specimens between these two groups was statistically significant (3.90 (3.45–4.45) in the control group vs. 4.90 (4.60–5.50) in the experimental group; $P < 0.001$). It was noted that DFSPs in the experimental group showed significantly more intensive fluorescent signals within tumor sites. On the other side, tumor size calculated by the largest diameter did not differ between these two groups (5.78 ± 1.53 in the control group vs. 5.83 ± 1.46 in the experimental group, $P = 0.76$). The data from both groups displayed that there was a positive correlation of maximum tumor size in cross-sections between integrated H&E photomicrographs and NIRF imaging (rs = 0.989, $P < 0.001$, for the control group; rs = 0.996, $P < 0.001$, for the experimental group). Representative cases in each group are shown in Figure 3.

To compare with rapid frozen pathology, some corresponding parameters of intraoperative "specimen view" were recorded. Firstly, there was a statistically significant decrease in examining time between rapid frozen-section diagnoses and NIR fluorescence imaging of specimen views (47.85 ± 10.82 min vs. 10.21 ± 3.46 min, $P < 0.001$). In addition, the number of surgical margins evaluated by NIRF imaging of specimen view was considerably increased compared with that by rapid frozen-section diagnosis (5.00 (5.00–5.00) vs. 13.00 (10.00–16.00), $P < 0.001$).

## Discussion

Intraoperative NIRF imaging by SWIG technique based on EPR effect has been investigated in the navigation for tumor radical resection in recent years. The EPR effect hypothesizes that after a certain time period, high-intensity ICG is still retained in tumor cells due to enhanced permeability of tumor vasculature, whereas fluorescent imaging of normal tissue has disappeared. Singhal et al. (18) analyzed NIRF imaging of murine tumor models, that infused with various doses from 0.71 to 10 mg/kg of ICG at different timepoints between immediately after injection up to 72 h later. They concluded ICG for NIRF imaging of non-hepatic solid tumors was optimal when dosed at 5 mg/kg and 24 h prior to surgery. Subsequently, surgeons performed clinical researches to observe NIRF imaging of a variety of solid tumors using SWIG technique. In 2016, the first-in-human study (20) enrolled 15 patients infused with a 5 mg/kg dose of ICG 24 h preoperatively. Their results displayed that 12/15 gliomas were visualized with the NIRF imaging, with a sensitivity of 98% and specificity of 45% to confirm malignant areas in gadolinium-enhancing specimens. Similar results were later validated in brain metastases (24), pituitary adenomas (26), and intracranial meningiomas (21), pulmonary metastasectomy (23), breast lumpectomy (28) and other malignant tumors, in which the doses of ICG have varied between 5 mg/kg to 2.5 mg/kg. Newton et al. (22) stratified patients by tumor histology and investigated the optimal dose of ICG in second window technique. They demonstrated that higher dose ICG (4–5 mg/kg) is optimal for intraoperative NIRF imaging of lung cancers and lower dose ICG (2–3 mg/kg) is superior for non-primary lung cancers caused by decreased background fluorescence signal. Based on research

TABLE 2 Test characteristics of intraoperative NIRF imaging for gross tumor and tumor bed in the control group.

| Group | NIRF imaging | Pathologic diagnosis | | Test statistic (95% CI) | | | |
|---|---|---|---|---|---|---|---|
| | | Positive | Negative | Sensitivity | Specificity | PPV | NPV |
| Control group | Positive | 16 | 4 | 100% (75.9%–100%) | 75.0% (47.4%–91.7%) | 80.0% (55.7%–93.4%) | 100% (69.9%–100%) |
| | Negative | 0 | 12 | | | | |
| Experimental group | Positive | 20 | 1 | 100% (80.0%–100%) | 93.8% (67.7%–99.7%) | 95.2% (74.1%–99.8%) | 100% (74.7%–100%) |
| | Negative | 0 | 15 | | | | |

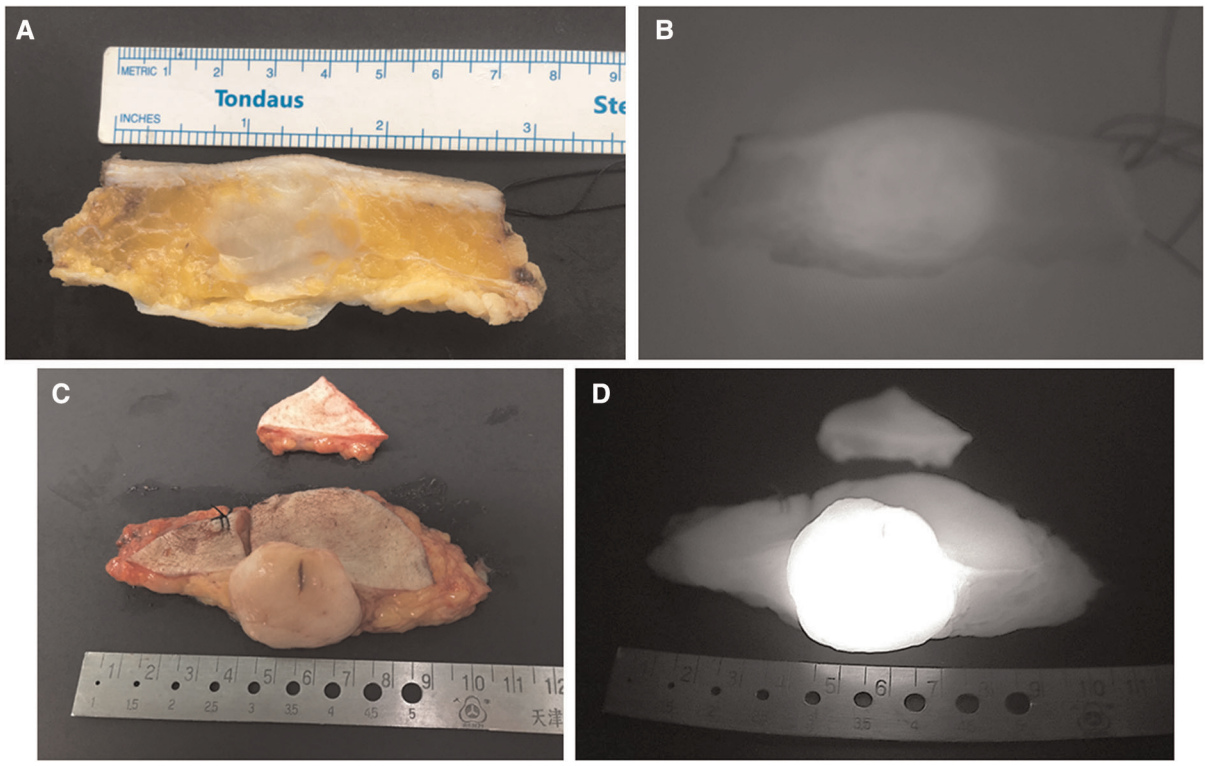


FIGURE 3
Representative images of cross-sectional specimen. (A) Ex vivo brightfield image and (B) ex vivo NIRF image of representative cross-section in the control group. (C) Ex vivo brightfield image and (D) ex vivo NIRF image of representative cross-section in the experimental group.

evidence and empirical data, we assume that the optimal dose of ICG injection correlates with tumor characteristics and parameters of NIRF imaging device.

DFSP is a common type of soft tissue sarcomas (STSs). In theory, ICG as macromolecule is liable to be accumulated within the DFSP, characterized by capsule or pseudocapsule neoplasm surrounded by avascular subcutaneous fat tissue. At present, radical resection with at least 2 cm surgical margins is primary treatment to minimize the risk of local recurrence. To our knowledge, this is the first clinical trial to display intraoperative NIRF fluorescence imaging of DFSP. We designed traditional SWIG technique as control group. Firstly, we compared the low-dose SWIG technique with conventional high dose group in terms of the accuracy of identifying malignant tissue by NIRF views of gross tumor and tumor bed. NIRF imaging in the experimental group demonstrated similar sensitivity (100% vs. 100% in the control group), higher specificity (93.8% vs. 75.0% in the control group), increased PPV (95.2% vs. 80.0% in the control group) and similar NPV (100% vs. 100% in the control group). In both groups, all gross tumors were detected by NIRF imaging. 3 positive fluorescent signals were observed from tumor bed views in experimental group, two of which were confirmed as residual DFSP tissue. In contrast, 4 positive fluorescent signals in tumor beds were validated as non-malignant tissue in the control group. Therefore, we assumed that low-dose SWIG technique appeared to be more sensitive in visualizing tumor bed. Secondly, we analyzed fluorescent signals in cross-sectional specimens. The TBRs of dissected cross-sections in the experimental group was significantly higher than in the control group (4.90 (4.60–5.50) vs. 3.90 (3.45–4.45), $P = 0.000$). Hence, we conclude that the low-dose SWIG technique (25 mg/patient) displayed an improved performance of identifying DFSP lesions by intraoperative NIRF visualization system.

Our NIRF visualization system has more sensitive femtomolar probe detecting fluorescent dye at a concentration of 300 pm/L, the light source output of three homologous wavelength and the camera with three channels. The highly sensitive NIRF optical system decreases the dosage of contrast agent from 5 mg/kg to 0.2 mg/kg, which is one of the reasons why we chose 25 mg ICG in one ampoule as the dose in the experimental group. Besides, the images are processed to reduce background signal by a convolutional neural network approach. Therefore, compared to previous reports, our NIRF imaging system is capable of producing more favorable outcome than conventional SWIG technique.

Although the incidence of lethal complication is less than 0.1%, the iodine, a main component of ICG, is liable to

induce a severe allergic reaction, even shock and death. Since the number of patients in our study was small, we didn't analyze the incidence of drug allergy. However, 1 patient had a mild skin rush during ICG administration in the control group. Take a patient with a weight of 65 kg as an example. The ICG in the control group costs 1,458 RMB (162 × 9), and that in the experimental group spends 162 RMB, which is obviously a very different cost. Given that drug safety, convenience of drug administration, and inpatient cost, 25 mg ICG as a single bolus has also a distinct advantage over high-dose infusion (2.5–5.0 mg/kg ICG).

Even so, there are still some issues to address. Firstly, 25 mg ICG are suitable for patients with normal body mass index (BMI). The individualized dosage in modified SWIG technique should be verified in the following study. Secondly, the inclusion criteria stipulated that only patients with DFSPs were recruited in our study. In fact, intraoperative NIRF imaging using this low-dose SWIG technique might play a positive role in visualizing other malignant soft tissue tumors, such as other types of sarcomas and cutaneous squamous carcinomas. **Figure 4** shows a case of apocrine carcinoma. Fluorescent signal demonstrated remarkable consistency with the contour of tumor in H&E slides. In the further, we will investigate this modified low-dose SWIG method for guiding the resections in other types of malignant neoplasms originated from soft tissues. As far as we know, some research referring to this low-dose SWIG technique in the field of other cancer therapy, such as lung cancer and breast cancer, is also ongoing. Especially for breast cancer locating in trunk and surrounded by adipose tissue, this modified approach is very meaningful in the surgical navigation for lumpectomy.

Besides a great deal of confidence in the prospect of low-dose SWIG technique for NIRF imaging, we also discovered that intraoperative NIRF imaging with SWIG technique could evaluate resected specimen in a more efficient, thorough, and quantitative manner.

At present, some problems in traditional histopathologic diagnosis remain to be solved. Firstly, there are several classification schemes of surgical margins in soft tissue sarcomas, such as the Musculoskeletal Tumor Society (MSTS) classification (29), the American Joint Committee on Cancer (AJCC) classification (27), and the Toronto Margin Context Classification (TMCC) (30), which involve the information of margin status, anatomic barrier and metric distance. Whichever classification is applied, the histopathological examinations just inspect few topical margins, which is obviously inadequate for assessing gross resection specimen, especially for those huge tumors. Moreover, intraoperative frozen-section diagnosis is incapable of offering precise margin distance and prolongs operative time to some degree.

In the present study, we dissected surgical specimen into multiple cross-sections and scanned cross-sectional specimens in sequence using NIRF imaging with SWIG technique before rapid frozen-section histopathology. There was a significant increase in the number of surgical margins assessed by NIRF imaging of specimen views compared to that by rapid frozen-

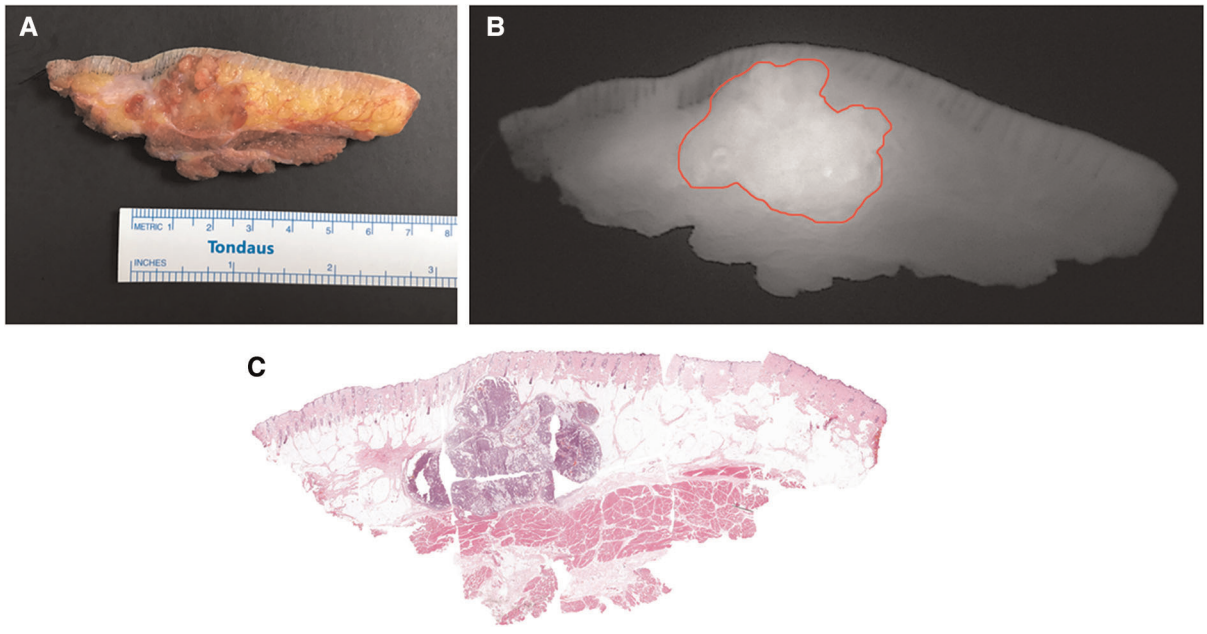


FIGURE 4
Cross-sectional specimen in a case of apocrine carcinoma. (**A**) Ex vivo brightfield image. (**B**) Ex vivo NIRF image. (**C**) Intact H&E photomicrograph integrated from multiple sections.

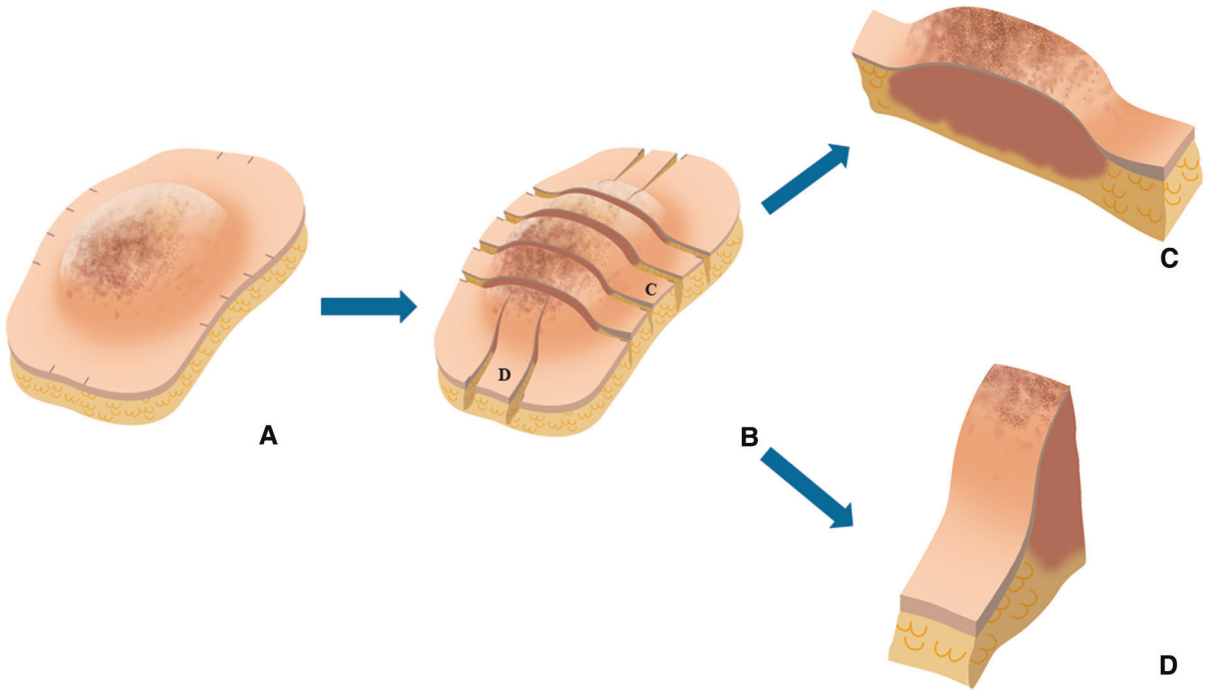


FIGURE 5
The schematic diagram of inspecting intact surgical specimen in the future.

section diagnoses (13.00 (10.00–16.00) vs. 5.00 (5.00–5.00), $P = 0.000$). The average examining time of rapid frozen-section diagnoses was 47 min, which was evidently longer than intraoperative NIRF imaging of specimen views with a mean time of 10 min. Technically, since the NIRF imaging has the advantage of rapid scanning, it is capable of inspecting the whole resected specimen within a few minutes. This efficient approach of evaluating gross surgical specimen could increase the number of positive margins along with a great amount of cross-section scanning. Additionally, NIRF imaging can offer more detailed information about tumor size and margin distance in every cross-section, which is impossible in rapid frozen diagnosis. In our study, the data in both groups displayed that there was a positive correlation of largest diameters of malignant tissue in cross-sections between integrated H&E photomicrographs and NIRF imaging of specimen views ($rs = 0.989$, $P = 0.000$, for the control group; $rs = 0.996$, $P = 0.000$, for the experimental group). Although margin distances were not analyzed in our research, the measurement of margin distance is feasible and beneficial for surgeons, especially when resected margins are suspicious.

We limited the quantity of dissected cross-sections at the current stage, so that the pathologists could assess the intact tumors before sampling. We plan to dissect surgical specimens from comprehensive and multidimensional viewpoints in the future study. Furthermore, we will proceed with investigating whether intraoperative NIRF imaging has potential in assisting pathologists with improving the performance of histopathologic diagnosis. Figure 5 shows a schematic diagram of inspecting intact surgical specimen in the future. For instance, under the direction of specimen views, how to efficiently assess gross surgical specimens, how to accurately harvest suspicious margins, and how to acquire more detailed parameters of metric distance.

## Conclusions

To our knowledge, this was the first time that low-dose SWIG technique was investigated in NIRF imaging. The low-dose SWIG technique demonstrated improved accuracy of detecting tumor fluorescent signal in the intraoperative navigation of DFSP radical resection compared with conventional SWIG technique. Taking into consideration the benefit of drug safety, convenience of drug administration, and inpatient cost, we assume that this modified approach has a good prospect for extensive clinical application. Additionally, our research was the first to explore the potential application of intraoperative NIRF imaging for evaluating resected specimens. Further investigations of NIRF imaging using low-dose SWIG technique will focus on the following issues: a refinement in ICG dosage, broadening clinical application in a variety of malignant tumors, as well

as optimizing NIRF imaging of specimen view for assisting pathologic diagnosis.

## Data availability statement

The original contributions presented in the study are included in the article/Supplementary Materials, further inquiries can be directed to the corresponding author/s.

## Ethics statement

The studies involving human participants were reviewed and approved by the Medical Ethics Committee of the Chinese PLA General Hospital. The patients/participants provided their written informed consent to participate in this study.

## Author contributions

Study conception and design: YH, YDH, LC. Acquisition of data: LC, GFW, XL, YQS. Analysis and interpretation of data: LC, WWP, DKZ, WQJ, YQK, ZQT, RT, YH, YDH. Drafting of manuscript: LC, YH, YDH. All authors contributed to the article and approved the submitted version.

## Acknowledgments

The preclinical research was completed in Plastic Surgery Hospital (Institute), CAMS, PUMC and supported by a program under award number Y2018001.

## Synopsis

This is the first study to demonstrate that a low-dose SWIG technique could improve near-infrared fluorescence image-guided dermatofibrosarcoma protuberans resection. Otherwise, intraoperative NIRF imaging with SWIG technique could evaluate resected specimen in an efficient, thorough, and quantitative manner.

## Conflict of interest

The authors declare that the research was conducted in the absence of any commercial or financial relationships that could be construed as a potential conflict of interest.

## Publisher's note



## References

1. Ugurel S, Kortmann R, Mohr P, Mentzel T, Garbe C, Breuninger H S1 guidelines for dermatofibrosarcoma protuberans (DFSP)—update 2018. *J Ger Soc Dermatol.* (2019) 17(6):663–8. doi: 10.1111/ddg.13849

2. Molina A, Duprat Neto J, Bertolli E, da Cunha IW, Fregnani JHTG, Figueiredo PHM Relapse in dermatofibrosarcoma protuberans: a histological and molecular analysis. *J Surg Oncol.* (2018) 117(5):845–50. doi: 10.1002/jso.25039

3. Sambri A, Caldari E, Fiore M, Zucchini R, Giannini C, Pirini MG Margin assessment in soft tissue sarcomas: review of the literature. *Cancers.* (2021) 13 (7):1687. doi: 10.3390/cancers13071687

4. Wang S, Ezaldein H, Delost G, Tripathi R, Stamey C, Neudecker M Safety and efficacy of mohs micrographic surgery in children and adolescents: a systematic review. *Dermatol Surg.* (2020) 46(7):880–4. doi: 10.1097/dss.0000000000002282

5. Charalambides M, Yannoulias B, Malik N, Mann JK, Celebi P, Veitch D A review of mohs micrographic surgery for skin cancer. Part 1: melanoma and rare skin cancers. *Clin Exp Dermatol.* (2022) 47(5):833–49. doi: 10.1111/ced.15081

6. Di Carlo H, Maruf M, Massanyi E, Shah B, Tekes A, Gearhart JP. 3-Dimensional magnetic resonance imaging guided pelvic floor dissection for bladder exstrophy: a single arm trial. *J Urol.* (2019) 202(2):406–12. doi: 10.1097/ju.0000000000000210

7. Scherer M, Zerweck P, Becker D, Kihm L, Jesser J, Beynon C The value of intraoperative MRI for resection of functional pituitary adenomas-a critical assessment of a consecutive single-center series of 114 cases. *Neurosurg Rev.* (2022) 45(4):2895–907. doi: 10.1007/s10143-022-01810-7

8. Zúñiga W, Jones V, Anderson S, Echevarria A, Miller NL, Stashko C Raman spectroscopy for rapid evaluation of surgical margins during breast cancer lumpectomy. *Sci Rep.* (2019) 9(1):14639. doi: 10.1038/s41598-019-51112-0

9. Bosma SE, Cleven AHG, Dijkstra PDS. Can navigation improve the ability to achieve tumor-free margins in pelvic and sacral primary bone sarcoma resections? A historically controlled study. *Clin Orthop Relat Res.* (2019) 477(7):1548–59. doi: 10.1097/CORR.0000000000000766

10. Fragoso Costa P, Fendler W, Herrmann K, Sandach P, Grafe H, Grootendorst M Radiation protection and occupational exposure on [Ga]Ga-PSMA-11 based cerenkov luminescence imaging procedures in robot assisted prostatectomy. *J Nucl Med.* (2021) 63(9):1349–56. doi: 10.2967/jnumed.121.263175

11. Bousquet E, Provost J, Zola M, Spaide R, Mehanna C, Behar-Cohen F. Mid-phase hyperfluorescent plaques seen on indocyanine green angiography in patients with central serous chorioretinopathy. *J Clin Med.* (2021) 10(19):4525. doi: 10.3390/jcm10194525

12. Chen H, Wang Y, Xie Z, Zhang L, Ge Y, Yu J Application effect of ICG fluorescence real-time imaging technology in laparoscopic hepatectomy. *Front Oncol.* (2022) 12:819960. doi: 10.3389/fonc.2022.819960

13. Lin H, Wang Y, Zhou J, Yang Y, Xu X, Ma D Tomoelastography based on multifrequency MR elastography predicts liver function reserve in patients with

hepatocellular carcinoma: a prospective study. *Insights Imaging*. (2022) 13(1):95. doi: 10.1186/s13244-022-01232-5

14. He K, Hong X, Chi C, Cai C, An Y, Li P Efficacy of near-infrared fluorescence-guided hepatectomy for the detection of colorectal liver metastases: a randomized controlled trial. *J Am Coll Surg*. (2022) 234(2):130–7. doi: 10.1097/xcs.0000000000000029

15. Dumitru D, Ghanakumar S, Provenzano E, Benson JR. A prospective study evaluating the accuracy of indocyanine green (ICG) fluorescence compared with radioisotope for sentinel lymph node (SLN) detection in early breast cancer. *Ann Surg Oncol*. (2022) 29(5):3014–20. doi: 10.1245/s10434-021-11255-9

16. Geierlehner A, Horch R, Ludolph I, Arkudas A. Intraoperative blood flow analysis of DIEP vs. ms-TRAM flap breast reconstruction combining transit-time flowmetry and microvascular indocyanine green angiography. *J Pers Med*. (2022) 12(3):482. doi: 10.3390/jpm12030482

17. Ishizawa T, Fukushima N, Shibahara J, Masuda K, Tamura S, Aoki T Real-time identification of liver cancers by using indocyanine green fluorescent imaging. *Cancer*. (2009) 115(11):2491–504. doi: 10.1002/cncr.24291

18. Jiang JX, Keating JJ, Jesus EM, Judy RP, Madajewski B, Venegas O Optimization of the enhanced permeability and retention effect for near-infrared imaging of solid tumors with indocyanine green. *Am J Nucl Med Mol Imaging*. (2015) 5(4):390–400.

19. Wu J. The enhanced permeability and retention (EPR) effect: the significance of the concept and methods to enhance its application. *J Pers Med*. (2021) 11(8):771. doi: 10.3390/jpm11080771

20. Lee J, Thawani J, Pierce J, Zeh R, Martinez-Lage M, Chanin M Intraoperative near-infrared optical imaging can localize gadolinium-enhancing gliomas during surgery. *Neurosurgery*. (2016) 79(6):856–71. doi: 10.1227/neu.0000000000001450

21. Lee J, Pierce J, Thawani J, Zeh R, Nie S, Martinez-Lage M Near-infrared fluorescent image-guided surgery for intracranial meningioma. *J Neurosurg*. (2018) 128(2):380–90. doi: 10.3171/2016.10.Jns161636

22. Newton A, Predina J, Corbett C, Frenzel-Sulyok LG, Xia L, Petersson EJ Optimization of second window indocyanine green for intraoperative near-infrared imaging of thoracic malignancy. *J Am Coll Surg*. (2019) 228(2):188–97. doi: 10.1016/j.jamcollsurg.2018.11.003

23. Predina J, Newton A, Corbett C, Shin M, Sulfyok LF, Okusanya OT Near-infrared intraoperative imaging for minimally invasive pulmonary metastasectomy for sarcomas. *J Thorac Cardiovasc Surg*. (2019) 157(5):2061–9. doi: 10.1016/j.jtcvs.2018.10.169

24. Teng C, Cho S, Singh Y, De Ravin E, Somers K, Buch L Second window ICG predicts gross-total resection and progression-free survival during brain metastasis surgery. *J Neurosurg*. (2021) 135(4):1–10. doi: 10.3171/2020.8.Jns201810

25. Teng C, Huang V, Arguelles G, Zhou C, Cho SS, Harmsen S Applications of indocyanine green in brain tumor surgery: review of clinical evidence and emerging technologies. *Neurosurg Focus*. (2021) 50(1):E4. doi: 10.3171/2020.10.Focus20782

26. Vergeer R, Theunissen R, van Elk T, Schmidt I, Postma MR, Tamasi K Fluorescence-guided detection of pituitary neuroendocrine tumor (PitNET) tissue during endoscopic transsphenoidal surgery available agents, their potential, and technical aspects. *Rev Endocr Metab Disord*. (2022) 23(3):647–57. doi: 10.1007/s11154-022-09718-9

27. Hermanek P, Wittekind C. The pathologist and the residual tumor (R) classification. *Pathol Res Pract*. (1994) 190(2):115–23. doi: 10.1016/s0344-0338(11)80700-4

28. Keating J, Tchou J, Okusanya O, Fisher C, Batiste R, Jiang J Identification of breast cancer margins using intraoperative near-infrared imaging. *J Surg Oncol*. (2016) 113(5):508–14. doi: 10.1002/jso.24167

29. Enneking W, Spanier S, Goodman MA. A system for the surgical staging of musculoskeletal sarcoma. *Clin Orthop Relat Res*. (1980) 153:106–20. doi: 10.1097/00003086-198011000-00013

30. Gerrand C, Wunder J, Kandel R, O'Sullivan B, Catton CN, Bell RS Classification of positive margins after resection of soft-tissue sarcoma of the limb predicts the risk of local recurrence. *J Bone Joint Surg Br*. (2001) 83(8):1149–55. doi: 10.1302/0301-620x.83b8.12028

frontiers | Frontiers in Oncology

TYPE Mini Review
PUBLISHED 25 November 2022
DOI 10.3389/fonc.2022.1005929



OPEN ACCESS

EDITED BY
Beatrice Aramini,
University of Bologna, Italy

REVIEWED BY
Federico Raveglia,
ASST-Monza, Italy
Davide Tosi,
IRCCS Ca 'Granda Foundation
Maggiore Policlinico Hospital, Italy
Paola Ciriaco,
San Raffaele Scientific Institute
(IRCCS), Italy

*CORRESPONDENCE
Alberto Testori
alberto.testori@
cancercenter.humanitas.it

SPECIALTY SECTION
This article was submitted to
Surgical Oncology,
a section of the journal
Frontiers in Oncology

RECEIVED 28 July 2022
ACCEPTED 03 November 2022
PUBLISHED 25 November 2022

CITATION
Mangiameli G, Testori A, Cioffi U,
Alloisio M and Cariboni U (2022)
Extracorporeal membrane
oxygenation support in
oncological thoracic surgery.
*Front. Oncol.* 12:1005929.
doi: 10.3389/fonc.2022.1005929



# Extracorporeal membrane oxygenation support in oncological thoracic surgery

Giuseppe Mangiameli[1,2], Alberto Testori[1]*, Ugo Cioffi[3], Marco Alloisio[1,2] and Umberto Cariboni[1]

[1]Division of Thoracic Surgery, IRCCS Humanitas Research Hospital, Rozzano, Milan, Italy, [2]Department of Biomedical Sciences, Humanitas University, Milan, Italy, [3]Department of Surgery, University of Milan, Milan, Italy

The use of extracorporeal lung support (ECLS) during thoracic surgery is a recent concept that has been gaining increasing approval. Firstly introduced for lung transplantation, this technique is now increasingly adopted also in oncological thoracic surgical procedures. In this review, we focus on the cutting-edge application of extracorporeal membrane oxygenation (ECMO) during oncological thoracic surgery. Therefore, we report the most common surgical procedures in oncological thoracic surgery that can benefit from the use of ECMO. They will be classified and discussed according to the aim of ECMO application. In particular, the use of ECMO is usually limited to certain lung surgery procedures that can be resumed such as in procedures in which an adequate ventilation is not possible such as in single lung patients, procedures where conventional ventilation can cause conflict with the surgical field such as tracheal or carinal surgery, and conventional procedures requiring both ventilators and hemodynamic support. So far, all available evidence comes from centers with large experience in ECMO and major thoracic surgery procedures.

KEYWORDS

ECMO, thoracic surgery, oncological surgery, lung cancer, NSCLC

## Introduction

The use of extracorporeal lung support (ECLS) during thoracic surgery is a recent concept that has been gaining increasing approval. Extracorporeal membrane oxygenation (ECMO) is a mechanical ECLS normally adopted in surgery to remove $CO_2$, oxygenate, or provide hemodynamic support or a combination thereof during demanding cardiovascular procedures (1). In particular, ECMO involves the use of a centrifugal pump to drive blood from the patient through an externalized membrane oxygenator system for carbon dioxide and oxygen exchange before returning to the

patient. Two different forms of ECMO are actually available: veno-venous (V-V) and veno-arterial (V-A) (see Figure 1).

Veno-venous (V-V) ECMO is the most common ECLS system adopted in thoracic surgery.

Indeed, V-V ECMO is used in severe and refractory adult respiratory failure and requires only peripherally placed venous catheters. Blood is drained from and reinfused into central veins. Thus, V-V ECMO allows excellent oxygenation of vital organs by an inflow directed to the right atrium.

Veno-arterial (V-A) ECMO is used for hemodynamic support with or without respiratory failure because, in addition to assisting in gas exchange, it can increase cardiac output. In this configuration, blood is drained from the venous side and reinfused in the arterial system to provide hemodynamic support. The quality of oxygenation to the vital organs depends on the insertion site of the inflow cannula: (i) low in case of peripheral V-A ECMO and (ii) optimal in case of central V-A ECMO. According to specific indications, these ECLS assistances can be introduced peripherally or centrally (2) by using a minimal amount of heparinization compared to CPB (3).

ECMO was initially introduced in the field of thoracic surgery thanks to lung transplantation (4), during which more thoracic surgeons gained increasing experience allowing widespread use in the oncological field as well (5). The spread of ECMO in oncological surgery has also been justified by the fact that the ECMO systems have a significantly lower impact than the traditional cardiopulmonary bypass (CPB) in producing transient immunosuppression, preventing the spread or growth of hidden malignant cells (6). Furthermore, according to several authors, tumor cells contaminated in the CPB reservoir blood might spread through the arterial cannula, representing a risk for tumor dissemination (6, 7).

To date, the use of ECMO is usually limited to some oncological lung surgery procedures exclusively requiring an adequate ventilation support or associated with a hemodynamic support. Thus, only few data are reported in literature suggesting a favorable result for ECMO in general nontransplant thoracic surgery.

In this article, we briefly report an overview about the state of art of the application of ECMO in oncological thoracic surgery. In particular, we report the most common surgical procedures in oncological thoracic surgery that can benefit from the use of ECMO. They will be classified and discussed according to the aim of ECMO application.

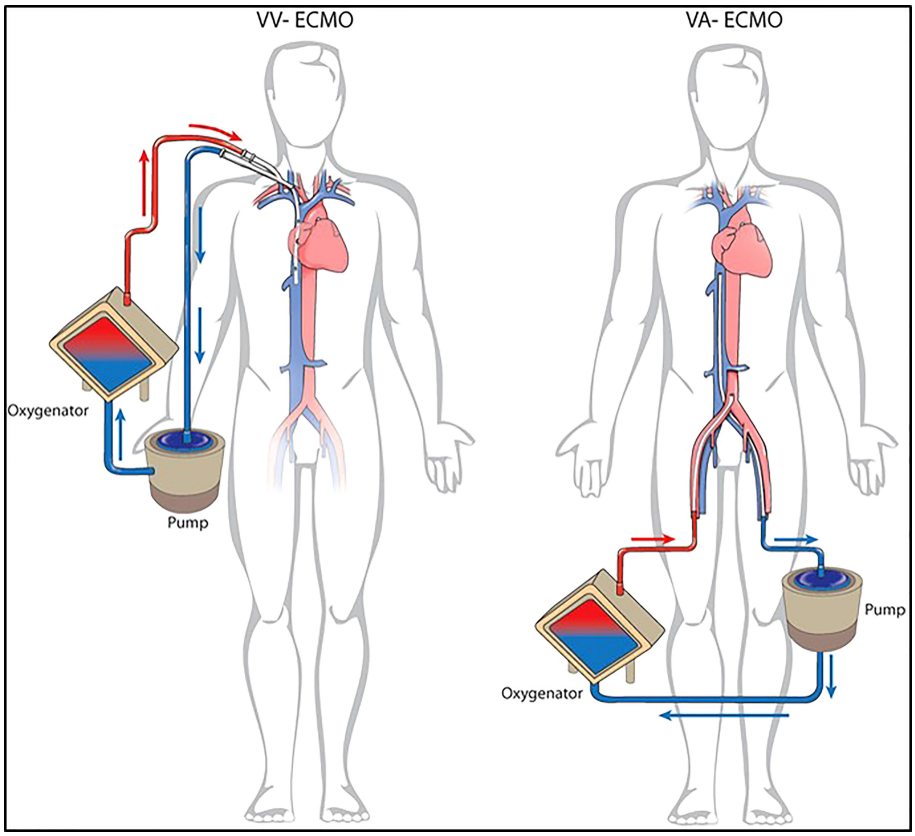


FIGURE 1
Different configuration for ECLS. V-V ECMO and V-A ECMO.

## Procedures requiring an adequate ventilation

In this setting, the use of ECMO is usually limited to certain lung surgery procedures where adequate ventilation is not otherwise feasible. In these cases, V-V ECMO is the most common procedure used because a cardiovascular support is not mandatory (8). Based on the clinical status and the medical history of surgical candidates, two common scenarios are usually possible.

### Surgery in patients with a history of previous extensive contralateral pulmonary resection including pneumonectomy

In this scenario, thoracic surgery is usually performed by using short intermittent apneic phases; thus, multiple atypical lung resections or a planned anatomical resection with radical lymph node dissection could be challenging due to the limited surgical exposure.

To date, several case reports have confirmed that V-V ECMO is a suitable ECLS technique for improving hematosis during surgery when performing lung resections in one-lung patients after pneumonectomy compared to severe respiratory failure patients with problematic one-lung ventilation (3, 8).

Redwan et al. reported one of the most important experiences with the intraoperative use of ECLS; in particular, he reports the adoption of different veno-venous low-flow and high-flow modes adapted to the individual patient requirements. There are two possible scenarios (9).

The first one involves patients who have previously undergone pneumonectomy. In these patients, performing an anatomical resection with radical lymph node dissection could be a challenge. In a no- ECMO setting, these patients usually undergo surgery with short intermittent apneic phases, and the subsequent limited surgical exposure might affect the oncological accuracy. Interestingly, Redwan et al. have reported the use of apneic phases up to 45 min under low-flow V-V ECLS in combination with apneic oxygenation when performing anatomical segmentectomy with radical lymph node dissection in three patients affected by NSCLC and history of previous pneumonectomy (two left sided and one right sided) (9).

The second scenario involves patients scheduled for a planned extensive surgery to the nonoperated lung with a history of previous extensive contralateral lung resection leading to an impairment of lung function and a decline in alveolar gas exchange surface. In these cases, a conventional single-lung ventilation during the entire surgical time may be inadequate and an intermittent double-lung ventilation is needed to maintain sufficient gas exchange. The practical surgical problem due to intermittent ventilation is the consequent reinflating of the lung that interferes with an optimal atelectatic state, which is essential to perform accurate oncological resection especially for multi-lobar metastasectomy. Therefore, in such cases, the German group reports the adoption of a high-flow V-V ECLS that allowed safe and extensive metastasectomy under optimal lung atelectasis in a patient affected by adenoid cystic carcinoma of the mandibular gland with bilateral pulmonary metastases and a history of previous extensive contralateral thoracic surgery (left lower lobe lobectomy and triple-wedge resections of the left upper lobe). He presented with multiple right-sided metastases in all three lobes. In this case, an extensive metastasectomy was performed including multiple atypical lung resections and two anatomical segmentectomies, under optimal lung atelectasis without any respiratory impairment (9).

### Surgery in patients having severely compromised pulmonary function

In patients having severely compromised pulmonary function, conventional single-lung ventilation may be problematic mainly due to hyperinflation and bronchial obstruction. In chronically pathological lungs, the intraoperative high-pressure ventilation could cause additional trauma, leading to complications such as secondary induced pneumothorax, prolonged air leakage, or barotrauma.

The use of ECMO for supporting a compromised pulmonary function during surgery was first reported in nononcological cases. For example, the use of V-V ECMO has been reported in cases of ARDS or respiratory failure allowing, under single-lung ventilation, limited lung resection (atypical resection or segmentectomy) for nononcological diseases (aspergillosis or lung abscess) (10, 11).

In the oncological field, the application of ECMO is rare. The first useful and safe adoption of a V-V ECLS in performing an oncological lung resection in a patient having a severe compromised lung function was reported by Redwan et al. (12).

In this scenario, the strategy adopted was the placement of a single-site cannulation low-flow V-V ECMO providing a sufficient intraoperative support assuring " protective" single-lung ventilation and avoiding additional barotrauma, which usually is a consequence of a high -pressure single ventilation of a pathological lung. Furthermore, by adopting the strategy of a single-site venous cannulation, all the described possible complications due to the arterial cannulation were avoided.

In particular, they reported a challenging surgical procedure performed in a 75-year-old male patient with a long-standing history of chronic obstructive pulmonary disease (Gold stage IV) and severe bullous emphysema. The surgery was a right lower lobe lobectomy and en bloc S6 segmentectomy, but due to tumor central localization with invasion of the lateral wall of the

bronchus intermedius and pulmonary artery, bronchial and right pulmonary artery sleeve resection with reimplantation of the middle lobe bronchus was necessary. The entire procedure was performed under uncomplicated single-lung ventilation thanks to the low-flow V-V ECMO support through a double-lumen twin-port cannula. Bronchial and vascular anastomoses were performed under an apnea phase of 30 min to enable optimal surgical exposure without any respiratory or hemodynamic changes. At the end of the procedure, the patient was normally extubated in the operating room and ECLS was successfully removed. The postoperative course was uneventful and the patient was discharged on the 16 th postoperative day but needed postsurgical intensive respiratory therapy.

The same strategy was adopted by Redwan et al. to perform a VATS right upper lobectomy in a 69- year-old woman having a squamous cellular carcinoma of the right upper lobe (cT2N0) and 33% of predicted FEV1 (9).

Logically, this type of ECMO indication for supporting patients with severe respiratory disease is limited in the oncological field because ECMO allows one to safely perform surgery but the preoperative severe respiratory status is not reversible and usually worsened by surgery.

All cited studies are reported in Table 1.

## Procedures requiring an obstacle-free surgical field

ECMO is the ECLS of choice for the treatment of T4 NSCLC presenting with carinal extension requiring complex tracheobronchial reconstruction. The main limitation of conventional ventilation during complex tracheobronchial reconstruction is the presence of disturbing lines or tubes that obstruct the operative field. In these circumstances, hemodynamic stability or cardioplegia is not necessary and a good oxygenation in addition to removal of $CO_2$ and a complete ventilator support could entirely be assured by ECMO (13). According to the type of tracheobronchial resection and the need to extend or not the surgical resection to the descending aorta or atrium, the use of both V-V and V-A ECMO has been reported in literature.

Initially, sporadic case reports and small cohort studies have reported the successful use of ECLS for tracheal surgical or endoscopic procedures (14, 15). One of the first and larger shared experiences in this field of ECMO application is reported by Lang et al. This Austrian surgical group has reported their experience with intraoperative V-A ECMO in performing complex tracheobronchial resection procedures in 10 patients with thoracic malignancies with excellent results in terms of mortality (0%) and R0 resection rate (89%) (16, 17).

In 2021, Koryllos et al. reported a series of 24 patients undergoing combined complex lung, carinal, aortal, or left atrial resections for oncological reasons by using intraoperative ECMO (16). They performed eight carinal resections, reporting a 78% complete resection (R0) rate and a 25% 30-day mortality. The authors report that the use of V-V ECMO for total respiratory support enabled an excellent surgical field exposure without any required interruption for mechanical ventilation. Furthermore, this strategy allows the reduction of intraoperative ventilation trauma in a group of patients with a high risk of postoperative ARDS, which is a common complication previously reported in these complex tracheobronchial procedures (17, 18). Finally, none of the patients required a V-A cannulation for additional circulatory support.

Recently, Spaggiari et al. have reported their preliminary results of ECMO-assisted tracheal sleeve pneumonectomy (TSP) for cancer in six patients (19). It is a significant experience considering that all the procedures were performed in an oncological setting and, in the last 10 years, only three studies have reported ECMO-assisted TSP for lung cancer, with only three patients described (12, 17, 20).

TABLE 1 Studies reporting the use of ECMO in oncological procedures requiring an adequate ventilation.

| Author | Year | No. of pts | Indications | Lung resection | ECMO type | Rationale |
|---|---|---|---|---|---|---|
| Redwan (9, 12) | 2015 | 3 | NSCLC | Segmentectomy (IIr, IIIr, VIIIl) | V-V low flow | Previous pneumectomy |
| | | 2 | NSCLC | Extended RLL with right PA sleeve resection, reimplantation of the ML bronchus and en bloc segmentectomy (II)<br>RUL lobectomy | V-V low flow | Hypercapnia massive emphysema |
| | | 2 | Lung metastases | Extensive metastasectomy<br>Multiple wedge resection of the LUL | V-V high flow | Previous extensive metastasectomy of the left lung<br>Previous left-sided single-lung transplantation due to end-stage fibrosis with nonfunctioning right fibrotic lung |

NSCLC, non-small cell lung cancer; r, right; l, left; V-V, veno-venous; RLL, right lower lobectomy; ML, middle lobe; RUL, right upper lobectomy; LUL, left upper lobectomy; PA, pulmonary artery.

TSP for treating lung cancer is an old procedure described by Abbot in 1950 (21); this technique is reserved for exceptional cases presenting tracheal carina involvement. This operation is extremely challenging for thoracic surgeons, anesthesiologists, and pulmonologists because of intra- and postoperative management. Several intraoperative strategies have been described to assure a correct ventilation during this type of surgery in these patients, each of these presenting specific limitations.

The cross-field ventilation through a classical endotracheal tube has some major difficulties such as the closure of the left upper bronchus due to its different anatomical length in the patients, the continuous tube dislocation, the possible blood lung aspiration during the dislocation of the tube, and the ischemic damage of the proximal end of the main bronchus due to balloon overinflating.

Similarly, other proposed ventilation strategies, such as intermitted cross-field ventilation, "apneic oxygenation", or jet ventilation, have some limitations, such as intraoperative hypercapnia, the occurrence of lung atelectasis, which can facilitate postoperative infective complications, or possible submucosal endobronchial cancer dissemination (19, 22).

As reported by Spaggiari et al., ECMO-assisted surgery assures adequate respiratory support, hemodynamic stability, an improved brain and myocardial oxygenation, and a lower risk of bleeding complications with a "clean" surgical field without cross-field tubes.

During the time of ECMO activation, the use of modern heparin-coated vascular cannulas prevents episodes of deep venous thrombosis and, additionally, they can be maintained in the case of postoperative instability or if needed. Finally, the theoretical risk of tumor cell spread during ECMO is negligible, considering the absence of the cardiotomy reservoir and the fact that ECMO is a closed circulatory system starting only after significant vessel ligation and lung removal. In their reported experience, they did not observe cannula- related complications or complications during ECMO assistance. The mean duration of assistance was short (38 min); it did not require excessive anticoagulation, and the rapid normalization of coagulation after ECMO use avoided any risk of bleeding. According to the authors, the use of ECMO during carina resection and tracheobronchial reconstruction improved surgical results. The reported advantages of this strategy are the following: the anastomosis can be completed efficiently; technical errors that could be fatal in the postoperative period can be avoided; the lack of left main bronchus manipulation by the endotracheal tube reduces ischemic damage of the stump, probably reducing the risk of dehiscence; the lack of contralateral lung atelectasis due to ventilation overpressure in the cross-field ventilation; and the inevitable passage of blood within the left main bronchus during the intervention due to the continuous manipulation of the bronchus for ventilation.

Recently, Martinod has reported the long-term follow-up and results of his series of 35 adult patients subjected to airway replacement using stented aortic matrices. In this series, 29 patients (82.9%) were operated for malignant lesions, and the use of V-V ECMO was reported in 4 (11.4%) out of 35 patients (23). All cited studies are reported in Table 2.

## Procedures requiring both ventilatory and hemodynamic support

As previously mentioned, V-A ECMO is the ECLS of choice for procedures that require both ventilatory and hemodynamic support. Usually, a very limited number of reports have considered the use of V-A ECMO in patients undergoing non-cardiac surgery (20, 26).

Two different scenarios are usually reported in literature for this type of ECMO indication.

The first one involves T4 NSCLC patients or patients affected by large sarcoma who need a simple lung resection or complex tracheobronchial reconstructions associated with the resection of the great vessels of the left atrium. Usually, surgery for centrally located cancers with wide infiltration of the left atrium or the descending aorta is related to challenging intraoperative conditions, making the adoption of an ECLS attractive for thoracic surgeons (27).

In this case, according to Klepetko's experience, V-A ECMO should be considered a safe alternative to CPB, avoiding its disadvantage when performing this type of extended surgery. Notably, in 2011, Klepetko et al. reported a series of nine cases of thoracic malignancies: in three of them, V-A ECMO was used to perform two descending aorta resections (in two patients affected by NSCLC) and one inferior vena cava resection (in one patient affected by synovial sarcoma) in addition to lung surgery. Based on their experience, the authors recommend that ECMO should also be used in performing resection of great vessels, with the traditional CPB support reserved for open resection of either the left or the right atrium, resection of the aortic arch, or central resection of the pulmonary trunk (16).

Similarly, Koryllos et al. in their series of 24 patients reported the use of V-A ECMO in two particular patient groups. The first involved resections of the left lung and the descending aorta ($n = 7$) and the second involved resections of the lung and left atrium ($n = 9$).

In the first group of patients, a V-A ECMO was the chosen ECLS support in estimating challenging cases with a setting for partial circulatory support (50% of the cardiac output) during longer periods of aortic clamping. Otherwise, in cases of left atrial tumor infiltration, a VV-A- ECMO setting for total circulatory support was the adopted strategy during surgery (24).

The second scenario involved patients affected by early-stage lung cancer with severe heart failure who would be excluded from surgery (the standard treatment) because of prohibitive perioperative risk (27–29). In these cases, ECMO could be a suitable option by assuring both circulatory and respiratory support.

TABLE 2 Studies reporting the use of ECMO in oncological procedures requiring an obstacle-free surgical field or both ventilatory and hemodynamic support.

| Author | Year | No. of pts | Indications | Lung resection | ECMO type | Rationale |
|---|---|---|---|---|---|---|
| Lang (17) | 2015 | 10 | NSCLC: 7<br>Carcinoid:2<br>Adenoid cystic carcinoma: 1 | Complex bronco-tracheal reconstructions | V-A | Avoiding cross-field or jet ventilation |
| Redwan (9) | 2015 | 1 | NSCLC | Left-sided pneumonectomy with carinal sleeve resection | V-V | Avoiding cross-field or jet ventilation to the right lung |
| Koryllos (24) | 2021 | 8 | NSCLC | Complex bronco-tracheal reconstructions | V-V | Avoiding cross-field or jet ventilation to the right lung |
| Spaggiari (19) | 2021 | 6 | NSCLC | Left-sided pneumonectomy with carinal sleeve resection | V-V | Avoiding cross-field or jet ventilation to the right lung |
| Costantino (20) | 2019 | 1 | NSCLC | Left-sided pneumonectomy with carinal sleeve resection | V-A | Avoiding cross-field or jet ventilation to the right lung |
| Mazzella (22) | 2021 | 1 | NSCLC | Right-sided pneumonectomy with carinal sleeve resection | V-V | Avoiding cross-field or jet ventilation to the right lung |
| Martinod (23) | 2022 | 4 | Non reported | Airway replacement using stented aortic matrices | V-V | Avoiding cross-field or jet ventilation |
| Lang (17) | 2015 | 3 | NSCLC: 2<br>Sarcoma: 1 | Descending aorta<br>Inferior vena cava | V-A | Hemodynamic support |
| Koryllos (24) | 2021 | 6<br>9 | NSCLC: 6<br>NSCLC:7<br>Sarcoma: 2 | Descending aorta<br>Left atrium<br>Left atrium | V-A | Hemodynamic support |
| Novellis (25) | 2022 | 1 | NSCLC | ULL with pulmonary artery angioplasty. | V-A | Hemodynamic support |

NSCLC, non-small cell lung cancer; V-A, veno-arterial; V-V, veno-venous; ULL, upper left lobectomy.

Recently, Novellis et al. reported the use of V-A ECMO as a tool to provide temporary cardiac support in a patient with severe impaired ejection fraction (EF) affected by resectable lung cancer and described the benefits of this new method (25). In particular, they reported the intraoperative fast-track use of V-A ECMO in a stage cIIA lung cancer patient with arterial infiltration and severe postischemic dilated cardiomyopathy (EF: 23%) subjected to a left upper lobectomy with angioplasty of pulmonary artery (25). Immediately after surgery, the circuit was removed, the heparin reversal was not administered, and the patient was extubated 3 h later in the intensive care unit. Finally, the patient was discharged in good general condition after an uneventful postoperative course (25).

According to the authors, when hemodynamic support is the main indication for the use of an ECLS device, V-A ECMO offers the most favorable profile because it completely supports the hemodynamic and respiratory function. In their experience, this fast- track strategy allowed the mitigation of all of the complications (bleeding, infection, thrombosis, and ischemia) usually associated with prolonged V-A ECMO support. The use of fast- track V-A ECMO enables fragile patients to be supported during the most challenging phase of the entire perioperative course. In fact, because hypotension, hypercapnia, hypoxia, pulmonary hypertension, tachycardia, and bleeding are more commonly observed intraoperatively than postoperatively, it is reasonable that the hemodynamic support should be maximal intraoperatively. Nevertheless, the cardiac risk in a patient with severe impaired EF remains higher than in a healthier population and can be mitigated only with meticulous postoperative monitoring. All cited studies are reported in Table 2.

## Conclusion

The concept of ECMO-assisted noncardiac oncological thoracic procedures is becoming increasingly attractive. Emerging evidence supports the use of ECMO as both respiratory and circulatory support to facilitate stable intraoperative conditions for satisfying the main goal of oncological R0 resection in case of complex tracheobronchial, atrial, or combined lung-aortic resections and to allow surgery in patients with respiratory limitations or cardiological comorbidities. In these latter cases (impaired lung and/or cardiac function), ECLS allows a safe surgical resection, but it cannot reverse baseline clinical conditions of the patients and

modify their high postoperative mortality rate. To date, all the available evidence comes from centers with large experience in ECMO and major thoracic surgery procedures.

## Author contributions

GM and UCa contributed to conception and design of the study. GM wrote the first draft of the manuscript. All authors contributed to manuscript revision, read, and approved the submitted version.

## Acknowledgments

We thank Dr. Gerardo Cioffi, native speaker, for reviewing the English language.

## Conflict of interest

The authors declare that the research was conducted in the absence of any commercial or financial relationships that could be construed as a potential conflict of interest.

The reviewer FR declared a past co-authorship with the author UCi to the handling editor.

## Publisher's note



## References

1. Abrams D, Combes A, Brodie D. Extracorporeal membrane oxygenation in cardiopulmonary disease in adults. *J Am Coll Cardiol* (2014) 63(25 Pt A):2769–78. doi: 10.1016/j.jacc.2014.03.046

2. Reeb J, Olland A, Massard G, Falcoz PE. Extracorporeal life support in thoracic surgery. *Eur J Cardiothorac Surg* (2018) 53(3):489–94. doi: 10.1093/ejcts/ezx477

3. Rinieri P, Peillon C, Bessou JP, Veber B, Falcoz PE, Melki J, et al. National review of use of extracorporeal membrane oxygenation as respiratory support in thoracic surgery excluding lung transplantation. *Eur J Cardiothorac Surg* (2015) 47 (1):87–94. doi: 10.1093/ejcts/ezu127

4. Mangiameli G, Arame A, Boussaud V, Petitti T, Rivera C, Pricopi C, et al. Lung transplantation in childhood and adolescence: unicentric 14-year experience with sex matching as the main prognosticator. *Eur J Cardiothorac Surg* (2016) 49 (3):810–7. doi: 10.1093/ejcts/ezv243

5. Mangiameli G, Voulaz E, Testori A, Cariboni U, Alloisio M. Surgical treatment of locally advanced T4 non small cell lung cancer with mechanical circulatory support. *Curr Chall Thorac Surg* (2020). doi: 10.21037/ccts-20-131

6. Hasegawa S, Otake Y, Bando T, Cho H, Inui K, Wada ,H. Pulmonary dissemination of tumor cells after extended resection of thyroid carcinoma with cardiopulmonary bypass. *J Thorac Cardiovasc Surg* (2002) 124:635–6. doi: 10.1067/mtc.2002.125060

7. Pinto CA, Marcella S, August DA, Holland B, Kostis JB, Demissie ,K. Cardiopulmonary bypass has a modest association with cancer progression: A retrospective cohort study. *BMC Cancer* (2013) 13:519. doi: 10.1186/1471-2407-13-519

8. Oey IF, Peek GJ, Firmin RK, Waller DA. Post-pneumonectomy video-assisted thoracoscopic bullectomy using extra-corporeal membrane oxygenation. *Eur J Cardiothorac Surg* (2001) 20(4):874–6. doi: 10.1016/s1010-7940(01)00896-x

9. Redwan B, Ziegeler S, Freermann S, Nique L, Semik M, Lavae-Mokhtari M, et al. Intraoperative veno-venous extracorporeal lung support in thoracic surgery: a single-centre experience. *Interact Cardiovasc Thorac Surg* (2015) 6):766–72. doi: 10.1093/icvts/ivv253

10. Souilamas R, Souilamas JI, Alkhamees K, Hubsch JP, Boucherie JC, Kanaan R, et al. Extracorporeal membrane oxygenation in general thoracic surgery: a new single veno-venous cannulation. *J Cardiothorac Surg* (2011) 6:52. doi: 10.1186/1749-8090-6-52

11. Brenner M, O'Connor JV, Scalea TM. Use of ECMO for resection of post-traumatic ruptured lung abscess with empyema. *Ann Thorac Surg* (2010) 90 (6):2039–41. doi: 10.1016/j.athoracsur.2010.01.085

12. Redwan B, Semik M, Dickgreber N, Ziegeler S, Fischer S. Single site cannulation veno-venous extracorporeal lung support during pulmonary resection in patients with severely compromised pulmonary function. *ASAIO J* (2015) 61(3):366–9. doi: 10.1097/MAT.0000000000000193

13. de Perrot M, Fadel E, Mercier O, Mussot S, Chapelier A, Dartevelle P. Long-term results after carinal resection for carcinoma: does the benefit warrant the risk? *J Thorac Cardiovasc Surg* (2006) 131(1):81–9. doi: 10.1016/j.jtcvs.2005.07.062

14. Lei J, Su K, Li XF, Zhou YA, Han Y, Huang LJ, et al. ECMO-assisted carinal resection and reconstruction after left pneumonectomy. *J Cardiothorac Surg* (2010) 5:89. doi: 10.1186/1749-8090-5-89

15. Fica M, Suarez F, Aparicio R, Suarez C. Single site venovenous extracorporeal membrane oxygenation as an alternative to invasive ventilation in post-pneumonectomy fistula with acute respiratory failure. *Eur J Cardiothorac Surg* (2012) 41:950–2. doi: 10.1093/ejcts/ezr103

16. Lang G, Taghavi S, Aigner C, Charchian R, Matilla JR, Sano A, et al. Extracorporeal membrane oxygenation support for resection of locally advanced thoracic tumors. *Ann Thorac Surg* (2011) 92(1):264–70. doi: 10.1016/j.athoracsur.2011.04.001

17. Lang G, Ghanim B, Hötzenecker K, Klikovits T, Matilla JR, Aigner C, et al. Extracorporeal membrane oxygenation support for complex tracheo-bronchial procedures. *Eur J Cardiothorac Surg* (2015) 47(2):250–5. doi: 10.1093/ejcts/ezu162

18. Byrne JG, Leacche M, Agnihotri AK, Paul S, Bueno R, Mathisen DJ, et al. The use of cardiopulmonary bypass during resection of locally advanced thoracic malignancies: a 10-year two-center experience. *Chest* (2004) 125(4):1581–6. doi: 10.1378/chest.125.4.1581

19. Spaggiari L, Sedda G, Petrella F, Venturino M, Rossi F, Guarize J, et al. Preliminary results of extra-corporeal membrane oxygenation assisted tracheal sleeve pneumonectomy for cancer. *Thorac Cardiovasc Surg* (2021) 69:240–5. doi: 10.1055/s-0040-1714071

20. Costantino CL, Geller AD, Wright CD, Ott HC, Muniappan A, Mathisen DJ, et al. Carinal surgery: A single-institution experience spanning 2 decades. *J Thorac Cardiovasc Surg* (2019) 157(5):2073–2083.e1. doi: 10.1016/j.jtcvs.2018.11.130

21. Abbott OA. Experiences with the surgical resection of the human carina, tracheal wall, and contralateral bronchial wall in cases of right total pneumonectomy. *J Thorac Surg* (1950) 19:906–22. doi: 10.1016/S0096-5588(20)31703-7

22. Mazzella A, Bertolaccini L, Petrella F, Spaggiari L. Veno-venous extracorporeal membrane oxygenation-assisted right tracheal-sleeve pneumonectomy. *Interact Cardiovasc Thorac Surg* (2021) 33(4):649–51. doi: 10.1093/icvts/ivab124

23. Martinod E, Radu DM, Onorati I, Portela AMS, Peretti M, Guiraudet P, et al. Airway replacement using stented aortic matrices: Long-term follow-up and results of the TRITON-01 study in 35 adult patients. *Am J Transplant* (2022). doi: 10.1111/ajt.17137

24. Koryllos A, Lopez-Pastorini A, Galetin T, Defosse J, Strassmann S, Karagiannidis C, et al. Use of extracorporeal membrane oxygenation for major cardiopulmonary resections. *Thorac Cardiovasc Surg* (2021) 69(3):231–9. doi: 10.1055/s-0040-1708486

25. Novellis P, Monaco F, Landoni G, Rossetti F, Carretta A, Gregorc V, et al. Venoarterial extracorporeal membrane oxygenation support in lung cancer resection. *Ann Thorac Surg* (2022) 113(3):e191–3. doi: 10.1016/j.athoracsur.2021.05.040

26. Kusstermann J, Gehrmann A, Kredel M, Wurmb T, Roewer N, Muellenbach RM. Akutes lungenversagen und septische kardiomyopathie. *Anaesthesist* (2013) 62(8):639–43. doi: 10.1007/s00101-013-2213-7

27. Dartevelle PG, Mitilian D, Fadel E. Extended surgery for T4 lung cancer: a 30 years' experience. *Gen Thorac Cardiovasc Surg* (2017) 65(06):321–8. doi: 10.1007/s11748-017-0752-6

28. Postmus PE, Kerr KM, Oudkerk M, Senan S, Waller DA, Vansteenkiste J, et al. ESMO guidelines committee. early and locally advanced non-small-cell lung cancer (NSCLC): ESMO clinical practice guidelines for diagnosis, treatment and follow-up. *Ann Oncol* (2017) 28(suppl_4):iv1–iv21. doi: 10.1093/annonc/mdx222

29. Flu WJ, van Kuijk JP, Hoeks SE, Kuiper R, Schouten O, Goei D, et al. Prognostic implications of asymptomatic left ventricular dysfunction in patients undergoing vascular surgery. *Anesthesiology* (2010) 112(6):1316–24. doi: 10.1097/ALN.0b013e3181da89ca

frontiers | Frontiers in Oncology

TYPE Original Research
PUBLISHED 19 December 2022
DOI 10.3389/fonc.2022.1065303



OPEN ACCESS

EDITED BY
Jeroen Van Vugt,
Erasmus Medical Center, Netherlands

REVIEWED BY
Mirza Pojskic,
University Hospital of Giessen and Marburg, Germany
Cordula Maria Netzer,
University Hospital of Basel, Switzerland

*CORRESPONDENCE
Feng Wei
weifeng@bjmu.edu.cn

†These authors have contributed equally to this work and share first authorship

SPECIALTY SECTION
This article was submitted to Surgical Oncology, a section of the journal Frontiers in Oncology

RECEIVED 09 October 2022
ACCEPTED 30 November 2022
PUBLISHED 19 December 2022

CITATION
Hu P, Du S, Wei F, Zhai S, Zhou H, Liu X and Liu Z (2022) Reconstruction after resection of C2 vertebral tumors: A comparative study of 3D-printed vertebral body versus titanium mesh. *Front. Oncol.* 12:1065303. doi: 10.3389/fonc.2022.1065303



# Reconstruction after resection of C2 vertebral tumors: A comparative study of 3D-printed vertebral body versus titanium mesh

Panpan Hu[1†], Suiyong Du[2†], Feng Wei[1*], Shuheng Zhai[1], Hua Zhou[1], Xiaoguang Liu[1] and Zhongjun Liu[1]

[1]Department of Orthopedics and Beijing Key Laboratory of Spinal Disease Research, Peking University Third Hospital, Beijing, China, [2]Department of Spine Surgery, 521 Hospital of Norinco Group, Xi'an, China

**Background:** Surgical resection of C2 vertebral tumors is challenging owing to the complex anatomy of C2 vertebrae and the challenges to surgical exposure. Various surgical approaches are available, but some are associated with excessively high risks of complications. An additional challenge is reconstruction of the upper cervical spine following surgery. In the last decade, additive-manufacturing personalized artificial vertebral bodies (AVBs) have been introduced for the repair of large, irregular bony defects; however, their use and efficacy in upper cervical surgery have not been well addressed. Therefore, in this study, we compared instrumented fixation status between patients who underwent conventional titanium mesh reconstruction and those who underwent the same resection but with personalized AVBs.

**Methods:** We performed a retrospective comparative study and recruited a single-institution cohort of patients with C2 vertebral tumors. Clinical data and imaging findings were reviewed. Through data processing and comparative analysis, we described and discussed the feasibility and safety of surgical resection and the outcomes of hardware implants. The primary outcome of this study was instrumented fixation status.

**Results:** The 31 recruited patients were divided into two groups. There were 13 patients in group A who underwent conventional titanium mesh reconstruction and 18 group B patients who underwent personalized AVBs. All patients underwent staged posterior and anterior surgical procedures. In the cohort, 9.7% achieved total en bloc resection of the tumor, while gross total resection was achieved in the remaining 90.3%. The perioperative complication and mortality rates were 45.2% and 6.5%, respectively. The occurrence of perioperative complications was related to the choice of anterior approach ($p < 0.05$). Group A had a higher complication rate than group B ($p < 0.05$). Four patients (4/13, 30.8%) developed hardware problems during the follow-up

period; however, this rate was marginally higher than that of group B (1/18, 5.6%).

**Conclusions:** Total resection of C2 vertebral tumors was associated with a high risk of perioperative complications. The staged posterior and retropharyngeal approaches are better surgical strategies for C2 tumors. Personalized AVBs can provide a reliable reconstruction outcome, yet minor pitfalls remain that call for further modification.

KEYWORDS

**primary spine tumor, C2 vertebra, total resection, 3D printing, titanium mesh, artificial vertebral body**

# 1 Introduction

The C2 vertebral body is one of the most common sites of primary spinal tumors; yet, this area has complicated anatomic conditions, with the existence of large arteries, excessive venous plexi, and important neurological structures (1). Technically, it is difficult to perform total en bloc resection (TER) of tumors in the C2 vertebral body. To achieve this surgical goal, surgeons generally choose between a combined or staged anterior and posterior approach to fully expose the lesion (2–5). Gokaslan and colleagues described the procedure of a single posterior TER of C2 vertebral tumors, with the two cases both receiving satisfactory outcomes (6, 7). Some additional authors have also described techniques of the single anterior approach (transoral, transmandibular, or retropharyngeal) for C2 vertebral tumors, whereas most of the cases barely achieved intralesional or gross total resection (GTR) (8–11).

Regardless of the surgical approach, the TER of C2 vertebral tumors is technically demanding and accompanied by a high risk of severe complications including cerebrospinal fluid leakage, vascular ruptures, paralysis of the diaphragm, respiratory dysfunction, ventilator dependence, wound problems such as an unhealed pharyngeal wall, and neurological deficits (3, 4, 7, 12–14). Moreover, hardware problems and even failures have been shown to be excessively high. Wei et al. (2016) reported that nearly 50% of their cases involving TER of C2 vertebral tumors had problems of bony malunion and disunion, and one-third of the cases had fixation failure (4). In an impressive case report by Rhines and colleagues (2005), the patient developed apparent migration of the graft and plate during the hospital stay; thus, an emergent revision was arranged (12). Singh et al. (2020) have also described their experience with the technique of modified titanium mesh and iliac crest graft, with solid fusion achieved after 18 months of follow-up (15). In 2016, Xu et al. introduced a customized 3D-printed artificial vertebral body (AVB) to reconstruct the upper cervical spine after the total resection of C2 Ewing sarcoma (16). Personalized 3D-printed AVBs have since then been widely utilized in column reconstruction after the resection of spinal tumors (10, 17–22). However, considering that few centers can perform TER of C2 tumors and/or have access to 3D-printed AVBs, there is a lack of specific comparative studies, and the efficacy and superiority of personalized AVBs have therefore not been fully addressed. Thus, in this study, we conducted a comparative analysis between 3D-printed AVBs and conventional titanium constructs.

# 2 Materials and methods

## 2.1 Patient inclusion

This was a retrospective comparative study. Patients with C2 vertebral tumors were reviewed from our institutional database of spinal tumors, and all patients were screened for eligibility. The inclusion criteria were as follows: (1) undergoing GTR or TER, (2) receiving anterior column reconstruction using either titanium meshes or AVBs, and (3) being regularly followed up until death or beyond 12 months. This study recruited 31 consecutively treated patients between January 2009 and December 2020. According to the methods of anterior reconstruction, two groups were allocated: group A, titanium mesh; and group B, personalized AVBs. Clinical records and imaging data of the recruited patients were reviewed and analyzed. The study was approved and supervised by our institutional ethics committee and all participants provided informed consent.

## 2.2 Preoperative evaluation and preparation

The routine preoperative imaging set included plain radiography, computed tomography (CT), CT angiography

(CTA), magnetic resonance imaging (MRI), and positron emission tomography- CT. CTA was necessary to determine the position of the vertebral arteries (VA). In this case series, CT-guided biopsy was performed for pathological diagnosis. For patients with a large tumor mass or potential involvement of the VA, preoperative embolization of tumor lesions and feeding vessels was performed to reduce intraoperative blood loss.

The preparation of personalized AVBs has been reported previously (22). After acquiring the patients' 1-mm-thin layer CT scans, the data were imported into MIMICS software (version 15.0; Materialize, Leuven, Belgium) for prosthesis design. This procedure was performed under the supervision of senior surgeons. The porous prosthesis was fabricated from Ti6Al4V powder by electron beam melting (Arcam EBM System; Arcam, Mölndal, Sweden). The diameters of the pores and wires were set at 600 ± 200 μm and 550 ± 200 μm, respectively, and the average porosity rate was 50%–80%.

## 2.3 Surgical procedures

All patients underwent staged posterior and anterior surgeries to achieve GTR or TER goals. The surgery was performed by our senior authors, namely, the FW and ZL teams. During the posterior procedure, the most important goal was to isolate the neurological structures and the VA. First, we resected the C2 lamina and lateral masses and exposed the spinal cord and bilateral nerve roots. Subsequently, the C2 transverse foramen was gently palpated using nerve probes, and its posterior and lateral walls were carefully removed in a piecemeal manner. Generally, a 1-mm Kerrison rongeur is first used to open a fissure, and then a high-speed drill or ultrasonic bone scalpel can be employed under the tight protection of the VA. After completing this step, we were able to remove the bilateral pedicles from the vertebral body. In some cases, it was necessary to ligate one side of the VA during the surgery to achieve TER of the tumor lesion. Posterior fixation was accomplished using an occipital or C1–C4/C5 screw-rod system.

The anterior procedure is typically completed through the high retropharyngeal and transoral approaches (Figure 1). However, in case #A8, we used an aggressive transmandibular approach to achieve intralesional resection of the C2 chordoma (Supplementary Table). During the anterior procedures, we predominantly performed extracapsular dissection to avoid minimal residual tumors. First, we transected the bilateral musculus longus coli to expose the transverse process and carefully probed the transverse foramen. Then, we resected the anterior and lateral walls and isolated the VA using a Kerrison rongeur with or without powered tools. Generally, we transected the odontoid process at the cranial end, although this may have constituted intralesional manipulation in some cases. At the caudal end, we removed the C2/3 or C3/4 intervertebral discs to preserve an intact tumor margin. At this time, the entire vertebral body was released and removed as an entire mass.

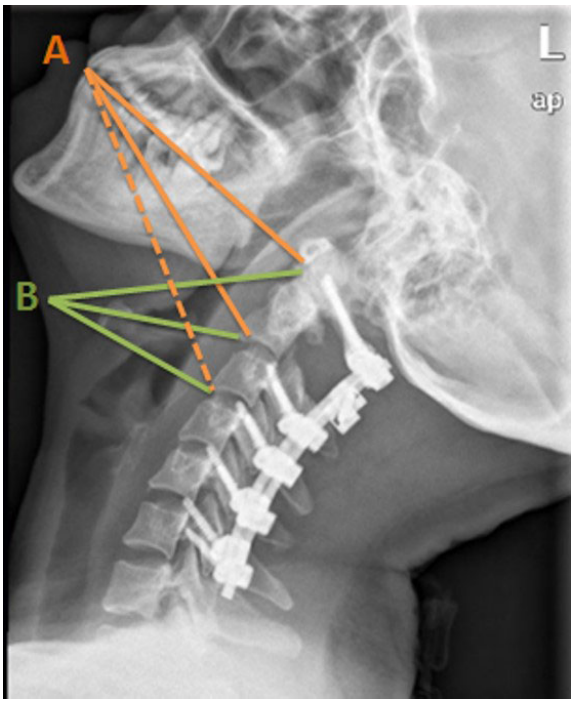


FIGURE 1
Illustration of longitudinal exposure range. Orange lines **(A)** represent the transoral approach: solid lines indicate areas that this approach was able to reach and the dotted line refers to the areas out of reach. Green lines **(B)** indicate where this approach can reach.

## 2.4 Anterior column reconstruction

In group A, we used cylindrical titanium mesh with a plate or stand-alone modified mesh (Figure 2A). In group B, patient-tailored AVBs were fabricated by 3D printing (Figure 2B). The choice of anterior reconstruction material was not randomized. Customized AVBs have been used in most cases since 2015, before which titanium mesh had been used exclusively.

## 2.5 Follow-up and data collection

The patients were regularly followed up at our clinic, with visit windows of 3, 6, and 12 months after the operation and lifelong assessments conducted annually. At each visit, we evaluated symptomatic improvement and performed imaging examinations including radiography, CT, and MRI. Positron emission tomography-CT was only indicated when evidence of tumor relapse emerged.

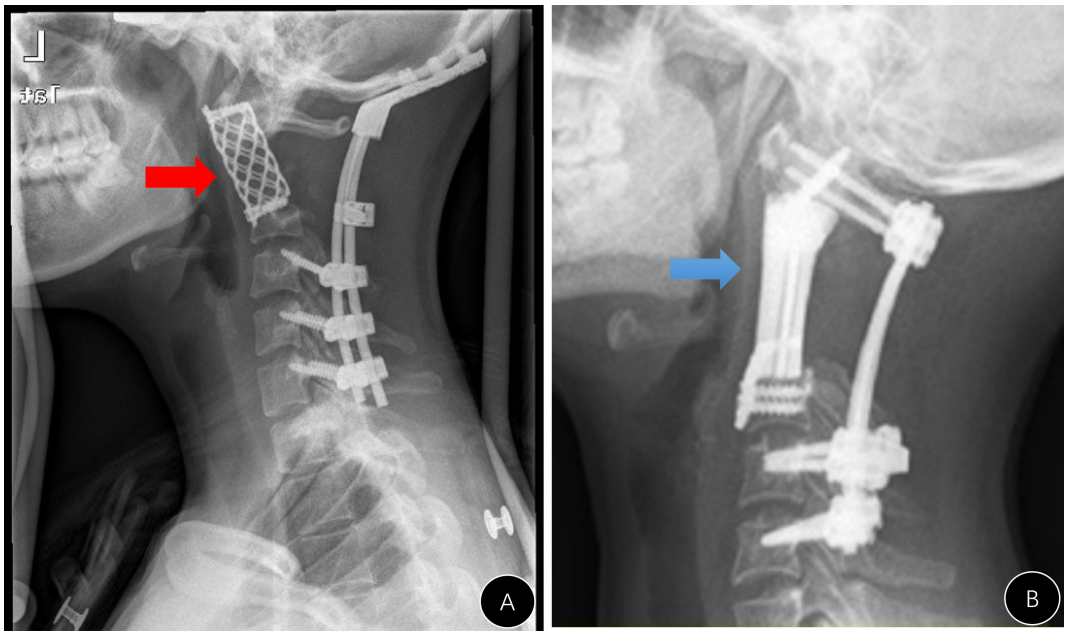


FIGURE 2
Two different anterior reconstruction materials. **(A)** Stand-alone titanium mesh; **(B)** 3D-printing artificial vertebral body.

This study used instrumented fixation as the primary outcome indicator. Other data collected included those regarding demographics, surgical details, complications, tumor pathologies, staging [using the Enneking and Weinstein–Boriani–Biagini systems (23) systems], and patient survival status.

## 2.6 Statistical analysis

Data analysis was performed using IBM SPSS Statistics for Windows Version 20 (IBM Corp., Armonk, NY, USA). Data were presented as percentage, mean ± standard deviation, or median (range). The Student's *t*-test and Pearson's $\chi^2$ test (or Fisher's exact test) were used to compare different groups. Statistical significance was set at $p < 0.05$.

# 3 Results

## 3.1 Demographics and pathologies

The detailed data for each case are presented in the Supplementary Table. There were 13 cases in group A and 18 in group B. The average patient age was 43.3 years in group A and 38.2 years in group B (Table 1). Neck pain was the most common clinical complaint, and other symptoms included neurological deficits (six cases), torticollis (two cases), dysphagia, and dyspnea. Pathologically, this cohort included 14 cases of chordoma, 11 cases of giant cell tumor, 2 cases of osteoblastoma, and 1 case each of paraganglioma, Ewing sarcoma, hemangiopericytoma, and Schwannoma. Two patients died after the postoperative hospital stay, and the other patients were followed up beyond 12 months.

## 3.2 Surgery-related data

In group A, all patients underwent midline incision, and anterior procedures included retropharyngeal (three cases), transoral (seven cases), transmandibular (one case), and combined approaches (two cases) (Table 1). All patients who underwent posterior procedures received screw-rod fixation. The anterior reconstruction materials included a modified titanium mesh in eight cases (Figure 3) and a mesh plus locking plate in five. Additionally, we sacrificed the unilateral nerve root in five patients and ligated one side of the VA in three because of tumor invasion. Specifically, six patients (46.2%) underwent tracheotomy during the operation for better respiratory management, and one underwent preoperative vascular embolization to reduce intraoperative blood loss (case #A4). After the operation, 10 patients (76.9%) wore a halo vest (the majority for a minimum of 3 months) to consolidate the internal fixation.

In group B, 17 patients (94.4%) underwent the retropharyngeal approach and 1 (#B4) underwent the transoral

TABLE 1 Summary of data and comparison between the two groups.

| Items | | Group A ($n$ = 13) | Group B ($n$ = 18) | $p$-values |
|---|---|---|---|---|
| Age (years) | | 43.3 ± 3.7 | 38.2 ± 3.8 | 0.356 |
| Pathologies ($n$) | | Chordoma: 6 | Chordoma: 8 | |
| | | GCT: 3 | GCT: 8 | |
| | | OB: 2 | PGL: 1 case | |
| | | HPC: 1 | ES: 1 | |
| | | Schwannoma: 1 | | |
| Surgical approaches | | | | |
| | Posterior | mid-line: 13 | mid-line: 18 | |
| | Anterior | RP: 3 | RP: 17 | |
| | | TO: 7 | TO: 1 | |
| | | TM: 1 | | |
| | | TO/RP: 1 | | |
| | | TO/TC: 1 | | |
| Fixation and reconstruction | | | | |
| | Posterior | Screw-rod: 13 | Screw-rod: 18 | |
| | Anterior | Mesh alone: 8 | AVB: 18 | |
| | | Mesh/LP: 5 | | |
| Bleeding volume (ml) | | | | |
| | Posterior | 896 ± 150 | 625 ± 80 | 0.098 |
| | Anterior | 1,384 ± 232 | 603 ± 132 | 0.008* |
| Operative time (min) | | | | |
| | Posterior | 265.9 ± 68.7 | 239.8 ± 34.6 | 0.325 |
| | Anterior | 269.9 ± 91.6 | 222.1 ± 37.0 | 0.138 |
| Tumor margins ($n$) | | | | |
| | Intralesional | 13 | 15 | |
| | Marginal | 0 | 3 | |
| Halo vest ($n$) | | 10 | 3 | 0.003* |
| Complicated events ($n$) | | 9 | 5 | 0.022* |
| Hardware problems ($n$) | | 4 | 1 | 0.060 |

*Significantly different at $p < 0.05$.
GCT, giant cell tumor; OB, osteoblastoma; PGL, paraganglioma; HPC, hemangiopericytoma; ES, Ewing sarcoma; RP, retropharyngeal; TO, transoral; TM, transmandibular; TC, transcervical; AVB, artificial vertebral body; LP, locking plate.

approach during the anterior procedures. Personalized AVBs were used as exclusive column constructs (Figure 4). During the operation, we ligated one side of the VA (case #B5) because of an inadvertent injury. One patient underwent preoperative vascular embolization to reduce intraoperative blood loss (case #B7). After the operation, only three patients (16.7%) wore the halo vest for 3– 8 weeks, which was a lower number than in group A ($p < 0.05$).

## 3.3 Postoperative and follow-up events

Perioperative complications developed in 14/31 patients (45.2%) (Table 1). The major complications included cerebrospinal fluid leakage (5/31 cases, 16.1%), wound problems (8/31 cases, 25.8%), cardiac events (case #A8), and vascular events (case #A11 and #B12). Three patients (3/18, 16.7%) in group B had respiratory dysfunction after the

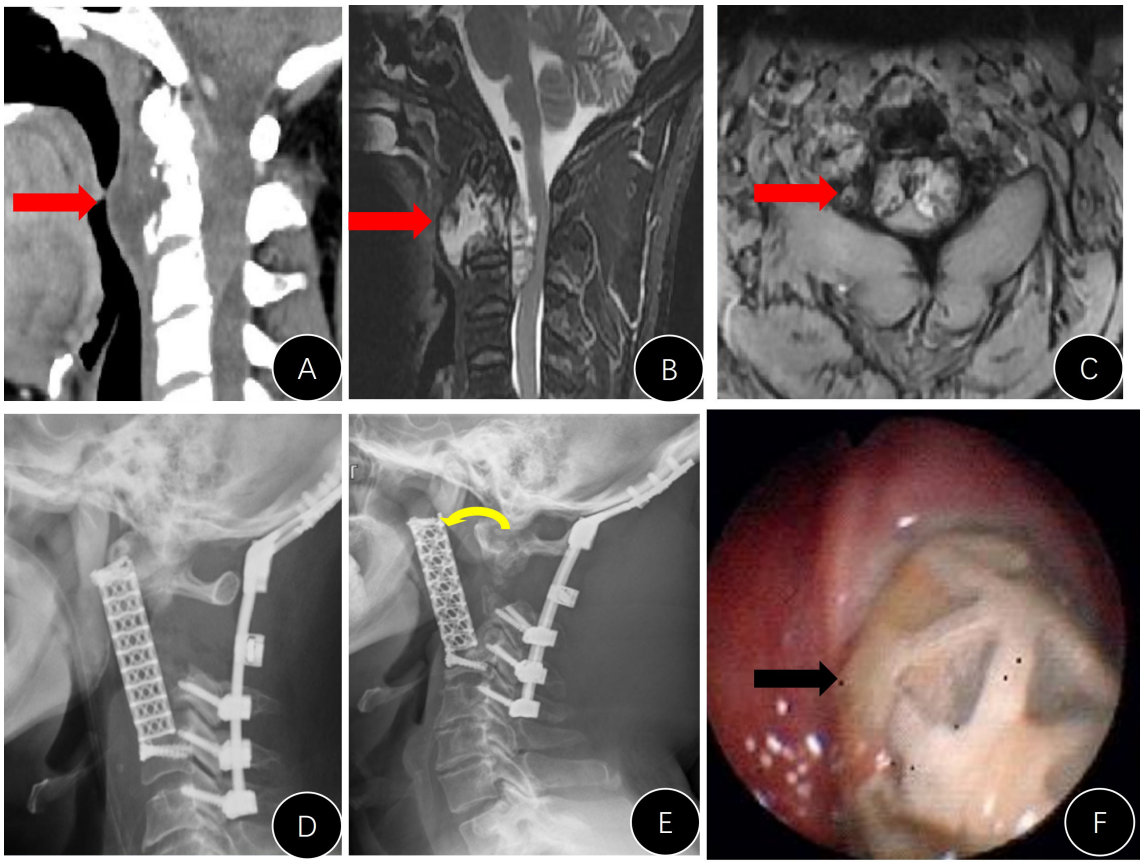


FIGURE 3
Presentation of #A9. **(A–C)** Preoperative CT and MRI images; **(D)** postoperative lateral x-ray; **(E)** lateral x-ray 3 years after the operation (anterior rotation of the titanium mesh); **(F)** unhealing of the pharyngeal wall with mesh exposure.

operation and required a temporary tracheotomy, one of whom died of respiratory failure and septic shock (case #B16). In group A, one patient (case #A11) died of postoperative hemorrhagic shock. This patient showed consistent drainage of fresh blood and signs of circulatory dysfunction; emergency exploratory surgery was performed, yet an active bleeding spot could not be detected. Thus, the patient unfortunately died of hemorrhagic shock. The overall mortality rate in the cohort was 6.5% (2/31).

Patients in group A had a higher incidence of perioperative complications than those in group B ($p < 0.05$, Table 1), and patients who underwent retropharyngeal approaches (30.0%, 6/20) had a lower incidence of perioperative complications than those who underwent transoral and transmandibular approaches (72.7%, 8/11) ($p = 0.022$).

## 3.4 Internal fixation outcomes

During follow-up, there were four cases (4/13, 30.8%) in group A with emerging internal instrument-related complications (Table 1). This ratio was marginally higher than that in group B ($p = 0.060$, Table 1). The stand-alone titanium mesh in case #A1 was observed to be malpositioned during the follow-up, and the modified meshes in cases #A3 and #A9 (Figure 3E) did not have a solid anchor at the cranial end and moved forward. Additionally, the titanium mesh in case #A6 did not fuse at all and completely loosened, and the posterior rods became broken. The broken rods were replaced during the revision operation, but the mesh was left untouched (Figure 5).

Only one case in group B presented with an instrument problem (case #B7). We found it difficult to nail the C1 screws during the operation and had to leave them malpositioned (Figure 6). However, the AVB in this patient did not loosen or move during follow-up.

# 4 Discussion

To the best of our knowledge, this report contains one of the largest single-center cohorts of C2 vertebral primary tumors. In

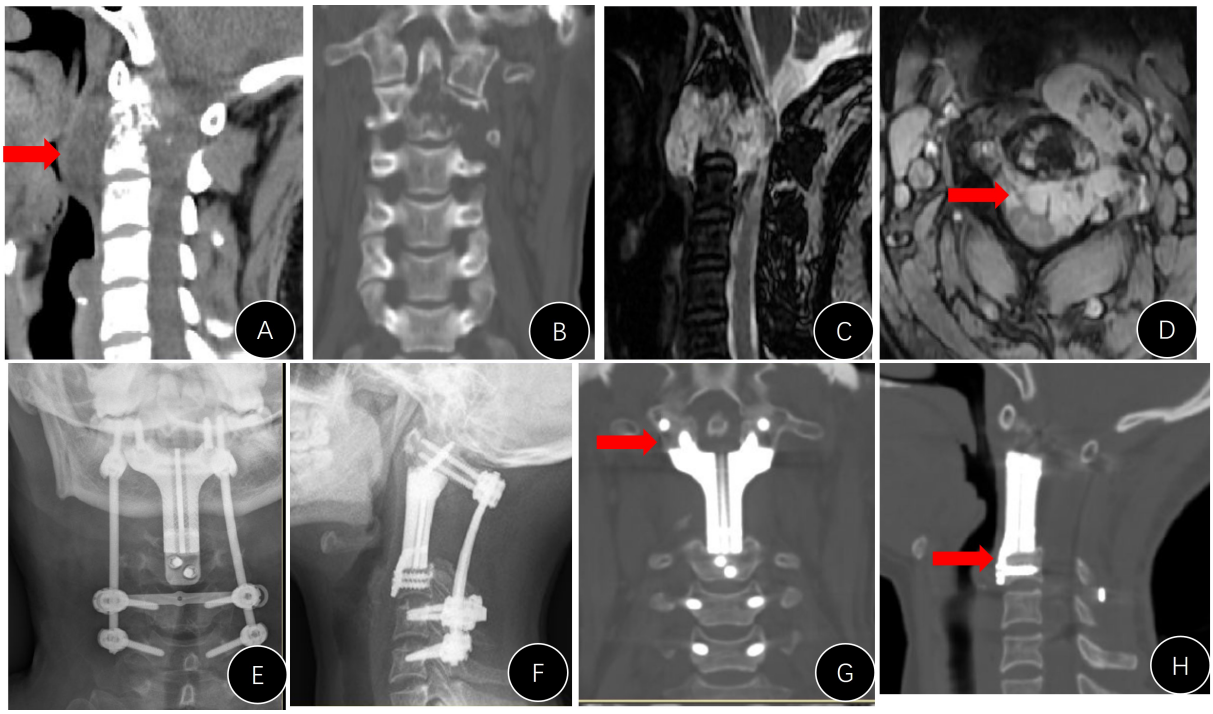


FIGURE 4
Presentation of case #B15. **(A–D)** Preoperative CT and MRI images; **(E, F)** postoperative x-rays; **(G, H)** CT reconstruction films 1 year later, indicating that the implant was well attached to the C1 lateral mass and superior endplate of C3.

addition, this article provides a comparative study between 3D-printed AVBs and conventional titanium constructs and demonstrates the efficacy and merits of AVBs with more solid evidence.

However, total resection of C2 vertebral tumors was associated with a high risk of perioperative complications. Staged posterior and retropharyngeal approaches were shown to be better surgical strategies for C2 tumors. Personalized AVBs can provide a reliable reconstruction outcome, yet minor pitfalls remain.

## 4.1 Surgical challenges and risks

Conventional radiotherapy is usually ineffective as a primary or adjuvant therapy after intralesional resection of malignant or aggressive tumors such as chordomas and GCT (24). However, more evidence has shown that modern radiotherapy techniques, such as stereotactic radiotherapy, provide durable local control as adjuvant therapy or even as the primary treatment for cases that are unable to undergo surgical resection (25). Theoretically, TER is the principal surgical goal for aggressive primary spinal tumors (14, 26, 27). A study based on the AOSpine Knowledge Forum Tumor database (28) revealed that an Enneking-appropriate (EA) surgical strategy for chordoma can significantly decrease locoregional recurrence and prolong the overall survival of patients. Although we attempted EA surgeries in all recruited patients, only three cases (9.7%, 3/31) achieved marginal TER. According to Zhong et al. (2021), TER can be achieved only for tumors localized within the vertebral body or odontoid process (29).

Owing to the complex anatomic structure of C2 and the existence of VA, resection surgery for C2 vertebral tumors is technically demanding and has an excessively high risk of complications (2–4, 7, 12–14). In this series, nearly half of the patients developed moderate-to-severe perioperative complications. This ratio is much higher than that for tumor resection surgery in other spinal segments (14, 20, 22). In our study, all patients underwent sequential posterior and anterior approaches to acquire more space for surgical manipulation and direct visual supervision. In previous studies, two-stage surgeries had a higher total bleeding volume than single-staged surgeries (6, 7, 9, 10). However, this strategy is still a better choice for most C2 vertebral tumors as it spares internal time for physical recovery between the two procedures.

Injury to the VA is one of the most severe complications in the resection of C2 vertebral tumors. In this study, the risk of inadvertent VA injury and ligation was high, and one case died of massive blood loss. Preoperative VA embolization can reduce operative bleeding, but it is difficult to perform in the upper cervical

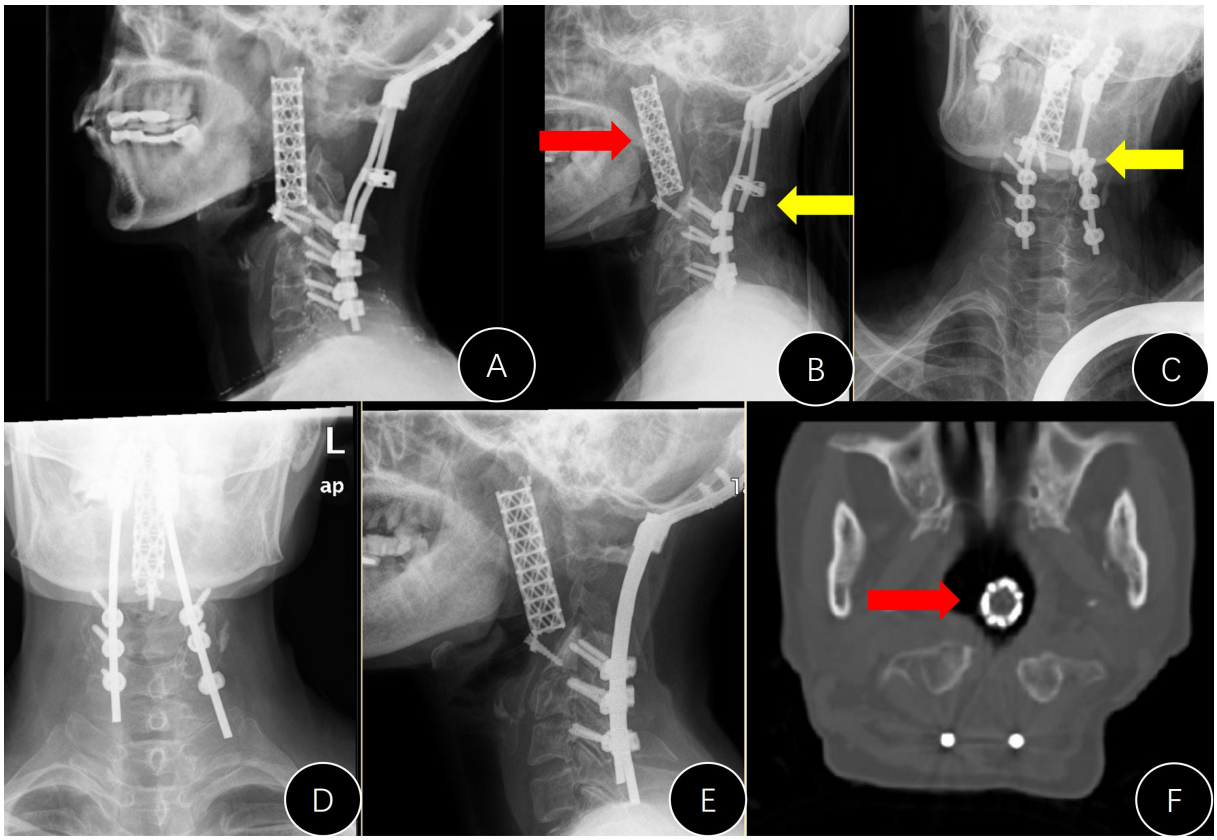


FIGURE 5
Presentation of case #A6. **(A)** Postoperative lateral x-ray; **(B, C)** x-rays 7 years later (anterior movement of titanium mesh and the breaking of both rods); **(D, E)** revision surgery to replace the rods; **(F)** mesh shifted into the pharyngeal cavity.

area (30, 31). According to Johns Hopkins (2020), the sacrifice of VA is only chosen in cases of complete encasement of the artery (32). Therefore, there are two important concerns regarding VA sacrifice: (1) it is technically possible to perform TER of C2 vertebral tumors and (2) VA is completely encased by the tumor. Otherwise, we should avoid arbitrarily sacrificing the VA.

## 4.2 Surgical approaches matter and retropharyngeal approach is safe

Previous studies have introduced a variety of surgical approaches for the upper cervical spine such as posterior, lateral/far-lateral, retropharyngeal, bilateral transcervical, transoral, endoscopic endonasal, and circumglossal approaches (2–4, 8–13, 33–36). In our center, we choose a posteroanterior approach as it provides a better visual field and simplifies surgical techniques (21, 22). In this series, wound healing was the most frequent complication and was approach-related. We found that patients who underwent transoral/transmandibular procedures had a higher risk of perioperative complications. Steinberger et al. (2016) reviewed the safety of the transoral approach to the cervical spine in 126 patients (13). They found that this approach carries significant risks for morbidity (21.4%) and mortality (2.4%). In previous case reports on the transmandibular approach, the risk of approach-related complications was extremely high (8, 12, 33–35).

The retropharyngeal approach, also termed the high cervical or submandibular approach, is one of the safest and most effective methods to access the upper cervical spine as it provides wide exposure and feasibility for instrumentation, allowing for extension to the lower cervical spine (11). Yang et al. (2011) adopted a combined retropharyngeal-posterior approach in a cohort of 11 C2 tumors and found that one major and two minor approach-related complications occurred (2). Thus, we recommend the retropharyngeal approach for anterior procedures in most cases. However, this approach may not easily expose the C1 anterior arch and odontoid process in some cases. Endoscopic visualization may facilitate surgical manipulation (37).

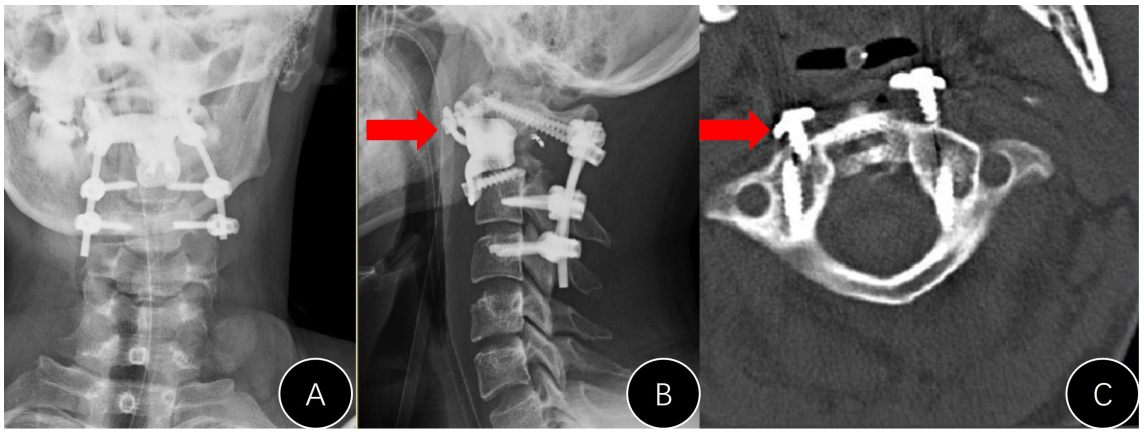


FIGURE 6
Presentation of case #B7. **(A, B)** Postoperative x-rays (unsatisfactory cranial attachment to C1 anterior arch); **(C)** CT film revealed that the cranial screws were not completely nailed in.

### 4.3 Personalized AVBs: Better choice with minor pitfalls

3D-printed AVBs are ideal materials for large bone defects after the surgical resection of spinal tumors (10, 17–22). Biomechanical analysis revealed that the load of the head is transmitted *via* the bilateral C1/2 joints and then redistributes this two-column load into a three-column system of the subaxial spine (38). Thus, conventional or modified cylindrical titanium meshes do not comply with this biomechanical role well. Personalized titanium-alloy AVBs are fabricated with high fidelity to the structure of bony defects and can play an axial biomechanical role perfectly. Finite element analysis has shown that personalized AVB can increase the stability of the upper cervical segment and produce less stress on the C3 endplate than the Harms-modified mesh (39).

After a long history of AVB application in 2014 (16, 18, 20–22), we found that personalized AVB can superbly mimic the structures of resected tumor lesions and thus provide a reliable reconstruction of the column. At the same time, 3D-printed AVBs could provide immediate stability due to perfect structural conformability and spared the long-lasting use of the halo vest after the operation (Table 1). More importantly, the microstructure of AVBs mimics porous cancellous bone and heavily elevates osseointegration between the host bone and implants (40). In addition, the porous structure of AVBs facilitates the possibility of loading pharmaceuticals such as rhBMP-2, hydroxyapatite, antibiotics, and anti-tumor drugs (41, 42).

In this single-center comparative study, the risk of hardware problems in AVB patients was marginally lower than that in conventional titanium meshes. However, we noticed some minor pitfalls during our study. For example, we found it difficult to nail C1 screws in (case #B7) because of the block of the mandible. We believe that an embedded oblique screw trajectory may prevent this problem. Thus, the current design of personalized AVB requires additional modifications in the future.

### 4.4 Limitations

To begin with, the sample size of this study was small, and the results of the statistical analysis call for cautious interpretation. Additionally, considering its retrospective nature, this study does not provide evidence of high-level quality to address the superiority of personalized AVB but rather a case series. Furthermore, some patients received a short to medium follow-up period, while the results of this study require long-term examination.

## Data availability statement

The original contributions presented in the study are included in the article/Supplementary Material. Further inquiries can be directed to the corresponding author.

## Ethics statement

The studies involving human participants were reviewed and approved by Peking University Third Hospital Ethics

Committee Board. The patients/participants provided their written informed consent to participate in this study.

## Author contributions

PH and SD designed the study, reviewed the patients, collected and processed the clinical data, and drafted the manuscript. FW designed the study, selected the patients, processed the data, and supervised the study. SZ and HZ reviewed the patients and collected the data. XL and ZL supervised the data collection and processing. All authors reviewed and approved this manuscript.

## Funding

This study was funded by the National Natural Science Foundation of China (grant number: 82172395; recipient: FW) and the Natural Science Foundation of Beijing Municipality (grant number: 7222813; recipient: FW).

## Conflict of interest

The authors declare that the research was conducted in the absence of any commercial or financial relationships that could be construed as a potential conflict of interest.

## Publisher's note

All claims expressed in this article are solely those of the authors and do not necessarily represent those of their affiliated organizations, or those of the publisher, the editors and the reviewers. Any product that may be evaluated in this article, or claim that may be made by its manufacturer, is not guaranteed or endorsed by the publisher.

## Supplementary material

The Supplementary Material for this article can be found online at: https://www.frontiersin.org/articles/10.3389/fonc.2022.1065303/full#supplementary-material

## References

1. Choi D, Melcher R, Harms J, Crockard A. Outcome of 132 operations in 97 patients with chordomas of the craniocervical junction and upper cervical spine. *Neurosurgery* (2010) 66(1):59–65. doi: 10.1227/01.NEU.0000362000.35742.3D

2. Yang X, Wu Z, Xiao J, Teng H, Feng D, Huang W, et al. Sequentially staged resection and 2-column reconstruction for C2 tumors through a combined anterior retropharyngeal-posterior approach: surgical technique and results in 11 patients. *Neurosurgery* (2011) 69(2 Suppl Operative):184–93. doi: 10.1227/NEU.0b013e31821bc7f9

3. Zhou H, Jiang L, Wei F, Yu M, Wu F, Liu X, et al. Chordomas of the upper cervical spine: clinical characteristics and surgical management of a series of 21 patients. *Chin Med J* (2014) 127(15):2759–64. doi: 10.3760/cma.j.issn.0366-6999.20132077

4. Wei F, Liu Z, Liu X, Jiang L, Dang G, Passias PG, et al. An approach to primary tumors of the upper cervical spine with spondylectomy using a combined approach: Our experience with 19 cases. *Spine* (2018) 43(2):81–8. doi: 10.1097/BRS.0000000000001007

5. Yang J, Yang XH, He SH, Jiao J, Jia Q, Hu JB, et al. A novel reconstruction using a combined anterior and posterior approach after axis tumor spondylectomy. *Clin Spine Surg* (2020) 33(7):E299–306. doi: 10.1097/BSD.0000000000001039

6. McLoughlin GS, Sciubba DM, Suk I, Bydon A, Witham T, Wolinsky JP, et al. Resection of a retropharyngeal craniovertebral junction chordoma through a posterior cervical approach. *J Spinal Disord Tech* (2010) 23(5):359–65. doi: 10.1097/BSD.0b013e3181aaca99

7. Bydon M, de la Garza-Ramos R, Suk I, McCarthy E, Yamada Y, Wolinsky JP, et al. Single-staged multilevel spondylectomy for en bloc resection of an epithelioid sarcoma with intradural extension in the cervical spine: Technical case report. *Oper Neurosurg* (2015) 11(4):E585–93. doi: 10.1227/NEU.0000000000000961

8. DeMonte F, Diaz EJr, Callender D, Suk I. Transmandibular, circumglossal, retropharyngeal approach for chordomas of the clivus and upper cervical spine. *Tech Note Neurosurg Focus* (2001) 10(3):E10. doi: 10.3171/foc.2001.10.3.11

9. Ricciardi L, Sturiale CL, Izzo A, Pucci R, Valentini V, Montano N, et al. Submandibular approach for single-stage craniovertebral junction ventral decompression and stabilization: A preliminary cadaveric study of technical feasibility. *World Neurosurg* (2019) 127:206–12. doi: 10.1016/j.wneu.2019.04.038

10. Suchomel P, Buchvald P, Barsa P, Froehlich R, Choutka O, Krejzar Z, et al. Single-stage total c-2 intralesional spondylectomy for chordoma with three-column reconstruction. technical note. *J Neurosurg Spine* (2007) 6(6):611–8. doi: 10.3171/spi.2007.6.6.17

11. Alshafai NS, Gunness VRN. The high cervical anterolateral retropharyngeal approach. *Acta Neurochir Suppl* (2019) 125:147–9. doi: 10.1007/978-3-319-62515-7_21

12. Rhines LD, Fourney DR, Siadati A, Suk I, Gokaslan ZL. En bloc resection of multilevel cervical chordoma with c-2 involvement. case report and description of operative technique. *J Neurosurg Spine* (2005) 2(2):199–205. doi: 10.3171/spi.2005.2.2.0199

13. Steinberger J, Skovrlj B, Lee NJ, Kothari P, Leven DM, Guzman JZ, et al. Surgical morbidity and mortality associated with transoral approach to the cervical spine. *Spine* (2016) 41(9):E535–40. doi: 10.1097/BRS.0000000000001320

14. Yamazaki T, McLoughlin GS, Patel S, Rhines LD, Fourney DR. Feasibility and safety of en bloc resection for primary spine tumors: a systematic review by the spine oncology study group. *Spine* (2009) 34(22 Suppl):S31–8. doi: 10.1097/BRS.0b013e3181b8b796

15. Singh PK, Agrawal M, Mishra S, Agrawal D, Sawarkar D, Jagdevan A, et al. Management of C2 body giant cell tumor by innovatively fashioned iliac crest graft and modified cervical mesh cage used as plate. *World Neurosurg* (2020) 140:241–6. doi: 10.1016/j.wneu.2020.05.182

16. Xu N, Wei F, Liu X, Jiang L, Cai H, Li Z, et al. Reconstruction of the upper cervical spine using a personalized 3D-printed vertebral body in an adolescent with Ewing sarcoma. *Spine* (2016) 41(1):E50–4. doi: 10.1097/BRS.0000000000001179

17. Xiao JR, Huang WD, Yang XH, Yan WJ, Song DW, Wei HF, et al. En bloc resection of primary malignant bone tumor in the cervical spine based on 3-dimensional printing technology. *Orthop Surg* (2016) 8(2):171–8. doi: 10.1111/os.12234

18. Wei F, Li Z, Liu Z, Liu X, Jiang L, Yu M, et al. Upper cervical spine reconstruction using customized 3D-printed vertebral body in 9 patients with primary tumors involving C2. *Ann Transl Med* (2020) 8(6):332. doi: 10.21037/atm.2020.03.32

19. Hunn SAM, Koefman AJ, Hunn AWM. 3D-printed titanium prosthetic reconstruction of the C2 vertebra: Techniques and outcomes of three consecutive cases. *Spine* (2020) 45(10):667–72. doi: 10.1097/BRS.0000000000003360

20. Dang L, Liu Z, Liu X, Jiang L, Yu M, Wu F, et al. Sagittal en bloc resection of primary tumors in the thoracic and lumbar spine: feasibility, safety and outcome. *Sci Rep* (2020) 10(1):9108. doi: 10.1038/s41598-020-65326-0

21. Wei F, Xu N, Li Z, Cai H, Zhou F, Yang J, et al. A prospective randomized cohort study on 3D-printed artificial vertebral body in single-level anterior cervical

corpectomy for cervical spondylotic myelopathy. *Ann Transl Med* (2020) 8 (17):1070. doi: 10.21037/atm-19-4719

22. Zhou H, Liu S, Li Z, Liu X, Dang L, Li Y, et al. 3D-printed vertebral body for anterior spinal reconstruction in patients with thoracolumbar spinal tumors. *J Neurosurg Spine* (2022), 1–9. doi: 10.3171/2022.1.SPINE21900

23. Boriani S, Weinstein JN, Biagini R. Primary bone tumors of the spine. terminology and surgical staging. *Spine* (1997) 22(9):1036–44. doi: 10.1097/00007632-199705010-00020

24. Boriani S, Bandiera S, Biagini R, Bacchini P, Boriani L, Cappuccio M, et al. Chordoma of the mobile spine: fifty years of experience. *Spine* (2006) 31(4):493–503. doi: 10.1097/01.brs.0000200038.30869.27

25. Jin CJ, Berry-Candelario J, Reiner AS, Laufer I, Higginson DS, Schmitt AM, et al. Long-term outcomes of high-dose single-fraction radiosurgery for chordomas of the spine and sacrum. *J Neurosurg Spine* (2019) 18:1–10. doi: 10.3171/2019.7.SPINE19515

26. Hsieh PC, Gallia GL, Sciubba DM, Bydon A, Marco RA, Rhines L, et al. En bloc excisions of chordomas in the cervical spine: review of five consecutive cases with more than 4-year follow-up. *Spine* (2011) 36(24):E1581–7. doi: 10.1097/BRS.0b013e318211839c

27. Kerr DL, Dial BL, Lazarides AL, Catanzano AA, Lane WO, Blazer DG3rd, et al. Epidemiologic and survival trends in adult primary bone tumors of the spine. *Spine J* (2019) 19(12):1941–9. doi: 10.1016/j.spinee.2019.07.003

28. Gokaslan ZL, Zadnik PL, Sciubba DM, Germscheid N, Goodwin CR, Wolinsky JP, et al. Mobile spine chordoma: results of 166 patients from the AOSpine knowledge forum tumor database. *J Neurosurg Spine* (2016) 24(4):644–51. doi: 10.3171/2015.7.SPINE15201

29. Zhong N, Yang M, Ma X, Gao X, Ye C, Yang J, et al. Early major complications after radical resection of primary C2-involved upper cervical chordoma through the combined anterior retropharyngeal-posterior approach: Incidence and risk factors. *World Neurosurg* (2021) 154:e790–6. doi: 10.1016/j.wneu.2021.08.001

30. Patsalides A, Leng LZ, Kimball D, Marcus J, Knopman J, Laufer I, et al. Preoperative catheter spinal angiography and embolization of cervical spinal tumors: Outcomes from a single center. *Interv Neuroradiol* (2016) 22(4):457–65. doi: 10.1177/1591019916637360

31. Ogungbemi A, Elwell V, Choi D, Robertson F. Permanent endovascular balloon occlusion of the vertebral artery as an adjunct to the surgical resection of selected cervical spine tumors: A single center experience. *Interv Neuroradiol* (2015) 21(4):532–7. doi: 10.1177/1591019915590072

32. Westbroek EM, Pennington Z, Ehresman J, Ahmed AK, Gailloud P, Sciubba DM. Vertebral artery sacrifice versus skeletonization in the setting of cervical spine tumor resection: Case series. *World Neurosurg* (2020) 139:e601–7. doi: 10.1016/j.wneu.2020.04.071

33. Konya D, Ozgen S, Gerçek A, Celebiler O, Pamir MN. Transmandibular approach for upper cervical pathologies: report of 2 cases and review of the literature. *Turk Neurosurg* (2008) 18(3):271–5.

34. Neo M, Asato R, Honda K, Kataoka K, Fujibayashi S, Nakamura T. Transmaxillary and transmandibular approach to a C1 chordoma. *Spine* (2007) 32(7):E236–9. doi: 10.1097/01.brs.0000259210.58162.29

35. Ozpinar A, Liu JJ, Whitney NL, Tempel ZJ, Choi PA, Andersen PE, et al. Anterior spinal reconstruction to the clivus using an expandable cage after C2 chordoma resection *Via* a labiomandibular glossotomy approach: A technical report. *World Neurosurg* (2016) 90:372–9. doi: 10.1016/j.wneu.2016.02.115

36. Baldassarre BM, Di Perna G, Portonero I, Penner F, Cofano F, Marco R, et al. Craniovertebral junction chordomas: Case series and strategies to overcome the surgical challenge. *J Craniovertebr Junction Spine* (2021) 12(4):420–31. doi: 10.4103/jcvjs.jcvjs_87_21

37. Hsu W, Kosztowski TA, Zaidi HA, Gokaslan ZL, Wolinsky JP. Image-guided, endoscopic, transcervical resection of cervical chordoma. *J Neurosurg Spine* (2010) 12(4):431–5. doi: 10.3171/2009.10.SPINE09393

38. Jeszenszky D, Fekete TF, Melcher R, Harms J. C2 prosthesis: anterior upper cervical fixation device to reconstruct the second cervical vertebra. *Eur Spine J* (2007) 16(10):1695–700. doi: 10.1007/s00586-007-0435-6

39. Zheng Y, Wang J, Liao S, Zhang D, Zhang J, Ma L, et al. Biomechanical evaluation of a novel integrated artificial axis: A finite element study. *Med (Baltimore)* (2017) 96(47):e8597. doi: 10.1097/MD.0000000000008597

40. Zhang T, Wei Q, Zhou H, Jing Z, Liu X, Zheng Y, et al. Three-dimensional-printed individualized porous implants: A new "implant-bone" interface fusion concept for large bone defect treatment. *Bioact Mater* (2021) 6(11):3659–70. doi: 10.1016/j.bioactmat.2021.03.030

41. Zhang T, Wei Q, Fan D, Liu X, Li W, Song C, et al. Improved osseointegration with rhBMP-2 intraoperatively loaded in a specifically designed 3D-printed porous Ti6Al4V vertebral implant. *Biomater Sci* (2020) 8(5):1279–89. doi: 10.1039/c9bm01655d

42. Jing Z, Zhang T, Xiu P, Cai H, Wei Q, Fan D, et al. Functionalization of 3D-printed titanium alloy orthopedic implants: a literature review. *BioMed Mater* (2020) 15(5):052003. doi: 10.1088/1748-605X/ab9078

frontiers | Frontiers in Surgery

TYPE Original Research
PUBLISHED 23 January 2023
DOI 10.3389/fsurg.2022.1035315



OPEN ACCESS

EDITED BY
Jeroen Van Vugt,
Erasmus Medical Center, Netherlands

REVIEWED BY
Birkan Bozkurt,
Başakşehir Çam & Sakura City Hospital Organ Transplant Center, Turkey
Matteo Donadon,
Università degli Studi del Piemonte Orientale, Italy

*CORRESPONDENCE
Xiaofeng Jiang
jiangxiaofeng008@163.com

SPECIALTY SECTION
This article was submitted to Surgical Oncology, a section of the journal Frontiers in Surgery

RECEIVED 02 September 2022
ACCEPTED 29 November 2022
PUBLISHED 23 January 2023

CITATION
Zhang X, Huang Z, Lu H, Yang X, Cao L, Wen Z, Zheng Q, Peng H, Xue P and Jiang X (2023) Identification of resection plane for anatomical liver resection using ultrasonography-guided needle insertion.
Front. Surg. 9:1035315.
doi: 10.3389/fsurg.2022.1035315



# Identification of resection plane for anatomical liver resection using ultrasonography-guided needle insertion

Xin Zhang, Zhenhui Huang, Haiwu Lu, Xuewei Yang, Liangqi Cao, Zilong Wen, Qiang Zheng, Heping Peng, Ping Xue and Xiaofeng Jiang*

Department of Hepato-Biliary-Pancreatic Surgery, The Second Affiliated Hospital of Guangzhou Medical University, Guangzhou, China

**Purposes:** To set up an easy-handled and precise delineation of resection plane for hepatic anatomical resection (AR).
**Methods:** Cases of AR using ultrasonography-guided needle insertion to trace the target hepatic vein for delineation of resection planes [new technique (NT) group, $n = 22$] were retrospectively compared with those without implementation of this surgical technique [traditional technique (TT) group, $n = 29$] in terms of perioperative courses and surgical outcomes.
**Results:** The target hepatic vein was successfully exposed in all patients of the NT group, compared with a success rate of 79.3% in the TT group ($P < 0.05$). The average operation time and intraoperative blood loss were $280 \pm 32$ min and $550 \pm 65$ ml, respectively, in the NT group. No blood transfusion was required in either group. The postoperative morbidities (bile leakage and peritoneal effusion) were similar between groups. No mortality within 90 days was observed.
**Conclusions:** Ultrasonography-guided needle insertion is a convenient, safe and efficient surgical approach to define a resection plane for conducting AR.

KEYWORDS
hepatocellular carcinoma, ultrasonography, anatomical resection, hepatic vein, liver

## Introduction

Hepatectomy is the first-line therapeutic option for hepatocellular carcinoma (HCC) and hepatolithiasis (intrahepatic stones, IHS), which are endemic in the Asia-Pacific region (1, 2). Anatomical resection (AR) is widely accepted as superior to non-anatomical resection in terms of surgical outcomes and survival for patients with HCC, considering that portal tumor thrombosis and intrahepatic metastasis are responsible for recurrence and poor prognosis after curative hepatic resection (3, 4). Also, AR is more effective for bleeding control and parenchymal preservation, and thus more beneficial for reducing postoperative morbidity and mortality. Identifying the major vascular structures in relation to the affected liver tissue, determining the segments that must be resected, and precisely proceeding with resection following the anatomical margins are critical for effective AR with minimal blood loss and optimal preservation of liver function.

Hepatic veins are intrahepatic veins that drain blood into the inferior vena cava (IVC). AR is commonly based on liver sections and segments defined using

Couinaud's classification, which divides the liver into eight segments based on three major hepatic veins (right, middle, and left) and the planes passing along the portal vein bifurcation. Identification of hepatic veins as an important landmark for segment delimitation is therefore essential for AR (5). The accumulated evidence has demonstrated the importance of careful review of hepatic vein anatomy and planning of AR accordingly (6, 7). Preoperative computed tomography (CT)/magnetic resonance imaging (MRI) and intraoperative ultrasonography have been valuable tools in recognizing these venous landmarks and delineating resection margins (8, 9). Surgical planning based on a three-dimensional (3D) model reconstructed from imaging has emerged as a promising approach to optimize the surgical procedure (10). However, despite the implementation of adjuvant imaging techniques, in clinical practice exact delineation of resection planes intraoperatively remains challenging. In the present study, we developed a simple technique for defining resection planes for AR in a precise manner. In this method, with the aid of intraoperative ultrasonography, a needle is inserted into the liver toward the target hepatic vein to create a resection plane for exposure of the hepatic vein. The feasibility and efficacy of this technique for creating resection planes for AR was assessed.

# Methods

This study was approved by the ethics committee of the Second Affiliated Hospital of Guangzhou Medical University. Informed consent was obtained from all patients. The use of ultrasonography-guided needle insertion to identify the resection plane in AR was initiated in January 2017, and as of July 2018, a total of 22 patients had undergone AR with this new technique (NT group). AR with this new technique was the preferred choice, unless the patient had a condition contraindicating the use of this approach, such as poor coagulation function or the absence of an appropriate puncture position. Another 29 patients who underwent liver resection without implementation of this new technique during the same period were used as reference cases [traditional technique (TT) group]. The surgeries in this study were all completed by Jiang's team, which was experienced and skillful in liver resection. The medical records of these patients were retrospectively reviewed, and the operation time, blood loss, transfusion rate, postoperative complications, and hospital stay were compared between the groups.

## Surgical procedures

The extent of AR was decided based on the size, number, and location of the lesions. For right or left hemi-hepatectomy, after mobilization of the liver according to the affected liver sections to be resected, selective ligation of portal veins and liver arteries was performed. For patients of the NT group, the resection plane was determined using the following steps. In step 1, intraoperative ultrasonography (BK Medical, Denmark) was performed to visualize the middle hepatic vein (MHV) and assess the appropriate position for needle insertion. In step 2, under ultrasonography guidance, a 21-G needle (Chiba, Japan) was inserted into the liver toward the MHV, as illustrated in **Figure 1A**. The insertion of the needle was confirmed under ultrasonography (**Figures 1B**, **2**). A resection plane was defined by the inserted needle and the MHV (see **Supplementary Video**). Afterwards, parenchyma transection was initiated along

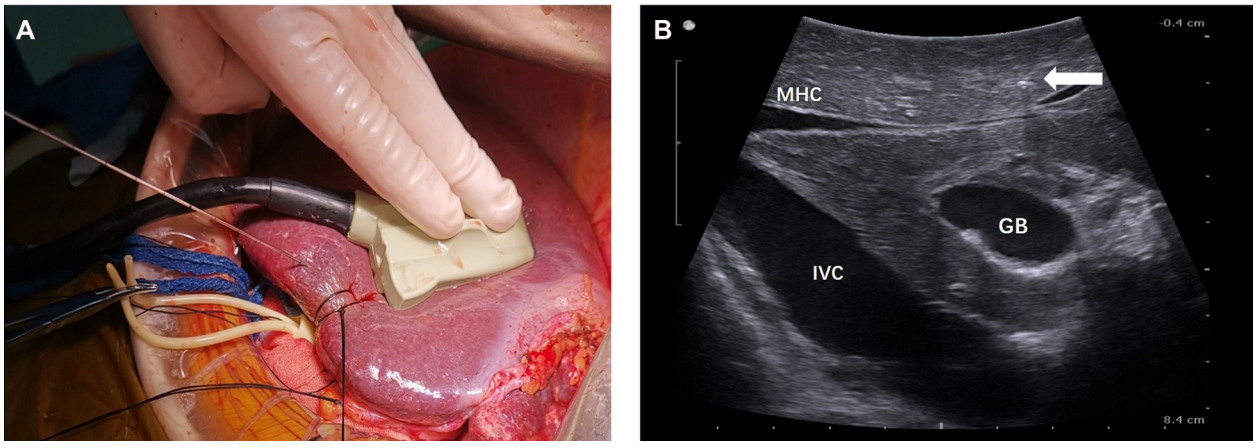


FIGURE 1
(A) Intraoperative view showing insertion of a 21-G needle into the liver toward MHV under ultrasonography guidance after ligation of the left portal vein and liver artery. (B) Intraoperative ultrasonography image showing the resection plane determined according to the MHV and the inserted needle (white arrow). The IVC may also be included in the resection plane. IVC, inferior vena cava; MHV, middle hepatic vein; GB, gallbladder.

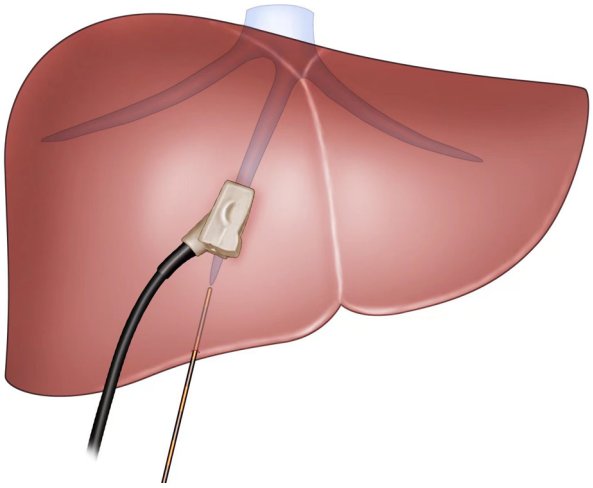

FIGURE 2
The view showing insertion of a 21-G needle into the liver toward MHV under ultrasonography guidance. MHV: middle hepatic vein.

the needle and continued until the MHV was reached with a cavitron ultrasonic surgical aspirator (CUSA, Integra, NJ, United States; Figure 3). In patients of the NT group receiving segmentectomy, to delineate the hepatic segment for AR, methylene blue was injected through the corresponding portal vein under ultrasonography guidance. Subsequently, a 21-G needle was inserted toward the corresponding hepatic vein and a resection plane was determined using the same approach described above.

In patients of the TT group, similar surgical techniques were used for AR, except for the method used to define the resection plane. Methylene blue was used to delineate the resection plane, and the resection line on the hepatic surface was marked with electrocautery under ultrasonography guidance.

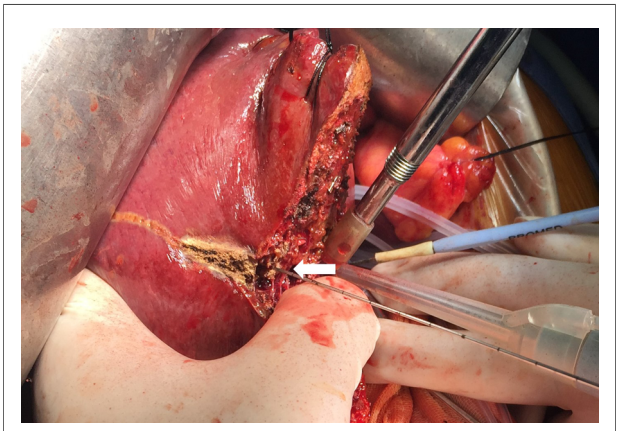

FIGURE 3
Intraoperative view showing parenchyma transection by a CUSA guided by the inserted needle (arrow) in a patient receiving left semi-hepatectomy.

## Statistical analysis

Continuous variables are expressed as mean ± standard deviation (SD) values, and categorized variables are expressed as percentages. Group differences were determined using Student's *t*-test for normally distributed variables and Mann–Whitney *U*-test if the variable did not follow a normal distribution. $\chi^2$ or Fisher's exact tests were used for comparison of categorical variables when appropriate. All statistical analyses were performed using SPSS 19.0 software (IBM SPSS Inc., IL, United States). *P* values <0.05 were considered statistically significant.

# Results

The primary outcome measure was the success rate of target hepatic vein exposure. The secondary outcome measures reflected the feasibility and safety of the approach which included the operation time, amount of blood loss, rate of blood transfusion, duration of hospital stay, postoperative morbidity and mortality. Table 1 summarizes the clinical, surgical, and outcome characteristics of the patients included in this study. No obvious differences were found between the NT and TT groups in terms of age, lesion types, size of tumor, number of tumor and types of resection.

TABLE 1 Baseline characteristics and surgical outcomes of patients.

| | NT group (*n* = 22) | TT group (*n* = 29) | *P* |
|---|---|---|---|
| Age (years) | 49 ± 6 | 53 ± 2 | >0.05 |
| Disease, *n* (%) | | | |
| HCC | 12 (54.5) | 16 (55.2) | >0.05 |
| IHS | 10 (45.5) | 13 (44.8) | |
| Type of resection | | | >0.05 |
| Hemihepatectomy | 11 | 13 | |
| Extended hemihepatectomy | 2 | 2 | |
| Sectionectomy | 5 | 6 | |
| Segmentectomy | 4 | 8 | |
| Resection plane, *n* (%) | 22 (100) | 23 (79.3) | <0.05* |
| Operation time (min) | 280 ± 32 | 250 ± 15 | >0.05 |
| Blood loss (ml) | 550 ± 65 | 600 ± 25 | >0.05 |
| Transfusion rate, *n* | 0 | 0 | >0.05 |
| Hospital stay (day) | 9.5 ± 1.5 | 10.5 ± 2 | >0.05 |
| Bile leakage, *n* (%) | 1 (4.5) | 2 (6.9) | >0.05 |
| Peritoneal effusion, *n* (%) | 2 (9.1) | 2 (6.9) | >0.05 |

HCC, hepatocellular carcinoma; IHS, intrahepatic stones; TT, traditional technique; NT, new technique.
*Significant difference.

The attempt to define the resection plane for AR failed in one patient because of the occurrence of needle drop during the transection procedure, and this case was therefore not included in the NT group. After this event, we replaced the 20-cm-long needle with a 15-cm-long needle. Resection to expose the target hepatic veins as guided by the needle insertion method succeeded in all 22 patients of the NT group, while the success rate was significantly less at only 79.3% in the TT group ($P < 0.05$). An intraoperative view from a patient undergoing left hepatectomy for IHS in the NT group showed that the MHV was exposed after transection along the resection plane guided by the needle (**Figures 4A**, **5**). The MHV, right hepatic vein (RHV), and IVC were exposed after segment 8 resection using the needle insertion method (**Figures 4B**, **6**). In a patient with HCC in the NT group, the RHV was not identified under ultrasonography guidance. In this patient, resection planes guided by needles toward the vein of segment 6 (V6) and vein of segment 7 (V7) were created. The MHV, V6, and V7 were exposed after resection of segments 5 and 8 in this patent (**Figures 7**, **8**).

The operation duration did not differ significantly between the NT and TT groups. The intraoperative blood loss volume was lower in the NT group than in the TT group, but the difference was not statistically significant. No blood transfusion was required in either group. The average duration of hospital stay of patients in the NT group was shorter but not significantly different compared with that for patients in the TT group.

The postoperative hospital morbidity rates were 9.1% in both the NT and TT groups ($P > 0.05$). No death was reported during the first 90 days after operation in either group.

## Discussion

AR is a technically challenging surgical procedure because of the potential risk of massive hemorrhage during surgical resection due to the complicated hepatic vascular anatomy. Over recent decades, significant technical advances have contributed to the reduction of perioperative hemorrhage, including better delineation of resection planes with the aid of preoperative and intraoperative imaging techniques, and more techniques available for inflow and outflow occlusion. In this study, patients received AR with these now considered

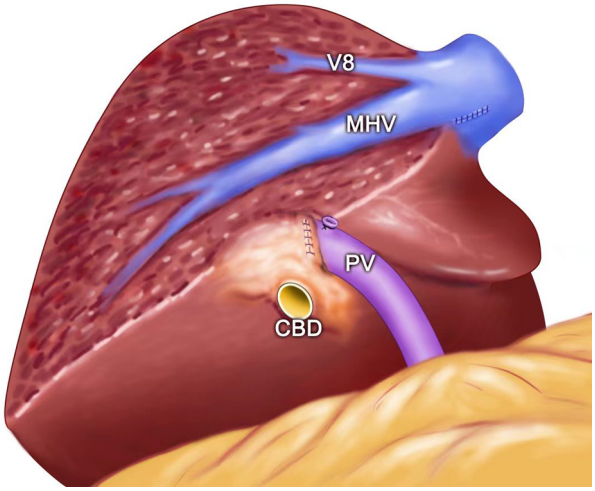


FIGURE 5
The view showing the MHV being exposed after left semi-hepatectomy for intrahepatic stones. MHC, middle hepatic vein; PV, portal vein; V8, vein of segment 8; CBD: common bile duct.

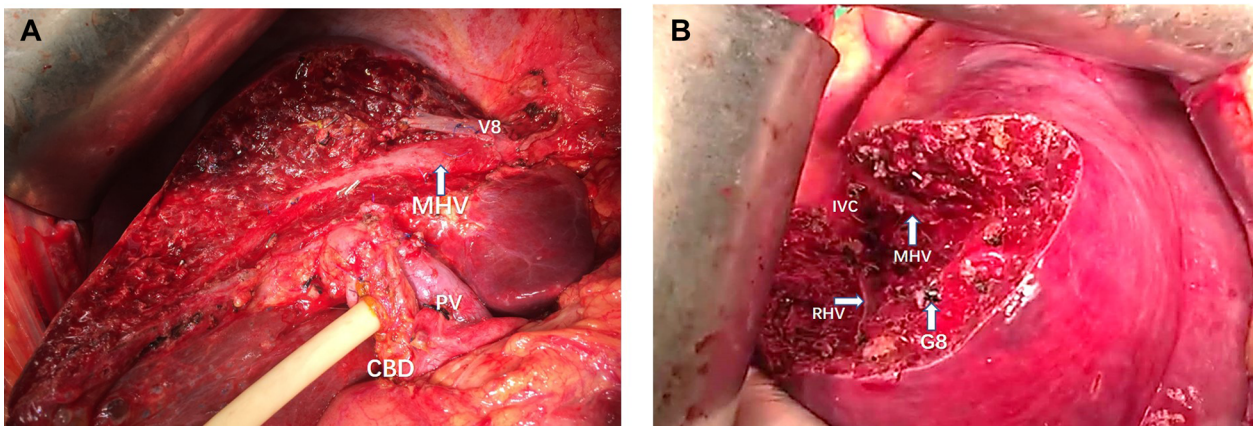


FIGURE 4
(A) Intraoperative view showing the MHV being exposed after left semi-hepatectomy for intrahepatic stones. (B) Intraoperative view showing the MHV, RHV, and IVC being exposed after segment 8 resection guided by the inserted needle. MHC, middle hepatic vein; PV, portal vein; CBD, common bile duct; RHV, right hepatic vein; IVC, inferior vena cava; V8, vein of segment 8; G8, Glisson's 8.

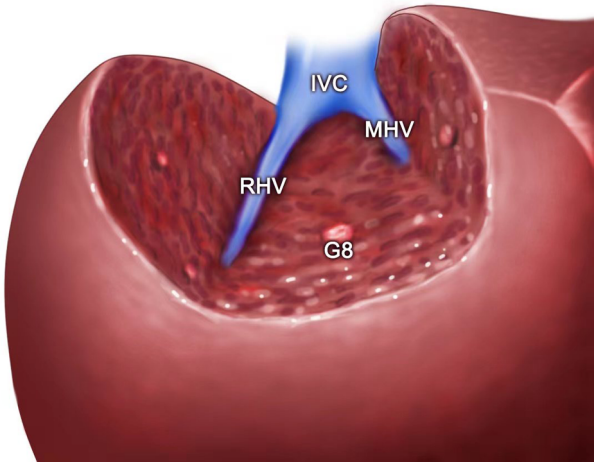


FIGURE 6
The view showing the MHV, RHV, and IVC being exposed after segment 8 resection guided by the inserted needle. MHC, middle hepatic vein; RHV, right hepatic vein; IVC, inferior vena cava; G8, Glisson's 8.

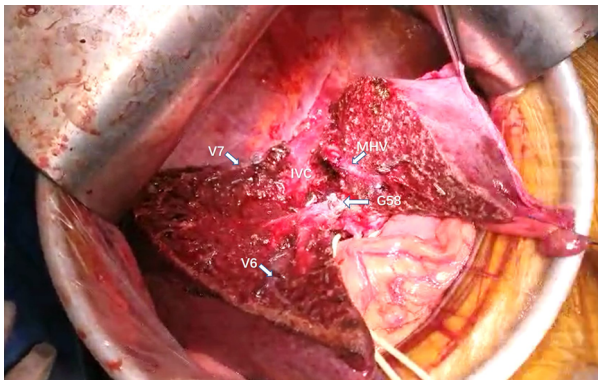


FIGURE 7
Intraoperative view showing the MHV, IVC, V6, and V7 being exposed after segment 5 and segment 8 resection for HCC. MHC, middle hepatic vein; V6, vein of segment 6; V7, vein of segment 7; IVC, inferior vena cava; G58, Glisson's 5 and 8.

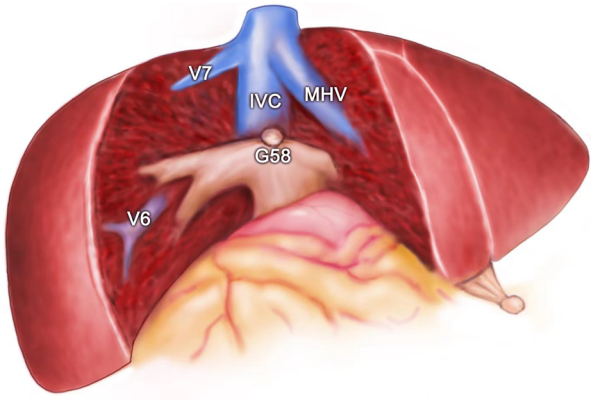


FIGURE 8
The view showing the MHV, IVC, V6, and V7 being exposed after segment 5 and segment 8 resection for HCC. MHC, middle hepatic vein; V6, vein of segment 6; V7, vein of segment 7; IVC, inferior vena cava; G58, Glisson's 5 and 8.

standard-of-care surgical procedures, and the results were satisfactory for all patients in terms of perioperative hemorrhage, given that blood transfusion was not required for any patients who received AR.

Intrahepatic metastasis of HCC occurs mainly through the portal vein route. AR can not only eliminate the tumor but also remove the independent hepatic segment where the tumor is located as well as the portal vein branch within the hepatic segment, so as to completely remove the lesion and reduce the likelihood of tumor recurrence (7). AR can achieve the expected safe margin for tumor patients and can completely remove the diseased bile duct for patients with hepatolithiasis, thus reducing the incidence of postoperative biliary leakage. Studies have shown that compared with non-anatomical resection, AR can reduce the recurrence of tumors and improve survival (11–13). Therefore, AR should be considered the first choice for hepatectomy for HCC.

However, AR has not been accepted as a standard surgical treatment for HCC worldwide. One important reason is that the demarcation planes between liver segments are irregular, which is particularly evident in the right liver. It is not easy to accurately identify the demarcation plane during resection to execute true AR. According to Makuuchi (14), hepatic segmental/subsegmental resection must proceed precisely along the hepatic segmental boundary and fully expose the hepatic veins in order to be called AR. Active exposure of hepatic veins may avoid injury and reduce the risk of bleeding. Although satisfactory surface markers can be obtained by ligating the hepatic pedicle or injecting dye into the portal vein, the ischemia boundary within liver parenchyma is not obvious, and dye is prone to contaminate the contralateral side through cross-sectional leakage, thus blurring the boundary. As a consequence, the transection from the line marked on the surface of the liver may not be precisely along the direction towards the deep inside hepatic veins. In our study, not surprisingly, transection through the resection plane defined by the surface markers failed to expose the target hepatic vein in 20.7% of patients in the TT group. The hepatic vein, as the demarcation between liver lobes and segments, is a natural marker of the intrahepatic plane. Makuuchi chose to obtain the surface ischemia line by staining or regional block of hepatic pedicle, transect 1 cm down to find the subbranch of hepatic vein, and then separate the liver parenchyma down to the trunk of hepatic veins (14). However, when dissecting liver

parenchyma, the subbranches of target hepatic vein encountered initially are relatively thin and vulnerable to injury. It may not only lead to bleeding and gas embolism, but could also lead to a loss of direction of the target hepatic vein, making it more difficult to expose the target hepatic vein. Moreover, in order to avoid damage to the branches of the target hepatic vein, the surgeon must be sufficiently meticulous, which may prolong the surgical procedure. To overcome this challenge, we developed a simple surgical procedure to define the resection plane for AR. Our results demonstrated the feasibility and efficacy of this approach based on a success rate of 100% for exposing the target hepatic veins.

In this study, we inserted a 21-G needle into the liver toward the direction of the target hepatic vein under the guidance of intraoperative ultrasonography. Based on the theorem that two intersecting lines determine one plane, the target hepatic vein and inserted needle make up a resection plane expected to expose the hepatic vein. A key step to ensure this resection plane passes through the hepatic vein is to have both the hepatic vein and inserted needle visualized as a line rather than a dot on the ultrasound screen. After the resection plane was established, we transected the liver parenchyma using a CUSA by following the inserted needle until the hepatic vein was reached. AR was carried out by tracking the hepatic vein until IVC exposure. These hepatic veins created the resection planes for AR. Our clinical experience demonstrated that compared with the traditional approach to identify the resection planes for AR, this method is straightforward and relatively easy to follow. In all patients in the NT group, all major hepatic veins were successfully exposed using this approach during the AR procedure. Notably, in one case in which the RHV was not visualized on the ultrasonography image, we easily established resection planes towards the V6 and V7 to achieve complete tumor resection. This demonstrated the flexibility of this method in the operative procedure in the case of anatomical variation.

The intraoperative blood loss and operation duration in the NT group were similar to those in the TT group, indicating that this ultrasonography-guided needle insertion method does not negatively affect the risk for hemorrhage or prolong the operation time. The postoperative hospital morbidity was similar between groups, and no mortality within 90 days of operation was recorded in either group, supporting the safety of this needle insertion procedure in AR for liver disease.

Another strength of this study is the use of the 21-G needle, which is widely used and not expensive in clinical settings. This method is therefore applicable and affordable in resource-poor regions. Indocyanine green (ICG) fluorescence-guided liver resection has emerged as a promising approach for AR by real-time illuminating anatomical landmarks of the liver (15, 16). However, this technique requires special equipment and reagents as well as complex surgical skills in portal vein puncture, which limits its application, especially in less developed regions.

To our best knowledge, this is the first report describing AR using an inserted needle to create resection planes for hepatic vein exposure under ultrasonography guidance. A previous study applied a needle insertion method for hepatic resection (17), but in that study, the needle was used to mark the distance from the tumor to the resection margin to guarantee adequate hepatic transection.

In conclusion, the ultrasonography-guided needle insertion method is a feasible and efficient procedure for identifying resection planes for AR. This technique provides a convenient and flexible approach for tracing hepatic veins during AR. Although our study is preliminary with its retrospective nature and small number of patients, we believe that the promising results observed in this study should lead to more researches. Further evaluation of the use of this technique in laparoscopic liver resection is expected.

## Data availability statement

The original contributions presented in the study are included in the article/**Supplementary Material**, further inquiries can be directed to the corresponding author.

## Conflict of interest

The authors declare that the research was conducted in the absence of any commercial or financial relationships that could be construed as a potential conflict of interest.

## Publisher's note



## Supplementary material

The Supplementary Material for this article can be found online at: https://www.frontiersin.org/articles/10.3389/fsurg.2022.1035315/full#supplementary-material.

# References


1. Grandhi MS, Kim AK, Ronnekleiv-Kelly SM, Kamel IR, Ghasebeh MA, Pawlik TM. Hepatocellular carcinoma: from diagnosis to treatment. *Surg Oncol*. (2016) 25:74–85. doi: 10.1016/j.suronc.2016.03.002

2. Li SQ, Liang LJ, Peng BG, Hua YP, Lv MD, Fu SJ, et al. Outcomes of liver resection for intrahepatic stones: a comparative study of unilateral versus bilateral disease. *Ann Surg*. (2012) 255:946–53. doi: 10.1097/SLA.0b013e31824dedc2

3. Moris D, Tsilimigras DI, Kostakis ID, Ntanasis-Stathopoulos I, Shah KN, Felekouras E, et al. Anatomic versus non-anatomic resection for hepatocellular carcinoma: a systematic review and meta-analysis. *Eur J Surg Oncol*. (2018) 44:927–38. doi: 10.1016/j.ejso.2018.04.018

4. Li SQ, Hua YP, Shen SL, Hu WJ, Peng BG, Liang LJ. Segmental bile duct-targeted liver resection for right-sided intrahepatic stones. *Medicine*. (2015) 94:e1158. doi: 10.1097/MD.0000000000001158

5. Strasberg SM. Nomenclature of hepatic anatomy and resections: a review of the Brisbane 2000 system. *J Hepatobiliary Pancreat Surg*. (2005) 12:351–5. doi: 10.1007/s00534-005-0999-7

6. Makuuchi M, Hasegawa H, Yamazaki S. Ultrasonically guided subsegmentectomy. *Surg Gynecol Obstet*. (1985) 161:346–50.

7. Xiao L, Li JW, Zheng SG. Laparoscopic anatomical segmentectomy of liver segments VII and VIII with the hepatic veins exposed from the head side (with videos). *J Surg Oncol*. (2016) 114:752–6. doi: 10.1002/jso.24411

8. Ferrero A, Lo Tesoriere R, Russolillo N, Vigano L, Forchino F, Capussotti L. Ultrasound-guided laparoscopic liver resections. *Surg Endosc*. (2015) 29:1002–5. doi: 10.1007/s00464-014-3762-9

9. Torzilli G, Procopio F. State of the art of intraoperative ultrasound in liver surgery: current use for resection-guidance. *Chirurgia*. (2017) 112:320–5. doi: 10.21614/chirurgia.112.3.320

10. Soon DS, Chae MP, Pilgrim CH, Rozen WM, Spychal RT, Hunter-Smith DJ. 3D Haptic modelling for preoperative planning of hepatic resection: a systematic review. *Ann Med Surg*. (2016) 10:1–7. doi: 10.1016/j.amsu.2016.07.002

11. Viganò L, Procopio F, Mimmo A, Donadon M, Terrone A, Cimino M, et al. Oncologic superiority of anatomic resection of hepatocellular carcinoma by ultrasound-guided compression of the portal tributaries compared with nonanatomic resection: an analysis of patients matched for tumor characteristics and liver function. *Surgery*. (2018) 164:1006–13. doi: 10.1016/j.surg.2018.06.030

12. Xu HW, Liu F, Hao XY, Wei YG, Li B, Wen TF, et al. Laparoscopically anatomical versus non-anatomical liver resection for large hepatocellular carcinoma. *HPB*. (2020) 22:136–43. doi: 10.1016/j.hpb.2019.06.008

13. Okamura Y, Sugiura T, Ito T, Yamamoto Y, Ashida R, Ohgi K, et al. Anatomical resection is useful for the treatment of primary solitary hepatocellular carcinoma with predicted microscopic vessel invasion and/or intrahepatic metastasis. *Surg Today*. (2021) 51:1429–39. doi: 10.1007/s00595-021-02237-1

14. Makuuchi M. Surgical treatment for HCC–special reference to anatomical resection. *Int J Surg*. (2013) 11(Suppl 1):S47–49. doi: 10.1016/S1743-9191(13)60015-1

15. Ishizawa T, Fukushima N, Shibahara J, Masuda K, Tamura S, Aoki T, et al. Real-time identification of liver cancers by using indocyanine green fluorescent imaging. *Cancer*. (2009) 115:2491–504. doi: 10.1002/cncr.24291

16. Nakaseko Y, Ishizawa T, Saiura A. Fluorescence-guided surgery for liver tumors. *J Surg Oncol*. (2018) 118:324–31. doi: 10.1002/jso.25128

17. Izumi R, Shimizu K, Kiriyama M, Hashimoto T, Yagi M, Yamaguchi A, et al. Hepatic resection guided by needles inserted under ultrasonographic guidance. *Surgery*. (1993) 114:497–501.

frontiers | Frontiers in Surgery

TYPE Original Research
PUBLISHED 24 January 2023
DOI 10.3389/fsurg.2023.1097642



OPEN ACCESS

EDITED BY
Jeroen Van Vugt,
Erasmus Medical Center, Netherlands

REVIEWED BY
Chenyu Sun,
AMITA Health, United States
Mubashir Ayaz Ahmed,
AMITA Health St Joseph Hospital, United States

*CORRESPONDENCE
Yun Wang
✉ wydzs@aliyun.com

SPECIALTY SECTION
This article was submitted to Surgical Oncology, a section of the journal Frontiers in Surgery

RECEIVED 14 November 2022
ACCEPTED 06 January 2023
PUBLISHED 24 January 2023

CITATION
Duan J, Yi J and Wang Y (2023) Exploitation of a shared genetic signature between obesity and endometrioid endometrial cancer.
Front. Surg. 10:1097642.
doi: 10.3389/fsurg.2023.1097642



# Exploitation of a shared genetic signature between obesity and endometrioid endometrial cancer

Junyi Duan[1], Jiahong Yi[2] and Yun Wang[3]*

[1]First Clinical Medical College, Shanxi Medical University, Taiyuan, China, [2]Sun Yat-Sen University Cancer Center, Sun Yat-Sen University, Guangzhou, China, [3]Department of Obstetrics and Gynecology, The 985th Hospital of The People's Liberation Army Joint Logistic Support Force, Taiyuan, China

**Aims:** The findings in epidemiological studies suggest that endometrioid endometrial cancer (EEC) is associated with obesity. However, evidence from gene expression data for the relationship between the two is still lacking. The purpose of this study was to explore the merits of establishing an obesity-related genes (ORGs) signature in the treatment and the prognostic assessment of EEC.
**Methods:** Microarray data from GSE112307 were utilized to identify ORGs by using weighted gene co-expression network analysis. Based on the sequencing data from TCGA, we established the prognostic ORGs signature, confirmed its value as an independent risk factor, and constructed a nomogram. We further investigated the association between grouping based on ORGs signature and clinicopathological characteristics, immune infiltration, tumor mutation burden and drug sensitivity.
**Results:** A total of 10 ORGs were identified as key genes for the construction of the signature. According to the ORGs score computed from the signature, EEC patients were divided into high and low-scoring groups. Overall survival (OS) was shorter in EEC patients in the high-scoring group compared with the low-scoring group ($P < 0.001$). The results of the Cox regression analysis showed that ORGs score was an independent risk factor for OS in EEC patients (HR = 1.017, 95% confidence interval = 1.011–1.023; $P < 0.001$). We further revealed significant disparities between scoring groups in terms of clinical characteristics, tumor immune cell infiltration, and tumor mutation burden. Patients in the low-scoring group may be potential beneficiaries of immunotherapy and targeted therapies.
**Conclusions:** The ORGs signature established in this study has promising prognostic predictive power and may be a useful tool for the selection of EEC patients who benefit from immunotherapy and targeted therapies.

KEYWORDS

endometrioid endometrial cancer, obesity-related genes, weighted gene coexpression network analysis, immune correlation analyses, targeted treatment

## Introduction

Endometrial cancer (EC) is the most prevalent tumor in the female genital system, and its morbidity and mortality are gradually increasing (1). Despite significant advances in various aspects of EC management, the accumulating disease burden of EC has not been reversed. Molecular typing based on genomic features has deepened our understanding of EC and as a result, clinical practice has changed as a result. It is critical to further analyze The Cancer Genome Atlas (TCGA) data to improve our understanding of EC and to address rising morbidity and mortality (2).

Obesity is a growing hazard attracting tremendous attention. Meanwhile, its association with EC and the impact of weight loss on the prevention and prognosis of EC have been the focus of gynecologic oncologists and patients (3). The results of traditional observational studies and

Mendelian randomization analyses showed that the risk of EC increases with increasing Body Mass Index (BMI) and was much more relevant than other tumors. Correspondingly, bariatric surgery was effective in reducing the risk of EC (4–6). Epidemiological data demonstrated a correlation between obesity and EC, but evidence from transcription profiling is still inadequate.

This study focused on endometrioid EC (EEC), the pathological subtype that is more strongly associated with obesity (7). Obesity-related genes (ORGs) were identified by microarray data from obese women, and subsequently the ORGs signature was established in EEC patients. We analyzed the ORGs scoring groups in terms of clinical characteristics, immune function, and drug sensitivity. Through this study, we hope to better understand the potential mechanisms of EEC and obesity, find novel biomarkers that can be applied for screening and treatment, delineate subgroups to seek potential beneficiaries of targeted therapy, and take a step further toward precision medicine for EEC.

# Methods

## Data source

Series GSE112307 from the Gene Expression Omnibus (GEO) database was utilized to identify ORGs (8). Microarray data from GSE112307 were derived from 54 paired subcutaneous adipose tissues from 27 moderately obese women, collected before or after a calorie-restricted diet. The GEOquery and illuminaHumanv3.db R packages were applied for data download and gene annotation. RNA sequencing, tumor somatic mutation and clinical data from EEC patients were manually downloaded from the TCGA portal. TPM data were extracted from the RNA sequencing data for signature construction and functional analyses, and the maftools and XML R packages were used to collate mutation and survival data.

## Identification of ORGs

Weighted gene co-expression network analysis (WGCNA) is an algorithm that explores the relationship between expression and phenotype data based on correlation coefficients (9). In this study, WGCNA was used to identify gene modules associated with obesity and was implemented using the limma and WGCNA R packages. First, we performed sample clustering and removed abnormal samples. The correlation between genes was calculated. The appropriate $\beta$ was then selected based on correlation coefficients to build the matrix and evaluate the correlation of gene expression patterns. On the basis of this, gene hierarchical and module clustering was performed to determine the correlation between gene modules and obesity based on the eigenvalues of the gene modules and the obesity or not of the samples. We then performed functional enrichment analysis and visualization of gene modules highly associated with obesity, using the clusterProfiler, org.Hs.eg.db and enrichplot R packages.

## Training and testing of ORGs signature

The samples of EEC are divided, half for the training cohort and half for the test cohort. ORGs associated with the prognosis of EEC patients were screened by univariate Cox regression in the training cohort. Subsequently, the least absolute shrinkage and selection operator (LASSO) regression was applied to further select variables and avoid model overfitting. Finally, a prognostic ORGs signature was established using stepwise multivariate Cox regression. ORGs score was calculated for each sample according to the following equation:

$$\text{ORGs score} = \sum_i \text{coefficient}(\text{ORGs}_i) \times \text{expression}(\text{ORGs}_i).$$

The differences between the ORGs scoring groups were assessed by scatter plots and principal component analysis (PCA). The log-rank test was performed to compare overall survival (OS) between the two groups. The above analyses were validated in the test cohort and in the entire cohort. The survminer, survival, glmnet, ggplot2, pheatmap, and scatterplot3d R packages were utilized for training and testing of the ORGs signature.

## Correlation analysis of clinical features

We performed Cox regression analysis to elucidate whether ORGs score was independent of other relatively complete clinicopathological characteristics (age, race, FIGO stage and tumor grade) and visualized as forest plots. In addition, we examined the predictive power of ORGs signature in different clinical subgroups. We integrated the available clinical information to develop a nomogram using regplot, rms and survivor R packages. The accuracy of the nomogram was assessed using calibration curves.

## Correlation analysis of immune function

Single-sample gene set enrichment analysis (ssGSEA) was used to assess the infiltration and function of immune cells. We then investigated the differences in immune checkpoint gene expression between ORGs groups. Immune and stromal infiltration in the tumor microenvironment was evaluated in two groups based on the ESTIMATE algorithm (10).

## Gene mutation analysis

Somatic mutation data from TCGA were collated and analyzed using the maftools R package. The 15 genes with the highest tumor mutation frequency (TMF) in each ORGs group were visualized by waterfall plots. The tumor mutation burden (TMB) was calculated for each sample. After establishing subgroups based on median TMB, we compared the survival differences between TMB groups and confirmed the prognostic value of ORGs groups in TMB subgroups. The cBioPortalData R package was applied to download data about the microsatellite instability (MSI) status of EEC patients. Whereafter, differences in MSI status in ORGs groups, differences in ORGs score in MSI subgroups, and differences in prognosis were analyzed.

## Drug sensitive analysis

The oncopredict R package was implemented to predict drug response in ORGs groups (11). Half maximal inhibitory concentrations (IC50) of antitumor drugs were calculated based on data from the Genomics of Drug Sensitivity in Cancer (12).

## Statistical analysis

The entire analysis was implemented using R (version 4.0.3). Cox regression and survival analyses were performed by the survivor and survminer R packages. The pheatmap R package was used to draw heat maps. Wilcoxon rank sum test was applied to test the discrepancies between quantitative data. We applied Pearson correlation analysis to calculate the correlation coefficients. $P < 0.05$ was considered statistically significant.

# Results

## Identification and functional annotation of obesity-related genes

The flow plot of this study was summarized in **Figure 1**. A gene clustering dendrogram was generated based on the GSE112307 dataset using WGCNA (**Figure 2A**). The expression matrix was divided into six gene modules, and the dark red module containing 1,148 genes was significantly associated with obesity and identified as ORGs (**Figure 2B**). The results of enrichment analysis showed that ORGs were significantly enriched in pathways related to fatty acid metabolism and biological oxidation, and were involved in transmembrane transport of substances in the form of enzymes and transporters (**Figures 2C,D**).

## Training and testing of the ORGs signature

A total of 399 cases from the TCGA database were included in this study and were equally divided into training and test groups. Univariate regression analysis of ORGs combined with transcriptomic data and clinical data showed that a total of 36 ORGs were significantly associated with prognosis in EEC patients ($P < 0.001$, **Figure 3A**). We then conducted LASSO and stepwise multivariate Cox regression for prognosis-related ORGs. Finally, 10 key ORGs were identified for the construction of the prognostic signature (**Figures 3B,C**). The ORGs score was calculated according to the following equation, and the training cohort was divided into high- and low-scoring groups according to the median of the ORGs score: YIPF1 × 0.017847 + SULT1A2 × 1.8463 + SRGAP3 × 0.082928 + OR6B2 × 5.6732 + LRRC31 × 0.078038 + FMOD × 0.0014647 + FAM222B × 0.033231 + DHRS7B × 0.032636 + DGAT2 × 0.10261 + ANG × 0.025124. The PCA plot illustrated the distribution of differences between the two ORGs groups (**Figure 3D**). The survival time and survival status of ORGs score in EEC patients were shown as scatter plots, where the survival time decreased and the number of deaths increased with increasing ORGs score (**Figure 3E**). The expression of key genes of ORGs signature and their correlation with ORGs groups are shown by heat map (**Figure 3F**). Kaplan-Meier curves demonstrated significant differences in survival between ORGs groups ($P = 0.003$, **Figure 3G**). Similar results were observed in the testing cohort and the entire cohort, which verified the strong and robust predictive power of ORGs signature (**Figures 4A–H**).

## Correlation analysis of clinical characteristics

The results of univariate and multivariate Cox regression analyzes demonstrated that the ORGs score was an independent risk factor that affected the prognosis of patients with EEC (**Figures 5A,B**). Receiver operating characteristic curve (ROC) analysis and the C index curves demonstrated the strong predictive power of the ORG

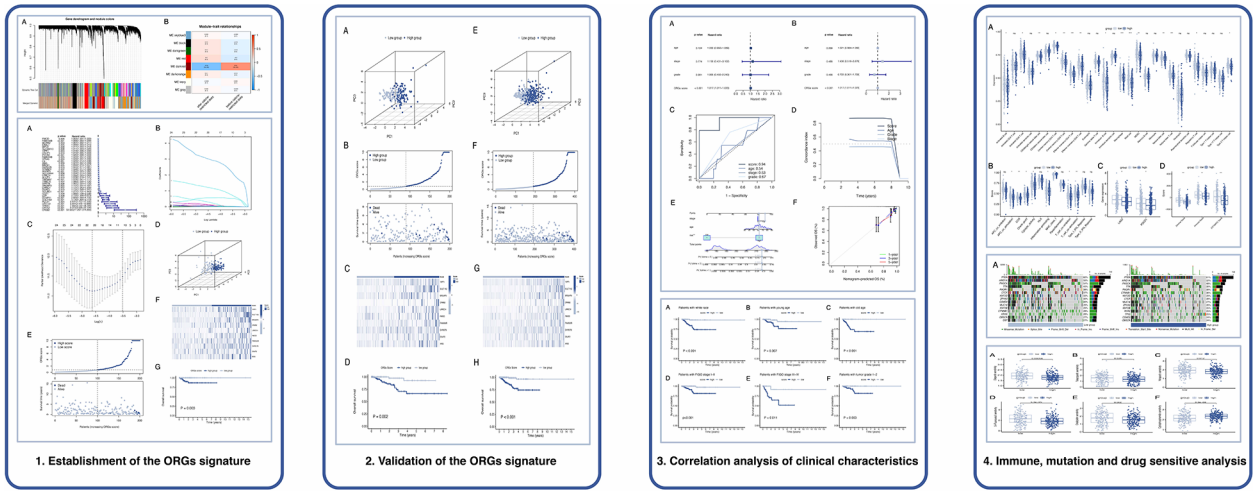


FIGURE 1
The flow plot of this study.

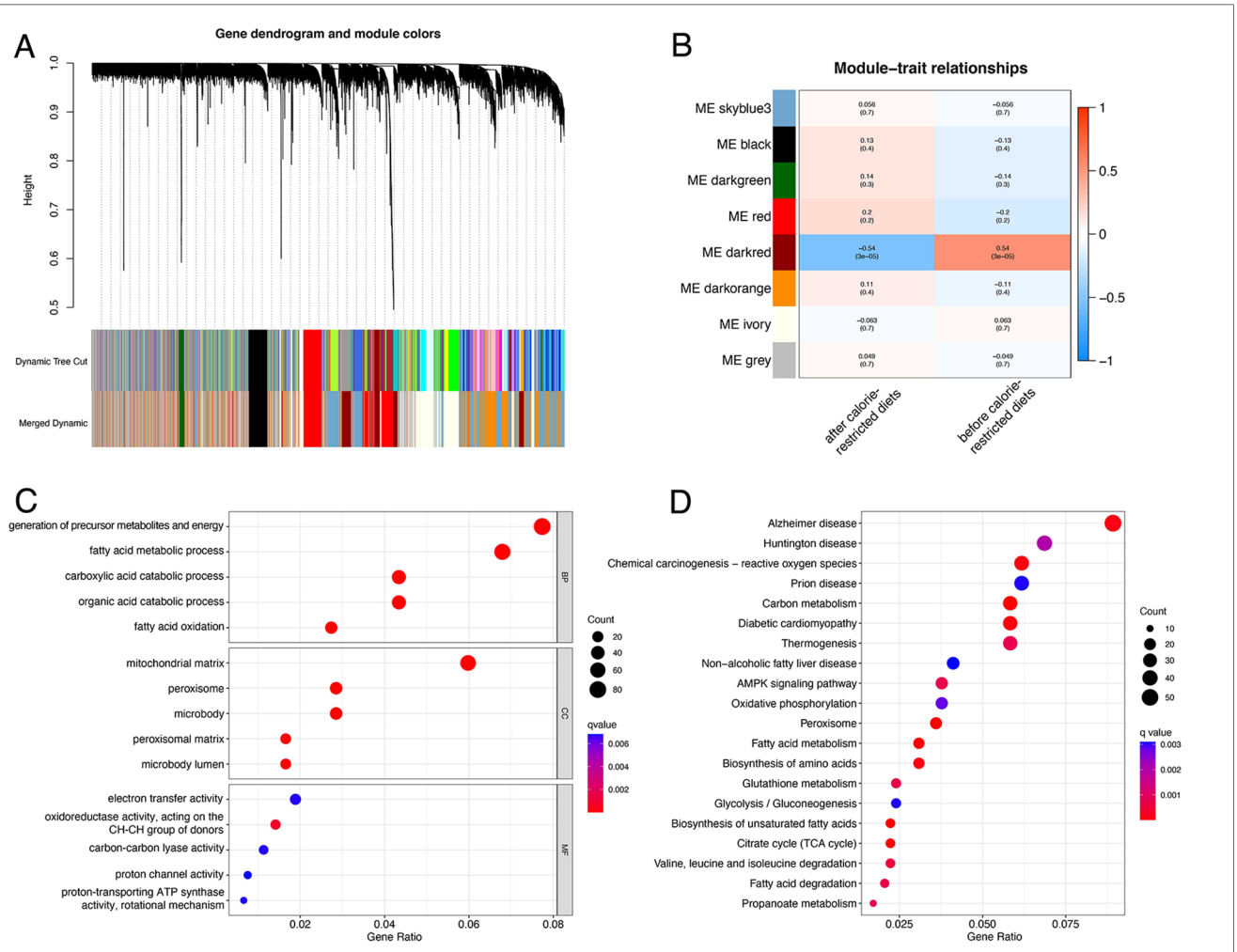


FIGURE 2
Identification and functional annotation of ORGs. (**A**) The cluster dendrogram of ORGs in obesity. (**B**) Correlation of WGCNA modules and obesity. (**C**) GO analysis of ORGs. (**D**) KEGG analysis of ORGs. ORGs, obesity-related genes. WGCNA, weighted gene co-expression network analysis. GO, Gene Ontology. KEGG, Kyoto Encyclopedia of Genes and Genomes.

score compared to other clinicopathological characteristics (Figures 5C, D). Integrating the ORGs score and relatively complete clinical characteristics including age, race, FIGO stage, and tumor stage, we constructed a nomogram to predict 1-year, 3-year, and 5-year survival rates after diagnosis in EEC patients (Figure 5E). We also plotted calibration curves to confirm the agreement between the predictions of the nomogram and actual observations (Figure 5F). To further confirm the prognostic value of ORGs signature, we performed subgroup analyzes of different clinicopathological characteristics of EEC patients in the entire cohort. The results showed that ORGs grouping was associated with the prognosis of patients with EEC among those white, of different age, different tumor grade, different FIGO stage, and different BMI ($P < 0.05$; Figures 6A–I). This suggests that the ORGs signature retains valid predictive power across subgroups of age, race, BMI, FIGO stage, and tumor grade.

## Correlation analysis of immune function

To investigate the relationship between ORGs grouping and immune status, ssGSEA was performed for each immune cell subset and functional pathway. Activated B cell, Activated CD8 T cell, CD56bright natural killer cell, Central memory CD4 T cell, Central memory CD8 T cell, Effector memory CD4 T cell, Effector memory CD8 T cell, Immature B cell, Macrophage, Mast cell, MDSC, Natural killer cell, Natural killer T cell, Regulatory T cell, and Type 2 T helper cell were significantly elevated in the low-scoring group compared to the counterpart (Figure 7A). The immune function score showed that the low-scoring group was more active in APC co stimulation, CCR, Check-point, Cytolytic activity, Inflammation-promoting, MHC class I, T cell co-inhibition, and T cell co-stimulation (Figure 7B). Furthermore, we analyzed the expression of immune checkpoint genes between the two groups and found that the immune checkpoint genes LAG3 and PD-1 were more expressed in the low-scoring group (Figure 7C). In addition, we calculated the tumor microenvironment (TME) score according to the ESTIMATE algorithm. Likewise, the results revealed a higher infiltration of stromal cells and immune cells in the low-scoring group (Figure 7D).

## Gene mutation analysis

By waterfall graphs, we visualized somatic mutations in different ORGs groups (Figure 8A). PTEN, ARID1A, PIK3CA, and TTN were

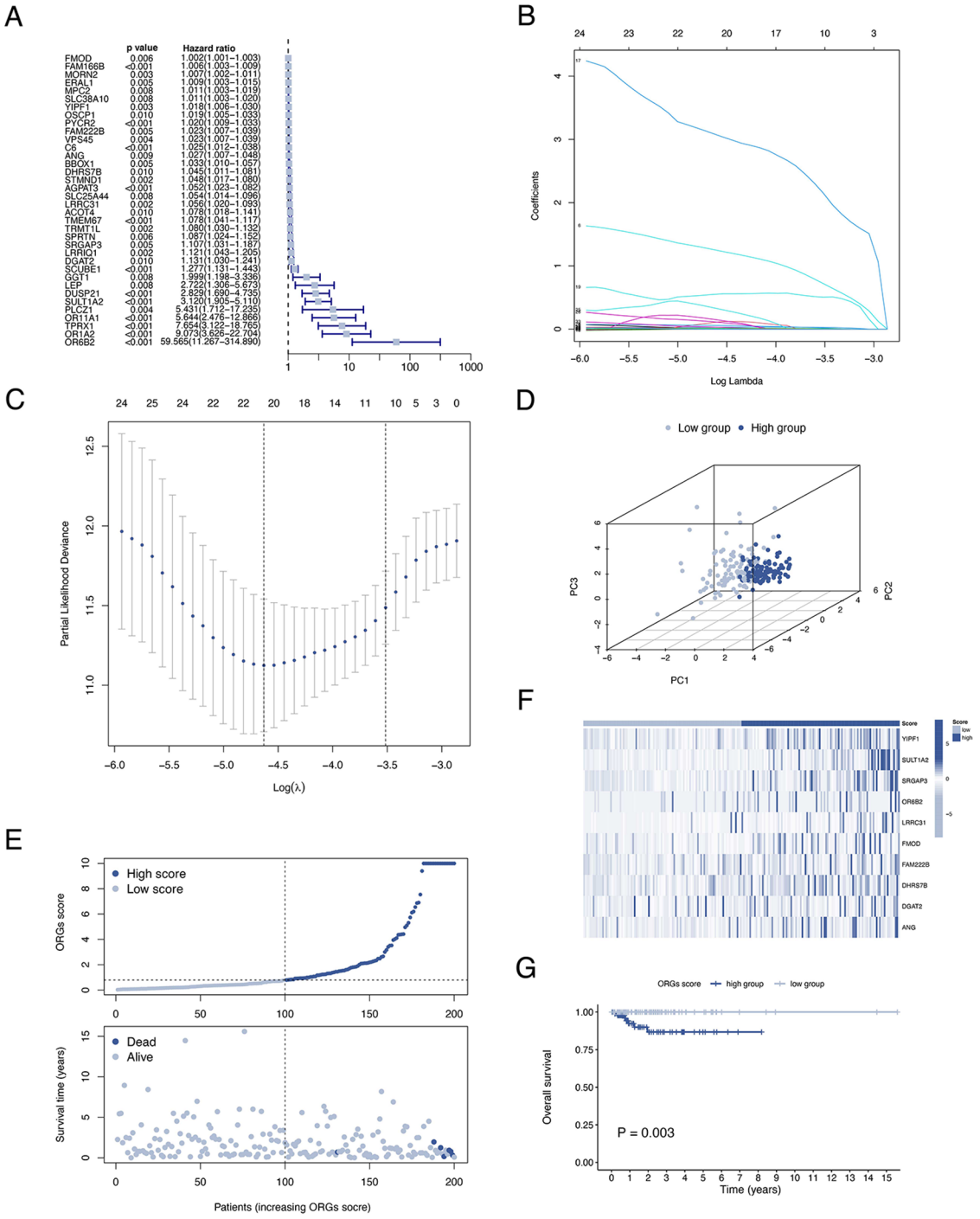


FIGURE 3
Establishment of the ORGs signature in the train cohort. (**A**) Univariate Cox regression analysis for screening prognostic ORGs. (**B**,**C**) LASSO regression analysis for variable selection and avoid overfitting. (**D**) PCA plot for different ORGs scoring groups. (**E**) Scatter diagram for the ORGs score and survival status of EEC patients. (**F**) Heat map for the key 10 ORGs expression with ORGs grouping. (**G**) Kaplan–Meier curves of survival difference between two groups. ORGs, obesity-related genes. LASSO, least absolute shrinkage and selection operator. PCA, principal component analysis. EEC, endometrioid endometrial cancer.

mutated frequently in the EEC and more frequently in the low-scoring group. After that, we calculated the tumor mutation burden in each group and observed no significant difference in TMB levels between ORGs groups (**Figure 8B**). Grouped by median TMB, patients with high TMB had a better prognosis ($P = 0.045$, **Figure 8C**). In the subgroup with low TMB, the ORGs score had prognostic predictive value (**Figure 8D**). In addition, we analyze the correlation between MSI and ORGs score. The histogram illustrated the discrepancies in the distribution of MSI status in the different scoring groups. The proportion of high-frequency MSI (MSI-H) was higher in patients with low ORGs score (**Figure 8E**). Patients with

10.3389/fsurg.2023.1097642

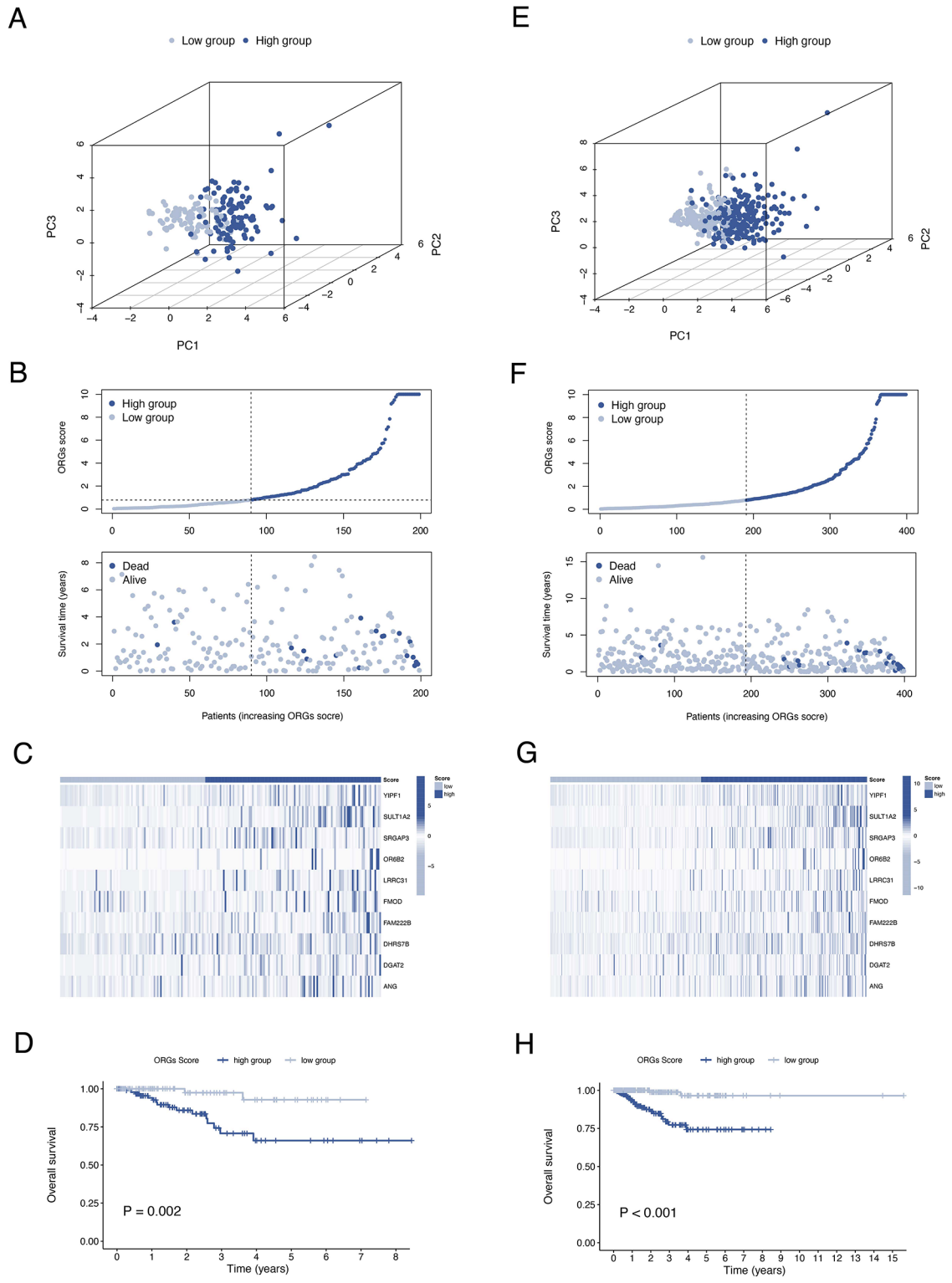


FIGURE 4
Validation of the ORGs signature in the test cohort and the entire cohort. PCA plot (**A**), scatter plot (**B**), heat map (**C**), and Kaplan–Meier curves (**D**) for the test cohort. PCA plot (**E**), scatter plot (**F**), heat map (**G**), and Kaplan–Meier curves (**H**) for the entire cohort. ORGs, obesity-related genes. PCA, principal component analysis.

MSI-H had lower ORGs score compared with microsatellite stability (MSS) patients ($P = 0.047$, Figure 8F). The ORGs score has prognostic value in patients with MSI-H and MSS (Figures 8G,H).

## Drug sensitive analysis

Drug sensitivity analysis revealed significant differences in ORGs scoring group among various gynecologic antitumor drugs including

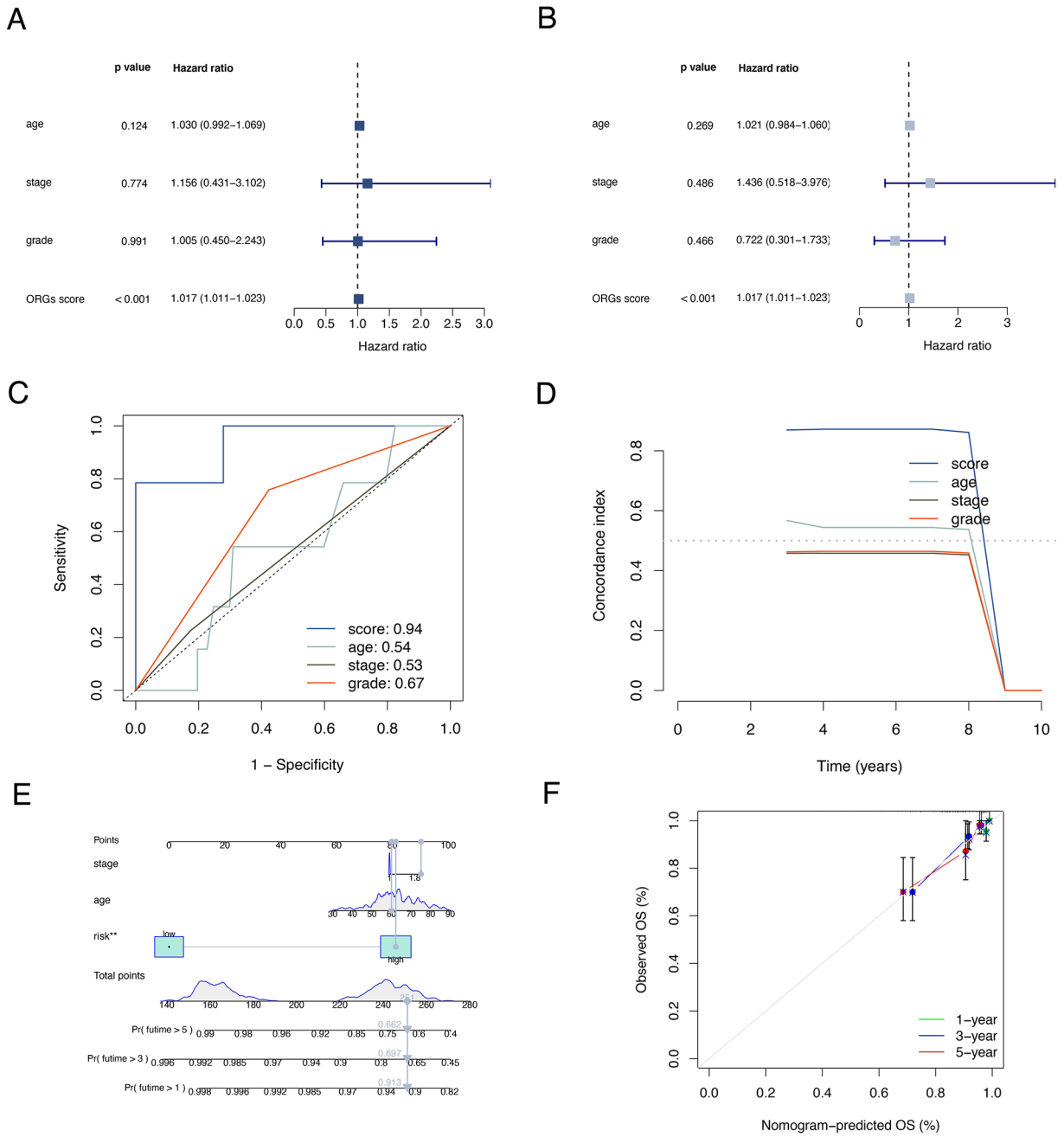


FIGURE 5
Correlation analyses of clinical features. Univariate (A) and multivariate (B) Cox regressions of ORGs score, age, tumor grade, and FIGO stage. The ROC (C) and C-index (D) of ORGs score, age, tumor grade, and FIGO stage. (E) The nomogram for predicting prognosis of EEC patients. (F) The calibration curves of the nomogram. ORGs, obesity-related genes. FIGO, the International Federation of Gynecology and Obstetrics. ROC, receiver operating characteristic curve. EEC, endometrioid endometrial cancer.

olaparib, talazoparib, niraparib, 5-fluorouracil, oxaliplatin, and cyclophosphamide (**Figures 9A–F**).

## Discussion

Unlike other reproductive system tumors that threaten women's life and health, EC is a serious disease burden as its morbidity and mortality are increasing year by year. This could be due to the combined effects of an aging population, a decrease in benign hysterectomy, and the prevalence of obesity (13). As one of the most important factors associated with the development of EC, obesity seriously affects the prognosis of patients with EC by making surgery and perioperative management more difficult and increasing the risk of comorbidities and complications (7). The current view is that EEC is the subtype most strongly associated with obesity. Analyzing the association between obesity and EEC based on gene expression data will help us to better understand

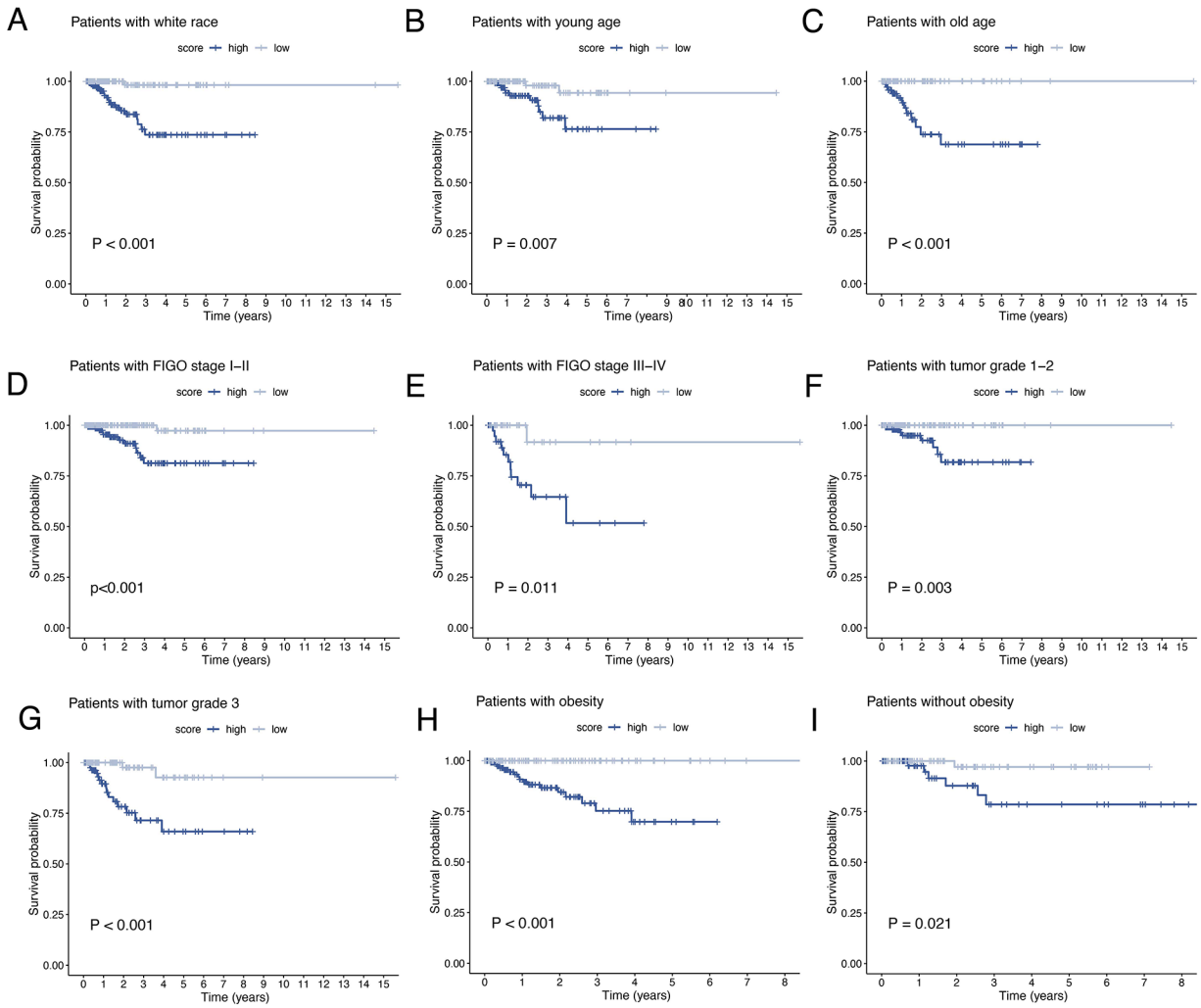


FIGURE 6
Subgroup analysis of EEC patients. Kaplan–Meier curves of patients with white race (A), age < 65 (B), age ≥ 65 (C), FIGO stage I–II (D), FIGO stage III–IV (E), tumor grade 1–2 (F), tumor grade 3 (G), BMI ≥ 30 (H), BMI < 30 (I). EEC, endometrioid endometrial cancer. FIGO, the International Federation of Gynecology and Obstetrics. BMI, body mass index.

potential mechanisms, select more appropriate therapeutic regimens for patients with different molecular characteristics, and improve the prognosis of EEC patients.

In this study, a gene module significantly associated with obesity was identified using WGCNA based on the GSE6008 data. The enrichment analysis of the module genes showed significant enrichment in fatty acid metabolism and biooxidation pathways. Subsequently, we constructed an ORGs signature using RNA sequencing data from EEC samples in TCGA. Subsequently, extracting RNA sequencing data from EEC samples in TCGA, we constructed a signature of ORGs including *ANG*, *SULT1A2*, *DGAT2*, *YIPF1*, *SRGAP3*, *LRRC31*, *FMOD*, *OR6B2*, *DHRS7B*, and *FAM222B*. *ANG*-encoding proteins belong to the ribonuclease A superfamily and have been widely reported to be associated with the invasion and progression of various cancers. In colorectal cancer, *ANG* cleavage produces tRNA-derived stress-induced small RNAs (tiRNAs) that promote colorectal cancer metastasis (14). Meanwhile, elevated expression of ANG was found to affect endometrial angiogenesis in hyperinsulin-treated mice (15). Integrating previous reports and bioinformatics analysis, we hypothesized that *ANG* expression is associated with obesity and involved in EC progression by affecting tumor angiogenesis. *SULT1A2* encodes phenol sulfotransferases involved in hormone metabolism and has been reported to be associated with the prognosis of patients with HER2-positive breast cancer (16). Also, as estrogen-dependent tumors, the development of EEC may be influenced by *SULT1A2* expression. *DGAT2* encodes a key enzyme that catalyzes the synthesis of triglycerides and has been reported to be involved in the reprogramming of lipid metabolism in tumor cells, driving tumor progression (17). Similarly, the correlation between *YIPF1*, *SRGAP3*, *LRRC31*, *FMOD* and various tumors has been reported in the literature (18–21). However, the correlation between *OR6B2*, *DHRS7B*, *FAM222B*, and tumors has been little explored. In future studies, we should experimentally investigate their role in the development of EEC.

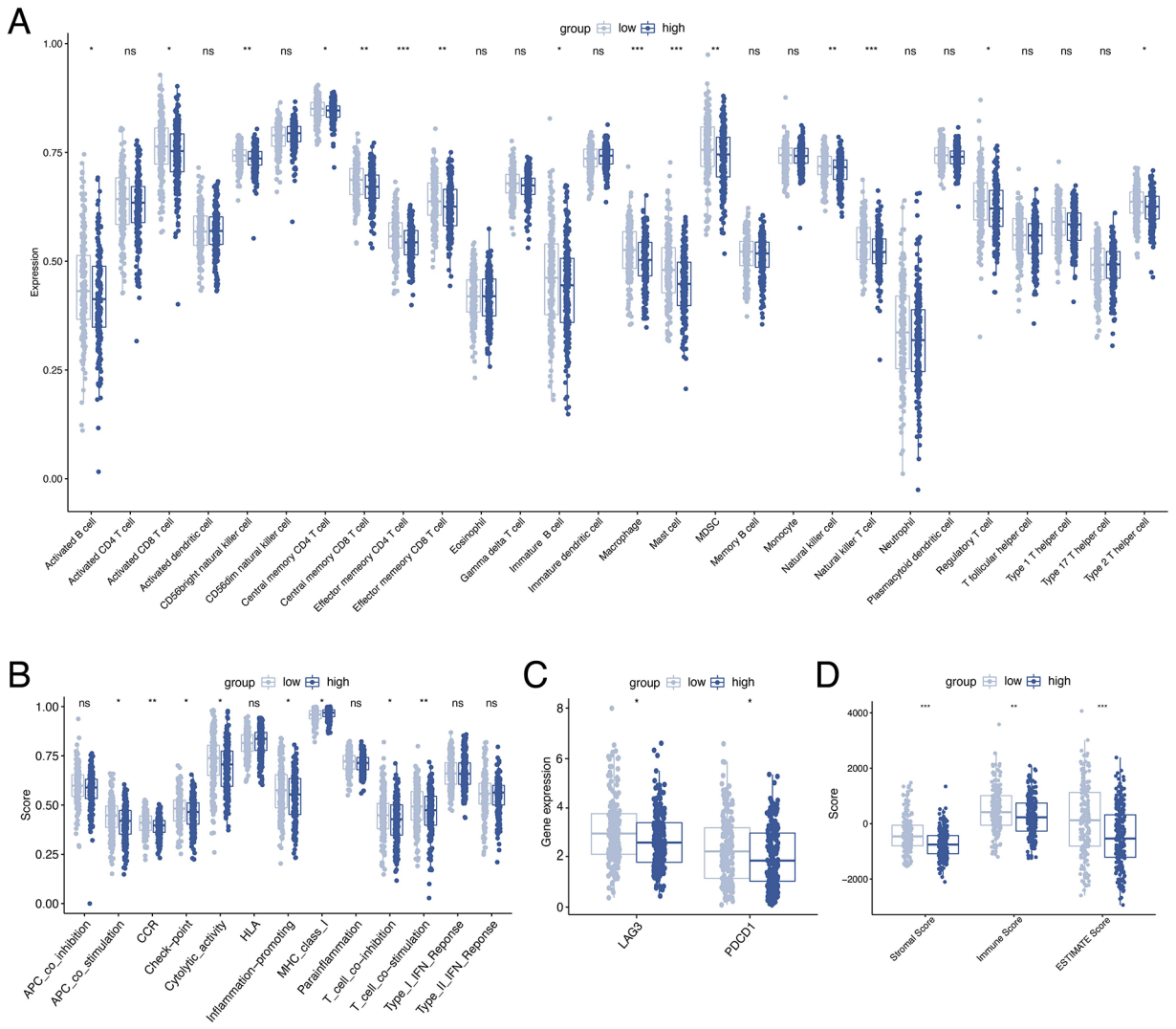


FIGURE 7
Analysis of immune activity. Comparison of the discrepancy of immune cell infiltration (A) and immune function (B) between two groups based on ssGSEA. (C) Differences in the expression of LAG-3 and PD-1 between the two groups. (D) TME analysis based on the ESTIMATE algorithm. ssGSEA, single-sample gene set enrichment analysis. TME, tumor microenvironment.

According to the ORGs score, EEC patients were divided into two groups. PCA and survival analysis demonstrated the differences in the distribution between the two groups and the prognostic value of the ORGs signature. We then applied Cox regression and ROC analysis to clarify the value of the ORGs score as an independent risk factor for EEC patients. Subgroup analysis demonstrated that ORGs score-based grouping maintained considerable survival predictive power in different clinical subgroups. Integrating age, FIGO stage, tumor grade, and ORGs score, we further developed a prognostic nomogram to stratify the prognosis of EEC patients to support clinical practice.

By analyzing somatic mutation data, we found discrepancies in gene mutation frequencies between ORGs groups. The frequency of *ARID1A* mutations was significantly higher in the low-scoring group. It was shown that *ARID1A* protein expression deletion occurred more frequently in high-grade EEC and was associated with activation of the PI3K/AKT pathway (22, 23). The higher frequency of *CTNNB1* mutations in the high-scoring group, with reduced expression of its encoded protein $\beta$-catenin, was involved with disease progression and associated with poor prognosis (24, 25). The TMB was calculated using mutation data and found that the ORGs score still had the ability to stratify the prognosis in the low-TMB group.

Currently, immunotherapy for EC is a popular concern among gynecological oncologists. Immune checkpoint blockers (ICBs) activate the immune system to kill tumors by relieving T-cell suppression through binding to their targets (26). Based on the findings of Keynote 028 and Keynote 158, the current view is that ICBs are beneficial for recurrent or metastatic EC patients with TMB-H, MSI-H and PD-1/PD-L1-positive (27–29). This study revealed differences in immune cell infiltration, PD-1 expression, and MSI status between the ORGs groups. Innate and specific immune cells were more infiltrated in the low-

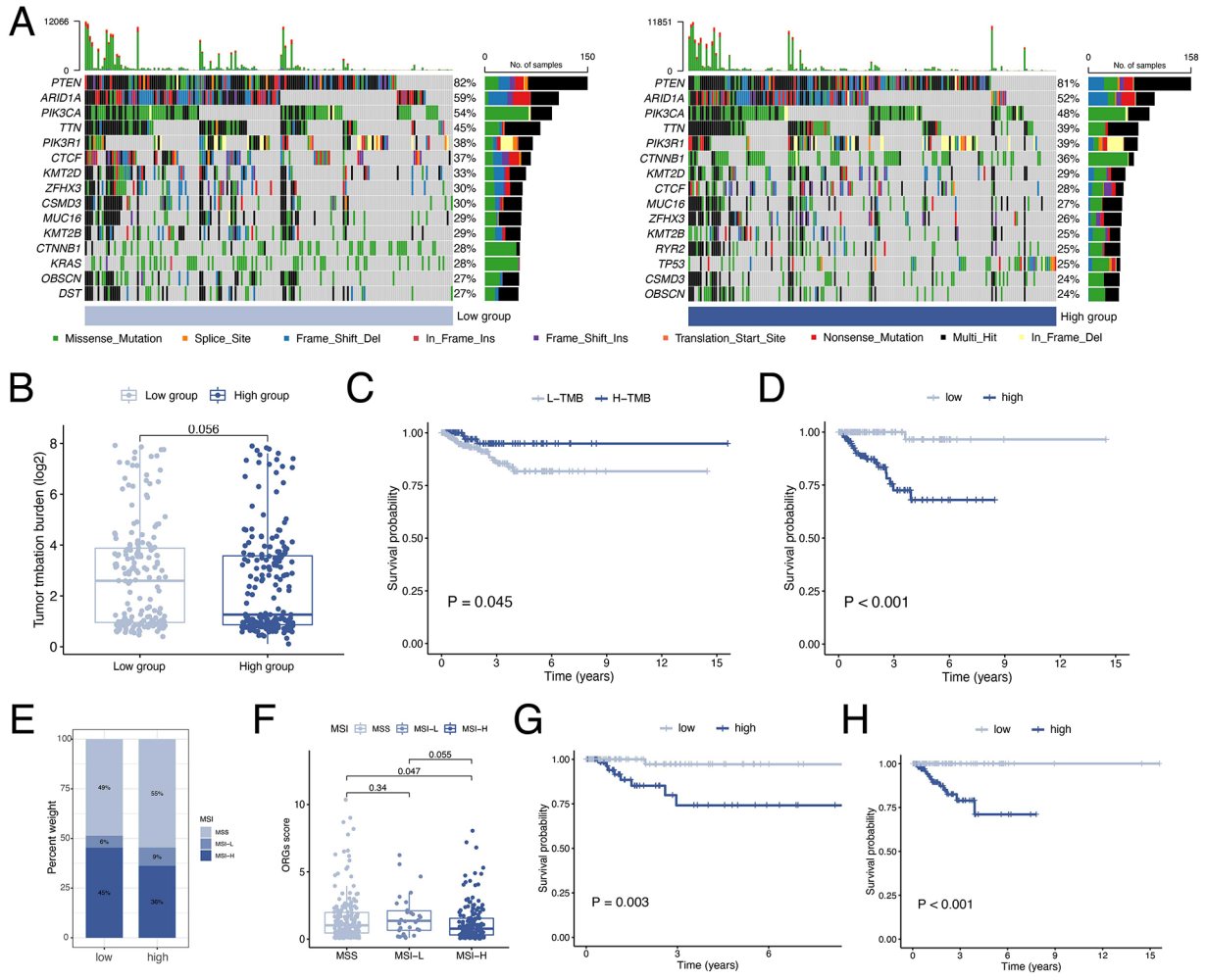


FIGURE 8
Analyses of mutation data. (**A**) Visualization of somatic mutations in different ORGs groups. (**B**) Differential analysis of TMB in ORGs scoring groups. (**C**) Kaplan–Meier curves of survival differences between the high- and low-TMB groups. (**D**) Kaplan–Meier curves of survival differences between ORGs scoring groups in low-TMB patients. (**E**) Distribution of MSI status in the different scoring groups. (**F**) Differential analysis of the ORGs score in patients with different MSI status. Kaplan–Meier curves of survival differences between ORGs scoring groups in patients with MSI-H (**G**) and MSS (**H**). ORGs, obesity-related genes. TMB, tumor mutation burden. MSI, microsatellite instability. MSI-H, high microsatellite instability. MSS, microsatellite stable.

scoring group, and PD-1 expression and MSI-H proportion were higher. Given the survival discrepancies between different ORGs groups in each MSI subgroup, we speculate that integrating ORGs score, MSI status, TMB levels, and immune checkpoint gene expression might allow further screening of EEC patients and precise targeting of immunotherapy benefit populations.

Considering the promising results of poly (ADP-ribose) polymerase inhibitors (PARPi) in the maintenance treatment of ovarian cancer, numerous studies have converged on the possibility of PARPi application in the treatment of EC (30, 31). The results of our sensitivity analysis for commonly used gynecologic antineoplastic agents showed that the ORGs groups differed in drug sensitivity for a variety of PARPi, including olaparib, niraparib and talazoparib. The possibility of ORGs score for screening potential PARPi beneficiaries and the mechanism of correlation between ORGs and PARPi still needs to be clarified by further studies.

There are unavoidable limitations to this study. The data used to construct and validate the model were obtained from retrospective public databases and the conclusions of this study should be further validated by prospective data. In addition, the hypotheses established based on the results of immune, mutation and drug sensitivity analyses need to be further confirmed by functional experiments.

## Conclusion

In the present study, the ORGs signature was established and analyzed in terms of clinical characteristics, mutation data, immune correlation and drug sensitivity, which found new

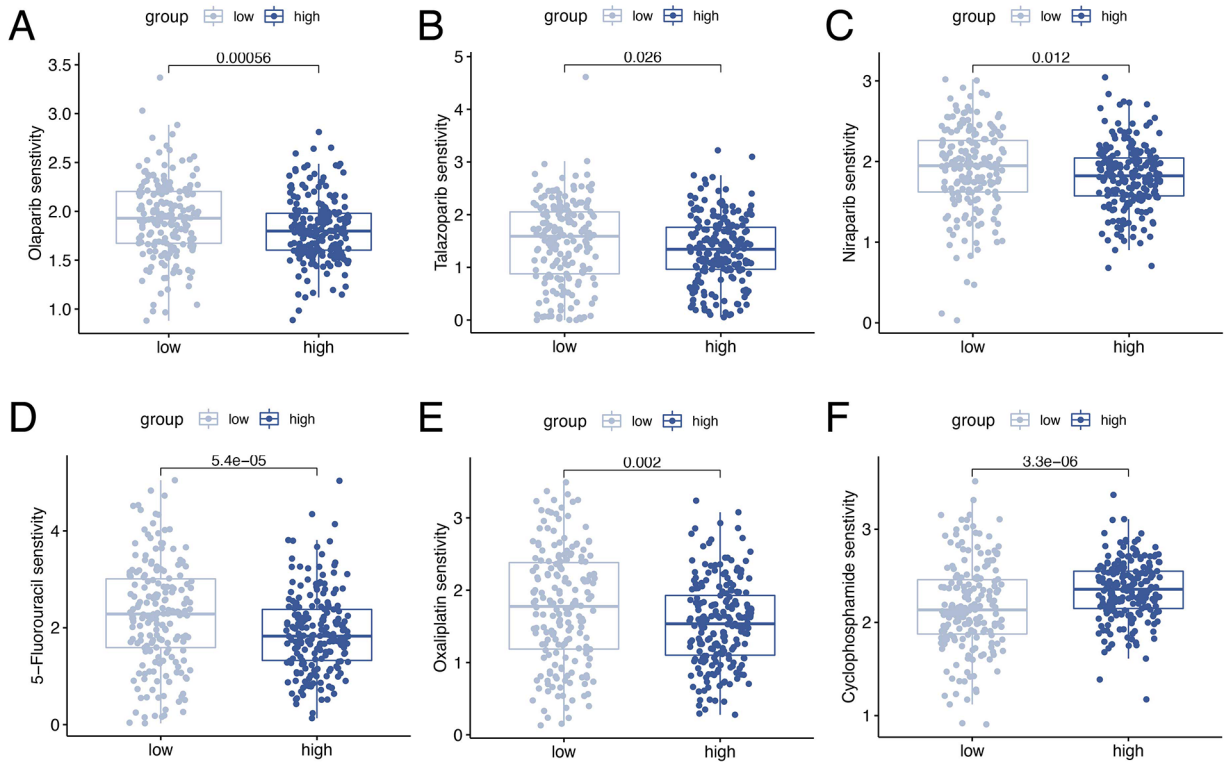


FIGURE 9
Drug sensitivity analyses. Analysis of drug sensitivity differences in olaparib (A), talazoparib (B), niraparib (C), 5-fluorouracil (D), oxaliplatin (E), and cyclophosphamide (F).

biomarkers for exploring the underlying mechanisms of obesity and EEC and provided new insights into the precise treatment of EEC patients.

## Data availability statement

The original contributions presented in the study are included in the article/Supplementary Material, further inquiries can be directed to the corresponding author/s.

## Author contributions

JD: Project development, data analysis, manuscript writing. JY: Data analysis, manuscript writing. YW: Project development, manuscript writing. All authors contributed to the article and approved the submitted version.

## Acknowledgments

The authors would like to thank TCGA and GEO for providing accessible public data.

## Conflict of interest

The authors declare that the research was conducted in the absence of any commercial or financial relationships that could be construed as a potential conflict of interest.

## Publisher's note

All claims expressed in this article are solely those of the authors and do not necessarily represent those of their affiliated organizations, or those of the publisher, the editors and the reviewers. Any product that may be evaluated in this article, or claim that may be made by its manufacturer, is not guaranteed or endorsed by the publisher.

## References

1. Lu KH, Broaddus RR. Endometrial cancer. *N Engl J Med.* (2020) 383(21):2053–64. doi: 10.1056/NEJMra1514010

2. Kandoth C, Schultz N, Cherniack AD, Akbani R, Liu Y, Shen H, et al. Integrated genomic characterization of endometrial carcinoma. *Nature.* (2013) 497(7447):67–73.

3. Wan YL, Beverley-Stevenson R, Carlisle D, Clarke S, Edmondson RJ, Glover S, et al. Working together to shape the endometrial cancer research agenda: the top ten unanswered research questions. *Gynecol Oncol*. (2016) 143(2):287–93. doi: 10.1016/j.ygyno.2016.08.333

4. Bhaskaran K, Douglas I, Forbes H, dos-Santos-Silva I, Leon DA, Smeeth L. Body-mass index and risk of 22 specific cancers: a population-based cohort study of 5·24 million UK adults. *Lancet*. (2014) 384(9945):755–65. doi: 10.1016/S0140-6736(14)60892-8

5. Lauby-Secretan B, Scoccianti C, Loomis D, Grosse Y, Bianchini F, Straif K. Body fatness and cancer–viewpoint of the IARC working group. *N Engl J Med*. (2016) 375 (8):794–8. doi: 10.1056/NEJMsr1606602

6. Larsson SC, Burgess S. Causal role of high body mass index in multiple chronic diseases: a systematic review and meta-analysis of Mendelian randomization studies. *BMC Med*. (2021) 19(1):320. doi: 10.1186/s12916-021-02188-x

7. Onstad MA, Schmandt RE, Lu KH. Addressing the role of obesity in endometrial cancer risk, prevention, and treatment. *J Clin Oncol*. (2016) 34(35):4225–30. doi: 10.1200/JCO.2016.69.4638

8. Dao MC, Sokolovska N, Brazeilles R, Affeldt S, Pelloux V, Prifti E, et al. A data integration multi-omics approach to study calorie restriction-induced changes in insulin sensitivity. *Front Physiol*. (2018) 9:1958. doi: 10.3389/fphys.2018.01958

9. Langfelder P, Horvath S. WGCNA: an R package for weighted correlation network analysis. *BMC Bioinformatics*. (2008) 9:559. doi: 10.1186/1471-2105-9-559

10. Yoshihara K, Shahmoradgoli M, Martínez E, Vegesna R, Kim H, Torres-Garcia W, et al. Inferring tumour purity and stromal and immune cell admixture from expression data. *Nat Commun*. (2013) 4:2612. doi: 10.1038/ncomms3612

11. Maeser D, Gruener RF, Huang RS. Oncopredict: an R package for predicting in vivo or cancer patient drug response and biomarkers from cell line screening data. *Brief Bioinform*. (2021) 22(6):bbab260. doi: 10.1093/bib/bbab260

12. Yang W, Soares J, Greninger P, Edelman EJ, Lightfoot H, Forbes S, et al. Genomics of drug sensitivity in cancer (GDSC): a resource for therapeutic biomarker discovery in cancer cells. *Nucleic Acids Res*. (2013) 41(Database issue):D955–61. doi: 10.1093/nar/gks1111

13. Crosbie EJ, Kitson SJ, McAlpine JN, Mukhopadhyay A, Powell ME, Singh N. Endometrial cancer. *Lancet*. (2022) 399(10333):1412–28. doi: 10.1016/S0140-6736(22)00323-3

14. Li S, Shi X, Chen M, Xu N, Sun D, Bai R, et al. Angiogenin promotes colorectal cancer metastasis via tiRNA production. *Int J Cancer*. (2019) 145(5):1395–407. doi: 10.1002/ijc.32245

15. Chen W, Lu S, Yang C, Li N, Chen X, He J, et al. Hyperinsulinemia restrains endometrial angiogenesis during decidualization in early pregnancy. *J Endocrinol*. (2019) 243(2):137–48. doi: 10.1530/JOE-19-0127

16. Gao C, Li H, Zhou C, Liu C, Zhuang J, Liu L, et al. Survival-Associated metabolic genes and risk scoring system in HER2-positive breast cancer. *Front Endocrinol*. (2022) 13:813306. doi: 10.3389/fendo.2022.813306

17. Almanza A, Mnich K, Blomme A, Robinson CM, Rodriguez-Blanco G, Kierszniowska S, et al. Regulated IRE1$\alpha$-dependent decay (RIDD)-mediated reprograming of lipid metabolism in cancer. *Nat Commun*. (2022) 13(1):2493. doi: 10.1038/s41467-022-30159-0

18. Lahoz A, Hall A. A tumor suppressor role for srGAP3 in mammary epithelial cells. *Oncogene*. (2013) 32(40):4854–60. doi: 10.1038/onc.2012.489

19. Alshabi AM, Vastrad B, Shaikh IA, Vastrad C. Identification of crucial candidate genes and pathways in glioblastoma multiform by bioinformatics analysis. *Biomolecules*. (2019) 9(5):201. doi: 10.3390/biom9050201

20. Khan FU, Owusu-Tieku NYG, Dai X, Liu K, Wu Y, Tsai HI, et al. Wnt/β-catenin pathway-regulated fibromodulin expression is crucial for breast cancer metastasis and inhibited by aspirin. *Front Pharmacol*. (2019) 10:1308. doi: 10.3389/fphar.2019.01308

21. Chen Y, Jiang T, Zhang H, Gou X, Han C, Wang J, et al. LRRC31 Inhibits DNA repair and sensitizes breast cancer brain metastasis to radiation therapy. *Nat Cell Biol*. (2020) 22(10):1276–85. doi: 10.1038/s41556-020-00586-6

22. Wiegand KC, Lee AF, Al-Agha OM, Chow C, Kalloger SE, Scott DW, et al. Loss of BAF250a (ARID1A) is frequent in high-grade endometrial carcinomas. *J Pathol*. (2011) 224(3):328–33. doi: 10.1002/path.2911

23. Takeda T, Banno K, Okawa R, Yanokura M, Iijima M, Irie-Kunitomi H, et al. ARID1A Gene mutation in ovarian and endometrial cancers (review). *Oncol Rep*. (2016) 35(2):607–13. doi: 10.3892/or.2015.4421

24. Dou Y, Kawaler EA, Cui Zhou D, Gritsenko MA, Huang C, Blumenberg L, et al. Proteogenomic characterization of endometrial carcinoma. *Cell*. (2020) 180 (4):729–48.e26. doi: 10.1016/j.cell.2020.01.026

25. Ledinek Ž, Sobočan M, Knez J. The role of CTNNB1 in endometrial cancer. *Dis Markers*. (2022) 2022:1442441. doi: 10.1155/2022/1442441

26. Gómez-Raposo C, Merino Salvador M, Aguayo Zamora C, de Santiago B G, Sáenz E C. Immune checkpoint inhibitors in endometrial cancer. *Crit Rev Oncol Hematol*. (2021) 161:103306. doi: 10.1016/j.critrevonc.2021.103306

27. Ott PA, Bang YJ, Berton-Rigaud D, Elez E, Pishvaian MJ, Rugo HS, et al. Safety and antitumor activity of pembrolizumab in advanced programmed death ligand 1-positive endometrial cancer: results from the KEYNOTE-028 study. *J Clin Oncol*. (2017) 35 (22):2535–41. doi: 10.1200/JCO.2017.72.5952

28. Marabelle A, Le DT, Ascierto PA, Di Giacomo AM, De Jesus-Acosta A, Delord JP, et al. Efficacy of pembrolizumab in patients with noncolorectal high microsatellite instability/mismatch repair-deficient cancer: results from the phase II KEYNOTE-158 study. *J Clin Oncol*. (2020) 38(1):1–10. doi: 10.1200/JCO.19.02105

29. Marabelle A, Fakih M, Lopez J, Shah M, Shapira-Frommer R, Nakagawa K, et al. Association of tumour mutational burden with outcomes in patients with advanced solid tumours treated with pembrolizumab: prospective biomarker analysis of the multicohort, open-label, phase 2 KEYNOTE-158 study. *Lancet Oncol*. (2020) 21(10):1353–65. doi: 10.1016/S1470-2045(20)30445-9

30. Musacchio L, Caruso G, Pisano C, Cecere SC, Di Napoli M, Attademo L, et al. PARP Inhibitors in endometrial cancer: current Status and perspectives. *Cancer Manag Res*. (2020) 12:6123–35. doi: 10.2147/CMAR.S221001

31. Banerjee S, Moore KN, Colombo N, Scambia G, Kim BG, Oaknin A, et al. Maintenance olaparib for patients with newly diagnosed advanced ovarian cancer and a BRCA mutation (SOLO1/GOG 3004): 5-year follow-up of a randomised, double-blind, placebo-controlled, phase 3 trial. *Lancet Oncol*. (2021) 22(12):1721–31. doi: 10.1016/S1470-2045(21)00531-3

frontiers | Frontiers in Oncology

TYPE Systematic Review
PUBLISHED 30 January 2023
DOI 10.3389/fonc.2023.1083285



OPEN ACCESS

EDITED BY
Marek Minarik,
Elphogene, s.r.o, Czechia

REVIEWED BY
Manuela Gariboldi,
Fondazione IRCCS Istituto Nazionale Tumori, Italy
Dalong Pang,
Georgetown University, United States

*CORRESPONDENCE
Jan M. van Rees
j.vanrees@erasmusmc.nl

SPECIALTY SECTION
This article was submitted to Surgical Oncology, a section of the journal Frontiers in Oncology

RECEIVED 28 October 2022
ACCEPTED 09 January 2023
PUBLISHED 30 January 2023

CITATION
van Rees JM, Wullaert L, Grüter AAJ, Derraze Y, Tanis PJ, Verheul HMW, Martens JWM, Wilting SM, Vink G, van Vugt JLA, Beije N and Verhoef C (2023) Circulating tumour DNA as biomarker for rectal cancer: A systematic review and meta-analyses.
*Front. Oncol.* 13:1083285.
doi: 10.3389/fonc.2023.1083285



# Circulating tumour DNA as biomarker for rectal cancer: A systematic review and meta-analyses

Jan M. van Rees[1]*, Lissa Wullaert[1], Alexander A. J. Grüter[2], Yassmina Derraze[2], Pieter J. Tanis[1], Henk M. W. Verheul[3], John W. M. Martens[3], Saskia M. Wilting[3], Geraldine Vink[4,5], Jeroen L. A. van Vugt[1], Nick Beije[3] and Cornelis Verhoef[1]

[1]Department of Surgical Oncology and Gastrointestinal Surgery, Erasmus MC Cancer Institute, Rotterdam, Netherlands, [2]Department of Surgery, Amsterdam University Medical Centres (UMC), Vrije Universiteit Amsterdam, Department of Surgery, Cancer Center Amsterdam, Amsterdam, Netherlands, [3]Department of Medical Oncology, Erasmus MC Cancer Institute, Rotterdam, Netherlands, [4]Department of Medical Oncology, University Medical Center Utrecht, Utrecht University, Utrecht, Netherlands, [5]Department of Research and Development, Netherlands Comprehensive Cancer Organisation, Utrecht, Netherlands

**Background:** Circulating tumour DNA (ctDNA) has been established as a promising (prognostic) biomarker with the potential to personalise treatment in cancer patients. The objective of this systematic review is to provide an overview of the current literature and the future perspectives of ctDNA in non-metastatic rectal cancer.

**Methods:** A comprehensive search for studies published prior to the 4th of October 2022 was conducted in Embase, Medline, Cochrane, Google scholar, and Web of Science. Only peer-reviewed original articles and ongoing clinical trials investigating the association between ctDNA and oncological outcomes in non-metastatic rectal cancer patients were included. Meta-analyses were performed to pool hazard ratios (HR) for recurrence-free survival (RFS).

**Results:** A total of 291 unique records were screened, of which 261 were original publications and 30 ongoing trials. Nineteen original publications were reviewed and discussed, of which seven provided sufficient data for meta-analyses on the association between the presence of post-treatment ctDNA and RFS. Results of the meta-analyses demonstrated that ctDNA analysis can be used to stratify patients into very high and low risk groups for recurrence, especially when detected after neoadjuvant treatment (HR for RFS: 9.3 [4.6 – 18.8]) and after surgery (HR for RFS: 15.5 [8.2 – 29.3]). Studies investigated different types of assays and used various techniques for the detection and quantification of ctDNA.

**Conclusions:** This literature overview and meta-analyses provide evidence for the strong association between ctDNA and recurrent disease. Future research should focus on the feasibility of ctDNA-guided treatment and follow-up strategies in rectal cancer. A blueprint for agreed-upon timing, preprocessing, and assay techniques is needed to empower adaptation of ctDNA into daily practice.

KEYWORDS

**Ctdna (circulating tumour DNA), cfDNA (circulating free DNA), rectal cancer, minimal residual disease (MRD), liquid biopsy**

# Introduction

Rectal cancer is a worldwide cause of cancer-related mortality, with a global incidence of approximately 732,200 new cases per year (1). The introduction of combined neoadjuvant (chemo)radiotherapy and total mesorectal excision (TME) has significantly reduced the local recurrence rate, though distant recurrence rates remain around 30% (2). Recurrences are likely to derive from residual locoregional disease after surgery or subclinical metastatic disease (minimal residual disease) (3). These micrometastases are undetectable by the currently used imaging techniques. Carcinoembryonic antigen (CEA) is a widely accepted tumour marker in the follow-up of colorectal cancer, but is imperfect due to the limited accuracy of this test to detect recurrence, mostly owing to its high rate of false positive results (4, 5). Consequently, there is an urgent need for novel techniques to detect minimal residual disease after standard treatment, in order to identify those patients who are at high risk for recurrent disease.

Classification of these patients would enable a 'tailored' postoperative treatment approach, in which patients could be stratified into groups who may benefit from additional treatment or, otherwise, less intensive surveillance.

Circulating tumour DNA (ctDNA) is a component of the total amount of cell-free DNA (cfDNA), and it presumed that this ctDNA is shed into the bloodstream by necrotising cancer cells. Measurement of ctDNA in peripheral blood samples has been established as a promising biomarker, with the potential to optimise tailored treatment in cancer patients (6–8). In recent years, ctDNA has been investigated in various cancer types and settings, and is considered to be an important diagnostic tool for the detection of minimal residual disease after surgery. The potential clinical utility of ctDNA has already been established in certain fields. In stage II colon cancer, ctDNA-guided treatment resulted in a reduction in the number of patients receiving adjuvant therapy when compared to conventional stratification methods, whilst not altering the risk of recurrence (9). For rectal cancer, research establishing the true clinical value of ctDNA-guided treatment has yet to be conducted. In addition, there is still a lack of consensus whether the use of adjuvant chemotherapy is justified in rectal cancer patients, and postoperative treatment regimens differ per country (10, 11).

During curative treatment of rectal cancer, there are several methods and time points when ctDNA could be measured in peripheral blood samples. At diagnosis and before any treatment, the amount of ctDNA could be associated with the extent of the disease. During or after neoadjuvant treatment, changes in the level ctDNA could be associated with response or progression. Finally, the presence of ctDNA after surgery is an indication of minimal residual disease. The conceivable added value of ctDNA in rectal cancer is its potential application as a guide for therapy selection. Herein, patients who are stratified as high-risk for recurrence could, for example, be treated with adjuvant systemic therapy, while patients without detectable ctDNA after neoadjuvant treatment and surgery might be suitable for less intensive follow-up regimes.

In literature, several methods have been described to analyse the presence of ctDNA in peripheral blood samples, with different recommendations regarding pre-analytical conditions (12–14). In rectal cancer, two main ctDNA detection techniques are measuring the absolute number of cfDNA or identifying tumour-specific somatic mutations (15). These mutations are usually detected using polymerase chain reaction (PCR) or next-generation sequencing (NGS). Although PCR is a viable option to detect a small number of already known somatic mutations, the main advantage of NGS is the possibility to interrogate multiple genes at once, and it does not necessarily require prior knowledge of a specific mutation profile. Both techniques could either be applied to the unique mutations of the patient's tumour (i.e., *tumour-informed with specific panel*) or to a universal panel of genes commonly mutated in (colorectal) cancer patients (i.e., *tumour-agnostic*). Finally, a universal panel could be used that is evaluated by the patients' tumour tissue (i.e., *tumour-informed with predefined panel*). Given the heterogeneity in measurement techniques of ctDNA, a summary of the applied techniques in previous studies may provide insight in suitable approaches for specific purposes.

The aim of this literature review is to provide an overview of the current evidence and ongoing trials in the field of ctDNA in non-metastatic rectal cancer.

# Methods

This systematic review and meta-analyses were conducted according to the PRISMA guidelines (Preferred Reporting Items for Systematic Reviews and Meta-analysis). A comprehensive search was performed in five databases (Embase, Medline, Cochrane, Web of Science and Google Scholar), including potential studies published prior to the 4$^{th}$ of October 2022. Only English-written, peer-reviewed clinical studies that investigated the association between ctDNA and oncologic outcomes in non-metastatic rectal cancer patients were included. Non-original articles (i.e. review articles and meta-analyses) and case reports were excluded. The complete search term performed on the 4$^{th}$ of October 2022 is shown in Supplementary 1.

## Study selection and quality assessment

Screening of the articles was performed by two independent authors (JR, LW) and disagreement was resolved through joint assessment and in collaboration with a third reviewer (NB). Quality assurance was performed by two individual reviewers (JR, LW) according to the Quality In Prognosis Studies tool (QUIPS) (16). Three categories of risk of bias were considered as the outcome of the QUIPS tool, being low, moderate and high risk of bias. The outcomes of the quality assessment using the QUIPS tool were visualised using the Risk-of-bias VISualization (robvis) tool (17). In case of disagreement, joint evaluation was performed, and a third reviewer (SW) was approached when deemed necessary. Study characteristics like study design, sample size and specifications about the ctDNA assessment (collection time points, target, assay type, quantification method, whether the technique was NSG or PCR based and whether it was tumour informed) were collected.

## Meta-analyses

Meta-analyses were performed using the generic inverse-variance method using a random-effects model. Herein, only studies that reported hazard ratios with either confidence intervals or p-values, for recurrence-free survival (RFS) or disease-free survival (DFS) were included. Studies that did not report appropriate or sufficient data for the pooled analysis were separately discussed. Outcomes of interest included: hazard ratios (HR), 95% confidence intervals (CI), $I^2$ values for heterogeneity, and p-values, in which a value <0.05 was considered statistically significant. Meta-analyses and figures were established from Review Manager (RevMan) version 5.4.1, The Cochrane Collaboration, 2020.

# Results

A total of 480 records were retrieved by the systematic search, of which 189 were duplicates, 261 were original publications and 30 were ongoing trials (Figure 1). All 291 unique studies and trials were screened for eligibility, after which 270 publications were excluded by reading title and abstract. Reasons for exclusion were reports of conference abstracts, case reports, (systematic) reviews, studies that did not include patients with rectal cancer, and studies that had not investigated clinical outcomes. The full text of twenty-one studies was assessed, of which two additional studies were excluded due to a lack of distinction between colon and rectal cancer, and due to an analysis of circulating tumour cells, which was ineligible for the current meta-analysis. A total of nineteen studies is discussed in this literature review, of which seven were included in the meta-analysis. For each included study a quality assurance was performed according to the QUIPS tool, as shown in Supplementary 2. Study characteristics, including outcome measures and the number of patients, are reported in Table 1.

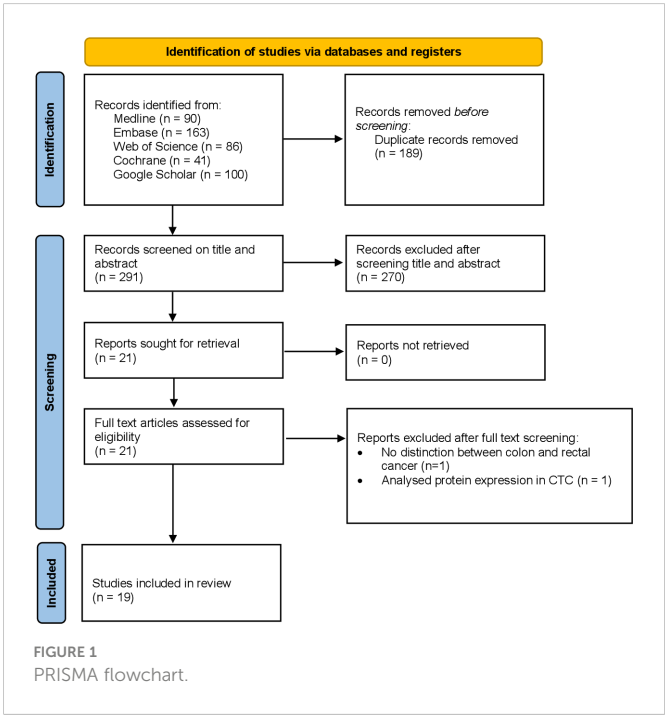


FIGURE 1
PRISMA flowchart.

Nine out of nineteen (47%) included studies were considered high risk of bias, six (32%) received a low risk of bias score, and four studies (22%) a moderate risk of bias. High risk of bias was mostly due to bias in prognostic factor measurement and attrition, as depicted in the graph in Supplementary 3. ctDNA measurement techniques varied greatly among included studies. Most frequently used quantification methods were digital droplet PCR (ddPCR), real time PCR (qRT-PCR) and next generation sequencing (NGS). Five studies designed their panel based on the unique tumour and patient (tumour informed – tumour specific). Four studies applied a tumour informed predefined panel, and ten adopted a tumour agnostic approach. Liu et al. investigated multiple ctDNA techniques (22). All studies in this review only included patients with locally advanced rectal cancer (LARC). No eligible studies were found that included non-LARC patients.

## Original articles

All included studies were either prospective or retrospective cohort studies. A total of 1598 patients undergoing treatment for LARC were included, with sample sizes ranging from 25 to 159 patients. The methods for ctDNA analyses (assay type, quantification method, tumour-informed or -agnostic) are described in Table 1. Twelve studies (63%) used a mutation-specific panel, of which nine were tumour-informed. Seven other studies measured total cfDNA concentration. Nine studies quantified ctDNA with a PCR-based technique. NGS was the chosen technique in eight studies, and another two studies used the direct fluorescent assay (dFA). Time points at which ctDNA was measured varied, and are reported from baseline (defined as before the start of any treatment) up until last follow-up after definite treatment. Additional details regarding plasma isolation, cfDNA isolation, and pre-processing conditions can be found in Supplementary 4.

## ctDNA and treatment outcomes in rectal cancer (cfDNA concentration studies)

The earliest study in the systematic search reporting clinical outcomes, published in 2008, investigated changes in cfDNA levels before and after neoadjuvant chemoradiation in patients with LARC using quantitative real-time polymerase chain reaction (qRT-PCR) (18). No association was found between baseline cfDNA levels and tumour response, but the study showed that patients who responded to chemoradiation had a decrease in cfDNA levels (median 2.2 ng/mL), whereas in patients without response, cfDNA levels significantly increased (median 5.1 ng/mL) (P = 0.006). The authors concluded that cfDNA concentration could be used for therapy monitoring in patients with rectal cancer undergoing preoperative chemoradiation, and these findings were repeatedly confirmed in several other exploratory studies (19–21, 36).

10.3389/fonc.2023.1083285

TABLE 1 Study characteristics.

| Author, year | Study design | Patients | Assay type | NSG / PCR | Tumour informed | Time points (s) | Outcome (binary) | Risk of Bias |
|---|---|---|---|---|---|---|---|---|
| Zitt et al. (18) | Prospective cohort, single centre | LARC, 26 | cfDNA concentration | PCR | Agnostic | BL, post-CRT, end treatment | Treatment response | High |
| Agostini et al. (19) | Prospective pilot study | LARC, 67 | cfDNA concentration | PCR | Agnostic | BL, post-CRT | Treatment response | High |
| Sun et al. (20) | Prospective cohort, single centre | LARC, 34 | Multiple | PCR | Agnostic | BL, post-CRT | Treatment response | High |
| Boysen et al. (21) | Retrospective cohort | LARC, 75 | cfDNA concentration | PCR | Agnostic | Post-CRT | Both | High |
| Liu et al. (22) | Prospective cohort, multicentre | LARC, 82 | Mutation-specific panel | NGS | Both | During and post-NAT | Long-term (oncologic) survival | Low |
| Sclafani et al. (23) | Prospective cohort, multicentre | LARC, 97 | Mutation-specific panel | PCR | Tumour informed (predefined panel) | BL | Both | High |
| Schou et al. (24) | Prospective cohort, single centre | LARC, 123 | cfDNA concentration | dFA | Agnostic | BL, after induction chemotherapy, after CRT, serial samples 5 years after surgery | Long-term (oncologic) survival | High |
| Tie et al. (25) | Prospective cohort, multicentre | LARC, 159 | Mutation-specific panel | NGS | Tumour informed (tumour specific) | BL, post-CRT, post-surgery | Long-term (oncologic) survival | Low |
| Appelt et al. (26) | Prospective cohort, multicentre | LARC, 146 | cfDNA concentration | PCR | Agnostic | BL | Long-term (oncologic) survival | High |
| Guo et al. (27) | Unknown | LARC, 194 | Promoter genes | NGS | Agnostic | BL | Treatment response | High |
| Khakoo et al. (28) | Prospective cohort, single centre | LARC, 47 | Mutation-specific panel | PCR | Tumour informed (tumour specific) | BL, mid CRT, post-CRT, after surgery | Both | Low |
| Murahashi et al. (29) | Prospective cohort, single centre | LARC, 85 | Mutation-specific panel | NGS | Agnostic | BL, post-NAT, post-surgery | Both | Moderate |
| Pazdirek et al. (30) | Prospective cohort, single centre | LARC, 36 | Mutation-specific panel | PCR | Tumour informed (predefined panel) | BL, during CRTx | Long-term (oncologic) survival | Moderate |
| Zhou et al. (31) | Prospective cohort, multicentre | LARC, 106 | Mutation-specific panel | NGS | Tumour informed (tumour specific) | BL, during CRT, presurgery, and postsurgery | Long-term (oncologic) survival | Low |
| McDuff et al. (32) | Retrospective cohort | LARC, 29 | Mutation-specific panel | PCR | Tumour informed (tumour specific) | BL, preoperatively, and postoperatively | Both | Moderate |
| Vidal et al. (33) | Prospective cohort, multicentre | LARC, 119 | Mutation-specific panel | NGS | Agnostic | BL, during nCRT, and after surgery | Both | Moderate |
| Wang et al. (34) | Prospective cohort, single centre | LARC, 72 | Mutation-specific panel | NGS | Tumour informed (predefined panel) | BL, post-NAT | Both | Low |
| Roesel et al. (35) | Prospective cohort, multicentre | LARC, 25 | Mutation-specific panel | NGS | Tumour informed (predefined panel) | T0: first day of radiotherapy<br>Tend: last day of radiotherapy<br>T4: 4 weeks after radiotherapy<br>T7: 7 weeks after radiotherapy<br>Top: day of surgery<br>Tpost-op: 3-7 days after surgery<br>TIMV: mesenteric vein sample during surgery | Treatment response | Low |

*(Continued)*

TABLE 1 Continued

| Author, year | Study design | Patients | Assay type | NSG / PCR | Tumour informed | Time points (s) | Outcome (binary) | Risk of Bias |
|---|---|---|---|---|---|---|---|---|
| Truelsen et al. (36) | Prospective cohort, single centre | LARC, 76 | cfDNA concentration | dFA | Agnostic | BL, mid therapy and at end of therapy | Treatment response | High |

BL, baseline; cfDNA, cell-free DNA; CRT, chemoradiotherapy; dFA, direct fluorescence assay; LARC, locally advanced rectal cancer; NAT, neoadjuvant treatment; NSG, next generation sequencing; PCR, polymerase chain reaction.

## ctDNA and long-term oncologic survival outcomes in rectal cancer (cfDNA concentration studies)

Besides the use of cfDNA for response outcomes, cfDNA was investigated as predictor for long-term (oncological) outcomes as well. In 2017, Boysen et al. were the first to find an association between the level of pre-surgery cfDNA and the risk of recurrence after surgery (21). In this study including 75 patients with LARC, the level of cfDNA was quantified by ddPCR and expressed as copy number of beta 2 microglobulin. The median levels of cfDNA for patients with recurrent disease were 13,000 copies/mL compared to 5200 copies/mL for non-recurrent patients (p = 0.08).

In line with this, Schou et al. demonstrated, in a study with 123 participants, that patients with baseline cfDNA levels above the 75th quartile measured by a direct fluorescent assay, had a higher risk of local or distant recurrence and shorter time to recurrence compared with patients with plasma cfDNA below the 75th percentile (HR = 2.48, 95% CI: 1.3–4.8, P = 0.007) (24). The same applied to DFS (HR = 2.43, 95% CI: 1.27–4.7, P = 0.015). In a subgroup analysis with 71 patients who received induction chemotherapy (capecitabine and oxaliplatin (CAPOX)) before chemoradiation, the prognostic impact of plasma levels of cfDNA remained significant for time to recurrence and DFS. In multivariate analysis, a high cfDNA level was significantly associated with time to progression and DFS. During follow-up, the association remained significant regardless of time point for sample analysis.

Finally, Appelt et al. found that fractional abundance of hypermethylation of the neuropeptide Y gene in cfDNA (meth-cfDNA), could be used as baseline prognostic marker as well (26). They showed in 146 LARC patients that meth-cfDNA, determined by quantitative PCR on baseline, was associated with a significantly worse overall survival (adjusted HR: 2.08, 95% CI: 1.23-1.51) and distant metastases rate (55% *vs*. 72% at 5 y, p=0.01).

## ctDNA and long-term oncologic survival outcomes in rectal cancer (mutation-specific assay studies)

While multiple studies described the prognostic value of cfDNA concentrations, an important downside is that these assays lack the ability to discriminate between cfDNA from healthy cells and cfDNA directly derived from the tumour (ctDNA). Especially in the context of MRD detection, there is a need for tests with high specificity.

Therefore, in recent years, more and more studies utilising techniques that can specifically detect ctDNA have increasingly been described (22, 25, 28–35). The largest study conducted so far by Tie et al., including 159 patients with LARC, has demonstrated that ctDNA status could be used to classify groups as very high and low risk for recurrence (25). Somatic mutations in individual patient's tumours were identified *via* massively parallel sequencing of 15 genes commonly mutated in colorectal cancer, after which personalised assays were designed to quantify ctDNA in plasma samples. Prior to neoadjuvant (chemo)radiotherapy 122 (77%) patients had detectable ctDNA. After surgery, 19 patients (12%) had detectable ctDNA of which 58% recurred during follow-up (median 24 months). In contrast, recurrence occurred in only 8.6% of the patients without detectable ctDNA (HR 13, 95% CI 5.5-31, p<0.001). The prognostic value of detectable ctDNA for recurrence was even stronger in patients with a high pathological stage (ypT3-4 and ypN1-2), demonstrated by recurrence rates up to 89% after 2 years in patients with detectable ctDNA after surgery combined with pathologically staged lymph node metastases. This study also showed that the predictive value of ctDNA was strong when measured after treatment. No difference in RFS was observed between patients with detectable ctDNA and those without detectable ctDNA before treatment (HR 1.1; 95% CI: 0.42 - 3.0). However, for the post-treatment measurements, the Kaplan-Meier estimates of RFS at 3 years were 50% (95% CI: 28% - 88%) and 85% (95% CI: 79% - 93%) for the postchemoradiation ctDNA-positive and ctDNA-negative groups respectively, and 33% (95% CI: 16% - 72%) and 87% (95% CI: 79% - 95%) for the postoperative ctDNA-positive and ctDNA-negative groups. This study also demonstrated that postoperative CEA (≥5.0 ng/ml) was also a predictor for recurrence (adjusted HR 5.1, 95% CI: 1.3 - 18), but that in patients with normal CEA, postoperative detectable ctDNA remained associated with a high risk of recurrence (HR 8.8, 95% CI 3.2 – 24; P<0.001).

Another prospective multicentre study also investigated the predictive value of ctDNA analysed by targeted NGS at different time points before and during treatment in 106 LARC patients undergoing chemoradiation (31). Mutations in cfDNA were only called as somatic mutations if these mutations were also present in the primary tumour, which was also subjected to targeted NGS. ctDNA was detected in 75% of patients at baseline, 16% during chemoradiation, 11% before surgery, and 7% after surgery. Again, detectable ctDNA after surgery was the strongest predictive factor for distant metastasis (HR 25.30, 95% CI 1.475-434.0), compared to one cycle after the initiation of chemoradiation (HR 6.635, 95% CI: 1.240-35.50), and 7 weeks after chemoradiation (before surgery) (HR 19.82, 95% CI: 2.029-193.7). However, these subgroup analyses were underpowered (only 6 patients had detectable ctDNA in the postoperative ctDNA group).

Khakoo et al. investigated the role of ctDNA by tracking up to three somatic variants that were found in tumour tissue in plasma using ddPCR in patients with LARC (28). They showed that all three

patients with detectable ctDNA after surgery had recurrent disease compared with none of the 20 patients with undetectable ctDNA (P = 0.001). Similar results were found in a study conducted by McDuff et al. (32) In this study, NGS was used to identify mutations in the primary tumour, and mutation-specific ddPCR were used to assess mutation fraction in ctDNA. The study found that all four LARC patients with detectable postoperative ctDNA recurred (positive predictive value = 100%), whereas only two of 15 patients with undetectable ctDNA recurred (negative predictive value: 87%). The hazard ratio for RFS at a median follow-up of 20 month was 12 in patients with detectable postoperative ctDNA (P = 0.007). Another study of 119 LARC patients demonstrated that post-operative ctDNA testing with a tumour-agnostic customised NGS panel targeting 422 cancer-related genes, in combination with a high-risk pathological feature (perineural invasion, tumour deposits, vascular invasion, and lymph node metastasis), was able to predict the recurrence of all six patients that were analysed in this risk group (HR 90, 95% CI: 17 – 479 compared to undetectable ctDNA and no high risk features) (34).

Another prospective cohort study conducted by Murahashi et al. used NGS on a cfDNA panel with 14 target genes to investigate the association of ctDNA on preoperative treatment response and postoperative recurrence in 85 LARC patients (29). A significant association was found between changes in ctDNA before and after neoadjuvant treatment (≥80% change in cfDNA versus < 80% change in cfDNA) and pathological complete response (OR 8.5; 95% CI: 1.4–163). In addition, the rate of recurrent disease was significantly higher in patients with high levels of postoperative ctDNA (≥0.5%) than in those with low levels of ctDNA (<0.5%) (HR 17.1, 95% CI: 1.0-282). In this study, postoperative CEA (≥5.0 ng/ml) was also independently associated with recurrence (adjusted HR: 6.9, 95% CI 1.6–29), and all four patients that had a combination of detectable ctDNA and CEA had disease relapse (HR: 34, 95% CI: 0.4 - 2631).

The phase II GEMCAD 1402 study, including 72 patients with LARC undergoing total neoadjuvant treatment (fluorouracil, leucovorin, and oxaliplatin with or without aflibercept, followed by chemoradiation and surgery), also evaluated ctDNA as biomarker to predict tumour response and survival outcome (33). ctDNA was detectable using a tumour-agnostic CRC-specific NGS assay (Guardant reveal) integrating somatic mutations and epigenomic signatures in 83% of patients at baseline and in 15% following total neoadjuvant treatment (pre-surgery). Baseline ctDNA detection was not associated with poor survival outcomes, but detectable ctDNA just before surgery (after total neoadjuvant treatment) was significantly associated with systemic recurrence, shorter DFS (HR, 4; P = 0.033), and shorter overall survival (HR, 23; P < 0.0001). The predictive value of detectable ctDNA after surgery was not investigated in this study.

Finally, an exploratory study by Liu et al. analysed three different ctDNA techniques in LARC patients in samples taken after neoadjuvant treatment (22). The three ctDNA assays were: 1. a tumour-informed personalized assay, 2. a tumour-agnostic targeted assay of genes frequently mutated in CRC, and 3. a copy number alteration-based approach. All three investigated techniques were associated with a poor RFS. The personalised assay targeting tumour-informed mutations was significantly associated with an increased risk of recurrence (HR = 27.38; log-rank P < 0.0001), the universal panel of genes frequently mutated in colorectal cancer (HR = 5.18; log-rank P = 0.00086), and the low depth sequencing for copy number alterations (CNAs) analysis showed a compromised performance in predicting recurrence (HR = 9.24; log-rank P = 0.00017). Of note, this study was not powered to detect differences between the three assays.

## Alternative cfDNA and ctDNA techniques

Alternative methods to enable the use of cfDNA in clinical practice have been described as well. Guo et al. analysed gene promoter coverage in cfDNA of 20 patients with LARC (both 10 patients with- and without pathological complete response), in order to predict tumour expression status and subsequently patients' response to chemoradiation (27). Thus, this study did not investigate mutations (ctDNA), but determined the relative coverage of gene promoter regions in the cfDNA. In a letter to the editor, they propose a classifier of promoters with differential coverage between cfDNA of patients with and without pathological complete response, and validated the use of this prediction technique in 194 LARC patients. The classifier resulted in an AUC of 0.89 (0.83-0.94) to discriminate patients with and without pathological response, but no external validation of this classifier was performed.

Sclafani et al. used ctDNA to assess KRAS/BRAF mutations in baseline blood samples from 114 patients with LARC, and compared these to mutations in tumour tissue (23). Notably, in 26 patients the ctDNA analysis revealed a KRAS mutation that was not previously found in tumour tissue using standard PCR-based techniques. However, a more sensitive technique (ddPCR) and additional analysis of a different tissue section revealed that 22 of these 26 "newly" detected plasma mutations were already detectable in the tumour in hindsight. In this study, no association between the presence of KRAS/BRAF in ctDNA and clinical outcomes was found.

## Meta-analyses

The association between recurrence-free survival and: 1) the presence of ctDNA after neoadjuvant treatment (chemoradiation with or without systemic treatment), 2) the presence of ctDNA after curative intent surgery were investigated in meta-analyses. Results are summarised in Figures 2, 3. The pooled hazard ratio for ctDNA presence after neoadjuvant treatment was 9.26 (95% CI: 4.56 – 18.84) compared to those patients who were without detectable ctDNA after neoadjuvant treatment. After surgery, patients with detectable ctDNA had increased risk for recurrence, compared to patients without detectable ctDNA (HR 15.54, 95% CI: 8.23 – 29.34).

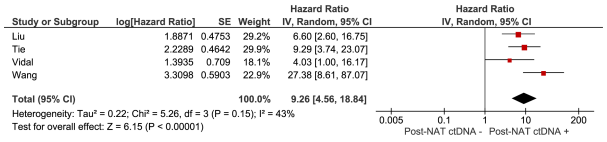


FIGURE 2
Meta-analysis of the association between recurrence-free survival and the presence of ctDNA after neoadjuvant treatment (chemoradiation with or without systemic treatment).

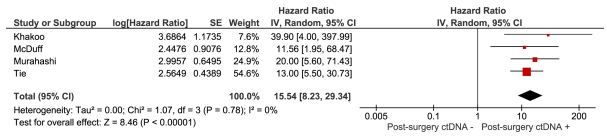


FIGURE 3
Meta-analysis of the association between recurrence-free survival and the presence of ctDNA after curative intent surgery.

## Ongoing ctDNA trials in rectal cancer

Two interventional trials were found in the systematic search investigating the use of ctDNA in patients with rectal cancer, being the DYNAMIC-RECTAL trial (ACTRN12617001560381) and the SYNCOPE study (NCT04842006). The aim of the DYNAMIC-RECTAL trial was to randomise 408 patients to either a ctDNA-informed arm and a standard of care arm (37). In the ctDNA-informed arm, patients would receive adjuvant chemotherapy if ctDNA was detected, or a not detected in the presence of a high-risk tumour (based on the standard pathology risk assessment of the tumour). In the standard of care arm, the decision regarding adjuvant chemotherapy was based on the standard pathology risk assessment of the tumour. Recruitment of this study terminated early, as accrual slowed down due to the COVID-19 pandemic and the total neoadjuvant treatment approach in this population was adopted. Therefore, the target number could not be reached within the planned recruitment period.

The SYNCOPE study randomises 93 rectal cancer patients into a group of patients that will be treated with novel precision methods, being ctDNA and organoid-guided adjuvant therapy, and a group of patients that will undergo conventional treatment strategy. Primary outcomes are RFS and the number of patients with detectable ctDNA in the postoperative sample of patients in the conventional treatment arm who are not assigned to chemotherapy.

# Discussion

The aim of this literature review was to provide an overview of the current evidence and ongoing trials in the field of ctDNA in non-metastatic rectal cancer. Studies have consistently shown the strong association between detectable ctDNA after treatment and unfavourable prognosis. It can be concluded from these results that ctDNA analysis from peripheral blood samples, especially detected after surgery with curative intent, stratifies patients into two groups: one with a very high risk for recurrence, another with a low risk for recurrence. Thus far, there are no rectal cancer trials published, that have investigated ctDNA-guided adjuvant treatment in a randomised setting.

Based on our systematic search, this systematic review is the first to pool long-term oncological survival outcomes in a meta-analysis. A systematic review by Boyson et al. included nine single arm studies with a total of 615 patients undergoing chemoradiation for rectal cancer and investigated the relation between ctDNA and clinical outcomes (15). Eight of the nine studies showed some degree of correlation between ctDNA and either response to chemoradiation, risk of recurrence or disease-free survival. A second systematic review also included nine studies and investigated the association between clinical outcomes and ctDNA at different time points (at diagnosis, after chemoradiation, and after surgery) (38). No association was found between treatment response and ctDNA status at baseline. Studies reporting the prognostic impact of ctDNA after chemoradiation and before surgery showed varying results. All five studies reporting outcomes of detectable ctDNA postoperative and clinical outcomes, found an association between ctDNA positivity after surgery and worse survival. This review demonstrated that post-operative ctDNA is the most predictive prognostic factor of all investigated time points. A third systematic review investigating different ctDNA measurement techniques on predictive and prognostic outcomes in LARC patients, concluded that detection of ctDNA at different time points of treatment was consistently associated with worse prognosis, but that the ideal method and timing for the liquid biopsy still needed to be defined (39).

Although all studies found a positive correlation between ctDNA and treatment and oncological outcomes, various methods to analyse ctDNA were used, including those with quantitative (e.g. absolute cfDNA concentration) and qualitative (tumour-specific somatic mutations) measurements. Articles that utilized quantitative analyses were generally published between 2008-2018, and were considered relatively inferior because quantitative tests do not have the ability to discriminate tumour DNA from physiological circulating DNA from non-cancerous cells. More recent studies often used qualitative techniques that are able to specifically detect tumour-specific cfDNA. These mutation-specific analyses are nowadays considered as technique of choice, and are acceptable in terms of costs (40). Differences in qualitative analyses exist as well, as was shown as shown by Liu et al. (22) This study revealed that minor differences in the sensitivity of ctDNA are observed when different gene panels and techniques for ctDNA quantification are used, in which a personalised assay targeting tumour-informed mutations was suggested to yield the best performance. However, tumour-informed assays are more expensive and labour-intensive as they require sequencing of the tumour and subsequent design of tumour-specific assays. This can be challenging, especially in a setting where the turnaround time for clinical decision-making needs to be short and will be accompanied by higher costs. A tumour-agnostic method is likely to have a faster turnaround time, as it is easier to conduct, and is accompanied by lower costs. Currently, well-powered studies in a real-world setting comparing all assays with regard to its sensitivity, specificity and turnaround time are lacking.

Another controversy in ctDNA analysis is the optimal timing of measurement to detect MRD after surgery, as it has been suggested that an abundance of surgery-induced cfDNA fragments could hamper the detection of ctDNA from the tumour (41). In a study by Hendriksen et al., it was shown that cfDNA levels in patients with colorectal cancer were increased by threefold during the first week after surgery (median 3.6-fold increase, mean: 4.0, 95% CI 2.90–5.37, P = 0.0005), and slowly decreased over the next 3 weeks. Notably, it was assumed that in five of the eight patients, ctDNA was falsely measured as being negative, as these patients were ctDNA positive in all other measurements in which ctDNA surgery-induced cfDNA fragments were not increased. Therefore, to maximize sensitivity of the measurement, one could argue to only measure ctDNA at least

four weeks after surgery. On the other hand, when the results of the ctDNA analyses have clinical consequences, e.g. ctDNA-based adjuvant therapy, results ought to be known within the timeframe that consolidation treatment will still be sufficient. Typically, most ctDNA assays are accompanied by an additional four weeks turnover time from blood withdrawal to definite results (42), so the typical timeframe of a maximum of 8 or 12 weeks from surgery to start with adjuvant treatment could be endangered when delaying the ctDNA result too long (43–45). A balance between test sensitivity, and considerations regarding turnaround times inherent to different methods, should be considered for each clinical implication and setting.

Precision biomarkers to predict postoperative outcomes, such as ctDNA, could contribute to the ongoing debate whether additional treatment should be considered after rectal cancer surgery. The role of adjuvant systemic treatment in rectal cancer has not been established globally; practice differs between Europe and the USA, and between European countries as well. In the Netherlands, adjuvant chemotherapy is not recommended for any stage (46). There are only a few randomised controlled trials on adjuvant chemotherapy for rectal cancer available, which yielded conflicting results (47). The fact that the benefit of adjuvant chemotherapy has not yet been demonstrated, is likely related to a dilution effect, and it might very well be true that a subgroup of patients will benefit from additional treatment. Therefore, it would certainly be of interest to explore whether high-risk patients based on ctDNA detected in postoperative peripheral blood samples might benefit from adjuvant treatment. A trial randomising patients with detectable ctDNA into an adjuvant treatment group and a follow-up group is warranted. Such a trial should be able to answer the important question whether ctDNA-guided adjuvant treatment is beneficial in rectal cancer.

Another potential opportunity of ctDNA-guided treatment is the ability to tailor follow-up strategies based on patients' individual risk of recurrence. As intensive follow-up does not appear to improve overall and cancer-specific survival and quality of life in colorectal cancer, there seems to be an incentive to reduce surveillance after curative surgery (46, 48, 49). Studies have demonstrated that ctDNA outperforms CEA in (colo)rectal cancer patients to detect relapsing disease (5, 25, 31, 50). Therefore, ctDNA-based risk prediction for recurrence may very well be an excellent biomarker to stratify patients without detectable DNA into a less intensive and decentralised surveillance programme in the home environment or even earlier discharge of standard follow-up. This could eventually improve health-related quality of life, cause a reduction in health-related and societal costs as well as anxiety in cancer patients, without compromising oncological outcomes. Further research would be needed to investigate whether this ctDNA-guided follow-up approach is feasible in rectal cancer.

Finally, novel technical advances highlight the promise of several tumour-agnostic ways to detect ctDNA (i.e. without prior tissue-based information) in the future. For example, recent results highlight the merit of circulating cell free (cf)DNA methylation analyses for both detection and classification of many cancer types, including colorectal cancer (51–54). Next to methylation profiling, recently discovered "fragmentomics" also shows great promise for the sensitive detection of cancer using cfDNA (55–57). Both cfDNA methylation profiling and fragmentomics capture information from a much broader spectrum of the circulating tumour genome, theoretically enabling a higher analytical sensitivity for the detection of minute traces of ctDNA in case of MRD. Supporting this notion, combining features from different molecular levels was shown to have complementary value for MRD detection in colorectal cancer (58).

In conclusion, in rectal cancer patients treated with neoadjuvant treatment and surgery, a very strong association was found between post-treatment detectable ctDNA and recurrent disease as well as overall survival. Randomised controlled trials are needed to investigate whether this ctDNA-informed risk classification could be used during clinical decision making for the purpose of patient-tailored treatment.

## Data availability statement

The original contributions presented in the study are included in the article/Supplementary Material. Further inquiries can be directed to the corresponding author.

## Author contributions

All authors have significantly contributed to this work. JR, LW, AG, YD, CV, NB were involved in writing the introduction, the systematic search, and the article selection process. JR, LW, NB, JV, SW conducted the quality assessment of the included articles and methodology. GV, PT, HV, JM, CV were part of the writing committee. The manuscript was drafted by JM, LW, AG, YD, and corrected by NB, JV, SW, GV, PT, HV, JM, CV. Supervision was provided by SW, NB and CV. All authors contributed to the article and approved the submitted version.

## Conflict of interest

The authors declare that the research was conducted in the absence of any commercial or financial relationships that could be construed as a potential conflict of interest.

## Publisher's note



## Supplementary material

The Supplementary Material for this article can be found online at: https://www.frontiersin.org/articles/10.3389/fonc.2023.1083285/full#supplementary-material

# References


1. Ferlay J, Colombet M, Soerjomataram I, Parkin DM, Piñeros M, Znaor A, et al. Cancer statistics for the year 2020: An overview. *Int J Cancer* (2021) 149(4):778–89. doi: 10.1002/ijc.33588

2. van Gijn W, Marijnen CA, Nagtegaal ID, Kranenbarg EM, Putter H, Wiggers T, et al. Preoperative radiotherapy combined with total mesorectal excision for resectable rectal cancer: 12-year follow-up of the multicentre, randomised controlled TME trial. *Lancet Oncol* (2011) 12(6):575–82. doi: 10.1016/S1470-2045(11)70097-3

3. Badia-Ramentol J, Linares J, Gómez-Llonin A, Calon A. Minimal residual disease, metastasis and immunity. *Biomolecules* (2021) 11(2):130. doi: 10.3390/biom11020130

4. Litvak A, Cercek A, Segal N, Reidy-Lagunes D, Stadler ZK, Yaeger RD, et al. False-positive elevations of carcinoembryonic antigen in patients with a history of resected colorectal cancer. *J Natl Compr Canc Netw* (2014) 12(6):907–13. doi: 10.6004/jnccn.2014.0085

5. Reinert T, Henriksen TV, Christensen E, Sharma S, Salari R, Sethi H, et al. Analysis of plasma cell-free DNA by ultradeep sequencing in patients with stages I to III colorectal cancer. *JAMA Oncol* (2019) 5(8):1124–31. doi: 10.1001/jamaoncol.2019.0528

6. Diaz LAJr., Bardelli A. Liquid biopsies: Genotyping circulating tumor DNA. *J Clin Oncol* (2014) 32(6):579–86. doi: 10.1200/JCO.2012.45.2011

7. Bettegowda C, Sausen M, Leary RJ, Kinde I, Wang Y, Agrawal N, et al. Detection of circulating tumor DNA in early- and late-stage human malignancies. *Sci Trans Med* (2014) 6(224):224ra24–ra24. doi: 10.1126/scitranslmed.3007094

8. Schøler LV, Reinert T, Ørntoft MW, Kassentoft CG, Árnadóttir SS, Vang S, et al. Clinical implications of monitoring circulating tumor DNA in patients with colorectal cancer. *Clin Cancer Res* (2017) 23(18):5437–45. doi: 10.1158/1078-0432.CCR-17-0510

9. Tie J, Cohen JD, Lahouel K, Lo SN, Wang Y, Kosmider S, et al. Circulating tumor DNA analysis guiding adjuvant therapy in stage II colon cancer. *New Engl J Med* (2022) 386(24):2261–27. doi: 10.1056/NEJMoa2200075

10. Bujko K, Glynne-Jones R, Bujko M. Does adjuvant fluoropyrimidine-based chemotherapy provide a benefit for patients with resected rectal cancer who have already received neoadjuvant radiochemotherapy? a systematic review of randomised trials. *Ann Oncol* (2010) 21(9):1743–50. doi: 10.1093/annonc/mdq054

11. Breugom AJ, van Gijn W, Muller EW, Berglund Å, van den Broek CBM, Fokstuen T, et al. Adjuvant chemotherapy for rectal cancer patients treated with preoperative (chemo)radiotherapy and total mesorectal excision: A Dutch colorectal cancer group (DCCG) randomized phase III trial. *Ann Oncol* (2015) 26(4):696–701. doi: 10.1093/annonc/mdu560

12. Dasari A, Morris VK, Allegra CJ, Atreya C, Benson AB 3rd, et al. ctDNA applications and integration in colorectal cancer: An NCI colon and rectal-anal task forces whitepaper. *Nat Rev Clin Oncol* (2020) 17(12):757–70. doi: 10.1038/s41571-020-0392-0

13. Connors D, Allen J, Alvarez JD, Boyle J, Cristofanilli M, Hiller C, et al. International liquid biopsy standardization alliance white paper. *Crit Rev Oncology/Hematology* (2020) 156:103112. doi: 10.1016/j.critrevonc.2020.103112

14. van Dessel LF, Beije N, Helmijr JC, Vitale SR, Kraan J, Look MP, et al. Application of circulating tumor DNA in prospective clinical oncology trials - standardization of preanalytical conditions. *Mol Oncol* (2017) 11(3):295–304. doi: 10.1002/1878-0261.12037

15. Boysen AK, Schou JV, Spindler KLG. Cell-free DNA and preoperative chemoradiotherapy for rectal cancer: A systematic review. *Clin Transl Oncol* (2019) 21(7):874–80. doi: 10.1007/s12094-018-1997-y

16. Hayden JA, van der Windt DA, Cartwright JL, Côté P, Bombardier C. Assessing bias in studies of prognostic factors. *Ann Intern Med* (2013) 158(4):280–6. doi: 10.7326/0003-4819-158-4-201302190-00009

17. McGuinness LA, Higgins JPT. Risk-of-bias VISualization (robvis): An r package and shiny web app for visualizing risk-of-bias assessments. *Res Synthesis Methods* (2020) 12(1):55–61. doi: 10.1002/jrsm.1411

18. Zitt M, Müller HM, Rochel M, Schwendinger V, Zitt M, Goebel G, et al. Circulating cell-free DNA in plasma of locally advanced rectal cancer patients undergoing preoperative chemoradiation: A potential diagnostic tool for therapy monitoring. *Dis Markers* (2008) 25(3):159–65. doi: 10.1155/2008/598071

19. Agostini M, Pucciarelli S, Enzo MV, Del Bianco P, Briarava M, Bedin C, et al. Circulating cell-free DNA: A promising marker of pathologic tumor response in rectal cancer patients receiving preoperative chemoradiotherapy. *Ann Surg Oncol* (2011) 18(9):2461–8. doi: 10.1245/s10434-011-1638-y

20. Sun W, Sun Y, Zhu M, Wang Z, Zhang H, Xin Y, et al. The role of plasma cell-free DNA detection in predicting preoperative chemoradiotherapy response in rectal cancer patients. *Oncol Rep* (2014) 31(3):1466–72. doi: 10.3892/or.2013.2949

21. Boysen AK, Wettergren Y, Sorensen BS, Taflin H, Gustavson B, Spindler KLG. Cell-free DNA levels and correlation to stage and outcome following treatment of locally advanced rectal cancer. *Tumor Biol* (2017) 39(11). doi: 10.1177/1010428317730976

22. Liu W, Li Y, Tang Y, Song Q, Wang J, Li N, et al. Response prediction and risk stratification of patients with rectal cancer after neoadjuvant therapy through an analysis of circulating tumour DNA. *eBioMedicine* (2022) 78:103945. doi: 10.1016/j.ebiom.2022.103945

23. Sclafani F, Chau I, Cunningham D, Hahne JC, Vlachogiannis G, Eltahir Z, et al. KRAS and BRAF mutations in circulating tumour DNA from locally advanced rectal cancer. *Sci Rep* (2018) 8(1):1445. doi: 10.1038/s41598-018-19212-5

24. Schou JV, Larsen FO, Sørensen BS, Abrantes R, Boysen AK, Johansen JS, et al. Circulating cell-free DNA as predictor of treatment failure after neoadjuvant chemo-radiotherapy before surgery in patients with locally advanced rectal cancer. *Ann Oncol* (2018) 29(3):610–5. doi: 10.1093/annonc/mdx778

25. Tie J, Cohen JD, Wang Y, Li L, Christie M, Simons K, et al. Serial circulating tumour DNA analysis during multimodality treatment of locally advanced rectal cancer: A prospective biomarker study. *Gut* (2019) 68(4):663–71. doi: 10.1136/gutjnl-2017-315852

26. Appelt AL, Andersen RF, Lindebjerg J, Jakobsen A. Prognostic value of serum NPY hypermethylation in neoadjuvant chemoradiotherapy for rectal cancer: Secondary analysis of a randomized trial. *Am J Clin Oncol Cancer Clin Trials* (2020) 43(1):9–13. doi: 10.1097/COC.0000000000000609

27. Guo ZW, Xiao WW, Yang XX, Yang X, Cai GX, Wang XJ, et al. Noninvasive prediction of response to cancer therapy using promoter profiling of circulating cell-free DNA. *Clin Transl Med* (2020) 10(5):e174. doi: 10.1002/ctm2.174

28. Khakoo S, Carter PD, Brown G, Valeri N, Picchia S, Bali MA, et al. MRI Tumor regression grade and circulating tumor DNA as complementary tools to assess response and guide therapy adaptation in rectal cancer. *Clin Cancer Res* (2020) 26(1):183–92. doi: 10.1158/1078-0432.CCR-19-1996

29. Murahashi S, Akiyoshi T, Sano T, Fukunaga Y, Noda T, Ueno M, et al. Serial circulating tumour DNA analysis for locally advanced rectal cancer treated with preoperative therapy: Prediction of pathological response and postoperative recurrence. *Br J Cancer* (2020) 123(5):803–10. doi: 10.1038/s41416-020-0941-4

30. Pazdirek F, Minarik M, Benesova L, Halkova T, Belsanova B, Macek M, et al. Monitoring of early changes of circulating tumor DNA in the plasma of rectal cancer patients receiving neoadjuvant concomitant chemoradiotherapy: Evaluation for prognosis and prediction of therapeutic response. *Front Oncol* (2020) 10. doi: 10.3389/fonc.2020.01028

31. Zhou J, Wang C, Lin G, Xiao Y, Jia W, Xiao G, et al. Serial circulating tumor DNA in predicting and monitoring the effect of neoadjuvant chemoradiotherapy in patients with rectal cancer: A prospective multicenter study. *Clin Cancer Res* (2021) 27(1):301–10. doi: 10.1158/1078-0432.CCR-20-2299

32. McDuff SGR, Hardiman KM, Ulintz PJ, Parikh AR, Zheng H, Kim DW, et al. Circulating tumor dna predicts pathologic and clinical outcomes following neoadjuvant chemoradiation and surgery for patients with locally advanced rectal cancer. *JCO Precis Oncol* (2021) 5:123–32. doi: 10.1200/PO.20.00220

33. Vidal J, Casadevall D, Bellosillo B, Pericay C, Garcia-Carbonero R, Losa F, et al. Clinical impact of presurgery circulating tumor DNA after total neoadjuvant treatment in locally advanced rectal cancer: A biomarker study from the GEMCAD 1402 trial. *Clin Cancer Res* (2021) 27(10):2890–8. doi: 10.1158/1078-0432.CCR-20-4769

34. Wang Y, Yang L, Bao H, Fan X, Xia F, Wan J, et al. Utility of ctDNA in predicting response to neoadjuvant chemoradiotherapy and prognosis assessment in locally advanced rectal cancer: A prospective cohort study. *PLoS Med* (2021) 18(8):e1003741. doi: 10.1371/journal.pmed.1003741

35. Roesel R, Epistolio S, Molinari F, Saletti P, De Dosso S, Valli M, et al. A pilot, prospective, observational study to investigate the value of NGS in liquid biopsies to predict tumor response after neoadjuvant chemo-radiotherapy in patients with locally advanced rectal cancer: The LiBReCa study. *Front Oncol* (2022) 12:900945. doi: 10.3389/fonc.2022.900945

36. Truelsen CG, Kronborg CS, Sorensen BS, Callesen LB, Spindler KG. Circulating cell-free DNA as predictor of pathological complete response in locally advanced rectal cancer patients undergoing preoperative chemoradiotherapy. *Clin Transl Radiat Oncol* (2022) 36:9–15. doi: 10.1016/j.ctro.2022.06.002

37. Tie J. Use of circulating tumour DNA (ctDNA) results to inform the decision for adjuvant chemotherapy in patients with locally advanced rectal cancer who have been treated with pre-operative chemo-radiation and surgery. (2017).

38. Dizdarevic E, Hansen TF, Jakobsen A. The prognostic importance of ctDNA in rectal cancer: A critical reappraisal. *Cancers* (2022) 14(9):2252. doi: 10.3390/cancers14092252

39. Morais M, Pinto DM, Machado JC, Carneiro S. ctDNA on liquid biopsy for predicting response and prognosis in locally advanced rectal cancer: A systematic review. *Eur J Surg Oncol* (2022) 48(1):218–27. doi: 10.1016/j.ejso.2021.08.034

40. Pascual J, Attard G, Bidard FC, Curigliano G, De Mattos-Arruda L, Diehn M, et al. ESMO recommendations on the use of circulating tumour DNA assays for patients with cancer: A report from the ESMO precision medicine working group. *Ann Oncol* (2022) 33(8):750–68. doi: 10.1016/j.annonc.2022.05.520

41. Henriksen TV, Reinert T, Christensen E, Sethi H, Birkenkamp-Demtröder K, Gögenur M, et al. The effect of surgical trauma on circulating free DNA levels in cancer patients-implications for studies of circulating tumor DNA. *Mol Oncol* (2020) 14(8):1670–9. doi: 10.1002/1878-0261.12729

42. Chakrabarti S, Kasi AK, Parikh AR, Mahipal A. Finding Waldo: The evolving paradigm of circulating tumor DNA (ctDNA)-guided minimal residual disease (MRD) assessment in colorectal cancer (CRC). *Cancers (Basel)* (2022) 14(13):3078. doi: 10.3390/cancers14133078

43. Grothey A, Sobrero AF, Shields AF, Yoshino T, Paul J, Taieb J, et al. Duration of adjuvant chemotherapy for stage III colon cancer. *New Engl J Med* (2018) 378(13):1177–88. doi: 10.1056/NEJMoa1713709

44. André T, Meyerhardt J, Iveson T, Sobrero A, Yoshino T, Souglakos I, et al. Effect of duration of adjuvant chemotherapy for patients with stage III colon cancer (IDEA collaboration): Final results from a prospective, pooled analysis of six randomised, phase 3 trials. *Lancet Oncol* (2020) 21(12):1620–9. doi: 10.1016/S1470-2045(20)30527-1

45. Iveson TJ, Kerr RS, Saunders MP, Cassidy J, Hollander NH, Tabernero J, et al. 3 versus 6 months of adjuvant oxaliplatin-fluoropyrimidine combination therapy for colorectal cancer (SCOT): an international, randomised, phase 3, non-inferiority trial. *Lancet Oncol* (2018) 19(4):562–78. doi: 10.1016/S1470-2045(18)30093-7

46. *Dutch Colorectal Cancer Guideline, version 3.0* (2014). Available at: https://richtlijnen.nhg.org/files/2020-05/colorectaalcarcinoom.pdf. (accessed at 01-12-2022)

47. Breugom AJ, Swets M, Bosset JF, Collette L, Sainato A, Cionini L, et al. Adjuvant chemotherapy after preoperative (chemo)radiotherapy and surgery for patients with rectal cancer: A systematic review and meta-analysis of individual patient data. *Lancet Oncol* (2015) 16(2):200–7. doi: 10.1016/S1470-2045(14)71199-4

48. Galjart B, Höppener DJ, Aerts J, Bangma CH, Verhoef C, Grünhagen DJ. Follow-up strategy and survival for five common cancers: A meta-analysis. *Eur J Cancer* (2022) 174:185–99. doi: 10.1016/j.ejca.2022.07.025

49. Jeffery M, Hickey BE, Hider PN, See AM. Follow-up strategies for patients treated for non-metastatic colorectal cancer. *Cochrane Database Syst Rev* (2016) 11(11): CD002200. doi: 10.1002/14651858.CD002200.pub3

50. Tie J, Cohen JD, Lo SN, Wang Y, Li L, Christie M, et al. Prognostic significance of postsurgery circulating tumor DNA in nonmetastatic colorectal cancer: Individual patient pooled analysis of three cohort studies. *Int J Cancer* (2021) 148(4):1014–26. doi: 10.1002/ijc.33312

51. Liu MC, Oxnard GR, Klein EA, Swanton C, Seiden MV, Consortium C. Sensitive and specific multi-cancer detection and localization using methylation signatures in cell-free DNA. *Ann Oncol* (2020) 31(6):745–59. doi: 10.1016/j.annonc.2020.02.011

52. Shen SY, Singhania R, Fehringer G, Chakravarthy A, Roehrl MHA, Chadwick D, et al. Sensitive tumour detection and classification using plasma cell-free DNA methylomes. *Nature* (2018) 563(7732):579–83. doi: 10.1038/s41586-018-0703-0

53. Luo H, Zhao Q, Wei W, Zheng L, Yi S, Li G, et al. Circulating tumor DNA methylation profiles enable early diagnosis, prognosis prediction, and screening for colorectal cancer. *Sci Transl Med* (2020) 12(524):eaax7533. doi: 10.1126/scitranslmed.aax7533

54. Wu X, Zhang Y, Hu T, He X, Zou Y, Deng Q, et al. A novel cell-free DNA methylation-based model improves the early detection of colorectal cancer. *Mol Oncol* (2021) 15(10):2702–14. doi: 10.1002/1878-0261.12942

55. Cristiano S, Leal A, Phallen J, Fiksel J, Adleff V, Bruhm DC, et al. Genome-wide cell-free DNA fragmentation in patients with cancer. *Nature* (2019) 570(7761):385–9. doi: 10.1038/s41586-019-1272-6

56. Lo YMD, Han DSC, Jiang P, Chiu RWK. Epigenetics, fragmentomics, and topology of cell-free DNA in liquid biopsies. *Science* (2021) 372(6538):aaw3616. doi: 10.1126/science.aaw3616

57. Mouliere F, Chandrananda D, Piskorz AM, Moore EK, Morris J, Ahlborn LB, et al. Enhanced detection of circulating tumor DNA by fragment size analysis. *Sci Transl Med* (2018) 10(466):eaat4921. doi: 10.1126/scitranslmed.aat4921

58. Parikh AR, Van Seventer EE, Siravegna G, Hartwig AV, Jaimovich A, He Y, et al. Minimal residual disease detection using a plasma-only circulating tumor DNA assay in patients with colorectal cancer. *Clin Cancer Res* (2021) 27(20):5586–94. doi: 10.1158/1078-0432.CCR-21-0410

frontiers | Frontiers in Surgery

TYPE Original Research
PUBLISHED 08 February 2023
DOI 10.3389/fsurg.2023.1106137



OPEN ACCESS

EDITED BY
Jeroen Van Vugt,
Erasmus Medical Center, Netherlands

REVIEWED BY
Fabrizio Consorti,
Sapienza University of Rome, Italy
Guobing Yin,
Second Affiliated Hospital of Chongqing Medical University, China

*CORRESPONDENCE
Baoding Chen
✉ alphalife@163.com

SPECIALTY SECTION
This article was submitted to Surgical Oncology, a section of the journal Frontiers in Surgery

RECEIVED 23 November 2022
ACCEPTED 10 January 2023
PUBLISHED 08 February 2023

CITATION
Feng H, Chen Z, An M, Chen Y and Chen B (2023) Nomogram for preoperative prediction of high-volume lymph node metastasis in the classical variant of papillary thyroid carcinoma. Front. Surg. 10:1106137.
doi: 10.3389/fsurg.2023.1106137



# Nomogram for preoperative prediction of high-volume lymph node metastasis in the classical variant of papillary thyroid carcinoma

Huahui Feng, Zheming Chen, Maohui An, Yanwei Chen and Baoding Chen*

Department of Medical Ultrasound, The Affiliated Hospital of Jiangsu University, Zhenjiang, China

**Introduction:** The objective of our study was to construct a preoperative prediction nomogram for the classical variant of papillary thyroid carcinoma (CVPTC) patients with a solitary lesion based on demographic and ultrasonographic parameters that can quantify the individual probability of high-volume (>5) lymph node metastasis (HVLNM).

**Materials and methods:** In this study, a total of 626 patients with CVPTC from December 2017 to November 2022 were reviewed. Their demographic and ultrasonographic features at baseline were collected and analyzed using univariate and multivariate analyses. Significant factors after the multivariate analysis were incorporated into a nomogram for predicting HVLNM. A validation set from the last 6 months of the study period was conducted to evaluate the model performance.

**Results:** Male sex, tumor size >10 mm, extrathyroidal extension (ETE), and capsular contact >50% were independent risk factors for HVLNM, whereas middle and old age were significant protective factors. The area under the curve (AUC) was 0.842 in the training and 0.875 in the validation set.

**Conclusions:** The preoperative nomogram can help tailor the management strategy to the individual patient. Additionally, more vigilant and aggressive measures may benefit patients at risk of HVLNM.

KEYWORDS

papillary thyroid carcinoma, high-volume lymph node metastasis, risk factors, nomogram, ultrasonography

## Introduction

The prevalence of thyroid cancer is increasing worldwide (1). Notably, papillary thyroid carcinoma accounts for 85% of differentiated thyroid cancers with a high 10-year survival rate (2–4). CVPTC is the most prevalent variant and is believed to be a less aggressive histological subtype that has a lower risk for death and metastatic disease (5). Prophylactic central lymph node dissection remains controversial according to different guidelines (6–8). However, up to 50% of papillary thyroid carcinoma (PTC) patients develop lymph node metastasis (LNM) (9). Large-volume or high-volume LNM (HVLNM) was defined as >5 metastatic lymph nodes (8). Increasing evidence has shown that patients with HVLNM have poorer outcomes than those with small-volume LNM, which includes higher recurrence rates and lower disease-free survival (10, 11). Consequently, the latest American Thyroid Association (ATA) guidelines have determined clinical N1 disease or >5 pathological lymph nodes (less than 3 cm) as characteristics of patients with an intermediate risk for postoperative risk stratification (8).

Ultrasound (US) is the primary choice for routine thyroid examination and preoperative staging of thyroid cancer. Several associations have published reporting systems for the assessment of thyroid nodules based on ultrasonographic patterns that are helpful in diagnosing nodules (8, 12–14). However, due to the complex anatomical structure of the neck and the physical limitations of US, the diagnostic performance of preoperative US evaluation in detecting lymph node involvement in the cervical region, especially in the central compartment, is not particularly effective (15). Another reason that the detection rates of positive lymph nodes are low is that the procedure relies heavily on the proficiency of operators. Therefore, during the preoperative examination, the potential risks of LNM and HVLNM may be overlooked, further misleading the management of vulnerable patients.

Many studies have focused on the association between imaging patterns of thyroid nodules and LNM. A few studies have concentrated on the risk factors for HVLNM (16–20). Furthermore, in these studies, multifocal lesions and postoperative diagnosis were analyzed in most cases. And the association between preoperative ultrasonographic features and HVLNM, such as capsule morphology, has never been investigated thoroughly. Clinical decisions may be altered if feasible preoperative prediction models can be established, and more aggressive treatment modalities may be found suitable for some CVPTC patients.

Thus, this study aimed to construct a preoperative nomogram to predict HVLNM in CVPTC patients with a solitary lesion based on demographic and ultrasonographic features. Besides, the predictive value of the nomogram was assessed using a validation set consisting of the patients from the last 6 months of the cohort. The developed nomogram may help clinicians select a follow-up approach for the entire diagnosis and treatment process.

# Materials and methods

## Patient selection

This retrospective study was approved by the Ethics Committee of the Affiliated Hospital of Jiangsu University, and the requirement for written informed consent was waived. The records of 626 patients diagnosed with PTC between December 2017 and November 2022 were retrospectively assessed. These medical records were reviewed to collect data, including sex, age, final pathological diagnoses, and preoperative ultrasonographic findings. The inclusion criteria were as follows: (1) postoperative pathological diagnosis of CVPTC, (2) age ≥18 years, and (3) complete preoperative thyroid US. The exclusion criteria were as follows: (1) history of neck radiotherapy or thyroid surgery, (2) incomplete patient information in the hospital database, and (3) sonographic patterns unavailable for analysis. Preoperative fine-needle aspiration (FNA) and US were performed to eliminate suspicious lesions in the unresected thyroid tissue. Prophylactic central lymph node dissection (CLND) was performed in all patients, whereas lateral lymph node dissection (LLND) was performed based on preoperative imaging reports and US-guided FNA biopsy results for suspicious metastatic lymph nodes. Postoperative pathology is the gold standard for lymph node metastasis. HVLNM is defined as more than 5 positive metastatic lymph nodes on postoperative pathologic diagnosis. The flowchart of the patient selection process is shown in **Figure 1**.

## Preoperative US examination and image analysis

Two experienced radiologists independently assessed the US patterns of the suspicious nodules. When discrepancies emerged, a senior radiologist reviewed the images. Nodules were classified according to the 2020 Chinese Thyroid Imaging Reporting and Data System (C-TIRADS) (14). Ultrasonographic characteristics were further categorized as follows: tumor size (≤10 or >10 mm), composition (mixed or solid), echogenicity (hyperechoic, isoechoic, hypoechoic, or markedly hypoechoic), shape (wider than tall or taller than wide), margin (circumscribed or not circumscribed), calcifications (absent, microcalcifications, macrocalcifications, or mixed calcifications), vascular pattern (avascularity, peripheral, mainly peripheral, mainly central, or mixed vascularity), capsular contact (no contact, ≤50% or >50%), and ETE on US (absent or present). The tumor's size was defined by its maximum diameter on US. The tumor shape was evaluated based on the transverse dimension. Microcalcifications were defined as hyperechoic foci that were equal to or less than 1 mm in diameter. Calcifications >1 mm were classified as macrocalcifications (14). When microcalcifications and macrocalcifications presented simultaneously in a nodule, they were classified as mixed calcifications. Disruption of the thyroid capsule and gross invasion of the perithyroidal structures were defined as ETE on US. Bulging of the normal thyroid contour without capsule disruption would not be defined as ETE. The degree of capsular contact was calculated according to the proportion of the nodule perimeter in contact with the capsules on the images where the nodule was in greatest contact with the capsules (21). Vascular patterns were detected using color Doppler US.

## Statistical analysis

The entire group was divided into the training set and the validation set. Patients included from the last 6 months of the study period were used for the validation set. The developed model from the training set was then tested in the validation set. All statistical analyses were performed using SPSS version 29 and R programming language. Statistical significance was defined as $P < 0.05$. Categorical variables are presented as numbers (%). Univariate analysis was performed for categorical variables using the chi-squared test or Fisher's exact test. Variables with a *P*-value less than 0.05 in the univariate analysis were included in the multivariate analysis to establish a logistic regression model.

A nomogram was generated using independent predictors from the multivariate analysis to visualize the individual probability of HVLNM. The model discriminatory ability was determined using the area under the receiver operating characteristic (ROC) curve (AUC), known as the concordance index. An AUC of 1 represents a perfect model, whereas an AUC of 0.5 represents a random

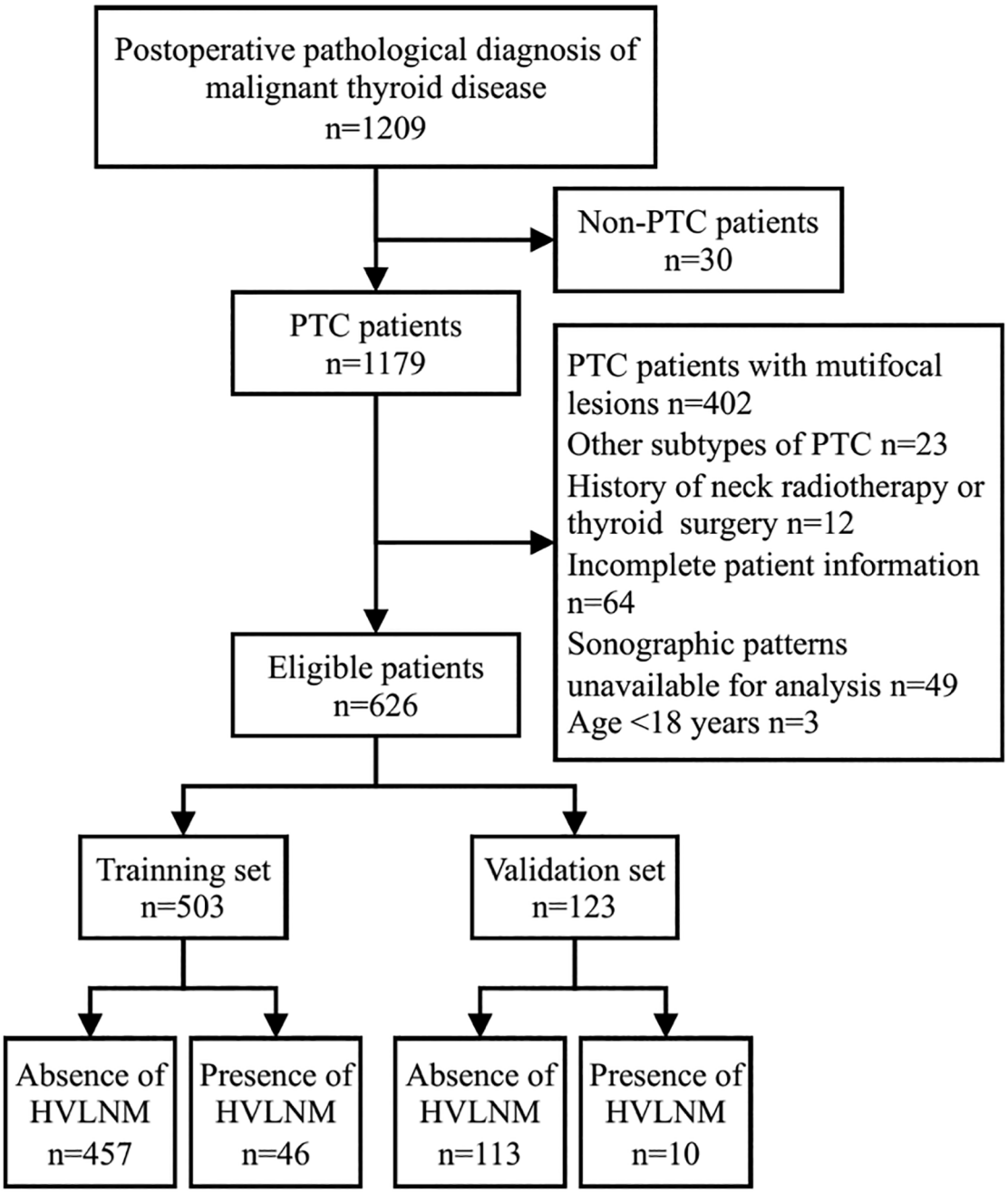


FIGURE 1
The flowchart of the patient selection process.

classifier. Calibration curves were plotted to compare the predicted versus actual probabilities. Decision curve analysis (DCA) was used to estimate the net benefit.

# Results

## Clinicopathological backgrounds

In this study, 626 patients with solitary CVPTC confirmed by postoperative pathology were included between December 2017 and November 2022. 503 patients between December 2017 and May 2022 constituted the training set, and 123 patients were allocated to the validation set between June 2022 and November 2022. Patients were divided into HVLNM and non-HVLNM groups according to the number of metastatic lymph nodes confirmed by postoperative pathology. A total thyroidectomy or near-total thyroidectomy was performed in 89 patients. Thyroid lobectomy with or without the isthmus was performed in 537 patients. After surgery, 46 (9.1%) cases in the training set and 10 (8.1%) cases in the validation set had HVLNM (Table 1). Baseline demographic and ultrasonographic characteristics were summarized in Table 1. The training set showed a good agreement with the validation set, except for a difference in the presence of ETE on US (Table 1).

10.3389/fsurg.2023.1106137

TABLE 1 Baseline demographic and ultrasonographic characteristics of patients with solitary CVPTC.

| Characteristics | | Total | Patient sets (%) | | *P*-value |
|---|---|---|---|---|---|
| | | | Training set | Validation set | |
| Sex | Female | 476 | 386 (76.7) | 90 (73.2) | 0.406 |
| | Male | 150 | 117 (23.3) | 33 (26.8) | |
| Tumor size | ≤10 mm | 414 | 333 (66.2) | 81 (65.9) | 0.942 |
| | >10 mm | 212 | 170 (33.8) | 42 (34.1) | |
| Composition | Mixed | 51 | 46 (9.1) | 5 (4.1) | 0.065 |
| | Solid | 575 | 457 (90.9) | 118 (95.9) | |
| Echogenicity | Hyperechoic | 15 | 11 (2.2) | 4 (3.3) | 0.076 |
| | Isoechoic | 51 | 37 (7.4) | 14 (11.4) | |
| | Hypoechoic | 402 | 318 (63.2) | 84 (68.3) | |
| | Markedly hypoechoic | 158 | 137 (27.2) | 21 (17.1) | |
| Shape | Wider than tall | 189 | 149 (29.6) | 40 (32.5) | 0.530 |
| | Taller than wide | 437 | 354 (70.4) | 83 (67.5) | |
| Margin | Circumscribed | 22 | 20 (4) | 2 (1.6) | 0.319 |
| | Not circumscribed | 604 | 483 (96) | 121 (98.4) | |
| Vascular pattern | Avascularity | 266 | 202 (40.2) | 64 (52) | 0.090 |
| | Peripheral vascularity | 144 | 117 (23.3) | 27 (22) | |
| | Mainly peripheral vascularity | 84 | 75 (14.9) | 9 (7.3) | |
| | Mainly central vascularity | 49 | 40 (8) | 9 (7.3) | |
| | Mixed vascularity | 83 | 69 (13.7) | 14 (11.4) | |
| ETE | Absent | 572 | 472 (93.8) | 100 (81.3) | <0.001 |
| | Present | 54 | 31 (6.2) | 23 (18.7) | |
| Capsular contact | No contact | 304 | 243 (48.3) | 61 (49.6) | 0.065 |
| | ≤50% | 240 | 201 (40) | 39 (31.7) | |
| | >50% | 82 | 59 (11.7) | 23 (18.7) | |
| Calcifications | Absent | 230 | 182 (36.2) | 48 (39) | 0.366 |
| | Microcalcifications | 316 | 261 (51.9) | 55 (44.7) | |
| | Macrocalcifications | 43 | 31 (6.2) | 12 (9.8) | |
| | Mixed calcifications | 37 | 29 (5.8) | 8 (6.5) | |
| C-TIRADS category | C-TIRADS 3 | 2 | 2 (0.4) | 0 (0) | 0.169 |
| | C-TIRADS 4A | 12 | 8 (1.6) | 4 (3.3) | |
| | C-TIRADS 4B | 73 | 58 (11.5) | 15 (12.2) | |
| | C-TIRADS 4C | 491 | 391 (77.7) | 100 (81.3) | |
| | C-TIRADS 5 | 48 | 44 (8.7) | 4 (3.3) | |
| Age | <40 | 217 | 174 (34.6) | 43 (35) | 0.906 |
| | 40–55 | 252 | 201 (40) | 51 (41.5) | |
| | ≥55 | 157 | 128 (25.4) | 29 (23.6) | |
| HVLNM | Absent | 570 | 457 (90.9) | 113 (91.9) | 0.724 |
| | Present | 56 | 46 (9.1) | 10 (8.1) | |

TABLE 2 Univariate analysis of risk factors for HVLNM in the training set.

| Characteristics | | Non-HVLNM (*N* = 457) | HVLNM (*N* = 46) | *P* |
|---|---|---|---|---|
| Sex | Female | 357 (92.5) | 29 (7.5) | <0.05 |
| | Male | 100 (85.5) | 17 (14.5) | |
| Age | <40 | 148 (85.1) | 26 (14.9) | <0.01 |
| | 40–55 | 189 (94) | 12 (6) | |
| | ≥55 | 120 (93.8) | 8 (6.2) | |
| Tumor size | ≤10 mm | 319 (95.8) | 14 (4.2) | <0.001 |
| | >10 mm | 138 (81.2) | 32 (18.8) | |
| Composition | Mixed | 36 (78.3) | 10 (21.7) | <0.01 |
| | Solid | 421 (92.1) | 36 (7.9) | |
| Echogenicity | Hyperechoic | 8 (72.7) | 3 (27.3) | 0.193 |
| | Isoechoic | 33 (89.2) | 4 (10.8) | |
| | Hypoechoic | 290 (91.2) | 28 (8.8) | |
| | Markedly hypoechoic | 126 (92) | 11 (8) | |
| Shape | Wider than tall | 128 (85.9) | 21 (14.1) | <0.05 |
| | Taller than wide | 329 (92.9) | 25 (7.1) | |
| Margin | Circumscribed | 19 (95) | 1 (5) | 0.795 |
| | Not circumscribed | 438 (90.7) | 45 (9.3) | |
| Vascular pattern | Avascularity | 186 (92.1) | 16 (7.9) | 0.116 |
| | Peripheral vascularity | 106 (90.6) | 11 (9.4) | |
| | Mainly peripheral vascularity | 70 (93.3) | 5 (6.7) | |
| | Mainly central vascularity | 38 (95) | 2 (5) | |
| | Mixed vascularity | 57 (82.6) | 12 (17.4) | |
| ETE | Absent | 438 (92.8) | 34 (7.2) | <0.001 |
| | Present | 19 (61.3) | 12 (38.7) | |
| Capsular contact | No contact | 234 (96.3) | 9 (3.7) | <0.001 |
| | ≤50% | 184 (91.5) | 17 (8.5) | |
| | >50% | 39 (66.1) | 20 (33.9) | |
| Calcifications | Absent | 172 (94.5) | 10 (5.5) | 0.128 |
| | Microcalcifications | 231 (88.5) | 30 (11.5) | |
| | Macrocalcifications | 29 (93.5) | 2 (6.5) | |
| | Mixed calcifications | 25 (86.2) | 4 (13.8) | |
| C-TIRADS category | C-TIRADS 3 | 1 (50.0) | 1 (50.0) | 0.064 |
| | C-TIRADS 4A | 7 (87.5) | 1 (12.5) | |
| | C-TIRADS 4B | 51 (87.9) | 7 (12.1) | |
| | C-TIRADS 4C | 361 (92.3) | 30 (7.7) | |
| | C-TIRADS 5 | 37 (84.1) | 7 (15.9) | |

The data are presented as *N* (%).

TABLE 3 Multivariate analysis of risk factors for HVLNM.

| Characteristics | OR | 95% CI | | *P*-value |
|---|---|---|---|---|
| | | Lower | Upper | |
| Age (<40) | 1 | - | - | 0.012 |
| Age (40–55) | 0.389 | 0.173 | 0.878 | 0.023 |
| Age (≥55) | 0.295 | 0.116 | 0.755 | 0.011 |
| Male sex | 3.396 | 1.579 | 7.304 | 0.002 |
| Tumor size >10 mm | 2.662 | 1.156 | 6.132 | 0.021 |
| Solid composition | 0.984 | 0.362 | 2.675 | 0.975 |
| Taller than wide | 0.956 | 0.443 | 2.060 | 0.908 |
| ETE | 5.087 | 1.897 | 13.638 | 0.001 |
| Capsular contact (no contact) | 1 | - | - | <0.001 |
| Capsular contact (≤50%) | 1.738 | 0.694 | 4.356 | 0.238 |
| Capsular contact (>50%) | 7.377 | 2.697 | 20.175 | <0.001 |

## Univariate and multivariate analyses of risk factors for HVLNM in CVPTC patients

In the training set, univariate analysis revealed that sex, age, tumor size, nodule composition and shape, ETE on US, and capsular contact were associated with HVLNM (Table 2). The incidence of HVLNM varied significantly among the three age groups. The incidences were 14.9% (26/174), 6% (12/201), and 6.2% (8/128), respectively. Moreover, capsular contact >50% presented a higher incidence than the other two groups (no contact and contact ≤50%). Tumor echogenicity, margin, calcifications, vascular pattern, and C-TIRADS category did not correlate with the presence of HVLNM.

Significant factors in the univariate analysis were then included in the multivariate analysis. Multivariate logistic regression analysis demonstrated that male sex (OR 3.396, 95% CI 1.579–7.304), tumor size >10 mm (OR 2.662, 95% CI 1.156–6.132), ETE on US (OR 5.087, 95% CI 1.897–13.638), and capsular contact >50% (OR 7.377, 95% CI 2.697–20.175) were independent risk factors for HVLNM. Compared with young patients (age <40 years), middle-aged (OR 0.389, 95% CI 0.173–0.878) and older patients (OR 0.295, 95% CI 0.116–0.755) had a lower risk of HVLNM (Table 3). Nagelkerke R square for the model was 0.305.

## Model construction and validation

The logistic regression analysis used all the independent factors to develop a predicting model. The AUC of the developed model in predicting HVLNM in the training set was 0.842 (95% CI 0.782–0.902). The sensitivity, specificity, positive predictive value, and negative predictive value of 0.804, 0.735, 0.234, and 0.974, respectively. In the validation set, the developed model acquired an AUC of 0.875 (95% CI 0.783–0.968) and yielded the sensitivity, specificity, positive predictive value, and negative predictive value of 0.900, 0.743, 0.237, and 0.988, respectively (Figure 2).

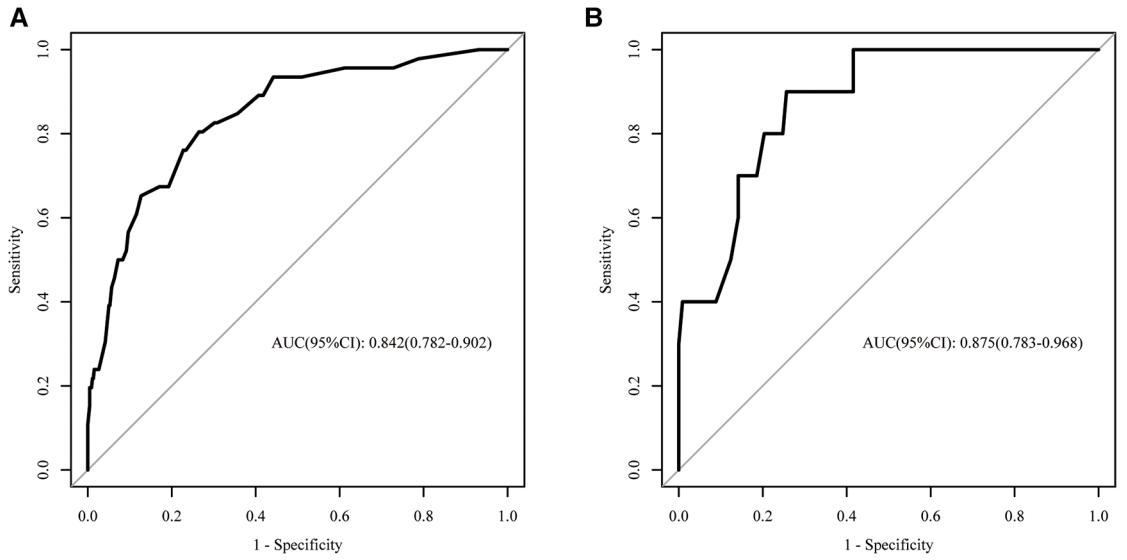


FIGURE 2
Receiver operating characteristics curves in the training set (A) and validation set (B).

A nomogram integrating all five significant factors was created. According to the analysis, capsular contact >50% was the most significant contributor to the prediction model, followed by ETE. The final scores were calculated by summing the total scores, and the risk rate of HVLNM was calculated (**Figure 3**). The calibration curves showed good agreement between the predicted and observed probabilities of HVLNM, with a mean absolute error of 0.017 and 0.034 (**Figure 4**). The DCA curves showed a threshold probability from 0.00 to 0.92 in the training set, suggesting a wide range of clinical utility (**Figure 4**).

## Discussion

Evidence has suggested that the prognosis of PTC was linked to the number and size of involved lymph nodes. Randolph et al. revealed a marked difference in the median risk of recurrence in pathological N1 patients between <5 positive nodes (4%, range 3%–8%) and >5 nodes (19%, range 7%–21%) (10). Moreover, an analysis based on data from the National Cancer Data Base and SEER database, showed that a higher number of metastatic lymph nodes (up to six metastatic) was associated with lower overall survival (HR 1.12, 95% CI 1.01–1.25). In contrast, no additional mortality risk was found with more positive nodes (HR 0.99, 95% CI, 0.99–1.05) (11). All these findings allude a more concerning message about HVLNM. Thus, the 2015 ATA guidelines have modified the clinical and pathological nodal status as a characteristic that can stratify the risk of recurrence in PTC patients. The status of more than five metastatic lymph nodes is classified as intermediate risk, indicating a >20% risk of recurrence (8).

Precise identification of patients with HVLNM preoperatively may facilitate the selection of rigorous screening and treatment protocols. However, the low diagnostic performance of lymph nodes in preoperative assessments is unfavorable for patients and physicians. It was reported that the diagnostic efficacy was unsatisfactory, with a pooled sensitivity between 0.31 and 0.35 for detecting involved lymph nodes in the central neck (22). Another

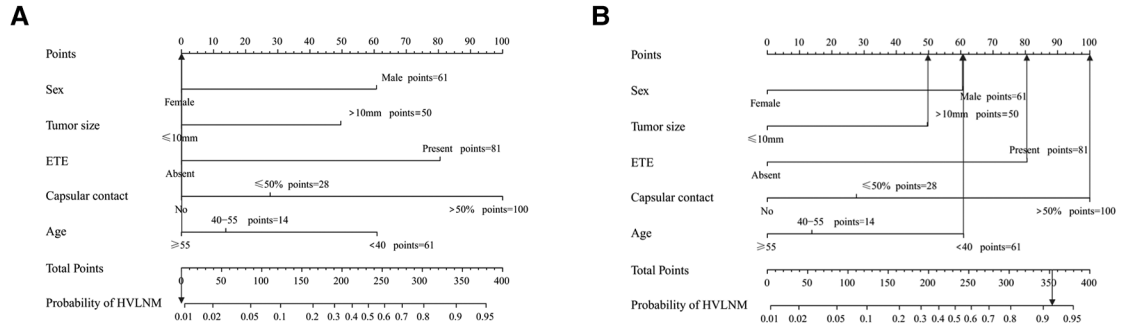


FIGURE 3
The use of the developed nomogram. (A) A 75-year-old lady diagnosed as non-HVLNM with a papillary thyroid microcarcinoma, extrathyroidal extension (–), capsular contact (–). The total score of this patient is 0 and the risk rate of HVLNM was <0.01. (B) A 37-year-old man diagnosed as HVLNM with a papillary thyroid macrocarcinoma, extrathyroidal extension (+), capsular contact (>50%). The total score of this patient is 353 and the risk rate of HVLNM was 91.6%.

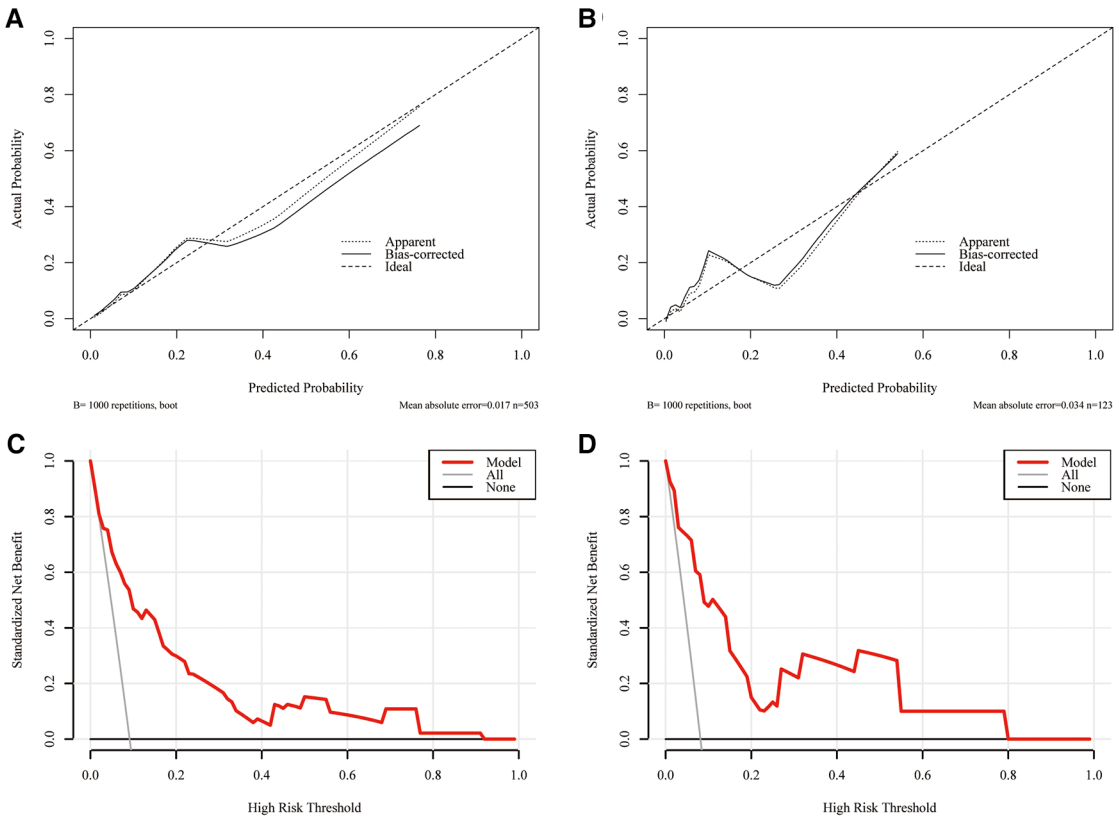


FIGURE 4
The calibration curves for comparing the predicted probabilities with actual probabilities and the DCA curves for estimating the net benefit of the prediction model. (A) The calibration curve in the training set; (B) the calibration curve in the validation set; (C) the DCA curve in the training set; (D) the DCA curve in the validation set.

meta-analysis reported that US + Computed Tomography and FNA cytology + FNA-thyroglobulin (FNA-Tg) showed good diagnostic performance (23). The limitations are that these methods are radiative or invasive. For these reasons, it would be helpful to establish a prediction model for PTC patients combined with demographic features and nodule characteristics using US.

In a previous study, preoperatively sonographic characteristics combined with serum Tg antibodies levels were found to help predict central LNM (CLNM) (24). Differently, our current study developed a preoperative nomogram based on preoperative sonographic patterns to visualize the prediction model for HVLNM in solitary CVPTC patients. The AUC was 0.842 in the training set and 0.875 in the validation set. Moreover, the HVLNM rate was found in 9.1% (46/503 cases) in the training set and 8.1% (10/123 cases) in the validation set, which was lower than that reported by Liu et al. (12.3%, 254/2,073 cases) (16). Different designs of the single lesion in this study, the inclusion criteria, or the sample capacity might have caused the divergence. When comparing the two groups in the training set, the data revealed that male sex, tumor size >10 mm, ETE on neck US, and capsular contact >50% were independent risk factors for HVLNM. Contrastingly, middle age and old age were significant protective factors. It is suggested that increased vigilance would be required for potential HVLNM patients.

There is no consensus regarding the impact of age on LNM, and age classification varies in different studies. Ito et al. pointed out that tumor progression was the greatest in young patients and the poorest in older patients with papillary thyroid microcarcinoma (PTMC), indicating that tumors presented increased aggressiveness in younger patients compared to older patients (25). A meta-analysis, including 9,369 PTC patients, reported that age <45 years increased the risk of lymph node metastasis (pooled OR 1.52, 95% CI 1.14–2.01, $P < 0.00001$) (26). In the study, age classification was consistent with that of two recent studies by Oh et al. and Shen et al. (19, 20). According to our data in the training set, people of middle age and older people groups had less than half the incidence of HVLNM compared to the young age group. Multivariate analysis revealed that middle-aged and older patients had lower rates of HVLNM than younger patients. In addition, studies have investigated age's influence on HVLNM in patients with PTMC and derived some approximations. For instance, Zhang et al. found that the risk of HVLNM in PTMC was significantly lower in patients of middle age (40–59 years) (OR 0.313, 95% CI 0.191–0.515) and older (≥60 years) patients (OR 0.085, 95% CI 0.012–0.633) (18). Another finding worth mentioning is that Liu et al. revealed that age ≥40 years was an independent protective factor (17). Similarly, elderly age (≥55 years) was also found to be a protective factor of high-volume CLNM within PTMC in Wei's study (27). However, age was not found to be significantly different among participants in a study of 2,073 patients with PTC using the cutoff of 55 years (16). Overall,

grouping by age varied in some studies; thus, detailed and well-recognized stratification of age groups may provide a more accurate risk assessment. Apart from age, our results demonstrated that the risk of HVLNM in males was 3.396 times higher than that in females (95% CI 1.579–7.304), indicating a similar adverse effect of male sex on LNM in previous studies (26).

Importantly, primary tumor size is the most intuitive parameter in the preoperative US that has long been analyzed in previous studies and included in several scoring schemes (AGES, AMES, and MACIS) (28–30). To distinguish PTMC and conventional papillary thyroid cancer, 10 mm is used as a benchmark. It has been proposed that tumors with a diameter larger than 10 mm have a higher incidence of invasion, LNM, and CLNM, thus requiring more radical tactics to improve outcomes (26, 31–33). Likewise, in our study, the HVLNM portion of patients with tumor size ≤10 mm was 4.2%, while in the >10 mm group was 18.8% in the training set. Multivariate analysis also demonstrated that a tumor diameter >10 mm significantly increased the risk of HVLNM.

Numerous studies have shown that ETE was recognized as a predictor of metastatic diseases, such as locoregional LNM and distant metastasis (34, 35). In addition, Feng et al. used the SEER database and single-center data to evaluate the correlation between demographic and clinicopathologic characteristics and CLNM in CVPTC patients (33). ETE on pathology was significantly different between the two groups (33). On the contrary, Tao et al. did not find significant associations of ETE with CLNM and lateral LNM (LLNM) in PTMC (36). However, the definition of ETE differed in some of these studies, and most were based on postoperative pathological results, which limited their utility in the presurgical setting. Lamartina et al. reported that by combining US signs of minimal or gross ETE and taking the presence of microscopic or gross ETE as a reference on histology, preoperative US achieved an accuracy of 81.5% (37). In addition, gross ETE is believed to have a higher incidence of tumor recurrence than microscopic ETE (38, 39). Accordingly, preoperative US signs of ETE are of great diagnostic importance. In our current study, the incidences of HVLNM were significantly different in terms of ETE. Nevertheless, further studies are still needed to determine the diagnostic criteria for ETE using US.

Few studies have estimated the degree of capsular contact and analyzed its impact on LNM in PTC (40–42). Animal and human studies suggested that lymphatic networks and vessels appeared denser at the periphery of the gland (43, 44). A study in Japan revealed that increased lymphatic density was also correlated with vascular endothelial growth factor-D expression and LNM in PTC patients (45). These findings could explain that the state of contact with the glandular capsule has facilitated the spread of the tumor to regional lymph nodes. Research in clinical practice concurred with these findings. Ye et al. found that capsular extension >50% was associated with LLNM in PTC (40). Kwak et al. found >25% contact with the adjacent capsule was a risk factor for LLNM in PTMC (46). Contrastingly. Lin et al. and Zeng et al. found no significant association between capsular contact and LLNM after multivariate logistic regression (47, 48). Different from previous studies, our study highlighted the association between capsular contact and HVLNM and found that capsular contact >50% was the most common in the HVLNM group in the training set, contributing the most to the prediction model. Since the all-around measurement is needed during the examination, real-time observation of US or dynamic images after the examination could benefit the analysis after the examination.

Despite the promising results, limitations remain in the current study. First, this was a retrospective case-control study at a single center, and selection bias was inevitable. Second, only a small number of patients had HVLNM, and comparisons were only made between the HVLNM and non-HVLNM groups, while factors related to other nodal statuses were not investigated. Moreover, our nomogram included only five factors, and potential variables might need to be analyzed and validated. Thus, a large-sample cohort study involving external validation from a multicenter study is required.

In conclusion, HVLNM is relatively uncommon in CVPTC patients with a solitary lesion. Male sex, larger tumor size (>10 mm), ETE on US, and capsular contact >50% increased the risk of HVLNM, whereas middle and old age were significant protective factors. These findings may be essential for implementing more vigilant and aggressive preoperative examinations and treatment strategies for CVPTC patients with a high risk of HVLNM based on the nomogram. Additionally, real-time US plays a vital role in preoperative assessment.

## Data availability statement

The raw data supporting the conclusions of this article will be made available by the authors, without undue reservation.

## Ethics statement

The studies involving human participants were reviewed and approved by the Ethics Committee of the Affiliated Hospital of Jiangsu University. The ethics committee waived the requirement of written informed consent for participation.

## Author contributions

HF and BC conceived and designed the study. ZC and MA acquired all the raw data. HF and ZC analyzed and interpreted the data. HF wrote and reviewed the manuscript. YC revised and edit the manuscript. All authors contributed to the article and approved the submitted version.

## Funding

This research was supported by the Zhenjiang Social Development Fund (SH2021028).

## Conflict of interest

The authors declare that the research was conducted in the absence of any commercial or financial relationships that could be construed as a potential conflict of interest.

## Publisher's note



## References

1. Cabanillas ME, McFadden DG, Durante C. Thyroid cancer. *Lancet*. (2016) 388:2783–95. doi: 10.1016/S0140-6736(16)30172-6

2. Torre LA, Bray F, Siegel RL, Ferlay J, Lortet-Tieulent J, Jemal A. Global cancer statistics, 2012. *CA Cancer J Clin*. (2015) 65:87–108. doi: 10.3322/caac.21262

3. Fagin JA, Wells SA. Biologic and clinical perspectives on thyroid cancer. *N Engl J Med*. (2016) 375:1054–67. doi: 10.1056/NEJMra1501993

4. Sciuto R, Romano L, Rea S, Marandino F, Sperduti I, Maini CL. Natural history and clinical outcome of differentiated thyroid carcinoma: a retrospective analysis of 1503 patients treated at a single institution. *Ann Oncol*. (2009) 20:1728–35. doi: 10.1093/annonc/mdp050

5. Chrisoulidou A, Boudina M, Tzemailas A, Doumala E, Iliadou PK, Patakiouta F, et al. Histological subtype is the most important determinant of survival in metastatic papillary thyroid cancer. *Thyroid Res*. (2011) 4(1):12. doi: 10.1186/1756-6614-4-12

6. Takami H, Ito Y, Okamoto T, Yoshida A. Therapeutic strategy for differentiated thyroid carcinoma in Japan based on a newly established guideline managed by Japanese society of thyroid surgeons and Japanese association of endocrine surgeons. *World J Surg*. (2011) 35:111–21. doi: 10.1007/s00268-010-0832-6

7. Haddad RI, Nasr C, Bischoff L, Busaidy NL, Byrd D, Callender G, et al. NCCN guidelines insights: thyroid carcinoma, version 2.2018. *J Natl Compr Canc Netw*. (2018) 16:1429–40. doi: 10.6004/jnccn.2018.0089

8. Haugen BR, Alexander EK, Bible KC, Doherty GM, Mandel SJ, Nikiforov YE, et al. 2015 American thyroid association management guidelines for adult patients with thyroid nodules and differentiated thyroid cancer: the American thyroid association guidelines task force on thyroid nodules and differentiated thyroid cancer. *Thyroid*. (2016) 26:1–133. doi: 10.1089/thy.2015.0020

9. Ito Y, Uruno T, Nakano K, Takamura Y, Miya A, Kobayashi K, et al. An observation trial without surgical treatment in patients with papillary microcarcinoma of the Thyroid. *Thyroid*. (2003) 13:381–7. doi: 10.1089/105072503321669875

10. Randolph GW, Duh QY, Heller KS, LiVolsi VA, Mandel SJ, Steward DL, et al. The prognostic significance of nodal metastases from papillary thyroid carcinoma can be stratified based on the size and number of metastatic lymph nodes, as well as the presence of extranodal extension. *Thyroid*. (2012) 22:1144–52. doi: 10.1089/thy.2012.0043

11. Adam MA, Pura J, Goffredo P, Dinan MA, Reed SD, Scheri RP, et al. Presence and number of lymph node metastases are associated with compromised survival for patients younger than age 45 years with papillary thyroid cancer. *J Clin Oncol*. (2015) 33:2370–5. doi: 10.1200/jco.2014.59.8391

12. Tessler FN, Middleton WD, Grant EG, Hoang JK, Berland LL, Teefey SA, et al. ACR thyroid imaging, reporting and data system (TI-RADS): white paper of the ACR TI-RADS committee. *J Am Coll Radiol*. (2017) 14:587–95. doi: 10.1016/j.jacr.2017.01.046

13. Ha EJ, Chung SR, Na DG, Ahn HS, Chung J, Lee JY, et al. 2021 Korean thyroid imaging reporting and data system and imaging-based management of thyroid nodules: Korean society of thyroid radiology consensus statement and recommendations. *Korean J Radiol*. (2021) 22:2094–123. doi: 10.3348/kjr.2021.0713

14. Zhou J, Yin L, Wei X, Zhang S, Song Y, Luo B, et al. 2020 Chinese guidelines for ultrasound malignancy risk stratification of thyroid nodules: the C-TIRADS. *Endocrine*. (2020) 70:256–79. doi: 10.1007/s12020-020-02441-y

15. Alabousi M, Alabousi A, Adham S, Pozdnyakov A, Ramadan S, Chaudhari H, et al. Diagnostic test accuracy of ultrasonography vs computed tomography for papillary thyroid cancer cervical lymph node metastasis: a systematic review and meta-analysis. *JAMA Otolaryngol Head Neck Surg*. (2022) 148:107–18. doi: 10.1001/jamaoto.2021.3387

16. Liu C, Zhang L, Liu Y, Xia Y, Cao Y, Liu Z, et al. Ultrasonography for the prediction of high-volume lymph node metastases in papillary thyroid carcinoma: should surgeons believe ultrasound results? *World J Surg*. (2020) 44:4142–8. doi: 10.1007/s00268-020-05755-0

17. Liu C, Liu Y, Zhang L, Dong Y, Hu S, Xia Y, et al. Risk factors for high-volume lymph node metastases in cN0 papillary thyroid microcarcinoma. *Gland Surg*. (2019) 8:550–6. doi: 10.21037/gs.2019.10.04

18. Zhang L, Yang J, Sun Q, Liu Y, Liang F, Liu Z, et al. Risk factors for lymph node metastasis in papillary thyroid microcarcinoma: older patients with fewer lymph node metastases. *Eur J Surg Oncol*. (2016) 42:1478–82. doi: 10.1016/j.ejso.2016.07.002

19. Shen G, Ma H, Huang R, Kuang A. Predicting large-volume lymph node metastasis in the clinically node-negative papillary thyroid microcarcinoma: a retrospective study. *Nucl Med Commun*. (2020) 41:5–10. doi: 10.1097/mnm.0000000000001119

20. Oh H-S, Park S, Kim M, Kwon H, Song E, Sung T-Y, et al. Young age and male sex are predictors of large-volume central neck lymph node metastasis in clinical N0 papillary thyroid microcarcinomas. *Thyroid*. (2017) 27:1285–90. doi: 10.1089/thy.2017.0250

21. Chung SR, Baek JH, Choi YJ, Sung T-Y, Song DE, Kim TY, et al. Sonographic assessment of the extent of extrathyroidal extension in thyroid cancer. *Korean J Radiol*. (2020) 21:1187–95. doi: 10.3348/kjr.2019.0983

22. Zhao H, Li H. Meta-analysis of ultrasound for cervical lymph nodes in papillary thyroid cancer: diagnosis of central and lateral compartment nodal metastases. *Eur J Radiol*. (2019) 112:14–21. doi: 10.1016/j.ejrad.2019.01.006

23. Wang SR, Li QL, Tian F, Li J, Li W-X, Chen M, et al. Diagnostic value of multiple diagnostic methods for lymph node metastases of papillary thyroid carcinoma: a systematic review and meta-analysis. *Front Oncol*. (2022) 12:990603. doi: 10.3389/fonc.2022.990603

24. Min Y, Huang Y, Wei M, Wei X, Chen H, Wang X, et al. Preoperatively predicting the central lymph node metastasis for papillary thyroid cancer patients with hashimoto's thyroiditis. *Front Endocrinol*. (2021) 12:713475. doi: 10.3389/fendo.2021.713475

25. Ito Y, Miyauchi A, Kihara M, Higashiyama T, Kobayashi K, Miya A. Patient age is significantly related to the progression of papillary microcarcinoma of the thyroid under observation. *Thyroid*. (2014) 24:27–34. doi: 10.1089/thy.2013.0367

26. Mao J, Zhang Q, Zhang H, Zheng K, Wang R, Wang G. Risk factors for lymph node metastasis in papillary thyroid carcinoma: a systematic review and meta-analysis. *Front Endocrinol*. (2020) 11:265. doi: 10.3389/fendo.2020.00265

27. Wei X, Min Y, Feng Y, He D, Zeng X, Huang Y, et al. Development and validation of an individualized nomogram for predicting the high-volume (>5) central lymph node metastasis in papillary thyroid microcarcinoma. *J Endocrinol Invest*. (2022) 45(3):507–15. doi: 10.1007/s40618-021-01675-5

28. Voutilainen PE, Siironen P, Franssila KO, Sivula A, Haapiainen RK, Haglund CH. AMES, MACIS and TNM prognostic classifications in papillary thyroid carcinoma. *Anticancer Res*. (2003) 23:4283–8.

29. Hay ID, Bergstralh EJ, Goellner JR, Ebersold JR, Grant CS. Predicting outcome in papillary thyroid carcinoma: development of a reliable prognostic scoring system in a cohort of 1779 patients surgically treated at one institution during 1940 through 1989. *Surgery*. (1993) 114:1050–8.

30. Hay ID, Grant CS, Taylor WF, McConahey WM. Ipsilateral lobectomy versus bilateral lobar resection in papillary thyroid carcinoma: a retrospective analysis of surgical outcome using a novel prognostic scoring system. *Surgery*. (1987) 102:1088–95.

31. Bilimoria KY, Bentrem DJ, Ko CY, Stewart AK, Winchester DP, Talamonti MS, et al. Extent of surgery affects survival for papillary thyroid cancer. *Ann Surg*. (2007) 246:375–81. doi: 10.1097/sla.0b013e31814697d9

32. Wu Z, Han L, Li W, Wang W, Chen L, Yao Y, et al. Which is preferred for initial treatment of papillary thyroid cancer, total thyroidectomy or lobotomy? *Cancer Med*. (2021) 10:1614–22. doi: 10.1002/cam4.3743

33. Feng Y, Min Y, Chen H, Xiang K, Wang X, Yin G. Construction and validation of a nomogram for predicting cervical lymph node metastasis in classic papillary thyroid carcinoma. *J Endocrinol Invest*. (2021) 44(10):2203–11. doi: 10.1007/s40618-021-01524-5

34. Póvoa AA, Teixeira E, Bella-Cueto MR, Melo M, Oliveira MJ, Sobrinho-Simões M, et al. Clinicopathological features as prognostic predictors of poor outcome in papillary thyroid carcinoma. *Cancers*. (2020) 12:3186. doi: 10.3390/cancers12113186

35. Vuong HG, Duong UNP, Pham TQ, Tran HM, Oishi N, Mochizuki K, et al. Clinicopathological risk factors for distant metastasis in differentiated thyroid carcinoma: a meta-analysis. *World J Surg*. (2018) 42:1005–17. doi: 10.1007/s00268-017-4206-1

36. Tao Y, Wang C, Li L, Xing H, Bai Y, Han B, et al. Clinicopathological features for predicting central and lateral lymph node metastasis in papillary thyroid microcarcinoma: analysis of 66 cases that underwent central and lateral lymph node dissection. *Mol Clin Oncol*. (2017) 6:49–55. doi: 10.3892/mco.2016.1085

37. Lamartina L, Bidault S, Hadoux J, Guerlain J, Girard E, Breuskin I, et al. Can preoperative ultrasound predict extrathyroidal extension of differentiated thyroid cancer? *Eur J Endocrinol*. (2021) 185:13–22. doi: 10.1530/eje-21-0091

38. Arora N, Turbendian HK, Scognamiglio T, Wagner PL, Goldsmith SJ, Zarnegar R, et al. Extrathyroidal extension is not all equal: implications of macroscopic versus microscopic extent in papillary thyroid carcinoma. *Surgery*. (2008) 144:942–8. doi: 10.1016/j.surg.2008.07.023

39. Yang J, Zhao C, Niu X, Wu S, Li X, Li P, et al. Predictive value of ultrasonic features and microscopic extrathyroidal extension in the recurrence of PTC. *Eur J Radiol*. (2022) 157:110518. doi: 10.1016/j.ejrad.2022.110518

40. Ye L, Hu L, Liu W, Luo Y, Li Z, Ding Z, et al. Capsular extension at ultrasound is associated with lateral lymph node metastasis in patients with papillary thyroid carcinoma: a retrospective study. *BMC Cancer*. (2021) 21:1250. doi: 10.1186/s12885-021-08875-5

41. Kamaya A, Tahvildari AM, Patel BN, Willmann JK, Jeffrey RB, Desser TS. Sonographic detection of extracapsular extension in papillary thyroid cancer. *J Ultrasound Med*. (2015) 34:2225–30. doi: 10.7863/ultra.15.02006

42. Lee DY, Hwang SM, An JH, Son KR, Baek SK, Kim SG, et al. Predicting extrathyroidal extension in patients with papillary thyroid microcarcinoma according to a BRAF mutation. *Clin Exp Otorhinolaryngol*. (2017) 10:174–80. doi: 10.21053/ceo.2015.01655

43. Rienhoff WF. The lymphatic vessels of the thyroid gland in the dog and in man. *Arch Surg*. (1931) 23:783–804. doi: 10.1001/archsurg.1931.01160110070003

44. Foschini MP, Papotti M, Parmeggiani A, Tallini G, Castaldini L, Meringolo D, et al. Three-dimensional reconstruction of vessel distribution in benign and malignant lesions of thyroid. *Virchows Arch*. (2004) 445:189–98. doi: 10.1007/s00428-004-1035-z

45. Yasuoka H, Nakamura Y, Zuo H, Tang W, Takamura Y, Miyauchi A, et al. VEGF-D expression and lymph vessels play an important role for lymph node metastasis in papillary thyroid carcinoma. *Mod Pathol*. (2005) 18:1127–33. doi: 10.1038/modpathol.3800402

46. Kwak JY, Kim E-K, Kim MJ, Son EJ, Chung WY, Park CS, et al. Papillary microcarcinoma of the thyroid: predicting factors of lateral neck node metastasis. *Ann Surg Oncol*. (2009) 16:1348–55. doi: 10.1245/s10434-009-0384-x

47. Zeng RC, Li Q, Lin KL, Zhang W, Gao EL, Huang GL, et al. Predicting the factors of lateral lymph node metastasis in papillary microcarcinoma of the thyroid in eastern China. *Clin Transl Oncol*. (2012) 14:842–7. doi: 10.1007/s12094-012-0875-2

48. Lin KL, Wang OC, Zhang XH, Dai XX, Hu XQ, Qu JM. The BRAF mutation is predictive of aggressive clinicopathological characteristics in papillary thyroid microcarcinoma. *Ann Surg Oncol*. (2010) 17:3294–300. doi: 10.1245/s10434-010-1129-6

frontiers | Frontiers in Oncology

TYPE Original Research
PUBLISHED 09 February 2023
DOI 10.3389/fonc.2023.1072775



OPEN ACCESS

EDITED BY
Beatrice Aramini,
University of Bologna, Italy

REVIEWED BY
Elavarasan Subramani,
University of Texas MD Anderson Cancer Center, United States
Yexiong Tan,
Eastern Hepatobiliary Surgery Hospital, China
Zeming Wu,
iPhenome Biotechnology (Dalian) Inc., China

*CORRESPONDENCE
Xiao Xu
zjxu@zju.edu.cn

†These authors have contributed equally to this work

SPECIALTY SECTION
This article was submitted to Surgical Oncology, a section of the journal Frontiers in Oncology

RECEIVED 17 October 2022
ACCEPTED 26 January 2023
PUBLISHED 09 February 2023

CITATION
Lin Z, Li H, He C, Yang M, Chen H, Yang X, Zhuo J, Shen W, Hu Z, Pan L, Wei X, Lu D, Zheng S and Xu X (2023) Metabolomic biomarkers for the diagnosis and post-transplant outcomes of AFP negative hepatocellular carcinoma.
*Front. Oncol.* 13:1072775.
doi: 10.3389/fonc.2023.1072775



# Metabolomic biomarkers for the diagnosis and post-transplant outcomes of AFP negative hepatocellular carcinoma

Zuyuan Lin[1,2,3,4†], Huigang Li[1,3,4†], Chiyu He[1,3,4†], Modan Yang[1,2,3,4], Hao Chen[1,3,4], Xinyu Yang[1,2,3,4], Jianyong Zhuo[1,3,5], Wei Shen[1,3,4], Zhihang Hu[1,3,4], Linhui Pan[1,3,5], Xuyong Wei[1,3,4], Di Lu[1,3,5], Shusen Zheng[2,4,5,6] and Xiao Xu[3,4,5,7*]

[1]Department of Hepatobiliary and Pancreatic Surgery, Affiliated Hangzhou First People's Hospital, Zhejiang University School of Medicine, Hangzhou, China, [2]The First Affiliated Hospital, Zhejiang University School of Medicine, Hangzhou, China, [3]Key Laboratory of Integrated Oncology and Intelligent Medicine of Zhejiang Province, Affiliated Hangzhou First People's Hospital, Zhejiang University School of Medicine, Hangzhou, China, [4]National Health Commission Key Laboratory of Combined Multi-organ Transplantation, Hangzhou, China, [5]Institute of Organ Transplantation, Zhejiang University, Hangzhou, China, [6]Department of Hepatobiliary and Pancreatic Surgery, Shulan (Hangzhou) Hospital, Zhejiang Shuren University School of Medicine, Hangzhou, China, [7]Zhejiang University School of Medicine, Hangzhou, China

**Background:** Early diagnosis for α-fetoprotein (AFP) negative hepatocellular carcinoma (HCC) remains a critical problem. Metabolomics is prevalently involved in the identification of novel biomarkers. This study aims to identify new and effective markers for AFP negative HCC.

**Methods:** In total, 147 patients undergoing liver transplantation were enrolled from our hospital, including liver cirrhosis patients (LC, n=25), AFP negative HCC patients (NEG, n=44) and HCC patients with AFP over 20 ng/mL (POS, n=78). 52 Healthy volunteers (HC) were also recruited in this study. Metabolomic profiling was performed on the plasma of those patients and healthy volunteers to select candidate metabolomic biomarkers. A novel diagnostic model for AFP negative HCC was established based on Random forest analysis, and prognostic biomarkers were also identified.

**Results:** 15 differential metabolites were identified being able to distinguish NEG group from both LC and HC group. Random forest analysis and subsequent Logistic regression analysis showed that PC(16:0/16:0), PC(18:2/18:2) and SM (d18:1/18:1) are independent risk factor for AFP negative HCC. A three-marker model of Metabolites-Score was established for the diagnosis of AFP negative HCC patients with an area under the time-dependent receiver operating characteristic curve (AUROC) of 0.913, and a nomogram was then established as well. When the cut-off value of the score was set at 1.2895, the sensitivity and specificity for the model were 0.727 and 0.92, respectively. This model was also applicable to distinguish HCC from cirrhosis. Notably, the Metabolites-Score was not correlated to tumor or body nutrition parameters, but difference of the score was statistically significant between different neutrophil-lymphocyte ratio (NLR) groups (≤5 vs. >5, P=0.012). Moreover, MG(18:2/0:0/0:0) was the only prognostic

biomarker among 15 metabolites, which is significantly associated with tumor-free survival of AFP negative HCC patients (HR=1.160, 95%CI 1.012-1.330, P=0.033).

**Conclusion:** The established three-marker model and nomogram based on metabolomic profiling can be potential non-invasive tool for the diagnosis of AFP negative HCC. The level of MG(18:2/0:0/0:0) exhibits good prognosis prediction performance for AFP negative HCC.

KEYWORDS

**hepatocellular carcinoma, cirrhosis, AFP, metabolomics, nomogram**

# 1 Introduction

Liver cancer ranks the 6th most prevalent cancer, and the related mortality ranks the 4th (1). Hepatocellular carcinoma (HCC) comprises around 80% of all the liver cancer cases. China has the heaviest HCC burden worldwide owing to the prevalence of Hepatitis B. HCC is characterized by insidious onset and rapid progress, and prone to metastasis (2). Therefore, many HCC patients are no longer suitable for surgical treatment when they are diagnosed. Most HCC evolves from liver cirrhosis (3). Distinguishing HCC from liver cirrhosis, especially in the early stage, is conducive to clinical decision-making and thus improves the prognosis. α-fetoprotein (AFP) is the most widely used serologic marker for the HCC diagnosis. However, its diagnostic power has been continuously challenged, because up to 50% of small HCC do not secrete AFP and it is elevated in only 20% of early stage HCC patients (4). Moreover, AFP may also deviate from normal value in cirrhosis or hepatitis patients (5). Therefore, the exploration for novel and effective biomarkers for AFP negative HCC is critically important.

Metabolomics is a high throughput and quantitative approach to measure the low-molecular-weight metabolites under specific conditions (6). It is capable of detecting metabolic changes in different pathological or physiological status, which has been an effective tool in disease diagnosis, mechanism study and drug screening (7). Currently, it has shown great promise as a means to identify new biomarkers for various types of cancer, including HCC (8). Acetylcarnitine was identified by metabolomic profiling as a serum diagnostic marker for HCC (9). Liu et al. identified 32 metabolites by metabolomics that altered between HCC and liver cirrhosis (LC), and achieve 100% sensitivity with these markers (10). Wu et al. even established a diagnostic model for HCC from LC based on GC/MS in urine sample (11). However, metabolomic profiling specific for AFP negative HCC is still needed to improve the diagnostic accuracy for HCC. In this study, we enrolled patients of different status related to HCC. By comparing the metabolomic profiling between groups, we successfully identified metabolites capable of screening out AFP negative HCC and further established a novel model.

# 2 Materials and methods

## 2.1 Study population and data collection

25 liver cirrhotic patients (LC group) and 122 HCC patients including 44 AFP negative HCC patients (NEG group), 78 HCC patients with AFP over 20 ng/ml (POS group) in the First Affiliated Hospital of Zhejiang University School of Medicine from April 2012 to December 2016 were enrolled in the study. All Patients in the LC and HCC group underwent liver transplantation and were diagnosed according to post-transplant pathological examination. The exclusion criteria included patients younger than 18 years, undergoing multiorgan transplantation or re-transplantation, or with missing essential data for analysis. Another cohort of 52 healthy control samples (HC group) collected from the same batch of individuals who underwent healthy examination. We collected the data including demographics, body mass index (BMI), pre- operative AFP level, alanine transaminase (ALT) level, aspartate transaminase (AST) level, morphological features (tumor number and largest tumor size), skeletal muscle index [SMI, to define sarcopenia (12)], neutrophil-lymphocyte ratio (NLR), post-transplant recurrence, and patients' survival for analysis. Informed consent was obtained from all the participants, and the study protocol was approved by the Human Ethics Committee of the hospital.

## 2.2 Sample preparation

Peripheral blood samples (EDTA-K2 anticoagulant) were collected from fasted patients or healthy volunteers in the morning of LT or healthy examination, and centrifuged at 3000 rpm for 10 min, then stored the plasma at −80°C, until use. The plasma samples were thawed at 4°C, and the quality control (QC) samples were prepared by pooling aliquots (10 μl) of each sample. Acetonitrile (800 μl) was added to the plasma (200 μl) sample and vortexed for 1 min. We then incubated the mixture at room temperature for 1 min and centrifuged it at 14000 rpm for 10 min at 4°C. The acquired clear supernatant was transferred to UPLC vials, and was then stored at 4°C until detection. The pretreatment of the QC samples was the same as that for the test samples.

## 2.3 UPLC–MS analysis of samples

We performed reversed-phase analysis on a Waters ACQUITY Ultra Performance LC system using an ACQUITY UPLC BEH C18 analytical column (i.d., 2.1 mm × 100 mm; particle size 1.7 mm; pore size, 130 Å). We then used water/formic acid (99.9:0.1 v/v) as mobile phase A and acetonitrile/formic acid (99.9:0.1 v/v) as mobile phase B. A linear gradient LC system (Waters, Milford MA) was optimized as follows: the composition of mobile phase B was changed from 3% to 80% in 7 min, reached 98% in 8 min and held for 5 min, and then reached 100% in 1 min and held for 3 min. The sample manager was kept at 4°C, with an injection volume of 2 µl for each analysis. The QC samples were injected at regular intervals (every 14 samples) throughout the analytical run. These inserted QC samples were used to evaluate the repeatability of sample pretreatment and monitor the stability of the LC–MS system during sequence analysis.

We used a Waters Q-TOF Premier mass spectrometer to perform the mass spectrometry in positive ion electrospray mode. The instrumental parameters were set as follows: The mass scan range was 50 m/z–1000 m/z using an accumulation time of 0.2 s per spectrum; the MS acquisition rate was set to 0.3 s with a 0.02 s inter scan delay; high-purity nitrogen was used as nebulizer and drying gas. The nitrogen drying gas was at a constant flow rate of 600 L/h, and the source temperature was set at 120°C. For the positive mode, the capillary voltage was set at 3.0 kV and the sampling cone voltage was set at 45.0 V. Argon was used as collision gas. MS/MS analysis was performed on the mass spectrometer set at different collision energies of 10 eV–50 eV according to the stability of each metabolite. The time of flight analyzer was used in V mode and tuned for maximum resolution (>10,000 resolving power at m/z 556.2771). The instrument was previously calibrated with sodium formate; the lock mass spray for precise mass determination was set by leucine enkephalin at 556.2771 m/z with concentration of 0.5 ng/L in the positive ion mode. All analyses were acquired using the lock spray to ensure accuracy and reproducibility.

## 2.4 Data processing and statistical analysis

We referred to our previously published metabolomic data (13). The dataset was generated based on the retention time, m/z, and normalized signal intensity of the peaks. The preprocessed data obtained by MassLynx were exported and analyzed using SIMCA-P 14.1 (Umetrics AB, Sweden). Firstly, principal component analysis (PCA) was introduced to evaluate the reliability of the resulting dataset (including QC samples). Secondly, supervised orthogonal partial least squares discriminant analysis (OPLS-DA) was performed to better distinguishing the two groups. Potential biomarkers of differentiating AFP negative HCC patients from LC and HC groups were selected according to the Variable Importance in the Projection (VIP) values, fold change (FC), and Wilcoxon Test. Statistical analysis including logistic regression and cox regression was performed using SPSS version 25.0 statistical software (SPSS inc. Chicago, IL, USA) and GraphPad Prism version 9 (GraphPad, La Jolla, CA, USA). Random forest analysis and nomogram construction were performed by R Version 3.6.1. Area under the time-dependent receiver operating characteristic curve (AUROC) were used to evaluate discriminative ability. The AUROC difference is performed using DeLong's test. The Hosmer-Lemeshow (HL) goodness-of-fit test was used to assess the calibration of the model. Mann-Whitney U test were used to compare the Metabolite-Score between different groups. Kaplan-Meier analysis and Breslow test were used to compare the survival between groups. $P < 0.05$ was considered statistically significant throughout the study.

# 3 Results

## 3.1 Baseline characteristics

147 patients included in this study underwent LT for HCC or cirrhosis treatment, and 52 healthy volunteers were also enrolled. Of all the patients with different liver diseases, 132 were male (89.8%) and 15 were female (10.2%), while 14 were male (26.9%) and 38 were female (73.1%) in healthy controls. The mean age in LC group and NEG group was 47.9 ± 9.8 and 53.2 ± 8.8 years, respectively (P=0.021). This could be explained by the fact that cirrhosis is an intermediate process of chronic hepatic disease developing to HCC. The AFP level in these two groups was 79.9 ± 275.4 and 8.4 ± 5.5 ng/mL, respectively (P=0.170). The difference of liver functions (including ALT and AST) was not significant between the two groups. Baseline features of all the study subjects including HC group and POS group were listed in Table 1, and particular features of tumor patients are listed in Supplementary Table S1.

TABLE 1 Baseline characteristics of patients with liver disease.

| | Liver cirrhosis (n=25) | AFP negative HCC (n=44) | AFP positive HCC (n=78) | Healthy controls (n=52) | P value* |
|---|---|---|---|---|---|
| Age (years) | 47.9 ± 9.8 | 53.2 ± 8.8 | 51.6 ± 8.1 | 37.8 ± 10.4 | 0.021 |
| Male gender, n (%) | 22 (88.0) | 40 (90.9) | 70 (89.7) | 14 (26.9) | 0.700 |
| AFP (ng/mL) | 79.9 ± 275.4 | 8.4 ± 5.5 | 7091.4 ± 15697.9 | 6.3 ± 23.4[#] | 0.170 |
| ALT (U/L) | 123.7 ± 197.6 | 64.1 ± 101.9 | 50.7 ± 54.8 | 17.6 ± 12.4 | 0.836 |
| AST (U/L) | 132.8 ± 249.3 | 94.9 ± 241.1 | 69.7 ± 62.5 | 20.4 ± 7.0 | 0.400 |

*P: Liver cirrhosis vs. AFP negative HCC group.
[#]: There was one case of missing data.
AFP, α-fetoprotein; HCC, hepatocellular carcinoma; ALT, alanine aminotransferase; AST, aspartate aminotransferase.

## 3.2 Metabolomic markers for AFP negative HCC

Metabolomic profiling was performed on the plasma of 52 healthy volunteers and 147 patients with HCC or cirrhosis, and general workflow of this study is listed as Figure 1A. The total ion chromatograms of a single sample from each group were acquired by the UPLC-MS platform. Using MZmine ver. 2.0 software, this pre-treatment revealed 1242 integral peaks following extraction ion chromatography detection in all samples, which was reported in our previous work (13). PCA plot (R2X=0.631, Q2 = 0.421) showed that QC sample cluster together, indicating the high stability and reproducibility of the instrument (Supplementary Figure S1). Besides, HC group showed an obvious separation from NEG HCC group and LC group, while NEG HCC group was roughly separated from LC group (Figure 1B).

In order to identify metabolomic markers for AFP negative HCC, pair-wise comparisons were performed among HC, LC and NEG group based on OPLS-DA models (Figures 1C–E) and Wilcoxon Test. Validation of the OPLS-DA model of LC and NEG group was obtained from 200 permutation tests (Supplementary Figures S2A–C). The validation plot demonstrated that the original model was valid: the Q2 regression line had a negative intercept, and the intercepts of R2 were lower than the original point to the right. S-plots of these OPLS-DA models were further investigated to acquire the correlation value of metabolites (Supplementary Figures S2D–F). Ions with a variable importance value (VIP) >1, fold change (FC) >1.5 and P<0.01 were selected. Thus, 116 overlapping ions were selected for further identification (Figure 2A). By excluding those ions with over one third cases of '0' value, 15 metabolites including MG (monoacylglyceride), PC (phosphatidylcholine), DG (diglyceride) and SM (sphingomyelin) were finally selected (Table 2 and Supplementary Table S2), and their VIP values and correlation values were also listed. In comparison to LC group, 4 metabolites (Chenodeoxycholic acid glycine conjugate, MG(18:2/0:0/0:0), 1-Oleoylglycerophosphoserine, PC(16:0/16:0)) were significantly decreased in NEG group, whereas 11 metabolites (DG(9M5/9M5/0:0), PC(22:6/16:0), SM(d18:1/18:1), LysoPC(17:0), LysoPC(16:0), PC(22:6/18:2), PC(18:2/18:2), 3-Methoxybenzenepropanoic acid, PC(18:2/20:4), 3-Carboxy-4-methyl-5-propyl-2-furanpropionic acid, PC(14:0/20:4)) were significantly elevated (Figure 2B).

The biological pathways involved in the metabolism of these 15 differential metabolites were determined by enrichment analysis using MetaboAnalyst. All matched pathways were shown according to p

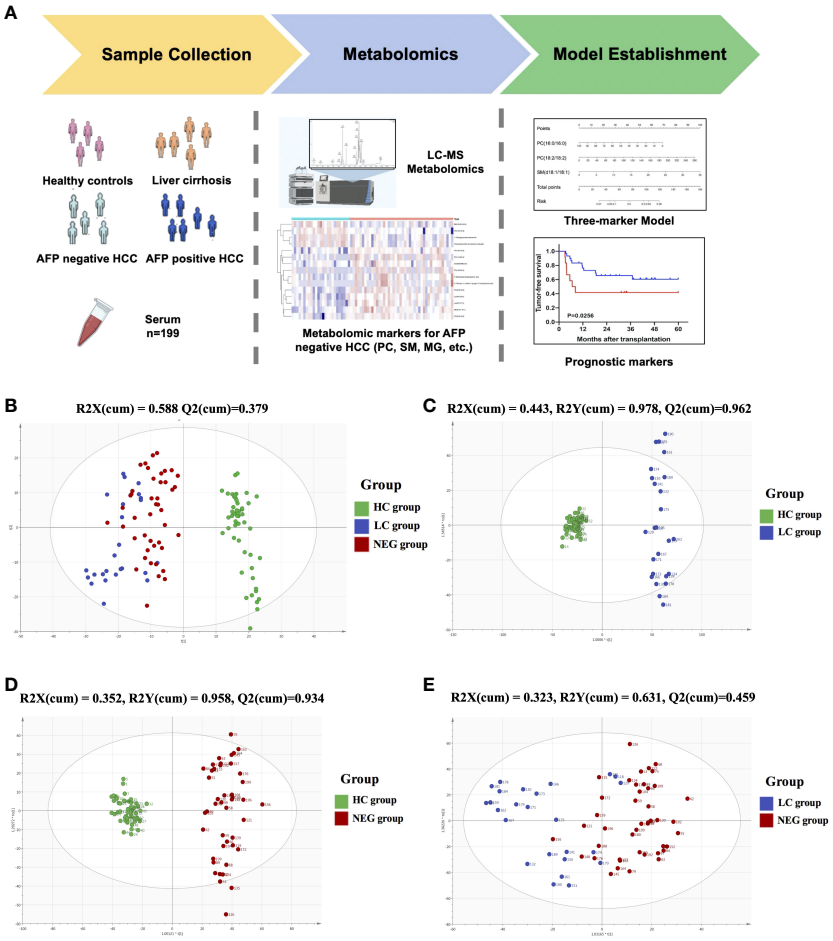


FIGURE 1
The metabolomics profiling for plasma samples. **(A)** General workflow for this study. **(B)** PCA score plot for 52 healthy controls, 25 liver cirrhosis patients, 122 HCC patients and 15 quality controls. **(C)** OPLS-DA score plot for HC and LC group. **(D)** OPLS-DA score plot for HC and NEG group. **(E)** OPLS-DA score plot for LC and NEG group.

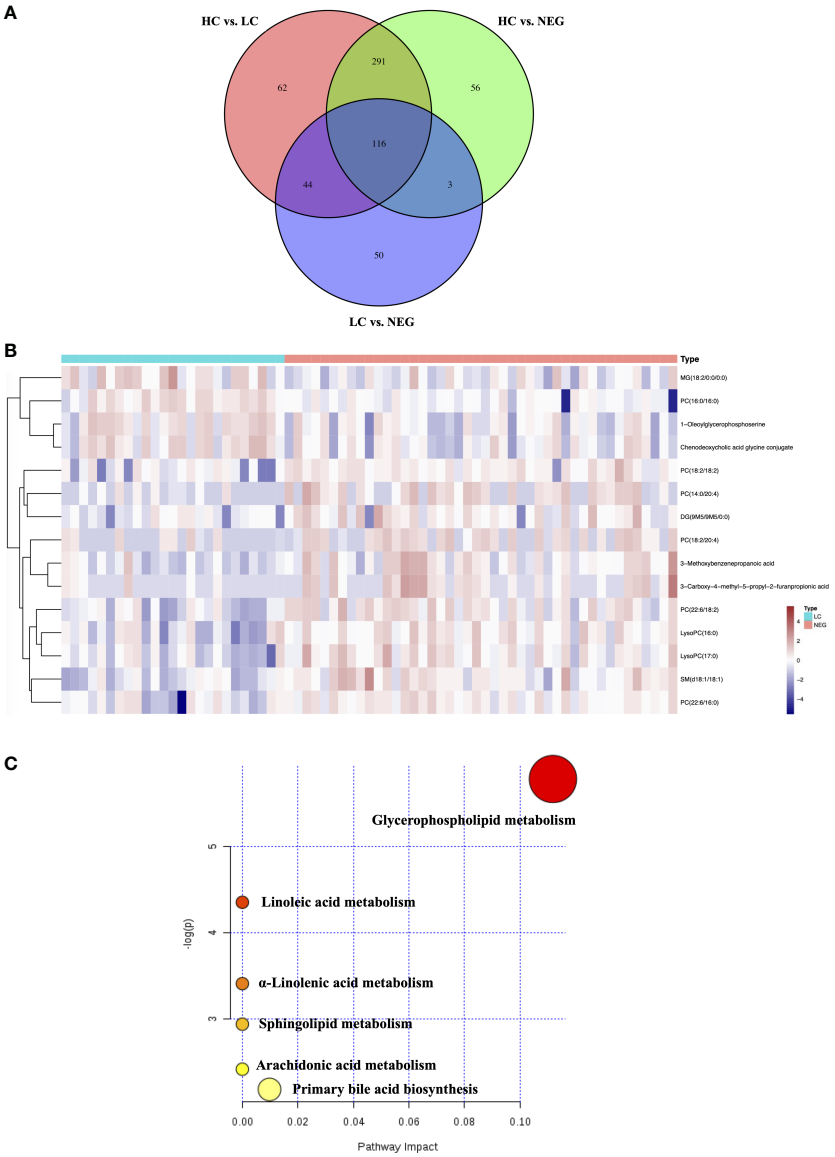


FIGURE 2
Differential metabolites for AFP negative HCC. **(A)** Venn diagram of the differential ions in HC vs. LC, HC vs. NEG and LC vs. NEG. **(B)** Heatmap of 15 differentially expressed metabolites between LC and NEG group according to the normalized intensity. **(C)** Summary of altered pathways AFP negative HCC patients compared to liver cirrhosis patients, as analyzed by MetaboAnalyst platform (https://www.metaboanalyst.ca/). .

values from the pathway enrichment analysis (y-axis) and pathway impact values from pathway topology analysis (x-axis) (14), with the most impacted pathways colored in red. One pathway was considered specifically related to AFP negative HCC, that is, glycerophospholipid metabolism (Figure 2C).

## 3.3 A novel model for the diagnosis of AFP negative HCC

Random forest (RF) analysis was further used to discriminate AFP negative HCC patient from liver cirrhosis patients based on 15-metabolites panel, which showed relatively low error rate of 25.49% in the training set. Moreover, the prediction of validation data based on training set RF models also yielded satisfactory results with error rate of 14.28% for LC vs. NEG. In order to identify potential biomarkers for AFP negative HCC, the top 7 ranked differential metabolites in the respective models were selected according to the mean decrease accuracy (MDA), which denoted the percent decrease in accuracy when the trial was performed in the absence of the metabolite (Figure 3A). The PCoA plot also showed these two groups of samples could almost cluster separately (Figure 3B). Subsequent Logistic regression analysis showed that PC(16:0/16:0), PC(18:2/18:2) and SM(d18:1/18:1) were independent risk factors distinguishing AFP negative HCC from liver cirrhosis patients (Supplementary Table S3). Thus, a three-marker model was constructed: Metabolites-Score = -0.071* PC(16:0/16:0) + 0.038* PC (18:2/18:2) + 0.293* SM(d18:1/18:1)-0.553.The ROC curve for the three-marker model was then constructed and a nomogram was then established as well (Figures 3C, D). The model showed good discrimination (AUROC=0.913, 95%CI 0.848-0.977, P<0.001) and calibration (HL P=0.739). According to the model, AFP negative

TABLE 2 Differential ions and referred metabolites between LC and NEG group.

| Ions | Mean (LC) | Mean (NEG) | logFC | P value | VIP value | Correlation value | Metabolites |
|---|---|---|---|---|---|---|---|
| var297 | 97.351 | 44.007 | -1.145 | 3.38E-03 | 1.336 | -0.631 | Chenodeoxycholic acid glycine conjugate |
| var499 | 7.985 | 3.980 | -1.004 | 1.15E-03 | 1.468 | -0.383 | MG(18:2/0:0/0:0) |
| var634 | 10.424 | 5.654 | -0.883 | 1.93E-04 | 1.468 | -0.677 | 1-Oleoylglycerophosphoserine |
| var690 | 60.707 | 34.012 | -0.836 | 1.08E-05 | 1.772 | -0.783 | PC(16:0/16:0) |
| var350 | 1.321 | 2.069 | 0.648 | 2.46E-03 | 1.226 | 0.335 | DG(9M5/9M5/0:0) |
| var265 | 69.075 | 111.190 | 0.687 | 5.81E-04 | 1.413 | 0.577 | PC(22:6/16:0) |
| var61 | 7.749 | 12.562 | 0.697 | 6.87E-06 | 1.419 | 0.473 | SM(d18:1/18:1) |
| var380 | 2.362 | 4.057 | 0.780 | 5.08E-04 | 1.387 | 0.557 | LysoPC(17:0) |
| var4 | 31.630 | 57.377 | 0.859 | 8.63E-04 | 1.347 | 0.528 | LysoPC(16:0) |
| var169 | 3.388 | 6.484 | 0.937 | 9.04E-06 | 1.545 | 0.574 | PC(22:6/18:2) |
| var325 | 24.917 | 51.680 | 1.052 | 1.94E-04 | 1.333 | 0.436 | PC(18:2/18:2) |
| var312 | 2.192 | 6.600 | 1.590 | 1.76E-04 | 1.184 | 0.346 | 3-Methoxybenzenepropanoic acid |
| var905 | 3.500 | 11.605 | 1.729 | 9.60E-04 | 1.191 | 0.472 | PC(18:2/20:4) |
| var898 | 0.150 | 0.645 | 2.107 | 2.50E-03 | 1.089 | 0.378 | 3-Carboxy-4-methyl-5-propyl-2-furanpropionic acid |
| var810 | 0.441 | 1.942 | 2.140 | 2.35E-04 | 1.360 | 0.547 | PC(14:0/20:4) |

FC, fold change; VIP, Variable Importance in the Projection; MG, monoacylglyceride; PC, phosphatidylcholine; DG: diglyceride; 9M5, 9-(3-methyl-5-pentylfuran-2-yl)nonanoic acid; SM, sphingomyelin.

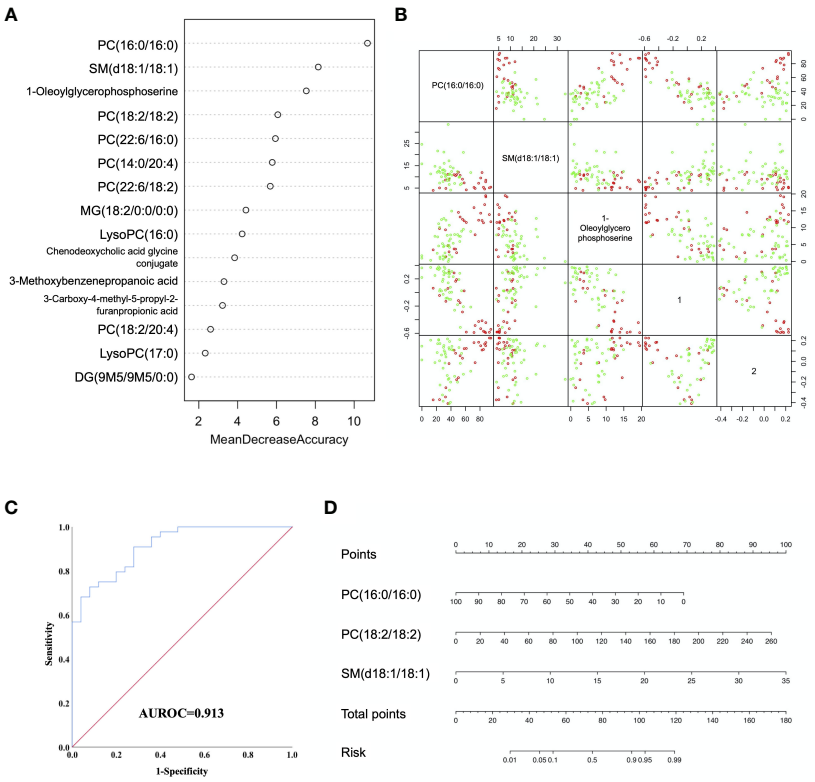


FIGURE 3
Diagnostic model for AFP negative HCC based on Random Forest (RF) analysis. **(A)** MDA plot of 15 differentially expressed metabolites based on RF analysis between LC and NEG group. **(B)** Predictors and PCoA plot based on RF analysis, and Scatter plots showing correlation distribution between each feature and PCoA1/2 axes. **(C)** ROC curve showing the ability of three-marker model to distinguish AFP negative HCC patients from liver cirrhosis patients. **(D)** Diagnostic nomogram for AFP negative HCC based on the three-marker model.

patients but with Metabolites-Score more than 1.2895 could be regarded as having a high risk of HCC. The sensitivity and specificity for the model were 0.727 and 0.92, respectively.

## 3.4 Model for the diagnosis of HCC

We further validated our three-marker model in all patients with HCC or cirrhosis. The diagnostic value of this model was assessed, showing a good discrimination (AUROC=0.912, 95%CI 0.857-0.967, P<0.001) and calibration (HL P=0.645). The cut-off value of Metabolites-Score was also set at 1.2895 with a sensitivity of 0.713 and a specificity of 0.92. To compare the diagnostic performance between our model and AFP, we also performed ROC analysis for AFP and the AUROC was 0.812 (95%CI 0.716-0.909, P<0.001). When the cut-off value was set at 3.7 ng/ml, the sensitivity and specificity were 0.91 and 0.6, respectively. Though the AUROC of our three-marker model was higher than that of AFP, the difference was not significant between them (ΔAUROC=0.1, P=0.13). By combining AFP with three-marker model, we are able to achieve a higher accuracy for diagnosis with an AUROC of 0.951 (95%CI 0.917-0.986, P<0.001, Figure 4) and a HL P value of 0.216. The diagnostic performance of the combination model was significantly better than three-marker model (ΔAUROC=0.039, P=0.006) or AFP along (ΔAUROC=0.139, P=0.014), with a positive predictive value of 0.981 and a negative predictive value of 0.575 (Supplementary Table S4).

## 3.5 Correlation between the metabolites-score and clinical parameters

We further explore the relationship between Metabolites-Score and clinical parameters, and 122 HCC patients were enrolled. We stratified all HCC patients into two groups according to AFP level (≤400 ng/mL and >400ng/mL), tumor number (single and multiple) and largest tumor size (≤5cm and >5cm), though no statistically significant difference in Metabolites-Score were found between any two groups (P>0.05, Figures 5A–C). In addition, we analyze the relationship between Metabolites-Score and body nutrition status in all HCC patients. In overweight patients group (BMI≥24kg/m$^2$), the Metabolites-Score was higher than that in normal weight patients group (BMI<24kg/m$^2$, 3.81 ± 3.13 vs. 2.99 ± 2.13, P=0.243, Figure 5D). In sarcopenic patient group, the Metabolites-Score was lower than that in non-sarcopenic patient group (2.56 ± 2.11 vs. 3.46 ± 2.60, P=0.155, Figure 5E). NLR, which represents patient immune status, was also included in the study. Patients with a NLR over 5 had significantly lower Metabolites-Score than patients with a NLR below 5 (2.14 ± 1.88 vs. 3.56 ± 2.60, P=0.012, Figure 5F).

## 3.6 Metabolomic markers predicting prognosis of AFP negative HCC in liver transplantation

After excluding the patients who died within two months, 42 AFP negative HCC patients were enrolled for prognostic analysis. 17 patients died during follow-up, with 1-, 3-, and 5-year overall survival (OS) rates of 92.9%, 62.8% and 52.2%, respectively. 18 patients were diagnosed with tumor recurrence during follow-up, with 1-, 3-, and 5-year tumor-free survival (TFS) rates of 66.5%, 58.9% and 54.7%, respectively. According to the univariable Cox regression analysis, MG(18:2/0:0/0:0) was the only metabolite having a moderate prediction capability for TFS (HR=1.160, 95%CI 1.012-1.330, P=0.033, Table 3). Based on the normalized peak intensity of MG (18:2/0:0/0:0), the patients were divided into low risk group (n=30) and high risk group (n=12). TFS and OS was significantly different

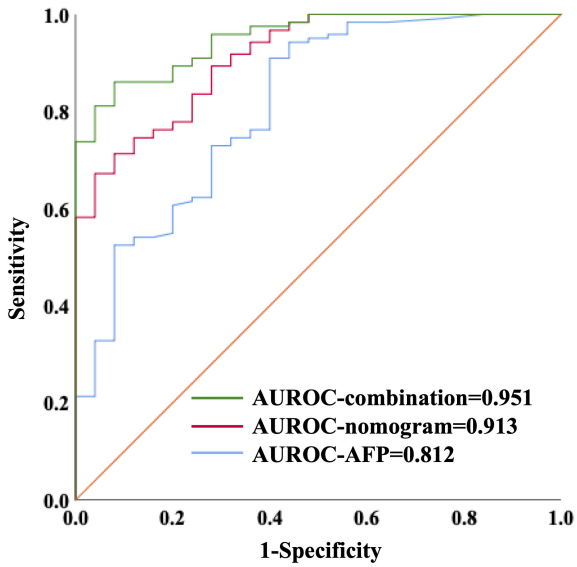


FIGURE 4
ROC curves showing diagnostic value of nomogram combining with AFP in distinguishing HCC patients from liver cirrhosis patients.

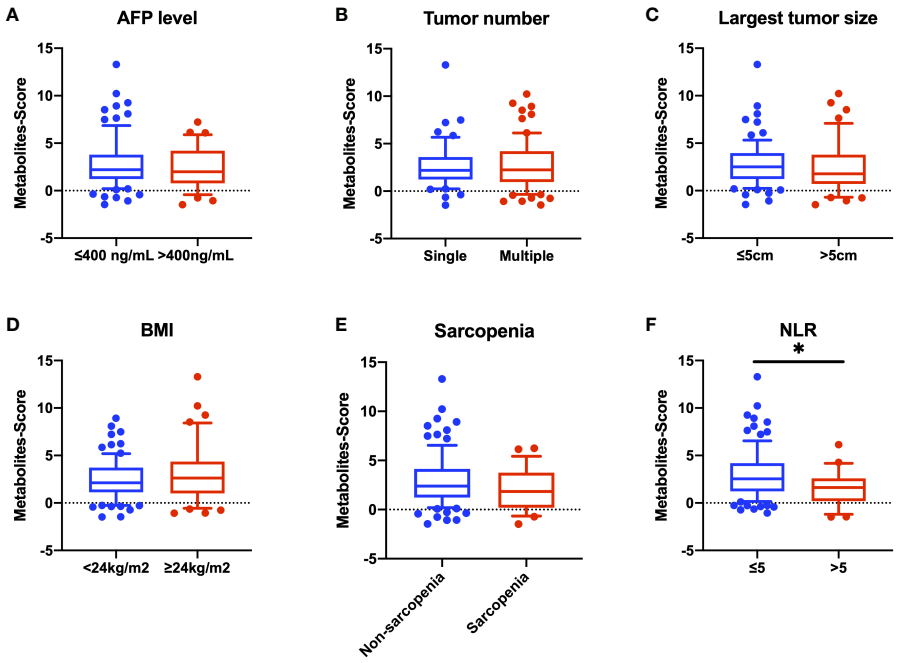


FIGURE 5
Comparison of Metabolites-Score in different groups divided by clinical parameters. Metabolites-Score showed no significant difference in groups divided by tumor parameters and body nutrition parameters, but was significantly correlated to NLR level. **(A)** Bar plot for AFP ≤ 400 ng/mL group vs. >400ng/mL group. **(B)** Bar plot for single tumor group vs. multiple tumor group. **(C)** Bar plot for largest tumor size ≤ 5 cm group vs. >5 cm group. **(D)** Bar plot for BMI<24kg/m2 group vs. ≥24kg/m2 group. **(E)** Bar plot for non-sarcopenia group vs. sarcopenia group. **(F)** Bar plot for NLR ≤ 5 group vs. >5 group. Data are expressed as median (10-90 percentile range) (*P < 0.05, Mann–Whitney U test).

between the two groups (P<0.05, Figures 6A, B), especially in early survival. We also validated the prognostic value of MG(18:2/0:0/0:0) in AFP positive HCC patients, but it showed no difference between low risk group (n=55) and high risk group (n=19, Supplementary Figures S3A, B).

## 4 Discussion

Multiple studies have reported that AFP negative HCC patients were less likely to feature aggressive tumors and were more likely to have a favorable long-term survival when compared with AFP

TABLE 3 Univariate Cox regression analysis for predictive factors of tumor-free survival.

| Ions | Metabolites | HR (95% CI) | P value |
|---|---|---|---|
| var690 | PC(16:0/16:0) | 0.977 (0.943-1.012) | 0.190 |
| var634 | 1-Oleoylglycerophosphoserine | 0.909 (0.797-1.037) | 0.156 |
| var325 | PC(18:2/18:2) | 0.994 (0.979-1.010) | 0.471 |
| var810 | PC(14:0/20:4) | 1.067 (0.816-1.394) | 0.637 |
| var61 | SM(d18:1/18:1) | 0.965 (0.876-1.063) | 0.465 |
| var4 | LysoPC(16:0) | 1.003 (0.990-1.016) | 0.681 |
| var169 | PC(22:6/18:2) | 0.959 (0.817-1.125) | 0.608 |
| var265 | PC(22:6/16:0) | 1.005 (0.995-1.016) | 0.329 |
| var499 | MG(18:2/0:0/0:0) | 1.160 (1.012-1.330) | 0.033 |
| var312 | 3-Methoxybenzenepropanoic acid | 1.031 (0.975-1.090) | 0.290 |
| var297 | Chenodeoxycholic acid glycine conjugate | 0.986 (0.971-1.002) | 0.078 |
| var380 | LysoPC(17:0) | 1.011 (0.779-1.312) | 0.933 |
| var905 | PC(18:2/20:4) | 1.028 (0.983-1.075) | 0.227 |
| var350 | DG(9M5/9M5/0:0) | 0.801 (0.480-1.335) | 0.395 |
| var898 | 3-Carboxy-4-methyl-5-propyl-2-furanpropionic acid | 1.359 (0.827-2.232) | 0.226 |

HR, hazard ratio; CI, confidence interval.

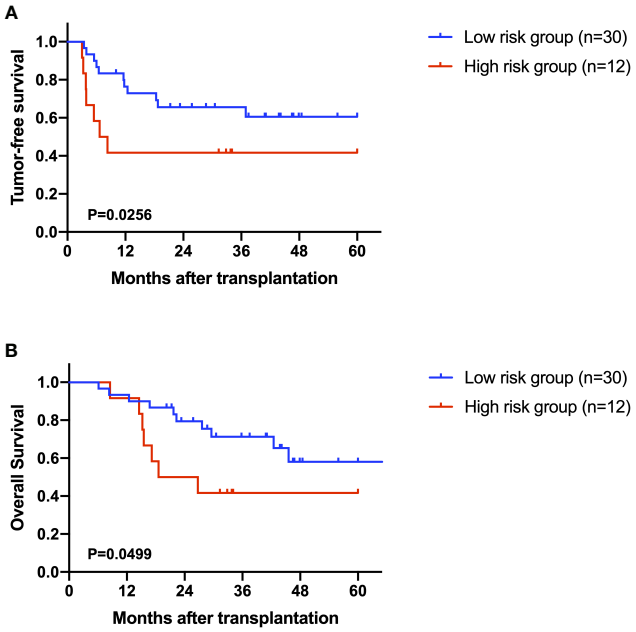


FIGURE 6
The role of MG(18:2/0:0/0:0) in the prediction of prognosis. **(A)** Kaplan-Miere plot of tumor-free survival in AFP negative HCC patients. **(B)** Kaplan-Miere plot of overall survival in AFP negative HCC patients.

positive HCC patients. Discrimination of AFP negative HCC from LC patients by noninvasive methods is important for clinical practice, which would help patients to get timely and appropriate treatment. A number of serum biomarkers carrying diagnostic potential, like des-gamma-carboxyprothrombin (DCP), and lens culinaris agglutinin-reactive AFP (AFP-L3), have been identified as complements to AFP (15). Furthermore, Xu et al. reported that the combination of AFP-L3 and glypican-3 (GPC3) achieved high diagnostic accuracy for low-AFP HCC patients, because single detection with AFP-L3 may not be sensible and accurate (16, 17). Combination of Dickkopf proteins (DKK1) and AFP also increased the diagnostic yield than using either marker alone (18, 19). Studies are still being carried out for optimal biomarkers for AFP negative HCC. Metabolomics has always been a method exploring new diagnostic markers for various liver diseases. Here, we performed metabolomic profiling on the plasma of healthy volunteers and patients with LC or HCC to select novel biomarkers. Our results showed that the combination of metabolomic biomarkers could be applied to distinguish AFP negative HCC patients and predict their outcomes.

In this study, we identified 15 markers able to discriminate AFP negative HCC from both LC and HC patients. These markers are associated with glycerophospholipid metabolism. Alterations in glycerophospholipid metabolism was involved in the progression of different kinds of cancer including HCC (20–22). It is reported that highly proliferating cancer cells need to continually provide glycerophospholipids particularly for membrane production by fatty acids synthesis (23). On the other hand, among the 15 markers, 8 of them are also significantly altered between POS and LC group, which indicated that involved metabolomic changes were common in HCC pathologically. Thus, targeting this pathway might be a promising strategy for HCC treatment. For instance, Sorafenib, which is the most common drug for targeted therapy in HCC, could preferentially affect glycerophospholipid metabolism (24). We further performed Random forest analysis and Logistic regression analysis to construct the novel model. The three-marker model is accurate to distinguish AFP negative HCC patients from liver cirrhosis patients. By combining AFP with this model, we are able to achieve higher accuracy for diagnosis with an AUROC of 0.951.

Our three-marker model contains two kinds of phosphatidylcholine (PC) and one kind of sphingomyelin (SM). Many studies have reported their association with cancer and other disorders, which is known to play an important role in biological function including cell proliferation, migration and apoptosis (25, 26). A recent study found that the generation of PC is a notable lipid signature in proliferating hepatocytes, which also showed a positive correlation to hepatic carcinogenesis (27). Sphingomyelin synthase (SMS) is reported to play a critical role in sphingolipid metabolism which is involved in oncogenesis and sorafenib resistance (28), though the direct function of SM in HCC has not been clearly elucidated. Nevertheless, different types of PCs also have diverse functions. Some studies indicating that PC showed opposite function in tumor progression and hepatic carcinogenesis (29, 30). Our research also reflected this contrary phenomenon, that is, increased PC(16:0/16:0) showed lower risk of HCC, while increased PC(18:2/18:2) had a positive relationship to the risk of HCC. Subsequently, we further studied the correlation between the Metabolites-Score and clinical parameters. Our results found that patients in different groups divided by tumor parameters (including AFP level, tumor number and largest tumor size) have close Metabolites-Score, which indicated our model is applicable to all kinds of HCC patients. As for body nutrition parameters, overweight (BMI≥24kg/m$^2$) and non-sarcopenic patients had relatively high Metabolites-Score, though without significant difference due to low sample size. Several studies reported that overweight and sarcopenic patients had distinctive lipidomic signatures like dysregulated SM and PC lipid species (31–33). Interestingly, our results found that NLR, an inflammatory marker, was significantly related to Metabolites-Score. NLR could partially represent

the balance between pro-tumor inflammation and anti-tumor immune reaction (34). It is reported that PC-derived lipid mediators could bind to receptors presented in diverse immune cells, thus inhibiting the antitumor immunity and promoting immunoregulation (35). Therefore, metabolomics or lipidomics is promising to identify novel biomarkers to reflect body immune status and metabolic status concurrently.

Also, we found that MG(18:2/0:0/0:0) was associated with both OS and TFS in AFP negative patients, though it was not applicable for all HCC patients. This finding indicated that MG(18:2/0:0/0:0) was a prognostic biomarkers specially for AFP negative HCC. MG(18:2/0:0/0:0) belongs to monoglyceride family, which is more correctly known as a monoacylglycerol. Yang et al. reported that the overexpression of monoglyceride lipase (MGLL), an enzyme converting monoacylglycerol to free fatty acids and glycerol, could suppress the migration of HCC cells (36). Thus, monoacylglycerol might accumulate in patients with advanced HCC due to the deficit of MGLL.

Our study still has some limitations. Firstly, non-targeted metabolomics has disadvantages such as inaccurate identification of metabolites, difficult to detect low abundance metabolites and so on. For new model establishment, the differential metabolites were relatively scarce. In spite of those disadvantages, we still provided a perspective on metabolic markers for AFP negative HCC and identified several lipid metabolism-associated markers. Hence, targeted metabolomics like lipidomics could be performed accordingly in the future. Secondly, due to the severe burden of HCC in China, the recurrence rate was relatively high in this study for the attempts in liver transplantation beyond the Milan criteria. Thus, those identified metabolites and the nomogram might not be completely suitable for western patient cohort. Another issue is its feasibility in clinical practice, so further external validation should be performed in future studies.

In conclusion, metabolomics profiling successfully identified metabolic markers and novel diagnostic nomogram for AFP negative HCC. The pre-operative plasma metabolite level was also efficient in the prediction of recurrence risk in liver transplantation for AFP negative HCC.

## Data availability statement

The original contributions presented in the study are included in the article/Supplementary Material. Further inquiries can be directed to the corresponding author.

## Ethics statement

The studies involving human participants were reviewed and approved by the First Affiliated Hospital, Zhejiang University School of Medicine. The patients/participants provided their written informed consent to participate in this study.

## Author contributions

Study concept and design: XX, SZ and DL; Acquisition of data: ZL, HL and CH; Analysis and interpretation of data: ZL, HL, CH, MY and DL; Drafting of the manuscript: ZL, HL, HC and DL; Critical revision of the manuscript for Important intellectual content: XX, SZ and XW; Statistical analysis: ZL, XY, JZ, WS and ZH; Obtained funding: XX and DL; Administrative, technical, or material support: WS, ZH and LP; Study supervision: XX. All authors contributed to the article and approved the submitted version.

## Funding

This work was supported Key Program, National Natural Science Foundation of China (No. 81930016), National Key Research and Development Program of China (No. 2021YFA1100500), the Major Research Plan of the National Natural Science Foundation of China (No.92159202), Young Program of National Natural Science Funds (No. 82000617) and the Construction Fund of Key Medical Disciplines of Hangzhou (OO20200093).

## Acknowledgments

We thank Ms. Cen and Ms. Xu for technical assistance and secretarial work.

## Conflict of interest

The authors declare that the research was conducted in the absence of any commercial or financial relationships that could be construed as a potential conflict of interest.

## Publisher's note



## Supplementary material

The Supplementary Material for this article can be found online at: https://www.frontiersin.org/articles/10.3389/fonc.2023.1072775/full#supplementary-material

# References


1. Bray F, Ferlay J, Soerjomataram I, Siegel RL, Torre LA, Jemal A. Global cancer statistics 2018: GLOBOCAN estimates of incidence and mortality worldwide for 36 cancers in 185 countries. *CA Cancer J Clin* (2018) 68(6):394–424. doi: 10.3322/caac.21492

2. Llovet JM, Montal R, Sia D, Finn RS. Molecular therapies and precision medicine for hepatocellular carcinoma. *Nat Rev Clin Oncol* (2018) 15(10):599–616. doi: 10.1038/s41571-018-0073-4

3. Llovet JM, Zucman-Rossi J, Pikarsky E, Sangro B, Schwartz M, Sherman M, et al. Hepatocellular carcinoma. *Nat Rev Dis Primers* (2016) 2:16018. doi: 10.1038/nrdp.2016.18

4. Fong ZV, Tanabe KK. The clinical management of hepatocellular carcinoma in the united states, Europe, and Asia: A comprehensive and evidence-based comparison and review. *Cancer* (2014) 120(18):2824–38. doi: 10.1002/cncr.28730

5. Wong RJ, Ahmed A, Gish RG. Elevated alpha-fetoprotein: Differential diagnosis - hepatocellular carcinoma and other disorders. *Clin Liver Dis* (2015) 19(2):309–23. doi: 10.1016/j.cld.2015.01.005

6. Gomase V, Changbhale S, Patil S, Kale K. Metabolomics. *Curr Drug Metab* (2008) 9 (1):89–98. doi: 10.2174/138920008783331149

7. Zhang A, Sun H, Yan G, Han Y, Ye Y, Wang X. Urinary metabolic profiling identifies a key role for glycocholic acid in human liver cancer by ultra-performance liquid-chromatography coupled with high-definition mass spectrometry. *Clin Chim Acta* (2013) 418:86–90. doi: 10.1016/j.cca.2012.12.024

8. Liesenfeld DB, Habermann N, Owen RW, Scalbert A, Ulrich CM. Review of mass spectrometry-based metabolomics in cancer research. *Cancer Epidemiol Biomarkers Prev* (2013) 22(12):2182–201. doi: 10.1158/1055-9965.EPI-13-0584

9. Lu Y, Li N, Gao L, Xu YJ, Huang C, Yu K, et al. Acetylcarnitine is a candidate diagnostic and prognostic biomarker of hepatocellular carcinoma. *Cancer Res* (2016) 76 (10):2912–20. doi: 10.1158/0008-5472.Can-15-3199

10. Liu Y, Hong Z, Tan G, Dong X, Yang G, Zhao L, et al. NMR and LC/MS-based global metabolomics to identify serum biomarkers differentiating hepatocellular carcinoma from liver cirrhosis. *Int J Cancer* (2014) 135(3):658–68. doi: 10.1002/ijc.28706

11. Wu H, Xue R, Dong L, Liu T, Deng C, Zeng H, et al. Metabolomic profiling of human urine in hepatocellular carcinoma patients using gas chromatography/mass spectrometry. *Analytica chimica Acta* (2009) 648(1):98–104. doi: 10.1016/j.aca.2009.06.033

12. Itoh S, Yoshizumi T, Kimura K, Okabe H, Harimoto N, Ikegami T, et al. Effect of sarcopenic obesity on outcomes of living-donor liver transplantation for hepatocellular carcinoma. *Anticancer Res* (2016) 36(6):3029–34.

13. Lu D, Yang F, Lin Z, Zhuo J, Liu P, Cen B, et al. A prognostic fingerprint in liver transplantation for hepatocellular carcinoma based on plasma metabolomics profiling. *Eur J Surg Oncol* (2019) 45(12):2347–52. doi: 10.1016/j.ejso.2019.07.004

14. Xia J, Wishart DS. Web-based inference of biological patterns, functions and pathways from metabolomic data using MetaboAnalyst. *Nat Protoc* (2011) 6(6):743–60. doi: 10.1038/nprot.2011.319

15. Chen H, Zhang Y, Li S, Li N, Chen Y, Zhang B, et al. Direct comparison of five serum biomarkers in early diagnosis of hepatocellular carcinoma. *Cancer Manag Res* (2018) 10:1947–58. doi: 10.2147/CMAR.S167036

16. Shu H, Li W, Shang S, Qin X, Zhang S, Liu Y. Diagnosis of AFP-negative early-stage hepatocellular carcinoma using fuc-PON1. *Discovery Med* (2017) 23(126):163–8.

17. Eltaher SM, El-Gil R, Fouad N, Mitwali R, El-Kholy H. Evaluation of serum levels and significance of soluble CD40 ligand in screening patients with hepatitis c virus-related hepatocellular carcinoma. *Eastern Mediterr Health J* (2016) 22(8):603–10.

18. Erdal H, Gul Utku O, Karatay E, Celik B, Elbeg S, Dogan I. Combination of DKK1 and AFP improves diagnostic accuracy of hepatocellular carcinoma compared with either marker alone. *Turkish J Gastroenterol Off J Turkish Soc Gastroenterol* (2016) 27(4):375–81. doi: 10.5152/tjg.2016.15523

19. Vongsuvanh R, van der Poorten D, Iseli T, Strasser SI, McCaughan GW, George J. Midkine increases diagnostic yield in AFP negative and NASH-related hepatocellular carcinoma. *PloS One* (2016) 11(5):e0155800. doi: 10.1371/journal.pone.0155800

20. Cala MP, Aldana J, Medina J, Sanchez J, Guio J, Wist J, et al. Multiplatform plasma metabolic and lipid fingerprinting of breast cancer: A pilot control-case study in Colombian Hispanic women. *PloS One* (2018) 13(2):e0190958. doi: 10.1371/journal.pone.0190958

21. Zang HL, Huang GM, Ju HY, Tian XF. Integrative analysis of the inverse expression patterns in pancreas development and cancer progression. *World J Gastroenterol* (2019) 25(32):4727–38. doi: 10.3748/wjg.v25.i32.4727

22. Zhou X, Zheng R, Zhang H, He T. Pathway crosstalk analysis of microarray gene expression profile in human hepatocellular carcinoma. *Pathol Oncol Res POR* (2015) 21 (3):563–9. doi: 10.1007/s12253-014-9855-x

23. Dolce V, Rita Cappello A, Lappano R, Maggiolini M. Glycerophospholipid synthesis as a novel drug target against cancer. *Curr Mol Pharmacol* (2011) 4(3):167–75. doi: 10.2174/1874467211104030167

24. Zheng JF, Lu J, Wang XZ, Guo WH, Zhang JX. Comparative metabolomic profiling of hepatocellular carcinoma cells treated with sorafenib monotherapy vs. *Sorafenib-Everolimus Combination Ther Med Sci Monit Int Med J Exp Clin Res* (2015) 21:1781–91. doi: 10.12659/msm.894669

25. Insausti-Urkia N, Solsona-Vilarrasa E, Garcia-Ruiz C, Fernandez-Checa JC. *Sphingomyelinases and liver diseases* Vol. 10. *Biomolecules* (2020) 10(11):1497. doi: 10.3390/biom10111497

26. Paul B, Lewinska M, Andersen J. Lipid alterations in chronic liver disease and liver cancer. *JHEP Rep Innovation Hepatol* (2022) 4(6):100479. doi: 10.1016/j.jhepr.2022.100479

27. Hall Z, Chiarugi D, Charidemou E, Leslie J, Scott E, Pellegrinet L, et al. Lipid remodeling in hepatocyte proliferation and hepatocellular carcinoma. *Hepatology* (2021) 73(3):1028–44. doi: 10.1002/hep.31391

28. Taniguchi M, Okazaki T. The role of sphingomyelin and sphingomyelin synthases in cell death, proliferation and migration-from cell and animal models to human disorders. *Biochim Biophys Acta* (2014) 1841(5):692–703. doi: 10.1016/j.bbalip.2013.12.003

29. Sakakima Y, Hayakawa A, Nagasaka T, Nakao A. Prevention of hepatocarcinogenesis with phosphatidylcholine and menaquinone-4: *in vitro* and *in vivo* experiments. *J Hepatol* (2007) 47(1):83–92. doi: 10.1016/j.jhep.2007.01.030

30. Sakakima Y, Hayakawa A, Nakao A. Phosphatidylcholine induces growth inhibition of hepatic cancer by apoptosis *via* death ligands. *Hepatogastroenterology* (2009) 56(90):481–4.

31. Anjos S, Feiteira E, Cerveira F, Melo T, Reboredo A, Colombo S, et al. Lipidomics reveals similar changes in serum phospholipid signatures of overweight and obese pediatric subjects. *J Proteome Res* (2019) 18(8):3174–83. doi: 10.1021/acs.jproteome.9b00249

32. Mayneris-Perxachs J, Mousa A, Naderpoor N, Fernández-Real J, de Courten B. Low AMY1 copy number is cross-sectionally associated to an inflammation-related lipidomics signature in overweight and obese individuals. *Mol Nutr Food Res* (2020) 64 (11):e1901151. doi: 10.1002/mnfr.201901151

33. Hinkley J, Cornnell H, Standley R, Chen E, Narain N, Greenwood B, et al. Older adults with sarcopenia have distinct skeletal muscle phosphodiester, phosphocreatine, and phospholipid profiles. *Aging Cell* (2020) 19(6):e13135. doi: 10.1111/acel.13135

34. Qi X, Li J, Deng H, Li H, Su C, Guo X. Neutrophil-to-lymphocyte ratio for the prognostic assessment of hepatocellular carcinoma: A systematic review and meta-analysis of observational studies. *Oncotarget* (2016) 7(29):45283–301. doi: 10.18632/oncotarget.9942

35. Saito R, Andrade L, Bustos S, Chammas R. Phosphatidylcholine-derived lipid mediators: The crosstalk between cancer cells and immune cells. *Front Immunol* (2022) 13:768606. doi: 10.3389/fimmu.2022.768606

36. Yang X, Zhang D, Liu S, Li X, Hu W, Han C. KLF4 suppresses the migration of hepatocellular carcinoma by transcriptionally upregulating monoglyceride lipase. *Am J Cancer Res* (2018) 8(6):1019–29.

frontiers | Frontiers in Oncology

TYPE Clinical Trial
PUBLISHED 27 February 2023
DOI 10.3389/fonc.2023.1101162



OPEN ACCESS

EDITED BY
Jeroen Van Vugt,
Erasmus Medical Center, Netherlands

REVIEWED BY
Zhaohui Tang,
Shanghai Jiao Tong University, China
Jiliang Shen,
Zhejiang University, China

*CORRESPONDENCE
Chong Zhong
zhongchong1732@gzucm.edu.cn

†These authors have contributed equally to this work

SPECIALTY SECTION
This article was submitted to Surgical Oncology, a section of the journal Frontiers in Oncology

RECEIVED 17 November 2022
ACCEPTED 03 February 2023
PUBLISHED 27 February 2023

CITATION
Fang C, Luo R, Zhang Y, Wang J, Feng K, Liu S, Chen C, Yao R, Shi H and Zhong C (2023) Hepatectomy versus transcatheter arterial chemoembolization for resectable BCLC stage A/B hepatocellular carcinoma beyond Milan criteria: A randomized clinical trial. *Front. Oncol.* 13:1101162. doi: 10.3389/fonc.2023.1101162



# Hepatectomy versus transcatheter arterial chemoembolization for resectable BCLC stage A/B hepatocellular carcinoma beyond Milan criteria: A randomized clinical trial

Chongkai Fang[1,2,3†], Rui Luo[1,2,3†], Ying Zhang[1,2,3], Jinan Wang[1,2,3], Kunliang Feng[1,2,3], Silin Liu[1,2,3], Chuyao Chen[1,2,3], Ruiwei Yao[1,2,3], Hanqian Shi[1,2,3] and Chong Zhong[1,2,3*]

[1]The First Clinical Medical School, Guangzhou University of Chinese Medicine, Guangzhou, China, [2]The First Affiliated Hospital, Guangzhou University of Chinese Medicine, Guangzhou, China, [3]Lingnan Medical Research Center of Guangzhou University of Chinese Medicine, Guangzhou, China

**Background:** Hepatectomy is the recommended option for radical treatment of BCLC stage A/B hepatocellular carcinoma (HCC) that has progressed beyond the Milan criteria. This study evaluated the efficacy and safety of preoperative neoadjuvant transcatheter arterial chemoembolization (TACE) for these patients.

**Methods:** In this prospective, randomized, open-label clinical study, BCLC stage A/B HCC patients beyond the Milan criteria were randomly assigned (1:1) to receive either neoadjuvant TACE prior to hepatectomy (NT group) or hepatectomy alone (OP group). The primary outcome was overall survival (OS), while the secondary outcomes were progression-free survival (PFS) and adverse events (AEs).

**Results:** Of 249 patients screened, 164 meeting the inclusion criteria were randomly assigned to either the NT group (n = 82) or OP group (n = 82) and completed follow-up requirements. Overall survival was significantly greater in the NT group compared to the OP group at 1 year (97.2% vs. 82.4%), two years (88.4% vs. 60.4%), and three years (71.6% vs. 45.7%) (p = 0.0011) post-treatment. Similarly, PFS was significantly longer in the NT group than the OP group at 1 year (60.1% vs. 39.9%), 2 years (53.4% vs. 24.5%), and 3 years (42.2% vs. 24.5%) (p = 0.0003). No patients reported adverse events of grade 3 or above in either group.

**Conclusions:** Neoadjuvant TACE prolongs the survival of BCLC stage A/B HCC patients beyond the Milan criteria without increasing severe adverse events frequency.

**Clinical trial registration:** https://www.chictr.org.cn/, identifier ChiCTR2200055618.

KEYWORDS

hepatocellular carcinoma, neoadjuvant treatment, transcatheter arterial chemoembolization, hepatectomy, survival, Milan criteria

# Introduction

Hepatocellular carcinoma (HCC) is the sixth most prevalent cancer and the third most common cause of cancer-related death worldwide (1, 2). Current treatments for HCC include surgical resection, liver transplantation, and local radiofrequency ablation, of which hepatectomy is the most frequently used method for radical treatment. However, the recurrence rate is approximately 50%–60% at 2 years and 80% at 5 years, and the median survival time after recurrence without additional therapeutic interventions is only 2.7 to 4.0 months (3–7). Therefore, it is necessary to explore additional treatments to improve survival among this patient group. Barcelona Clinic Liver Cancer (BCLC) staging is a common clinical standard for assessing clinical progression and treatment selection according to tumor size, tumor number, degree of liver function, and general physical condition (8). The recommended treatments for very early and early BCLC stages (0 and A) include surgical resection, local radiofrequency ablation, and liver transplantation, while the recommended treatments for intermediate stage (B) included transcatheter arterial chemoembolization (TACE) (9). The Milan criteria are widely used for evaluating eligibility for liver transplantation to treat early-stage liver cancer transplantation, but most patients are beyond Milan criteria by the time of diagnosis (10, 11). Moreover, some patients meeting the Milan criteria miss the opportunity for liver transplantation while waiting for a suitable donor. Also, liver cancer progresses quickly, so changes in size and location can increase the risks of surgery. Therefore, for patients with stage A/B liver cancer beyond Milanese standard BCLC, we use neoadjuvant TACE to control tumor progression before surgical resection. In our preliminary clinical observation, this treatment not only reduced the risks of surgery but also improved overall survival (OS).

Nevertheless, preoperative TACE remains controversial for resectable HCC. Some investigators have reported that preoperative TACE increases the risk of tumor cells metastasizing into the bloodstream without improving the survival in patients with resectable solitary HCC (12). In contrast, others have reported that preoperative TACE combined with hepatectomy improves both OS and progression-free survival (PFS) of patients with giant HCC compared to hepatectomy alone (13). Therefore, it is essential to evaluate if preoperative TACE can benefit patients with BCLC stage A/B HCC who are beyond Milan criteria.

This prospective clinical trial of patients diagnosed with BCLC stage A/B HCC beyond Milan criteria was designed to evaluate the clinical safety and efficacy of TACE combined with hepatectomy prior to hepatectomy alone.

# Methods

## Trial design

This open-label, phase III, randomized, parallel study was conducted at the First Affiliated Hospital of Guangzhou University of Chinese Medicine (Guangzhou, China) and Sun Yat-Sen Cancer Center (Guangzhou, China). Patients with HCC beyond Milan criteria were randomized to receive neoadjuvant TACE plus hepatectomy (NT group) or hepatectomy alone (OP group). The study was conducted in accordance with the Declaration of Helsinki and CSCO Clinical Practice Guidelines and was approved by the First Affiliated Hospital of Guangzhou University of Chinese Medicine Institutional Review Board and Ethics Committee (IRB approval number: NO.ZYYECK [2019] 163). All patients participated voluntarily and provided informed written consent. Patients meeting the eligibility criteria (below) were randomized at a 1:1 ratio using a sealed envelope system. An application for registration was submitted to the Chinese Clinical Trial Registry (https://www.chictr.org.cn/, trail number: ChiCTR2200055618).

## Eligibility criteria

Inclusion criteria were as follows: (1) 18–75 years of age; (2) Eastern Cooperative Oncology Group performance score (ECOG PS) of 0 or 1; (3) BCLC A/B stage exceeding the Milan criteria; (4) HCC lesion(s) not previously treated with local or systematic therapy; (5) meeting criteria for Child Pugh class A live score; (6) no distant metastasis, organ dysfunction, or other contraindications to liver resection; (7) laboratory tests meeting the acceptance criteria for TACE and liver resection; (8) no allergy to any TACE agent; (9) informed written consent; and (10) no concomitant antitumor therapy or enrollment in other clinical trials.

The exclusion criteria were as follows: (1) mixed tumors exhibiting other features; (2) recurrent HCC or other simultaneously occurring malignancies; (3) received alternatives to TACE or palliative resection for anticancer treatment before

hepatectomy; (4) serious major organ dysfunction; (5) lack of clinical and follow-up data; and (6) death from unrelated causes.

## Neoadjuvant TACE

Patients in the NT group received at least two times TACE before hepatectomy. Hepatic angiography was performed by inserting a catheter through the femoral artery using the Seldinger technique. After assessing the hepatic vascular anatomy, TACE was performed selectively through the left or right hepatic artery, or the tumor-feeding artery when technically possible (as there was a need for super selective catheterization in some cases). Epirubicin (30 mg/m$^2$) and lipiodol (5–20 ml) emulsions were injected into the tumor, with a lipiodol dose set according to tumor diameter. The manufacturer of chemotherapeutic agents allowed diverse selection due to TACE was performed at different hospitals. Approximately 4–6 weeks after the initial therapy, a complete assessment was conducted consisting of a physical examination, routine blood analysis, and computed tomography (CT) scan. Based on this review and patient condition, the decision was made to perform the second cycle of TACE.

After neoadjuvant therapy, we estimated the efficiency of TACE by radiography based on the Modified Response Evaluation Criteria In Solid Tumors (mRECIST). If the patient was diagnosed with progressive disease (PD) or could not accept the hepatectomy, we would suggest the appropriate advice for the subsequent therapy. On the contrary, if the patient achieved complete remission (CR), partial remission (PR), or stable disease (SD), resection was recommended as the first optional treatment.

## Partial hepatectomy

Anatomic resection was conducted using Pringle's maneuver to limit liver blood volume inflow and thereby reduce uncontrolled bleeding. Briefly, an elastic tourniquet was tightened around the entire hepatoduodenal ligament with occlusive time set according to liver function (up to 30 min if the liver function was excellent).

## Follow-up

Patients were evaluated at least every 3 months during the first 2 years post-hepatectomy and every 6 months thereafter. If patients could not review their tumor condition, we actively connect with them by telephone or mail for follow-up. Ultrasonography, chest X-ray, CT, magnetic resonance imaging (MRI), serum alpha-fetoprotein (AFP) measurement, liver function tests, and blood analyses were conducted routinely as part of the standard diagnostic process. After detecting a suspected recurrence/metastasis, further tests were performed, including hepatic angiography or biopsy. Recurrence/metastasis was confirmed by cytologic/histologic evidence or noninvasive diagnostic criteria established by the European Association for the Study of Liver. All patients with recurrence were subsequently treated by our hospital's multi-disciplinary team according to tumor location, liver function, and physical condition.

We strictly recorded every adverse event (AE) during the whole stage of treatment. AEs associated with TACE and hepatectomy were evaluated according to National Cancer Institute Common Terminology Criteria for Adverse Events v4.0.

## Statistical analyses

The primary outcome measure was OS from the day the patient was randomly assigned to a treatment group until the date of death from any cause, while the secondary outcomes were PFS and AEs.

From our retrospect research, the OS of 3 years between the NT and OP groups was approximately 66% and 40%, respectively. Following the principle that the primary outcome should get 90% statistical power and differ between intervention groups by one-sided $\alpha = 0.05$, we recruited 249 patients and randomized eligible patients equally into the NT and OP groups. Assuming 10% loss to follow-up, we estimated that it would require 81 cases per group randomized by PASS [Hintze, J. (2011). PASS 11, NCSS, LLC, Kaysville, UT, USA. www.ncss.com]. Survival was plotted using the Kaplan–Meier method and compared between groups using the log-rank test, while Cox proportional hazards analysis was conducted to calculate hazard ratios (HRs) with 95% confidence intervals (CIs). Survival curves and forest plot were drawn and analyzed using GraphPad Prism version 8.0.1 for Windows (GraphPad Software San Diego, CA, USA). AEs were compared between groups by independent samples *t*-test. Subgroup analyses included sex, age, tumor size, cirrhosis, AFP, and hepatitis B or C virus (HBV or HCV) infection as potential prognostic factors. These analyses were conducted using SPSS software version 25 (Chicago, IL, USA). $p < 0.05$ was considered statistically significant for all tests.

# Results

## Patient characteristics and treatment

Between 2 April 2020, and 2 April 2021, 249 patients were screened, and 172 (intention-to-treat population) were randomly assigned to receive neoadjuvant therapy prior to hepatectomy (n = 86) or hepatectomy alone (n = 86). In the NT group, one patient lacked pathology evidence, and three patients accepted other therapies. In the OP group, two patients lacked the pathology evidence, and two patients received other treatments. Finally, the efficacy and safety analyses included 82 patients in each group (Figure 1).

Baseline demographic and disease characteristics did not differ significantly between groups with the exception of higher cirrhosis incidence in the OP group (Table 1).

10.3389/fonc.2023.1101162

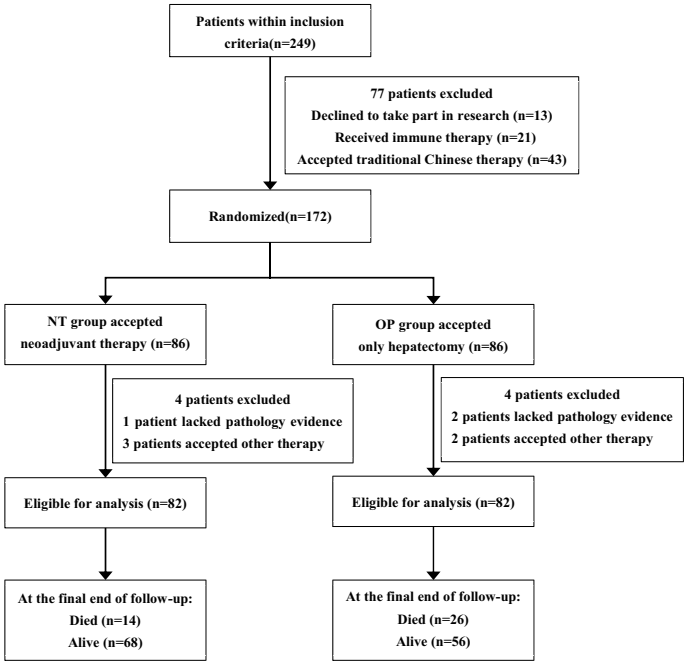


FIGURE 1
Patient enrollment and randomization to treatment groups.

TABLE 1 Clinical characteristics of patients in the neoadjuvant group (NT group) and hepatectomy alone group (OP group).

| | | Total | NT group | OP group | p-Value |
|---|---|---|---|---|---|
| Patients (n) | | 164 | 82 | 82 | - |
| **Gender (n%)** | **male** | 141 (86.0%) | 68 (82.9%) | 73 (89.0%) | 0.261 |
| | **female** | 23 (14.0%) | 14 (17.1%) | 9 (11.0%) | |
| **Age (n%)** | **<65** | 137 (83.5%) | 71 (86.6%) | 66 (80.5%) | 0.292 |
| | **≥65** | 27 (16.5%) | 11 (13.4%) | 16 (19.5%) | |
| **BCLC (n%)** | **BCLC A** | 107 (65.2%) | 53 (64.6%) | 54 (65.9%) | 0.87 |
| | **BCLC B** | 57 (34.8%) | 29 (35.4%) | 28 (34.1%) | |
| **Number of tumor (s)** | **Single** | 106 (64.6%) | 53 (64.6%) | 53 (64.6%) | 1 |
| | **Multiple** | 58 (35.4%) | 29 (35.4%) | 29 (35.4%) | |
| **Maximum diameter of tumor (cm)** | **≤5cm** | 25 (15.2%) | 12 (14.6%) | 13 (15.9%) | 0.828 |
| | **>5cm** | 139 (84.8%) | 70 (85.4%) | 69 (84.1%) | |
| **Hepatitis B/C infection** | **Y** | 145 (88.4%) | 73 (89.0%) | 72 (87.8%) | 0.807 |
| | **N** | 19 (11.6%) | 9 (11.0%) | 10 (12.2%) | |
| **Cirrhosis** | **Y** | 59 (36.0%) | 19 (23.2%) | 40 (48.8%) | 0.001 |
| | **N** | 105 (64.0%) | 63 (76.8%) | 42 (51.2%) | |
| **Differentiation of tumor** | **1** | 6 (3.7%) | 6 (7.3%) | 0 (0%) | 0.401 |
| | **2** | 90 (54.9%) | 43 (52.4%) | 47 (57.3%) | |
| | **3** | 68 (41.5%) | 33 (40.2%) | 35 (42.7%) | |
| **Child-Pugh (n%)** | **A** | 164 (100%) | 82 (100%) | 82 (100%) | – |
| | **B** | 0 (0%) | 0 (0%) | 0 (0%) | |

*(Continued)*

TABLE 1 Continued

| | | Total | NT group | OP group | p-Value |
|---|---|---|---|---|---|
| **AFP** | **<400** | 89 (54.3%) | 39 (47.6%) | 50 (61.0%) | 0.085 |
| | **≥400** | 75 (45.7) | 43 (52.4%) | 32 (39.0%) | |
| **Serum biomarker** | **NEU** | 4.05 (2.98–5.20) | 4.07 (3.02–5.53) | 3.99 (2.93–4.71) | 0.26 |
| | **WBC** | 6.51 (5.27–7.88) | 6.30 (5.24–7.95) | 6.67 (5.29–7.73) | 0.784 |
| | **HGB** | 146 (133.3–156) | 143 (133–152) | 148 (138–159) | 0.107 |
| | **PLT** | 213 (164.3–279.3) | 216 (169–301) | 208 (161–274) | 0.436 |
| | **ALT** | 38.3 (26.7–60.7) | 37.55 (25.00–59.50) | 39.45 (28.92–63.10) | 0.379 |
| | **ALB** | 42.5 (40.3–44.5) | 41.85 (39.67–44.00) | 43.15 (40.57–44.95) | 0.107 |
| | **TB** | 12.7 (10.1–15.6) | 13.0 (10.5–16.3) | 12.3 (9.3–15.3) | 0.076 |
| | **PT** | 11.8 (11.3–12.6) | 12.0 (11.3–12.8) | 11.6 (11.2–12.5) | 0.091 |
| | **CREA** | 75.9 (65.1–85.5) | 76.60 (62.35–86.25) | 75.35 (66.82–85.17) | 0.653 |

AFP, alpha-fetoprotein; NEU, neutrophil; WBC, white blood cells; HGB, hemoglobin; PLT, platelet count; ALT, alanine aminotransferase; ALB, albumin; TBil, total bilirubin; PT, prothrombin time; CREA, creatinine.

## Efficacy analysis

By 2 April 2021, there were 14 deaths and 31 recurrences in the NP group compared to 26 deaths and 48 recurrences in the OP group. Overall survival was higher in the NT group compared to the OP at 1 year (97.2% vs. 82.4%), 2 years (88.4% vs. 60.4%), and 3 years (71.8% vs. 45.7%) post-treatment (HR 0.3602 [95% CI, 0.1914 to 0.6779]; p = 0.0011) (Figure 2A). Progression-free survival was also greater in the NT group compared to the OP at 1 year (60.1% vs. 39.9%), 2 years (53.4% vs. 24.5%), and 3 years (42.2% vs. 24.5%) post-treatment (HR 0.4525 [95% CI, 0.2891 to 0.7082]; p = 0.0003) (Figure 2B). Among patients with (earlier) BCLC A stage disease, OS was higher in the NT group than the OP group at 1 year (95.6% vs. 83.6%), 2 years (82.9% vs. 63.6%), and 3 years (73.3% vs. 50.3%) post-treatment (HR 0.3893 [95%CI, 0.1788 to 0.8474]; p = 0.0159) (Figure 3A). Similarly, PFS was higher among NT group patients with BCLC A stage disease compared to OP group patients with BCLC A stage disease at 1 year (63.7% vs. 45.7%), 2 years (57.4% vs. 23.7%), and 3 years (50.2% vs. 23.7%) post-treatment (HR 0.442 [95%CI, 0.2493 to 0.7834]; p = 0.0044) (Figure 3B). Among patients with intermediate BCLC B stage disease as well, OS was higher in the NT group at 1 year (100% vs. 97.6%), 2 years (91.8% vs. 64.3%), and 3 years (68% vs. 38.6%) post-treatment (HR 0.2592 [95%CI, 0.0844 to 0.7996]; p = 0.0063) (Figure 4A), as was PFS at 1 year (53.3% vs. 28.9%), 2 years (45.7% vs. 28.9%), and 3 years (30.5% vs. 28.9%) post-treatment (HR 0.4606 [95% CI, 0.2238–0.9481]; p = 0.0244) (Figure 4B).

There are subgroup analyses of patient outcomes in Figure 5 (Figure 5). Utmost patients can have better OS and PFS benefits from the NT group. Although some accepted neoadjuvant therapy patients take the disadvantage for OS with these characters, such as age <65, patients of BCLC B stage, tumor size ≤5 cm, cirrhosis,

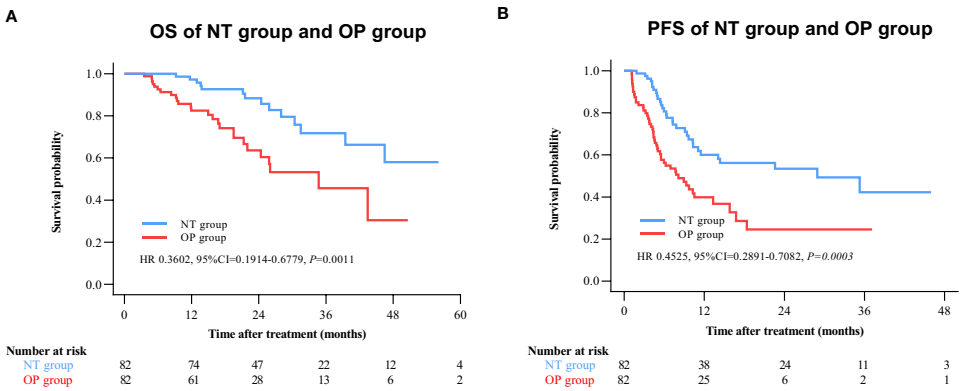


FIGURE 2
Kaplan–Meier survival curves of the neo-adjuvant plus hepatectomy (NT) group and hepatectomy alone (OP) group. **(A)** Overall survival (OS). **(B)** Progression-free survival (PFS).

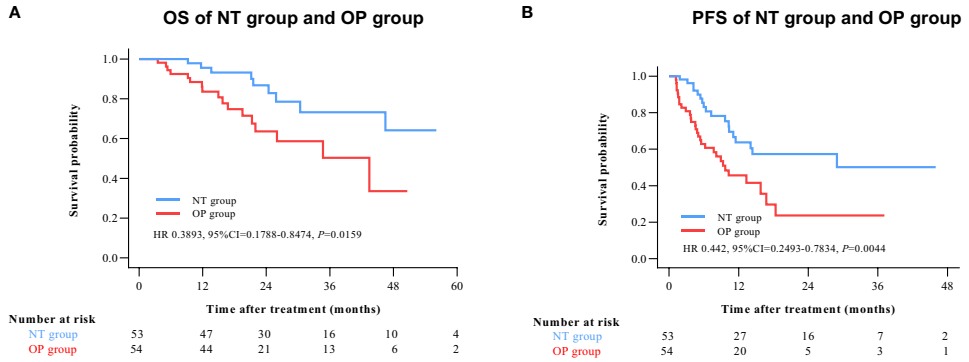


FIGURE 3
Kaplan–Meier survival curves of BCLC A patients in the NT and OP groups. **(A)** Overall survival (OS). **(B)** Progression-free survival (PFS).

high-level differentiation, positive MVI, and AFP <400. Similarly, gender, tumor size ≤5cm, without HBV/HCV infection, none of cirrhosis, low or middle level differentiation, positive MVI, and AFP<400 appeared to influence the advantages of neo-adjuvant therapy on PFS, but again without statistical significance.

## Safety analysis

There were no significant differences in individual AE frequencies between NT and OP groups (Table 2). Moreover, all AEs were mild and treated during hospitalization. In both groups, the most common AEs were pain, hyperbilirubinemia, anemia, and elevated serum liver enzymes.

# Discussion

Liver transplantation and hepatectomy are the current curative treatments for HCC but only HCC patients who meet the Milan/UCSF criteria are eligible for liver transplantation and those beyond the Milan/UCSF criteria are at higher risk of recurrence after hepatectomy (14, 15). In China, few patients receive successful liver transplantation due to a shortage of donors and high incidence of HBV, which is exclusionary according to the Milan criteria (16). Further, patients may progress beyond the Milan criteria while waiting for liver transplantation.

There are several neoadjuvant therapies that may improve outcome for HCC patients. In addition to preoperative TACE, several new potential adjuvant or first-line therapies are available for HCC, including Locally Active Agent for Tumor Treatment and Eradication (LATTE), another percutaneous locoregional therapy. Compared to TACE, LATTE is relatively simple, requiring only an ultrasound to inject chemotherapy drugs into the tumor tissue. For patients, it may enable liver transplantation or hepatectomy, decrease surgical risk, and reduce the financial burden on patients. However, additional safety and efficacy data are required (17). Immunotherapy, such as immune checkpoint inhibitors (PD-1 and PD-L1), is another potential treatment, but many patients are insensitive to single immunotherapy cycles.

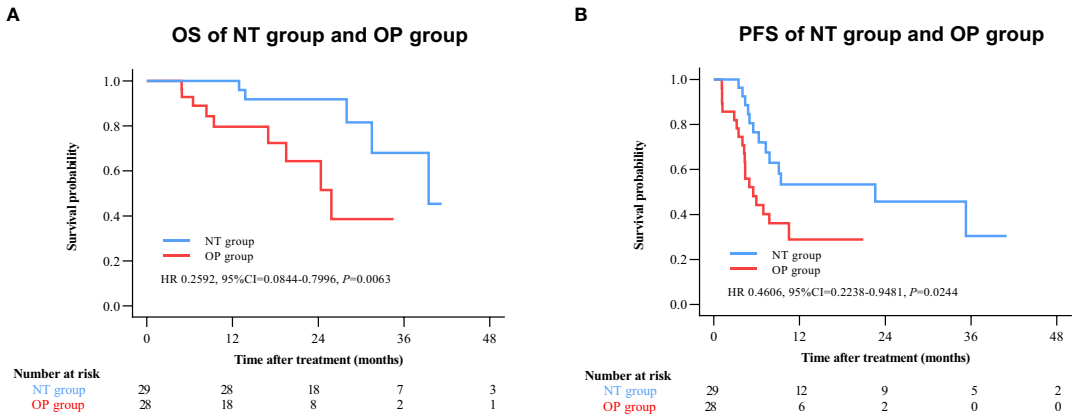


FIGURE 4
Kaplan–Meier survival curves of BCLC B patients in the NT and OP groups. **(A)** Overall survival (OS). **(B)** Progression-free survival (PFS).

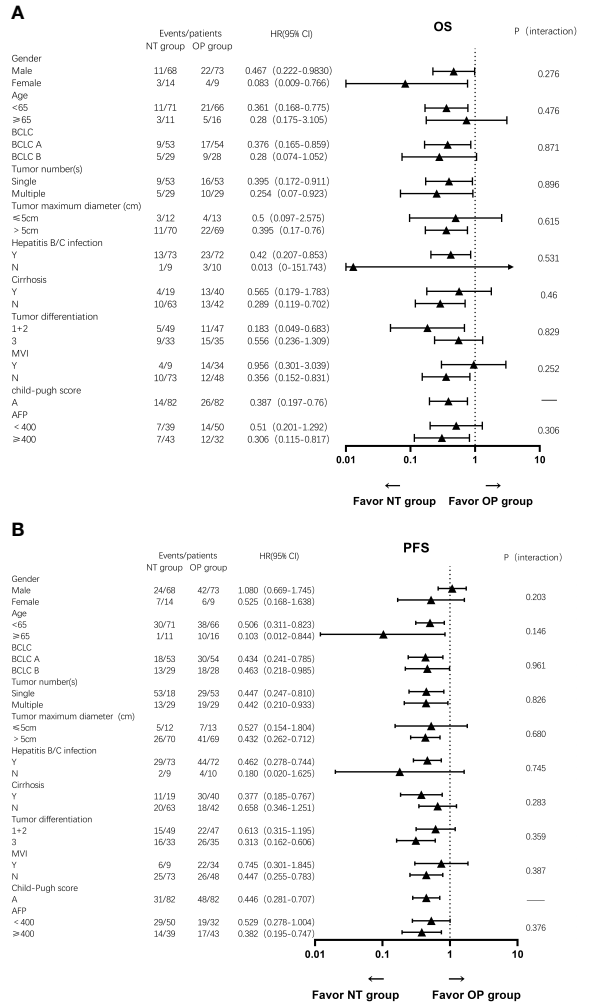


FIGURE 5
Subgroup analysis of **(A)** OS and **(B)** PFS for patients in the NT and OP groups.

Therefore, combination therapy, including novel drugs, may be a more promising research area. Recently, immunotherapy based on natural killer (NK) cells has been examined for liver cancer treatment (18, 19).

Moreover, imaging examination is essential to visually observe tumor response in patients before surgery. Radiomics can transform images into high-dimensional mineable data to monitor the differentiation in the tumor tissue and adjacent tissue, providing objective criteria for the study (20). A recent research has proved that BCLB stage, serum of AFP, tumor location, and other factors are significant factors for tumor response after TACE in HCC patients, which is similar to our findings (21). Therefore, establishing a clinical-radiological model through screening clinical data combined with radiomics may predict the survival in clinical treatment (22).

Neoadjuvant treatment is mainly applied for patients with unresectable HCC, while the safety and efficacy of its application in patients with resectable HCC remains controversial (23). Neoadjuvant TACE is one of the effective treatments for patients with unresectable HCC, potentially creating opportunities for liver resection (24). For this study, we substantiated that preoperative neoadjuvant TACE in patients with resectable HCC with multifocal lesions or large isolated lesions larger than 5 cm provided better survival benefit. In addition, this study shows that neoadjuvant TACE has admissible safety record and is well tolerated.

TACE is widely acknowledged as one of the most effective local treatments for patients with unresectable HCC. However, it is controversial whether patients with resectable HCC should receive preoperative TACE preoperatively. Some studies have reported that preoperative TACE has adverse effects, such as perihepatic adhesions that make surgery more difficult, increase the risk of liver injury and liver failure, or delay surgery, thereby allowing continued tumor growth (25–27). Further, a meta-analysis concluded that HCC patients undergoing hepatectomy do not necessarily derive a survival advantage from preoperative TACE (28). Therefore, it is critical to identify those patient groups most likely to benefit from neoadjuvant TACE (29–33). A study by Guo (11) and colleagues using propensity score matching found that preoperative TACE improved RFS ($p = 0.002$) and OS ($p = 0.003$) in the patients. In our study as well, patients with resectable BCLC A stage HCC beyond the Milan criteria who received preoperative TACE achieved a significant survival advantage in OS and PFS at 1, 2, and 3 years post-treatment, although there was a decreasing trend after 3 years. The efficacy of preoperative TACE for patients with resectable HCC beyond the Milan criteria may also be related to the number of TACE sessions, as it has been suggested that more than two TACE sessions can improve the clinical outcomes of HCC patients (25, 34) In this study, patients in the NT group received at least two preoperative neoadjuvant TACE, which may also account for the better survival benefit.

We also found no statistically significant differences in AE frequency profile between NT and OP groups, indicating that hepatectomy was the main cause of postoperative complications. Similar to previous reports on hepatectomy, most of the complications were grade 1 or 2, most frequently liver dysfunction, anemia, and hypoproteinemia (35). Thus, neoadjuvant TACE is safe and well tolerated by HCC patients with resectable tumors but beyond the Milan criteria.

This study has several limitations. First, cirrhosis was less common in the NT group, which may have contributed to the improved outcome. However, subgroup analyses indicated that neither influenced the group difference in OS or PFS. Second,

TABLE 2 Summary of treatment-related adverse events.

| | NT group (n = 82) | | | | OP group (n = 82) | | | | p-Value |
|---|---|---|---|---|---|---|---|---|---|
| | Grade 1 | Grade 2 | Grade 3 | Grade 4 | Grade 1 | Grade 2 | Grade 3 | Grade 4 | |
| ALT | 29 | 4 | 2 | 0 | 32 | 8 | 4 | 1 | 0.588 |
| ALB | 36 | 0 | 0 | 0 | 33 | 0 | 0 | 0 | – |
| Tbil | 20 | 15 | 2 | 0 | 24 | 24 | 8 | 0 | 0.324 |
| CREA | 2 | 0 | 0 | 0 | 2 | 2 | 0 | 0 | 0.221 |
| HGB | 26 | 13 | 1 | 0 | 38 | 12 | 0 | 0 | 0.332 |
| PLT | 6 | 3 | 0 | 0 | 2 | 3 | 0 | 0 | 0.334 |
| Infection | 3 | 0 | 0 | 0 | 4 | 0 | 1 | 0 | 0.408 |
| Pain | 4 | 0 | 0 | 0 | 16 | 1 | 0 | 0 | 0.619 |
| Edema | 7 | 0 | 0 | 0 | 8 | 2 | 0 | 0 | 0.208 |
| Emesis | 3 | 1 | 0 | 0 | 2 | 0 | 0 | 0 | 0.439 |
| Nausea | 0 | 1 | 0 | 0 | 1 | 2 | 0 | 0 | 0.505 |
| Neutropenia | 3 | 0 | 0 | 0 | 0 | 0 | 0 | 0 | – |
| Cough | 4 | 4 | 0 | 0 | 7 | 3 | 0 | 0 | 0.387 |
| Constipation | 8 | 0 | 0 | 0 | 4 | 1 | 0 | 0 | 0.188 |
| Diarrhea | 3 | 0 | 0 | 0 | 7 | 0 | 0 | 0 | – |
| Hemorrhage | 1 | 1 | 2 | 0 | 1 | 0 | 1 | 1 | 0.525 |
| Hypertension | 1 | 0 | 1 | 0 | 2 | 1 | 1 | 0 | 0.687 |

patients were recruited from two clinical centers in China, which may have introduced selection bias, especially from ethnicity. The efficacy and safety of preoperative neoadjuvant TACE for patients with resectable BCLC stage A/B HCC beyond the Milan criteria should be evaluated in different ethnic populations and between patients with and without cirrhosis.

In conclusion, this study suggests that preoperative neoadjuvant TACE can improve the survival rate of patients with resectable BCLC stage A/B HCC beyond the Milan criteria.

## Data availability statement

The original contributions presented in the study are included in the article/supplementary material. Further inquiries can be directed to the corresponding authors.

## Ethics statement

The studies involving human participants were reviewed and approved by the First Affiliated Hospital of Guangzhou University of Chinese Medicine. The patients/participants provided their written informed consent to participate in this study. Written informed consent was obtained from the individual(s) for the publication of any potentially identifiable images or data included in this article.

## Author contributions

Conception: CF and CZ; Financial support: CZ; Collection and assembly of data: CF, RL, KF, JW, CC, and RY; Data analysis and interpretation: CF, RL, YZ, and HS; Manuscript writing: CF, RL, JW, and SL. All authors contributed to the article and approved the submitted version.

## Funding

This work was supported by the National Natural Science Foundation of China (NSFC 82274526), “First-class universities and disciplines of the world” and high-level university discipline reserve talent cultivation project of Guangzhou University of Chinese Medicine (A1-2601-22-415-023), the Guangzhou Municipal Science and Technology Project (202102010406), the Innovation Project of the First Affiliated Hospital of Guangzhou University of Chinese Medicine (2019IIT18) and the Natural Science Foundation of Guangdong Province (2023A1515011069).

## Conflict of interest

The authors declare that the research was conducted in the absence of any commercial or financial relationships that could be construed as a potential conflict of interest.

## Publisher's note



## References

1. Sung H, Ferlay J, Siegel RL, Laversanne M, Soerjomataram I, Jemal A, et al. Global Cancer Statistics 2020: GLOBOCAN Estimates of Incidence and Mortality Worldwide for 36 Cancers in 185 Countries. *CA Cancer J Clin* 2021, 71(3):209–49. doi: 10.1001/jamaoncol.2017.3055

2. Cao W, Chen H-D, Yu Y-W, Li N, Chen W-Q Changing profiles of cancer burden worldwide and in China: a secondary analysis of the global cancer statistics 2020. *Chinese Medical Journal* 2021, 134(7):783–91. doi: 10.1097/CM9.0000000000001474

3. Imamura H, Matsuyama Y, Tanaka E, Ohkubo T, Hasegawa K, Miyagawa S, et al. Risk factors contributing to early and late phase intrahepatic recurrence of hepatocellular carcinoma after hepatectomy. *J Hepatol* (2003) 38(2):200–7. doi: 10.1016/S0168-8278(02)00360-4

4. Llovet JM, Fuster J, Bruix J. Intention-to-treat analysis of surgical treatment for early hepatocellular carcinoma: resection versus transplantation. *Hepatology* (1999) 30 (6):1434–40. doi: 10.1002/hep.510300629

5. Zeng H, Chen W, Zheng R, Zhang S, Ji JS, Zou X, et al. Changing cancer survival in China during 2003-15: a pooled analysis of 17 population-based cancer registries. *Lancet Glob Health* (2018) 6(5):e555–67. doi: 10.1016/S2214-109X(18)30127-X

6. Llovet JM, Bustamante J, Castells A, Vilana R, MdC A, Sala M, et al. Natural history of untreated nonsurgical hepatocellular carcinoma: rationale for the design and evaluation of therapeutic trials. *Hepatology* (1999) 29(1):62–7. doi: 10.1002/hep.510290145

7. Villa E, Moles A, Ferretti I, Buttafoco P, Grottola A, Del Buono M, et al. Natural history of inoperable hepatocellular carcinoma: estrogen receptors' status in the tumor is the strongest prognostic factor for survival. *Hepatology* (2000) 32(2):233–8. doi: 10.1053/jhep.2000.9603

8. Bruix J, Reig M, Sherman M. Evidence-based diagnosis, staging, and treatment of patients with hepatocellular carcinoma. *Gastroenterology* (2016) 150(4):835–53. doi: 10.1053/j.gastro.2015.12.041

9. Han K, Kim JH. Transarterial chemoembolization in hepatocellular carcinoma treatment: Barcelona clinic liver cancer staging system. *World J Gastroenterol* (2015) 21 (36):10327–35. doi: 10.3748/wjg.v21.i36.10327

10. Famularo S, Di Sandro S, Giani A, Bernasconi DP, Lauterio A, Ciulli C, et al. Treatment of hepatocellular carcinoma beyond the Milan criteria. a weighted comparative study of surgical resection versus chemoembolization. *HPB (Oxford)* (2020) 22(9):1349–58. doi: 10.1016/j.hpb.2019.12.011

11. Guo C, Zou X, Hong Z, Sun J, Xiao W, Sun K, et al. Preoperative transarterial chemoembolization for barcelona clinic liver cancer stage A/B hepatocellular carcinoma beyond the milan criteria: a propensity score matching analysis. *HPB (Oxford)* (2021) 23(9):1427–38. doi: 10.1016/j.hpb.2021.02.006

12. Tao Q, He W, Li B, Zheng Y, Zou R, Shen J, et al. Resection versus resection with preoperative transcatheter arterial chemoembolization for resectable hepatocellular carcinoma recurrence. *J Cancer* (2018) 9(16):2778–85. doi: 10.7150/jca.25033

13. Li C, Wang M-D, Lu L, Wu H, Yu J-J, Zhang W-G, et al. Preoperative transcatheter arterial chemoembolization for surgical resection of huge hepatocellular carcinoma (≥ 10 cm): a multicenter propensity matching analysis. *Hepatol Int* (2019) 13(6):736–47. doi: 10.1007/s12072-019-09981-0

14. Mazzaferro V, Regalia E, Doci R, Andreola S, Pulvirenti A, Bozzetti F, et al. Liver transplantation for the treatment of small hepatocellular carcinomas in patients with cirrhosis. *N Engl J Med* (1996) 334(11):693–9. doi: 10.1056/NEJM199603143341104

15. Yao FY, Ferrell L, Bass NM, Watson JJ, Bacchetti P, Venook A, et al. Liver transplantation for hepatocellular carcinoma: expansion of the tumor size limits does not adversely impact survival. *Hepatology* (2001) 33(6):1394–403. doi: 10.1053/jhep.2001.24563

16. Mi S, Jin Z, Qiu G, Xie Q, Hou Z, Huang J. Liver transplantation in China: Achievements over the past 30 years and prospects for the future. *Biosci Trends* (2022) 16(3):212–20. doi: 10.5582/bst.2022.01121

17. Albadawi H, Zhang Z, Altun I, Hu J, Jamal L, Ibsen KN, et al. Percutaneous liquid ablation agent for tumor treatment and drug delivery. *Sci Transl Med* (2021) 13 (580):1–12. doi: 10.1126/scitranslmed.abe3889

18. Chew V, Chen J, Lee D, Loh E, Lee J, Lim KH, et al. Chemokine-driven lymphocyte infiltration: an early intratumoural event determining long-term survival in resectable hepatocellular carcinoma. *Gut* (2012) 61(3):427–38. doi: 10.1136/gutjnl-2011-300509

19. Chu J, Gao F, Yan M, Zhao S, Yan Z, Shi B, et al. Natural killer cells: a promising immunotherapy for cancer. *J Transl Med* (2022) 20(1):240. doi: 10.1186/s12967-022-03437-0

20. Bell M, Turkbey EB, Escorcia FE. Radiomics, radiogenomics, and next-generation molecular imaging to augment diagnosis of hepatocellular carcinoma. *Cancer J* (2020) 26(2):108–15. doi: 10.1097/PPO.0000000000000435

21. Chen M, Cao J, Hu J, Topatana W, Li S, Juengpanich S, et al. Clinical-radiomic analysis for pretreatment prediction of objective response to first transarterial chemoembolization in hepatocellular carcinoma. *Liver Cancer* (2021) 10(1):38–51. doi: 10.1159/000512028

22. Zhao Y, Wang N, Wu J, Zhang Q, Lin T, Yao Y, et al. Radiomics analysis based on contrast-enhanced MRI for prediction of therapeutic response to transarterial chemoembolization in hepatocellular carcinoma. *Front In Oncol* (2021) 11:582788. doi: 10.3389/fonc.2021.582788

23. Benson AB, D'Angelica MI, Abbott DE, Anaya DA, Anders R, Are C, et al. Hepatobiliary cancers, version 2.2021, NCCN clinical practice guidelines in oncology. *J Natl Compr Canc Netw* (2021) 19(5):541–65. doi: 10.6004/jnccn.2021.0022

24. Zhang Y, Huang G, Wang Y, Liang L, Peng B, Fan W, et al. Is salvage liver resection necessary for initially unresectable hepatocellular carcinoma patients downstaged by transarterial chemoembolization? ten years of experience. *Oncologist* (2016) 21(12):1442–9. doi: 10.1634/theoncologist.2016-0094

25. Zhang Z, Liu Q, He J, Yang J, Yang G, Wu M. The effect of preoperative transcatheter hepatic arterial chemoembolization on disease-free survival after hepatectomy for hepatocellular carcinoma. *Cancer* (2000) 89(12):2606–12. doi: 10.1002/1097-0142(20001215)89:12<2606::AID-CNCR13>3.0.CO;2-T

26. Arslan M, Degirmencioglu S. Risk factors for postembolization syndrome after transcatheter arterial chemoembolization. *Curr Med Imaging Rev* (2019) 15(4):380–5. doi: 10.2174/1573405615666181122145330

27. Wei ZQ, Zhang YW. Transcatheter arterial chemoembolization followed by surgical resection for hepatocellular carcinoma: a focus on its controversies and screening of patients most likely to benefit. *Chin Med J (Engl)* (2021) 134(19):2275–86. doi: 10.1097/CM9.0000000000001767

28. Cheng X, Sun P, Hu QG, Song ZF, Xiong J, Zheng QC. Transarterial (chemo) embolization for curative resection of hepatocellular carcinoma: a systematic review and meta-analyses. *J Cancer Res Clin Oncol* (2014) 140(7):1159–70. doi: 10.1007/s00432-014-1677-4

29. Llovet JM, Mas X, Aponte JJ, Fuster J, Navasa M, Christensen E, et al. Cost effectiveness of adjuvant therapy for hepatocellular carcinoma during the waiting list for liver transplantation. *Gut* (2002) 50(1):123–8. doi: 10.1136/gut.50.1.123

30. Lau WY, Ho SK, Yu SC, Lai EC, Liew CT, Leung TW. Salvage surgery following downstaging of unresectable hepatocellular carcinoma. *Ann Surg* (2004) 240(2):299–305. doi: 10.1097/01.sla.0000133123.11932.19

31. Chen XP, Hu DY, Zhang ZW, Zhang BX, Chen YF, Zhang WG, et al. Role of mesohepatectomy with or without transcatheter arterial chemoembolization for large centrally located hepatocellular carcinoma. *Digestive Surg* (2007) 24(3):208–13. doi: 10.1159/000102901

32. Chapman WC, Majella Doyle MB, Stuart JE, Vachharajani N, Crippin JS, Anderson CD, et al. Outcomes of neoadjuvant transarterial chemoembolization to downstage hepatocellular carcinoma before liver transplantation. *Ann Surg* (2008) 248 (4):617–25. doi: 10.1097/SLA.0b013e31818a07d4

33. Zhang Q, Xia F, Mo A, He W, Chen J, Zhang W, et al. Guiding value of circulating tumor cells for preoperative transcatheter arterial embolization in solitary Large hepatocellular carcinoma: A single-center retrospective clinical study. *Front Oncol* (2022) 12:839597. doi: 10.3389/fonc.2022.839597

34. Georgiades C, Geschwind JF, Harrison N, Hines-Peralta A, Liapi E, Hong K, et al. Lack of response after initial chemoembolization for hepatocellular carcinoma: does it predict failure of subsequent treatment? *Radiology* (2012) 265(1):115–23. doi: 10.1148/radiol.12112264

35. Aoki T, Kubota K, Matsumoto T, Nitta H, Otsuka Y, Wakabayashi G, et al. Endoscopic liver surgery study group of J: Safety assessment of laparoscopic liver resection: A project study of the endoscopic liver surgery study group of Japan. *J Hepatobiliary Pancreat Sci* (2021) 28(6):470–8. doi: 10.1002/jhbp.917

frontiers | Frontiers in Oncology

TYPE Original Research
PUBLISHED 16 March 2023
DOI 10.3389/fonc.2023.1072106



OPEN ACCESS

EDITED BY
Beatrice Aramini,
University of Bologna, Italy

REVIEWED BY
Hao Liu,
University of Pittsburgh Medical Center, United States
Yan-Shen Shan,
National Cheng Kung University, Taiwan

*CORRESPONDENCE
Kosei Takagi
kotakagi15@gmail.com

SPECIALTY SECTION
This article was submitted to Surgical Oncology, a section of the journal Frontiers in Oncology

RECEIVED 17 October 2022
ACCEPTED 06 March 2023
PUBLISHED 16 March 2023

CITATION
Takagi K, Noma K, Nagai Y, Kikuchi S, Umeda Y, Yoshida R, Fuji T, Yasui K, Tanaka T, Kashima H, Yagi T and Fujiwara T (2023) Impact of cancer-associated fibroblasts on survival of patients with ampullary carcinoma.
*Front. Oncol.* 13:1072106.
doi: 10.3389/fonc.2023.1072106



# Impact of cancer-associated fibroblasts on survival of patients with ampullary carcinoma

Kosei Takagi[1]*, Kazuhiro Noma[1], Yasuo Nagai[1], Satoru Kikuchi[1], Yuzo Umeda[1], Ryuichi Yoshida[1], Tomokazu Fuji[1], Kazuya Yasui[1], Takehiro Tanaka[2], Hajime Kashima[1], Takahito Yagi[1] and Toshiyoshi Fujiwara[1]

[1]Department of Gastroenterological Surgery, Okayama University Graduate School of Medicine, Dentistry, and Pharmaceutical Sciences, Okayama, Japan, [2]Department of Pathology, Okayama University Graduate School of Medicine, Dentistry, and Pharmaceutical Sciences, Okayama, Japan

**Background:** Cancer-associated fibroblasts (CAFs) reportedly enhance the progression of gastrointestinal surgery; however, the role of CAFs in ampullary carcinomas remains poorly examined. This study aimed to investigate the effect of CAFs on the survival of patients with ampullary carcinoma.

**Materials and methods:** A retrospective analysis of 67 patients who underwent pancreatoduodenectomy between January 2000 and December 2021 was performed. CAFs were defined as spindle-shaped cells that expressed α-smooth muscle actin (α-SMA) and fibroblast activation protein (FAP). The impact of CAFs on survival, including recurrence-free (RFS) and disease-specific survival (DSS), as well as prognostic factors associated with survival, was analyzed.

**Results:** The high-α-SMA group had significantly worse 5-year RFS (47.6% vs. 82.2%, p = 0.003) and 5-year DSS (67.5% vs. 93.3%, p = 0.01) than the low-α-SMA group. RFS (p = 0.04) and DSS (p = 0.02) in the high-FAP group were significantly worse than those in the low-FAP group. Multivariable analyses found that high α-SMA expression was an independent predictor of RFS [hazard ratio (HR): 3.68; 95% confidence intervals (CI): 1.21–12.4; p = 0.02] and DSS (HR: 8.54; 95% CI: 1.21–170; p = 0.03).

**Conclusions:** CAFs, particularly α-SMA, can be useful predictors of survival in patients undergoing radical resection for ampullary carcinomas.

KEYWORDS

**ampullary carcinoma, carcinomas of the papilla of Vater, cancer-associated fibroblast, outcome, survival, recurrence**

# 1 Introduction

Ampullary carcinomas of the duodenum are rare neoplasms that arise in the ampulla of Vater. Surgical resection is a standard treatment for ampullary carcinoma, and relatively good prognosis has been reported after radical resection (1, 2). Histologically, ampullary carcinoma can be divided into three subtypes: intestinal, and pancreatobiliary, and mixed types (3, 4). As several studies have reported the better prognosis and non-invasive nature of the intestinal type, the prognostic role of the histological subtypes has been currently recognized (5). However, the morphology and immunohistochemical features of ampullary carcinomas have been poorly investigated, owing to its rarity (3, 4).

The tumor microenvironment or stroma is a multicellular system consisting of mesenchymal, endothelial, and hematopoietic cells in the extracellular matrix (6). Cancer-associated fibroblasts (CAFs) are key components of the tumor microenvironment with various functions, including cancer initiation and progression (7). Markers of fibroblast subtypes include α-smooth muscle actin (α-SMA) and fibroblast activation protein (FAP) (8). The clinical implications of CAFs as biomarkers and potential targets for prevention and treatment have been discussed in gastrointestinal oncology (9, 10). However, the role of CAFs in ampullary carcinoma has rarely been investigated.

This study aimed to investigate the presence of CAFs in patients with ampullary carcinoma. We also evaluated the effect of CAFs on the survival of patients with ampullary carcinoma.

# 2 Materials and methods

## 2.1 Patients

We retrospectively reviewed 78 patients with ampullary carcinoma who underwent pancreatoduodenectomy at our institution between January 2000 and December 2021. The study protocol was approved by the Institutional ethics committee (approval no. 2110-003), and was conducted in accordance with the Declaration of Helsinki.

## 2.2 Data extraction

Clinicopathological data were extracted from our database: age, sex (male or female), body mass index, American Society of Anesthesiologists (ASA) physical status (grade 1, 2, or 3), hypertension, diabetes mellitus, preoperative biliary drainage, operative time, estimated blood loss, postoperative outcome [major complication defined as Clavien grade ≥3 (11) and mortality), pathological factors evaluated by the General Rules for Clinical and Pathological Studies on Cancer of the Biliary Tract of Japan (12) (T and N factors), histopathologic subtype evaluated by a pathologist (intestinal, pancreatobiliary, and mixed type) (13), recurrence (absence or presence), status at the last follow-up (survival or death), and cause of death (primary disease-related or others).

## 2.3 Immunohistochemical analysis

We employed a previously reported protocol for evaluating CAFs (14–16). First, the presence of tumor cells was confirmed by hematoxylin and eosin (H&E) staining. Sections on the microslides were deparaffinized with xylene, hydrated using a diluted alcohol series, and immersed in H2O2 with methanol to quench endogenous peroxidase activity. To reduce nonspecific staining, each section was blocked with a serum-free protein block (Dako, Agilent Technologies, Santa Clara, CA, USA) for 15 min. After heat-mediated antigen retrieval with Tris/EDTA buffer, the sections were incubated with anti-SMA antibody (1:1000 dilution; Sigma-Aldrich, St. Louis, MO, USA) or anti-FAP antibody (1:250 dilution; Abcam, Cambridge, UK) diluted in Dako REAL Antibody Diluent (Dako, Agilent Technologies, Santa Clara, CA, USA) and incubated overnight at 4° C. The sections were then incubated with Envision+ anti-mouse/rabbit antibodies (Dako, Agilent Technologies, Santa Clara, CA, USA) for 30 min at RT. The chromogen used was liquid DAB+ (Dako, Agilent Technologies, Santa Clara, CA, USA). The sections were visualized with a 3,3'-diaminobenzidine tetrahydrochloride solution, and nuclei were counterstained with Meyer's hematoxylin. CAFs were defined as spindle-shaped cells expressing α-SMA or FAP, and evaluated using an area index calculated in low-magnification fields using ImageJ software (http://rsb.info.nih.gov/ij/). Three fields, including stromal cells per sample, were carefully selected to evaluate CAFs. The mean value obtained from each sectioned tissue sample was defined as the area index. The α-SMA and FAP positive rates were calculated as each area index. In this study, the median values of the area index for α-SMA and FAP were used as cut-off values to define the low and high groups.

## 2.4 Endpoints

The primary endpoint was the prognostic factors for survival after surgery. The secondary endpoint was survival after surgery, focusing on CAFs. The recurrence-free (RFS) and disease-specific (DSS) survival rates were analyzed.

## 2.5 Statistics

RFS and DSS rates were investigated using the Kaplan–Meier method, and the log-rank test was used to evaluate differences between the groups. DSS was defined as the duration from surgery to the date of death as a result of the primary disease. Patients who died of causes unrelated to the primary disease were excluded.

The prognostic factors associated with RFS and DSS were investigated using a Cox proportional hazards model with hazard ratios (HR) and 95% confidence intervals (CI). As a significant correlation between α-SMA and FAP was found, the multivariable analyses were generated by including α-SMA and FAP separately. In Model 1, relevant factors, including α-SMA, were included in the multivariable analyses. In Model 2, the multivariable analyses included relevant factors, including FAP.

JMP version 11 software (SAS Institute, Cary, NC, USA) was used for statistical analyses.

# 3 Results

## 3.1 Study cohort

Of the 78 patients, 67 were available for immunohistochemical analysis. The characteristics of 67 patients are shown in Table 1. Pathological T factors included Tis (n = 10), T1 (n = 21), T2 (n = 22), and T3 (n = 17). Lymph node metastases were observed in 14 patients (21%). Histopathologic subtypes of ampullary carcinoma included the intestinal (n = 36, 54%), pancreatobiliary (n = 20, 30%), and mixed type (n = 11, 16%). Postoperative recurrence was observed in 17 patients (25%) during a mean follow-up period of 5.3 years.

## 3.2 CAF expression

CAFs were identified as stromal cells expressing α-SMA and FAP. The mean (standard deviation [SD]) area indices for α-SMA and FAP were 11.0 (10.5) and 6.9 (9.6), respectively (Figure 1). Using the median area indices for α-SMA and FAP, the cut-off values were set at 7.1 for α-SMA and 1.2 for FAP. Microscopic images of H&E, anti-α-SMA, and FAP staining, as well as the images generated using Image J, are shown in Figure 2. The area index of α-SMA significantly correlated with that of FAP ($r^2 = 0.55$; $p < 0.001$), as shown in Figure 3.

## 3.3 Association of CAF expression with histopathologic subtype

Relationship between CAF expression and histopathologic subtype of ampullary carcinoma is depicted in Table 2. A significant difference was found in the mean (SD) area index for α-SMA and FAP between three groups: 4.8 (5.9) and 2.2 (5.8) in the intestinal type; 19.1 (9.9) and 12.8 (10.1) in the pancreatobiliary type; and 16.0 (10.8) and 11.1 (11.0) in the mixed type. The high-α-SMA and high-FAP was 25% and 19% in the intestinal type, 90%

TABLE 1 Clinicopathological characteristics of patients with ampullary carcinoma.

| | Patients (n = 67) |
|---|---|
| **Demographic variables** | |
| Age (year) | 70.3 (9.2) |
| Sex (male/female) | 40 (60)/27 (40) |
| BMI (kg/m$^2$) | 22.0 (3.5) |
| ASA-PS (1–2/3) | 56 (84)/11 (16) |
| Hypertension | 27 (40) |
| Diabetes mellitus | 19 (28) |
| Preoperative biliary drainage | 35 (52) |
| **Perioperative factors** | |
| Operative time (min) | 420 (87) |
| Blood loss (mL) | 374 (347) |
| Major complication (presence/absence) | 8 (13)/59 (87) |
| Mortality (presence/absence) | 0 (0)/67 (100) |
| **Pathological factors** | |
| T factor (Tis/1/2/3) | 7 (10)/21 (31)/22 (33)/17 (25) |
| Lymph node metastasis (presence/absence) | 14 (21)/53 (79) |
| **Histopathologic subtype** | |
| Intestinal type | 36 (54) |
| Pancreatobiliary type | 20 (30) |
| Mixed type | 11 (16) |
| **Cancer-associated fibroblasts** | |
| α-SMA (n = 66) | 11.0 (10.5) |
| FAP | 6.9 (9.6) |
| Recurrence (presence/absence) | 17 (25)/50 (75) |

Data are presented as mean (± standard deviation) or number (percentage).
BMI, body mass index; ASA-PS, American Society of Anesthesiologists physical status.

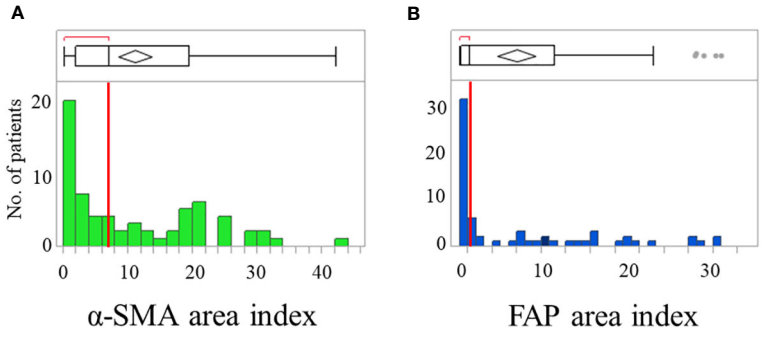


FIGURE 1
Distribution of patients showing α-smooth muscle actin (α-SMA) **(A)** and fibroblast activation protein (FAP) **(B)** area index. Box plots show median with the interquartile range; whiskers give the range.

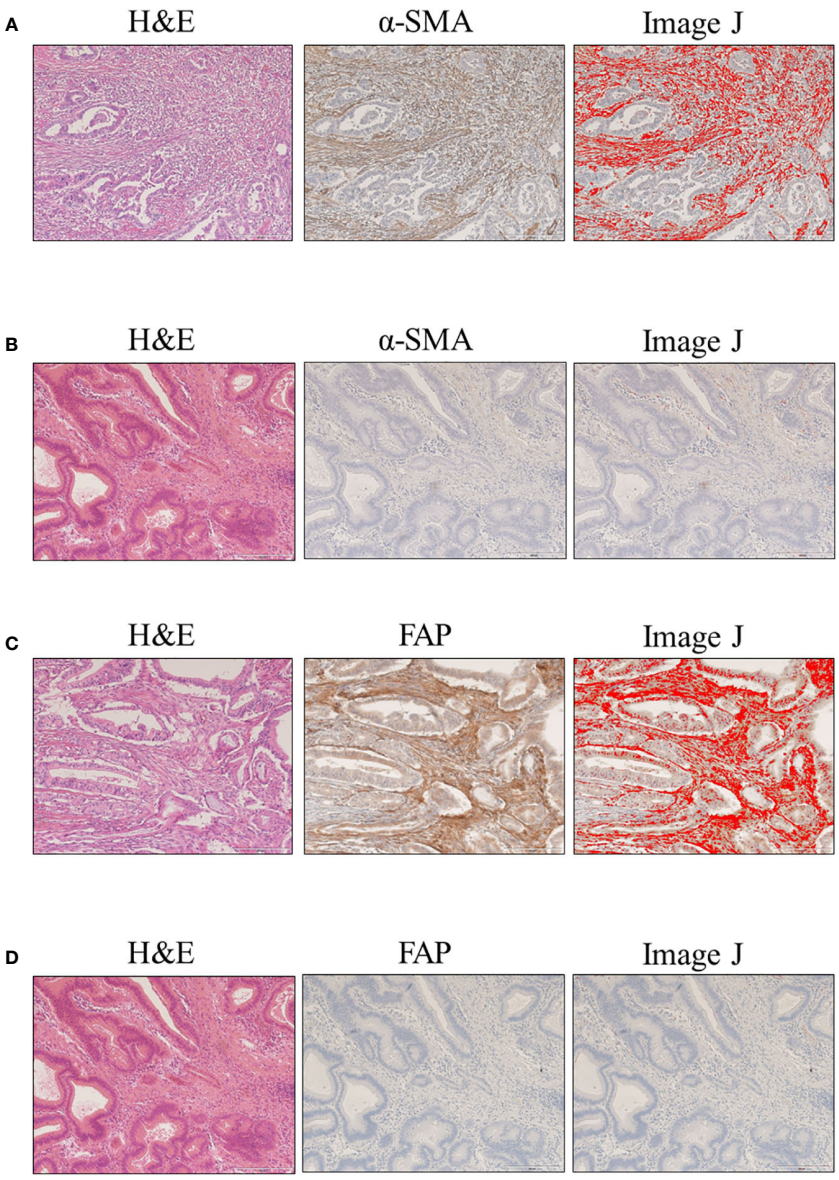


FIGURE 2
Evaluation of α-smooth muscle actin (α-SMA) and fibroblast activation protein (FAP) expression in clinical samples of ampullary carcinoma. Microscopic images with hematoxylin and eosin (H&E), cancer-associated fibroblasts (CAF) staining, and Image J: **(A)** high α-SMA expression; **(B)** low α-SMA expression; **(C)** high FAP expression; and **(D)** low FAP expression.

and 80% in the pancreatobiliary type, and 73% and 91% in the mixed type, respectively.

## 3.4 Association of CAF expression with survival

The 5-year RFS and DSS rates were 63.9% and 78.5%, respectively. RFS and DSS curves stratified by α-SMA and FAP are shown in Figure 4. Patients with high α-SMA expression had a significantly worse RFS than those with low α-SMA expression (5-year RFS, 47.6% vs. 82.2%; p = 0.003; Figure 4A). Furthermore, the 5-year DSS rates in the low- and high-α-SMA groups were 93.3% and 67.5%, respectively, with a significant difference between the groups (p = 0.01; Figure 4B). Regarding the effect of FAP on survival, the high-FAP group had significantly worse RFS (5-year RFS, 53.5% vs. 73.7%; p = 0.04; Figure 4C) and DSS (5-year DSS, 65.7% vs. 94.4%; p = 0.02; Figure 4D) than the low-FAP group.

## 3.5 Prognostic factors associated with survival

The results of the univariate and multivariable analyses for investigating the prognostic factors of RFS are shown in Table 3. Univariate analyses revealed that α-SMA, FAP, and lymph node metastasis were significant factors, but histopathologic subtypes were not an independent factor. In model 1, multivariable analysis

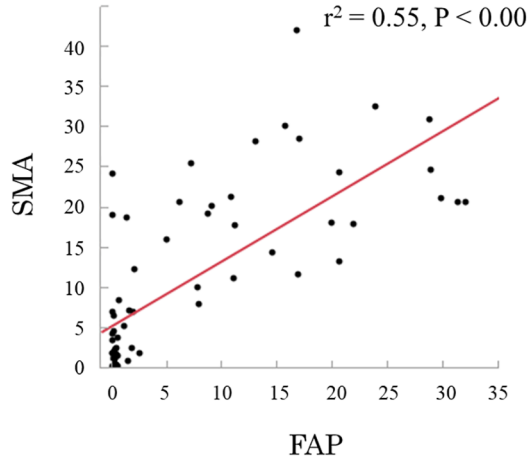


FIGURE 3
Relationship between smooth muscle actin (α-SMA) and fibroblast activation protein (FAP), showing a linear correlation ($r^2$ = 0.55; p < 0.001).

revealed that high α-SMA expression was an independent predictor (HR: 3.68; 95% CI: 1.21–12.4; p = 0.02). In contrast, high FAP was not an independent index for RFS in model 2.

Table 4 shows the results of the univariate and multivariable analyses for DSS. Univariate analyses identified high α-SMA (HR: 9.48; p = 0.005) and FAP (HR: 4.50; p = 0.03) as independent predictors of DSS. However, only high α-SMA level (HR: 8.54; 95% CI: 1.21–170; p = 0.03) was a significant factor associated with DSS in the multivariable analyses.

## 3.6 CAF expression and clinicopathological parameters

The relationship between α-SMA expression and clinicopathological parameters is shown in Table 5. No significant differences were found between the low- and high-α-SMA groups in terms of the demographic variables. High α-SMA expression was significantly associated with advanced T stage as well as higher incidences of lymph node metastases and recurrence. In fact, the low α-SMA group had lymph node metastasis in only one patient (3%) and no recurrence after surgery.

# 4 Discussion

This study is the first to investigate the significance of CAFs in patients undergoing pancreatoduodenectomy for ampullary carcinoma. We found CAFs in ampullary carcinoma. Furthermore, our results revealed that CAFs, especially α-SMA, are significantly associated with survival after radical resection.

Interesting association of CAF expression with histopathologic subtype of ampullary carcinoma was detected in this study. A novel finding included that the intestinal type was associated with a lower area index of α-SMA as well as FAP compared to those of the pancreatobiliary and mixed types (Table 2). Similar to previous reports (5), prognosis in the intestinal type was better than those in the pancreatobiliary and mixed types (Supplementary Figure 1). Moreover, multivariable analyses revealed that CAF expression was a stronger predictor of survival than histopathologic subtypes. Further research would be required to examine the interaction between CAF and histopathologic subtypes.

The present study reveals a strong relationship between CAFs and survival. Patients with high α-SMA and FAP expression had significantly worse RFS and DSS (Figure 4), in line with previous reports in gastrointestinal surgical oncology (14, 15). Moreover, our multivariable analyses suggested that α-SMA was an independent predictor of RFS and DSS after surgery (Tables 3, 4). There was a significant association between α-SMA expression and pathological factors (Table 5). Based on the relationship between α-SMA expression and advanced tumor stages, the findings of multivariable analyses can be explained. Briefly, patients with high α-SMA expression had more advanced tumors and a higher incidence of lymph node metastases, leading to worse RFS and DSS.

The role of CAFs has recently gained widespread attention in the field of cancer biology. CAF biology is mediated through direct and paracrine interactions of cellular and acellular compartments (9). The role of CAFs in cancer invasion and metastasis has been investigated over the past few years. A recent review reported the association of CAFs with cancer invasion and metastasis that occurs through extracellular matrix deposition and remodeling, epithelial-mesenchymal transition in cancer cells, and secretion of growth factors supporting cancer cells (17). Furthermore, potential CAF-targeted therapeutic strategies have been suggested (6, 14–17). There are ongoing clinical trials investigating the efficacy of CAF-targeted therapies combined with existing therapies (8, 18–20).

TABLE 2 Association of CAF expression with histopathologic subtype of ampullary carcinoma.

| | Intestinal type (n = 36) | Pancreatobiliary type (n = 20) | Mixed type (n = 11) | p-value |
|---|---|---|---|---|
| α-SMA (n = 66) | 4.8 (5.9) | 19.1 (9.9) | 16.0 (10.8) | <0.001 |
| Low | 28 | 2 | 3 | <0.001 |
| High | 7 | 18 | 8 | |
| FAP | 2.2 (5.8) | 12.8 (10.1) | 11.1 (11.0) | <0.001 |
| Low | 29 | 4 | 1 | <0.001 |
| High | 7 | 16 | 10 | |

Data are presented as mean (± standard deviation) or number.

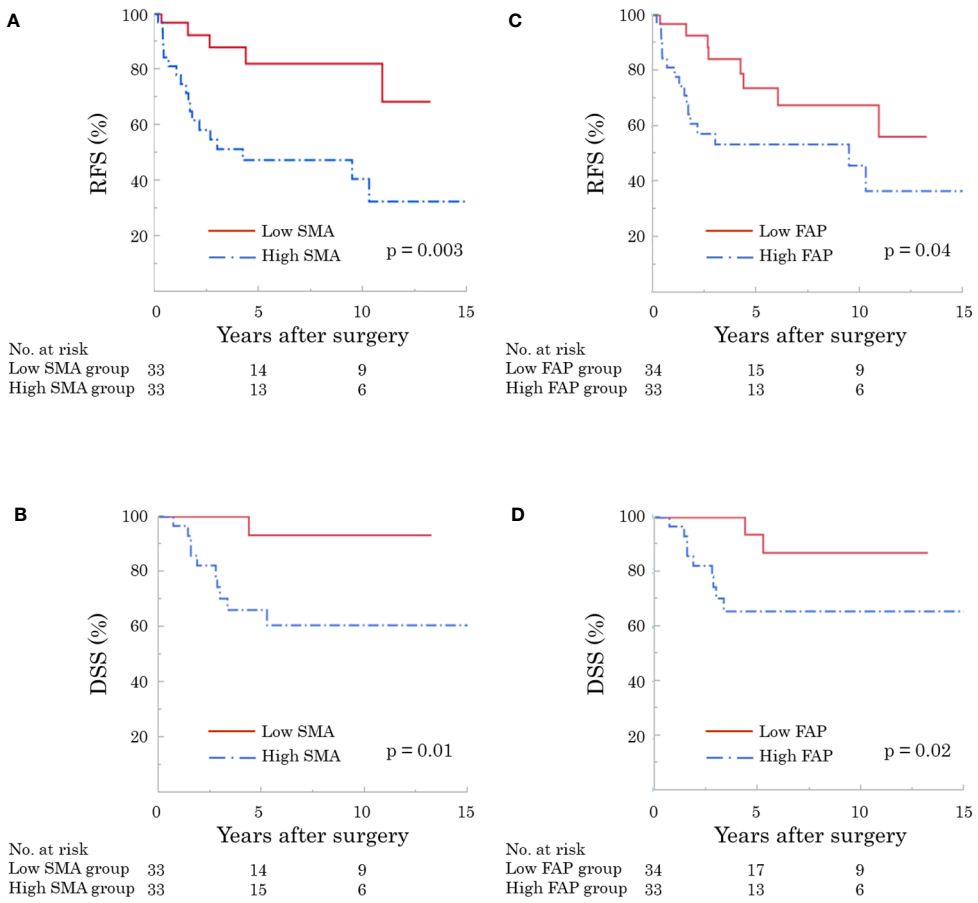


FIGURE 4
Recurrence-free (RFS) and disease-specific survival (DSS) according to expression of cancer-associated fibroblasts (CAF). The high α-smooth muscle actin (α-SMA) group had significantly worse RFS [**(A)** p = 0.003] and DSS [**(B)** p = 0.01]. In addition, patients with high fibroblast activation protein (FAP) showed significantly worse RFS [**(C)** p = 0.04] and DSS [**(D)** p = 0.02].

TABLE 3 Univariate and multivariable analyses of prognostic factors associated with recurrence-free survival.

| | Univariate analysis | | | Multivariable analysis (Model 1) | | | Multivariable analysis (Model 2) | | |
|---|---|---|---|---|---|---|---|---|---|
| Variable | HR | 95% CI | p-value | HR | 95% CI | p-value | HR | 95% CI | p-value |
| αSMA | | | | | | | | | |
| Low | 1 | | | | | | | | |
| High | 3.94 | 1.57–12.0 | 0.003 | 3.68 | 1.21–12.4 | 0.02 | | | |
| FAP | | | | | | | | | |
| Low | 1 | | | | | | 1 | | |
| High | 2.31 | 1.01–5.69 | 0.047 | | | | 2.03 | 0.75–5.57 | 0.15 |
| Sex | | | | | | | | | |
| Female | 1 | | | 1 | | | 1 | | |
| Male | 1.39 | 0.61–3.44 | 0.44 | 2.09 | 0.86–5.49 | 0.11 | 2.00 | 0.82–5.29 | 0.13 |
| Age (years) | | | | | | | | | |
| < 70 | 1 | | | | | | | | |

*(Continued)*

10.3389/fonc.2023.1072106

TABLE 3 Continued

| | Univariate analysis | | | Multivariable analysis (Model 1) | | | Multivariable analysis (Model 2) | | |
|---|---|---|---|---|---|---|---|---|---|
| Variable | HR | 95% CI | p-value | HR | 95% CI | p-value | HR | 95% CI | p-value |
| ≥ 70 | 1.85 | 0.81–4.58 | 0.14 | | | | | | |
| BMI (kg/m$^2$) | | | | | | | | | |
| < 25 | 1 | | | | | | | | |
| ≥ 25 | 0.50 | 0.08–1.71 | 0.30 | | | | | | |
| ASA-PS | | | | | | | | | |
| Grade 1–2 | 1 | | | | | | | | |
| Grade 3 | 1.52 | 0.44–4.06 | 0.47 | | | | | | |
| Major complication | | | | | | | | | |
| Absence | 1 | | | | | | | | |
| Presence | 1.50 | 0.43–4.02 | 0.48 | | | | | | |
| T factor | | | | | | | | | |
| < T3 | 1 | | | 1 | | | 1 | | |
| T3 | 1.65 | 0.67–3.79 | 0.27 | 0.81 | 0.29–2.10 | 0.67 | 0.98 | 0.37–2.45 | 0.97 |
| Lymph node metastasis | | | | | | | | | |
| Absence | 1 | | | 1 | | | 1 | | |
| Presence | 3.23 | 1.34–7.42 | 0.01 | 2.38 | 0.87–6.34 | 0.09 | 2.88 | 1.11–7.25 | 0.03 |
| Histopathologic subtype | | | | | | | | | |
| Intestinal type | 1 | | | | | | | | |
| Pancreatobiliary type | 2.75 | 1.10–6.97 | 0.03 | | | | | | |
| Mixed type | 2.75 | 0.84–8.01 | 0.09 | | | | | | |

HR, hazard ratio; CI, confidence interval; BMI, body mass index; ASA, American Society of Anesthesiologists.

TABLE 4 Univariate and multivariable analyses of prognostic factors associated with disease-specific survival.

| | Univariate analysis | | | Multivariable analysis (Model 1) | | | Multivariable analysis (Model 2) | | |
|---|---|---|---|---|---|---|---|---|---|
| Variable | HR | 95% CI | p-value | HR | 95% CI | p-value | HR | 95% CI | p-value |
| αSMA | | | | | | | | | |
| Low | 1 | | | 1 | | | | | |
| High | 9.48 | 1.81–174 | 0.005 | 8.54 | 1.21–170 | 0.03 | | | |
| FAP | | | | | | | | | |
| Low | 1 | | | | | | 1 | | |
| High | 4.50 | 1.16–29.6 | 0.03 | | | | 2.92 | 0.57–22.1 | 0.21 |
| Sex | | | | | | | | | |
| Female | 1 | | | | | | | | |
| Male | 2.01 | 0.58–9.19 | 0.28 | | | | | | |
| Age (years) | | | | | | | | | |
| < 70 | 1 | | | | | | | | |
| ≥ 70 | 1.62 | 0.49–6.18 | 0.44 | | | | | | |

*(Continued)*

10.3389/fonc.2023.1072106

TABLE 4 Continued

| | Univariate analysis | | | Multivariable analysis (Model 1) | | | Multivariable analysis (Model 2) | | |
|---|---|---|---|---|---|---|---|---|---|
| Variable | HR | 95% CI | p-value | HR | 95% CI | p-value | HR | 95% CI | p-value |
| BMI (kg/m$^2$) | | | | | | | | | |
| < 25 | 1 | | | | | | | | |
| ≥ 25 | 0.58 | 0.03–3.06 | 0.58 | | | | | | |
| ASA-PS | | | | | | | | | |
| Grade 1–2 | 1 | | | 1 | | | 1 | | |
| Grade 3 | 4.69 | 1.20–16.1 | 0.03 | 4.42 | 0.94–20.6 | 0.06 | 3.67 | 0.82–15.9 | 0.09 |
| Major complication | | | | | | | | | |
| Absence | 1 | | | | | | | | |
| Presence | 2.16 | 0.47–7.52 | 0.29 | | | | | | |
| T factor | | | | | | | | | |
| < T3 | 1 | | | 1 | | | 1 | | |
| T3 | 2.14 | 0.62–7.11 | 0.22 | 0.56 | 0.12–2.42 | 0.44 | 0.79 | 0.19–3.16 | 0.74 |
| Lymph node metastasis | | | | | | | | | |
| Absence | 1 | | | 1 | | | 1 | | |
| Presence | 2.55 | 0.67–8.45 | 0.16 | 1.59 | 0.40–5.68 | 0.49 | 1.92 | 0.47–7.12 | 0.34 |
| Histopathologic subtype | | | | | | | | | |
| Intestinal type | 1 | | | | | | | | |
| Pancreatobiliary type | 4.50 | 1.18–21.4 | 0.03 | | | | | | |
| Mixed type | 3.49 | 0.46–21.2 | 0.20 | | | | | | |

HR, hazard ratio; CI, confidence interval; BMI, body mass index; ASA, American Society of Anesthesiologists.

TABLE 5 Relationship between αSMA expression and clinicopathological parameters.

| | Low α-SMA (n = 33) | High α-SMA (n = 33) | p-value |
|---|---|---|---|
| Demographic variables | | | |
| Age (year) | 69.9 (9.6) | 70.8 (8.9) | 0.74 |
| Sex (male/female) | 21 (64)/12 (36) | 18 (55)/15 (45) | 0.45 |
| BMI (kg/m$^2$) | 22.6 (4.1) | 21.5 (2.7) | 0.14 |
| ASA-PS (1–2/3) | 29 (88)/4 (12) | 23 (70)/7 (30) | 0.32 |
| Pathological factors | | | |
| T stage (Tis/1/2/3) | 7 (21)/17 (52)/9 (27)/0 (0) | 0 (0)/4 (12)/13 (39)/16 (48) | <0.001 |
| Lymph node metastasis (presence/absence) | 1 (3)/32 (97) | 12 (36)/21 (64) | <0.001 |
| Histopathologic subtype | | | |
| Intestinal type | 28 (85) | 7 (21) | <0.001 |
| Pancreatobiliary type | 2 (6) | 18 (55) | |
| Mixed type | 3 (9) | 8 (24) | |
| Recurrence (presence/absence) | 0 (0)/33 (100) | 16 (48)/17 (52) | <0.001 |

Data are presented as mean (± standard deviation) or number (percentage).
BMI, body mass index; ASA-PS, American Society of Anesthesiologists Physical Status.

Current extensive research has demonstrated subtypes of CAFs including pro-tumor or anti-tumor characteristics. Recent studies have supported the evidence for CAF heterogeneity in pancreatic ductal adenocarcinoma, showing several subpopulations of CAFs such as myofibroblastic CAFs (myCAFs), inflammatory CAFs (iCAFs), and antigen-presenting CAFs (apCAFs) (21, 22). However, the role of CAFs subtypes of ampullary carcinoma has not yet been investigated.

Translating the results of this study into clinical practice is important. The assessment of CAF expression can be easy and useful for detecting high-risk patients who could have poor long-term outcomes. Although the utility of adjuvant therapy for high-risk patients with ampullary carcinoma has been suggested (23), further studies are required to understand its biological features and histological characteristics and to develop an optimal therapeutic strategy to treat ampullary carcinoma (4). Therefore, evaluation of CAFs could be regarded as a novel treatment strategy in decision making for the introduction of adjuvant or first-line chemotherapy.

This study has several limitations, given that was a retrospective single-center study. The sample size was relatively small because of the rarity of the disease. Further studies with larger sample sizes are needed to clarify the role and efficacy of CAFs in ampullary carcinoma. The detailed mechanisms underlying the interaction between CAFs and prognosis are unknown. We suggest that CAFs promote epithelial-mesenchymal transition as well as cancer invasion and metastasis, including lymph node metastasis (17), leading to worse prognosis in patients with ampullary carcinoma. However, further studies should be performed to identify and delineate the interactions among CAFs, epithelial-mesenchymal transition, and cancer invasion.

## 5 Conclusion

The present study indicates that the assessment of CAFs can be helpful in evaluating cancer progression as well as in estimating survival after radical resection in patients with ampullary carcinoma.

## Data availability statement

The raw data supporting the conclusions of this article will be made available by the authors, without undue reservation.

## Ethics statement

The studies involving human participants were reviewed and approved by Okayama University Hospital. The ethics committee waived the requirement of written informed consent for participation.

## Author contributions

Concept and study design: KT, KN, and SK; Acquisition of data: KT, YN, YU, RY, TomF, KY, and HK; Pathological evaluation: TT; Drafting of the manuscript: KT; Critical revision of the manuscript for important intellectual content: KN, SK, YU, RY, TY and TosF. All authors contributed to the article and approved the final version of the article.

## Conflict of interest

The authors declare that the research was conducted in the absence of any commercial or financial relationships that could be construed as a potential conflict of interest.

## Publisher's note



## Supplementary material

The Supplementary Material for this article can be found online at: https://www.frontiersin.org/articles/10.3389/fonc.2023.1072106/full#supplementary-material

SUPPLEMENTARY FIGURE 1
Recurrence-free (RFS) and disease-specific survival (DSS) by histopathologic subtypes. The 5-year RFS showed 79.0% in the intestinal group, 43.6% in the pancreatobiliary group, and 53.9% in the mixed group (**A**; p = 0.046). The 5-year DSS included 91.8% in the intestinal group, 60.5% in the pancreatobiliary group, and 71.4% in the mixed group (**B**; p = 0.07).

## References

1. Takagi K, Nagai Y, Umeda Y, Yoshida R, Yoshida K, Fuji T, et al. Prognostic value of the regional lymph node station in pancreatoduodenectomy for ampullary carcinoma. *In Vivo* (2022) 36(2):973–8. doi: 10.21873/invivo.12789

2. Winter JM, Cameron JL, Olino K, Herman JM, de Jong MC, Hruban RH, et al. Clinicopathologic analysis of ampullary neoplasms in 450 patients: implications for surgical strategy and long-term prognosis. *J Gastrointest Surg* (2010) 14(2):379–87. doi: 10.1007/s11605-009-1080-7

3. Okano K, Oshima M, Suto H, Ando Y, Asano E, Kamada H, et al. Ampullary carcinoma of the duodenum: current clinical issues and genomic overview. *Surg Today* (2022) 52(2):189–97. doi: 10.1007/s00595-021-02270-0

4. Rizzo A, Dadduzio V, Lombardi L, Ricci AD, Gadaleta-Caldarola G. Ampullary carcinoma: An overview of a rare entity and discussion of current and future therapeutic challenges. *Curr Oncol* (2021) 28(5):3393–402. doi: 10.3390/curroncol28050293

5. Shin DW, Kim S, Jung K, Jung JH, Kim B, Ahn J, et al. Impact of histopathological type on the prognosis of ampullary carcinoma: A systematic review and meta-analysis. *Eur J Surg Oncol* (2023) 49(2):306–15. doi: 10.1016/j.ejso.2022.10.001

6. Liu T, Han C, Wang S, Fang P, Ma Z, Xu L, et al. Cancer-associated fibroblasts: an emerging target of anti-cancer immunotherapy. *J Hematol Oncol* (2019) 12(1):86. doi: 10.1186/s13045-019-0770-1

7. Noma K, Smalley KS, Lioni M, Naomoto Y, Tanaka N, El-Deiry W, et al. The essential role of fibroblasts in esophageal squamous cell carcinoma-induced angiogenesis. *Gastroenterology* (2008) 134(7):1981–93. doi: 10.1053/j.gastro.2008.02.061

8. Sahai E, Astsaturov I, Cukierman E, DeNardo DG, Egeblad M, Evans RM, et al. A framework for advancing our understanding of cancer-associated fibroblasts. *Nat Rev Cancer* (2020) 20(3):174–86. doi: 10.1038/s41568-019-0238-1

9. Kobayashi H, Enomoto A, Woods SL, Burt AD, Takahashi M, Worthley DL. Cancer-associated fibroblasts in gastrointestinal cancer. *Nat Rev Gastroenterol Hepatol* (2019) 16(5):282–95. doi: 10.1038/s41575-019-0115-0

10. Sunami Y, Häußler J, Zourelidis A, Kleeff J. Cancer-associated fibroblasts and tumor cells in pancreatic cancer microenvironment and metastasis: Paracrine regulators, reciprocation and exosomes. *Cancers (Basel)* (2022) 14(3):744. doi: 10.3390/cancers14030744

11. Clavien PA, Barkun J, de Oliveira ML, Vauthey JN, Dindo D, Schulick RD, et al. The clavien-dindo classification of surgical complications: five-year experience. *Ann Surg* (2009) 250(2):187–96. doi: 10.1097/SLA.0b013e3181b13ca2

12. Surgery JSoH-B-P. *Japanese Society of Hepato-Biliary-Pancreatic Surgery: General Rules for Clinical and Pathological Studies on Cancer of the Biliary Tract* (*7th edition*). Japan, Kanehiora Publ Corp., (2021).

13. Quero G, Laterza V, Fiorillo C, Menghi R, De Sio D, Schena CA, et al. The impact of the histological classification of ampullary carcinomas on long-term outcomes after pancreaticoduodenectomy: a single tertiary referral center evaluation. *Langenbecks Arch Surg* (2022) 407(7):2811–21. doi: 10.1007/s00423-022-02563-z

14. Ogawa T, Kikuchi S, Tabuchi M, Mitsui E, Une Y, Tazawa H, et al. Modulation of p53 expression in cancer-associated fibroblasts prevents peritoneal metastasis of gastric cancer. *Mol Ther Oncol* (2022) 25:249–61. doi: 10.1016/j.omto.2022.04.009

15. Kashima H, Noma K, Ohara T, Kato T, Katsura Y, Komoto S, et al. Cancer-associated fibroblasts (CAFs) promote the lymph node metastasis of esophageal squamous cell carcinoma. *Int J Cancer* (2019) 144(4):828–40. doi: 10.1002/ijc.31953

16. Kato T, Noma K, Ohara T, Kashima H, Katsura Y, Sato H, et al. Cancer-associated fibroblasts affect intratumoral CD8(+) and FoxP3(+) T cells *Via* IL6 in the tumor microenvironment. *Clin Cancer Res* (2018) 24(19):4820–33. doi: 10.1158/1078-0432.CCR-18-0205

17. Asif PJ, Longobardi C, Hahne M, Medema JP. The role of cancer-associated fibroblasts in cancer invasion and metastasis. *Cancers (Basel)* (2021) 13(18):4720. doi: 10.3390/cancers13184720

18. Murphy JE, Wo JY, Ryan DP, Clark JW, Jiang W, Yeap BY, et al. Total neoadjuvant therapy with FOLFIRINOX in combination with losartan followed by chemoradiotherapy for locally advanced pancreatic cancer: A phase 2 clinical trial. *JAMA Oncol* (2019) 5(7):1020–7. doi: 10.1001/jamaoncol.2019.0892

19. Hingorani SR, Zheng L, Bullock AJ, Seery TE, Harris WP, Sigal DS, et al. HALO 202: Randomized phase II study of PEGPH20 plus nab-Paclitaxel/Gemcitabine versus nab-Paclitaxel/Gemcitabine in patients with untreated, metastatic pancreatic ductal adenocarcinoma. *J Clin Oncol* (2018) 36(4):359–66. doi: 10.1200/JCO.2017.74.9564

20. Hofheinz RD, al-Batran SE, Hartmann F, Hartung G, Jäger D, Renner C, et al. Stromal antigen targeting by a humanised monoclonal antibody: an early phase II trial of sibrotuzumab in patients with metastatic colorectal cancer. *Onkologie* (2003) 26 (1):44–8. doi: 10.1159/000069863

21. Geng X, Chen H, Zhao L, Hu J, Yang W, Li G, et al. Cancer-associated fibroblast (CAF) heterogeneity and targeting therapy of CAFs in pancreatic cancer. *Front Cell Dev Biol* (2021) 9:655152. doi: 10.3389/fcell.2021.655152

22. Öhlund D, Handly-Santana A, Biffi G, Elyada E, Almeida AS, Ponz-Sarvise M, et al. Distinct populations of inflammatory fibroblasts and myofibroblasts in pancreatic cancer. *J Exp Med* (2017) 214(3):579–96. doi: 10.1084/jem.20162024

23. Vo NP, Nguyen HS, Loh EW, Tam KW. Efficacy and safety of adjuvant therapy after curative surgery for ampullary carcinoma: A systematic review and meta-analysis. *Surgery* (2021) 170(4):1205–14. doi: 10.1016/j.surg.2021.03.046

frontiers | Frontiers in Oncology

TYPE Review
PUBLISHED 26 September 2023
DOI 10.3389/fonc.2023.1241561



OPEN ACCESS

EDITED BY
Beatrice Aramini,
University of Bologna, Italy

REVIEWED BY
Noel Donlon,
Trinity College Dublin, Ireland
Giacomo Deiro,
University of Turin, Italy

*CORRESPONDENCE
D. Wagner
Doris.wagner@medunigraz.at

†These authors have contributed equally to this work

RECEIVED 16 June 2023
ACCEPTED 07 August 2023
PUBLISHED 26 September 2023

CITATION
Wagner D, Wienerroither V, Scherrer M, Thalhammer M, Faschinger F, Lederer A, Hau HM, Sucher R and Kornprat P (2023) Value of sarcopenia in the resection of colorectal liver metastases—a systematic review and meta-analysis.
*Front. Oncol.* 13:1241561.
doi: 10.3389/fonc.2023.1241561



# Value of sarcopenia in the resection of colorectal liver metastases—a systematic review and meta-analysis

D. Wagner*†, V. Wienerroither†, M. Scherrer, M. Thalhammer, F. Faschinger, A. Lederer, H. M. Hau, R. Sucher and P. Kornprat

Division for General, Visceral, and Transplantation Surgery, Department of Surgery, Medical University of Graz, Graz, Austria

**Introduction:** Sarcopenia is defined as a decline in muscle function as well as muscle mass. Sarcopenia itself and sarcopenic obesity, defined as sarcopenia in obese patients, have been used as surrogates for a worse prognosis in colorectal cancer. This review aims to determine if there is evidence for sarcopenia as a prognostic parameter in colorectal liver metastases (CRLM).

**Methods:** PubMed, Embase, Cochrane Central, Web of Science, SCOPUS, and CINAHL databases were searched for articles that were selected in accordance with the PRISMA guidelines. The primary outcomes were overall survival (OS) and disease-free survival (DFS). A random effects meta-analysis was conducted.

**Results:** After eliminating duplicates and screening abstracts ($n$ = 111), 949 studies were screened, and 33 publications met the inclusion criteria. Of them, 15 were selected after close paper review, and 10 were incorporated into the meta-analysis, which comprised 825 patients. No significant influence of sarcopenia for OS (odds ratio (OR), 2.802 (95% confidence interval (CI), 1.094–1.11); $p$ = 0.4) or DFS (OR, 1.203 (95% CI, 1.162–1.208); $p$ = 0.5) was found, although a trend was defined toward sarcopenia. Sarcopenia significantly influenced postoperative complication rates (OR, 7.905 (95% CI, 1.876–3.32); $p$ = 0.001) in two studies where data were available.

**Conclusion:** Existing evidence on the influence of sarcopenia on postoperative OS as well as DFS in patients undergoing resection for CRLM exists. We were not able to confirm that sarcopenic patients have a significantly worse OS and DFS in our analysis, although a trend toward this hypothesis was visible. Sarcopenia seems to influence complication rates but prospective studies are needed.

KEYWORDS

**colorectal liver metastases, colorectal cancer, liver metastases, overall survival, disease free survival, sarcopenia**

**Abbreviations:** CRC, colorectal cancer; CRLM, colorectal liver metastases; OS, overall survival; DFS, disease-free survival.

# Introduction

Colorectal cancer (CRC), with 1.8 million new cases diagnosed per year, has been found to be the fourth most incident cancer worldwide. It accounts for the second-most cancer-related deaths worldwide, which means 800,000 CRC-related deaths annually (1, 2).

Colorectal liver metastases (CRLM) are present in approximately 15% of CRC patients at the time of the primary diagnosis, and another 16% of patients develop CRLM throughout their 5-year follow-up after CRC treatment (3, 4). With a 5-year survival of about 16% of overall CRLM patients, this number increases in resectable situations to up to 50% (5).

Various risk factors for the development of CRC have been defined. One of the major risk factors appointed by the World Health Organization is obesity with a body mass index (BMI) above 30 kg/m$^2$ for adults (6, 7). It has been well described, and the rise of obesity in all industrial nations worldwide might also contribute to the higher incidences of CRC in these industrial populations (8, 9).

For obese patients, worse overall survival as well as higher incidences of CRLM and worse outcomes after CRLM resection has been shown, rebutting the "obesity paradox," which had been described earlier, stating that moderate obesity might even be protective for patients sustaining CRC (10, 11). However, there is still limited high-quality evidence on the real impact of obesity on perioperative as well as long-term outcomes after resection for CRLM.

Sarcopenia has been used as a surrogate for muscle wasting in previous years and is defined as a progressive and generalized skeletal muscle disorder that is associated with an increased likelihood of adverse outcomes (12, 13). It comprises not only a decline in muscle mass but also a decline in muscle function. Generally, sarcopenia has been found to be present in about 38% of cancer patients at the time of presentation; in CRC patients, about 39% of patients have been described as sarcopenic (14, 15). In metastatic CRC patients, even 44% have been identified in studies as having sarcopenia. On top of over a third of patients being sarcopenic at the time of diagnosis of CRC, treatment of CRC with chemotherapy often leads to a significant reduction in muscle mass on top of already prevalent sarcopenia, leading to CRLM patients, who usually receive chemotherapy prior to resection, offering an even worse premise for a potential resection to the individual patient (16, 17).

Unfortunately, sarcopenia is defined very heterogeneously in the present literature. The definition is mainly based on measures of muscle mass and/or muscle density on computed tomography (CT) imaging. Commonly used measures that have been described are the skeletal muscle index (SMI), the total psoas area (TPA), or the Hounsfield Average Calculation (HUAC). All of these parameters are measured on single cross-sectional CT images of the abdomen at the level of the transverse processes of the third lumbar vertebra (L3), normalized for height. The HUAC reflecting the muscle density is measured using the Hounsfield Units of the psoas muscles in the described images and normalizing the measures for the psoas muscles area. Low muscle density has been used as an indicator for intramuscular adipose tissue content (IMAC) and therefore poorer muscle quality (18–20).

Sarcopenia in obese patients—known as sarcopenic obesity—has emerged in recent years as an additional and sometimes more precise prognostic tool as these patients seem to be highly prone to complications. Sarcopenic obesity has been attributed to poor oncologic as well as surgical prognosis (21, 22).

We aimed to perform a systematic review of sarcopenia in the setting of colorectal liver metastases. The presented review was registered in the PROSPERO database (https://www.crd.york.ac.uk/prospero, ID: 432501).

# Methods

## Search strategy

The search for this review was performed according to the preferred reporting items for systematic reviews and meta-analysis (PRISMA) guidelines (23). The Cochrane Register of Controlled Trials (CENTRAL), Embase, the Web of Science, Medline, and Google Scholar were screened for the search string: "colorectal neoplasms" [MeSH Terms] OR "colorectal neoplasms" [Title/Abstract] OR "colorectal cancer" [Title/Abstract] OR "colorectal carcinoma" [Title/Abstract] OR "colorectal tumor" [Title/Abstract] OR "colorectal adenocarcinoma" [Title/Abstract]) AND ("liver neoplasms" [MeSH Terms] OR "liver neoplasms" [Title/Abstract] OR "liver metastases" [Title/Abstract] OR "hepatic metastases" [Title/Abstract] OR "metastatic liver disease" [Title/Abstract])) AND ("sarcopenia" [MeSH Terms] OR "sarcopenia" [Title/Abstract] OR "muscle wasting" [Title/Abstract] OR "muscle loss" [Title/Abstract] OR "muscle atrophy" [Title/Abstract]. The search was carried out on the 22nd day of May 2023 by Scherrer M and Wagner D.

## Inclusion criteria

Only original studies investigating humans were included in the analysis. Studies were only included if they reported outcomes of patients aged 18 years and above who underwent liver resection with curative intent for colorectal liver metastases or if specific outcomes for sarcopenic patients were reported. Studies that reported a defined outcome as recurrence, disease-free survival, or overall survival were included in further analysis.

Only studies that reported the exact outcome as the main objective, defined as the influence of sarcopenia on patients' survival and/or recurrence, were selected for further analysis.

## Exclusion criteria

We excluded case series, case reports, reviews, or editorials, as well as experimental research. Only studies written in English were considered for evaluation. Studies reporting from the same databases were limited to the most recent report. We also included outcomes that did not report in numbers and/or missing odds ratios or the possibility of deriving these odds ratios from reported numbers.

## Data sources and study selection

The authors F.F., S.M., and W.D. independently screened titles and abstracts to determine their eligibility for inclusion. Full texts were selected and screened upon identification after abstract reading.

## Data extraction

Eligible studies were selected for further assessment and data extraction. Data were extracted into a database. Data selected included author, publication date, country, number of participants, median age, methods of sarcopenia assessment, preoperative therapy if reported, including chemotherapy, operation method, type of liver resection, and follow-up (duration, reported overall survival or disease-free survival or both as well as perioperative outcomes).

## Quality assessment of included studies and meta-analysis

The quality assessment of the included studies was performed using the Quality in Prognosis Instrument (QUIPS) by three observers (D.W., M.S., and F.F.). The included 10 studies were analyzed using the instrument. The risk of bias was considered low if less than two items were rated as "low risk" or "moderate risk" in the respective assessment categories. Risk of bias was rated "high risk" if more than one item was rated high risk in the respective category (24).

## Statistical analysis

The statistical analysis was performed using SPSS Version 26.0 (SPSS Inc, Chicago, IL, USA). To compare the combined effects of hazard ratios (HR) and/or odds ratios (OR), an inverse approach was applied using 95% confidence intervals (CI) for survival and other outcome data. Heterogeneity was assessed using a random effects model and a $C^2$ test with a $p$-value of $< 0.1$ being considered significant. To assess the quantity of heterogeneity, $I^2$ statistics were used with a cutoff value of 50%, and odds ratios defined the difference of dichotome variables in the pooled studies (25).

# Results

## Description of included studies

The initial search led to 949 studies. After the removal of duplicates ($n$ = 838), 111 studies were screened, and a further 78 studies were excluded after abstract screening. The full publications of the remaining 33 studies were screened, and 15 were selected for inclusion into a close assessment. After an independent full-paper review by two investigators, five studies were excluded (no reporting of endpoints $n$ = 2, reporting of endpoints not in inclusion criteria $n$ = 3). The PRISMA Flow Chart is depicted in Figure 1.

So our search derived 10 studies with 1,619 participants that were included in the analysis. Studies were published between 2012 and 2022 and were published by Asian ($n$ = 3), European ($n$ = 6), and one US American study group (26–35). All studies were retrospective in nature. Databases for the reports had been compiled in a median of 108 months (range: 48–132 months) and mostly included all recipients who underwent CRLM resection in the respective centers and who had undergone preoperative imaging via CT scans, including the lumbar vertebral area at the level of L3. Only Yang et al. included patients who had undergone neoadjuvant treatment and therefore only investigated a limited number of patients who had undergone hepatic resection in their respective centers (33). The characteristics of the included studies are compiled in Table 1.

Six of the included studies reported primary tumor location (26–28, 31, 32, 34), and seven reported neoadjuvant and/or adjuvant chemotherapy as confounders (26–29, 33–35). All patients included underwent liver resection, whereas only five

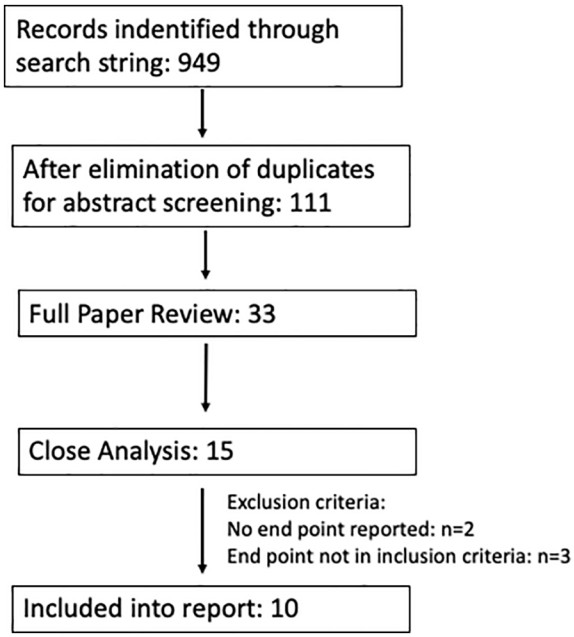


FIGURE 1
PRISMA flow chart of the search for the review.

TABLE 1 All characericstis of the included studies.

| Author | Year | Country | Sample size | Study design | Sarcopenia assessment | Cutoff values | Cutoff definition |
|---|---|---|---|---|---|---|---|
| Erikkson et al. | 2017 | Sweden | 97 | Retrospective | SMI | Males: 52.4 $cm^2/m^2$<br>Females: 38.5 $cm^2/m^2$ | Prado et al. |
| Vledder et al. | 2012 | The Netherlands | 196 | Retrospective | HU adipose tissue and skeletal muscle mass | Lowest quartile (sex-specific) | Statistical stratification |
| Kobayashi et al. | 2018 | Japan | 124 | Retrospective | SMI | Lowest quartile (sex spcific) | Stastitical stratification |
| Bajric et al. | 2022 | Austria | 355 | Retrospective | SMI | Males: 52.4 $cm^2/m^2$<br>Females: 38.5 $cm^2/m^2$ | Prado et al. |
| Lodewick et al. | 2015 | The Netherlands | 171 | Retrospective | SMI | Males: 43 $cm^2/m^2$ if BMI < 25; 53 $cm^2/m^2$ if BMI > 25<br>Females: 41 $cm^2/m^2$ | Martin et al. |
| Runkel et al. | 2021 | Germany | 94 | Retrospective | SMI | Males: 52.4 $cm^2/m^2$<br>Females: 38.5 $cm^2/m^2$ | Prado et al. |
| Liu et al. | 2022 | China | 182 | Retrospective | HUAC | HUAC < 22 | Statistical stratification |
| Pessia et al. | 2021 | Italy | 74 | Retrospective | SMI | Males: 43 $cm^2/m^2$ if BMI < 25; 53 $cm^2/m^2$ if BMI > 25<br>Females: 41 $cm^2/m^2$ | Martin et al. |
| Yang et al. | 2023 | China | 67 | Retrospective | SMI | Males: 52.4 $cm^2/m^2$<br>Females: 38.5 $cm^2/m^2$ | Prado et al. |
| Peng et al. | 2011 | USA | 259 | Retrospective | TPA | 500 $mm^2/m^2$ | Optimum stratification |

Study participation, sarcopenia measurement and cutoffs as well as reference for chosen cutoffs are outlined as is the year of publication stratified by the respective first author. SMI, skeletal muscle index; TPA, total psoas area; HU, Hounsfield units; HUAC, Hounsfield units average calculation.

studies stated the resection technique (26, 27, 31, 33, 35), and only one reported the operation method in detail (35).

Sarcopenia was identified to be prevalent in 825 patients in all studies. Baseline characteristics were outlined in nine of 10 studies included in the analysis according to nonsarcopenic and sarcopenic patients. In four of them, baseline characteristics differed significantly in age, BMI, adipose tissue, tumor markers, tumor location, and the neutrophil-to-lymphocyte ratio (26, 28, 29, 34). Yang et al. also focused on the progression of sarcopenia after neoadjuvant chemotherapy (33).

## Confounder and outcome assessment

Confounders assessed along with sarcopenia differed widely throughout the studies. All studies used age, BMI, tumor stage with TNM classification, ASA status, and gender as confounding variables. The outcome assessment in nine studies was defined as overall survival as well as disease-free survival (26–32, 34). Both were defined homogeneously throughout the nine studies as overall patient survival being the patient survival in the respective follow-up and disease-free survival being the recurrence-free survival in the respective follow-up. Only three studies (Runkel et al., Bajric et al., and Peng et al.) used postoperative morbidity and mortality as combined outcome endpoints, defining patients' 30-day morbidity using Clavien–Dindo classification (26, 31, 35). Of them, only Bajric and Peng et al. could be used for meta-analysis, as the difference between the sarcopenic and nonsarcopenic patients was not stated in Runkel et al., neither in number nor in statistical form (26, 31).

## QUIPS checklist

In the quality assessment using the QUIPS chart, five studies were rated as having an overall low risk for bias, three had a moderate bias risk and two showed a high risk for bias in the category study participation/selection of study participants and assessment for confounders. All results are compiled in Table 2.

## Sarcopenia assessment and definition

The definition of sarcopenia was very heterogeneous throughout the studies. Most of the included studies used the skeletal muscle index (SMI) to define sarcopenic patients ($n = 7$); four of these studies defined sarcopenia according to the established cutoffs by Prado et al., and two defined sarcopenia using the cutoff values defined by Martin et al. Only one study used statistical stratification to define the cutoffs and used the lowest quartile of their own patient set as a definition for sarcopenia. The other three studies used the total psoas area (TPA) with a cutoff derived by statistical stratification as a definition for sarcopenia, and only two studies incorporated muscle attenuation (i.e., intramuscular adipose tissue) in their primary definition for sarcopenia using the Hounsfield Units as a surrogate for muscle density.

10.3389/fonc.2023.1241561

TABLE 2 Data of the QUIPS assessment of the included studies.

| Author | Study participation | Study attrition | Prognostic factor measurement | Study confounding | Outcome measurements | Statistical analysis and reporting |
|---|---|---|---|---|---|---|
| **Erikkson et al.** | Moderate risk | Moderate risk | Low risk | Low risk | Low risk | Low risk |
| **Vledder et al.** | High risk | Moderate risk | Moderate risk | Moderate risk | Low risk | Low risk |
| **Kobayashi et al.** | Low risk | Moderate risk | Low risk | Moderate risk | Low risk | Moderate risk |
| **Bajric et al.** | Low risk | Moderate risk | Low risk | Moderate risk | Low risk | Low risk |
| **Lodewick et al.** | Moderate risk | Moderate risk | Moderate risk | Moderate risk | Low risk | Low risk |
| **Runkel et al.** | Moderate risk | Moderate risk | Low risk | Low risk | Low risk | Moderate risk |
| **Liu et al.** | Moderate risk | Moderate risk | Low risk | Moderate risk | Low risk | Low risk |
| **Pessia et al.** | Moderate risk | Moderate risk | Moderate risk | High risk | Low risk | Moderate risk |
| **Yang et al.** | Moderate risk | Moderate risk | Low risk | Low risk | Low risk | Low risk |
| **Peng et al.** | Moderate risk | Moderate risk | Moderate risk | Moderate risk | Low risk | Moderate risk |

## Meta-analysis of sarcopenia-related outcomes

The studies reported outcomes for a total of 825 patients. Sarcopenic patients therefore comprised 51% of overall patients. Sarcopenia assessment was heterogeneous throughout the studies, with most studies using SMI and cutoffs established by Prado et al. but not all.

Regression analysis of all aggregated data showed that sarcopenia was associated with postoperative overall survival, but no significance was reached due to selective outcome reporting (OR, 2.802 (95% CI, 1.094–1.11); $p$ = 0.4, Figure 2). In the subgroup analysis of studies that reported the influence of neoadjuvant therapy vs. studies that did not, no significant influence on overall survival was observed, although the death rate recorded as events influenced overall survival, especially in patients with neoadjuvant therapy (OR, 2.802 (95% CI, 1.094–1.11); $p$ = 0.4, Figure 3). No heterogeneity was found between the studies ($I^2$ = 0.28; $p$ = 0.6).

Concerning disease-free survival, which was reported in five studies, nonsarcopenia seemed better predictive but did not reach statistical significance due to heterogeneous reporting (OR, 1.203 (95% CI, 1.162–1.208); $p$ = 0.5; Figure 4).

Only two studies reported data on postoperative complications according to sarcopenia. The meta-analysis between these studies

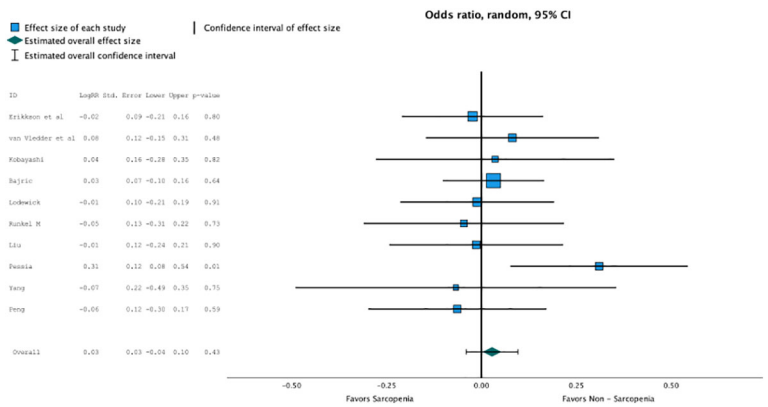


FIGURE 2
Regression analysis of all aggregated data showed that sarcopenia was associated with post operative overall survival, but no significance was reached due to selective outcome reporting (OR 2.802, CI95%1.094-1.11, p=0.4).

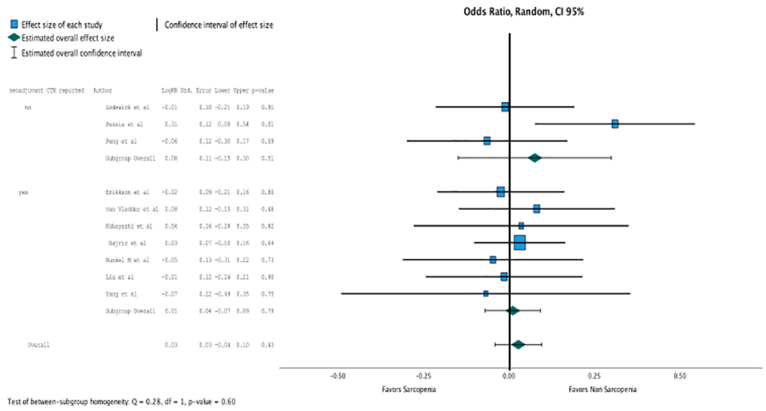


FIGURE 3
In the subgroup analysis of studies that reported the influence of neoadjuvant therapy vs. studies that did not, no significant influence on overall survival was observed. (OR 2.802, CI95% 1.094-1.11, p=0.4).

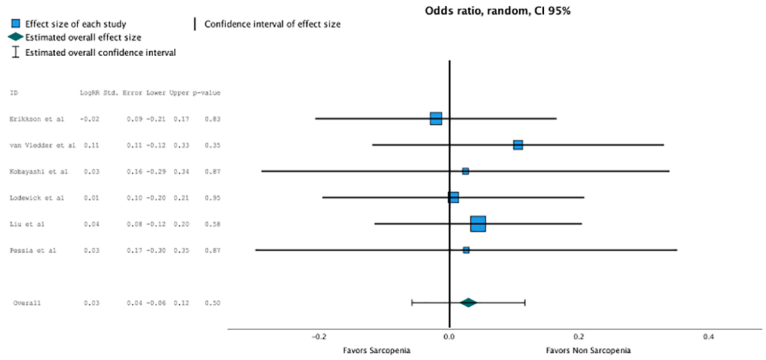


FIGURE 4
Non sarcopenia seemed better predictive for disease free survival but did not reach statistical significance due heterogenous reporting (OR 1.203, CI95% 1.162-1.208, p=0.5).

showed a high association of sarcopenia with postoperative complications (OR, 7.905 (95% CI, 1.876–3.32); $p = 0.001$; Figure 5).

## Discussion

To the best of our knowledge, this is the first meta-analysis that deals with the influence of sarcopenia on the outcome of patients who undergo liver resection for colorectal liver metastases (CRLM) alone. CRLM patients have been incorporated into previous meta-analyses (36, 37). However, due to the unique nature of CRLM and its rising incidence, preoperative assessment is more and more valued in this patient cohort (38). CRLMs are resected in up to 50% of cases. Recent guidelines for liver resection suggest incorporating prehabilitation into their recommendations for preoperative care of patients who undergo liver resection (39). Appropriate sarcopenia diagnosis and knowledge about the impact of sarcopenia on these patients might lead to optimization of preoperative patient care through optimization of prehabilitation and therefore contribute to better postoperative outcomes (19).

Sarcopenia is usually referred to as loss of muscle mass with loss of performance and impaired muscle strength (12, 13, 18). Performing a whole frailty or sarcopenia assessment is time-consuming. This fact often leads to the assessment being omitted or replaced by preoperative image analysis (40, 41). The definition of sarcopenia on preoperative images is still very heterogeneous, both through the working groups and the existing studies (39).

Our review not only confirmed this, but we were also able to display the heterogeneity systematically. Only 40% of the included studies used the same definition for sarcopenia (26, 27, 33, 35), even though 70% of the included studies used the same parameter to assess sarcopenia ($p = 0.05$). This not only is a significant difference; it also depicts the priority most clinicians usually have when it comes to sarcopenia assessment—to do it fast. This again stresses the high need in the clinical setting to have a readily available parameter. Williams et al. recently stressed this need from a perioperative patient management point of view (42). Until a concise and easily assessed parameter is available, sarcopenia will still be treated as a research parameter, although it is associated with dose-limiting toxicity in chemotherapy in other cancer patients

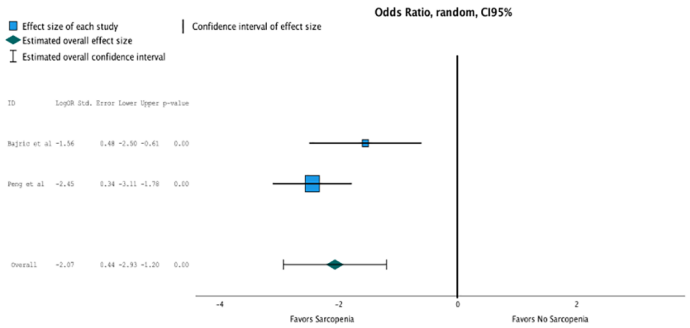


FIGURE 5
Only two studies reported data on postoperative complications according to sarcopenia. The meta analysis between these studies showed a high association of sarcopenia with postoperative complications (OR 7.905, CI95% 1.876-3.32, p=0.001).

(43). This was partially confirmed in the report by Yang et al., who clearly showed that patients who undergo neoadjuvant therapy do experience more pre- and postoperative sarcopenia and concomitantly higher morbidity and mortality rates (33).

Previous meta-analyses have found an association between overall survival and sarcopenia in patients who undergo loco-regional treatment for CRLM (44).

Although a trend toward sarcopenia was associated with lower overall survival rates in our patients, definitive significance was not observed among the included studies. Some studies have already shown this association. For example, Levolger et al. found poorer overall survival in patients undergoing resection of gastrointestnal malignancies.

Unfortunately, in this study, no report exists from an association of CRLM patients. In colorectal patients after resection, sarcopenia has been associated with poorer overall survival in studies by Trejo-Avila et al. This association was not as prominent in our meta-analysis, but it was observed (17).

Trejo-Avila et al. also performed a subanalysis on CRLM resection and postoperative complications. They found only a trend in association. Although we were only able to incorporate two studies into the meta-analysis, our association between sarcopenia and postoperative outcome was more prominent as compared to this previous study (26, 31).

Our analysis did not include studies that incorporated mixed populations due to their heterogenic nature in planning. This might explain this difference in one of our main findings compared to a recent meta-analysis incorporating all liver tumors (37, 45).

However, an association between sarcopenia and postoperative complications, according to Clavien–Dindo, has been reported in different resected tumors—for example, after gastrectomy (OR, 2.17 (95% CI, 1.53–3.08)) (16) or for colorectal cancer (OR, 1.82 (95% CI, 1.36–2.44)) (46). Similar patients with sarcopenia also showed limited survival in patients with pancreatic cancer (OR, 1.80 (95% CI, 1.42–2.29)) or esophageal cancer, as well as an association with higher complication rates (47).

After evaluation of the studies, we feel that the association between sarcopenia and worse postoperative outcomes after CRLM resection is clinically relevant and needs to be evaluated in prospective studies, including prehabilitation protocols prior to liver resection.

Why the association between postoperative complications and sarcopenia is so prominent in our meta-analysis can only be hypothesized. This might also be due to the fact that often multiple metastases are resected in one operation in CRLM patients. All studies that reported postoperative complications in our analysis detailed the complications, with biliary complications and bleeding complications the most prominent of the two studies that could be included in the meta-analysis (26, 31).

There is increased evidence that preoperative prehabilitation in the form of dietary supplements, protein supplementation, and exercise can improve muscle mass, function, and quantity (48). Studies showed that postoperative outcome was improved in patients who underwent resection for gastric cancer, and this is currently under prospective evaluation in these patients (49, 50). Also, chemotherapy tolerance as well as efficacy was ameliorated with the improvement of sarcopenia in recent reports (14, 47, 51).

However, our analysis has several limitations that need to be addressed. All the included studies were retrospective. Until now, no prospective analysis and follow-up of sarcopenic patients who undergo liver resection for CRLM exists. Despite the number of initially screened studies being high, only a limited number of studies could be selected for systematic review, and hence the quality of the analysis might be different in a higher study number setting. Also, the included studies were published over a relatively long period of time, between 2011 and 2023. This was also reflected in the quality of reporting of endpoints and in the quality assessment, with the studies that were reported recently showing lower risks for bias as compared to studies that had been reported earlier. All studies only measured sarcopenia using CT scans, whereas muscle performance seems to be crucial to defining real sarcopenia.

In conclusion, our meta-analysis showed that addressing sarcopenia seems to be beneficial for patients undergoing CRLM resections. A prospective study incorporating sarcopenia as muscle mass and muscle status and incorporating prehabilitation should be performed to accurately assess the value of sarcopenia in the setting of CRLM treatment with and without resection.

## Author contributions

DW, PK, VW, HH, RS: conzeptuatlization of review. DW, MS, FF, VW: search string, literature review, study selection. DW, MS, VW: QUIPS analysis. MS, FF: data extraction. DW, MS: meta analysis. All authors contributed to the article and approved the submitted version.

## Conflict of interest

The authors declare that the research was conducted in the absence of any commercial or financial relationships that could be construed as a potential conflict of interest.

## Publisher's note



## References

1. Rawla P, Sunkara T, Barsouk A. Epidemiology of colorectal cancer: incidence, mortality, survival, and risk factors. *Prz Gastroenterol* (2019) 14(2):89–103. doi: 10.5114/pg.2018.81072

2. Arhin N, Ssentongo P, Taylor M, Olecki EJ, Pameijer C, Shen C, et al. Age-standardised incidence rate and epidemiology of colorectal cancer in Africa: a systematic review and meta-analysis. *BMJ Open* (2022) 12(1):e052376. doi: 10.1136/bmjopen-2021-052376

3. Horn SR, Stoltzfus KC, Lehrer EJ, Dawson LA, Tchelebi L, Gusani NJ, et al. Epidemiology of liver metastases. *Cancer Epidemiol* (2020) 67:101760. doi: 10.1016/j.canep.2020.101760

4. McNally SJ, Parks RW. Surgery for colorectal liver metastases. *Dig Surg* (2013) 30 (4-6):337–47. doi: 10.1159/000351442

5. Manfredi S, Lepage C, Hatem C, Coatmeur O, Faivre J, Bouvier AM. Epidemiology and management of liver metastases from colorectal cancer. *Ann Surg* (2006) 244(2):254–9. doi: 10.1097/01.sla.0000217629.94941.cf

6. Ma Y, Yang Y, Wang F, Zhang P, Shi C, Zou Y, et al. Obesity and risk of colorectal cancer: a systematic review of prospective studies. *PloS One* (2013) 8(1):e53916. doi: 10.1371/journal.pone.0053916

7. Bluher M. Obesity: global epidemiology and pathogenesis. *Nat Rev Endocrinol* (2019) 15(5):288–98. doi: 10.1038/s41574-019-0176-8

8. Arroyo-Johnson C, Mincey KD. Obesity epidemiology worldwide. *Gastroenterol Clin North Am* (2016) 45(4):571–9. doi: 10.1016/j.gtc.2016.07.012

9. Stefan N, Haring HU, Hu FB, Schulze MB. Metabolically healthy obesity: epidemiology, mechanisms, and clinical implications. *Lancet Diabetes Endocrinol* (2013) 1(2):152–62. doi: 10.1016/S2213-8587(13)70062-7

10. Petrelli F, Cortellini A, Indini A, Tomasello G, Ghidini M, Nigro O, et al. Association of obesity with survival outcomes in patients with cancer: A systematic review and meta-analysis. *JAMA Netw Open* (2021) 4(3):e213520. doi: 10.1001/jamanetworkopen.2021.3520

11. Mintziras I, Miligkos M, Wachter S, Manoharan J, Maurer E, Bartsch DK. Reply letter to: "Response to: Sarcopenia and sarcopenic obesity are significantly associated with poorer overall survival in patients with pancreatic cancer: Systematic review and meta-analysis". *Int J Surg* (2019) 66:101–2. doi: 10.1016/j.ijsu.2019.02.017

12. Cruz-Jentoft AJ, Sayer AA. Sarcopenia. *Lancet* (2019) 393(10191):2636–46. doi: 10.1016/S0140-6736(19)31138-9

13. Cruz-Jentoft AJ, Bahat G, Bauer J, Boirie Y, Bruyere O, Cederholm T, et al. Sarcopenia: revised European consensus on definition and diagnosis. *Age Ageing* (2019) 48(1):16–31. doi: 10.1093/ageing/afy169

14. Pamoukdjian F, Bouillet T, Levy V, Soussan M, Zelek L, Paillaud E. Prevalence and predictive value of pre-therapeutic sarcopenia in cancer patients: A systematic review. *Clin Nutr* (2018) 37(4):1101–13. doi: 10.1016/j.clnu.2017.07.010

15. Surov A, Pech M, Gessner D, Mikusko M, Fischer T, Alter M, et al. Low skeletal muscle mass is a predictor of treatment related toxicity in oncologic patients. *A meta-analysis Clin Nutr* (2021) 40(10):5298–310. doi: 10.1016/j.clnu.2021.08.023

16. Xie H, Wei L, Liu M, Liang Y, Yuan G, Gao S, et al. Prognostic significance of preoperative prognostic immune and nutritional index in patients with stage I-III colorectal cancer. *BMC Cancer* (2022) 22(1):1316. doi: 10.1186/s12885-022-10405-w

17. Trejo-Avila M, Bozada-Gutierrez K, Valenzuela-Salazar C, Herrera-Esquivel J, Moreno-Portillo M. Sarcopenia predicts worse postoperative outcomes and decreased survival rates in patients with colorectal cancer: a systematic review and meta-analysis. *Int J Colorectal Dis* (2021) 36(6):1077–96. doi: 10.1007/s00384-021-03839-4

18. Cruz-Jentoft AJ, Baeyens JP, Bauer JM, Boirie Y, Cederholm T, Landi F, et al. Sarcopenia: European consensus on definition and diagnosis: Report of the European Working Group on Sarcopenia in Older People. *Age Ageing* (2010) 39(4):412–23. doi: 10.1093/ageing/afq034

19. Sayer AA, Cruz-Jentoft A. Sarcopenia definition, diagnosis and treatment: consensus is growing. *Age Ageing* (2022) 51(10). doi: 10.1093/ageing/afac220

20. Beaudart C, McCloskey E, Bruyere O, Cesari M, Rolland Y, Rizzoli R, et al. Sarcopenia in daily practice: assessment and management. *BMC Geriatr* (2016) 16 (1):170. doi: 10.1186/s12877-016-0349-4

21. Dieli-Conwright CM, Courneya KS, Demark-Wahnefried W, Sami N, Lee K, Buchanan TA, et al. Effects of aerobic and resistance exercise on metabolic syndrome, sarcopenic obesity, and circulating biomarkers in overweight or obese survivors of breast cancer: A randomized controlled trial. *J Clin Oncol* (2018) 36(9):875–83. doi: 10.1200/JCO.2017.75.7526

22. Baracos VE, Arribas L. Sarcopenic obesity: hidden muscle wasting and its impact for survival and complications of cancer therapy. *Ann Oncol* (2018) 29(suppl_2):ii1–9. doi: 10.1093/annonc/mdx810

23. Moher D, Shamseer L, Clarke M, Ghersi D, Liberati A, Petticrew M, et al. Preferred reporting items for systematic review and meta-analysis protocols (PRISMA-P) 2015 statement. *Syst Rev* (2015) 4(1):1. doi: 10.1186/2046-4053-4-1

24. Hayden JA, van der Windt DA, Cartwright JL, Cote P, Bombardier C. Assessing bias in studies of prognostic factors. *Ann Intern Med* (2013) 158(4):280–6. doi: 10.7326/0003-4819-158-4-201302190-00009

25. Leeflang MM. Systematic reviews and meta-analyses of diagnostic test accuracy. *Clin Microbiol Infect* (2014) 20(2):105–13. doi: 10.1111/1469-0691.12474

26. Bajric T, Kornprat P, Faschinger F, Werkgartner G, Mischinger HJ, Wagner D. Sarcopenia and primary tumor location influence patients outcome after liver resection for colorectal liver metastases. *Eur J Surg Oncol* (2022) 48(3):615–20. doi: 10.1016/j.ejso.2021.09.010

27. Eriksson S, Nilsson JH, Strandberg Holka P, Eberhard J, Keussen I, Sturesson C. The impact of neoadjuvant chemotherapy on skeletal muscle depletion and preoperative sarcopenia in patients with resectable colorectal liver metastases. *HPB (Oxford)* (2017) 19(4):331–7. doi: 10.1016/j.hpb.2016.11.009

28. Kobayashi A, Kaido T, Hamaguchi Y, Okumura S, Shirai H, Kamo N, et al. Impact of visceral adiposity as well as sarcopenic factors on outcomes in patients undergoing liver resection for colorectal liver metastases. *World J Surg* (2018) 42 (4):1180–91. doi: 10.1007/s00268-017-4255-5

29. Liu YW, Lu CC, Chang CD, Lee KC, Chen HH, Yeh WS, et al. Prognostic value of sarcopenia in patients with colorectal liver metastases undergoing hepatic resection. *Sci Rep* (2020) 10(1):6459. doi: 10.1038/s41598-020-63644-x

30. Lodewick TM, van Nijnatten TJ, van Dam RM, van Mierlo K, Dello SA, Neumann UP, et al. Are sarcopenia, obesity and sarcopenic obesity predictive of outcome in patients with colorectal liver metastases? *HPB (Oxford)* (2015) 17(5):438–46. doi: 10.1111/hpb.12373

31. Peng PD, van Vledder MG, Tsai S, de Jong MC, Makary M, Ng J, et al. Sarcopenia negatively impacts short-term outcomes in patients undergoing hepatic resection for colorectal liver metastasis. *HPB (Oxford)* (2011) 13(7):439–46. doi: 10.1111/j.1477-2574.2011.00301.x

32. Pessia B, ROmano L, Carlei F, Lazzari S, Vicentini V, Giuliani A, et al. Preoperative sarcopenia predicts survival after hepatectomy for colorectal metastases: a prospective observational study. *Eur Rev Med Pharmacol Sci* (2021) 25(18):5619–24.

33. Yang YR, Shi CS, Chang SW, Wu YY, Su YL, Lin GP, et al. The impact of sarcopenia on overall survival in patients with pan-RAS wild-type colorectal liver metastasis receiving hepatectomy. *Sci Rep* (2023) 13(1):6911. doi: 10.1038/s41598-023-33439-x

34. van Vledder MG, Levolger S, Ayez N, Verhoef C, Tran TC, Ijzermans JN. Body composition and outcome in patients undergoing resection of colorectal liver metastases. *Br J Surg* (2012) 99(4):550–7. doi: 10.1002/bjs.7823

35. Runkel M, Diallo TD, Lang SA, Bamberg F, Benndorf M, Fichtner-Feigl S. The role of visceral obesity, sarcopenia and sarcopenic obesity on surgical outcomes after liver resections for colorectal metastases. *World J Surg* (2021) 45(7):2218–26. doi: 10.1007/s00268-021-06073-9

36. Thormann M, Omari J, Pech M, Damm R, Croner R, Perrakis A, et al. Low skeletal muscle mass and post-operative complications after surgery for liver Malignancies: a meta-analysis. *Langenbecks Arch Surg* (2022) 407(4):1369–79. doi: 10.1007/s00423-022-02541-5

37. O'Connell RM, O'Neill M, Ríordáin MGO, Súilleabháin CBO, O'Sullivan AW. Sarcopaenia, obesity, sarcopaenic obesity and outcomes following hepatic resection for colorectal liver metastases: a systematic review and meta-analysis. *HPB (Oxford)* (2022) 24(11):1844–53. doi: 10.1016/j.hpb.2022.07.003

38. Bernardi L, Roesel R, Vagelli F, Majno-Hurst P, Cristaudi A. Imaging based body composition profiling and outcomes after oncologic liver surgery. *Front Oncol* (2022) 12:1007771. doi: 10.3389/fonc.2022.1007771

39. Joliat GR, Kobayashi K, Hasegawa K, Thomson JE, Padbury R, Scott M, et al. Guidelines for perioperative care for liver surgery: enhanced recovery after surgery (ERAS) society recommendations 2022. *World J Surg* (2023) 47(1):11–34. doi: 10.1007/s00268-022-06732-5

40. Chen F, Chi J, Liu Y, Fan L, Hu K. Impact of preoperative sarcopenia on postoperative complications and prognosis of gastric cancer resection: A meta-analysis of cohort studies. *Arch Gerontol Geriatr* (2022) 98:104534. doi: 10.1016/j.archger.2021.104534

41. Chianca V, Albano D, Messina C, Gitto S, Ruffo G, Guarino S, et al. Sarcopenia: imaging assessment and clinical application. *Abdom Radiol (NY)* (2022) 47(9):3205–16.

42. Williams DGA, Molinger J, Wischmeyer PE. The malnourished surgery patient: a silent epidemic in perioperative outcomes? *Curr Opin Anaesthesiol* (2019) 32(3):405–11. doi: 10.1097/ACO.0000000000000722

43. Bozzetti F. Chemotherapy-induced sarcopenia. *Curr Treat Options Oncol* (2020) 21(1):7. doi: 10.1007/s11864-019-0691-9

44. Levolger S, van Vledder MG, Muslem R, Koek M, Niessen WJ, de Man RA, et al. Sarcopenia impairs survival in patients with potentially curable hepatocellular carcinoma. *J Surg Oncol* (2015) 112(2):208–13. doi: 10.1002/jso.23976

45. Waalboer RB, Meyer YM, Galjart B, Olthof PB, van Vugt JLA, Grunhagen DJ, et al. Sarcopenia and long-term survival outcomes after local therapy for colorectal liver metastasis: a meta-analysis. *HPB (Oxford)* (2022) 24(1):9–16. doi: 10.1016/j.hpb.2021.08.947

46. Kelly KN, Iannuzzi JC, Rickles AS, Monson JR, Fleming FJ. Risk factors associated with 30-day postoperative readmissions in major gastrointestinal resections. *J Gastrointest Surg* (2014) 18(1):35–43; discussion -4. doi: 10.1007/s11605-013-2354-7

47. Capurso G, Pecorelli N, Burini A, Orsi G, Palumbo D, Macchini M, et al. The impact of nutritional status on pancreatic cancer therapy. *Expert Rev Anticancer Ther* (2022) 22(2):155–67. doi: 10.1080/14737140.2022.2026771

48. Lee JA, Young S, O'Connor V, DiFronzo LA. Safety and efficacy of an enhanced recovery protocol after hepatic resection. *Am Surg* (2020) 86(10):1396–400. doi: 10.1177/0003134820964492

49. Wada Y, Nishi M, Yoshikawa K, Takasu C, Tokunaga T, Nakao T, et al. Preoperative nutrition and exercise intervention in frailty patients with gastric cancer undergoing gastrectomy. *Int J Clin Oncol* (2022) 27(9):1421–7. doi: 10.1007/s10147-022-02202-z

50. Tully R, Loughney L, Bolger J, Sorensen J, McAnena O, Collins CG, et al. The effect of a pre- and post-operative exercise programme versus standard care on physical fitness of patients with oesophageal and gastric cancer undergoing neoadjuvant treatment prior to surgery (The PERIOP-OG Trial): Study protocol for a randomised controlled trial. *Trials* (2020) 21(1):638. doi: 10.1186/s13063-020-04311-4

51. Davis MP, Panikkar R. Sarcopenia associated with chemotherapy and targeted agents for cancer therapy. *Ann Palliat Med* (2019) 8(1):86–101. doi: 10.21037/apm.2018.08.02

# Frontiers in Oncology

**Advances knowledge of carcinogenesis and tumor progression for better treatment and management**

The third most-cited oncology journal, which highlights research in carcinogenesis and tumor progression, bridging the gap between basic research and applications to imrpove diagnosis, therapeutics and management strategies.

---

## Discover the latest Research Topics

See more →


**Frontiers**

Avenue du Tribunal-Fédéral 34
1005 Lausanne, Switzerland
frontiersin.org

**Contact us**

+41 (0)21 510 17 00
frontiersin.org/about/contact